

annual progress report

2009

ADVANCED VEHICLE TECHNOLOGY
ANALYSIS AND EVALUATION ACTIVITIES
AND HEAVY VEHICLE SYSTEMS
OPTIMIZATION PROGRAM

DEPARTMENT OF
ENERGY

Energy Efficiency &
Renewable Energy

**U.S. Department of Energy
Vehicle Technologies Program
1000 Independence Avenue, S.W.
Washington, DC 20585-0121**

FY 2009

Annual Progress Report for

**Advanced Vehicle Technology Analysis and Evaluation Activities and
Heavy Vehicle Systems Optimization Program**

**Submitted to:
U.S. Department of Energy
Energy Efficiency and Renewable Energy
Vehicle Technologies Program
Advanced Vehicle Technology Analysis and Evaluation**

Lee Slezak, Technology Manager

CONTENTS

I. INTRODUCTION.....	5
II. MODELING AND SIMULATION	14
A. Validation of Advanced Vehicles.....	14
B. Simulation Runs to Support GPRA/PDS	19
C. Evaluation of Technology Potential to Reach 40% Fuel Efficiency Improvement.....	29
D. PSAT Maintenance and Enhancements.....	35
E. Plug-and-Play Tool Development (Cooperative Research and Development Agreement with General Motors)	39
F. Impacts of Real-World Drive Cycles on PHEV Fuel Efficiency and Cost for Different Powertrain and Battery Characteristics.....	53
G. PHEV Vehicle Level Control Selection Based on Real World Drive Cycles.....	60
H. Instantaneous Optimization for a Multimode Transmission	67
I. Development of Models for Advanced Engines and Emission Control Components.....	74
J. Plug-in Hybrid Electric Vehicle (PHEV) Value Proposition Study.....	83
K. Plug-in Hybrid Electric Vehicle (PHEV) Market Introduction Study.....	92
L. Enabling High Efficiency Ethanol Engines (Delphi PHEV CRADA).....	97
M. Simulated Fuel Economy and Performance of Advanced Hybrid Electric and Plug-in Hybrid Electric Vehicle Technologies Using In-Use Travel Profiles	103
N. Predicting In-Use PHEV Fuel Economy from Standardized Test Cycle Results.....	108
O. Integrated Vehicle Thermal Management Systems Analysis/Modeling	113
P. Medium-Duty Plug-in Hybrid Electric Vehicle Analysis	118
Q. Energy Storage Life and Cost Study to Identify Cost-effective Vehicle Electrification.....	122
R. Medium and Heavy-Duty Vehicle Simulation	128
S. Medium Truck Duty Cycle (MTDC) Project	131
T. Technical and Market Penetration Challenges of Plug-in Hybrid Electric Vehicles	139
U. Predicted Impact of PHEVs to the U.S. Power System.....	151
III. INTEGRATION AND VALIDATION	161
A. Battery Hardware-in-the-Loop Testing	161
B. Peak Shaving-PHEV Battery Control Development & Vehicle.....	169
C. Impact of PHEV Design Strategies and Fuels on Fuel Economy and Emissions	176
IV. LABORATORY TESTING AND BENCHMARKING	184
A. Benchmarking and Validation of Hybrid Electric Vehicles.....	184
B. Benchmarking and Validation of Plug-in Hybrid Electric Vehicles	195
C. PHEV Test Methods and Procedures Development.....	210
D. PHEV Demonstration Program Prototype Vehicle Testing at APRF	215
E. Comparing PHEV Lab Test Data to On-Road Data.....	219
F. Maintain an On-Line HEV Test Results Database.....	227
G. Vehicle Test Procedure for Measuring Air Conditioning Fuel Use	231
V. OPERATIONAL AND FLEET TESTING	236
A. Plug-in Hybrid Electric Vehicle Testing by DOE's Advanced Vehicle Testing Activity (AVTA)	236
B. Hybrid Electric Vehicle Testing.....	258
C. Hydrogen Internal Combustion Engine (ICE) Vehicle Testing	272
D. Neighborhood Electric Vehicle Testing	277
E. Advanced Technology Medium and Heavy Vehicles Testing	281

VI. AERODYNAMIC DRAG REDUCTION 288
 A. DOE Project on Heavy Vehicle Aerodynamic Drag 288

VII. THERMAL MANAGEMENT 292
 A. Agreement # 14758 – Thermal Conditions Underhood: Nanofluids..... 292
 B. Agreement # 16824 – Efficient Cooling in Engines with Nucleate Boiling 298
 C. Agreement # 15529 - Erosion of Materials in Nanofluids 308
 D. Agreement #18494 – Nanofluid Development and Characterization..... 312
 E. CoolCab – Truck Thermal Load Reduction Project..... 317

VIII. FRICTION AND WEAR 323
 A. Boundary Lubrication Mechanisms 323
 B. Parasitic Energy Loss Mechanisms 331
 C. Agreement # 13723 - Residual Stresses in Thin Films* 341

I. INTRODUCTION

On behalf of the U.S. Department of Energy’s Vehicle Technologies (VT) Program, I am pleased to submit the Annual Progress Report for fiscal year 2009 for the Advanced Vehicle Technology Analysis and Evaluation (AVTAE) team activities.

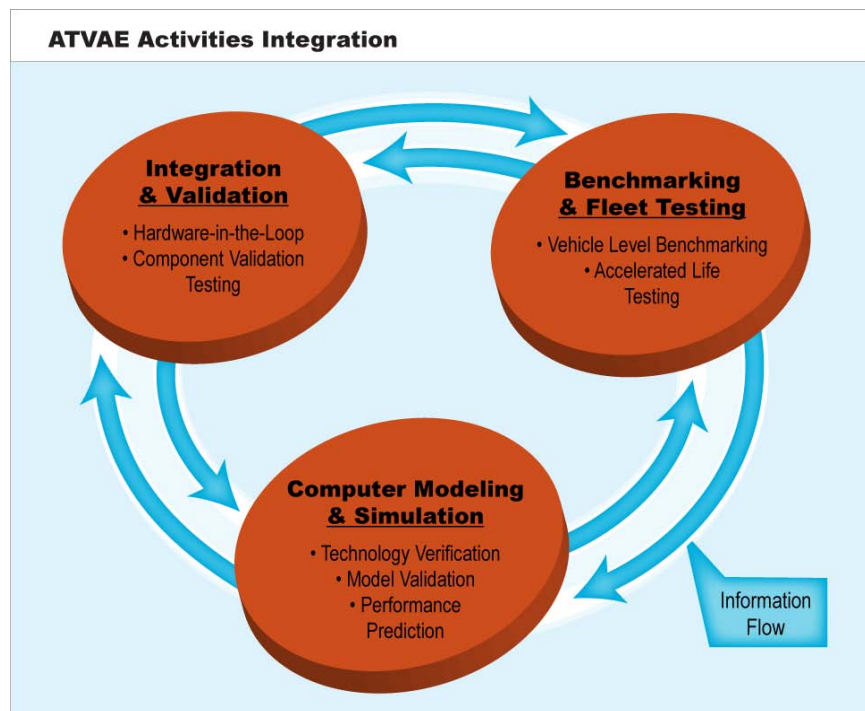
Mission

The AVTAE team’s mission is to evaluate the technologies and performance characteristics of advanced automotive powertrain components and subsystems in an integrated vehicle systems context, covering light to heavy platforms. This work is directed toward evaluating and verifying the targets of the VT technology R&D teams and to providing guidance in establishing roadmaps for achievement of these goals.

Objective

The prime objective of the AVTAE team activities is to evaluate VT Program targets and associated data that will enable the VT technology R&D teams to focus research on specific technology areas. The areas of interest are technologies that will maximize the potential for fuel efficiency improvements, as well as petroleum displacement, and tailpipe emissions reduction. AVTAE accomplishes this objective through a tight union of computer modeling and simulation, integrated component testing and emulation, and laboratory and field testing of vehicles and systems. AVTAE also supports the VT Program goals of fuel consumption reduction by developing and evaluating vehicle system technologies in the area of vehicle ancillary loads reduction.

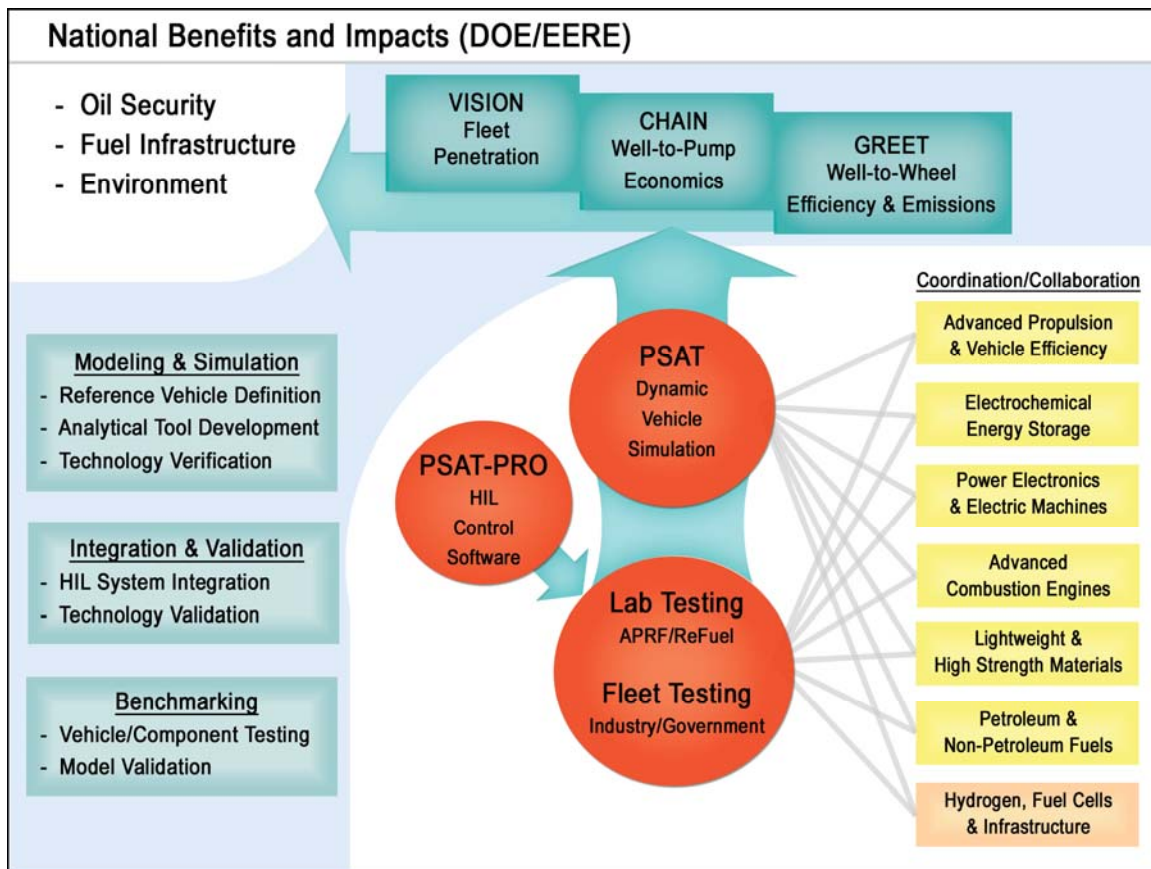
The integration of computer modeling and simulation, hardware-in-the-loop testing, vehicle benchmarking, and fleet evaluations is critical to the success of the AVTAE team. Each respective area feeds important information back into the other, strengthening each aspect of the team. A graphical representation of this is shown in the figure below.



Integration of AVTAE Computer Modeling and Testing Activities

FY 2009 AVTAE Activities

AVTAE provides an overarching vehicle systems perspective in support of the technology R&D activities of DOE’s VT and Hydrogen, Fuel Cells & Infrastructure Technologies (HFCIT) Programs. AVTAE uses analytical and empirical tools to model and simulate potential vehicle systems, validate component performance in a systems context, verify and benchmark emerging technology, and validate computer models. Hardware-in-the-loop testing allows components to be controlled in an emulated vehicle environment. Laboratory testing then provides measurement of progress toward VT technical goals and eventual validation of DOE-sponsored technologies at the Advanced Powertrain Research Facility for light- and medium-duty vehicles and at the ReFUEL Facility for heavy-duty vehicles. For this sub-program to be successful, extensive collaboration with the technology development activities within the VT and HFCIT Programs is required for both analysis and testing. Analytical results of this sub-program are used to estimate national benefits and and/or impacts of DOE-sponsored technology development, as illustrated in the figure below.



AVTAE Activities Providing Estimates of National Benefits and Impacts of Advanced Technologies

AVTAE is comprised of the following seven (7) main focus areas, each of which is described in detail in this report:

1. Modeling and Simulation

A unique set of tools has been developed and is maintained to support VT research. VISION, CHAIN, and GREET are used to forecast national-level energy and environmental parameters including oil use, infrastructure economics, and greenhouse gas contributions of new technologies, based on VT vehicle-level simulations that predict fuel economy and emissions using the Powertrain Systems Analysis Toolkit (PSAT) modeling tool. Dynamic simulation models (i.e., PSAT) are combined with DOE's specialized equipment and facilities to validate DOE-sponsored technologies in a vehicle context (i.e., PSAT-PRO control code and actual hardware components in a virtual vehicle test environment). Modeling and testing tasks are closely coordinated to enhance and validate models as well as ensure laboratory and field test procedures and protocols comprehend the needs of coming technologies.

PSAT (Powertrain Systems Analysis Toolkit) allows dynamic analysis of vehicle performance and efficiency to support detailed design, hardware development, and validation. A driver model attempts to follow a driving cycle, sending a torque demand to the vehicle controller, which, in turn sends a demand to the propulsion components (commonly referred to as "forward-facing" simulation). Dynamic component models react to the demand (using transient equation-based models) and feed back their status to the controller. The process iterates on a sub-second basis to achieve the desired result (similar to the operation of a vehicle). The forward architecture is suitable for detailed analysis of vehicles/propulsion systems and the realistic command-control-feedback capability is directly translatable to PSAT-PRO control software for testing in the laboratory. Capabilities include transient performance, efficiency and emissions (conventional, hybrid, plug-in hybrid and fuel cell vehicles), development and optimization of energy management strategies, and identification of transient control requirements.

PSAT-PRO (PSAT rapid control PROtotyping software) allows dynamic control of components and subsystems in Rapid Control Prototyping (RCP) or hardware-in-the-loop (HIL) testing. Hardware components are controlled in an emulated vehicle environment (i.e., a controlled dynamometer and driveline components) according to the control strategy, control signals, and feedback of the components and vehicle as determined using PSAT. The combination of PSAT-PRO and RCP/HIL is suitable for propulsion system integration and control system development, as well as rigorous validation of control strategies, components, or subsystems in a vehicle context (without building a vehicle). Capabilities include transient component, subsystem and dynamometer control with hardware operational safeguards compatible with standard control systems.

AUTONOMIE is a newly developed MATLAB based software environment and framework for automotive control system design, simulation and analysis. The software was developed under a Cooperative Research and Development Activity (CRADA) with General Motors and substantial input from other OEMs. One of the primary benefits of Autonomie is its Plug-and-Play foundation which allows integration of models of various degrees of fidelity and abstraction from multiple engineering software environments, including GT-Power®, AMESim®, CarSim®, and AVL-DRIVE®. Autonomie enables the development, sharing, and rapid application of models, control algorithms and processes from the entire automotive community. Autonomie uses a unique Graphical User Interface (GUI) to simplify the integration and configuration process and accelerate the selection of models to be evaluated. The program is currently in the BETA stage of development.

2. Integration and Validation

Hardware-in-the-loop (HIL) simulation provides a novel and cost effective approach to evaluating advanced automotive component and subsystem technologies. HIL allows actual hardware components

to be tested in the laboratory at a full vehicle level without the extensive cost and lead time of building a complete prototype vehicle. This task integrates modeling and simulation with hardware in the laboratory to develop/evaluate propulsion subsystems in a full vehicle level context.

The versatile Mobile Automotive Technology Testbed (MATT) was developed in FY 2008. MATT serves as a unique HIL platform for advanced powertrain technology evaluation in an emulated vehicle environment. The flexible chassis testbed allows researchers to easily replace advanced components or change the architecture of the powertrain in various hybrid configurations. MATT was developed to assist DOE in validating advanced technology. MATT was utilized in FY 2009 in a collaborative effort between ANL and the University of Tennessee to evaluate the impact of Hybrid control strategies on fuel economy and emissions, as detailed in this report. As the VT Program matures, the need to evaluate newly developed technology in a vehicle system context will become critical. Through the FreedomCAR and Fuels Partnership Vehicle System Analysis Technical Team (VSATT), MATT facilitates interactions between each of the other technical teams by providing a common platform for component integration and testing. Each specific set of technical targets and their impacts on the vehicle system can easily be studied using the MATT platform.

High energy traction battery technology is important to the successful development of plug-in hybrid electric vehicles. In support of plug-in hybrid electrical vehicle (PHEV) research, Argonne National Laboratory (ANL) has developed and implemented a battery hardware-in-the-loop simulator to test potential battery packs in vehicle level operating conditions. Research continued in this area in FY 2009 as ANL used PSAT to provide a virtual vehicle for a collaborative effort with Johnson Controls-Saft (JCS). This research used Battery Hardware in the loop (BHIL) to study the trade-offs between fuel efficiency and battery life with a cost analysis.

3. Laboratory Testing and Benchmarking

This section describes the activities related to laboratory validation of advanced propulsion subsystem technologies for advanced vehicles. In benchmarking, the objective is to extensively test production vehicle and component technology to ensure that VT-developed technologies represent significant advances over technologies that have been developed by industry. Technology validation involves the testing of DOE-developed components or subsystems to evaluate the technology in the proper systems context. Validation helps to guide future VT programs and facilitates the setting of performance targets.

Validation and benchmarking require the use of internationally accepted test procedures and measurement methods. However, many new technologies require adaptations and more careful attention to specific procedures. AVTAE engineers have developed many new standards and protocols, which have been presented to a wide audience such as FreedomCAR partners, other government laboratories, and the European Commission and are being adopted as industry standard testing procedures.

To date, over 110 PHEVs, HEVs, fuel cell vehicles, and propulsion subsystem components have been benchmarked or validated by the AVTAE team. The results of these evaluations have been used to identify needed areas of improvement for these advanced vehicles and technologies that will help bring them to market faster. They have also been used to identify the most promising new opportunity areas to achieve greater overall vehicle efficiencies at the lowest possible cost. The propulsion system hardware components: batteries, inverters, electric motors and controllers are further validated in simulated vehicle environments to ensure that they meet the vehicle performance targets established by the government-industry technical teams.

The major facility that supports these activities is the Advanced Powertrain Research Facility (APRF), a state-of-the-art automotive testing laboratory operated by ANL. A multi-dynamometer facility for testing components (such as engines and electric motors) and a four-wheel vehicle dynamometer that allows

accurate testing of all types of powertrain topologies. ANL utilizes its own correlation vehicle for test repeatability. This facility will undergo substantial upgrades in FY 2010 to prepare for additional ambient condition impact testing on BEVs, HEVs and PHEVs.

4. Operational and Fleet Testing

The Advanced Vehicle Testing Activity (AVTA), working with industry partners, accurately measures real-world performance of advanced technology vehicles via a testing regime based on test procedures developed with input from industry and other stakeholders. The performance and capabilities of advanced technologies are benchmarked to support the development of industry and DOE technology targets. The testing results provide data for validating component, subsystem, and vehicle simulation models and hardware-in-the-loop testing. Fleet managers and the public use the test results for advanced technology vehicle acquisition decisions. Idaho National Laboratory (INL) conducts light-duty testing activities in partnership with an industry group led by Electric Transportation Applications (ETA). Accelerated reliability testing provides reliable benchmark data of the fuel economy, operations and maintenance requirements, general vehicle performance, engine and component (such as energy storage system) life, and life-cycle costs. the needs of the testing partner; the tests are described below.

Baseline Performance Testing

The objective of baseline performance testing is to provide a highly accurate snapshot of a vehicle's performance in a controlled testing environment. The testing is designed to be highly repeatable. Hence it is conducted on closed tracks and dynamometers, providing comparative testing results that allow "apple-to-apple" comparisons within respective vehicle technology classes. The APRF at ANL is utilized for the dynamometer testing of the vehicles.

Fleet Testing

Fleet testing provides a real-world balance to highly controlled baseline performance testing. Some fleet managers prefer fleet testing results to the more controlled baseline performance or the accelerated reliability testing.

During fleet testing, a vehicle or group of vehicles is operated in normal fleet applications. Operating parameters such as fuel-use, operations and maintenance, costs/expenses, and all vehicle problems are documented. Fleet testing usually lasts one to three years and, depending on the vehicle technology, between 3,000 and 25,000 miles are accumulated on each vehicle.

For some vehicle technologies, fleet testing may be the only available test method. Neighborhood electric vehicles (NEVs) are a good example. Their manufacturer-recommended charging practices often require up to 10 hours per charge cycle, while they operate at low speeds (<26 mph). This makes it nearly impossible to perform accelerated reliability testing on such vehicles.

Accelerated Reliability Testing

The objective of accelerated reliability testing is to quickly accumulate several years or an entire vehicle-life's worth of mileage on each test vehicle. The tests are generally conducted on public roads and highways, and testing usually lasts for up to 36 months per vehicle. The miles to be accumulated and time required depend heavily on the vehicle technology being tested. For instance, the accelerated reliability testing goal for PHEVs is to accumulate 5,400 miles per vehicle in 7 months. The testing goal for HEVs is to accumulate 160,000 miles per vehicle within three years. This is several times greater than most HEVs will be driven in three years, but it is required to provide meaningful vehicle-life data within a useful time frame. Generally, two vehicles of each model are tested to ensure accuracy. Ideally, a larger sample size would be tested, but funding tradeoffs necessitate only testing two of each model to ensure accuracy.

Depending on the vehicle technology, a vehicle report is completed for each vehicle model for both fleet and accelerated reliability testing. However, because of the significant volume of data collected for the HEVs, fleet testing fact sheets (including accelerated reliability testing) and maintenance sheets are provided for the HEVs.

5. Aerodynamic Drag Reduction for Heavy Duty Vehicles

The primary goal of this focus area is to reduce Class 8 tractor-trailer aerodynamic drag for a significant improvement on fuel economy while satisfying regulatory and industry operational constraints. An important part of this effort is to expand and coordinate industry collaborations with DOE and establish buy-in through CRADAs and to accelerate the introduction of proven aerodynamic drag reduction devices into new vehicle offerings.

The primary approach in drag reduction is through the control of the tractor-trailer flow field and tractor-trailer integration. This will be achieved with geometry modifications, integration, and flow conditioning. These are essential components to develop and design the next generation of aerodynamically integrated tractor-trailer.

To accomplish this goal, Lawrence Livermore National Laboratory (LLNL) has established a unique team of experts from industry, university, and government laboratory to perform a full-scale (80'x120') wind tunnel test at NFAC/NASA Ames research facility. A number of drag reducing aerodynamic devices/concepts will be tested in addition to aerodynamic impact of low rolling resistance super single tires from Michelin. Three flow regions around the heavy vehicle are explored: trailer base, underbody, and tractor-trailer gap for application of drag reducing add-on devices. Many add-on devices will be tested, with two different tractors (standard and long sleeper) and three different trailers (28', 53', and 53' drop frame) for their individual performance and in combination with other devices.

6. Thermal Management for Heavy Duty Vehicles

Thermal management of heavy vehicle engines and support systems is a technology that addresses reduction in energy usage through improvements in engine thermal efficiency and reductions in parasitic energy uses and losses. Fuel consumption is directly related to the thermal efficiency of engines and support systems. New thermal management technologies with the potential for high impact on energy reduction are investigated and developed under this program. Technologies are targeted that can increase the percentage of mechanical work extracted from the combustion process and decrease the heat rejection to the environment. Some technologies impact the thermal efficiency directly while others reduce energy usage including, but not limited to, such areas as: reduction in weight, reduced size of auxiliary engine systems, reduction in power consumption of auxiliary systems, and reduced aerodynamic drag.

Components of this interrelated program, which are briefly described in the following paragraphs, include development and characterization of nanofluids, experimental measurements and theoretical analysis of heat transfer characteristics of nanofluids, investigation of the erosion effects of nanofluids, and work on evaporative cooling. The work is performed in collaboration with Michelin, Saint Gobain, Cummins, PACCAR, and TARDEC.

Development and Characterization of Nanofluids

The aim of this project is to develop the required chemistry to produce nanofluids with the largest enhancement of thermal conductivities. Addition of nanoparticles to a coolant (typically 50/50 ethylene glycol/water mixture) increases viscosity so that considerable effort is devoted to viscosity modifications. Additionally, the effect of nanoparticle material, size, volume concentration, suspension properties, and shape are explored because these properties determine the effectiveness of the coolant. These properties are investigated over a range of temperatures. Experimental results are compared with existent theories that are modified if necessary.

Heat Transfer

The most important property of a coolant is most likely its heat transfer coefficient. The heat transfer coefficients are determined for turbulent flow in a unique, ANL-designed and built, horizontal stainless steel tube apparatus. Experimental turbulent Reynolds number typically ranges from 3,000 to 13,000 with a Prandtl number range of 4.6 to 7.1, a velocity range of 1.8 to 5.4 m/s, and a nanofluid temperature range of 34 to 57°C. Results are compared to predictions from standard correlations for liquids and the correlations are modified if necessary.

Erosion

Nanofluids could potentially erode radiator materials. This experiment is designed to measure the material wastage of typical radiator materials and an automotive pump using very controlled conditions. Additionally, the power required to pump nanofluids can be measured and compared to power required to pump coolants without nanoparticles.

Nucleated Boiling

It is well known that boiling heat transfer coefficients are much higher than the convective heat transfer coefficient of the same fluid. However, in order to use boiling for cooling a truck radiator, the critical heat flux (CHF) must be avoided or severe damage would occur. Hence, this program is designed to measure the heat transfer coefficient and CHF of several possible coolants, compare the results to theories, and transfer the data to industry.

7. Friction and Wear for Heavy Duty Vehicles

Parasitic engine and driveline energy losses arising from boundary friction and viscous losses consume 10 to 15 percent of fuel used in transportation, and thus engines and driveline components are being redesigned to incorporate low-friction technologies to increase fuel efficiency of passenger and heavy-duty vehicles. The Friction and Wear Project, within the Heavy Vehicle Systems Optimization Program, supports research agreements/projects that focus on the development of advanced technologies required to improve the fuel efficiency and reliability of critical engine and driveline components, notably:

- Activities to experimentally investigate fundamental friction and wear mechanisms to provide the understanding required for developing advanced low-friction, fuel-efficient technologies.
- Activities to model and validate, component-by-component, the impact of friction on overall vehicle efficiency.
- Activities to develop advanced low friction technologies (materials, coatings, engineered surfaces, and advanced lubricants) required to improve engine and driveline efficiency and reliability/durability.

Boundary Layer Lubrication

Researchers at ANL have made significant progress on the development of modeling scuffing phenomena and the formation of protective tribofilms. In the first task, material pairs with a high CSI (contact severity index – a measure of resistance to scuffing) were evaluated. The mechanisms for scuffing in these material pairs were elucidated, providing a pathway for further improvement in scuffing resistance. The development of materials with enhanced scuffing resistance will facilitate the development of high-power-density components and systems. The second task involved characterization of low-friction boundary films produced from a model lubricant and fully formulated lubricant. Post-test analysis of the films by SEM, EDX, and FIB is ongoing. These analyses will provide information on the thickness, composition, and structure of highly desirable low-friction boundary films.

Parasitic Energy Losses

At ANL, researchers continued to use computer simulations of parasitic energy losses in diesel engines to guide fundamental research on low friction coatings and additive treatments. Work is underway to experimentally validate the models by tests with a fired, single-cylinder diesel rig outfitted with an

instrumented fixed-sleeve to measure the friction forces continuously as a function of crank angle. A piston component test rig was developed and brought on-line to validate the friction coefficient data used to model the parasitic friction losses, as well as to optimize advanced surface modification technologies for engine applications. Tests are underway to evaluate two technologies: a boric-acid-based lubricant additive and a surface texturing technique. Laboratory tests using the ring-on-liner rig indicated that friction can be significantly reduced by using boric-acid based additives.

Hard/SuperHard Nanocomposite Coatings

Researchers at ANL focused their effort toward further optimization and scale-up of ANL's superhard coating technology. In collaboration with a commercial coating company, ANL researchers produced superhard coatings on commercial-scale deposition systems and performed extensive tests to determine their mechanical and tribological properties. They also performed surface and structure analytical studies on the coatings produced on the commercial system to determine their structural morphology and chemical compositions. Tribological tests of such coatings at ANL confirmed their extreme resistance to wear and scuffing. Near-term future activities will focus on applying the coatings to a large variety of engine components (tappets, valve lifters, fuel injectors, piston rings, etc.) and testing them in actual engines.

Major projects which were conducted by the national laboratories in support of these areas in FY 2009 are described in this report. A summary of the major activities in each area is given first, followed by detailed reports on the approach, accomplishments and future directions for the projects. For further information, please contact the DOE Project Leader named for each project.

Future Directions for AVTAE

Near-term solutions for reducing the nation's dependence on imported oil, such as PHEVs, will require the development, integration, and control of vehicle components, subsystems, and support systems. These solutions will require exploration of high capacity energy storage and propulsion system combinations to get the most out of hybrid propulsion. Analysis and testing procedures at the national labs will be enhanced to study these advanced powertrains with simulation tools, component/subsystem integration, and hardware-in-the-loop testing. DOE-sponsored hardware developments will be validated at the vehicle level, using a combination of testing and simulation procedures.

In FY 2010, the AVTAE will continue to expand activities in the area of PHEV simulation and evaluation including further baseline performance testing of conversion and original equipment manufacturer (OEM) PHEVs, and validation of simulation models for PHEVs tested in the APRF. Field and laboratory testing will continue to be integrated with modeling/simulation tools. Fleet evaluation of PHEV conversion vehicles will continue; however, emphasis will be placed on establishing evaluation fleets of OEM production PHEVs. In FY 2008, DOE VT issued a solicitation for the purpose of establishing a PHEV demonstration fleet consisting of large volume manufacturers and OEMs as participants. This program launched in FY 2009 and will last for approximately three years. Deviation of test procedures for PHEVs will be completed, and a new PHEV test procedure will be submitted to SAE (J1711) in FY 2010. Work will focus on validation of these procedures.

In addition to the HEV and PHEV activities, a full range of simulation and evaluation activities will be conducted on Battery Electric Vehicles (EV) as they are brought to market by OEMs. Because EVs are dependent on a robust charging infrastructure for their operation and ultimate consumer acceptance, the AVTAE will greatly increase efforts to address issues related to codes and standards for EVs, charging infrastructure, and vehicle/grid integration. AVTAE FY 2010 activities will include the management, coordination, and data harvesting from 18 electric drive vehicle demonstration and education projects that were selected for \$400 million of American Reinvestment and Recovery Act funding under Transportation Electrification in FY 2009.

Heavy vehicle systems optimization work in the areas of aerodynamics, thermal management, and friction and wear will continue, but at a reduced effort level in FY 2010. The focus of these activities will revolve around cooperative projects with industry partners, in an attempt to bring developed technologies to market quickly.

Work on a revised vehicle cost model, incorporated into PSAT, will continue in FY 2010. Although the development of light vehicle simulation models will be essentially completed, the vehicle and component models, as well as their respective control strategies, will continually be updated and enhanced to reflect the progress of technology in the transportation sector. Validation of VT technologies for advanced power electronics, energy storage, and combustion engines will be ongoing as each technology progresses towards the targeted performance.

Inquiries regarding the AVTAE activities may be directed to the undersigned.



Lee Slezak

Technology Manager

Advanced Vehicle Technology Analysis and Evaluation

Vehicle Technologies Program

II. MODELING AND SIMULATION

A. Validation of Advanced Vehicles

Antoine Delorme (project leader), Philippe Abiven, Dominik Karbowski, Aymeric Rousseau
 Argonne National Laboratory
 9700 South Cass Avenue
 Argonne, IL 60439-4815
 (630) 252-7261; *arousseau@anl.gov*

DOE Technology Manager: Lee Slezak

Objectives

Validate the latest conventional, hybrid, and plug-in hybrid vehicles in Powertrain System Analysis Toolkit (PSAT).

Approach

- Gather component and vehicle assumptions.
- Develop the vehicle-level control strategy.
- Validate the model by comparing with available test data.

Accomplishments

- Validated heavy-duty conventional vehicles.
- Validated hybrid electric vehicles (HEVs) and plug-in hybrid electric vehicles (PHEVs) using proprietary data.

Future Directions

- Continue to validate models of the latest powertrain technologies.

Introduction

The objective of this project is to validate the latest vehicle powertrain configurations and component technologies to ensure the accuracy of the component data and vehicle-level control strategies used to evaluate fuel consumption benefits. The information obtained will support Department of Energy (DOE) research and development guidance.

Because no vehicle test data are available within DOE for validation of medium- and heavy-duty applications, test data from partnerships with West Virginia University and the U.S. Environmental Protection Agency (EPA) were used.

Vehicle Test Data Analysis

To validate the vehicle model, Argonne used a generic process shown in Figure 1. First, the test data from a text file are imported into a Matlab environment following a PSAT format. Then, each parameter is analyzed, the redundant signals are compared, and the missing signals are calculated.

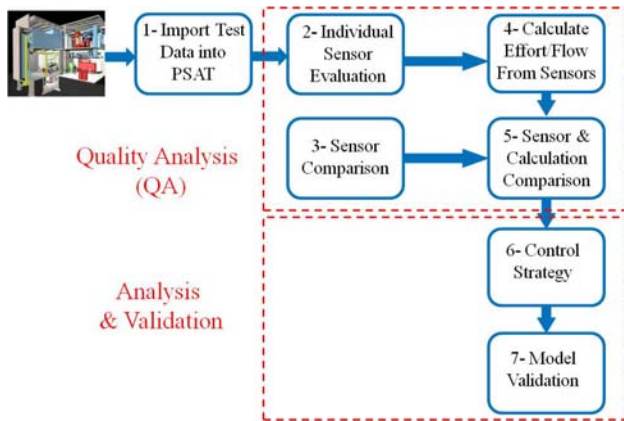


Figure 1. Test Data Analysis Process

The same process was implemented for the different validations considered below.

Ford PHEV Escape

A pre-production version of the Ford Escape PHEV was tested at Argonne’s Advanced Powertrain Research Facility. A previously validated Ford Escape HEV model was used as a starting point. The battery model and data were provided by Argonne’s Battery Group. The vehicle control strategy was analyzed and reproduced in simulation. The engine

ON/OFF and its operating conditions were matched with the test data. Because of the proprietary nature of the vehicle application, detailed information is not provided in this report.

Line-Haul Class 8 with West Virginia University

A model of a 1996 long-haul Peterbilt truck, tested at West Virginia University, was developed and validated. Figure 2 shows the Peterbilt truck used in this research. Table 1 presents the details of the vehicle configuration.



Figure 2. Peterbilt Truck

Table 1. Details of the Peterbilt Truck and Test Conditions

Description	Model Characteristics
Vehicle Manufacturer	Peterbilt
Vehicle Model Year	1996
Gross Vehicle Weight	20,909 kg/46,000 lb (tractor only) 36,364 kg/80,000 lb (assumed value with trailer)
Vehicle Tested Weight	25,455 kg/56,000 lb
Odometer Reading (mile)	441,097
Transmission Type	Manual
Transmission Configuration	18 speed
Engine Type	Caterpillar 3406E
Engine Model Year	1996
Engine Displacement (liter)	14.6
Number of Cylinders	6
Primary Fuel	D2
Test Cycle	Urban dynamometer driving schedule (UDDS) (also termed TEST_D)
Test Date	4/21/06

As for any validation, the critical aspect is to match the efforts and flows of the different components, along with the fuel rate, at every sample time of the test. Figure 3 shows a good correlation between the instantaneous fuel rates from simulation and test.

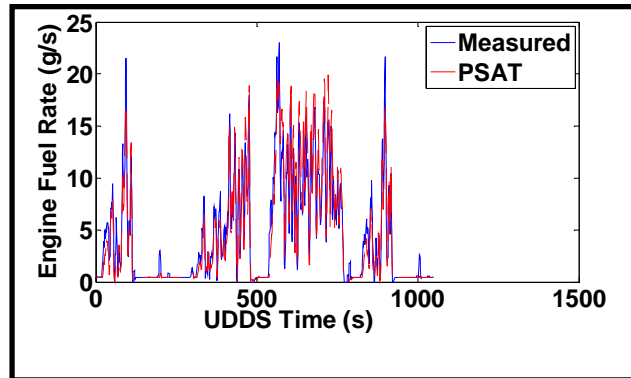


Figure 3. Peterbilt Truck Engine Fuel Rate Comparison

Table 2 provides a summary of the fuel consumption results for the test conditions considered.

Table 2. Peterbilt Truck PSAT Validation with Chassis (test weight 56,000 lb)

Parameters	Measured	Simulation	Error
UDDS Cycle (miles)	5.44	5.37	1.29
Fuel Economy (mpg)	3.82	3.82	0.00
Fuel Consumption (gal/100 miles)	26.17	26.17	0.00
Fuel Mass (kg)	4.58	4.52	1.31
Engine Fuel Rate (g/s)	4.40	4.30	1.27
CO ₂ (g/mile)	2639.8	2685.5	-1.73

Line-Haul Class 8 with EPA

In collaboration with EPA, Argonne validated another long-haul application. The vehicle, tested at SouthWest Research Institute (SwRI) was modeled in PSAT and validated using dynamometer test data. The truck is a Navistar ProStar with a Cummins ISX ST400 and a 10-speed manual transmission from EATON.

Figure 4 shows the close correlation between the simulated and measured engine speed. The other components’ effort and flow were matched as well, resulting in good comparison for the fuel economy for several cycles, as shown in Table 3.

The validation of the line-haul class 8 vehicle is ongoing; a new round of vehicle testing will be

performed at SwRI to address some remaining issues.

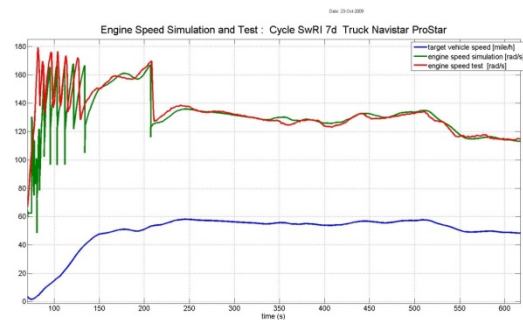


Figure 4. Navistar ProStar Truck Engine Speed Comparison

Table 3. Navistar ProStar Truck PSAT Validation – Fuel Economy (mpg)

Cycle	Measured	Simulation	Relative Error
7D	6.03	5.99	0.6
8D	7.31	7.1	2.8

Comparison with Other Published Studies

To further verify the validity of the model for medium- and heavy-duty applications, several analyses were performed to assess the impact of future technologies. Because of the lack of test data, the results were correlated with those contained in published studies.

Weight Reduction

Simulations were performed to assess the impact of gross vehicle weight rating (GVWR) reduction on fuel consumption. The baseline truck had a GVWR of 36,280 kg. The vehicle was simulated for different weights on the HHDDT65 (heavy heavy-duty diesel truck 65) drive cycle, which combines the various HHDDT cycles developed by the California Air Resources Board (CARB). The fuel consumption results and the percentage of fuel saved are shown in Figure 5, along with estimates by SwRI in the Northeast States Center for a Clean Air Future (NESCCAF) study.

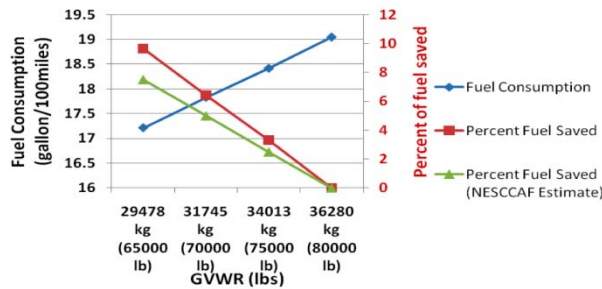


Figure 5. Impact of Gross Vehicle Weight Reduction on Fuel Consumption for a Class 8 Truck

The simulations show a 9.6% fuel consumption reduction when decreasing the GVWR from 80,000 to 65,000 lb. In other words, we can expect a 0.6% fuel saving for every 1,000-lb weight reduction. In comparison, the NESCCAF study estimate was 0.5%, and the Smartway estimate was 0.4%. It is important to keep in mind that the use of different

engine maps, transmissions, shifting schedules, drive cycles, or accessories can affect these estimates.

Rolling Resistance and Aerodynamic Reduction

Simulations were performed to assess the impact of drag coefficient reduction on fuel consumption. The baseline truck was a line-haul class 8 with a GVWR of 36,280 kg, a drag coefficient of 0.63, and a rolling resistance coefficient of 0.0068. The truck was simulated on the HHDDT65 cycle, and the simulation results were compared with those of other studies.

Figure 6 depicts the set of simulations that used a fixed rolling resistance of 0.0055. The drag coefficient varied from 0.63 to 0.4. Results show that reducing the drag coefficient leads to a 15.2% reduction in fuel consumption. In comparison, the NESCCAF study indicated a 14% fuel savings for the same scenario.

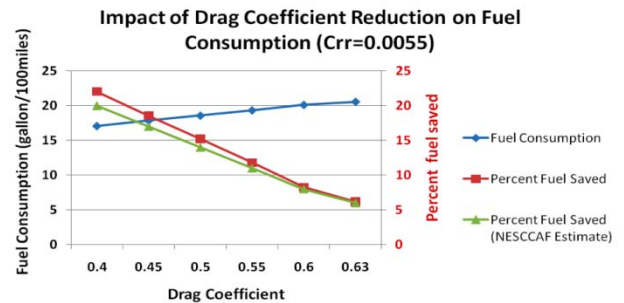


Figure 6. Impact of Drag Coefficient Reduction on Fuel Consumption (rolling resistance fixed at 0.0055)

Figure 7 shows a more aggressive scenario in which the rolling resistance value is set to 0.0045 and the drag coefficient is then reduced from 0.63 to 0.3. In this case, reducing the drag coefficient leads to a 26.7% reduction in fuel consumption. Again, these results are close to the NESCCAF estimates, which indicate a 24.6% fuel savings for this situation.

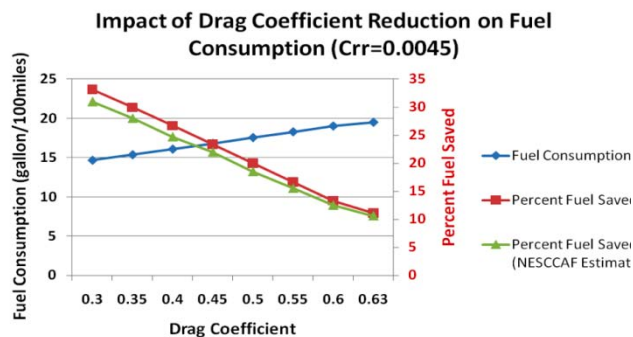


Figure 7. Impact of Drag Coefficient Reduction on Fuel Consumption (rolling resistance fixed at 0.0045)

Conclusion

Several vehicles were validated by using Argonne's Advanced Powertrain Research Facility and test data from government agencies (EPA) and universities. The validation of the Ford Escape PHEV and two line-haul class 8 vehicles demonstrated good correlation between tests and simulation.

The impacts of several key parameters, including weight, rolling resistance, and aerodynamics, were correlated with the results contained in published studies. The results from Argonne's simulation tools demonstrate improvements comparable to those found in other published studies.

The validation and correlation exercises demonstrate that PSAT is now ready for use in assessing the fuel consumption benefits of medium- and heavy-duty vehicles.

Publications/Presentations

N. Kim, R. Carlson, F. Jehlik, A. Rousseau, "Tahoe HEV Model Development in PSAT," SAE paper 2009-01-1307, SAE World Congress, Detroit, April 2009.

A. Rousseau, "Vehicle Model Validation, Presentation at DOE Annual Merit Review," May 2009.

A. Rousseau, "Update on Line-Haul Validation," Presentation to EPA, June 2009.

A. Rousseau, "Heavy-Duty Modeling and Simulation Update," Presentation to DOE, September 2009.

B. Simulation Runs to Support GPRA/PDS

Aymeric Rousseau (Project Leader), Antoine Delorme, Sylvain Pagerit, Phil Sharer
 Argonne National Laboratory
 9700 South Cass Avenue
 Argonne, IL 60439-4815
 (630) 252-7261; arouseau@anl.gov

DOE Technology Manager: Lee Slezak

Objectives

Simulate multiple vehicle platforms, configurations, and timeframes to provide fuel economy data for analysis in support of the Government Performance and Results Act (GPRA) of 1993.

Approach

Validate component and vehicle assumptions with Department of Energy (DOE) national laboratories and FreedomCAR Technical Teams.

Use automatic component sizing to run the study.

Accomplishments

Simulated and sized more than 1,000 vehicles.

Simulated new vehicles when assumptions or platforms were revised or when additional configurations or timeframes were requested.

Future Directions

Continue to provide analytical data to support GPRA in 2010.

Introduction

Through the Office of Planning, Budget, and Analysis, DOE's Office of Energy Efficiency and Renewable Energy (EERE) provides estimates of program benefits in its annual Congressional Budget Request. GPRA provided the basis for assessing the performance of Federally funded programs. Often referred to as "GPRA Benefits Estimates," these estimates represent one piece of EERE's GPRA implementation efforts—documenting some of the economic, environmental, and security benefits (or outcomes) that result from achieving program goals. The Powertrain System Analysis Toolkit (PSAT) was used to evaluate the fuel economy of numerous vehicle configurations (including conventional, hybrid electric vehicles [HEVs], plug-in HEVs [PHEVs], electric vehicles [EVs]), component technologies (gasoline, diesel, and hydrogen

engines, as well as fuel cells), and timeframes (current, 2010, 2015, 2030, and 2045). The uncertainty of each technology is taken into account by assigning probability values for each assumption.

Methodology

To evaluate the fuel efficiency benefits of advanced vehicles, the vehicles are designed on the basis of component assumptions. The fuel efficiency is then simulated on the Urban Dynamometer Driving Schedule (UDDS) and Highway Fuel Economy Test (HWFET). The vehicle costs are calculated from the component sizing. Both cost and fuel efficiency are then used to define the market penetration of each technology to finally estimate the amount of fuel saved. The process is highlighted in Figure 1. This report focuses on the first phase of the project: fuel efficiency and cost.

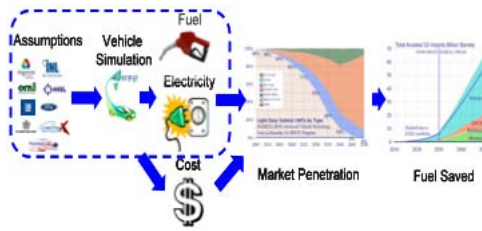


Figure 1. Process to Evaluate Fuel Efficiency of Advanced Technology Vehicles

To properly assess the benefits of future technologies, the following options were considered, as shown in Figure 2:

- Five vehicle classes: compact car, midsize car, small sport utility vehicle (SUV), medium SUV, and pickup truck.
- Five timeframes: current, 2010, 2015, 2030, and 2045.
- Five powertrain configurations: conventional, HEV, PHEV, fuel cell HEV, and EV.
- Four fuels: gasoline, diesel, hydrogen, and ethanol.

Overall, more than 1,000 vehicles were defined and simulated in PSAT. The current study does not include micro- or mild hybrids and does not focus on emissions.



Figure 2. Vehicle Classes, Timeframes, Configurations, and Fuels Considered

To address uncertainties, a triangular distribution approach (low, medium, and high) was employed, as shown in Figure 3. For each component, assumptions (e.g., regarding efficiency, power density) were made, and three separate values were defined to represent the (1) 90th percentile, (2) 50th percentile, and (3) 10th percentile. A 90%

probability means that the technology has a 90% chance of being available at the time considered. For each vehicle considered, the cost assumptions also follow the triangular uncertainty. Each set of assumptions is, however, used for each vehicle, and the most efficient components are not automatically the least-expensive ones. As a result, for each vehicle considered, we simulated three options for fuel efficiency. Each of these three options also has three values representing the cost uncertainties.

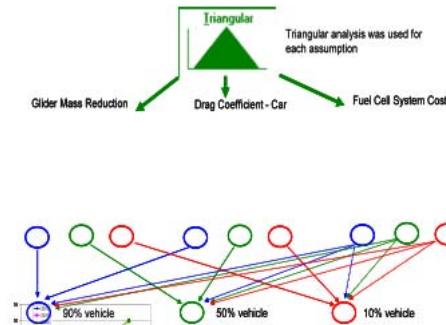


Figure 3. Uncertainty Process

The following paragraphs describe the assumptions and their associated uncertainties for each component technology.

Vehicle Technology Projections

The assumptions described below have been defined on the basis of inputs from experts and the FreedomCAR targets (when available).

Engines

Several state-of-the-art engines were selected for the fuels considered: gasoline, diesel, E85 FlexFuel, and hydrogen. The gasoline, diesel, and E85 FlexFuel engines used for current conventional vehicles were provided by automotive car manufacturers, while the port-injected hydrogen engine data were generated at Argonne. The engines used for HEVs and PHEVs are based on Atkinson cycles.

Different options were considered to estimate the evolution of each engine technology. Although linear scaling was used for gasoline, E85 (HEV applications only), and diesel engines, direct injection with linear scaling was considered for the hydrogen-fueled engine, and nonlinear scaling based on AVL’s work was used for gasoline and E85 (conventional applications). For the nonlinear

scaling, different operating areas were improved by different amounts, which resulted in changing the constant efficiency contours. The peak efficiencies of the different fuels and technologies are shown in Figure 4.

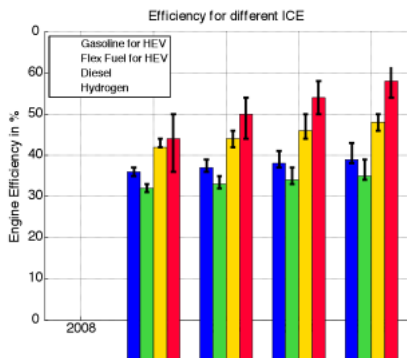


Figure 4. Engine Efficiency Evolution

Fuel Cell Systems

The fuel cell system model is based on the steady-state efficiency map. The values shown in Figure 5 include the balance of plant. The system is assumed to be gaseous hydrogen. In simulation, the additional losses due to transient operating conditions are not taken into account.

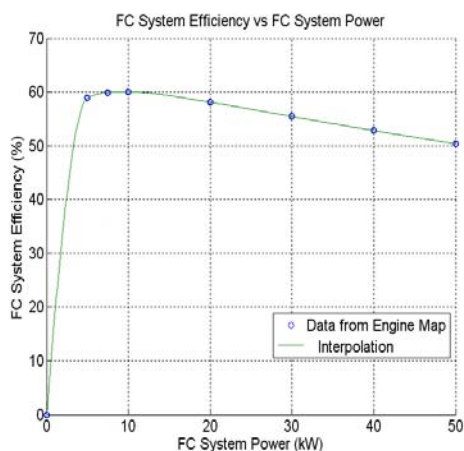


Figure 5. Fuel Cell System Efficiency versus Fuel Cell System Power from the System Map

Figure 6 shows the peak efficiencies of the fuel cell system and its cost. The peak fuel cell efficiency is currently assumed to be 55%, and it will rapidly increase to 60% by 2015. The efficiency value of 60% has already been demonstrated in laboratories and therefore is expected to be achieved soon in vehicles. The peak efficiencies remain constant in

the future because most research is expected to focus on reducing cost. The costs are projected to decrease from \$72/kW currently (values based on high production volume) to an average of \$38/kW in 2030 (uncertainty from \$26/kW to \$49/kW).

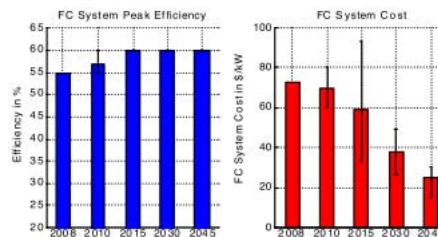


Figure 6. Fuel Cell System Efficiency and Cost

Hydrogen Storage Systems

The evolution of hydrogen storage systems is vital to the introduction of hydrogen-powered vehicles. Figure 7 shows the evolution of the hydrogen storage capacity.

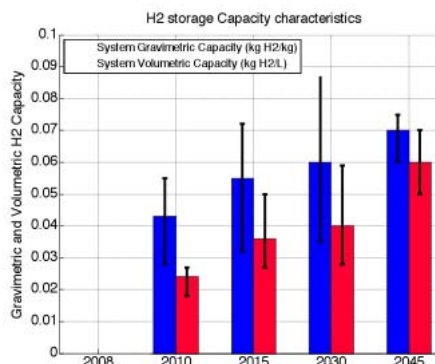


Figure 7. Hydrogen Storage Capacity in Terms of Quantity

One of the requirements for any vehicle in the study is that it must be able to travel 320 miles on the Combined Driving Cycle with a full fuel tank. The following ranges were selected:

- Reference, 2010, and 2015: 320 miles.
- 2030 and 2045: 500 miles.

Electric Machines

Figure 8 shows the electric machine peak efficiencies considered. The values for the current technologies are based on state-of-the-art electric machines currently used in vehicles. The electric

machine data from the Toyota Prius and Toyota Camry were used for the power-split HEV applications, while the Ballard IPT was selected for series fuel cell HEVs. Because the component is already extremely efficient, most of the improvements reside in cost reduction, as shown in Figure 9.

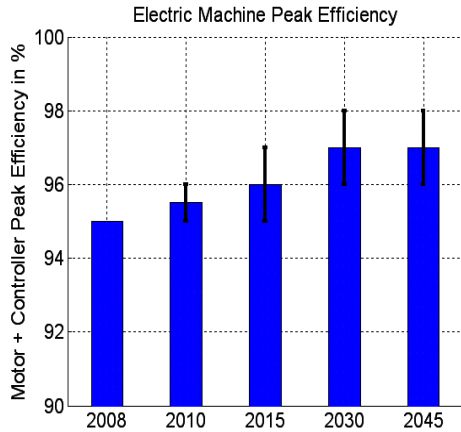


Figure 8. Electric Machine Peak Efficiency

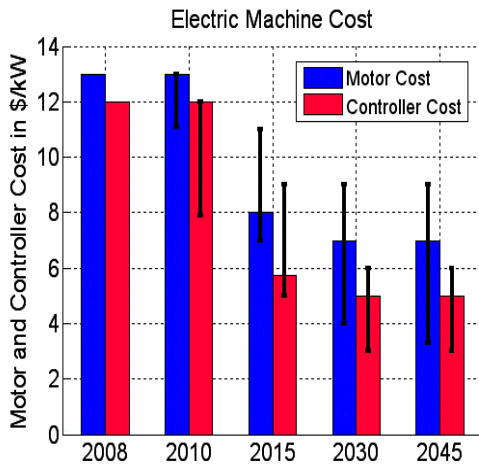


Figure 9. Electric Machine Cost

Energy Storage System

Energy storage systems are a key component in advanced vehicles. Although numerous studies are being undertaken with ultracapacitors, only batteries were taken into account in the study. All current vehicles are defined by using nickel metal hydride (NiMH) technology. The lithium ion (Li-ion) technology is introduced for the high case in 2010 and for the medium and high cases in 2015, before becoming the only one considered for later timeframes. For HEV applications, the NiMH is

based on the Toyota Prius battery pack, and the Li-ion is based on the 6-A·h battery pack from Saft. For PHEV applications, Argonne characterized the VL41M battery pack from Saft. Because each vehicle is sized for both power and energy in the case of a PHEV, a sizing algorithm was developed to design the batteries specifically for each application.

To ensure that the battery has similar performance at the beginning and end of life, the packs were oversized in terms of both power and energy, as shown in Figure 10. In addition, for PHEV applications, the state-of-charge (SOC) window (difference between maximum and minimum allowable SOC) increases over time, allowing a reduction of the battery pack, as shown in Figure 11.

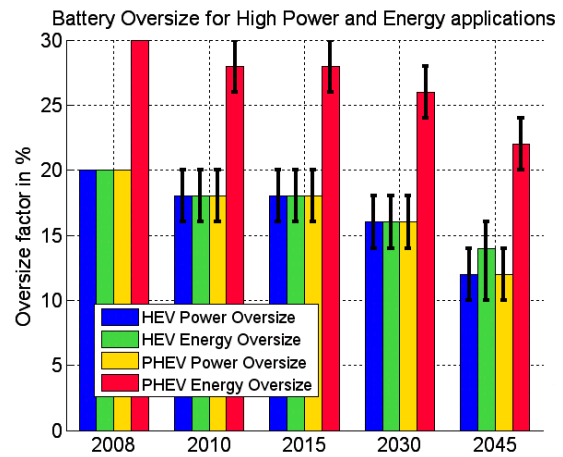


Figure 10. Battery Oversizing

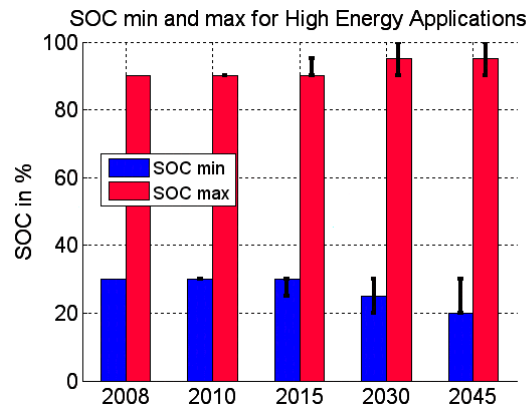


Figure 11. Battery SOC Window

Figures 12 and 13 show the cost of the battery packs for both high-power applications (\$/kW) and high-energy applications (\$/kWh).

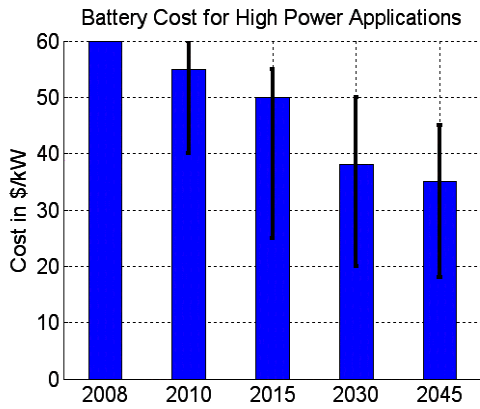


Figure 12. High-Power Battery Cost Projections

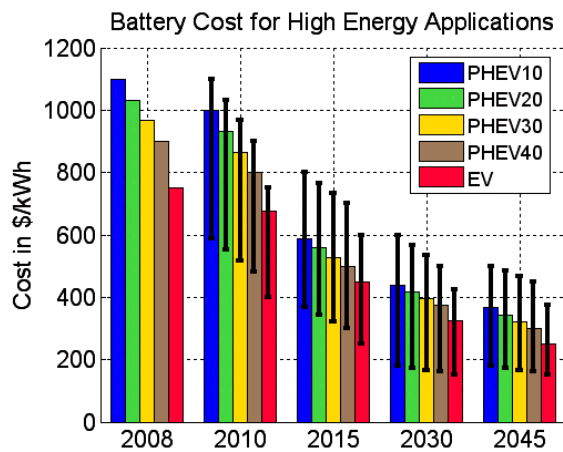


Figure 13. High-Energy Battery Cost Projections

Vehicle

As previously discussed, four vehicles classes were considered, as listed in Table 1.

Table 1. Vehicle Characteristics for Different Vehicle Classes

Vehicle Class	Glider Mass (Ref) (kg)	Frontal Area (Ref) in (m ²)	Tire	Wheel Radius (m)
Compact Car	800	2.15	P195/65/R15	0.317
Midsize car	990	2.2	P195/65/R15	0.317
Small SUV	1000	2.52	P225/75/R15	0.35925
Midsize SUV	1260	2.88	P235/70/R16	0.367
Pickup	1500	3.21	P255/65/R17	0.38165

Because of the improvements in material, the glider mass is expected to significantly decrease over time.

Although frontal area is expected to differ from one vehicle configuration to another (i.e., the electrical components will require more cooling capabilities), the reduction values were considered constant across the technologies. Figures 14 and 15 show the reduction in both glider mass and frontal area.

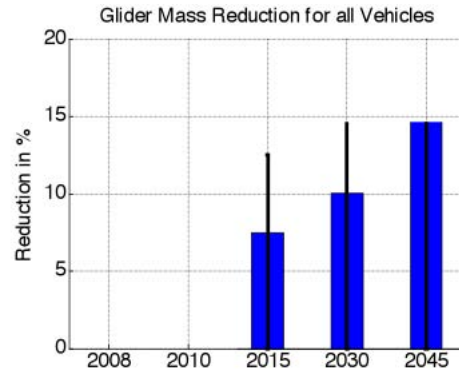


Figure 14. Glider Mass Reductions

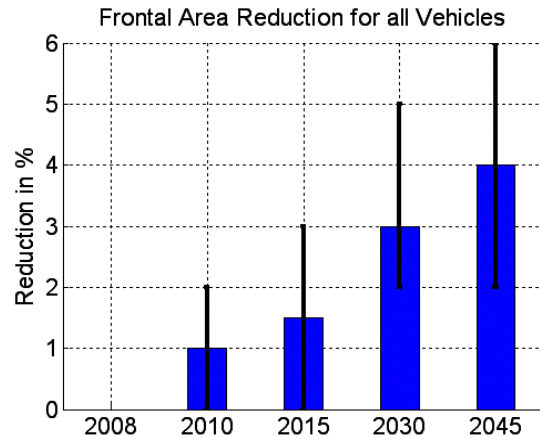


Figure 15. Frontal Area Reductions

Vehicle Powertrain Assumptions

All the vehicles have been sized to meet the same requirements:

- 0–100 km/h in 9 s +/-0.1.
- Maximum grade of 6% at 105 km/h at gross vehicle weight.
- Maximum vehicle speed of >160 km/h.

For all cases, the engine or fuel cell powers are sized to complete the grade without any assistance from the battery. For HEVs, the battery was sized to recuperate the entire braking energy during the

UDDS drive cycle. For the PHEV case, the battery power is defined as its ability to follow the UDDS in electric mode, while its energy is calculated to follow the trace for a specific distance. Because of the multitude of vehicles considered, an automated sizing algorithm was defined.

Input mode power-split configurations, similar to those used in the Toyota Camry, were selected for all HEV applications and PHEVs with low battery energies. Series configurations were used for PHEVs with high battery energies (e.g., 30 miles and up in EVs on the UDDS). The series fuel cell configurations use a two-gear transmission to allow them to achieve the maximum vehicle speed requirement. The vehicle-level control strategies employed for each configuration have been defined in previous publications.

Component Sizing

As shown in Figure 16, the engine power for all of the powertrains decreases over time. The power-split HEV is the one with the highest reduction in engine power: 20% from the reference case to the 2045 average case; whereas power for the conventional engine decreases by only 13%. The engine power is higher when the all-electric range (AER) increases because the power is determined based on acceleration and grade and because the different PHEVs (for the same fuel) vary from one to the other only by having a larger battery (and thus a heavier car).

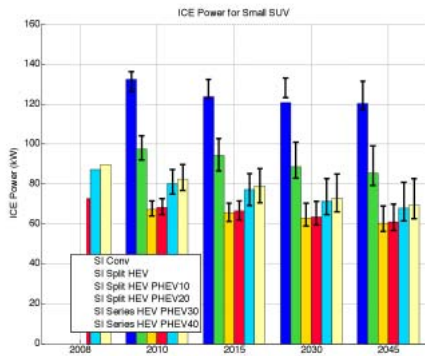


Figure 16. Engine Power for Gasoline Powertrains for Small SUV

The ICE (internal combustion engine) power changes linearly with the vehicle mass, as shown in Figure 17. The hydrogen and diesel points are on the

same line, but they do not cover the same mass range. For every 100-kg reduction in vehicle mass, the engine power decreases by approximately 10 kW.

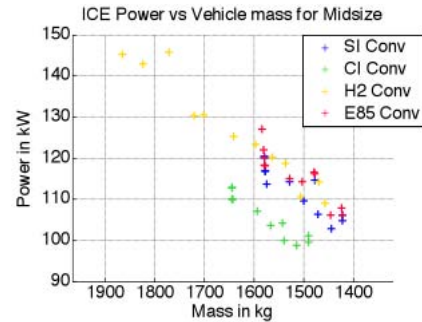


Figure 17. ICE Power as a Function of Vehicle Mass for Conventional Vehicle

Figure 18 shows the electric machine power for the gasoline HEVs and PHEVs. PHEVs require higher power because they must be able to follow the UDDS (low-energy batteries) or the US06 (high-energy batteries) in electric mode. Note that the vehicles can be driven in electric mode in the UDDS; the control strategy employed during fuel efficiency simulation is based on blended operation. However, the power in PHEVs does not increase significantly in comparison with HEVs because the input mode power-split configuration was considered. A decrease of 10 to 20 kW can be expected by 2045 as a result of component improvements.

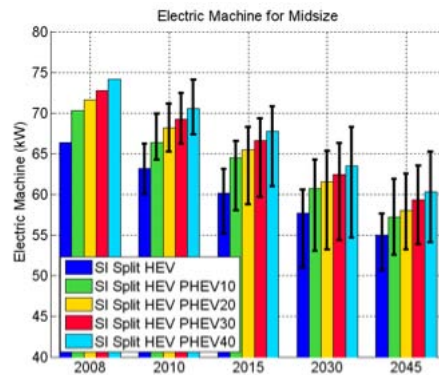


Figure 18. Electric Machine Power for Gasoline HEV and PHEVs for Midsize Vehicle

Figures 19 and 20 show the battery power and energy requirements for HEV, PHEV, and EV applications. The sensitivity of battery power to vehicle mass increases with the degree of

electrification (i.e., higher for EVs, then PHEVs, and finally HEVs). From an energy point of view, every 100-kg decrease for a PHEV40 (i.e., 40 miles on electric only on the UDDS) results in an approximately 2-kWh decrease in energy requirements.

- Split HEV: 18%
- Split PHEV: 14%
- Fuel Cell HEV: 25%
- Fuel Cell PHEV: 15%
- EV: 10%

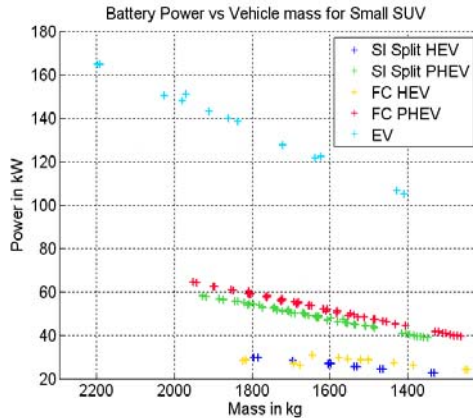


Figure 19. Battery Power

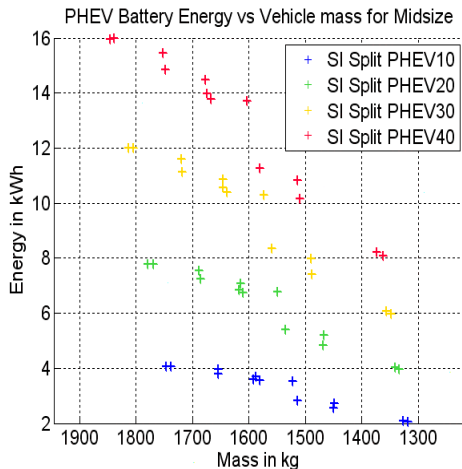


Figure 20. Battery Energy

Vehicle Simulation Results

The vehicles were simulated on both the UDDS and HWFET drive cycles. The fuel consumption values and ratios presented below are based on unadjusted values. The cold-start penalties were defined for each powertrain technology option on the basis of available data collected at Argonne’s dynamometer facility and in literature. The following cold-start penalties (on the 505 cycle at 20°C) were kept constant throughout the timeframes:

- Conventional: 15%

Impact of Different Fuels on Conventional Vehicles

Figure 21 shows the evolution of the fuel consumption for different fuels on a conventional midsize vehicle. All of the results are presented in gasoline fuel equivalent. As expected, the diesel engine achieves better fuel efficiency than the gasoline engine, but the difference between both technologies narrows with time because greater improvements are expected for gasoline engines.

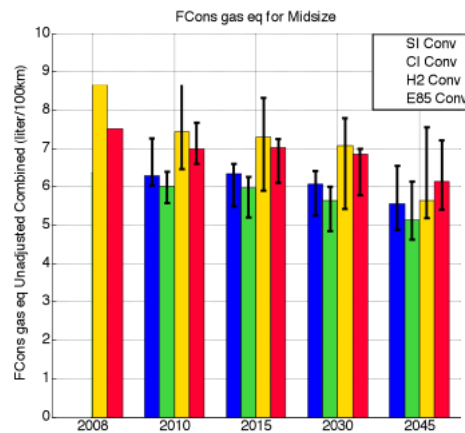


Figure 21. Gasoline-Equivalent Fuel Consumption (unadjusted for conventional midsize cars)

Hydrogen engines are penalized by the additional weight of the hydrogen storage system. With the introduction of direct-injection hydrogen engine technology combined with improved storage, hydrogen engines can compete with other fuels. It is also important to notice the large uncertainty related to hydrogen vehicles. Finally, the hydrogen storage efficiency is assumed to be 100%.

Ethanol engines are currently being designed to run on several fuels. When specifically designed to run on ethanol, these vehicles have the potential to achieve the best fuel efficiency.

Figure 22 shows the vehicle cost ratios between the different fuels for conventional vehicles. Diesel

engines are expected to remain more expensive than their gasoline counterparts, mostly due to after-treatments. Vehicles with hydrogen engines become competitive in the long term because storage will become less expensive.

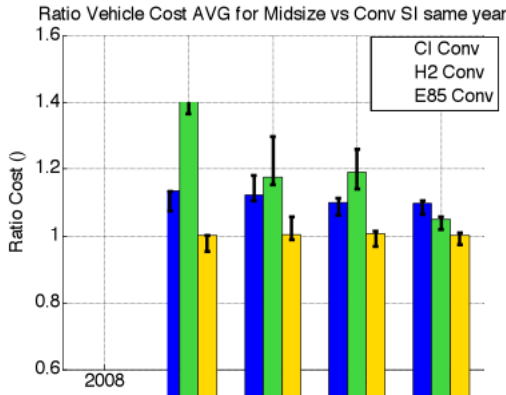


Figure 22. Conventional Vehicle Cost Ratio Compared with Conventional Gasoline Vehicles of the Same Year

Evolution of HEVs vs. Conventional Vehicles

The comparisons between power-split HEVs and conventional gasoline vehicles (same year, same case) in Figure 23 show that the ratios stay roughly constant for diesel, gasoline, and ethanol. Indeed, the gasoline HEV consumes between 25% and 30% less fuel than the conventional gasoline vehicle, whereas the diesel HEV consumes between 35% and 40% less fuel, and the ethanol HEV consumes between 20% and 25% less fuel. However, the hydrogen case shows more significant variations. In 2008, the hydrogen power-split vehicle consumes roughly 25% less fuel than the conventional gasoline vehicle; but in the 2045 average case, this advantage rises to 43% and even 47% in the high case. This analysis confirms that hydrogen vehicles will benefit more from hybridization in the future than will comparable conventional vehicles. In summary, the advances in component technology will equally benefit conventional vehicles and HEVs, except for the hydrogen engine, because of the additional benefits of hydrogen storage.

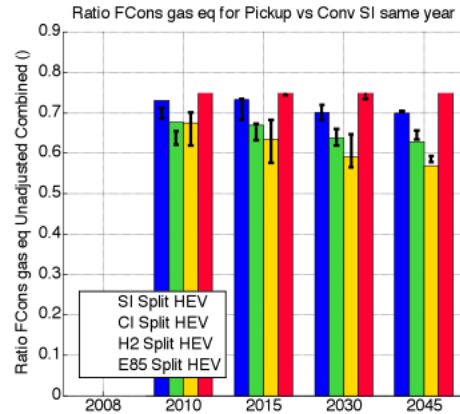


Figure 23. Ratio of Fuel Consumption Gasoline-Equivalent Unadjusted Combined in Comparison to the Conventional Gasoline Same Year, Same Case, for Pickup

Figure 24 shows the vehicle cost ratio between HEVs and conventional vehicles. As expected, HEVs remain more expensive than conventional vehicles, but the difference significantly decreases because costs associated with the battery and electric machine fall faster than those for conventional engines.

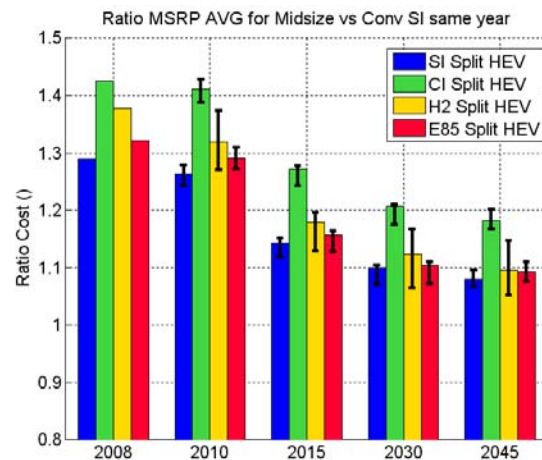


Figure 24. HEV Cost Ratio Compared with Conventional Gasoline Vehicle of the Same Year

Evolution of HEVs versus Fuel Cell HEVs

Figure 25 shows the fuel consumption comparison between HEVs and fuel cell HEVs for the midsize-car case. First, note that technology for fuel cell vehicles will continue to provide better fuel efficiency than the technology for the HEVs, with ratios above 1. However, the ratios vary over time, depending upon the fuel considered. The ratio for

the gasoline HEV increases over time because most improvements considered for the engine occur at low power and consequently do not significantly impact the fuel efficiency in hybrid operating mode. Both diesel and ethanol HEVs follow the same trend as gasoline HEVs.

Because of the larger improvements considered for the hydrogen engine, the hydrogen power split shows the best improvement in fuel consumption compared with the fuel cell technology. Indeed, in 2008, the hydrogen HEV consumes nearly 40% more fuel than the fuel cell HEV, but in the 2045 average case, this difference is reduced to 10%. If we consider the UDDS fuel consumption instead of the combined values, we find that the hydrogen power split consumes only 2.5% more fuel than a fuel cell HEV in the 2045 high case.

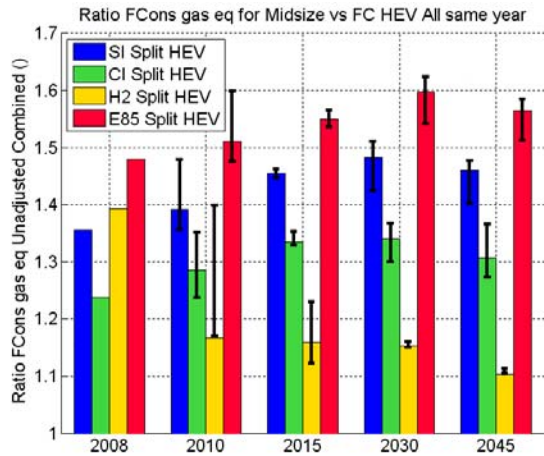


Figure 25. Ratio of Fuel Consumption Gasoline-Equivalent Unadjusted Combined in Comparison to the Fuel Cell HEV Same Year, Same Case for Midsize Vehicles

Figure 26 shows the vehicle cost comparison between HEVs and fuel cell HEVs. Note that the cost difference between both technologies is expected to decrease over time, with a ratio between 0.9 and 1.1 in 2030 and 2045.

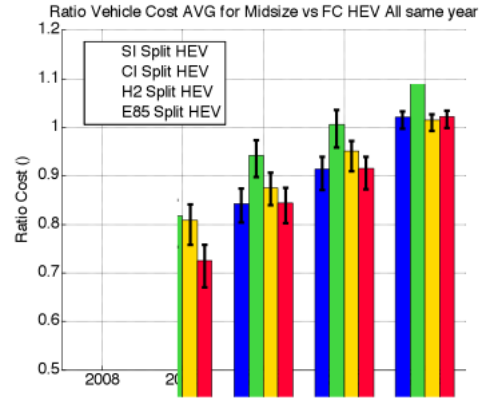


Figure 26. HEV Cost Ratio Compared with Fuel Cell HEV of the Same Year

Evolution of Hydrogen-Fueled Vehicles

As shown in Figure 27, in 2009, fuel cell HEVs consume about 49% less fuel than gasoline conventional vehicles, and this difference in fuel is almost constant for future technologies.

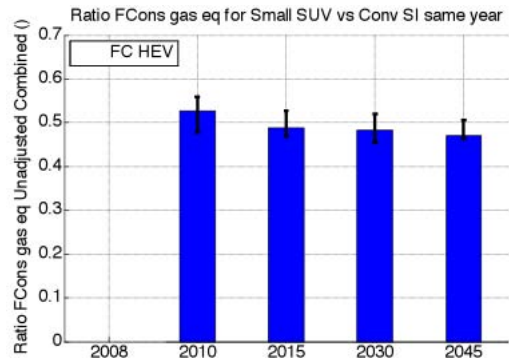


Figure 27. Ratio of Fuel Consumption (gasoline-equivalent, unadjusted combined) Compared with Conventional Gasoline Vehicle of the Same Year, Same Case, Small SUV

Fuel Consumption of Plug-in Hybrid Electric Vehicles

Figure 28 shows the fuel consumption of PHEVs compared with other technologies, including conventional vehicles and HEVs.

As the figure shows, significant fuel displacement can be achieved, especially for vehicle configurations with high-energy batteries.

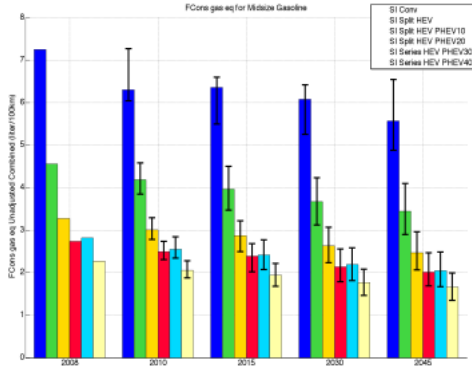


Figure 28. Fuel Consumption (gasoline-equivalent) for All Gasoline Midsize Vehicles (conventional, split HEV, and split PHEV [all ranges])

A. Delorme, A. Rousseau, P. Sharer, S. Pagerit, and T. Wallner, “Evolution of Hydrogen-Fueled Vehicles Compared to Conventional Vehicles from 2010 to 2045,” Society of Automotive Engineers (SAE) paper 2009-01-1008, SAE World Congress, Detroit, April 2009.

A. Delorme, S. Pagerit, P. Sharer, and A. Rousseau, “Cost Benefit Analysis of Advanced Powertrains from 2010 to 2045,” EVS24, Norway, May 2009.

A. Rousseau, “GPRA Results,” Presented at DOE Merit Review, May 2009.

Conclusions

More than 1,000 vehicles were simulated for different timeframes (to year 2045), powertrain configurations, and component technologies. Both their fuel economy and cost were assessed to estimate the potential of each technology. Each vehicle was associated with a triangular uncertainty. The simulations highlighted several points:

- The discrepancy between gasoline and diesel engines for conventional vehicles is narrowing with the introduction of new technologies, such as variable valve timing and low-temperature combustion.
- From a fuelefficiency perspective, HEVs maintain a relatively constant ratio compared with their conventional vehicle counterparts. However, the cost of electrification is expected to be reduced in the future, favoring the technology’s market penetration.
- Diesel vehicles will offer the lowest fuel consumption among the conventional powertrains in the near future.
- PHEVs offer the greatest potential to reduce fuel consumption, especially when using high-energy batteries.

Publications/Presentations

A. Delorme, S. Pagerit, and A. Rousseau, “Fuel Economy Potential of Advanced Configurations from 2010 to 2045,” IFP Conference, Paris, Nov. 2008.

C. Evaluation of Technology Potential to Reach 40% Fuel Efficiency Improvement

Aymeric Rousseau (project leader), Antoine Delorme, Dominik Karbowski, Phil Sharer
 Argonne National Laboratory
 9700 South Cass Avenue
 Argonne, IL 60439-4815
 (630) 252-7261; arouseau@anl.gov

DOE Technology Manager: Lee Slezak

Objectives

Evaluate available technologies to reach 40% improvement in fuel economy by 2016.

Approach

Gather component assumptions required for the specific study.

Size the components for each option considered.

Run simulations.

Compare results.

Accomplishments

Defined different combinations of technology options to reach 40% fuel economy.

Found that reaching 40% with conventional technology alone will require extremely aggressive improvements.

Future Directions

Develop tool to perform best selection of component technologies to meet Corporate Average Fuel Economy (CAFE) requirements from the point of view of cost effectiveness.

Introduction

The objective of the study is to assess the fuel economy potential and cost of several component and powertrain technologies that would support a 40% fuel economy improvement compared with current technologies (model year 2009). Argonne simulated several component technologies, along with powertrain configurations, to determine their respective fuel consumption. Uncertainties associated with each assumption were determined.

Methodology

The simulations were performed with the Powertrain System Analysis Toolkit (PSAT) using a similar process to CAFE:

- Employ two drive cycles (Urban Dynamometer Driving Schedule [UDDS] and Highway Fuel Economy Test [HWFET]).
- Use U.S. Environmental Protection Agency (EPA) weighting of 55/45.
- All values are unadjusted.

The plug-in hybrid electric vehicle (PHEV) fuel economies were defined on the basis of the latest known version of SAE J1711 using the National

Highway Traffic Safety Administration (NHTSA) utility factors.

The following powertrain configurations are considered based on existing and planned vehicles:

- Conventional vehicles
- Micro Hybrid Electric Vehicles (HEV)
- Mild HEVs
- Full HEVs
- PHEVs (Power split technology was considered for 10 and 20 miles all-electric range [AER] applications, whereas series technology was used for 30 and 40 miles AER).

The potential of each technology was assessed using a three-point uncertainty analysis (low, medium, and high). The vehicle characteristics (e.g., mass, power, energy) were specifically designed to meet the following vehicle technical specifications (VTS):

- 0 to 60 mph in less than 11 s for midsize cars and 9 s for the other classes.
- Maximum vehicle speed greater than 100 mph.
- 6% grade at 65 mpg at gross vehicle weight (GVW) without support from energy storage.

Several assumptions differ from the CAFE procedure:

- The CAFE standards have been developed based on the assumption that there will be no weight reduction (because of safety requirements from NHTSA). In our assumptions, some weight reduction was considered.
- The definitions of the vehicle classes used for CAFE are different than the ones for EPA.

Results

Tables 1 through 6 show the results for each vehicle class. The fuel economy values are unadjusted and include cold-start penalties. The fuel economy ratios are defined as follows: Ratio = Fuel Economy Gasoline-Equivalent Configuration Considered/Fuel Economy Gasoline-Equivalent 2009 Conventional Gasoline

The diesel vehicles utilize the following ratio: Ratio (Diesel) = Diesel Fuel Economy Configuration Considered/Fuel Economy Gasoline-Equivalent 2009 Conventional Gasoline

1. Compact Cars

The compact car fueled by conventional gasoline (used for reference) achieves 35 mpg (unadjusted) on the combined drive cycle (Table 1).

The analysis shows that, while advanced conventional vehicles have the potential to increase fuel economy, electric drive technologies will be required to meet the 40% target. Configurations that include small degrees of hybridization would have to be introduced in greater numbers to meet the requirements.

2. Midsize Cars

For midsize vehicles, two cases were considered to evaluate the impact of vehicle performance (Table 2):

- Vehicles are sized for a 0- to 60-mph acceleration in 9 s.
- Vehicles are sized for a 0- to 60-mph acceleration in 11 s.

For the series PHEV vehicles (30 and 40 miles AER), the acceleration time stays the same in both cases (approximately 8 s) because the electric machine is sized to achieve a US06 cycle without the help of the engine. Consequently, when we combine the power of the sized electric machine to the engine power (sized on grade requirement) for the acceleration test, the vehicle cannot be slower than 8 s. For similar reasons, diesel power split HEVs cannot achieve a 0- to 60-mph acceleration test slower than 10.3 s. In this case, the engine power is sized on the grade requirement, and the battery is sized to recover all regenerative braking on a UDDS cycle.

When combining these two requirements, the acceleration time cannot be slower than approximately 10.3 seconds.

Table 1. PSAT Fuel Economy and Cost Results for a Compact Car in 2016

Drivetrain Configuration	Fuel Economy Ratio Compared to Reference			Additional Retail Price Equivalent (RPE) Cost (\$)	0- to 60-mph Acceleration Time (sec.)
	Low	Medium	High		
Gasoline					
Conventional	1.06	1.20	1.33	97 – 1,482	9.0
Micro HEV	1.11	1.26	1.40	360 – 1,745	9.0
Mild HEV	1.12	1.29	1.42	1,159 – 2,544	9.0
Full HEV	1.65	1.83	2.08	3,772 – 4,292	9.0
PHEV (10 miles AER)	2.33	2.58	2.90	5,344 – 6,204	9.0
PHEV (20 miles AER)	2.74	3.11	3.53	6,248 – 7,489	9.0
PHEV (30 miles AER)	2.63	2.96	3.46	11,597 – 14,058	7.9–8.0
PHEV (40 miles AER)	3.27	3.67	4.19	12,685 – 15,787	7.8–8.0
Diesel					
Conventional (gasoline-equivalent ratio)	1.16	1.31	1.38	2,913 – 4,297	9.0
Conventional (diesel -equivalent ratio)	1.30	1.45	1.54		
Full HEV (gasoline-equivalent ratio)	1.75	1.96	2.21	6,656 – 7,230	9.0
Full HEV (diesel-equivalent ratio)	1.95	2.18	2.46		

Table 2. PSAT Fuel Economy and Cost Results for a Midsize Car in 2016 (sized for a 9-s acceleration time)

Drivetrain Configuration	Fuel Economy Ratio Compared to Reference			Additional RPE Cost (\$)	0- to 60-mph Acceleration Time (sec.)
	Low	Medium	High		
Gasoline					
Conventional	1.06	1.21	1.33	125 – 1457	9.0
Micro HEV	1.11	1.27	1.39	394 – 1727	9.0
Mild HEV	1.14	1.30	1.41	1193 – 2525	9.0
Full HEV	1.66	1.85	2.12	3957 – 4630	9.0
PHEV (10 miles AER)	2.28	2.56	2.95	5524 – 6553	9.0
PHEV (20 miles AER)	2.74	3.08	3.64	6534 – 7998	9.0
PHEV (30 miles AER)	2.65	3.05	3.54	12127 – 15030	7.9-8.0
PHEV (40 miles AER)	3.31	3.78	4.37	13385 – 16927	7.8-8.0
Diesel					
Conventional (gasoline-equivalent ratio)	1.20	1.32	1.44	2927 – 4071	9.0
Conventional (diesel-equivalent ratio)	1.33	1.47	1.60		
Full HEV (gasoline-equivalent ratio)	1.74	1.97	2.25	6899 – 7670	9.0
Full HEV (diesel-equivalent ratio)	1.94	2.19	2.50		

Table 3. PSAT Fuel Economy and Cost Results for a Midsize Car in 2016 (sized for an 11-s acceleration time)

Drivetrain Configuration	Fuel Economy Ratio Compared to Reference			Additional RPE Cost (\$)	0 to 60 mph Acceleration Time (sec.)
	Low	Medium	High		
Gasoline					
Conventional	1.04	1.13	1.28	169–1,537	11.0
Micro HEV	1.10	1.18	1.35	439–1,807	11.0
Mild HEV	1.11	1.20	1.36	1,237–2,605	11.0
Full HEV	1.63	1.83	2.08	3,596–4,123	10.9–11.0
PHEV (10 miles AER)	2.13	2.40	2.75	5,283–6,181	11.1
PHEV (20 miles AER)	2.55	2.87	3.38	6,331–7,613	11.0–11.1
PHEV (30 miles AER)	2.46	2.83	3.29	12,360–15,263	7.9–8.0
PHEV (40 miles AER)	3.07	3.50	4.06	13,618–17,160	7.8–8.0
Diesel					
Conventional (Gasoline equivalent ratio)	1.18	1.24	1.42	2,834–3,987	11.0
Conventional (Diesel equivalent ratio)	1.31	1.38	1.58		
Full HEV (Gasoline equivalent ratio)	1.70	1.92	2.16	6,732–7,289	10.1–10.3
Full HEV (Diesel equivalent ratio)	1.89	2.13	2.41		

a. Vehicles Sized for a 9-second Acceleration Test

The 2009 midsize car fueled by conventional gasoline (used for reference) achieves 32 mpg (unadjusted) on the combined drive cycle and performed a 0- to 60-mph acceleration in 9 s.

Comparison of Table 2 with Table 1 shows comparable fuel economy ratios for both vehicle classes.

b. Vehicles Sized for a 11-sec. Acceleration Test

The 2009 midsize car fueled by conventional gasoline (used for reference) achieves 34.5 mpg (unadjusted) on the combined drive cycle and achieved a 0- to 60-mph acceleration in 11.1 s.

Comparison of Table 3 with Table 2 shows that lowering performance also lowers the fuel economy ratio.

c. Different Ways to Reach 40% Fuel Economy Improvement with Non-HEVs

In this section, we explore a few ways to reach a 40% fuel economy improvement for conventional midsize cars in 2016 compared with the 2009 gasoline conventional reference. Table 2 shows that a conventional gasoline midsize car could reach up to a 33% fuel economy improvement in 2016 considering the highest uncertainty case. By changing some vehicle component technologies, particularly the engine, it is possible to reach 40% improvement without hybridization. Table 4 provides the vehicle assumptions for the different options considered.

The Option 1 vehicle uses the same vehicle assumptions as the default 2016 case, but the engine efficiency map is improved linearly by 5%. In this case, the fuel economy improvement can reach 39% compared with the 2009 vehicle. Most of this vehicle’s components are using very aggressive improvement assumptions. For instance, the gearbox used is an 8-speed automatic, the glider mass is reduced by 12.5% compared with 2009, the drag coefficient is reduced by 15%, and rolling resistance is reduced by 12.5%.

In the Option 2 vehicle, the 40% fuel economy improvement was reached (41%) mainly because of the use of turbocharging for the engine. The engine used is similar to the default 2016 case (spray-guided gasoline direct injection [GDI] + cam phasers), except for turbocharging. However, if turbocharging was the only assumption changed from the default 2016 case, the fuel economy improvement would have been greater than the 40% target. This is why, in addition to the engine technology change, we also chose to be less aggressive on the glider mass reduction, which was reduced by 7.5% instead of 12.5% in the default

2016 case (916 kg vs. 866 kg). (Remark: The frontal area is expected to keep increasing as a result of several factors, including the height of the passengers. As such, maintaining a constant value is considered to be most probable scenario.)

3. Small SUVs

The 2009 small conventional gasoline SUV used for reference achieves 28.9 mpg (unadjusted) on the combined drive cycle.

Table 4. Two Different Options to Reach 40% FE Improvement for Conventional Gasoline Vehicles

	Reference 2009	Default 2016 High Case	2016 Option 1	2016 Option 2
Engine technology	Port Fuel Injected 34.5% Peak Efficiency	Spray Guided GDI + Cam Phasers	Spray Guided GDI + Cam Phasers + 5% IMEP Improvement	Spray Guided GDI + Cam Phasers + Turbo Charging
Glider Mass (kg)	990	866	866	916
Frontal Area (m2)	2.2	2.2	2.2	2.2
Drag Coefficient	0.3	0.255	0.255	0.255
Gearbox	5-Speed Auto	8-Speed Auto	8-Speed Auto	8-Speed Auto
Rolling Resistance	0.008	0.007	0.007	0.007
Unadjusted Combined Fuel Economy Ratio	1.0	1.33	1.39	1.41

Table 5. PSAT Fuel Economy and Cost Results for a Small SUV in 2016

Drivetrain Configuration	Fuel Economy Ratio Compared to Reference			Additional RPE Cost (\$)	0 to 60 mph Acceleration Time (sec.)
	Low	Medium	High		
Gasoline					
Conventional	1.05	1.18	1.30	128 – 1510	9.0
Micro HEV	1.09	1.24	1.36	398 – 1779	9.0
Mild HEV	1.11	1.26	1.38	1196 – 2578	9.0
Full HEV	1.53	1.74	1.98	4237 – 4962	9.0
PHEV (10 miles AER)	2.13	2.40	2.75	6239 – 7390	9.0
PHEV (20 miles AER)	2.52	2.91	3.30	7340 – 9102	9.0
PHEV (30 miles AER)	2.37	2.71	3.16	13242 – 16662	7.9-8.0
PHEV (40 miles AER)	2.92	3.35	3.84	14685 – 18931	7.8-8.0
Diesel					
Conventional (gasoline-equivalent ratio)	1.21	1.32	1.41	2806 – 4249	9.0
Conventional (diesel -equivalent ratio)	1.35	1.47	1.59		
Full HEV (gasoline-equivalent ratio)	1.67	1.89	2.13	7219 – 7860	9.0
Full HEV (diesel-equivalent ratio)	1.86	2.10	2.37		

Table 6. PSAT Fuel Economy and Cost Results for a Midsize SUV in 2016

Drivetrain Configuration	Fuel Economy Ratio Compared to Reference			Additional RPE Cost (\$)	0 to 60 mph Acceleration Time
	Low	Medium	High		
Gasoline					
Conventional	1.04	1.23	1.30	358 – 1597	9.0
Micro HEV	1.09	1.29	1.36	628 – 1867	9.0
Mild HEV	1.11	1.31	1.37	1,426 – 2665	9.0
Full HEV	1.56	1.73	1.93	3,942 – 4894	9.0
PHEV (10 miles AER)	2.19	2.41	2.67	6,221 – 6989	9.0
PHEV (20 miles AER)	2.60	2.84	3.16	7,577 – 9477	9.0
PHEV (30 miles AER)	2.43	2.72	3.09	14,305 – 17997	7.9–8.0
PHEV (40 miles AER)	3.00	3.30	3.72	16,047 – 20621	7.8–8.0
Diesel					
Conventional (gasoline-equivalent ratio)	1.25	1.39	1.45	2085 – 3295	9.0
Conventional (diesel -quivalent ratio)	1.39	1.54	1.62		
Full HEV (gasoline-equivalent ratio)	1.71	1.92	2.11	6989 – 7908	9.0
Full HEV (diesel-equivalent ratio)	1.91	2.13	2.35		

4. Midsize SUVs

The 2009 midsize SUV conventional gasoline used for reference achieves 24.1 mpg unadjusted on the combined drive cycle.

Conclusion

The impact of several technologies and powertrain configurations was analyzed for several vehicle classes. The analysis demonstrates that the implementation of electric drive technology will be required to achieve 40% fuel economy improvements by 2016.

This study did not consider product renewal cycles or capital constraints.

The number of advanced vehicles required to achieve this target will depend on the degree of hybridization of the vehicles.

Publications/Presentations

A Rousseau, and A. Delorme, “Evaluation of Technologies to Reach 40% Fuel Economy Improvement by 2016,” DOE Report, July 2009.

D. PSAT Maintenance and Enhancements

Aymeric Rousseau (project leader), Shane Halbach, Sylvain Pagerit, Phil Sharer, Dominik Karbowski, Jason Kwon, Ram Vijayagopal
 Argonne National Laboratory
 9700 South Cass Avenue
 Argonne, IL 60439-4815
 (630) 252-7261; *arousseau@anl.gov*

DOE Technology Manager: Lee Slezak

Objectives

Enhance and maintain the Powertrain System Analysis Toolkit (PSAT) as needed to support the Department of Energy (DOE), the user community, and hardware-in-loop/rapid control prototyping (HIL/RCP) projects.

Approach

Use the feedback from PSAT users to implement new features.

Enhance PSAT capabilities to support DOE studies.

Accomplishments

Validated the use of PSAT for new MathWorks releases.

Added state-of-the-art component data from national laboratories and original equipment manufacturers (OEM).

Added new powertrain configurations.

Modified the tool to enhance medium- and heavy-duty capabilities.

Included J1711 plug-in hybrid electric vehicle (PHEV) test procedure utility factor.

Future Directions

Transfer the latest models, processes, and features to AUTONOMIE.

Introduction

To better support DOE and its users, several new features have been implemented in PSAT. Some of the most significant accomplishments are described below.

Results

The Vehicle Systems Analysis Team at Argonne National Laboratory has implemented many new features to support the U.S. DOE research and development activities. The tool is now available to simulate medium- and heavy-duty vehicles

applications. The latest version of PSAT now runs with MathWorks release R2007b and later on several PC operating systems.

Operating Systems

A significant amount of work was done to ensure that PSAT runs on several operating systems, including Windows XP and VISTA.

Some special attention was paid to solve issues between MathWorks and Windows interactions since PSAT launches Matlab.

Graphical User Interface

In addition to supporting issues reported by users, one of the main additions to the software is the implementation of the preliminary J1711 PHEV test procedure (Figure 1).

M. Duoba (at Argonne) has led the SAE J1711 PHEV test procedure. Since the fuel consumption of PHEVs is dependent on distance, the integration of the utility factor (UF) is an integral part of the process. The use of two energy sources—liquid and electricity—was also taken into account.

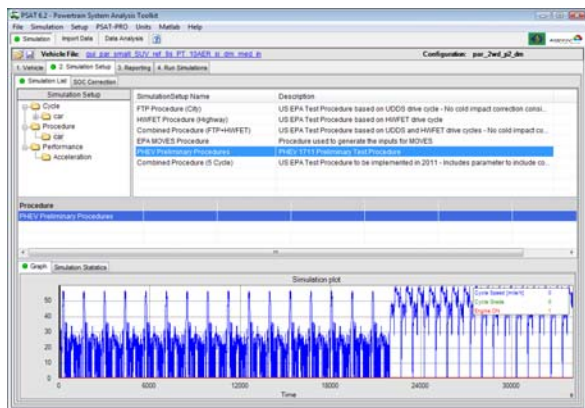


Figure 1. J1711 PHEV Test Procedure GUI

Additional Powertrain Configurations

Several new powertrain configurations were implemented on the basis of specific user requests. In addition, two configurations currently in production were added:

- Pre-transmission with two clutches; one before and one after the electric machine.
- Several conventional and hybrid configurations were modified to handle a large number of axes to support medium- and heavy-duty activities (Figure 2).

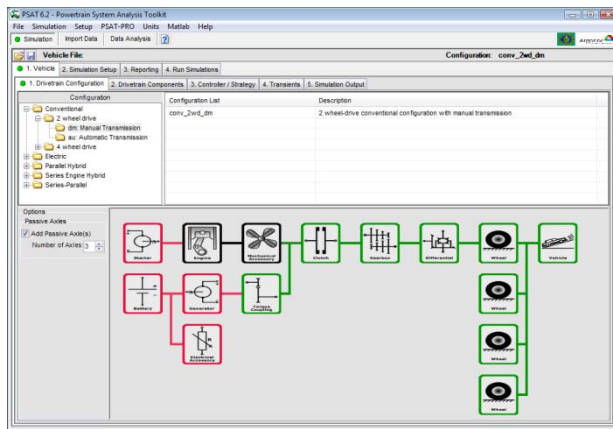


Figure 2. Heavy-Duty Configuration Example

Component Data

State-of-the-art component data were implemented from both universities and companies.

For example, DOE national laboratories provided the GM 2.2-L SIDI GM engine from Argonne’s dynamometer testing facility. The companies using PSAT also provided proprietary engine (i.e., ethanol, twin turbocharger), battery, and electric machine data.

Most of the focus was on gathering state-of-the-art data for medium- and heavy-duty applications. Since few data are publicly available, the data were provided by the OEMs. This effort will continue in the future, focusing especially on missing information, such as accessory loads.

In addition, several drive cycles from both light- and heavy-duty vehicles were added. For example, Oak Ridge National Laboratory (ORNL) provided real world drive cycles for Class 8 long-haul applications. Several additional heavy-duty cycles were also added from different OEMs and the Hybrid Truck Users Forum (HTUF). Finally, additional real world drive cycles were added from the Chicago area.

EcoCAR Competition

Because of the emphasis on modeling and simulation during the early stages of the competition, GM provided a significant amount of data to the different teams. All of the models were modified to follow PSAT nomenclature and then implemented into PSAT.

The reference conventional vehicle model was developed and validated by using component and vehicle data from GM (Figure 3). The teams use the vehicle model as reference for any further improvements.

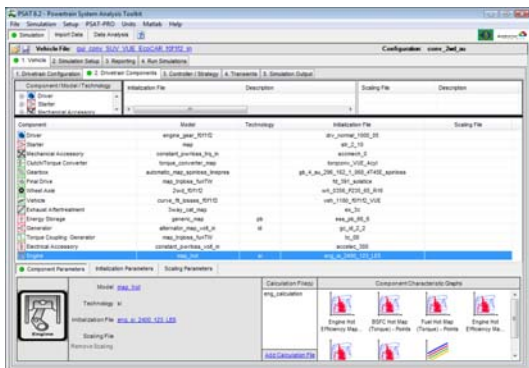


Figure 3. Reference EcoCAR Vehicle Model

Control Strategies

Vehicle-level control strategies were modified for medium- and heavy-duty applications. One of the main modifications includes adding a battery state-of-charge (SOC) regulation algorithm when the vehicle idles. This feature is necessary for such applications as utility trucks or long haul where trucks stay in the same location for a significant amount of time.

A new shifting algorithm was created with inputs from OEMs to represent specific requirements of medium- and heavy-duty applications (Figure 4). The StateFlow algorithm was modified to allow gear skipping during upshift and downshift. Members of the group visited OEMs to test drive several trucks so they could better understand how shifting was performed.

Since torque converters in medium- and heavy-duty vehicles do not lock up and release under the same conditions as in light-duty vehicles, a specific algorithm was developed in collaboration with OEMs. Two generic sets of torque converter specifications were also generated on the basis of proprietary OEM data, including speed and torque ratio, as well as K-factor.

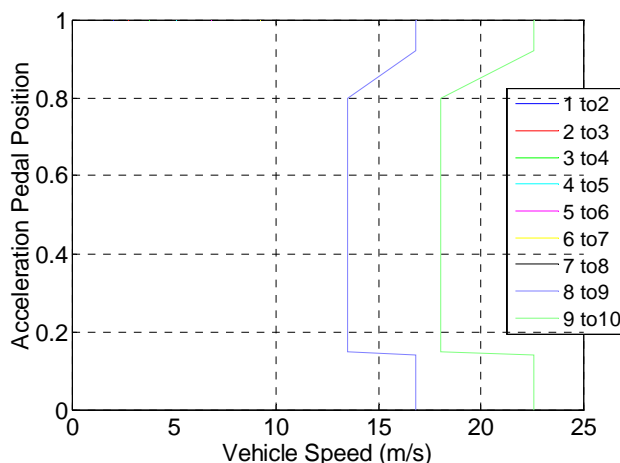


Figure 4. Shifting Curve Example for 10-Speed Long Haul

The long-haul engine algorithm was modified to allow Jake braking during deceleration. Engine data were implemented from OEMs to properly represent the engine’s negative torque.

Several changes and new control strategies were implemented for hybrid electric vehicles (HEVs), including an instantaneous optimization algorithm for the GM 2 Mode. The algorithm selects the proper mode and the operating points of the different components within each one to minimize fuel consumption while maintaining acceptable SOC.

Users’ Community

The PSAT users’ community has been continuously growing for the past five years and currently reaches more than 130 companies worldwide with more than 600 users. More than 20 additional companies adopted PSAT in 2009.

The PSAT development effort has focused on understanding the needs of its users and developing features that would allow researchers to be more efficient and consequently introduce advanced technologies to the market more quickly.

Conclusions

The latest version of PSAT includes numerous new features that were developed on the basis of feedback from DOE and the user community.

These enhancements are focused on component models and data, as well as vehicle control strategies.

The tool has been enhanced to support medium- and heavy-duty applications and is now ready to support U.S. DOE studies in this area.

Publications/Presentations

PSAT V6.2 SP1 Documentation, January 2009.

PSAT V6.2 SP1 Training Material (set of 9 presentations), January 2009.

E. Plug-and-Play Tool Development (Cooperative Research and Development Agreement with General Motors)

Aymeric Rousseau (project leader), Shane Halbach, Sylvain Pagerit, Phil Sharer, Ram Vijayagopal, Larry Michaels, Chuck Folkerts
 Argonne National Laboratory
 9700 South Cass Avenue
 Argonne, IL 60439-4815
 (630) 252-7261; *arousseau@anl.gov*

DOE Technology Manager: Lee Slezak

Objectives

Develop tool architecture and environment for plug-and-play hardware and software models to include control system design in the upfront, math-based design and analysis.

Approach

Enable efficient, seamless math-based control system design process.

Enable efficient reuse of models.

Enable sharing of modeling expertise across the organization.

Establish industry standard for architecture and model interfaces.

Accomplishments

Developed first beta version of the software.

Developed a process to import legacy code automatically into new nomenclature.

Developed a process to communicate with the CMSynergy database to upload and download files.

Applied tool capabilities with General Motors (GM) to low-level component control development.

Future Directions

Generate first public version of the tool.

Expand the use of Autonomie within GM and other original equipment manufacturers (OEM).

Position Autonomie for future use in medium- and heavy-duty vehicle regulations or policy options.

Introduction

Building hardware is expensive. Traditional design paradigms in the automotive industry often delay control system design until late in the process, in some cases requiring several costly hardware iterations. In order to reduce costs and improve time to market, greater emphasis must be placed on modeling and simulation. This imperative will only become truer as time passes because of the

increasing complexity of vehicles, the growing number of vehicle configurations, and larger numbers of people working on projects—all of which complicate design choices. To fully realize the benefits of math-based design, the models created must be as flexible and reusable as possible.

Placing greater reliance on modeling and simulation does come at some cost. Even if institutional inertia can be overcome, new processes must be put in

place to facilitate communication between all of the different model creators and consumers, as well as to handle an increase in the number of project files, which can become quite significant and overwhelming.

Consider the case of an average automotive OEM. Within a single OEM, there may be several subgroups carrying out modeling and simulation efforts. In years past, each subgroup typically would have had its own set of models, each with its own modeling conventions. For example, a subgroup working on battery hardware may have a custom vehicle model for plugging its battery model into for testing. Another subgroup may have its own vehicle model for plugging in an electric machine model. An altogether different group in charge of the control logic has its own vehicle model. None of the subgroups can share or reuse its models because they all use different naming conventions, model organizations, numbers of ports, and other conventions. Not only is it a waste of time for subgroups to duplicate each other's work, it can also introduce errors. For example, the control logic subgroup might have its own engine plant models that are not the same as the ones used by the engine plant modelers.

Now consider that each of these subgroups may have different models (e.g., for comparing one battery technology to another, or hot maps versus cold maps), models of different fidelities (e.g., a high-level model might be good for an architecture decision making study, but not for testing control logic), and different versions of one model (e.g., version 1 had some issues, which were fixed in version 2). All of these conditions hold true as well for the other associated files, such as initialization or configuration files. So each independent subgroup might have hundreds of individual files to manage. This situation could be even worse for a parts supplier who might have all of these problems, as well as additional levels of versioning, to deal with to conform to the modeling standards of its various customers.

In a perfect world, automotive subject matter experts (SME) would create libraries of models within their domain (engine, transmission, battery, etc.). These libraries would contain models of varying degrees of complexity depending on their intended use. However, the models would comply with robust standards, allowing them to be used interchangeably. In this way, all model users would have access to the exact models they needed, allowing users to move quickly from high-concept feasibility studies to physical confirmation, with full trust in the ultimate results.

Autonomie is a software package designed to support this ideal use of modeling and simulation for math-based automotive control system design. Autonomie supports the assembly and use of models from design to simulation to analysis with complete plug-and-play capabilities. Models in the standard format create building blocks, which are assembled at run time into a simulation model of a vehicle, system, subsystem, or component, to simulate. All parts of the graphical user interface (GUI) are designed to be flexible to support architectures, systems, components, and processes not yet envisioned. This feature allows the software to be molded to individual uses, so it can grow as requirements and technical knowledge expand. This flexibility also allows for implementation of legacy code, including models, controller code, processes, and post-processing equations. A library of useful and tested models and processes are included as part of the software package that can be accessed immediately to support a full range of simulation and analysis tasks. Autonomie also includes a configuration and database management front end to facilitate the storage, versioning, and maintenance of all required files, such as the models themselves, the model's supporting files, test data, and reports.

A standardized modeling architecture is needed to ensure interoperability of the various models. In this case, the standard would include common terminology; a hierarchical view of the model; certain standard levels in that hierarchy; various definition files, such as initialization and post-processing files; and common extensible markup language (XML) files to control it all. The standard would also dictate a way to lay out the ports of the individual models for ease of understanding.

The model building feature constructs a Simulink® (MathWorks) model diagram using information provided by the GUI in an XML file, known as the run file, as well as information given in layout files. The run file is the culmination of all the information the user has provided through the GUI. The pieces of this file are used by the automated model building feature, such as the user-selected vehicle configuration files. The configuration files contain information about the relative position of systems and their interconnections. The layout files contain information about translating relative to absolute position and about other peripheral blocks and systems that are involved in connection routing and contribute to the overall style, look, and feel of the Simulink model.

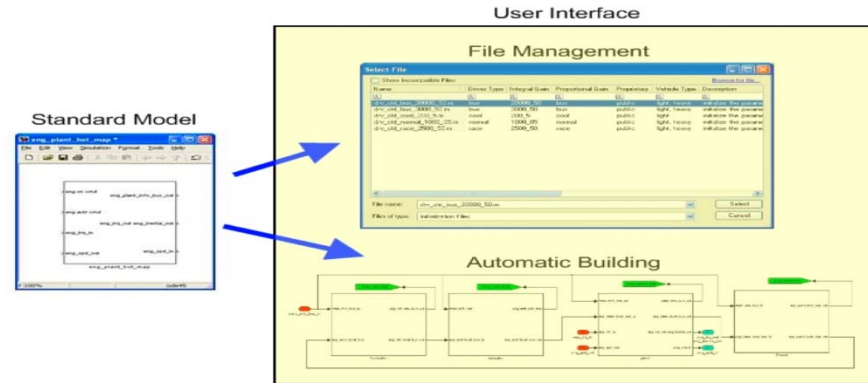


Figure 1. Simulation Management Concepts

Layout files have three different levels of abstraction. Static layout files are a direct translation of the style of a Simulink model into the XML Argonne Model Description Specification (XAMDS) and cannot be used across systems. Dynamic layout files have XAMDS elements that are resolved at build time and other elements that are only library elements. These files have greater flexibility and can be used across many different systems of a given category. Abstract dynamic layouts have a structure that is determined at build time. These files have the most flexible structure and can be used across many different categories of systems.

Each file managed by the system is associated with an XML file, which contains the metadata used to manage the file. XML was chosen for its flexibility and for its wide usage in the software industry. XML is easy to read by software and humans alike. As a language, it is specifically designed to create domain- and application-specific sublanguages and to pass information easily between software. In this case, we will be using it to pass information both between different parts of our program but also between different users of the overall modeling system. These XML files contain all of the information necessary to achieve true plug-and-play capability and are explored in detail later in this paper. They are collectively known as “definition

files” because they are used to fully flesh out and define the object to be modeled.

Finally, a GUI must control all of the different files and pieces for ease of use. Given the amount of information that will be available to choose from, it would be easy for a user to be overwhelmed. The Autonomie GUI works seamlessly with the pieces to provide quick access to the correct files, with integrated compatibility checks to guide the user as much as possible. In addition, the GUI will integrate with a central database to provide common offline model storage and file version control.

Architecture

All systems in the vehicle architecture can be logically categorized as either a containing system or a terminating system (Figure 2). Containing systems consist of one or more subsystems as well as optional files to define that system. They do not contain models; they only describe the structure of interconnections of systems and subsystems. Terminating systems consist of a model that defines the behavior of the system and any files needed to provide inputs or calculate outputs. Terminating system models contain the equations that describe the mathematical functions of the system or subsystem.

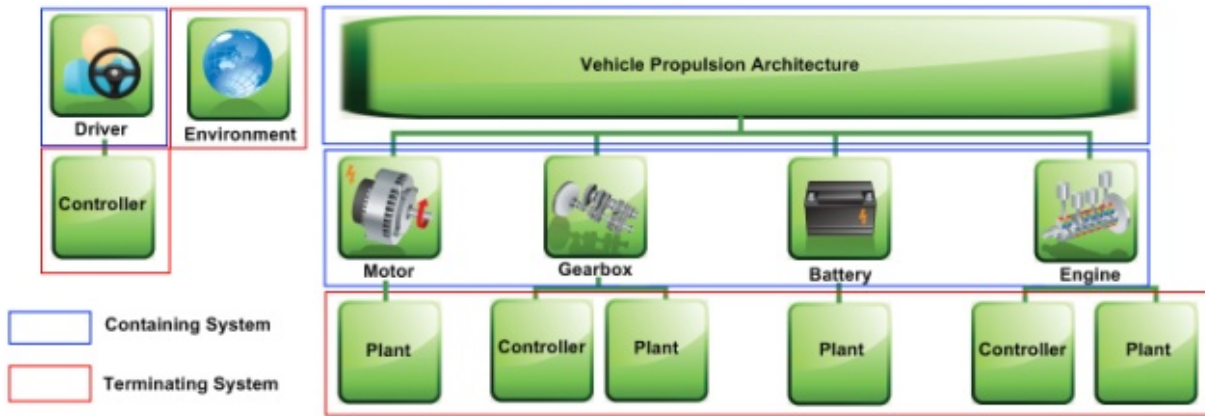


Figure 2. Container and Terminating Systems

Both of these types of systems are arranged in a hierarchical fashion to define the vehicle to be simulated. To avoid confusion, it is a best practice to mimic the structure of the actual hardware as much as possible. For example, low-level component controllers should be grouped with the components that they control and should be located at different levels of the hierarchy where applicable. Also, only systems that actually appear in the vehicle should be represented. In other words, there is no need to represent unused components or empty controllers.

In addition to simplifying the architecture, this philosophy will allow for easy transfer of systems among users and will fully support hardware-in-the-loop, software-in-the-loop, and rapid-control prototyping, if desired.

The relative positions of the systems, as well as connections between the systems and bus information, are contained in an architecture description file known as a configuration file. The use of an XML file to contain this information ensures that no restrictions are placed on the layouts of the systems. This file structure allows complete flexibility on the part of the system modeler. Any

organization is possible, as long as the systems can be characterized by effort and flow inputs and outputs. However, to simulate vehicles, a particular organization is suggested to avoid confusion and to help standardize layouts. Following this organization will allow for maximum reusability, both within an organization as well as externally among companies or universities.

At the top level is a vehicle system containing the following systems: environment, driver, vehicle propulsion controller (VPC) for advanced powertrain vehicles (such as hybrids or plug-in hybrids) that require a vehicle-level controller, and a vehicle propulsion architecture (VPA) (Figure 3). The VPA system will contain whichever powertrain components are required to simulate the vehicle, such as engine, battery, and wheels. Under any component system there should be a standard layout for systems, known as the controller, actuator, plant, and sensor (CAPS) configuration (Figure 4). Any or all of the four CAPS level systems may be present. For example, if a system to be simulated does not contain any actuators or sensors, only the controller and plant systems would be present. Many systems do not have independent controllers and may therefore contain only a plant system.

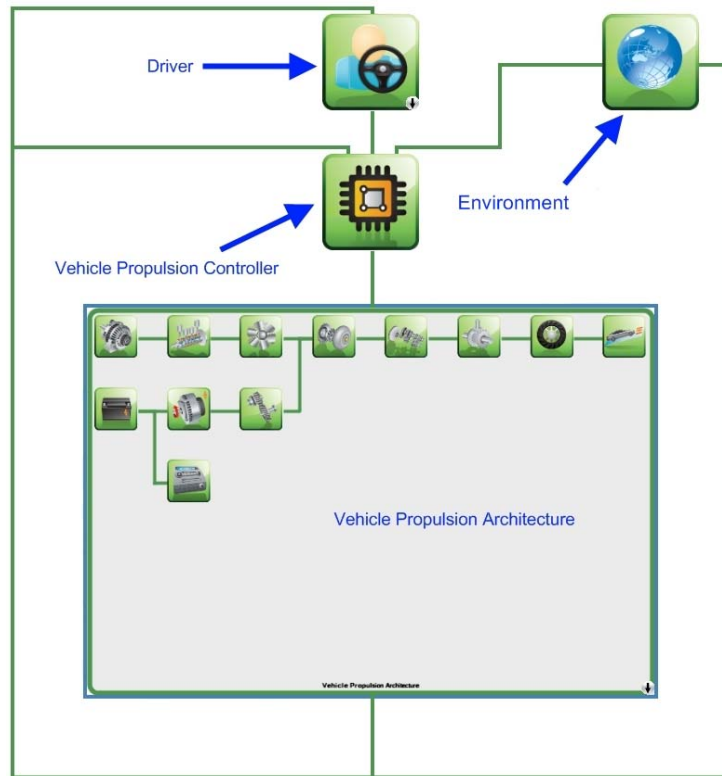


Figure 3. Top-level Vehicle Layout

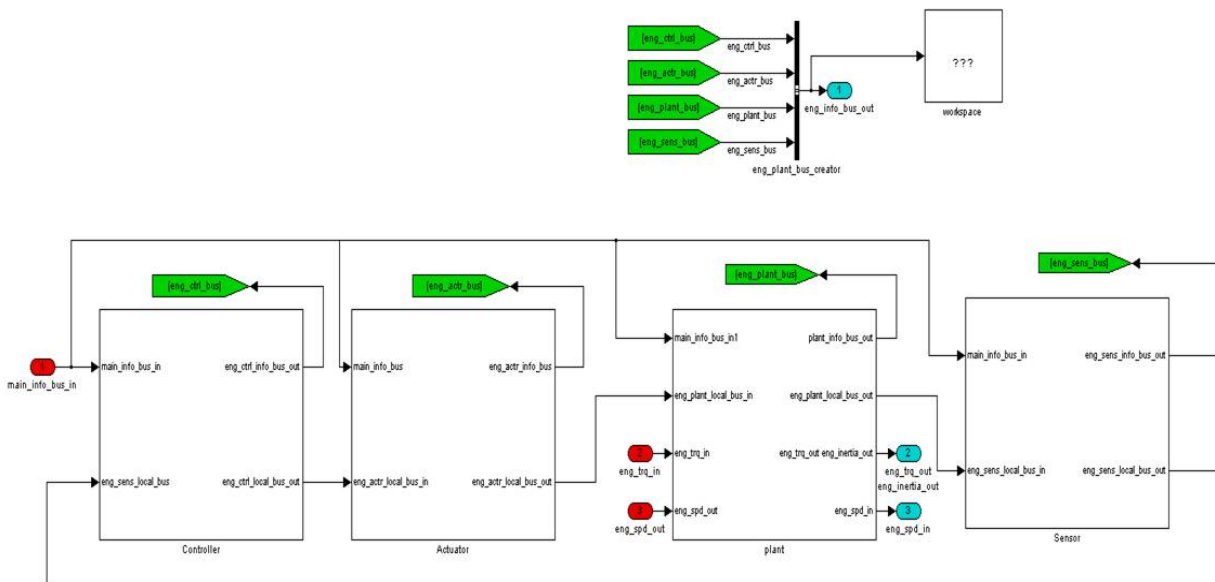


Figure 4. Controller Actuator, Plant, and Sensor Configuration for an Engine System

Depending on the fidelity of the model, additional and more detailed levels may be specified under the

CAPS level. For example, if individual pieces of an engine plant have been modeled, such as a cooling

subsystem or an exhaust subsystem, they would become subsystems of the engine plant system.

Note that the general philosophy of mimicking the actual vehicle hardware as closely as possible takes precedence. Although the standard is fairly generic, subsystems should be created where necessary, and deviations from the standard are acceptable only when required for consistency with a physical system (Figure 5).

System Definition

Several files can be specified to fully define a system: initialization files, preprocessing files, and post-processing files. In addition, a model file can be specified for a lowest or “leaf-level” (terminating) system (Figure 6).

Initialization and preprocessing files are evaluated to provide input values to a model. Initialization data are a set of constants. Preprocessing data are also used to initialize a model; however, these data require some processing or equations to arrive at a

final value. Only model files that require input parameters require initialization data, so initialization and preprocessing files are always optional. Post-processing files are evaluated at the end of the simulation run to calculate additional values used for analysis. The values from these files cannot be used as inputs for models.

In most cases, initialization and preprocessing files are specified on a terminating system, and the values apply directly to the model defining the system on which they are placed. In some instances, it makes sense to have the files on a containing system. For example, a parent system may need to aggregate information from all of its subsystems to calculate a value. Also note that these files are provided in a list. That is, multiple files of the same type can be specified on a system, allowing common information to be broken out into a separate file to avoid duplication. For a calculation performed for multiple systems, for example, a separate post-processing file can be created and selected on all of the appropriate systems.

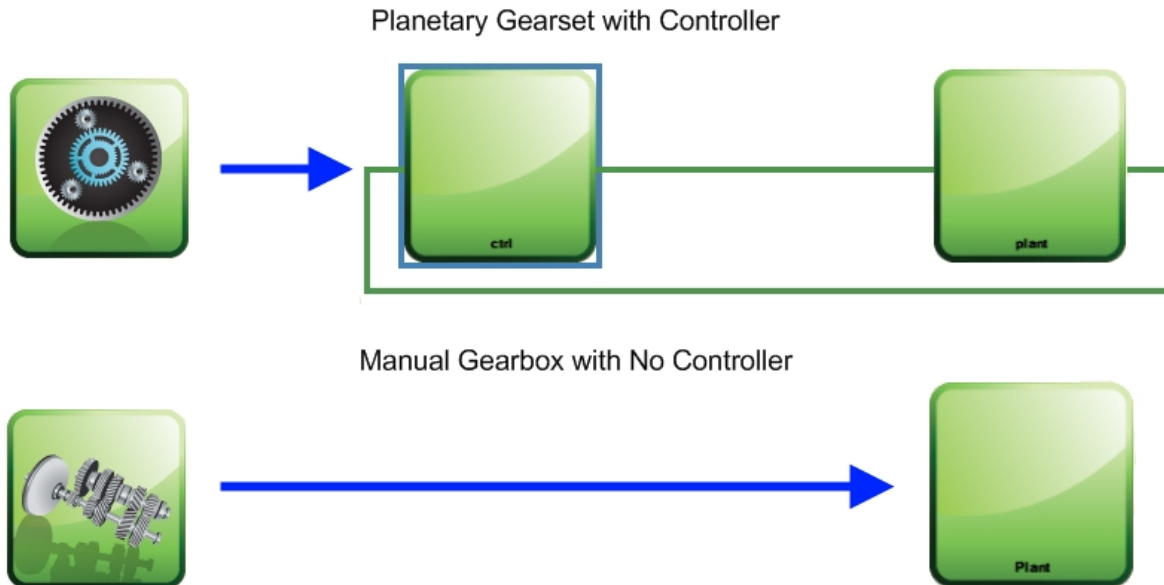


Figure 5. Controller Placement Consistent with Physical Hardware

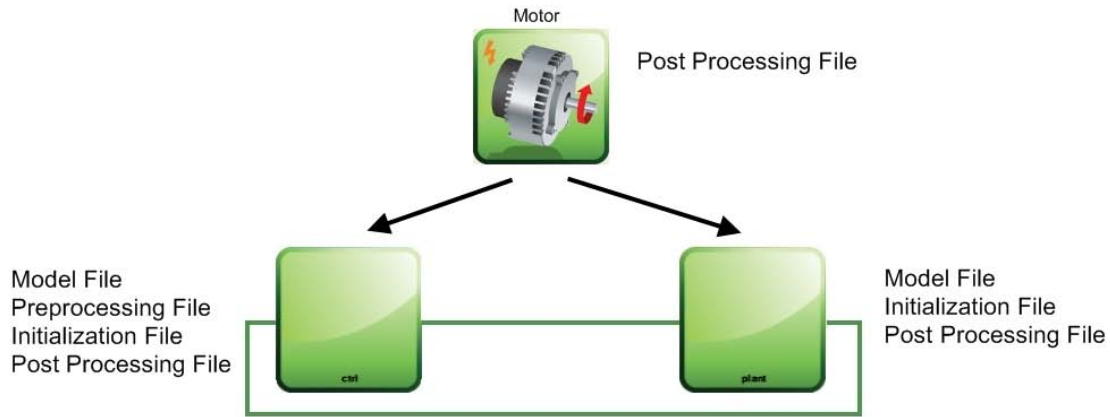


Figure 6. Motor with Example Definition Files Selected

Models can be specified on terminating systems only. This means that in most cases the models are specified at the CAPS level. Model files are created by using Matlab/Simulink and represent one system. In order to further capitalize on full reusability, the models are created with a common format and based on Bond Graph concepts. The ports on the left side of the model are input ports, which are used to transmit information from the previous system. The ports on the right side of the model are output ports and are used to transmit information to the next system.

The top pair of ports represent information flowing through the systems or shared between systems and subsystems. For example, information from another system, including commands (e.g., engine on/off, gear number), may be received on the input, and simulated variables may be passed on to the output (e.g., torque, rotational speed, current, voltage). An engine plant in the standard CAPS layout may receive command information from the controller or actuator system to its left and send out information about its state to the sensor block to its right (Figure 7).

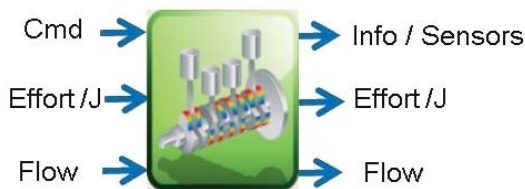


Figure 7. Example Engine Plant Block with Ports

The second pair of ports carry the “effort variables” (e.g., voltage or torque) through the system. The third pair of ports carry the “flow variables” (e.g., current or speed) through the system.

If a model does not participate in the propulsion of the vehicle and thus does not have an effort and flow, it will only contain the information-passing ports (the top pair).

Simulink Building

The model files created for the terminating systems need to be combined in a way that allows simulation in Simulink. One option is to create every possible combination of the systems and save each complete vehicle as a separate model file. This option quickly becomes infeasible when one considers the staggering number of combinations. Not only are we dealing with a number of different components, which is already overwhelming, but we must also consider different levels of fidelity and model versions for each component. Changing the version of a single component model would result in a new version of the entire vehicle. This method is clearly storage intensive and impractical.

A second option is to save every model in its own file and manage a library of the models. This approach would be an improvement over the first option; however, it still presents some difficulties. When a user wishes to create a new vehicle, he or she has to select all of the appropriate models from the library and connect them by hand into a vehicle

context. Not only is this manual process time consuming, but it also introduces many opportunities for error. Consider an engine control unit (ECU) model for autocode generation that can have more than 2,000 inputs and outputs. Connecting all of them manually virtually guarantees errors. It also requires some outside solution for model library management (such as searching, versioning, and ensuring compatibility).

Autonomie uses a novel approach that combines the second option with an automated building process. This design gives the user the flexibility of saving and versioning models independently without the headache of manually connecting everything. Users select the correct files in a user interface, and the automatic building uses metadata associated with the models to create the correct connections. This GUI also uses the metadata to facilitate the other necessary functions, such as compatibility checks and file selection.

Using an automated build procedure also provides other advantages. In some cases, models are not free to use any architecture or naming convention. A model might be used for interfacing with hardware or for automatic code generation, which may impose certain restrictions. In some cases, it might not be feasible to convert legacy models to a new format because of time or budget constraints. In those cases,

the automatic building can isolate rogue models by automatically placing blocks before and after them to perform certain conversions (Figure 8), such as variable name conversions, unit conversions, and data type conversions. As such, the Autonomie system can be used with legacy models with minimum modification.

Metadata

Each definition file (model, initialization, preprocessing, and post-processing) requires an associated metadata file to provide additional information (Figure 9). Metadata files are the mechanisms by which the definition files are managed. The information provided in metadata files serves three main purposes, as described in the following paragraphs.

First, the metadata are used to ensure that everything is explicitly specified. For example, each parameter on a file is fully qualified with information about data type, unit, and range. This means that users of the definition files do not need to make assumptions or learn archaic or confusing modeling conventions—neither does the software. Removing the reliance on this sort of institutional knowledge reduces opportunities for errors and allows files to be shared between divisions or companies, even when they do not agree on the naming convention.

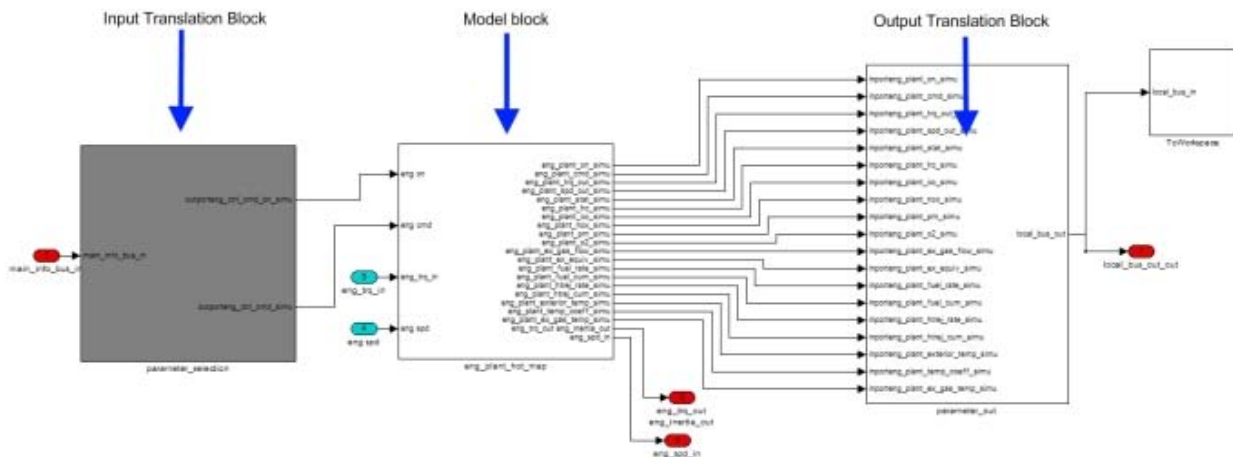


Figure 8. Automatic Input and Output Translation Blocks

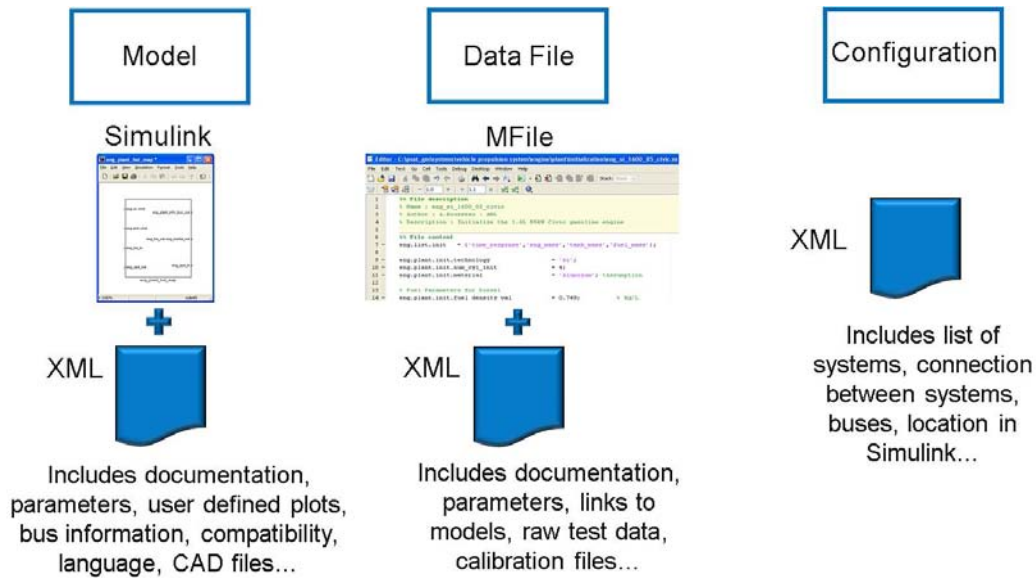


Figure 9. Metadata Files

Second, metadata allow reusability and transferability of files by enabling automatic compatibility checks among types of information, such as input and output variables, file types, and related files that may be needed for compatibility. In this way, systems can be used as black boxes: as long as the interfaces defined in the metadata files are satisfied, the system can be expected to work in a vehicle context. Model creators can be confident that their models are used appropriately, and model consumers can plug-and-play without needing to know the inner workings of the models.

Third, the metadata adds a level of user friendliness by providing a location for “helper information,” such as a description and a display name. Modelers can use this information to find a model they are looking for and to gain a quick understanding of what the file represents. Other such helper information could include a proprietary field; links to related files such as documentation, CAD drawings, test data, or validation reports; and a field to hold the level of modeling fidelity.

Because the list of potentially useful pieces of data is infinite, metadata files also contain a set of key/value pairs known as properties. These properties allow model creators to add any piece of information relevant to a model, even new types of data that were not anticipated by the software

developers. In this manner, the model can always display the type of data that is of interest to a user without restricting the model creator in any way.

User Interface

In order to fully define an object to simulate (e.g., a vehicle), we have to specify a tremendous amount of information and deal with many files. The number of files only increases when you consider the need for seamless cooperation of different versions of the same file and different levels of fidelity, each requiring its own supporting files. Therefore, a GUI to manage these file libraries is critical.

Autonomie is a software environment with a GUI that manages this complexity and makes it possible for novice users as well as experts to quickly find the files they need, stitch them together into a cohesive simulation, execute standard work processes, and perform database management functions without becoming overwhelmed.

Considering the concept of containing systems and terminating systems, a vehicle model has a logical hierarchical structure: the vehicle contains the VPA system, which contains component systems (such as an engine), which contain plants, on down to the lowest level of systems, which themselves contain models. Autonomie has two ways of displaying this

information: (1) in a tree format in the Project window and (2) as a series of icons representing systems that can be “drilled down on” to navigate deeper into the structure (Figure 10).

A system is always the basic unit of the structure. This definition helps keep the systems logically encapsulated, which in turn manages complexity. A user who is not an engine expert does not need to know how many levels there are under an engine system, how many models the functionality is broken down into, or where the models are. Rather, a user only needs to know that he or she has an engine system, which as long as the inputs and outputs of that system are satisfied, will work with any other systems in the vehicle.

In order to facilitate this system mindset, the System Properties window (Figure 10) always displays information about the selected system. Properties of the system are selected here, including definition files and, for a terminating system, a model file.

Each system can be selected in turn until all of the information is filled in and the vehicle model is complete for simulation.

GUI XML Files

There are several XML files that the GUI uses to help the user abstract all of the pieces for easier management. The first file type is a system file. This file represents one block on the GUI and everything contained within it, including any definition files or parameters that have been overridden in the GUI for the system, as well as all subsystems below this level. A system can be saved at any level. In this way, a user can save a piece of completed vehicle to be reused later or to be transferred to someone else. For example, one user might find it convenient to save an entire engine system, containing both a controller and a plant, while another user may only save the engine plant, so that it can be reused later with various controllers.

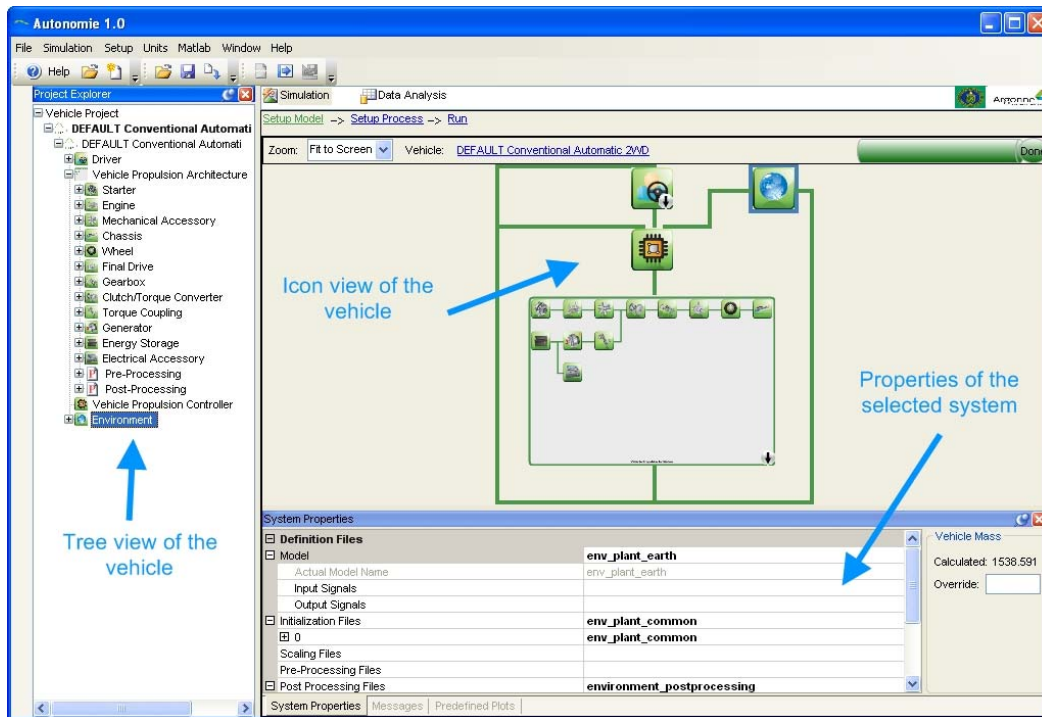


Figure 10. Vehicle in Autonomie

Once the various system files are completed and saved, users need not concern themselves with the details. They can quickly select pre-built pieces into

a completed vehicle. This feature avoids work duplication because each subgroup does not have to create its own representation of a system for its

particular modeling efforts. It also allows component experts, such as battery experts, to focus on the areas they are familiar with, while still being able to evaluate their component both as a stand-alone system as well as within a vehicle context (Figure 11). Systems can be exported and transferred that way, or the systems can be shared through the database. Autonomie includes as many pre-built systems as possible to give users a “jump start” into creating vehicles from scratch.

A vehicle file is logically much the same: it represents a system file saved at the top level, containing all other systems. An Autonomie vehicle would contain driver, environment, VPC and VPA subsystems, and all of their associated subsystems. Selecting a completed vehicle would allow a user to proceed immediately to the next step, which is to define the process to run, such as selecting a drive cycle. As with the system models, Autonomie includes as many pre-built vehicle models as possible. Most users will probably start with a pre-built vehicle and modify it.

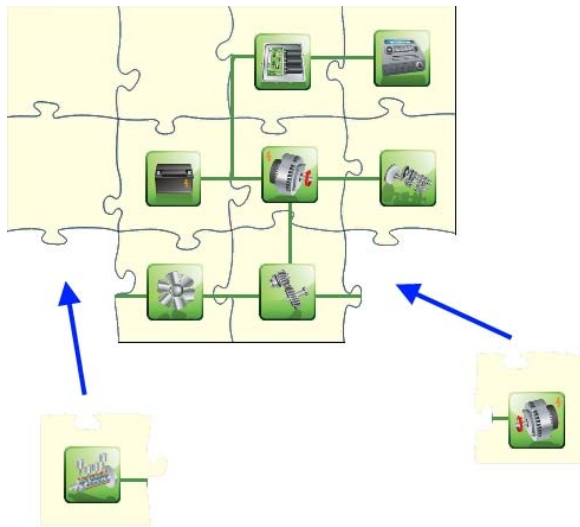


Figure 11. A Powertrain Is Assembled by System Experts

The final XML file is the run file, which contains all the information to recreate both the vehicle and the selected processes. The process information is the only difference between this file and a vehicle file (Figure 12). Given a run file, Autonomie will duplicate the simulation, provided none of the underlying definition files has changed in the interim.

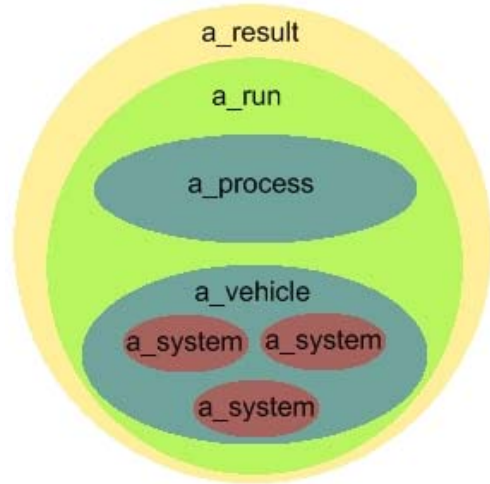


Figure 12. XML File Relationships

Once familiar with the use of these files, users can save their work at any level: system, vehicle, or run. These files help to encapsulate work so that users can focus on just their areas of expertise, and not get bogged down in the details. These files can be transferred between people to facilitate collaboration and reuse.

Finding Files in the GUI

In order to support the use of GUI files, they also contain the same types of information as the definition files, such as display name, description, proprietary designation, and properties. Properties are key/value pairs of information that a file creator or modeler believes are useful to identify that file. For example, engine system files might have properties that specify displacement or number of cylinders, and battery system files might have properties that specify chemistry type or peak power. Vehicle files might have properties that specify powertrain type or transmission type (manual, automatic, etc.).

The GUI uses the information in any metadata file (definition file or GUI file) to help a user search for a file. Because the architecture is generic, there is no way to know what sorts of information might be useful to a person trying to locate a particular file. For this purpose, the GUI uses the metadata values specified as properties to create a search dialog (Figure 13). The GUI also performs some initial filtering behind the scenes, so that only files that are compatible with the currently selected system are

displayed. That way, the dialog is always context sensitive, and the user can select from among files that are relevant without having to perform additional filtering.

When the GUI compiles the list of files to show in the dialog, it combines all of the properties of the files to create the columns of the dialog. The dialog is created on the fly every time it is displayed, and the layout of the dialog changes based on what it is showing. Only columns interesting and useful to finding those particular files are displayed. If, in the future, it becomes apparent that another piece of data would be useful for finding a file, it can simply be added to the appropriate metadata files, and the dialog will display it as a column with no code changes. In addition, these columns can be sorted or filtered to quickly and efficiently use the provided data to narrow in on the appropriate files.

Database Management

One of the critical areas of math-based design and simulation is file library management. As previously mentioned in this paper, the number of required files is staggering.

The number of files should begin to decrease as the various users and SMEs start to conform to the standard, merging their common files and getting rid

of redundancy. However, during this process, people may have access to many new files that they did not create. This situation adds yet another layer of complexity to the file selection process: not only are there hundreds or thousands of files, but the searcher is looking at files with which he or she is not familiar.

A database is required to manage all of these files, preferably a “source control” system that can inherently manage versioning. Autonomie provides a front end (Figure 14) that will interact with this database system in a way that is meaningful to an Autonomie user. If a user elects to download a vehicle file, the GUI would know to download all of the definition files needed to load that vehicle into Autonomie. This GUI is designed to support the typical database use cases: searching for files, mediating user access control, transferring files from the database to the working area, uploading from the working area to the database, checking out files for modification and checking them in, and making comparisons between local versions of files versus the version in the database.

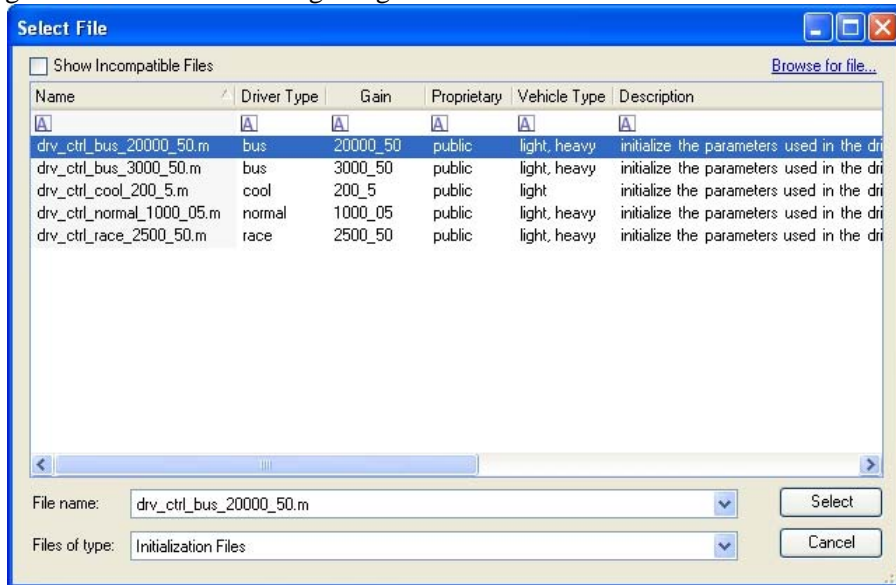


Figure 13. Using User-Defined Information to Find Files

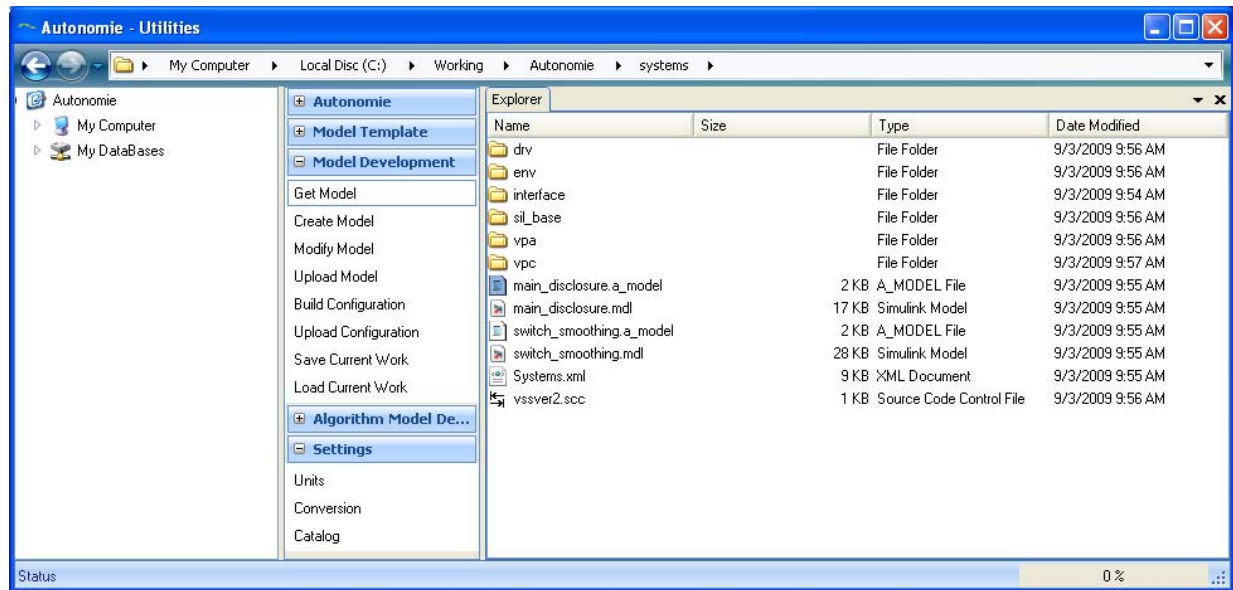


Figure 14. Database Utility

Consider the workflow for a model developer who wishes to create a new model to be used by others. First, the model must be created in Simulink. Assuming the model is in the proper format, the user next needs to create the proper XML metadata file to support its usage. In this case, the database utility provides a GUI so that the modeler can fill in all of the required information and generate the correct XML file. The modeler must then upload the new model, along with its metadata definition file, to the database so that the model is available to other users.

The database utility has been designed with the same flexibility as the rest of Autonomie, allowing several places for customization. For example, a plug-in can be created to allow the database utility GUI to connect to any “source control” provider. Also, custom processes can be added if the user has certain logic that needs to be executed, such as certain review and approval protocols that must be met before allowing a check in.

Simulations/Processes

When most vehicle modelers think about running a simulation, they immediately think about a driving cycle (i.e., a vehicle speed trace). However, this conception represents a limited view of what sort of simulations can be run with the Autonomie tool. To test a single component, it might be more appropriate to exercise the model with some other sort of input, such as a power profile. Some simulations may be more like a process, such as

those used in component sizing, parameter tuning, or optimization, which might require running multiple simulations. Other processes might not have any sort of trace input at all, such as a preliminary test to make sure the model builds correctly.

Autonomie uses the word “process” to include all of these different types of simulations under one umbrella. A process specifies the sequences of preprocessing and post-processing steps. One process can contain another process, creating a new process that is a composition of the two. For example, using the Autonomie process for a Five-Cycle Procedure and the process for an Autonomie optimization routine, a new composition process—a Five-Cycle Procedure wrapped in an optimization—can be defined. This composition operation can involve any number of processes. The Autonomie “process building” function mimics the structure of the Autonomie “system building” function. The GUI automatically completes process composition just before run time. Metafiles that define the architecture and steps of a process facilitate the development of composite processes.

A process is defined by an XML file. Each step has a Matlab .m file that is wrapped by a metadata file, known as a “process step info” file.

The process step info file lists the name of the associated .m file, as well as the usual display name, description, and proprietary fields. It also contains information about the parameters that the .m file accepts, including a default value for each parameter. The process file lists all of the process steps in order, and it can also specify overrides to the parameter values. In addition, an editor can be provided as an optional plug-in and will be displayed in the GUI. Providing an editor leads to flexibility, because it allows users to graphically change parameters at run time. For example, an editor that allows for the selection of a drive cycle can provide a visual representation of that drive cycle. Finally, the process and all of its parameter values are written, along with all of the vehicle information, into the run file.

This loose definition of a process allows users to create their own processes, including editors displayed in the GUI for the process steps. The possibilities are endless, allowing users to apply the Autonomie software in ways the tool developers have not yet even imagined.

Conclusions

To reduce costs, the automotive industry must embrace a math-based control system design for modeling, simulation, testing, and analysis. This paper proposes an ideal modeling process, wherein SMEs produce libraries of high-quality models in varying levels of fidelity for use throughout an organization and across the automotive industry. These models connect seamlessly for maximum reusability and flexibility, making collaboration quick and easy. The models developed by these experts can be used from the beginning to the end of the design process, from high-level configuration sorting studies, to code testing with production software (such as software-in-the-loop, hardware-in-the-loop, or rapid-control prototyping), and, finally, to solving production problems. Reuse of models is promoted, and costly duplication and redundancy activities throughout the development process are eliminated.

To arrive at this ideal and efficient virtual development process, we apply certain techniques, such as a standardized modeling architecture, on-demand model building, associated XML definition files, and GUIs for managing models. The

techniques described in this paper will allow modelers to navigate the challenges of executing a comprehensive strategy of math-based control system design for modeling, simulation, testing, and analysis with success, thus shortening time to market and reducing costs.

Publications/Presentations

A. Rousseau, "Accelerating the Development and Introduction of New Technologies through Model Based Design," October 2009, DOE.

A. Rousseau, "Autonomie Plug&Play Software Architecture," Presentation to DOE Merit Review, May 2009.

A. Rousseau, "Autonomie Overview," June 2009 (presented to OEMs, VSATT, and other potential users).

A. Rousseau, "Autonomie Project Review," Presentation to GM Gate Review, July 2009.

A. Rousseau, S. Halbach, and L. Michaels, "Autonomie Training," Presentations, September 2009.

S. Halbach, P. Sharer, S. Pagerit, C. Folkerts, and A. Rousseau, "Model Architecture, Methods, and Interfaces for Efficient Math-Based Design and Simulation of Automotive Control Systems," SAE 2010 World Congress.

F. Impacts of Real-World Drive Cycles on PHEV Fuel Efficiency and Cost for Different Powertrain and Battery Characteristics

Aymeric Rousseau (project leader), Ayman Moawad, Phil Sharer
 Argonne National Laboratory
 9700 South Cass Avenue
 Argonne, IL 60439-4815
 (630) 252-7261; arouseau@anl.gov

DOE Technology Manager: Lee Slezak

Objectives

Evaluate the impacts of different component sizes and vehicle control strategies on plug-in hybrid electric vehicle (PHEV) fuel efficiency by using realworld drive cycles.

Assess the cost benefits of different component requirements, vehicle powertrain configurations, and control strategies.

Approach

Define vehicles with different battery energy, from low to high values for all-electric range (AER).

Implement different control strategies to assess their benefits on real world drive cycles.

Analyze the electrical and fuel consumption levels on real world drive cycles.

Perform cost benefit analysis based on current and future cost values of the different components and fuels.

Accomplishments

Evaluated different component requirements for PHEV applications on several AER options.

Assessed fuel efficiency potential and cost for each vehicle and control option.

Future Directions

Implement new vehicle powertrain configurations and fuels.

Refine cost benefit analysis and implement net present value (NPV).

Refine study with additional realworld driving cycles.

Compare fuel consumption results to PHEV SAE J1711 procedure.

Define component cost requirements to meet several payback scenarios.

Introduction

PHEVs have demonstrated great potential with regard to petroleum displacement. Since the benefits of PHEV technology rely heavily on the battery, the development of new generations of advanced batteries with a long life and low cost is critical. To address this goal, the U.S. Department of Energy

(DOE), as part of the FreedomCAR and Fuel Partnership, is funding the development and testing of battery technologies.

Previous studies that focused on the impact of standard drive cycles or powertrain configurations demonstrated the need to further evaluate driving behaviors. Argonne National Laboratory has been working in collaboration

with the U.S. Environmental Protection Agency (EPA), which has been interested in realworld fuel economy in the past few years. This paper addresses the impact of realworld drive cycles on PHEV fuel efficiency and cost.

Vehicle Description

The vehicle class used represents a midsize sedan. The main characteristics are defined in Table 1.

Table 1. Main Vehicle Characteristics

Glider mass (kilograms [kg])	990
Frontal area (square meters [m2])	2.2
Coefficient of drag	0.29
Wheel radius (meter [m])	0.317
Tire rolling resistance	0.008

Two vehicle configurations were selected, depending on the degree of electrification:

- An input power split with a fixed ratio between the electric machine and the transmission, similar to the Camry hybrid electric vehicle (HEV), was used for HEVs and for PHEVs with low energy (i.e., 4- and 8-kWh total battery energy).
- A series engine configuration was selected for PHEVs with large energy (12- and 16-kWh battery energy cases).

Component Sizing

To quickly size the component models of the powertrain, an automated sizing process was developed. A flowchart illustrating the sizing process logic is shown in Figure 1. Unlike conventional vehicles, which have only one variable (engine power), PHEVs have two variables (engine power and electric power). In this case, the engine is sized to meet the gradeability requirements.

To meet the AER requirements, the battery power is sized to follow a specific driving cycle while in the all-electric mode. The batteries for the power-split configurations are sized to follow the Urban Dynamometer Drive Schedule (UDDS), while the series configurations are based on the more aggressive US06. In addition, the vehicle can capture the entire energy from regenerative braking during deceleration.

In previous studies, the battery energy was sized to meet required AER. In this case, four battery energy values were selected: 4, 8, 12, and 16 kWh total.

Vehicle mass is calculated by adding the mass of each component to the mass of the glider. The mass of each component is defined on the basis of its specific energy and power densities.

To maintain an acceptable battery voltage (around 200 V), the algorithm will change the battery capacity rather than the number of cells to meet the AER requirements. To do so, a scaling algorithm was developed that properly designs the battery for each specific application.

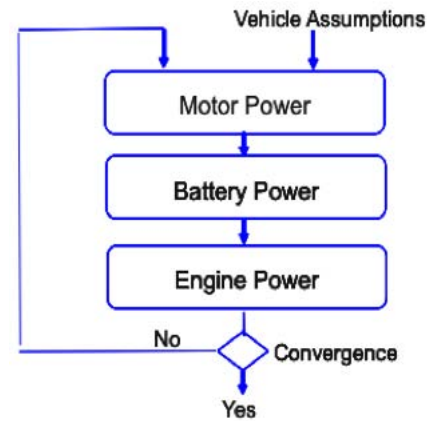


Figure 1. Process for Sizing PHEV Components

Finally, the PHEV will operate in electric-only mode at a higher vehicle speed than will regular hybrids. The architecture therefore needs to be able to start the engine at a high vehicle speed. In the power-split configuration, the generator is used to start the engine. Because all of those elements are linked to the wheels via the planetary gear system, researchers need to make certain that the generator (the speed of which increases linearly with vehicle speed when the engine is off) still has enough available torque—even at a speed above 50 mph—to start the engine in a timely fashion.

For the HEV powertrain, the battery is sized to capture the regenerative braking energy from the UDDS. The engine and both electric machines are sized to meet both gradeability (6% at 65 mph at gross vehicle weight) and performance requirements (0 to 60 mph under 9 s). The control strategy used has been validated against vehicle test data from

Argonne National Laboratory's Advanced Powertrain Research Facility (APRF).

Drive Cycle Description and Analysis

The EPA has measured many real world drive cycles. In 2005, more than 100 different drivers in Kansas City participated in the study. The user vehicles (model year 2001 and later) were instrumented, and their driving statistics were collected for the duration of a day. While several measurements were taken, only vehicle speed was used as part of this analysis. Speed was collected on a second-by-second basis independently through the onboard diagnostic (OBD) port, as well as from a GPS device. The OBD speed data were favored over the GPS when both were available. Data were collected on conventional as well as hybrid vehicles, but for reasons of simplicity, we have chosen to examine the speed from the conventional vehicles only, although there were minor differences in driving. Figure 2 shows an example of real world drive cycles. The maximum acceleration and deceleration of each trip were analyzed to ensure data validity.

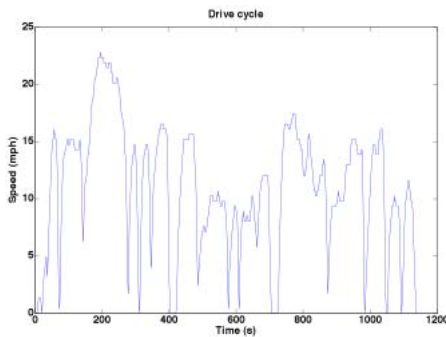


Figure 2. Example of Real world Drive Cycles

Fuel Efficiency Results

Reference Conventional Vehicle

Each vehicle is simulated on all of the real world drive cycles. A histogram showing the distribution of the results was generated, as shown in Figure 3. The mean value achieved for the reference vehicle is 6.61 l/100 km.

To compare different powertrain configurations, a kernel density function is defined.

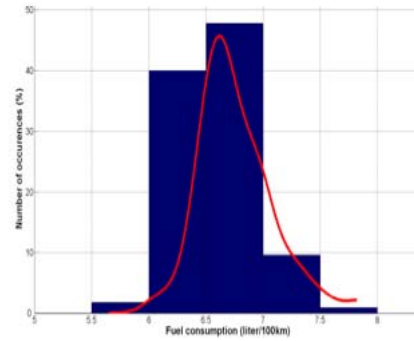


Figure 3. Conventional Vehicle Fuel Economy Distribution

Drivetrain Configuration Comparison

Different control strategies were implemented depending on the powertrain configuration considered. Each control option is briefly described below.

Electric vehicle/charge sustaining (EV/CS) (Thermostat) Strategy — The EV/CS control strategy was implemented for the series configuration. The controller has been designed to drive as long as possible by using energy from the battery, which depletes its state-of-charge (SOC) from 90% SOC to 30% SOC. The engine turns on only if the road load exceeds the power capability of either the battery or the motor. Once the battery reaches charge sustaining (CS), the engine is used as a thermostat to regulate the SOC.

Load Engine Power Strategy (Load following) — A power threshold, depending on the battery SOC, is used to turn the engine ON. As a result, the engine can be turned ON during charge-depleting (CD). To maximize charge depletion, when operating, the engine only provides the requested wheel power without recharging the battery.

Optimum Engine Power Strategy — Similarly to the previous control, the engine is turned ON based on a variable power threshold. However, the strategy attempts to restrict the engine operating region close to the peak efficiency of the engine. As a result, the engine might be used to recharge the battery during charge depleting mode.

These different options were selected to provide an acceptable tradeoff between the number of engine

ONs and fuel efficiency. Figure 4 shows the mean values of both electrical and fuel consumption rates for the different powertrain options. As is evident, the lowest levels of fuel consumption are achieved for the largest rates of electrical consumption. As demonstrated in previous studies, the fuel and electrical consumption rates have a linear relationship.

When analyzing both series configurations, smaller fuel consumption is achieved when using a 16-kWh total battery energy as compared to a 12-kWh (average of 0.9 l/100 km vs. 0.7 l/100 km).

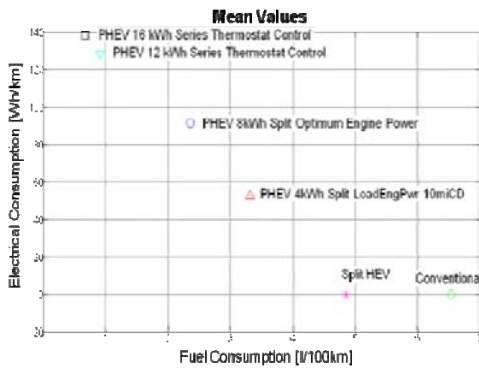


Figure 4. Comparison of the Mean Values for the Different Configurations Considered

Figure 5 provides the kernel distribution curves for the fuel consumption of each powertrain option. It is evident that with the increases in available battery energy, the standard deviation increases. This result is because of the fact that the engine operation becomes less dependent on the drive cycle with increased available battery energy.

For the largest battery energy, a significant portion of the drive cycles are driven in electric only mode.

Figure 6 provides the kernel distribution curves for the electrical consumption of each powertrain option. The lowest battery energy (4 kWh) has the lowest standard deviation. This result can be explained by the fact that the battery is used mainly for low power applications because of the control strategy selected. Both medium battery energy cases (8 and 12 kWh) provide the widest standard variation as the battery is used for both low and medium power requirements.

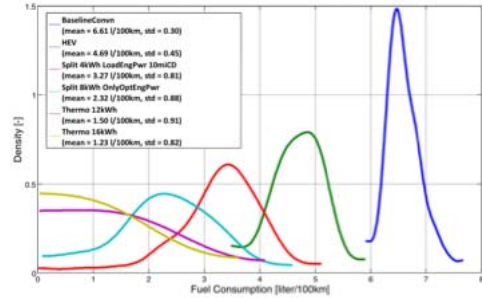


Figure 5. Fuel Consumption Comparison

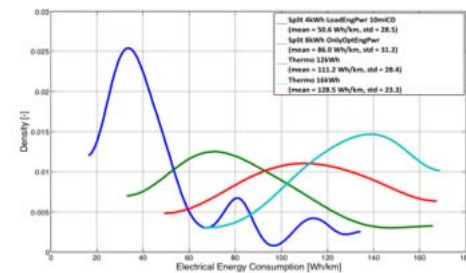


Figure 6. Electrical Consumption Comparison

Figure 7 shows the impact of battery energy size on root mean square (RMS) current. As is evident, the RMS current significantly increases from HEVs to PHEVs, along with the distribution width. The highest battery capacities lead to higher battery RMS current, which will affect the battery life.

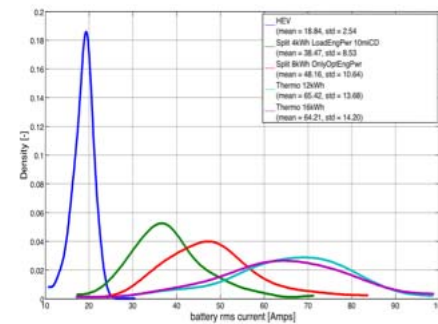


Figure 7. Impact of Battery Size on RMS Current

Figure 8 shows the distribution of the percentage of usable energy consumed at the end of a daily trip. While the energy is totally consumed for the low-energy batteries (60% and 56%, respectively, for the 4- and 8-kWh battery cases), some available energy remains for the larger batteries because of trips of short distances. As a result, the driver will carry

energy that will not be used, thus penalizing the vehicle’s fuel efficiency.

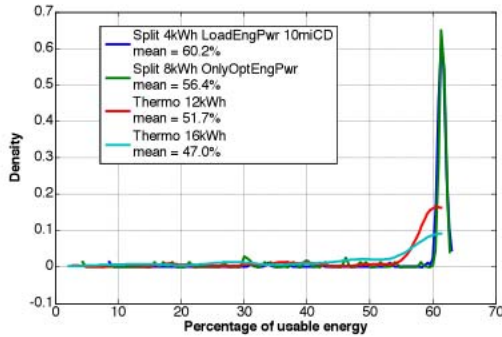


Figure 8. Percentage of Usable Energy at the End of Daily Trips

Impact of Distance on Consumption

Figure 9 provides the fuel consumption for each daily drive and vehicle powertrain. The total volume of fuel consumed by each drivetrain configuration for running all of the cycles was computed and is summarized in Table 2.

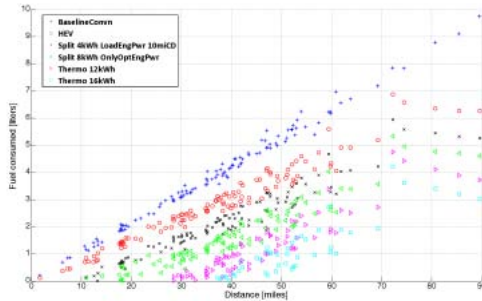


Figure 9. Fuel Consumption as a Function of Distance

Table 2. Fuel Consumed Total

Drivetrain Configuration	Volume (L)	Decrease vs. conventional (%)
Conventional	454	—
HEV	328	27.6
PHEV 4-kWh	238	47.5
PHEV 8-kWh	172	62
PHEV 12-kWh	99	78
PHEV 16-kWh	54	88

As Table 2 shows, significant gains are achieved with the HEV configurations. These gains, however,

are lower than those usually found when simulating standard drive cycles.

An additional 20% is achieved by using a 4-kWh battery. The gains from adding further battery capacities decrease when going from 8 to 16 kWh, with only a 10% increase from 12 to 16 kWh.

Figure 10 provides the electrical consumption for each daily drive. For daily drive with short electrical distances (less than 15 miles), the electrical consumption of PHEVs is similar across powertrain options. This result is likely because these cycles are characterized by low power demand and consequently can be performed in the all-electric mode for the most part. The largest discrepancies are noticed for medium distances (15 to 25 miles). These drive cycles are characterized by both low and large power demands. As a result, while the power-split 8-kWh option will lead to engine ON, the series configurations will continue to operate in all-electric mode, resulting in higher electrical consumption—and consistent with the electrical consumption distribution shown in Figure 6.

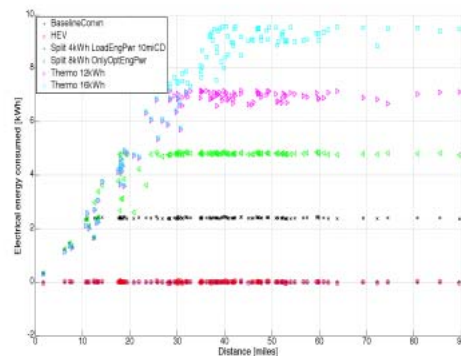


Figure 10. Electrical Consumption as a Function of Distance

Finally, for the longest distances, both series configurations provide similar behavior because the control strategy favors the use of electrical energy.

Cost/Benefit Analysis

The cost of the vehicle is defined by the size of the different components, both for power and energy. The vehicle costs used to calculate the payback are presented in Table 3.

Figure 11 shows “break-even” lines for the assumptions considered. The HEV break-even point is 7.5 years, while the PHEVs range from 8 to 12.5 years.

Table 3. Vehicle Cost

Parameter	Vehicle Cost (\$)
Conventional	17,245
HEV	20,029
PHEV 4-kWh	21,881
PHEV 8-kWh	23,709
PHEV 12-kWh	27,487
PHEV 16-kWh	29,338

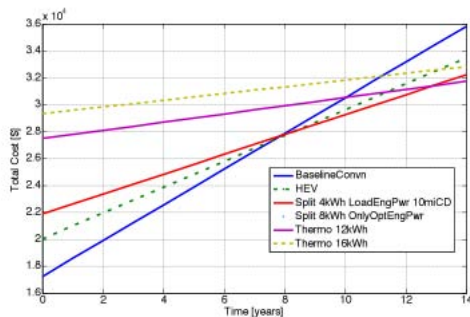


Figure 11. Break-even Line vs. Conventional

Figure 12 shows the payback as a function of distance for the different vehicles compared to the conventional powertrain. The results below are provided for an electrical cost of 0.09\$/kWh and a fuel cost of \$4/gallon (gal). As Figure 12 shows, a longer daily drive distance can significantly reduce payback time. On the basis of the assumptions considered, a consumer should drive at least 30 miles per day to realize an acceptable payback period (ranging from as high as six years down to four years for small energy batteries, and from as high as eight years down to six years for larger battery energies).

In addition, HEVs are more cost effective than the PHEV 4 kWh for daily driving distances of longer than 30 miles, but the order is reversed for shorter distances. When driving long distances (greater than 40 miles), both series configurations achieve similar payback as the additional battery cost is compensated for by fuel efficiency benefits.

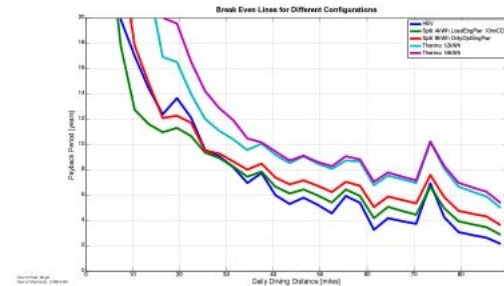


Figure 12. Payback as a function of Distance vs. Conventional

Figure 13 shows the payback as a function of distance for the different PHEVs as compared to the hybrid powertrain. In that case, the payback time as expected is longer than it is for the conventional vehicle. Since both HEV and PHEV technologies achieve better rates of payback when driving distances are longer, when comparing PHEVs to HEVs, the payback does not vary as much as a function of distance once the high-energy battery is depleted. Payback is close to 8 years for low-energy batteries and 11 years for larger batteries.

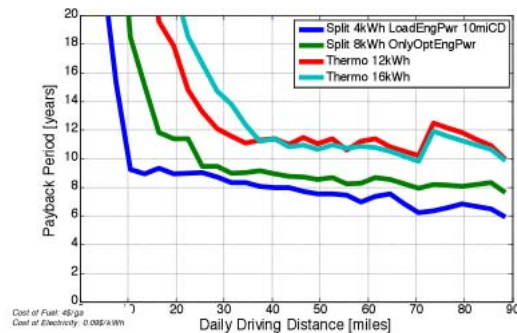


Figure 13. Payback as a function of Distance vs. HEV

Figure 14 shows the impact of fuel cost to payback period for a constant electricity cost of \$0.09/kWh. To achieve an acceptable payback, the price of fuel should be at least \$4.00/gal, with daily driving distances of 30 to 40 miles. Moving from a fuel price of \$4.00/gal to \$5.00/gal leads to a reduction in the payback period by one year on average.

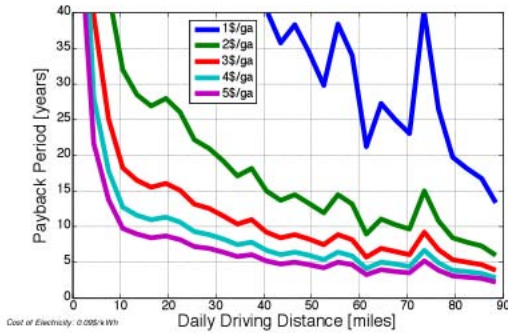


Figure 14. Impact of Fuel Cost on Payback Period (Split PHEV 4kWh)

Conclusions

Different powertrain configurations, including conventional vehicles, HEVs, and several PHEVs, have been simulated on more than 100 real world daily drive cycles. The power-split configuration was selected for the HEV and PHEV 4- and 8-kWh cases, while the series option was used for the largest battery energies (12 and 16 kWh).

The simulation results demonstrated significant fuel economy gains both with HEVs and PHEVs, with fuel displacement increasing linearly with available electrical energy.

However, it appears that the benefits, when adding 4 kWh of battery energy, seem to decrease between the 12 and 16-kWh range because of the distribution of the daily driving distances.

Since the drive cycles have different characteristics based on distance, the benefits of each vehicle configuration depend on how far the vehicle is driven. While the electrical consumption is similar for shorter and longer driving distances, the main differences occur during medium trips (15 to 25 miles).

Based on the assumptions considered, the cost of PHEVs remains high, requiring further research and development into batteries. In addition, higher fuel prices would help achieve a practical payback period.

Publications/Presentations

M. Fellah, G. Singh, and A. Rousseau, S. Pagerit, "Impact of Real-World Drive Cycles on PHEV

Battery Requirements," SAE paper 2006-01-0377, SAE World Congress, Detroit, Michigan, April 2009.

A. Rousseau, "PHEV Component Requirements," Presentation at DOE Merit Review, May 2009.

A. Moawad, G. Singh, S. Hagspiel, M. Fellah, and A. Rousseau, "Real World Drive Cycles on PHEV Fuel Efficiency and Cost for Different Powertrain and Battery Characteristics," EVS24, Norway, May 2009.

G. Faron, S. Pagerit, and A. Rousseau, "Evaluation of PHEVs' Fuel Efficiency and Cost Using Monte Carlo Analysis," EVS24, Norway, May 2009.

A. Rousseau, A. Moawad, G. Singh, S. Hagspiel, and M. Fellah, "Impact of Real World Drive Cycles on PHEV Fuel Efficiency and Cost for Different Powertrain and Battery Characteristics," AABC 2009, Long Beach, California, June 2009.

G. PHEV Vehicle Level Control Selection Based on Real World Drive Cycles

Aymeric Rousseau (project leader), Dominik Karbowski, and Ayman Moawad

Argonne National Laboratory

9700 South Cass Avenue

Argonne, IL 60439-4815

(630) 252-7261; arouseau@anl.gov

DOE Technology Manager: Lee Slezak

Objective

Evaluate the impact of different vehicle control strategies on the fuel efficiency of plug-in hybrid electric vehicles (PHEV) by using real world drive cycles.

Approach

Define vehicles with different battery energy (all-electric range).

Implement different control strategy philosophies to assess their benefits for real world drive cycles.

Analyze the electrical and fuel consumption levels on real world drive cycles.

Accomplishments

Assessed the fuel efficiency potential for each vehicle and control option.

Selected vehicle level control philosophies and control parameters to minimize fuel consumption, while maintaining an acceptable drive quality and battery life.

Future Directions

Further analyze the selection of the control strategy philosophy and its parameters for different travel distances.

Refine the study with additional real world drive cycles.

Introduction

PHEVs have demonstrated great potential with regard to petroleum displacement. Previous studies have demonstrated the need to consider the total trip distance to optimize fuel consumption. In this study, several vehicle-level control strategy algorithms are implemented on four midsize PHEVs. The parameters of each control are then tuned to achieve different charge-depleting (CD) ranges on the Urban Dynamometer Driving Schedule (UDDS). The impacts on fuel consumption, engine ON/OFF events, and the battery root mean squared (RMS) are analyzed to determine the most appropriate control/parameter combinations for each vehicle and to maintain acceptable drive quality.

Vehicle Description

The vehicle class used represents a midsize sedan. The main characteristics are defined in Table 1.

Table 1. Main Vehicle Characteristics

Glider mass (kg)	990
Frontal area (m ²)	2.2
Coefficient of drag	0.29
Wheel radius (m)	0.317
Tire rolling resistance	0.008

Two vehicle configurations were selected, depending on the degree of electrification:

- An input power split with a fixed ratio between the electric machine and the transmission, similar to the Camry hybrid electric vehicle (HEV), was used for HEVs and PHEVs with low energy (4-kWh and 8-kWh total battery energy).
- A series engine configuration was selected for PHEVs with high energy (12-kWh and 16-kWh battery energy cases).

Vehicle Level Control Strategy Development

Different control strategies were implemented, depending on the powertrain configuration that was considered. Each control option is briefly described below.

Load Engine Power Strategy (load following)

A power threshold, depending on the battery state-of-charge (SOC), is used to turn the engine ON. As a result, the engine can be turned ON during CD. As shown in Figure 1, to maximize charge depletion, when ON, the engine provides only the requested wheel power without recharging the battery.

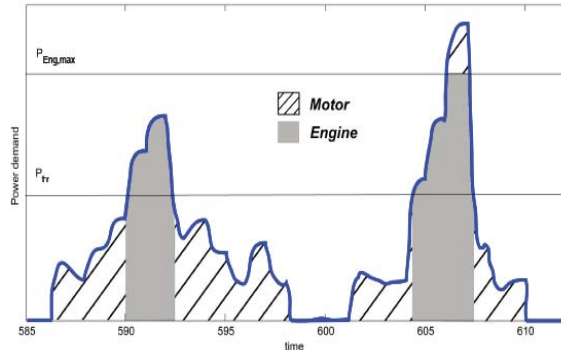


Figure 1. Load Following Vehicle Control

Differential Engine Power Strategy

As shown in Figure 2, the electric machine supplies all the power demanded by the system up to a predefined threshold. After exceeding the threshold, the motor continues to supply the threshold value, and the engine runs to supply the incremental power demand.

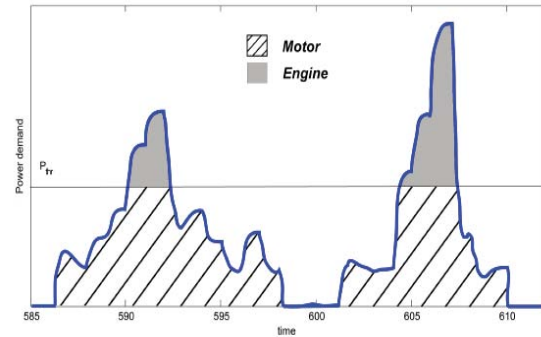


Figure 2. Differential Engine Power Vehicle Control

Optimum Engine Power Strategy

Similar to the previous control, the engine is turned on based on a variable power threshold. However, the strategy attempts to restrict the engine-operating region close to the peak efficiency of the engine (Figure 3). As a result, the engine might be used to recharge the battery during CD.

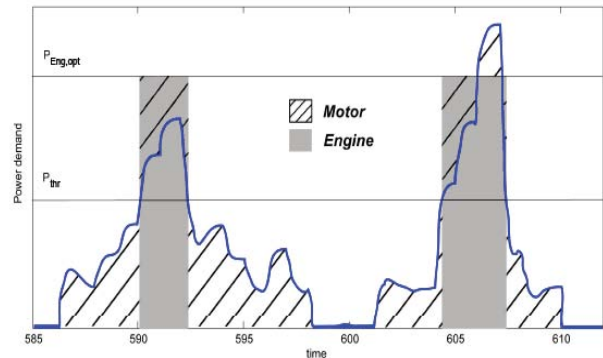


Figure 3. Optimum Engine Power Vehicle Control

EV/CS (thermostat) Strategy

The EV/CS control strategy was implemented for the series configuration. The controller has been designed to drive as long as possible by using energy from the battery, which depletes its SOC from 90% to 30%. The engine turns on only if the road load exceeds the power capability of either the battery or the motor. Once the battery reaches charge-sustaining (CS), the engine is used as a thermostat to regulate the SOC.

For each vehicle control strategy and each vehicle, the power threshold leading to engine ON was tuned to obtain a 10-, 20-, 30-, 40-, and 50-mile CD range on the UDDS cycle. The 4-kWh configuration has a

10.47-mile EV range on the UDDS, while the 8 kWh configuration range was 21.64 miles. The maximum power threshold for the engine is the maximum continuous power of the electric machine, as shown in Equation 1.

$$P_{thr,max} (4\text{-kWh vehicle}) = P_{mot,max} (4\text{-kWh vehicle}) = 34.6 \text{ kW, and}$$

$$P_{thr,max} (8\text{-kWh vehicle}) = P_{mot,max} (8\text{-kWh vehicle}) = 35.2 \text{ kW.}$$

Equation 1

The minimum power threshold is set to 3 kW. The threshold is sized with a secant method algorithm and a tolerance of 0.5 mile for the CD range. An example of vehicle level control strategy parameters is shown in Table 2.

Figure 4 summarizes the vehicle configurations, battery energies, control strategy philosophies, and parameters analyzed in the study.

Fuel Efficiency Results

Fuel Consumption

Figure 5 shows the mean values from running the different vehicle and control options on the real

world drive cycles from Kansas City, as provided by the U.S. Environmental Protection Agency (EPA). A significant spread of the fuel consumptions occurs for the same vehicles. For example, the mean fuel consumption of the power split with 4-kWh battery energy ranges from 2.6 l/100 km to 5.5 l/100 km because of impacts such as driving distance and driver aggressiveness.

While all the different combinations were simulated, only the best couple of options from a fuel consumption standpoint are presented below. In general, all the vehicle-level controls tuned for long CD distances led to higher fuel consumptions.

Table 2. Power Threshold Parameters: Load Following Engine Power Strategy

CD range	P _{threshold} (4 kWh)	P _{threshold} (8 kWh)
10 miles	P _{thr,max} = 34,600 W	P _{thr,max} = 35,200 W
20 miles	18,918 W	P _{thr,max} = 35,200 W
30 miles	15,296 W	22,045 W
40 miles	12,662 W	18,726 W
50 miles	11,310 W	17,275 W

Figure 4. Summary of the Considered Configurations and Controls

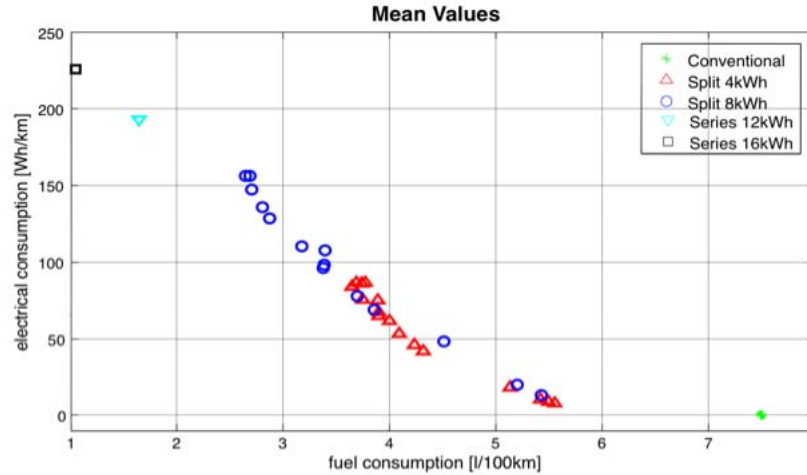


Figure 5. Summary of the Control Strategy Impact on Mean Fuel Consumption

Figure 6 depicts the distribution of the four control strategies that achieved the lowest fuel consumption for the power split with a 4-kWh battery. The differential engine power strategy tuned for 10-s and 20-s CD on the UDDS achieves the lowest fuel consumption, with the 20-mile case being the most efficient. While most engineers believe that the battery should be discharged as quickly as possible to minimize fuel consumption, this result highlights the need to take driving distance into account during the control strategy development process.

However, the difference between the four controllers is small. As a consequence, additional parameters must be considered to make an appropriate selection.

Electric Consumption

Figure 7 shows the distribution of the electrical consumption for the same four control strategies. All the batteries display similar behavior, with the highest density close to 40 Wh/km. This is explained by the fact that a PHEV with low battery energy will tend to use the electricity during low power demands, thereby leading to smaller electrical consumptions.

To select the final vehicle controls, the number of engine ON and battery RMS was taken into account.

Number of Engine Starts

Figure 8 shows the distribution of the number of engine starts per kilometer. The optimum engine power strategy has a lower number of starts compared with the other configurations. This is expected because the engine is used at higher power.

Battery RMS Current Evaluation

Figure 9 depicts the distribution of the battery RMS current, which has an impact on the battery life. The differential engine power control strategy tuned for a 20-mile CD has a much lower battery RMS current than the other options.

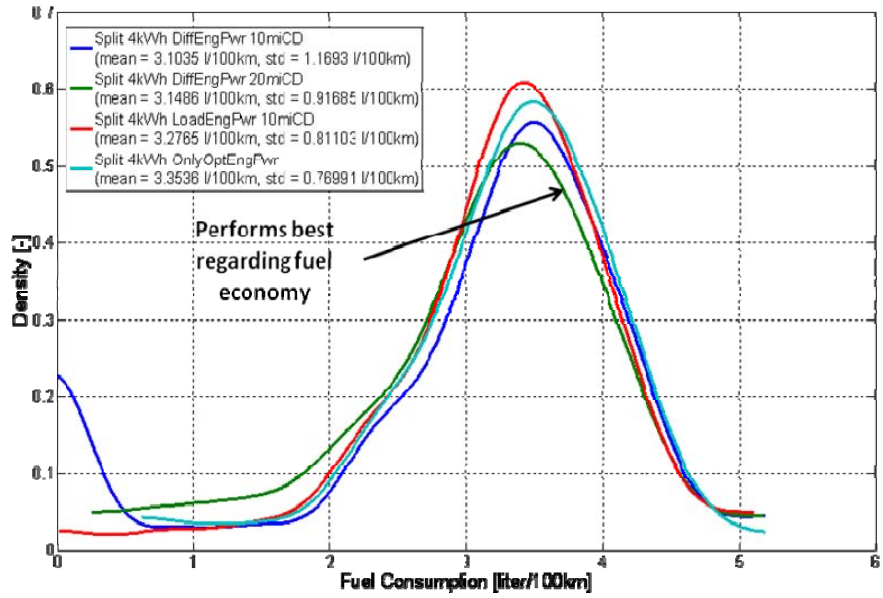


Figure 6. Fuel Consumption Distribution: Example of 4-kWh Split

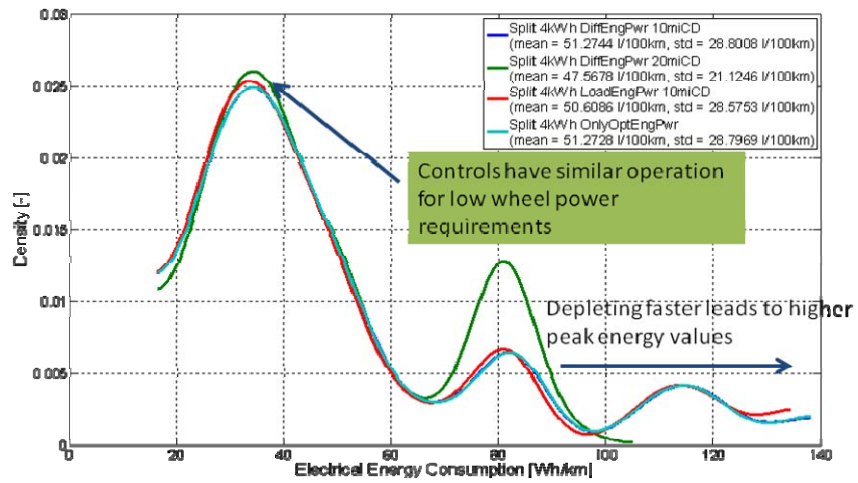


Figure 7. Electrical Consumption Distribution: Example of 4-kWh Split

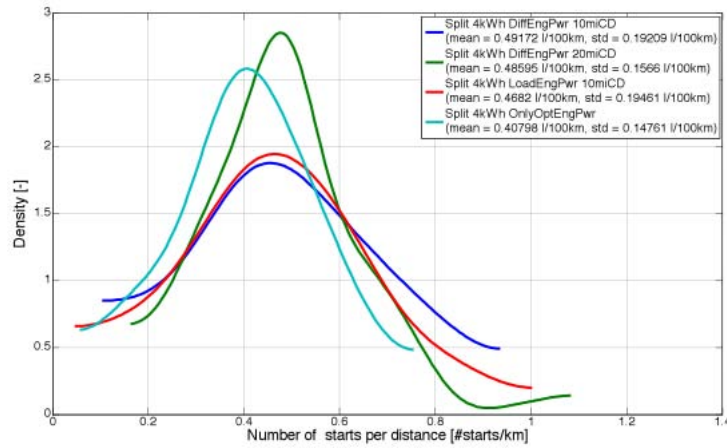


Figure 8. Impact of Control on the Engine Start Number: Example of 4-kWh Split

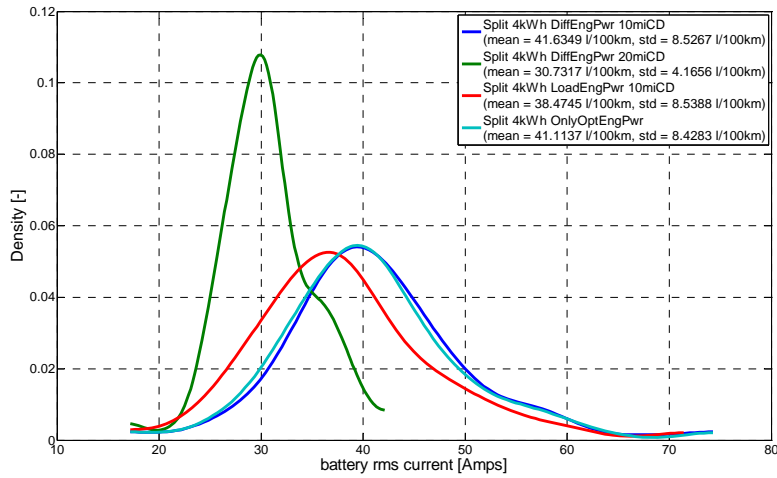


Figure 9. Impact of Control on the Battery RMS Current: Example of 4-kWh Split

Control Strategy Selection

Figure 10 details the mean values of both electrical and fuel consumptions for the selected control strategies of the different powertrain options. The lowest fuel consumption reductions are achieved for the largest electrical consumptions. As demonstrated in previous studies, the fuel and electrical consumptions have a linear relationship.

While the series configurations share the thermostat controller, both power split options (4 kWh and 8 kWh) use different control philosophies: the Load Engine Power for the 4 kWh and the Optimum Engine Power for the 8 kWh.

was analyzed for both fuel consumption and electrical consumption. The most promising options were then compared based on engine ON/OFF and battery RMS current.

While the series configurations share the thermostat controller, different vehicle level control strategies have been selected for the power split configurations based on the battery energy.

Publications/Presentations

S. Hagspiel, G. Singh, and A. Rousseau, “Impact of Vehicle Level Control Strategies on PHEV Fuel Efficiency,” presentation to the U.S. Department of Energy, January 2009.

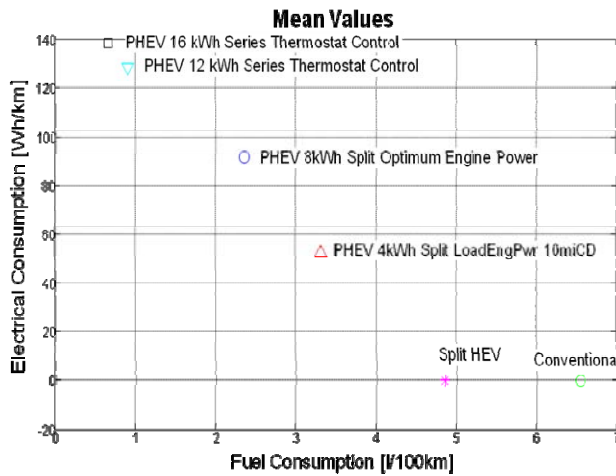


Figure 10. Comparison of the Mean Values for the Different Controls Selected

Conclusion

Four midsize PHEV vehicles, along with their HEV and conventional counterparts, were modeled. Both a power split configuration (for low battery energy cases) and a series configuration (for high battery energy) were selected. For each option, several vehicle level control strategies were developed. The main parameter influencing the CD distance was tuned to achieve different CD ranges on the UDDS cycle. The vehicles were simulated on more than 110 real world drive cycles provided by the EPA.

The results demonstrated that, while the battery should always be “empty” at the end of a trip, depleting it as fast as possible will not consistently lead to the lowest fuel consumption, especially for low-energy vehicles. Each vehicle control option

H. Instantaneous Optimization for a Multimode Transmission

Dominik Karbowski (project leader), Namdoo Kim, Jason Kwon, and Aymeric Rousseau
Argonne National Laboratory
9700 South Cass Avenue
Argonne, IL 60439-4815
(630) 252-7261; arousseau@anl.gov

DOE Technology Manager: Lee Slezak

Objective

Develop an instantaneous optimization algorithm for a multimode transmission.

Approach

Define the algorithm to minimize fuel consumption while maintaining acceptable computing power.

Develop and implement the algorithm while maintaining acceptable drive quality.

Run a simulation to analyze fuel consumption.

Accomplishments

Developed and implemented an instantaneous algorithm in the Powertrain Systems Analysis Toolkit (PSAT).

Analyzed the results using the previously validated model of the GM Tahoe 2-Mode.

Future Directions

Compare the instantaneous optimization with the rule-based approaches.

Modify the algorithm to include engine ON/OFF and additional logic.

Introduction

Hybrid electric vehicles (HEV) offer significant fuel economy improvements through the use of at least two different energy storage systems. The primary source of power, generally an internal combustion engine, is coupled to an energy storage system to avoid the most inefficient conventional vehicle operating conditions, including idling, low load. While numerous configurations have been studied over the years, most of the current production vehicles, including the Toyota Prius and Ford Escape, are based on the input power-split configuration. With the power-split, the use of a single planetary gearset along with two electric machines allows decoupling of the engine and the vehicle speeds. When the engine is ON, the control is based on operating the engine close to its best

efficiency curve while maintaining the battery state-of-charge (SOC) within an acceptable range. While the power-split configuration allows for significant fuel savings, its application for larger and/or more powerful vehicles is limited, as it would require very powerful electric machines to operate through the entire vehicle speed range. Consequently, Toyota and Lexus have opted to add a third electric machine in the rear axle. In addition, the system can be less efficient during energy recirculation. Another option is multimode transmissions, which include several electrically variable transmission (EVT) modes, along with potentially fixed gears. Allison Transmission first implemented a 2-mode transmission in buses, and General Motors (GM) recently added it to its full-size line of hybrid trucks and sport utility vehicles (SUV). In the latter, the transmission has two EVT modes and four fixed

gears, but it is still known as a 2-mode. While the study can be applied to any multimode transmission, the Chevrolet Tahoe was used.

The Tahoe’s greater number of modes (a total of six) includes two EVT and four fixed gear modes, which leads to greater flexibility and control complexity. The question becomes not only how each component should be operated to minimize fuel consumption, but also which mode should be selected. To address this issue, rule-based approaches can be implemented. However, this requires an intimate understanding of the system, and the tuning of each control parameter must be carefully adjusted from each specific set of component data and vehicle application. Another control technique is instantaneous optimization, which is currently implemented in the GM Tahoe HEV. One approach is the Equivalent Consumption Minimization Strategy, which optimizes the component operating conditions at each time step based on a cost function, including fuel and electric power. In this paper, a partial instantaneous optimization will be implemented.

Vehicle Description

In 2008, GM introduced the Chevrolet Tahoe, the first hybrid full-sized SUV. The vehicle features an exclusive 2-mode transmission that includes two electric machines, three planetary geartrains, and four clutches. It has all the advantages (i.e., all-electric mode, regenerative braking, torque assist, etc.) of a full hybrid vehicle, while preserving the towing capacities of the conventional version (Figure 1).

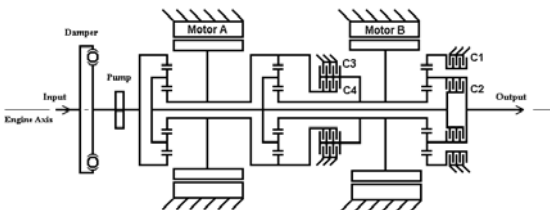


Figure 1. GM Tahoe Hybrid 2-Mode Transmission

The main vehicle characteristics are summarized in Table 1.

Table 1. Vehicle Specifications

Parameter	Value
Estimated test weight	2,685 kg
Wheel radius	0.401 m
Final drive ratio	3.08
Planetary gear ratio (Zs:Zr)	0.357:0.69, 0.69:1.357, 0.505:1.357
Motor peak power/torque	60 kW/307 Nm @ 1,865 RPM
Engine	LFA 6.0L V8, cylinder deactivation
Engine peak power/torque	248 kW @ 4,500 RPM/526 Nm @ 4,370 RPM
Battery	288 V, 6.5 A•h, NiMH

The 2-mode transmission can operate in six different modes: two EVT and four fixed gear modes. The EVT modes are called input and compound split. In the fixed gear modes, the vehicle operating conditions are similar to a parallel configuration. Due to the multiple EVT modes, there are several mechanical points, thereby leading to a reduction of inefficient power recirculation. The fixed gear modes are critical in towing and grade conditions. In the Chevrolet Tahoe, the transmission is coupled to a 6-L V8 engine using cylinder deactivation, which further improves the vehicle fuel efficiency.

A validated model of the GM Tahoe HEV in PSAT was used for the study.

Control Strategy Development

Equations

In order to properly select or compute the torque demands, the controller uses equations that describe the system operations and links the states and demand outputs. They are usually a simplified version of the more detailed ones embedded in the plant models. For example, inertia effects are omitted.

The battery is connected to both electric machines, as well as to the electric accessories. Each electric machine input power (i.e., electric power, independent of the power flow) is a function of its torque and speed. That function is generally given by a look-up table. Equation 1 describes the relationship between torques, speeds, and battery power.

$$P_{ess}^{out} - P_{access} = P_{EM1}^{in}(\omega_{EM1}, T_{EM1}) + P_{EM2}^{in}(\omega_{EM2}, T_{EM2}) \tag{Equation 1}$$

In the case of a fixed gear mode, the speed and torque relationships are similar to those of a classic multispeed gearbox. They are given by Equations 2 and 3, with k_X^i being the multiplication ratio for component X . (X can be the engine or either electric machine.) This is depicted in Figure 2.

$$T_{gb}^{out} = k_{ICE}^i T_{ICE} + k_{EM1}^i T_{EM1} + k_{EM2}^i T_{EM2} \tag{Equation 2}$$

$$\begin{cases} \omega_{ICE} = k_{ICE}^i \omega_{gb}^{out} \\ \omega_{EM1} = k_{EM1}^i \omega_{gb}^{out} \\ \omega_{EM2} = k_{EM2}^i \omega_{gb}^{out} \end{cases}$$

$$\tag{Equation 3}$$

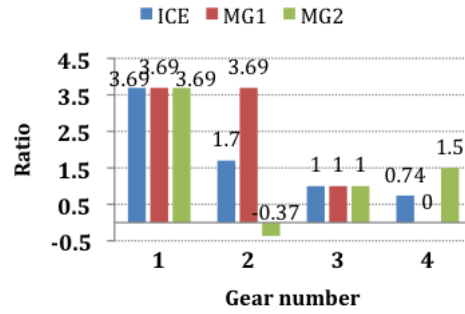


Figure 2. Fixed Gear Ratios for Each Traction Component

In the case of an EVT mode, the generic relationship between the torques and speeds is given by Equations 4 and 5 by using four factors (p_j , q_j , r_j , and s_j) that are specific to mode j . The ratios are defined in Tables 2 and 3.

$$\begin{bmatrix} T_{gb}^{out} \\ T_{ICE} \end{bmatrix} = \begin{bmatrix} p_j & q_j \\ r_j & s_j \end{bmatrix} \begin{bmatrix} T_{EM1} \\ T_{EM2} \end{bmatrix} \tag{Equation 4}$$

$$\tag{Equation 4}$$

$$\begin{bmatrix} \omega_{EM1} \\ \omega_{EM2} \end{bmatrix} = \begin{bmatrix} p_j & -r_j \\ q_j & -s_j \end{bmatrix} \begin{bmatrix} \omega_{gb}^{out} \\ \omega_{ICE} \end{bmatrix} \tag{Equation 5}$$

$$\tag{Equation 5}$$

Table 2. Definition of Reduced Ratio Variables

a	b	c	d	e	f
$\frac{Z_{R1}}{Z_{S1}}$	$\frac{Z_{S1} + Z_{R1}}{Z_{S1}}$	$\frac{Z_{R2}}{Z_{S1} + Z_{R2}}$	$\frac{Z_{S2}}{Z_{S1} + Z_{R2}}$	$\frac{Z_{S3} + Z_{R3}}{Z_{S3}}$	$\frac{Z_{R3}}{Z_{S3}}$

Table 3. Definition of Simplified Factors

	p	q	r	s
Mode 1	e	$\frac{bds}{1-bc}$	0	$\frac{a}{1-bc}$
Mode 2	$\frac{1-bc}{d}$	b	$-\frac{ac}{d}$	a

Algorithm Implementation

The engine ON/OFF and battery SOC control are defined by using a rule-based control, which consequently removes a degree of freedom by adding a constraint to the equations. At each time step, the battery power demand is known.

In a fixed gear mode, the only degree of freedom is the battery demand power split between both electric machines: either one can be used, or both can be used at the same time. As electric machine efficiency is generally better for higher torques, operating only one motor will probably lead to the optimal split when the speeds are the same (gears 1 and 3 or modes 3 and 5). When speeds are different (gear 2 or mode 4), the electric machine with the highest speed is selected. We will assume hereinafter that $x_{EM1} = 1$ for modes 3 to 5 (fixed gears 1 to 3), and $x_{EM1} = 0$ for mode 6 (fixed gear 4).

$$x_{EM1}(\mu \in \{3,4,5,6\}) = \begin{cases} 1 & \text{if } \mu \leq 5 \\ 0 & \text{if } \mu = 6 \end{cases} \tag{Equation 6}$$

$$\forall \mu \in \{3,4,5,6\} \quad c(\mu, t) = P_{ICE}^{in}(\omega_{ICE}, T_{ICE})$$

$$\omega_{ICE}, T_{ICE} \text{ s. a. } \begin{cases} \text{Eq. (1)(3)(4)} \\ P_{SS}^{out} = P_{SS}^{dmd}, T_{wh} = T_{drv}^{dmd@gbb} \\ x_{EM1} = x_{EM1}(\mu) \end{cases} \tag{Equation 7}$$

In EVT mode, it is not possible to make similar simplifications, as the non-linear electric power

equation comes into play with non-fixed component speeds. There is actually additional freedom in the control, since torque and speed can be selected. Given one variable (e.g., engine speed), it is possible to numerically solve the problem.

$$\forall \mu \in \{1,2\} \quad c(\mu, t) = \min_{\omega_{ICE}^{\min} \leq \omega_{ICE} \leq \omega_{ICE}^{\max}} P_{ICE}^{in}(\omega_{ICE}, T_{ICE}) \tag{Equation 8}$$

Eq.(1)(13)(14)
 $P_{SS}^{out} = P_{SS}^{dmd}, T_{gb}^{out} = T_{drv}^{dmd@gbb}$

Therefore, the optimization problem consists of finding the mode that minimizes the fuel rate at a given time (t), as described by Equation 9.

$$\mu_{opt}(t) = \underset{\mu}{\text{argmin}} \quad c(\mu, t) \tag{Equation 9}$$

This optimal mode is used only when the engine is ON. When it is OFF, there is no need for optimization, since there are no degrees of freedom.

Optimization Module

The principal role of the optimization module is to compute the costs associated with each mode, which involves computing the minimal fuel power associated with each mode and verifying whether each mode is possible. To perform those calculations, the operating points of each component are computed. They are later reused in the propelling controller, where it is necessary to have “targets,” thus avoiding code duplication. A switch also selects the fuel power for the current mode and feeds it back for comparison with the fuel power of each one of the remaining modes.

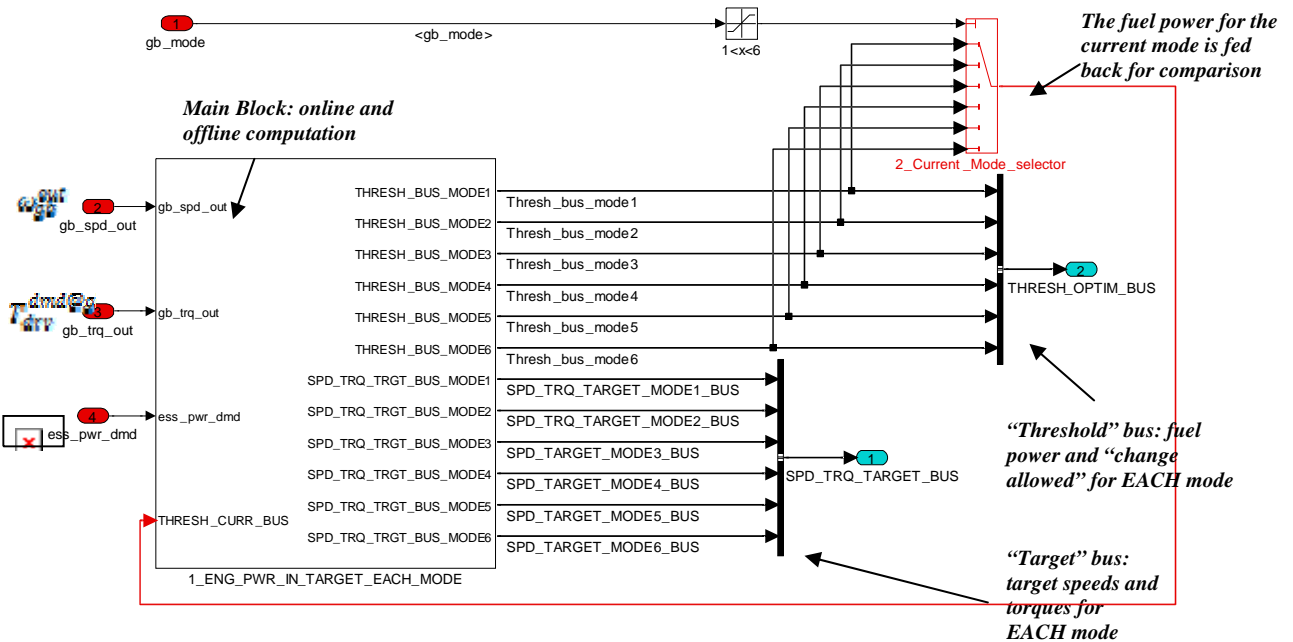


Figure 3. Optimization Module

Offline EVT Optimization

A Matlab function outputs an optimal engine speed look-up table that can be used in Simulink, indexed by gearbox output speed, battery power, and gearbox output torque. To compute that look-up table, a brute-force algorithm is used. All combinations of engine speed and electric machine torques are taken into consideration. Of all the solutions that verify Equations 1, 4, and 5, the one

with lowest fuel power is kept as a solution. The function is generic for any mode. The step sizes for torques and speeds can also be customized. It also reads the PSAT vehicle characteristics, such as engine efficiency and electric machine efficiency. The default steps are 10 rad/s for the gearbox output speed, 10 rad/s for the engine speed, and 1,000 W for battery power. It results in a 45,000 element map for mode 1 and 34,000 for mode 2. The look-up tables are depicted in Figures 4 and 5.

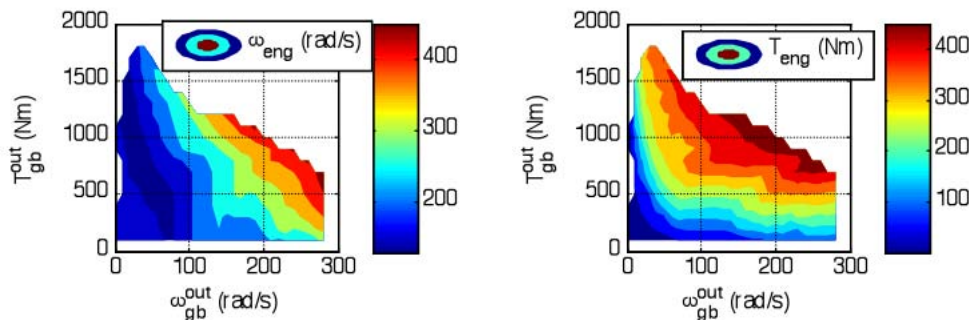


Figure 4. Look-up Tables Used in the Optimization Module: Optimal Engine Speed and Torque (mode 1; batterypower=0)

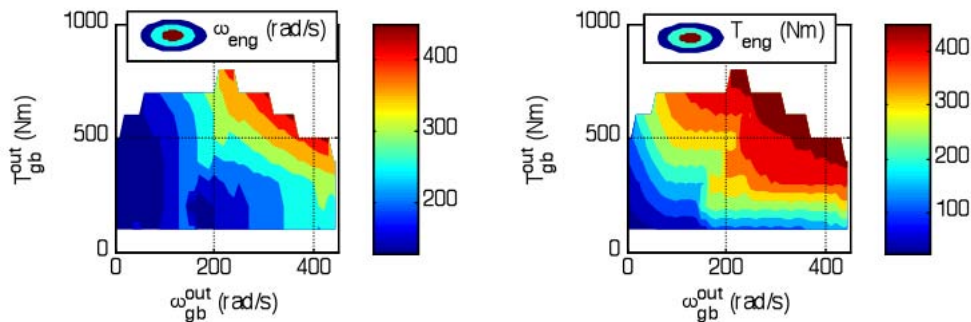


Figure 5. Look-up Tables Used in the Optimization Module: Optimal Engine Speed and Torque (mode 2; batterypower=0)

Results

Urban and Highway Cycles Operations

In urban driving, the vehicle alternates all-electric operations with hybrid mode (engine ON). Figure 6 depicts the mode, as well as engine torque and speed, on a portion of the urban cycle. The vehicle starts moving in all-electric mode before the engine kicks-in and starts to provide torque. The engine remains ON until the vehicle stops accelerating, at which point the driver power demand is low enough to allow an engine shut down. It starts again with the following acceleration.

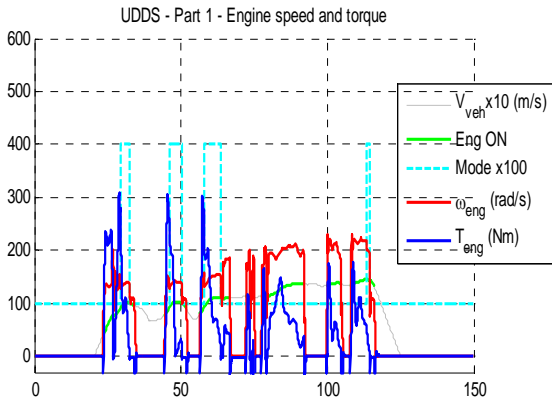


Figure 6. Engine Operations during the First 150 Seconds of the UDDS Cycle

On the Urban Dynamometer Driving Schedule (UDDS), as shown on Figure 7, the transmission mode that is used most often is the inputs split, since it is the only allowed mode in EV operation. The 4th mode (2nd fixed gear) is often used when the engine is ON. During the high speed

portions of the cycle, both highest gears (3rd and 4th fixed gears) are used.

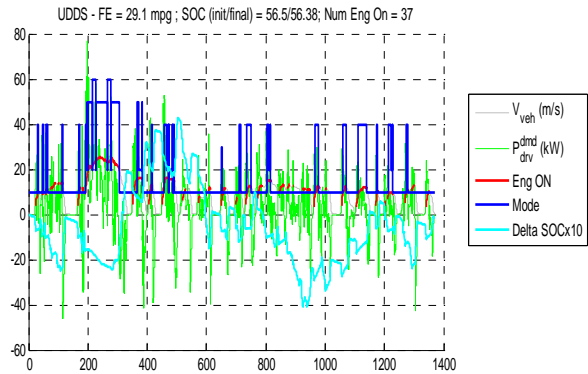


Figure 7. Vehicle Operation on the UDDS Cycle

As shown in Figure 8, the engine shuts down less frequently on the highway cycle.

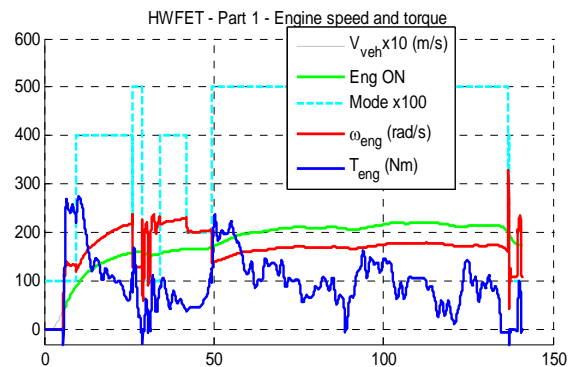


Figure 8. Engine Operations during the First 150 Seconds of the HWFET Cycle

Figure 9 shows that mode 5 (3rd fixed gear) is predominantly used during the first “hill” of the

cycle. The highest fixed gear is used on the second hill, which also corresponds to a higher speed area. The first mode (input split) is used only for some low-speed, low-acceleration areas or EV operation.

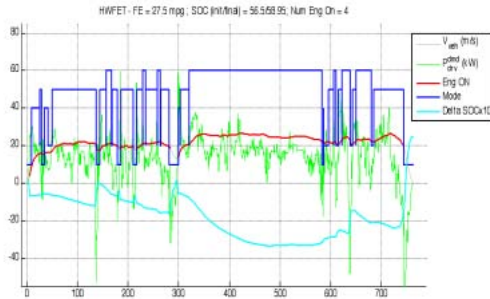


Figure 9. Vehicle Operation on the HWFET Cycle

Comparative Analysis

The vehicle was also simulated on other drive cycles: the New European Driving Cycle (NEDC), which is the European certification cycle; the LA92, which is a more aggressive urban cycle with some short highway cycles; and the US06, which is highly aggressive and predominantly at high speed. The fuel economy and consumption figures are reported in Table 4.

Table 4. Fuel Economy and Consumption for Various Standard Cycles (charge balanced)

	mpg	Km/L	L/100 km
UDDS	29.1	12.3	8.1
HWFET	27.8	11.8	8.5
NEDC	28.1	11.9	8.4
LA92	23.3	9.9	10.1
US06	19.5	8.3	12.1

In Figure 10, it can be seen that the repartition of used modes varies greatly as a function of drive cycles. Mode 1 is highly used in urban driving (UDDS, LA92, and NEDC). When the cycle is more aggressive, mode 2 is also used (LA92, US06). Highway cycles (NEDC, US06, and the Highway Fuel Economy Test [HWFET]) favor the use of fixed gears.

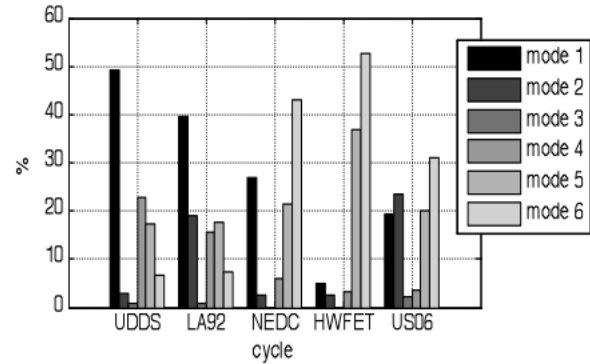


Figure 10. Share of Total Wheel Energy Spent in Each Mode for Various Cycles (while the engine is ON, and the drive torque demand is positive)

Conclusion

A practical implementation of instantaneous optimization for a multimode hybrid vehicle has been developed. It combines some classic hybrid-control rule-based functions (i.e., engine ON/OFF and battery SOC control) with an instantaneous optimization module that selects the mode with the greater fuel efficiency potential, as well as the most efficient operating point when in either EVT mode. It was demonstrated that the control performs well in various conditions, from the UDDS to the aggressive US06 cycles, with acceptable numbers of engine starts and mode changes. Further work will include the development of a different type of instantaneous optimization that will also encompass the battery power demand.

Publications/Presentations

D. Karbowski, J. Kwon, N. Kim, and A. Rousseau, "Instantaneous Optimized Controller for a Multimode Hybrid Electric Vehicle," SAE 2010 World Congress.

I. Development of Models for Advanced Engines and Emission Control Components

Principal Investigator: C. Stuart Daw

Oak Ridge National Laboratory (ORNL)

National Transportation Research Center

2360 Cherahala Boulevard

Knoxville, TN 37932

Voice: 865-946-1341; Fax: 865-946-1354; E-mail: dawcs@ornl.gov

DOE Technology Development Manager: Lee Slezak

Voice: 202-586-2335; E-mail: lee.slezak@ee.doe.gov

ORNL Program Manager: David E. Smith

Voice: 865-946-1324; Fax: 865-946-1262; E-mail: smithde@ornl.gov

Objectives

Develop component models that accurately reflect the drive performance, cost, fuel savings, and environmental benefits of advanced combustion engines and aftertreatment components as they could potentially be used in leading-edge hybrid electric and plug-in hybrid electric vehicles (HEVs and PHEVs).

Apply the above component models to help the Department of Energy (DOE) identify the highest HEV and PHEV research and development (R&D) priorities for reducing U.S. dependence on imported fuels as well as regulating pollutant emissions.

Approach

Develop and validate low-order, physically consistent computational models for emissions control devices including three-way catalysts (TWC), diesel oxidation catalysts (DOC), lean NO_x traps (LNT), diesel particulate filters (DPF), and selective catalytic reduction reactors (SCR) that accurately simulate HEV and PHEV performance under realistic steady-state and transient vehicle operation.

Develop and validate low-order, physically consistent computational models capable of simulating the power out and exhaust characteristics of advanced diesel and spark-ignition engines operating in both conventional and high-efficiency clean combustion (HECC) modes.

Develop and validate appropriate strategies for combined simulation of engine, aftertreatment, and exhaust heat recovery components in order to accurately account for and compare their integrated system performance in conventional, HEV, and PHEV powertrains.

Translate the above models and strategies into a form compatible with direct utilization in available vehicle systems simulation software.

Leverage the above activities as much as possible through inclusion of experimental engine and aftertreatment data and models generated by other DOE activities.

Accomplishments

Added and validated a TWC model to the Powertrain Systems Analysis Toolkit (PSAT), which can account for catalyst light-off and extinction in stoichiometric hybrid vehicles.

Added and validated a catalyzed DPF lean exhaust aftertreatment model to PSAT that is able to account for particulate matter (PM) filtration and filter regeneration in lean hybrid vehicles.

Constructed a new diesel oxidation catalyst model for PSAT to account for lean-exhaust oxidation in lean hybrid vehicles.

Constructed a new coolant heat storage system (CHSS) model for PSAT to simulate exhaust heat recovery in both stoichiometric and lean hybrid vehicles.

Constructed a combination of DOC plus catalyzed DPF lean exhaust after-treatment models for PSAT to simulate the fuel economy and emissions reduction in lean hybrid vehicles.

Demonstrated the impact of TWC on emission reduction in stoichiometric engine-based HEVs and PHEVs using PSAT.

Demonstrated the impact of DOC, catalyzed DPF, and LNT on fuel penalty and emissions reduction in lean engine-based HEVs and PHEVs using PSAT.

Tested the effect of CHSS, together with TWC or LNT, on fuel consumption and emission reduction in stoichiometric and lean engine based HEVs and PHEVs using PSAT.

Tested preliminary the engine maps for the uDev 1.9-L research diesel engine that is capable of HECC combustion and is being used as a common reference engine by the national labs and several universities.

Estimated preliminary full-range HECC engine maps for a Mercedes 1.7-L diesel engine that is expected to be capable of HECC over all engine operation conditions in an effort of understanding the ultimate potential of HECC employed in HEVs and PHEVs.

Demonstrated the usefulness of PSAT for making leading-edge integrated engine-aftertreatment concepts evaluations to the Crosscut Lean Exhaust Emissions reduction Simulation (CLEERS) Focus Groups and the DOE Diesel Crosscut Team.

Documented our methodology used for simulating engine cold and warm-start exhaust transients in an article to be published in the International Journal of Engine Research.

Future Directions

Continue refinement and testing of the PSAT DOC plus catalyzed DPF combination model and use it to assess the impact of various operating and control strategies on HEV and PHEV fuel efficiency and emissions performance.

Demonstrate Urea-SCR NO_x control in PSAT for diesel powered HEVs and PHEVs.

Test the effect of the combination of LNT plus Urea-SCR on NO_x control in PSAT for diesel powered HEVs and PHEVs.

Test the effect of the combination of LNT, DOC, and catalyzed DPF on PM control in PSAT for diesel powered HEVs and PHEVs.

Continue refinement and testing of a refined TWC model that includes NMOG oxidation.

Begin development of a HC trap model that can simulate HC storage at cold start and release at the following warm condition.

Demonstrate HEV simulations with lean direct-injected gasoline combustion.

Continue comparisons of diesel and gasoline HEV and PHEV fuel efficiency and emissions under the innovative combinations of emissions control devices.

Close coordination with Combustion MOU, ACEC, DCC Team, and CLEERS to ensure access to the latest engine/emissions technology information and industry needs

Introduction

Accurate predictions of the fuel efficiency and environmental impact of advanced vehicle propulsion and emissions control technologies are vital for making informed decisions about the optimal use of R&D resources and DOE programmatic priorities. One of the key modeling tools available for making such simulations is PSAT, maintained by the Argonne National Laboratory (ANL). A distinctive feature of PSAT is its ability to simulate the transient behavior of individual drivetrain components as well as their combined performance effects under realistic driving conditions. However, the accuracy of PSAT simulations ultimately depends on the accuracy of the individual component sub-models or maps. In some cases of leading-edge technology, such as with engines utilizing HECC and lean exhaust particulate and NO_x controls, the availability of appropriate component models or the data to construct them is very limited.

ORNL is a collaborator with ANL on the Vehicle Systems Analysis Technical Team (VSATT) and is specifically tasked with providing data and models that augment PSAT's capabilities. Specifically, ORNL's role has focused on the experimental measurement of performance data from advanced diesel engines and emissions controls components, as well as the incorporation of that data in the form of maps or low-order transient models that can be used in PSAT or other vehicle systems simulation software. In fiscal year (FY) 2009, the ORNL team concentrated its efforts in the following areas:

- Added and validated a TWC model to PSAT that accounts for catalyst light-off and extinction.
- Added and validated a catalyzed DPF model to PSAT that can account for PM filtration and filter regeneration.
- Constructed a new diesel oxidation catalyst model for PSAT to account for lean-exhaust oxidation.

- Constructed a new coolant heat storage system (CHSS) for PSAT to simulate waste heat recovery.
- Demonstrated a combination of DOC plus catalyzed DPF models in PSAT to simulate the fuel economy and emissions reduction.
- Demonstrated the impact of TWC on emission reduction in stoichiometric engine-based HEVs and PHEVs using PSAT.
- Demonstrated the impact of DOC, catalyzed DPF, and LNT on emission reduction in lean combustion engine-based HEVs and PHEVs using PSAT.
- Tested preliminary engine maps for the uDev 1.9-L research diesel engine that is capable of HECC combustion.
- Estimated preliminarily full HECC engine maps for a Mercedes 1.7-L diesel engine that is extended to be capable of HECC over the entire engine operation range.

Approach

Most current HEV and PHEV engines utilize stoichiometric engines, which are the predominant technology in most passenger cars in the United States today. In these engines, the fuel and air are balanced so that there is no excess oxygen present in the exhaust. With stoichiometric engines the emissions can be very effectively controlled with a three-way catalyst aftertreatment technology. The greatest needs for improving simulations of hybrid vehicles utilizing stoichiometric engines, involve the development of engine maps and models that accurately predict emissions and exhaust temperature as functions of speed and load under the highly transient conditions in normal drive cycles. Also, improved models are needed to capture the effects of start/stop transients in hybrid vehicles on the functioning of three-way catalysts. This is because the latter have been developed for more continuous engine operation than what occurs in hybrids.

Advanced combustion engines offer the potential for significantly increasing the fuel efficiency of hybrid

vehicles. These engines rely on lean combustion conditions (i.e., conditions where air is present in significant excess) and novel combustion states (e.g., HECC) where there is little or no flame present. While beneficial in reducing emissions, such lean combustion also involves larger and more drastic transient shifts in engine operation as driving demands change. Even though emissions are significantly reduced, they are still present in sufficient amounts to require exhaust aftertreatment subsystems for removing NO_x and PM.

Both NO_x and PM removal from lean exhaust involve complex transient and hysteretic interactions with the engine. The demands on the engine operation are further heightened by the need to periodically denitrate and desulfate LNTs and oxidize the carbonaceous particulate matter in DPFs. Simulation of such complicated behavior makes it necessary to build more sophisticated component models that exploit the known physics and chemistry of these devices as well as the best available experimental data.

Considering the above, the ORNL modeling team is building stoichiometric and lean aftertreatment component models for vehicle systems simulations that utilize proven approaches for simulating transient chemical reactors. The basic elements of these models include:

- Detailed time-resolved information on the flows, species, and temperatures entering the device.
- Differential, transient mass balances of key reactant species.
- Localized surface and gas-phase reaction rates.
- Differential, transient energy balances and temperatures within the device.
- Time resolved flow, species, and temperature for the gas stream exiting the device.

As much as possible, the descriptions of the internal reaction and transport processes are simplified to account for the dominant effects and physical limits while maintaining execution speeds acceptable for typical PSAT users. For example,

there are no cross-flow (i.e., radial) spatial gradients accounted for in the devices and the kinetics are defined in global form instead of elementary single reaction steps. This ‘in-between’ level of detail still allows for faithful simulation of the coupling of the after-treatment devices to both upstream and downstream components (arranged in any desired configuration). With the above information, it is also possible to determine both instantaneous and cumulative systems performance for any desired period.

Due to the greater complexity of engines, it is not practical to develop models with the same level of dynamic detail as in the aftertreatment component models. Instead, the usual approach for engine modeling relies on tabulated ‘maps’ developed from steady-state or pseudo-steady-state experimental engine-dynamometer data. Recently, it has been possible to develop maps that extend over both conventional and HECC operating ranges. Another key feature remaining to be added is an engine control sub-model that determines how the engine should operate (e.g., make transient shifts in combustion regime) in order to accommodate the needs of aftertreatment devices downstream. Typically, this also involves development of sensor models that indicate the state of the aftertreatment devices.

In future work, it is anticipated that experimental engine data can be supplemented with engine cycle simulations using large and complex engine simulation codes such as GT Power. This can account for many different effects and operating states that may be difficult to measure experimentally. It is expected that the results from these codes can be captured in more sophisticated formats (e.g., neural networks) than is possible with simple tabulated maps.

Results

Engine Mapping

We have improved the previously developed engine maps of the Saab BioPower flex-fuel vehicle using both gasoline and E85 fuels. The new maps were validated by using the highly simplified dynamic transform previously developed to relate the steady-state emissions values from the maps to transient engine exhaust properties and fuel economy. A detailed description of this transform and how we implement it for vehicle systems simulations has been

documented in an article accepted for publication in the International Journal of Engine Research [1]. As a test of the accuracy of this method for engine transient mapping, we predicted both gasoline and E85 fuel consumption for the Saab vehicle operating under an Urban Dynamometer Driving Schedule (UDDS) initiated by a cold start. The predicted fuel economy of 22.3 mpg for gasoline and 16.8 mpg for E85 are in good agreement with the experimentally measured values of 21.9 mpg and 16.2 mpg, respectively. Additional details for the predicted versus experimental comparison are provided in the article.

We also applied our simplified dynamic engine mapping transform to a 1.9-L research diesel engine that is capable of HECC combustion and is being extensively studied as a reference engine by the several national labs and universities. In an initial set of simulations, we assumed a conventional Honda Civic vehicle powered by this engine. Because this engine is currently able to achieve HECC only over a very narrow range of speed and load, we were only able to operate the engine intermittently in HECC. This significantly limited the benefits. For example, for hot-start UDDS operating conditions, the cumulative engine out NO_x emissions were 0.216 g/mi, and thus would still require lean NO_x aftertreatment to meet regulations. Subsequent HEV and PHEV simulations again demonstrated that the expected gains in fuel economy and emissions reduction from this intermittent form of HECC are rather limited. Clearly it will be important to expand the range of HECC for future HEV and PHEV applications.

To estimate the maximum potential value of expanded HECC, we created an idealized full-range HECC map for a 1.7-L Mercedes diesel engine. We did this by extrapolating the engine-out emissions ratios and exhaust temperature differences between HECC and conventional operation at low loads to the entire load range. Compared to the conventional Mercedes diesel engine performance, the full-range HECC Mercedes engine is estimated to reduce soot and NO_x emissions by up to 90%. On the other hand, CO and HC emissions from the full-range HECC map are considerably higher than the conventional

engine map. Thus the nature of the required emissions controls would need to be considerably altered for a fully capable HECC engine.

To improve systems studies accounting diesel engine particulate controls on HEVs and PHEVs, we extended the previous Mercedes 1.7 liter engine map to include additional operating states needed for catalyzed DPF regeneration. The map extension is based on data from engine-dynamometer-based catalyzed DPF experiments at ORNL [2]. The extended map specifically adds information about the transient engine exhaust composition and temperature for catalyzed DPF regeneration. This regeneration adjustment makes it possible to assess trade-offs between fuel penalty and emission control.

Aftertreatment Component Modeling

In collaboration with an OEM partner, we continued improving and validating our TWC model against transient OEM TWC measurements during chassis dynamometer studies of a new conventional gasoline vehicle operated under cold-start UDDS conditions. For validation purposes, we used TWC inlet species, temperature, and flow measurements from the OEM as inputs for our TWC model and predicted the expected TWC exit conditions. We then compared those predictions with the OEM exit measurements. For nominally stoichiometric fueling, we predicted net emissions of 0.837 g CO/mi, 0.149 g hydrocarbon HC/mi, and 0.157 g NO_x /mi compared to experimental values of 0.833 g CO/mi, 0.139 g HC/mi, and 0.157 g NO_x /mi.

Similar good agreements were obtained between predicted and measured TWC performance for the Saab Bio-Power flex-fuel vehicle. In this case, the simulations were implemented by assuming a PSAT library conventional Honda Civic power configuration equipped with TWC aftertreatment and Saab gasoline engine map.

Our catalyzed DPF model utilizes the basic framework of the previously developed non-catalyzed DPF model. Typically, most diesel engine particulate control systems use catalyzed DPFs, so this extension of the DPF capability is important for making realistic estimates of diesel hybrid vehicles. We compared the predicted results from the catalyzed DPF model with experimental diesel engine data reported in an open literature [3] over a range of loads. Predicted

particulate loadings under steady speed and load conditions have been typically less than 1% different from reported values.

Because diesel oxidation catalysts can have major impacts on DPF performance, we also constructed a simplified DOC component model for diesel hybrid studies. The simplified model accounts for three global reactions associated with lean exhaust, including (1) CO oxidation; (2) NO oxidation; and (3) HC oxidation. Comparisons between the model predictions and corresponding experimental data reported in an open literature [4] generally gave agreement within a few percent for all three reactions over a temperature range of 150 to 400 °C. To verify the correct functioning of our DOC model in PSAT, we simulated a conventional Honda Civic powered by 1.7-L Mercedes diesel engine over a UDDS cycle. The net CO and HC reduction achieved by the DOC during a cold start UDDS cycle is 80% and 72%, respectively. For hot start conditions both CO and HC are predicted to be reduced by more than 90%.

Component Model for Thermal Storage

We also developed a coolant heat storage system (CHSS) model to simulate waste heat recovery for stoichiometric and lean hybrid vehicles. The CHSS is able to store waste heat in a coolant tank and use the stored heat later to preheat the engine during cold start. In CHSS simulations, the CHSS is assumed to behave as an insulated tank connected with engine coolant system, which consists of the cylinder block, cabin heater, and radiator subsystems. Thus, the operating modes of CHSS will affect the temperature performance of coolant in cylinder block, cabin heater, and radiator. The major CHSS operating modes include engine preheat, engine warm-up, and energy recovery. In the engine preheat mode, stored waste heat goes directly to the cylinder block to raise engine temperature. During engine warm-up, waste heat flow to the storage tank is inhibited by closing the storage tank inlet valve and the engine thermostat valve. Energy recovery mode begins after engine warm-up is completed and the thermostat opens.

System Integration in Hybrid Vehicle Simulations

To quantify the potential benefits of utilizing lean engines (e.g., diesels or direct-injected gasoline engines) and coolant thermal storage in hybrid vehicles, we ran numerous simulations comparing various configurations of stoichiometric and lean PHEVs equipped with appropriate aftertreatment components. Figure 1 illustrates the simulated impact of CHSS on the fuel consumption and engine-out emissions from a Prius-type diesel-powered PHEV without aftertreatment. For visibility, the plot shows the first 300 s of a cold start UDDS drive cycle. The preheating engine using CHSS can boost diesel fuel economy by 2.8% while reducing both engine-out CO and HC emissions reduction by more than 14%. However, a slight increase of NO_x emissions occurs. Compared to the diesel PHEV, the impact of CHSS on the fuel mileage of the gasoline PHEV is 3.9%, and is better by a 2.8% for the diesel PHEV. The impact of CHSS on the fuel economy and emissions control in PHEVs with TWC or LNT was also investigated at a single cold start UDDS cycle. The results demonstrate that the fuel economy benefit achieved from the CHSS in a Prius-type diesel-powered PHEV with LNT could offset the fuel penalty caused by LNT regeneration in the single cold start UDDS cycle.

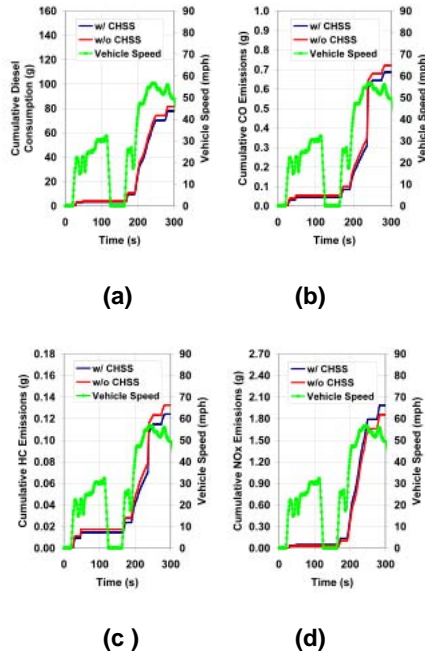
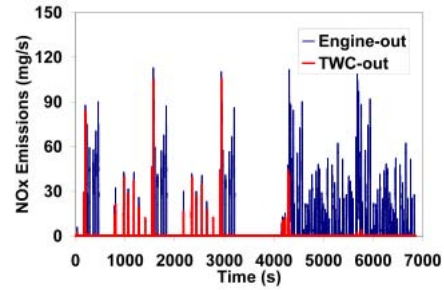
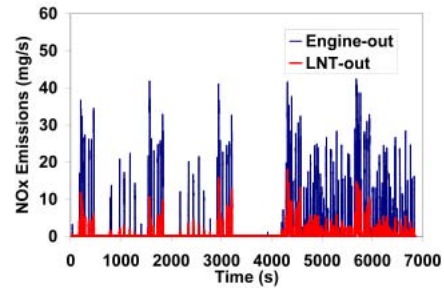


Figure 1. The first 300 seconds of the simulated impact of CHSS on fuel consumption and engine-out emissions for a Prius-type diesel-powered PHEV.

Figure 2 compares NO_x emissions from a Prius-type PHEV powered by a 1.5-L Prius engine (gasoline fueled) with a 1.5-L diesel PHEV. Both vehicles are equipped with appropriate aftertreatment (TWC for the gasoline car) and (only LNT for the diesel car) and are operated over five consecutive UDDS cycles beginning with a cold start. The cumulative tailpipe NO_x emissions are 0.11 g/mi for both PHEVs. The fuel economies are 113.8 mpg for gasoline and 132.4 mpg for diesel. Based on fuel energy content, the diesel powered PHEV still achieves approximately 3% higher energy efficiency than the gasoline-power PHEV, as shown in Figure 3.



(a) gasoline-powered PHEV with TWC



(b) diesel-powered PHEV with LNT

Figure 2. Simulation of engine-out and tailpipe NO_x emissions from gasoline-powered and diesel-powered PHEVs over five consecutive UDDS cycles beginning with a cold start.

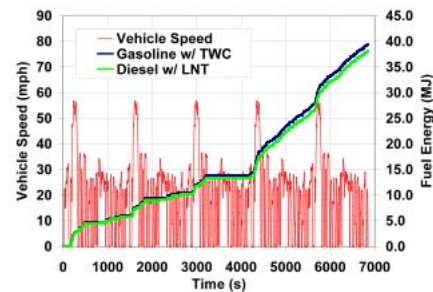
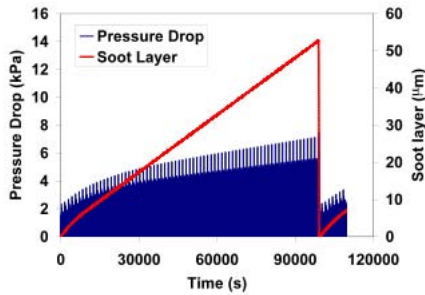


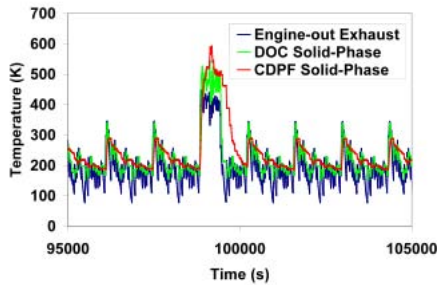
Figure 3. Simulation of fuel energy consumption for gasoline-powered and diesel-powered PHEVs over five consecutive UDDS cycles beginning with a cold start.

We further investigated the impact of combining the DOC and catalyzed DPF devices on fuel efficiency and emissions in a Prius-type HEV powered by a 1.5-L diesel engine. The aftertreatment train included a 0.7-L DOC and a 2.2-L catalyzed DPF. We based DPF regeneration control on pressure drop, triggering 10-minute regenerations when pressure drop exceeded a threshold of 7.5 kPa. For a simulation of 80 UDDS cycles, one DPF regeneration event occurred, which lasted 10 minutes. The effect of this regeneration, combined with the DPF pressure drop, resulted in a

2.1% fuel consumption penalty. Figure 4(a) shows the operating profile of DPF filtration and regeneration, as well as pressure drop. The DPF filtration efficiency is more than 98%. Figure 4(b) illustrates the predicted effect of DPF regeneration on temperature at different locations, and shows that DOC has a considerable impact on the temperature of the flow entering the DPF.



(a) 80 consecutive UDDS drive cycles



(b) 10 min catalyzed DPF regeneration

Figure 4. Simulation of the operating behavior of a combined DOC+catalyzed DPF installed in a diesel-powered PHEV.

Continuing from the HECC studies mentioned above, we used a hypothesized full-range HECC engine map to estimate the ultimate impact HECC operation on diesel HEVs and PHEVs equipped with DOC and catalyzed DPF devices. Our preliminary simulation results indicated that full implementation of HECC might be sufficient to achieve continuous passive regeneration of the CDPF without a need for active regeneration (Figure 5). The net fuel penalty for HECC particulate control was 0.33% compared to 2.1% for conventional combustion. We also obtained a similar estimate of the maximum potential impact of HECC on lean NO_x control and fuel penalty related to NO_x control. As shown in Figure 6, full-range HECC produced a dramatic reduction in

engine out NO_x, cutting the number of LNT regeneration events from eight to one over the entire UDDS cycle. The corresponding fuel penalty for NO_x control dropped from about 2.0% for conventional to about 0.2% for HECC, respectively.

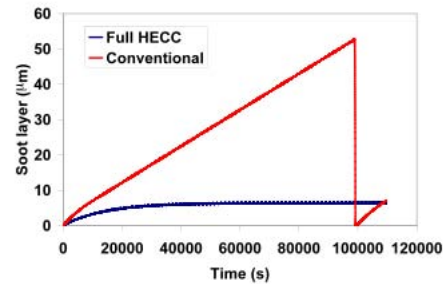


Figure 5. Simulation of the potential impact of full-range HECC on soot accumulation in a DOC+catalyzed DPF installed in a diesel PHEV over 80 consecutive UDDS cycles at a hot start.

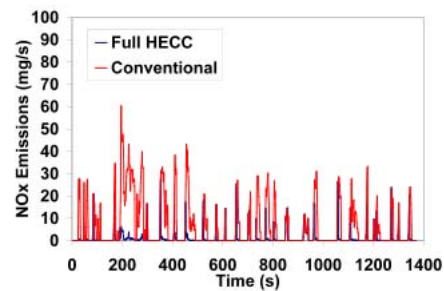


Figure 6. Simulation of the impact of full-range HECC on LNT NO_x emissions from a diesel PHEV over a single UDDS drive cycle with a hot start.

Clearly, full-range HECC engines could have a major impact on hybrid vehicle performance, but our first attempt at developing an extrapolated HECC map for diesel hybrids is rather crude and needs considerable refinement. However, we believe this preliminary exercise has been useful in helping to define the issues that need to be resolved in developing improved HECC engine maps for hybrid vehicle studies.

Conclusions

- A proposed methodology for modifying steady-state engine maps to account for cold- and warm-start transients has been successfully demonstrated for multiple light-duty engines, including both gasoline and diesel engines similar to those expected to be used in advanced hybrid vehicles.

- An idealized full-range HECC exhaust map for a 1.7-L Mercedes diesel engine was developed and utilized to estimate the potential impact of full HECC operation on hybrid vehicle fuel economy and emissions.
- A preliminary three-way catalyst component model was improved and validated with experimental data from multiple sources.
- A catalyzed DPF component aftertreatment model was developed from the non-catalyzed DPF model developed earlier, validated with literature data, and implemented in PSAT simulations of hybrid vehicles.
- A DOC component aftertreatment model was developed and validated to a limited extent to account for CO oxidation, NO oxidation, and HC oxidation.
- A coolant thermal storage component model (for waste heat recovery and more rapid aftertreatment catalyst light-off) was developed and implemented in PHEV systems simulations.
- PHEV simulations comparing diesel and gasoline-power vehicles equipped with appropriate NO_x control aftertreatments indicate that diesel vehicles will have modest efficiency advantages. However, these are reduced from what is ultimately possible due to emissions control fuel penalties.

Diesel Particulate Filter.” SAE 2003-01-0841.

4. A.P. Triana, “Development of Models to Study the Emissions, Flow, and Kinetic Characteristics from Diesel Oxidation Catalyst and Particulate Filters.” Dissertation, Michigan Technological University, 2005.

FY 2009 Publications/Presentations

1. Z. Gao, J.C. Conklin, C. S. Daw, and V.K. Chakravarthy, “A Methodology for Simulating Transient Engine Exhaust Temperature and Emissions in Vehicle Simulations”, Accepted by the International Journal of Engine Research.
2. Z. Gao, V.K. Chakravarthy, C.S. Daw and J.C. Conklin, “Lean NO_x Trap Modeling for Vehicle Systems Simulations”, Submitted to SAE 2010 World Congress.
3. Z. Gao, V.K. Chakravarthy, C.S. Daw and J.C. Conklin, “Hybrid vehicle simulations with LNT NO_x control”, 12th DOE Crosscut CLEERS Workshop, April 28-30, 2009 (<http://www.cleers.org>).
4. C.S. Daw, Z. Gao, V.K. Chakravarthy, J.C. Conklin, K.D. Edwards, R.M. Wagner, B.H. West “PHEV Engine and Aftertreatment Model Development”, DOE OVT Peer Review, May 20, 2009.

References

1. Z. Gao, J.C. Conklin, C. S. Daw, and V.K. Chakravarthy, “A Methodology for Simulating Transient Engine Exhaust Temperature and Emissions in Vehicle Simulations”, Accepted by the International Journal of Engine Research.
2. J. Parks, S. Huff, M. Kass and J. Storey, “Characterization of In-Cylinder Techniques for Thermal Management of Diesel Aftertreatment.” SAE 2007-01-3997.
3. C.T. Huynh, J.H. Johnson, S.L. Yang, S.T. Bagley and J.R. Warner, “A One-Dimensional Computational Model for Studying the Filtration and Regeneration Characteristic of a Catalyzed Wall-Flow

J. Plug-in Hybrid Electric Vehicle (PHEV) Value Proposition Study

Principal Investigator: Robert DeVault
Oak Ridge National Laboratory (ORNL)
Energy Sciences and Technology Division
Voice: 865-574-2020; E-mail: devaultrc@ornl.gov

DOE Technology Development Manager: Lee Slezak
Voice: 202-586-2335; E-mail: lee.slezak@ee.doe.gov

ORNL Program Manager: David E. Smith
Voice: 865-946-1324; Fax: 865-946-1262; E-mail: smithde@ornl.gov

Objective

Oak Ridge National Laboratory (ORNL), with the support of Sentech, Inc., General Electric (GE) Global Research, Electric Power Research Institute (EPRI), and the Center for Automotive Research at Ohio State University (OSU), will conduct a study to identify and evaluate value-added propositions needed to overcome the initial PHEV purchase cost barrier, resulting in a sustainable market that can thrive without the aid of state or Federal incentives or subsidies.

Approach

PHEV Value Proposition Workshop

Industry stakeholders brainstormed potential value propositions for PHEVs and projected several economic and technological characteristics of 2030.

Proposition Prioritization

Following the workshop, the project team prioritized the collected value propositions to determine which should be studied in subsequent phases.

Case Study Development

Details of the first case study, based in southern California, were selected (e.g., fuel prices, generation mix, vehicle characteristics). A second case study, located in the North American Electric Reliability Corporation (NERC) region formerly known as ECAR, is currently underway in Phase 2.

Model Development

A collection of models was agreed upon that was capable of analyzing all of the selected value propositions.

Exercise Models

Pre-defined parameters are entered into selected models for both case studies. Outputs are then either fed into additional models or are incorporated into final report.

Document Results in the Report

Conclusions from the initial case study were published in a PHEV Value Proposition Study Interim Report. Once Phase 2 is completed, a comprehensive report will be published.

Accomplishments

The initial case study, for southern California, concludes that the combined operating cost savings and societal benefits attainable with PHEVs will support a commercially viable and sustainable PHEV market by 2030.

Specifically, PHEVs owners in the studied region benefit from:

Fuel costs (both liquid and electricity) reduced by 55% and 33% compared to conventional vehicles and HEVs, respectively.

16% less total ownership cost than conventional vehicles; 4% less than HEVs.

Unique attributes (e.g., emergency backup power, mobile power, battery recycling credit).

The PHEV fleet of 2030 analyzed in this case study would enhance energy security and reduce environmental impacts by:

Decreasing gasoline consumption by 80% and 70% compared to conventional vehicles and HEVs, respectively.

Emitting 25% less carbon dioxide and total greenhouse gas emissions than conventional vehicles.

Consuming 40% and 10% less total energy than conventional vehicles and HEVs, respectively.

Potentially increasing utilization of domestic renewable resources.

Status of Milestones

The milestones as identified below have been met.

Milestones

#	Milestone Description	Due
1	Published PHEV Value Proposition Study Interim Report	January 2009
3	Kicked off Phase 2 of PHEV Value Proposition Study Monthly Reporting	July 2009

Future Directions

Finalize technical and market assumptions for second regional case study; use as inputs in collection of models (e.g., PSAT, GREET) to determine economic and environmental impacts of PHEVs in the region.

Analyze sensitivity of specific model inputs (e.g., fuel price, vehicle AER) for both case studies.

Compile results, conclusions, and recommendations into final report; publish in early 2010.

Introduction

PHEVs have gained interest over the past decade due to their high fuel economy, convenient low-cost recharging capabilities, and reduced use of petroleum. In fact, the Obama-Biden Agenda for Energy and the Environment has recently called for one million PHEVs to be on the road by 2015. Yet despite these potential benefits, the comparatively

high initial cost of PHEVs (primarily due to expensive batteries) presents a major market barrier to their widespread commercialization and adoption by consumers. Therefore, Sentech, Inc., ORNL, GE Global Research, EPRI, and OSU’s Center for Automotive Research conducted the initial phase of an in-depth study of the benefits, barriers, opportunities, and challenges of grid-connected PHEVs in order to identify potential value

propositions that will lead to a commercially viable market.

A Guidance & Evaluation Committee composed of representatives from various stakeholder organizations will contribute expertise throughout the study. Committee members include executives and entrepreneurs from the automotive, energy storage, utility, regulatory, and finance arenas. In addition, participation by Argonne National Laboratory (ANL), Pacific Northwest National Laboratory (PNNL), and National Renewable Energy Laboratory (NREL) has occurred.

Approach

PHEV Workshop

In December 2007, the project team conducted a workshop in Washington, D.C., where experts from the full range of industry stakeholders congregated to brainstorm potential business models that would promote a sustainable PHEV market with supporting infrastructure. Areas of interest included the operation (charge and discharge) of PHEVs, capabilities or functions of the PHEVs, different methods for financing and leasing PHEVs or their batteries, grid infrastructure and communication needs, and types of non-monetary incentives that would be valued by PHEV owners (i.e., access to high-occupancy vehicle [HOV] lanes). The outcome of this workshop was an extensive list of potential value propositions, assumptions, and a consensus vision of 2030 that would be applied to case studies. Key assumptions consensus vision for 2030 included:

- A 10% PHEV market penetration rate in 2030.
- A carbon “tax” associated with carbon emissions at \$30 per ton of CO₂ in current dollars.
- Most first generation PHEV chargers will only be capable of charging at 110V. Over time, dual voltage chargers will be introduced to accommodate quick charging, vehicle-to-grid (V2G), and vehicle-to-building (V2B) applications.
- Battery recycling capabilities will be in place due to regulations.

- Fuel economy of all vehicles will improve due to a 30% weight reduction by 2030.
- Three quarters of available fuel in 2030 will be E10, and one quarter will be E85. This roughly equates to an E30 average blend for use in this study.
- PHEVs in 2030 will have approximately 30 miles all-electric range (AER) equivalent (i.e. PHEV-30).
- PHEVs will be operated in “blended” mode (i.e., use most efficient blend of battery and internal combustion engine).

Initial Case Study Selection

Based on takeaways from the workshop, the project team chose southern California as the initial case study location. Reasons for this location selection include the state’s carbon policy, large number of early adopters of gasoline hybrids, high sales of hybrid vehicles, aggressive renewable portfolio standard (RPS) targets, and an emission-constrained dispatch of power plants in the Los Angeles air basin. These economic, environmental, social, and regulatory conditions are conducive to evaluating the potential advantages of PHEVs.

Assuming markets support steady growth of PHEV sales over the next two decades and additional interest of early adopters, PHEVs in this area are postulated to comprise about one million of the area’s private vehicles in 2030. They may be classified by a blended mileage description (e.g., 100 mpg, 150 mpg), an ownership cost (sum of costs per mile for fuel and electricity), or combination of the two that demonstrates a battery size equivalence of a PHEV-30.

The initial case study would investigate a PHEV “baseline” fleet of 2030 in order to focus on the primary goal of demonstrating lower operating costs for the driver. More advanced concepts, such as V2G and ancillary services that are secondary to basic operation and require preliminary modeling data, would be investigated in subsequent case studies. Based on this decision, the following seventeen value propositions were chosen for analysis in the initial case study:

- Fuel cost savings (with GPS-enabled fuel optimization dispatch)

- Tailgate/camping, limited household appliance backup (residential V2B)
- Opportunistic charging from any outlet
- Reduced vehicle maintenance costs
- Convenient charging locations (e.g., at airports, municipalities, etc.)
- Battery recycling credit
- Recognition of “social” responsibility
- Reduced petroleum imports
- Emissions reduction
- Responsive load – utility control of charger
- Increased use of renewable energy in generation mix
- Carbon “tax” equivalent
- Utility cost savings (capital or production) in \$/kWh for serving PHEVs
- Time dependent electricity pricing for PHEV owners
- Emergency back-up power for commercial facility (commercial V2B)
- Responsive load – V2B capability
- Reduced billing demand for commercial building (commercial V2B)

Analysis

This study’s overarching business model compares a PHEV-30 to both a hybrid electric vehicle (HEV) and conventional vehicle. Therefore, characteristics for each vehicle type were gathered to properly calculate desired outputs (e.g., fuel usage, emissions). Such properties include the base vehicle framework, breakdown of vehicle materials, the extent of power electronics and electric machinery (PE&EM) used, and the vehicle energy management strategy. For V2B applications, charge/discharge profiles of PHEVs arriving and parking at work have also been determined and used to help predict resulting building load and profiles. Finally, the project team also compiled a set of non-monetary value propositions in need of statistical consumer survey data.

Table 1 provides a summary breakdown of materials distribution and powertrain properties for a conventional vehicle, HEV, and PHEV-30 (all midsize sedans). The basis for cost calculations of individual vehicle components is listed in Table 2. Vehicles were anticipated to have a ten-year lifetime, and they were assumed to be driven on average 15,400 miles annually.

Table 1. Basic vehicle modeling parameters for mid-size sedan in 2030.

	Conventional	HEV	PHEV-30
Mass			
Glider Mass (kg) ¹	693	693	693
Engine/Transmission/ Final Drive/Wheels (kg)	441	374	374
PE&EM (kg)	-	44	44
Energy Storage (kg)	-	50	124
Fuel Subsystem (kg)	58	48	48
Total Vehicle Mass (kg)	1192	1209	1283
Total Vehicle Mass w/ 136 kg Cargo (approx. two passengers)	1328	1345	1419
Energy and Power			

¹ Glider mass = Vehicle– (Engine+Motor+Batteries+Transmission+Final Drive+Fuel Storage+Wheel) Based on 30% reduction in current glider mass as per DOE GPRA Study Results

Battery Energy (kWh)	-	-	14
Battery Power (kW) @ 95% state of charge	-	73	-
Engine Power (kW)	110	50	50
Motor Power (kW)	-	55	55

Table 2. Basis for vehicle cost calculations for mid-size sedan in 2030

	Conventional	HEV	PHEV-30
Manufacturer's Suggested Retail Price (MSRP)	\$21,390	-	-
Powertrain	Engine + Transmission + Motor/Inverter + Battery + Charging Plug		
Engine	\$14.5 x kW + \$531		
Transmission	\$12.5/kW		
Motor/Inverter	-	\$8/kW	
Battery	-	\$20/kW	\$200/kWh
Charging Plug	-	-	Parts/Labor
Glider	MSRP of conventional vehicle minus combined cost of engine and transmission		

Characteristics of the existing southern California utilities' power systems and the California Independent System Operator provided the initial data for the case study. The load forecasts, fuel price forecasts, and generation expansion plans for southern California were used to estimate the characteristics of the 2030 power system. However, the forecasted generation mix for 2030 was modified to incorporate a 30% RPS and any expected improvements to power generation technologies, such as increased efficiencies and reduced emissions. The Energy Information Agency (EIA) Annual Energy Outlook 2008 values, along with consensus from the workshop, were also used to simulate the effects of a carbon "tax," as well as fluctuating fuel and electricity prices. Southern California drive cycle data were also estimated to represent average work commutes and other trips.

A collection of modeling tools and techniques were carefully chosen to appropriately analyze inputs and calculate all desired outputs for the initial case study. Various models were borrowed from national laboratories, private industry, and government

agencies. In some cases, models have been modified to consider all relevant data. For instance, the project team used a modified version of ANL's Powertrain System Analysis Toolkit (PSAT) to properly simulate battery charge/discharge profiles and fuel usage in PHEVs. ANL's Greenhouse Gases, Regulated Emissions, and Energy Use in Transportation (GREET) model was also manipulated to calculate the potential carbon dioxide emissions for fleets of each vehicle type fleet using the average E30 blend. The Oak Ridge Competitive Electricity Dispatch (ORCED) model and OSU-CAR and GE in-house battery models were also utilized.

These analysis tools have been integrated into a macro business model (MBM) that weighs the costs and benefits associated with owning a PHEV over an HEV or conventional vehicle. The MBM is comprised of six primary components: *consumer financial cost and benefits, consumer preference data, societal benefits, utility benefits, commercial building owner benefits, and battery alternative design and ownership options.*

Technical Progress

An Interim Report documenting PHEV VPS Phase 1 activities was published in January 2009.

- Analysis conducted by ORNL, Sentech, OSU-CAR, GE, and EPRI.
- Results from the first regional case study set in southern California.
- Concluded a sustainable PHEV market can exist in 2030 (based on case study assumptions).

Phase 2 of the PHEV VPS kicked off in July '09.

- Includes second regional case study and sensitivity study on both regions

- Analysis is being conducted by ORNL, Sentech, OSU-CAR, and Taratec Corporation.

A PHEV Market Introduction Study to identify policies, incentives, and regulations that will help accelerate the sales of PHEVs over the next ten years is near completion.

- Analysis conducted by ORNL, Sentech, and DOE between Phase 1 and Phase 2 of the PHEV VPS.
- Analysis motivated in part by Phase 1 results that indicate viable PHEV market by 2030.
- Revisions currently being made to the final report.



Figure 1.

Conclusions

Benefits to the Consumer

To become commercially appealing, PHEVs must boast features that either increase consumer value or reduce the consumer cost. For example, operating cost savings attainable with a PHEV should match or outweigh the initial price premium over the competition. Results from the initial case study set in southern California demonstrate that the reduced operating costs of PHEVs accrued over a ten-year vehicle lifetime do indeed result in significant net cost savings over conventional vehicles and present a highly competitive alternative to HEVs.

Figure 3 displays the current purchase cost differences between each vehicle type, as well as the projected purchase cost in 2030. Both current and

2030 values are included to provide a frame of reference for anticipated technology advancements and economies of scale over the next two decades. As shown below, conventional vehicles are considered to have generally reached maturity. On the other hand, HEVs are expected to exhibit improvements in PE&EM, and PHEVs will likely see dramatic cost reductions in advanced batteries. With these savings, HEVs and PHEV-30s are expected to have price premiums of roughly \$1,200 and \$5,300 respectively, over conventional vehicles in 2030.

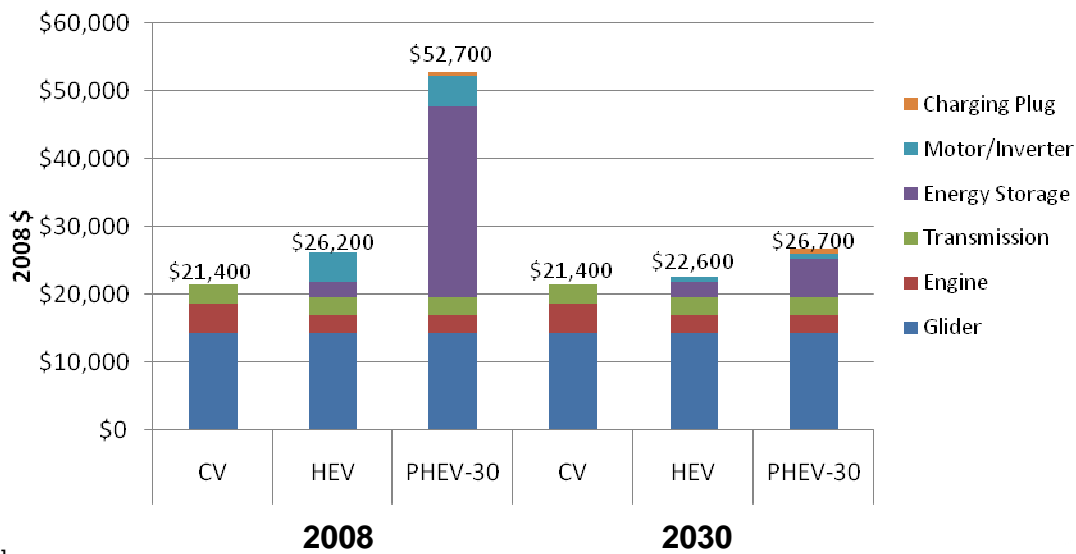
Operating costs to the owner are primarily comprised of fuel costs (from both liquid and electricity) among other factors. Case study results show that these combined fuel costs for a PHEV-30 are projected to be 6¢ per mile. This compares to projected conventional vehicle fuel cost of more than twice that, about 13.4¢ per mile; projected HEV

fuel cost is about 1.5 times that at about 9¢ per mile. Over the vehicle’s anticipated ten-year lifetime, this reduced cost per mile more than outweighs the anticipated vehicle purchase price premium over conventional vehicles. In fact, with all other factors constant, PHEVs are a better economic choice compared to conventional vehicles as long as E30 prices exceed \$2.22 per gallon. HEVs appear to offer marginally lower total ownership cost unless E30 prices exceed \$3.72 per gallon, in which case PHEVs become the most financially appealing option.

Case study results also indicate that PHEV-30s demonstrate slight reductions in scheduled maintenance costs relative to conventional vehicles and HEVs for several reasons. First, PHEV engines

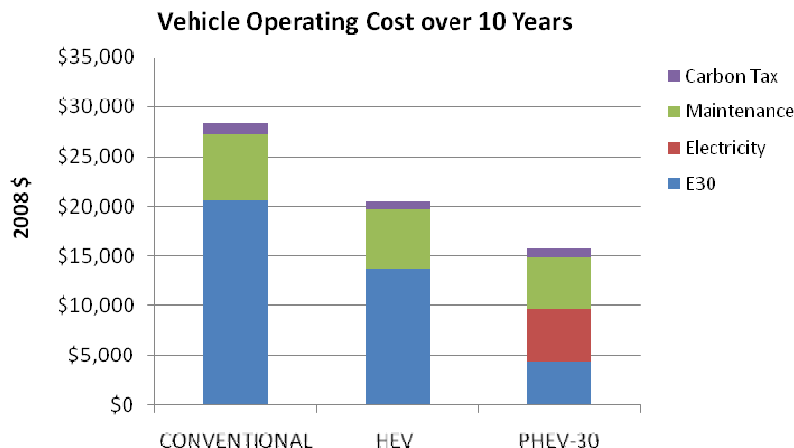
are operating for a lower percentage of the vehicle operating time. Thus, they may have longer intervals between oil changes and air filter replacements. Second, regenerative braking on HEVs and PHEVs reduces brake wear and the need for brake replacements. During the anticipated lifetime of the vehicle, PHEVs are estimated to save \$1,300 in scheduled maintenance costs. An anticipated recycling credit of approximately \$1,000 for an “end-of-life” lithium-ion battery pack also increases the PHEV’s competitive edge. Finally, the established carbon tax of \$30 per ton of carbon dioxide presents a slight savings to PHEV owners, since PHEV emissions are considerably lower than those of conventional vehicles. Figure 4 displays overall operating costs between the three vehicle types.

Vehicle Purchase Cost - Today vs. 2030



[1]
[2]

Figure 2. Overall vehicle purchase cost comparison for conventional vehicles, HEVs and PHEVs produced in both 2008 and 2030.



[3]

Figure 3. Overall vehicle operating cost comparison for conventional vehicles, HEVs and PHEVs in 2030 over the anticipated 10-year vehicle lifetime in southern California.

Benefits to Commercial Building Owners

Commercial building owners may also benefit from their employees’ plugging in at their workplace upon arrival in the morning. By charging the batteries when demands at the building are below peak, commercial building owners can use some of the power stored in the batteries to reduce their peak billing demand and thereby reduce their electric bill. By doing so, some of their electricity purchases could be shifted from afternoon peak prices to morning mid-peak prices, saving additional money. However, the total savings is dependent on the load shape of the facility and the utility’s rate structure. Vehicle owners will likely expect some form of compensation, either monetary rebates or non-monetary incentives (e.g., preferred parking spaces), for potential “wear and tear” on the battery. The building owner will also be expected to fully recharge the vehicle owners’ batteries to full charge at the close of most workdays. Only on days when the building electricity demand is at its greatest should vehicle owners not be expected to leave work with fully charged batteries. Overall, the net savings to the building owner will need to be sufficient to justify the capital and ongoing operations costs for the program.

As an example, for a large office building (greater than 1.5 MW peak demand) with up to fifty PHEVs available, the building owner(s) could purchase

extra power in the morning to recharge the batteries to full charge. In the afternoon, the building could then withdraw that power, squaring off each day’s peak. For example, if PHEVs began plugging in at 8 a.m., charged through the morning, and then released the same amount in the afternoon, then the building peak would drop to roughly 60 kW. Using current Southern California Edison and Los Angeles Department of Water and Power commercial rates, the savings from both reduced demand charge and lower cost energy purchases was \$1000 to \$2000 per month. By 2030, the amount will likely increase, but the amount of savings depends on the rate structure for the building.

Benefits to Society

In addition to monetary benefits, PHEVs are able to dramatically decrease dependence on foreign oil by substituting the majority of it with electricity. Case study results show that, on average, a single PHEV-30 will consume 80% less gasoline than conventional vehicles (~250 gallons annually) and 70% less gasoline than HEVs (~150 gallons annually). Assuming 60% of oil is imported over the next two decades, the southern California fleet of one million PHEVs in 2030 has the potential to reduce imported oil by approximately eight million barrels annually (if the PHEV fleet substituted for conventional vehicles) or by 4.5 million barrels annually (if the PHEV fleet substituted for HEVs).

PHEVs also demonstrate significant reductions in GHG emissions. Relative to conventional vehicles, PHEVs reduce both CO₂ emissions and overall GHGs by one quarter. CO₂ and GHG emissions were slightly higher in PHEVs than in HEVs. However, this is extremely dependent on the marginal generation mix and the ethanol blend that is used. In all cases evaluated, the PHEVs and the HEVs represent significant improvement in GHG emissions relative to conventional vehicles. PHEVs also consume significantly less total energy from a “well-to-wheel” perspective.

Benefits to Utilities

Analysis results show that the anticipated relatively slow penetration of PHEVs in the market in combination with smart charging that shifts demands to off-peak times leads to very little impact on overall peak electric demands while providing the utility with additional sales during off-peak times. The benefits to the utility include increased sales from idle capacity, thereby providing the potential to recover more of its fixed costs. If all PHEV owners choose to charge their vehicles during the period of peak demand (5 p.m. to 6 p.m. during the summer in southern California), then increased peak demands could have a negative effect on the grid. Such effects clearly show the benefit to the utility of providing incentives for customers to shift their charging times to nighttime.

FY 2009 Publications/Presentations

K. Genung, et al. Plug-In Hybrid Electric Vehicle Value Proposition Study: Interim Report: Phase 1 Scenario Evaluation, Oak Ridge National Laboratory/Sentech, Inc., January 2009. ORNL/TM-2008/076. http://apps.ornl.gov/~pts/prod/pubs/ldoc11390_phev_vps_phase_1_task_4__interim_report__2_.doc.

Stanton W. Hadley, Value Propositions, Presentation to the Austin Altcar Expo, October 17, 2008. http://apps.ornl.gov/~pts/prod/pubs/ldoc13443_austin_hadley_vps_v2.ppt.

K. Plug-in Hybrid Electric Vehicle (PHEV) Market Introduction Study

Principal Investigator: Robert DeVault
Oak Ridge National Laboratory (ORNL)
Energy Sciences and Technology Division
Voice: 865-574-2020; E-mail: devaultrc@ornl.gov

DOE Technology Development Manager: Lee Slezak
Voice: 202-586-2335; E-mail: lee.slezak@ee.doe.gov

ORNL Program Manager: David E. Smith
Voice: 865-946-1324; Fax: 865-946-1262; E-mail: smithde@ornl.gov

Objective

Oak Ridge National Laboratory (ORNL), Sentech, Inc., Pacific Northwest National Laboratory (PNNL)/University of Michigan Transportation Research Institute (UMTRI), and the U.S. Department of Energy (DOE) are conducting a Plug-in Hybrid Electric Vehicle (PHEV) Market Introduction Study to identify and assess the effect of potential policies, regulations, and temporary incentives as key enablers for a successful market debut.

Approach

The primary objective of the PHEV Market Introduction Study is to identify the most effective means for accelerating the commercialization of PHEVs in order to support national energy and economic goals. Ideally, these mechanisms would maximize PHEV sales while minimizing Federal expenditures. To develop a robust market acceleration program, individual incentives and policies must be examined in light of:

- Clarity and transparency of the market signals sent to the consumer.
- Expenditures and resources needed to support incentives and policies.
- Expected impacts on the market for PHEVs.
- Incentives that are compatible and/or supportive of each other.
- Complexity of institutional and regulatory coordination needed.
- Sources of funding.

Accomplishments

The timeframe over which market-stimulating incentives would be implemented—and the timeframe over which they would be phased out—are suggested. Possible sources of revenue to help fund these mechanisms are also presented. In addition, pinch points likely to emerge during market growth are identified and proposed solutions presented. Finally, modeling results from ORNL's plug-in hybrid electric (PHEV) Choice Model and UMTRI's Virtual Auto Motive Market Place (VAMMP) Model were used to quantify the expected effectiveness of the proposed policies, as well as to recommend a consensus strategy aimed at transitioning what begins as a niche industry into a thriving and sustainable market by 2030.

The project team would like to extend a special thank you to several industry stakeholders, including members of the study’s Guidance and Evaluation Committee² who participated in discussions on policies, incentives, and regulations that they expect to help accelerate the market for PHEVs in the short term.

Much appreciation is also due to DOE’s Jacob Ward for the extensive time spent exercising the ORNL PHEV Choice Model to meet the specifications and timeline of this project. In addition, expedited results from UMTRI’s VAMMP Model were achieved through its accelerated launch by John Sullivan.

Finally, results from the PHEV Market Introduction Study would not have been possible without DOE’s foresight to fund ORNL and PNNL/UMTRI to develop the PHEV Choice Model and VAMMP Model. Within DOE, funding is provided by the Vehicle Technologies Program and the Office of Electricity Delivery and Energy Reliability.

Milestones

#	Milestone Description	Due
1	PHEV Market Introduction Study Workshop	December 1-2, 2008
2	Published PHEV Market Introduction Study Interim Report	February 2010
3	Monthly Reporting	

² See list of Guidance and Evaluation Committee members at www.sentech.org/phev.

Introduction

The PHEV Market Introduction Study seeks to identify policy drivers that have the most potential for significantly boosting near-term sales of PHEVs with the least cost of implementation. This goal aligns with President Obama's recent call for one million plug-in hybrid cars to be on the road by 2015,³ which may be achievable by not only offering incentives for consumers to buy the vehicles, but by also persuading vehicle manufacturers to accelerate near-term production capacity plans to meet demand potentially created by these incentives.

The PHEV Market Introduction Study is a supplement to the PHEV Value Proposition Study,⁴ which concluded that PHEVs possess enough advantageous qualities to be competitive with conventional vehicles and hybrid electric vehicles (HEV) by 2030. This is due in large part to the significant operating cost reductions and improved convenience achieved by substituting less expensive electricity for the majority of gasoline use. In addition to reduced fuel costs, PHEVs demonstrate lower total lifecycle cost, reduced greenhouse gas (GHG) emissions, and many unique attributes (e.g., emergency backup power, mobile power, potential battery recycling credit, etc.).

Given the conclusion that a viable business case exists for PHEVs, focus has been directed toward developing a plan to successfully and efficiently accelerate the introduction of these vehicles into the market. Collaboration among ORNL, Sentech, Inc., UMTRI, and PNNL has led to the identification and assessment of how potential policies, regulations, and temporary incentives can be key enablers for a successful PHEV market debut. For each mechanism studied, the project team presents

- Concept(s) for implementation.
- Timeframe for implementation and phase out.

- Required revenue to initiate and sustain an incentive program.
- Alleviated market and technological pinch points.

Two consumer choice models were utilized in this study to help quantify the potential effectiveness of the investigated policies. Each model is designed to project PHEV market penetration using a unique approach (e.g., agent-based versus market-based models). In each model, PHEVs with all-electric ranges (AER) between 10 and 40 miles compete for market share against a variety of powertrains including conventional vehicles, diesels, and HEVs. Based on results from these models, a consensus strategy has been developed, aimed at transitioning what begins as a niche industry and grows into a thriving market by 2030.

Approach

PHEV stakeholders will be tasked with persuading consumers to modify driving behavior and possibly pay an initial price premium in exchange for much greater fuel efficiency and, therefore, long-term financial savings. Traditionally, policies, regulations, and temporary incentives have proven to be key enablers in helping to accelerate consumer adoption of alternative fuel vehicles (AFV). To best understand what strategies have been attempted or implemented for other AFVs (such as HEVs), a collection of past policies, incentives, and regulations (categorized as Federal, state/local, or private) was compiled in a PHEV Market Introduction Study Pre-Workshop Discussion Paper.⁵ Examples of potential market pinch points that PHEV industry stakeholders may face are also briefly described in this paper.

On December 1-2, 2008, a PHEV Market Introduction Study Workshop was held in Washington, D.C. The first day of the workshop focused on the identification of pinch points likely to

³ Obama-Biden Energy and Environment Agenda.

⁴ Visit www.sentech.org/phev for information, publications, and future work related to this study.

⁵ Sentech, Inc. et al. "PHEV Market Introduction Study: Pre-Workshop Discussion Paper." November 2008. http://www.sentech.org/phev/pdfs/MIS_Pre-Workshop_Summary_Report.pdf

have a significant effect on the early stages of PHEV market introduction. On the second day, participants brainstormed policies, incentives, and regulations that could help overcome the identified pinch points. Ideas ranged from the simple expansion of existing policies to include PHEVs (e.g., high-occupancy vehicle lane access) to a “feebate” system that rewards customers for purchasing fuel-efficient vehicles. Workshop findings have been collected and compiled by ORNL and Sentech, Inc. in the report, PHEV Market Introduction Study Summary of Workshop Results.⁶

Analysis

Two separate consumer choice models are used to simulate the market impacts of suggested policies, incentives, and regulations from the Workshop: the ORNL PHEV Consumer Choice Model and the VAMMP Model.

The ORNL PHEV Consumer Choice Model simulates competition of PHEVs against several other powertrains by placing values on specific vehicle attributes, consumer cost savings, and predefined market conditions. The ORNL model is a demand-driven model with no production capacity restraints incorporated. Therefore, the model may project high sales for a given incentive, even if the supply chain is not capable of producing enough vehicles to meet that demand.

The VAMMP Model, created through collaboration between UMTRI and PNNL, approaches market penetration projections from an agent-based perspective. In this model, four classes of decision-makers (consumers, government, fuel producers, and vehicle producers/dealers) interact with one another and the environment (especially the economic environment) based on their individual needs and/or organizational objectives. Similar to ORNL’s model, the VAMMP Model does not have production capacity constraints on new vehicles; a predetermined used vehicle market does exist, however.

⁶ Sentech, Inc. et al. “PHEV Market Introduction Study Summary of Workshop Results.”

Technical Progress

Using insights and recommendations from the PHEV Market Introduction Study Workshop, the two consumer choice models simulated sales of gasoline and diesel ICE vehicles, HEVs, PHEV-10s, PHEV-20s, and PHEV-40s. In addition, both passenger cars and light trucks were modeled. To establish a baseline for PHEV sales through 2020, a “current policy case” was created and used in this study to demonstrate what PHEV sales through 2020 would look like if no further funding or legislative action in support of PHEVs was taken beyond the current date. This current policy case accounts for the three major existing PHEV market accelerators:

- The Plug-In Vehicle Tax Credit (ARRA, Sec 1141, H.R.1) that offers between \$2,500-7,500 in tax credits to consumers, based on battery energy storage capacity.¹⁰
- \$2 billion in advanced battery manufacturing grants (ARRA, H.R.1) to domestic automotive, battery, and component manufacturers.¹¹
- \$400 million for electric drive vehicles and electrification infrastructure demonstration and evaluation projects (ARRA, H.R.1).

No additional PHEV-related policies, incentives, or regulations are included in the current policy case. Existing federal policies related to HEVs, however, are assumed to be in place through their anticipated phase-out periods.¹²

Conclusions

With existing policy measures, projections are:

- Approximately one million PHEVs on the road by end of 2015.

¹⁰ Established in Emergency Economic Stabilization Act of 2008; modified and extended in ARRA.

¹¹ Originally authorized but not funded under the Energy Independence and Security Act of 2007, Section 135.

Motor Vehicle Credit, Energy Policy Act of 2005, Section 1341.

- 425,000 PHEVs sold in 2015 (2.5% of LDVs sold).
- Additional policies should be considered in order to sustain market beyond PHEV tax credits.

PHEV-10s appear to offer most value for the cost (compared to PHEV-20s and PHEV-40s).

Policies that directly reduce the cost to the consumer appear to be most effective at increasing PHEV sales (e.g., state sales tax exemption, “Feebate Program,” annual operating cost allotments).

A 2¢ per gal increase in Federal gasoline tax would be sufficient to fund the implementation of all eight policies investigated.

Potential Market Pinch Points

- Supply chain insufficiencies: Ample production of batteries must be achieved to help drive down cost.
- Infrastructure readiness: There will be a need for simple and seamless PHEV charging equipment, both at residential and commercial
- Consumer Acceptance and Education: Ways to achieve maximum benefits of owning and operating PHEVs must be communicated to consumers.
- Price of Gasoline: The sense of urgency fades as gasoline prices decline

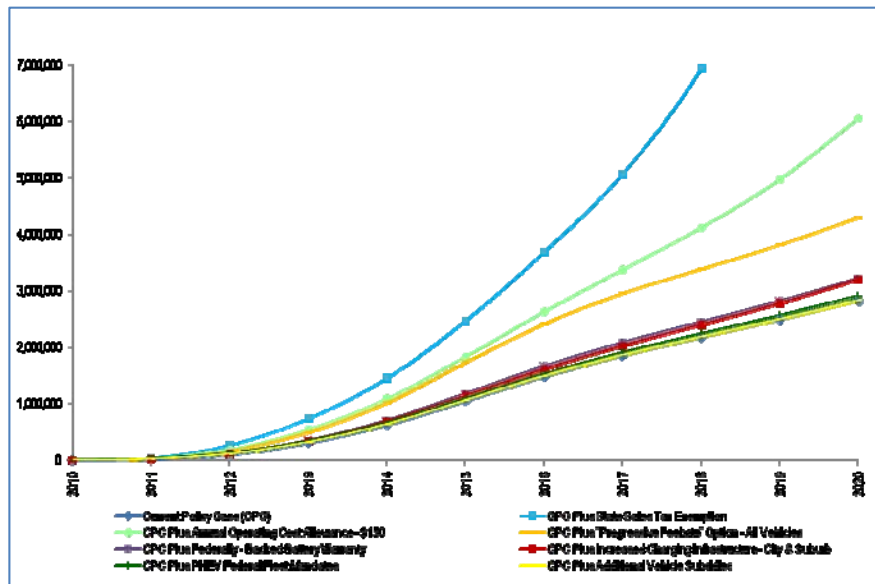


Figure1. PHEV Projected Cumulative Sales Units

L. Enabling High Efficiency Ethanol Engines (Delphi PHEV CRADA)

Principal Investigator: Robert M. Wagner

Oak Ridge National Laboratory (ORNL)

National Transportation Research Center

2360 Cherahala Boulevard

Knoxville, TN 37932

Voice: 865-946-1239; Fax: 865-946-1354; E-mail: wagnerm@ornl.gov

CRADA Partner: John A. MacBain, Keith Confer

Delphi Automotive Systems

Voice: 865-451-3739; E-mail: john.a.macbain@delphi.com

DOE Technology Development Manager: Lee Slezak

Voice: 202-586-2335; E-mail: lee.slezak@ee.doe.gov

ORNL Program Manager: David E. Smith

Voice: 865-946-1324; Fax: 865-946-1262; E-mail: smithde@ornl.gov

Objective

To explore the potential of ethanol-based fuels for improvements in drive-cycle efficiency and emissions based on simulation and experiments.

Approach

Make use of DI multi-cylinder engine with advanced powertrain components and controls for exploring the efficiency opportunities of ethanol and ethanol-blend fuels.

Construct representative vehicle model(s) for evaluating the efficiency of ethanol-based engines.

Develop advanced powertrain and component models in collaboration with Delphi Automotive Systems for integration into the Powertrain Systems Analysis Toolkit (PSAT) environment.

Simulate conventional and advanced powertrain systems for relevant drive cycles using engine data from an advanced ethanol engine developed for use with this activity.

Major Accomplishments

Multi-cylinder engine cell for evaluating ethanol efficiency potential and enabling technologies is near completion.

Ethanol engine build is underway with expected delivery to the Oak Ridge National Laboratory (ORNL) in early fiscal year (FY) 2009.

Engine maps from a Saab Bio-Power vehicle were validated for gasoline and ethanol fuels.

Conventional and advanced powertrains were simulated using Saab Bio-Power data (gasoline and ethanol) in split and parallel hybrid electric vehicle (HEV) models for relevant drive cycles.

Future Direction

Install an advanced ethanol engine at ORNL.

Baseline ethanol engine over speed/load range for use in PSAT powertrain simulations.

Simulate conventional and advanced (HEV and plug-in hybrid electric vehicle [PHEV]) powertrains using data from advanced ethanol engine data developed for this cooperative research and development agreement (CRADA).

Introduction

Ethanol has become of increasing interest in recent years because it is a large domestic energy resource with a potential to displace a significant portion of petroleum imported into the United States. The substantial subsidies and tax breaks for ethanol production and consumption reflect the desire of the U.S government to increase ethanol production as a way to make the country's energy portfolio more diverse and secure. Cellulosic ethanol may provide an additional step-change in reducing petroleum consumption by greatly expanding the quantity of feedstock available for ethanol production. It would also reduce the anthropogenic CO₂ emissions per vehicle mile that contribute to global warming due to the lower energy inputs associated with this technology.

Improved utilization of ethanol will require significant technical progress toward enabling higher efficiency. ORNL has considerable experience with non-traditional fuels and improving engine system efficiency for next generation of internal combustion engines. Delphi has extensive knowledge and experience in powertrain components and subsystems, along with real world issues associated with the implementation of ethanol-based fuels. Partnering, to combine ORNL and Delphi knowledge bases, is key to improving the efficiency and implementation of ethanol-based fuels.

This CRADA makes use of a direct-injection L850 engine, which has advanced Delphi components including a flexible valve train and open controller. This engine will be used in combination with modeling to improve the fundamental understanding of efficiency opportunities associated with ethanol and ethanol-gasoline blends.

This activity is co-funded by the Vehicle Technologies Fuels Utilization Subprogram. The Vehicle Systems portion of this CRADA will focus on drive-cycle estimations of efficiency and emissions based on simulation and experiments. Estimations will be performed for ethanol and ethanol blends with conventional and advanced powertrains to assess the full merit of the proposed research across a wide spectrum of powertrain technologies. To fully understand the value of the

research, overall vehicle efficiency impacts will be considered. PSAT will be the vehicle-level-modeling environment and allow for the dynamic analysis of vehicle performance and efficiency to support detailed design, hardware development, and validation.

Approach

Engine System Experiments

An advanced engine system has been developed to evaluate the efficiency potential of ethanol and ethanol blends through the use of advanced technologies developed by Delphi Automotive Systems. Engine maps developed with this engine will be used as input to vehicle systems modeling to characterize the potential of ethanol and ethanol blends with advanced engine and powertrain components.

Vehicle System Modeling

An essential aspect of the research is to evaluate the potential of optimized ethanol engines and their impacts on conventional and advanced powertrains. The vehicle modeling portion of the project is structured utilizing four principal tasks: (1) model development of a reference conventional vehicle and ethanol engine model, (2) development of advanced powertrain models utilizing gasoline and ethanol engine maps, (3) simulation of all respective vehicle models over pertinent drive cycles, and (4) development of a detailed final report including complete analysis and comparison of the results. These tasks are summarized below.

Development of representative midsized conventional vehicle model

A set of vehicle performance attributes, based on a 2007 Saab 9-5 BioPower sedan, were used as the basis for creating the complete conventional vehicle model. The results from this task established a reference for conventional vehicle performance, using both gasoline and ethanol (E85), for subsequent advanced powertrain variations to be compared against. The vehicle specifications used for creating the vehicle model are outlined in Table 1.

An integral part of this task was to create an ethanol engine model based on laboratory data collected at both ORNL’s Fuels, Engines, and Emissions Research Center (FEERC) and the Transportation Research Center (TRC). A Saab Bio-Power vehicle was available and has been tested at FEERC. Data from these tests were used to develop the ethanol engine model (map), and also provided a means of model validation. The Saab ethanol engine map also provides a secondary basis for comparison, i.e., the current production “state-of-the-art” for optimized flex-fuel engines.

Table 1. Main Specifications of the Saab BioPower Vehicle

<i>Component</i>	<i>Specifications</i>
Engine	Gasoline and E85 based on Saab BioPower data
Transmission	5-speed manual Ratios: [3.38, 1.76, 1.18, 0.89, 0.66]
Frontal Area	2.204 m ²
Final Drive Ratio	4.05
Drag Coefficient	0.290
Rolling Resist.	0.009 (plus speed-related term)
Wheel radius	0.3056 m

Development of mid-sized advanced powertrain vehicle models

In order to gain a broad understanding of the potential merits of the optimized ethanol engine, advanced powertrain models (such as HEVs and PHEVs) were identified and developed. Such powertrain configurations represent the most viable means of maximizing fuel economy in the near term.

Utilizing available component data from ORNL and industry, hybrid vehicle models that satisfy the Saab Bio-Power vehicle performance attributes were developed. The gasoline and ethanol engine models used for the conventional case were scaled in each powertrain application in order to approximate the performance of the conventional vehicle. These powertrains reflect the current technology available (in the case of HEVs) and proposed technology (in the case of PHEVs). The control system for each powertrain configuration was “optimized” so that a good estimation of the performance of each configuration could be determined. The base control strategy approach was to maximize the efficient use

of the engine, because this component is typically the weakest link in the “efficiency chain.”

Simulation of conventional and advanced powertrains over pertinent drive cycles

In order to understand the operational characteristics of the engine in different configurations, the models were exercised over drive cycles of various degrees of aggressiveness and transient characteristics. The drive cycles selected were the Urban Dynamometer Driving Schedule (UDDS), Highway Fuel Economy Test (HWFET), and the US06 cycles. A comparison of all data to the baseline conventional vehicle will then be performed.

Results

The conventional vehicle, based on the 2007 Saab 9-5 BioPower sedan, was modeled and validated against actual test data collected at ORNL and TRC in FY2008. Table 2 shows a comparison of the gasoline and ethanol fuel economy results for each drive cycle as a point of reference for comparison to the advanced powertrain simulation results.

Table 2. Fuel economy comparison for conventional model validation

<i>Facility</i>	<i>Fuel</i>	<i>Fuel Economy (MPG)</i>		
		FTP	HWFET	US06
ORNL	Gasoline	23.2	39.8	26.5
	E85	17.2	29.8	20.0
TRC	Gasoline	22.7	39.0	25.6
	E85	17.3	28.6	19.3
PSAT Conventional	Gasoline	22.4	40.0	25.4
	E85	17.2	29.7	18.4

Development of HEV and PHEV models has been completed. For these advanced powertrain cases, the following architectures were examined based on the 2007 Saab 9-5 BioPower vehicle:

- Power-split HEV
- Pre-transmission parallel HEV
- Pre-transmission parallel PHEV

Figure 1 represents a comparison of the fuel economy simulation results for the engine operating

on gasoline for the HEV powertrains. The engines for the HEV cases have been downsized in concert with the high-voltage traction drive in order for the vehicle to have the same performance characteristics as the conventional vehicle. As expected, there is a substantial increase in fuel economy for both HEV powertrains over the Federal Test Procedure (FTP) cycle due to engine-off operation during idle, and the effects of reduced fuel consumption due to downsizing. The power-split provides a substantial benefit due to increased operation at the engine's most efficient regions. The parallel HEV powertrain offers superior fuel economy over the HWFET cycle.

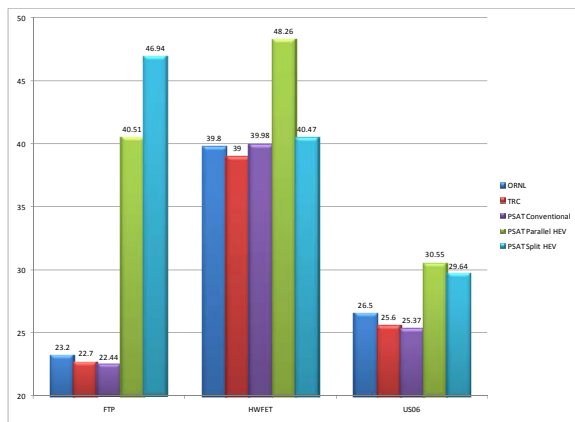


Figure 1. Comparison of HEV fuel economy results (MPG gasoline) compared to conventional vehicle

Figure 2 provides a comparison of the fuel economy simulation results for the engine operating on ethanol (E85) for the HEV powertrains. Similar results are shown here as compared to Figure 1. The advantages of hybrid operation are evident—particularly over the FTP cycle due to the large amount of stop-and-go operation. The power-split shows a notable increase in efficiency over the highway cycle while using E85.

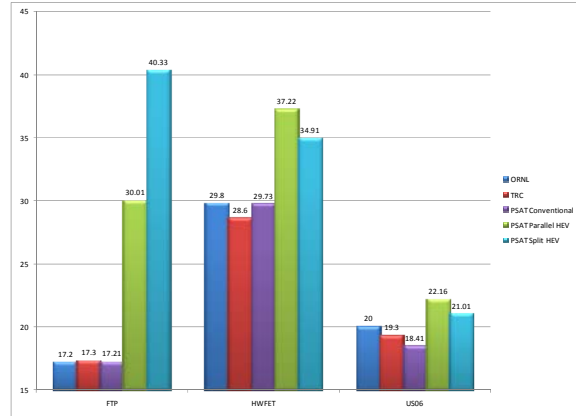


Figure 2. Comparison of HEV fuel economy results (mpg ethanol, E85) compared to conventional vehicle

In order to better understand how the engine operates in each of the powertrain architectures, engine torque density plots were created to show how the engine is used during each cycle. Figure 3 shows an example of these density plots for both the power-split and parallel HEV configurations during the FTP cycle. The power-split configuration is not speed constrained, and can operate at lower speed/higher load operation on the engine's most efficient operating points. The parallel HEV spends more time operating off the engine's maximum efficiency curve. While the torque operating points appear similar, the engine operation is very different between these respective architectures due to varied engine speeds (powertrain constrained) and the torque density plot does not give time series information (torque points not necessarily occurring at the same time).

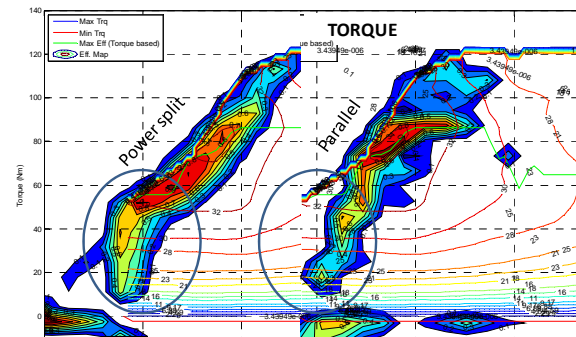


Figure 3. Example of conventional vehicle engine speed histogram (UDDS)

Conclusions

The second year of the CRADA has been focused on continuing to establish the tools for use in evaluating

the efficiency potential of ethanol-fueled engines in combination with advanced powertrain systems. Advanced powertrain HEV models have been developed and compared with conventional chassis dynamometer data from ORNL. PHEV models have been developed and simulations over the standard driving cycles are in progress. Data from prototype optimized ethanol engine will be incorporated into existing models for further analysis.

M. Simulated Fuel Economy and Performance of Advanced Hybrid Electric and Plug-in Hybrid Electric Vehicle Technologies Using In-Use Travel Profiles

Matthew Earleywine (Principal Investigator), Jeff Gonder, Tony Markel and Matthew Thornton
National Renewable Energy Laboratory
1617 Cole Boulevard
Golden, CO 80401-3393
(303) 275-4405; Matthew.Earleywine@nrel.gov

DOE Vehicle Systems Analysis Activity Manager: Lee Slezak
Voice: 202-586-2335; Fax: 202-586-1600; E-mail: Lee.Slezak@ee.doe.gov

Objective

Evaluate fuel economy and performance of plug-in hybrid electric vehicles (PHEVs) over in-use driving profiles and compare with standard certification cycles to better understand real world impacts on fuel economy and vehicle performance.

Compare performance of PHEVs with various energy storage capacities under real world driving situations.

Improve data processing methods for repairing and filtering travel activity data acquired using GPS technology.

Approach

Use GPS data collected from travel activity surveys to build driving profiles (in-use duty cycles), and gather statistics such as driving distances, maximum speeds, and average speeds.

Filter out extraneous and outlying data points in the GPS data sets.

Evaluate the performance of different types of advanced vehicles across all of the GPS driving profiles using vehicle simulation software.

Accomplishments

GPS data sets from Austin and San Antonio, TX have been filtered, repaired, and used to develop statistical drive cycle characteristics including daily vehicle miles of travel (VMT), percentage of vehicles on the road at any given time of day, maximum speed distribution, and average speed distribution.

Vehicle performance, fuel consumption, and electricity consumption has been evaluated in detail and compared to vehicle operation on the standard urban dynamometer driving schedule (UDDS) and Highway Fuel Economy Test (HWFET). In addition to overall vehicle performance, a separate evaluation was performed for both the charge-depleting (CD) mode and the charge-sustaining (CS) mode of vehicle operation.

The above-mentioned characteristics were evaluated using two different charging scenarios for the PHEVs: a base scenario and an opportunity charging scenario. The base scenario assumed the vehicle was fully charged at the beginning of the day and never recharged throughout the day. The opportunity charging scenario assumed that the vehicle started the day with a full charge and was plugged in again between each trip, leading to lower average daily liquid fuel consumption.

Future Directions

Perform similar evaluations using GPS travel activity data from other cities and regions of the country including multi-day data sets.

Partner with industry to design PHEVs statistically optimized for real world driving, rather than UDDS, HWFET, US06, or other standard driving profiles used to measure fuel economy.

Use demographic data to determine if there are relationships between demographic trends and driving patterns.

Incorporate changes in road grade into the simulations for more accurate results.

Improve GPS data processing methods.

Introduction

Recently, PHEV vehicles have become increasingly popular due to their high fuel economy and potential for reducing petroleum consumption. As per Environmental Protection Agency (EPA) standard methods, a vehicle's fuel economy is measured using standard driving cycles such as the UDDS and the HWFET. However, as new technologies and designs allow vehicles to become more fuel efficient, consumer behavior and driving profiles become more influential on the variation in actual fuel economy observed. That is, aggressive driving behavior not captured in standard drive cycles can greatly influence the actual fuel economy experienced by a given driver. This effect can be accentuated with advanced technology vehicles such as HEVs and PHEVs. In addition, in the case of PHEVs, the distance driven between opportunities to charge the vehicle greatly impacts the vehicle fuel use. For these reasons, use of real world driving profiles can help predict the actual fuel displacement benefits and the impact of advanced vehicle technology and design on fuel consumption.

Approach

The real world drive cycle data is obtained using GPS technology. GPS devices use satellites to calculate second-by-second information about vehicle position, speed, and distance traveled. The GPS data used for this study was gathered by the Texas Department of Transportation and consisted of a total of 784 vehicles in Austin and San Antonio, TX [1]. This GPS data was filtered and processed, and then used to generate 24-hour driving profiles for each vehicle in the study. Vehicle-level simulation tools were used to evaluate and compare

the simulated performance of different types of vehicles on these in-use drive cycles.

Six different vehicles were simulated on these cycles: a conventional vehicle (CV), an HEV, and four PHEVs. Of the four PHEVs, three of them had a parallel configuration, meaning that the internal combustion engine assisted the electric motor during times of high power demand. The three parallel PHEVs are referred to as PHEV10, PHEV20, and PHEV40 because they were designed to travel approximately 10, 20, and 40 miles, respectively, on the UDDS before using any fuel. The fourth PHEV was a series configuration, meaning that the electric motor provided all of the vehicle's power and the internal combustion engine was only used to sustain the charge of the batteries for longer distance driving. This vehicle is referred to as PHEV40s, and was designed to travel approximately 40 miles on the UDDS cycle before using any fuel.

Results

Of the two cities in this survey, the Austin data set contained 228 vehicles, and the San Antonio data set contained 556 vehicles. Figure 1 and Figure 2 show the daily driving distributions for the data from both Austin and San Antonio. The San Antonio data has a slightly higher percentage of vehicles that traveled at greater daily distances compared to Austin. This could be due to the fact that San Antonio is a larger city and covers a larger area. Therefore, people may tend to travel farther overall. The average daily driving distance in the Austin data was 34.27 miles, while it was 38.70 miles in the San Antonio data—yielding an overall average of 37.41 miles. The driving distributions followed similar trends to previous NREL studies, which included evaluations

of driving behavior and vehicle performance using GPS data in St. Louis, MO (Figure 3)[2].

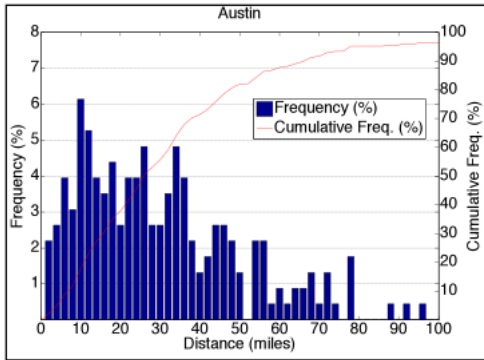


Figure 1. Daily Driving Distribution for Vehicles in Austin, TX

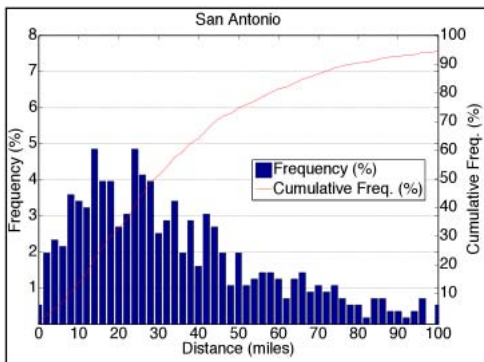


Figure 2. Daily Driving Distribution for Vehicles in San Antonio, TX

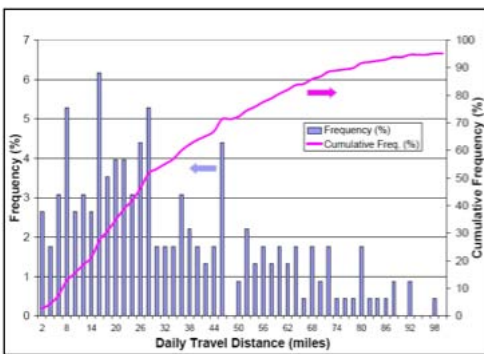


Figure 3. Daily Driving Distribution for Vehicles in St. Louis, MO [2]

Figure 4 shows the utility factor curves for Austin and San Antonio compared to the utility factor curve generated from the 2001 National Household Travel Survey (NHTS) data [3]. The utility factor is used to estimate the percentage of VMT covered for a specified CD range. For example, a vehicle

designed with a real world CD range of 50 miles would cover approximately 70% of the total VMT in the NHTS data set, 77% in San Antonio, and 82% in Austin. The Austin and San Antonio curves are significantly higher than the NHTS curve, which means that a higher percentage of vehicles in Austin and San Antonio travel shorter distances than in the NHTS survey. This could be because the vehicles in the Austin and San Antonio data sets represent mostly urban driving on a single weekday, while the NHTS would also include some rural driving.

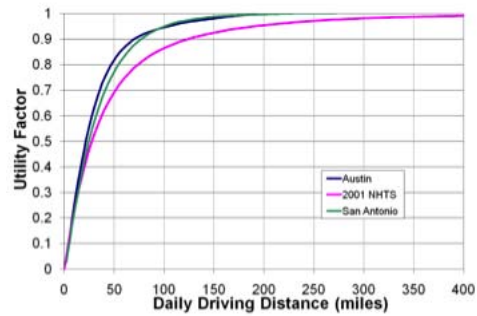


Figure 4. Utility Factor Curves for Austin and San Antonio Compared to 2001 NHTS Data

Tables 1 and 2 show the average fuel economy and electricity consumption from the vehicle simulations for all of the vehicles in both Austin and San Antonio. For the PHEVs it shows the fuel and electricity consumption for both the base case and the opportunity charging (opchg) case. The opportunity charging case is a best-case scenario. It assumes that the vehicle has the opportunity to be plugged in every time the vehicle is stopped for more than two minutes. Since most public parking lots don't have outlets in every stall to plug vehicles into, the base case is more likely representative of the real world. However, some consumers may make many trips throughout the day, returning home between each of trip. One example would be a stay-at-home parent, who shuttles their children from place to place and returns home in between trips. For this type of situation, the opportunity charging case may be a better representation. If public parking lots were to have outlets available to plug vehicles into, the fuel savings would be very significant, as shown

by the significant increase in fuel economy from the base case to the opportunity charging case.

Table 1. Fuel Economy and Electricity Consumption in Austin (Per Vehicle Average)

Austin				
Vehicle	mpg		Wh/mi	
	BASE	OPCHG	BASE	OPCHG
CV	23.05	n/a	n/a	n/a
HEV	34.68	n/a	n/a	n/a
PHEV10	47.26	78.19	150.21	269.32
PHEV20	59.03	100.48	225.10	308.94
PHEV40	93.09	119.48	308.30	325.98
PHEV40s	181.65	628.29	333.38	364.05

Table 2. Fuel Economy and Electricity Consumption in San Antonio (Per Vehicle Average)

San Antonio				
Vehicle	mpg		Wh/mi	
	BASE	OPCHG	BASE	OPCHG
CV	23.61	n/a	n/a	n/a
HEV	35.16	n/a	n/a	n/a
PHEV10	46.87	72.89	137.67	243.77
PHEV20	58.62	95.64	208.75	288.65
PHEV40	92.85	126.62	292.54	317.73
PHEV40s	149.19	435.89	315.62	357.09

Although the PHEVs were designed to travel 10, 20 and 40 miles respectively on the UDDS, approximately 98% of the daily travel profiles caused the parallel configured PHEVs to use fuel during CD mode. This means that 98% of the time, the internal combustion engine initially began using fuel because of high power demand, not because the state of charge of the energy storage system was too low. This is due to higher accelerations observed in the real world data compared to the UDDS cycle. For this reason over 65% of the profiles caused the engine in the parallel configured PHEVs to turn on within the first mile.

Conclusions

PHEVs consume significantly less fuel than CVs or HEVs, and have a potential to play a key role in reducing U.S. petroleum consumption and carbon emissions in the future. Computer simulations using GPS data to generate in-use driving profiles are a convenient and effective way to evaluate vehicle performance and fuel economy in the real world. These simulations can be used to size components such as the electric motors, internal combustion

engines, and energy storage systems. They can also be useful in optimizing control strategies and other vehicle designs.

The standard UDDS and HWFET cycles are by themselves poor representations of real world driving—particularly when it comes to predicting fuel use for PHEVs and when used as a base for evaluating vehicle designs. This is mainly due to aggressive driving and higher accelerations observed in the real world. The daily driving distance compared to the size of the energy storage system also plays a significant role in a PHEVs fuel economy, whereas a CV’s fuel economy is affected very little by daily driving distance.

Future research efforts will include performing similar simulations using GPS data from other regions of the country and from multi-day data sets. Vehicle performance in different regions could be compared to determine whether driving behavior varies based on region or geographic location. If there is a correlation, vehicles could be designed for optimal performance in the specific region in which they will be used.

Demographic data could also help determine whether different types of consumers have different driving habits. Again, if this is proven to be true, vehicles could be optimized for specific types of consumers. Preliminary studies by Argonne National Laboratory have already evaluated the relationship between population density and driving habits [4].

Future efforts should also incorporate changes in road grade into the simulations, as steep road grades will significantly impact vehicle power demands and in turn performance. This is especially important for very hilly regions, such as the mountainous west. NREL is currently working to integrate this feature into its database of in-use driving profiles.

References

1. Ojah, M., Pearson, D., 2006 Austin/San Antonio GPS-Enhanced Household Travel Survey, Texas Transportation Institute August 2008.
2. Gonder, J., Markel, T., Simpson, A., Thornton, M., “Using GPS Travel Data to Assess the Real World Driving Energy Use of Plug-In Hybrid

Electric Vehicles (PHEVs)", Transportation Research Board 86th Annual Meeting, January 2007.

3. 2001 NHTS Data (<http://nhts.ornl.gov>).
4. Santini, D., Vyas, A., "Population Density, LDV Miles, Speed, Travel Time, and Fuel Use – Net Effects on Location Choice in the U.S.", Transportation Research Board 88th Annual Meeting, January 2009.

N. Predicting In-Use PHEV Fuel Economy from Standardized Test Cycle Results

*Jeff Gonder (Principal Investigator), Aaron Brooker and Matthew Thornton
National Renewable Energy Laboratory (NREL)
1617 Cole Boulevard
Golden, CO 80401-3393
(303) 275-4462; Jeff.Gonder@nrel.gov*

*DOE Vehicle Systems Analysis Activity Manager: Lee Slezak
Voice: 202-586-2335; Fax: 202-586-1600; E-mail: Lee.Slezak@ee.doe.gov*

Objective

Estimate average in-use plug-in hybrid electric vehicle (PHEV) fuel and electricity consumption based on results from standardized cycle testing.

Establish a methodology to compare different PHEV designs on the basis of their expected real world performance (both with each other and with other vehicles, for which established methods exist to predict real world performance by adjusting standardized test results).

Approach

Identify issues by applying adjustments to PHEV performance results over standard test cycles.

Develop adjustment method(s) that could be applied to any PHEV design (based on theorizing impacts to PHEV operation in real-world driving relative to less-aggressive standard lab test cycles, as well as making simplifying assumptions for broader applicability).

Test out adjustment approach by applying methodology to PHEV data from standard cycle laboratory testing and comparing the adjusted estimates to observed on-road performance for a large number of PHEVs of the same design.

Accomplishments

Developed an approach for predicting in-use PHEV fuel economy based on adjusting raw fuel and electricity consumption results from laboratory testing over the standard historic city and highway test cycles.

Collaborated with two other national laboratories to validate the approach by applying it to actual PHEV data from standard cycle laboratory testing. The adjusted predictions for both fuel and electricity consumption agreed with the average on-road observations from a fleet of roughly 100 PHEVs of the same design (when accounting for how often the PHEVs in the fleet actually plug in to recharge their batteries).

Future Directions

Evaluate the methodology on other PHEV designs as substantial on-road test data becomes available for other vehicles.

Focus particularly on the adjustment method's impact for PHEVs with high electric power capability, and refine the method as needed. (The validation has so far only been possible on a single PHEV design, which utilizes a "blended" operating strategy while depleting the electricity stored from off-board charging. That is, occasionally blending in power from the vehicle's engine to satisfy aggressive driving demands).

Computer simulations of different PHEV models can support further method validation and refinement while awaiting on-road data from more PHEV designs. Simulations routinely calculate fuel and electricity consumption over standard test cycles, and can use real-world travel survey data to generate the comparable in-use estimates. (Other National Renewable Energy Laboratory [NREL] activities include analysis of data from surveys that use GPS devices to collect second-by-second travel data).

Introduction

Current rules for estimating miles per gallon of conventional vehicles do not work for PHEVs, which run on both electricity and a liquid fuel (e.g., gasoline). PHEV testing is further complicated by the fact that these vehicles operate in two different modes based on the distance they are driven. The initial charge-depleting (CD) mode uses energy from the large PHEV battery to propel the vehicle and consumes little or no liquid fuel. If the PHEV continues driving longer distances, it begins operating in a charge-sustaining (CS) mode and behaves much like a regular hybrid electric vehicle (HEV), where all net driving energy comes from the liquid fuel in the fuel tank. General consensus exists on PHEV testing techniques to account for the vehicles’ two sources of energy and two modes of operation. One question that remains, however, is how to adjust raw standardized cycle test results to best predict a PHEV’s average real world energy use.

The U.S. Code of Federal Regulations (CFR) describes the process for adjusting certification cycle test results for conventional vehicles and HEVs in order to better predict their real world fuel economy [1]. The outcome of the process is fairly straight forward and can be directly applied to the CS mode of PHEV operation where the vehicle behaves much like an HEV. The adjustment is shown visually on the right side of Figure 1 where the CS fuel consumption increases (fuel economy decreases) in real world operation relative to raw test results using historic certification drive cycles (which do not fully capture actual driving demands/ aggressiveness of today’s drivers).

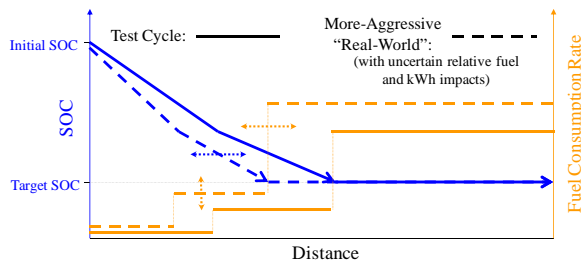


Figure 1. Added power demands can impact PHEV state-of-charge (SOC) depletion rate, distance to reach charge-sustaining operation, and fuel consumption rate.

As can be seen on the left side of the figure above, the PHEV behavior changes in real world versus certification cycle operation can be much more complicated during CD mode (where the state-of-charge [SOC] of the battery decreases). Not only can the PHEV’s fuel consumption rate change, but the electricity depletion rate out of the vehicle battery could change instead or in addition. Any change in the depletion rate would also change the distance that the vehicle travels in CD mode, which in turn impacts the utility factor (UF) used to combine together the CD and CS consumption measurements [2, 3].

Approach

Adjusting raw certification cycle test results in both modes of PHEV operation (in order to predict in-use fuel economy) requires making some simplifying assumptions. Figure 2 illustrates one approach developed at NREL, which assumes that PHEV fuel consumption during CD mode increases at the same rate as in CS mode when translating certification cycle test results into in-use predictions. The method further assumes no change in electricity depletion rate or distance driven in CD mode for in-use versus standard test cycles. For some PHEVs, such as those with significant power/acceleration capability solely using battery electricity, the vehicle will behave somewhat differently in the real world than the method assumes (i.e., depleting the battery faster rather than increasing fuel use in the example mentioned). Though the method penalizes such a vehicle with more CD fuel consumption than it would experience in the real world, it rewards the vehicle with a larger CD distance than actually achieved (and hence a smaller weighting for the much-higher-fuel-consuming CS mode). These two errors could potentially cancel each other out in the final combined calculation. Therefore, this needs to be further evaluated.

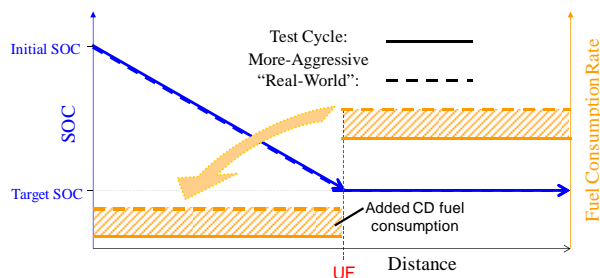


Figure 2. Method for applying adjustment equations to PHEVs.

During 2009, NREL partnered with Argonne National Laboratory (ANL) and Idaho National Laboratory (INL) to validate this adjustment method against on-road data on the only PHEV currently available in large numbers. INL monitors fleet fuel use of advanced technology cars as part of DOE’s Advanced Vehicle Testing Activity (AVTA), and has accumulated more than a year’s worth of data on roughly 100 PHEVs of the same design. Because of limited purpose-built PHEV availability, the cars used in this study were production Toyota Prius HEVs modified with PHEV kits by Hymotion (an aftermarket conversion company owned by A123 Systems). ANL had collected data on the same vehicle to evaluate PHEV test protocols over standard certification cycle speed profiles.

Results

Figure 3 illustrates the step-by-step process of applying the adjustment approach to the raw data from laboratory testing at ANL. The raw test results are provided on the far left side for the urban dynamometer driving schedule (UDDS) and the Highway Fuel Economy Test (HFET). The values indicated on the right half of the figure incorporate a UF weighting based on national driving statistics, and result in a composite PHEV rating that under-predicts fuel use and over-predicts electricity use (relative to the actual average in-use observations for the AVTA fleet). However, it has been shown that the AVTA vehicles (which are mostly operated by private fleets) drive longer distances and hence operate more in CS mode and less in CD mode than national driving statistics would predict [4].

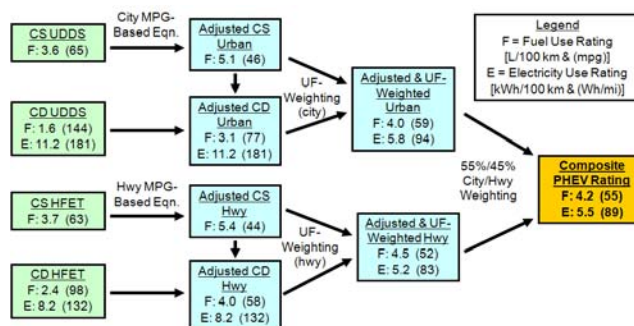


Figure 3. Step-by-step example application of the adjustment method.

To isolate evaluation of the adjustment methodology (intended to estimate the impact of real world driving aggressiveness), NREL next repeated the adjustment calculation steps using the AVTA fleet’s actual CD operating fraction for the UF weighting. As Figure 4 shows, this results in good agreement between the adjusted laboratory test estimates for fuel and electricity consumption relative to the actual on-road observations. Generating in-use estimates from the same UF weighting with no adjustment results in good agreement on the electricity consumption prediction, but poor agreement on fuel consumption.

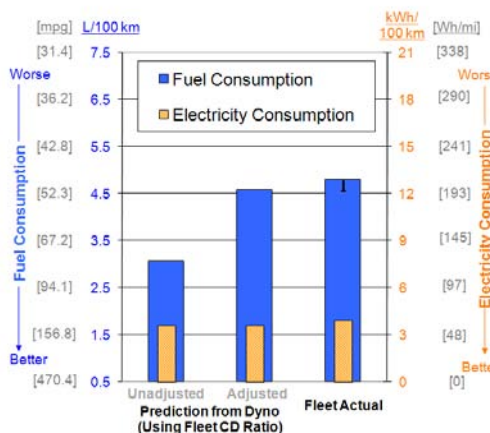


Figure 4. Comparison of predictions from laboratory testing to actual on-road results.

Conclusions

NREL has been developing techniques for adjusting standard cycle PHEV test results (which can be obtained from simulations or laboratory testing) in order to objectively estimate real-world fuel and electricity consumption for different PHEVs. Partnering with two other national laboratories

provided the opportunity to evaluate an adjustment method against actual operational data on a large number of PHEVs. After accounting for how frequently the PHEVs in the on-road comparison fleet actually plug in, the adjusted test cycle predictions for both fuel and electricity use agreed well with the average in-use observations.

While this finding is promising, the validation has so far only been possible on a single aftermarket conversion PHEV design. It will be important to repeat the analysis and refine the method once laboratory testing and substantial on-road fleet data become available for different PHEV designs—particularly those with greater electric driving capability. In the meantime, NREL plans to extend the analysis by simulating “virtual” fleets with a variety of PHEV powertrains operating on GPS driving profiles obtained from conventional vehicle travel surveys [5]. It should also be noted that while this process seeks to predict the average on-road fuel and electricity use from a large number of PHEVs, fuel economy will vary greatly based on how the vehicle is driven. It will be important to educate PHEV drivers on how to obtain the best results. Figure 5 highlights the large degree to which “your mileage may vary” in a PHEV by showing the average estimate for the vehicle in this study (using the presented adjustment approach and national driving distance estimates) along with two extremes on either side of the average that the vehicle could achieve [6].

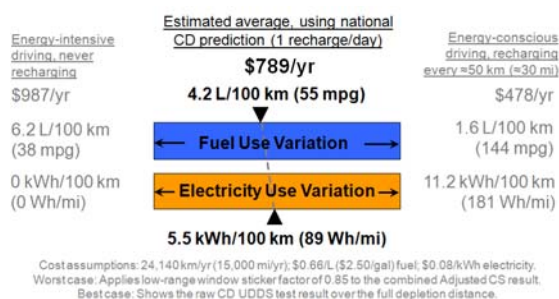


Figure 5. Example representation of the annual energy cost/use for the Hymotion Prius PHEV conversion.

References

1. United States Environmental Protection Agency, Fuel Economy Labeling of Motor Vehicles: Revisions to Improve Calculation of Fuel Economy Estimates; Final Rule, 40 CFR Parts 86 and 600, December 27, 2006, <http://www.epa.gov/fedrgstr/EPA->

- AIR/2006/December/Day-27/a9749.pdf.
2. J. Gonder and A. Simpson, “Measuring and reporting fuel economy of plug-in hybrid electric vehicles,” **World Electric Vehicle Association (WEVA) Journal**, vol. 1, May 2007.
3. SAE International, Surface Vehicle Information Report SAE J2841—Utility Factor Definitions for Plug-In Hybrid Electric Vehicles Using 2001 U.S. DOT National Household Travel Survey Data, March 2009.
4. M. Duoba, R. Carlson, F. Jehlik, J. Smart, and S. White, “Correlating dynamometer testing to in-use fleet results of plug-in hybrid electric vehicles,” *International Electric Vehicle Symposium 24*, Stavanger, Norway, 2009.
5. J. Gonder, T. Markel, M. Thornton, and A. Simpson, “Using global positioning system travel data to assess real-world energy use of plug-in hybrid electric vehicles,” *Transportation Research Record (TRR)*, *Journal of the Transportation Research Board (TRB)*, No. 2017, Dec. 2007.
6. J. Gonder, A. Brooker, R. Carlson, and J. Smart, “Deriving In-Use PHEV Fuel Economy Predictions from Standardized Test Cycle Results,” *Proceedings of the 5th IEEE Vehicle Power and Propulsion Conference (VPPC)*, Dearborn, MI, Sept. 2009.

O. Integrated Vehicle Thermal Management Systems Analysis/Modeling

Kevin Bennion (Principal Investigator) and Matthew Thornton
National Renewable Energy Laboratory
1617 Cole Boulevard
Golden, CO 80401-3393
(303) 275-4447; kevin.bennion@nrel.gov

DOE Vehicle Systems Analysis Activity Manager: Lee Slezak
Voice: 202-586-2335; Fax: 202-586-1600; E-mail: Lee.Slezak@ee.doe.gov

Objective

Develop paths for integrating power electronics and electric machine (PEEM) thermal management systems with other vehicle thermal management systems to reduce the total incremental cost of the PEEM system for electric drives in hybrid electric vehicle (HEV), plug-in hybrid electric vehicle (PHEV), fuel cell vehicle (FCV), and electric vehicle (EV) applications.

Approach

Quantify the integration potential in terms of temperature compatibility and misalignment of transient heat loads of proposed integrated vehicle thermal management systems.

Determine transient and continuous thermal loads based on existing vehicle simulation data over in-use drive cycles over a range of vehicle configurations.

Develop thermal, fluid, and heat exchanger models to evaluate the viability of alternative thermal management integration concepts.

Accomplishments

Developed analysis techniques to quantify the transient and continuous heat loads of individual components and integrated systems over in-use operating conditions.

Applied the developed analysis approach to the electric drive thermal management system to investigate potential integration opportunities with the internal combustion engine (ICE) and heating, ventilation, and air conditioning (HVAC) thermal management systems.

Documented the analysis in a Department of Energy (DOE) milestone and a publication is under review for the 2009 SAE World Congress.

Potential Future Directions

Collaborate with other Vehicle Technology (VT) Program areas such as the Advanced Power Electronics and Electric Machines (APEEM) activity to prototype concept designs with industry support.

Introduction

Vehicle thermal management (VTM) systems are critical in terms of safety, reliability, performance, and passenger comfort. VTM technologies must balance the needs of multiple vehicle systems that

may require heat for operation, require cooling to reject heat, or require operation within specified temperature ranges. The application of thermal management technologies to vehicle propulsion technologies dominated by conventional ICES developed gradually over approximately the last

hundred years, as shown by a 1919 patent related to engine cooling [1]. Changes in vehicle propulsion configurations away from systems dominated by ICEs—toward more electrically dominated systems with electric drives—affect the heat load balance within a vehicle and require new techniques to meet the multiple demands placed on VTM systems.

The additional thermal management requirements associated with electric drive systems are a recognized challenge in terms of the costs related to the thermal management hardware. The costs not only relate to dollars, but also weight and size. The difficulties arise from the impacts on vehicle mass, cargo space, component packaging space, and total component count. Due to the thermal management challenges, DOE supports research and development in thermal management of electric drive technologies through the VT Program. The research includes the energy storage system (ESS) and APEEM activities. Assumptions related to available coolant temperatures influence technology development through research goals, technical targets, and the ultimate direction of technology development. For this reason, there is a need to take a higher level vehicle system view of how cooling systems are integrated into an overall vehicle thermal management strategy.

Integrated vehicle thermal management (IVTM) is one pathway to address the cost, weight, and size challenges. IVTM looks at the total vehicle thermal management needs based on vehicle type and identifies opportunities to share or integrate thermal management systems. As the number of vehicle components that require active thermal management increase, so do the costs in terms of dollars, weight, component count, and package space. The cost increase is particularly true for advanced vehicle powertrains in HEVs and PHEVs, which contain additional critical components that require active cooling. One path for reducing the costs associated with electric drive systems, is the integration of the PEEM thermal management system with other existing thermal management systems on a vehicle.

The work conducted in fiscal year (FY) 2009 demonstrated techniques for quantifying the integrated system heat loads of combined systems and applied the techniques to vehicle electric drive systems. The work highlighted a potential

opportunity to create an integrated low-temperature liquid coolant loop incorporating the PEEM and air conditioning (AC) systems in contrast to a high temperature system integrating the PEEM and ICE cooling systems.

Approach

The approach consisted of three key areas. The first task required the selection of representative vehicle configurations with similar performance characteristics to provide a fair comparison across multiple powertrain configurations. The selection of representative vehicle configurations enabled the comparison of heat loads across components and vehicle propulsion technologies in terms of transient and continuous values. Past work performed at NREL describing a previously published set of vehicle configurations provided a consistent set of vehicle configurations [2]. The simulated vehicle results of over 227 real world or in-use conditions provided data for the heat load analysis.

Second, the techniques for evaluating the transient and continuous heat loads of individual components and integrated systems were applied to the electric drive thermal management system. The developed method compared the transient and continuous heat loads from the 227 in-use drive cycles. The approach resembled a procedure [3] to calculate battery pulse power requirements. A similar process was also applied by the DOE APEEM activity to examine PHEV impacts on PEEM systems [4]. The process of calculating the transient and continuous heat loads across all 227 in-use drive profiles involved computing a moving average of a specified heat load versus time signal. The moving average sample size varied over a range of filter time windows ranging from 2 seconds to 200 seconds. The resulting heat load curve quantified the peak transient and continuous heat loads over all 227 drive cycles for a specific vehicle configuration.

Finally, thermal and fluid system models provided the capability to investigate alternative arrangements of integrated thermal management systems within Aspen Plus and MATLAB. The models enabled analysis of performance impacts associated with heat loads, coolant flow rates, heat exchanger requirements, and ambient environmental conditions such as temperature and humidity. The heat exchanger performance requirements fed into a heat

exchanger sizing model. The heat exchanger sizing analysis checked that the heat exchanger size could reasonably be packaged in a vehicle application that integrated the PEEM system and AC system.

Results

The ability of the heat load curve to illustrate both the transient and continuous heating demonstrated the impact of combining multiple systems onto the same thermal management system. Two requirements illustrated the potential for combining thermal management systems. First, the coolant temperature specifications for the systems must be compatible. Second, the transient heat loads should not be time aligned.

The heat load for the integrated thermal management systems was not always the sum of the peak or continuous heat loads from the combined systems. Different components experienced peak heat loads at different times depending on their use. Misalignment of the peak heat loads led to a potential decrease in the net heat load, reducing the required heat exchanger weight and volume. Two integration options for the PEEM cooling system were investigated, and the results related to temperature compatibility and heat load misalignment are described below.

When combining the ICE and electric drive coolant loops, the individual component peak heat loads did not simply add because the transient peak heat loads often occurred at different times for the analyzed vehicle configurations. The results depend on the control strategy for the vehicle. Figure 1 provides an example with respect to the HEV and PHEV40 vehicle configurations. The figure compares three values. The first curve illustrates the heat load in the ICE coolant (dotted line). The second curve shows the addition of the individual ICE and the PEEM heat load curves (dashed line). Finally, the third solid curve highlights the integrated heat load, which added the heat loads in the time domain and generated the heat load curve using the proposed moving average technique on the combined heat loads. The integrated heat load curve (solid line) accounts for misalignment of peak heat loads.

While the integrated HEV system heat load resembled the sum of the individual heat load curves, they were not the same (Figure 1). Adding

the individual component heat load curves overestimated the combined heat load by assuming the transient heat loads were aligned. For transient conditions, the two curves were similar, but the continuous heat load for the integrated system more closely resembled the heat load from the ICE alone. The reduced heat load showed an opportunity to integrate the two systems without a large increase in the continuous cooling capacity of the thermal management system relative to the ICE cooling system. The integration could reduce the costs associated with the separate PEEM heat exchanger.

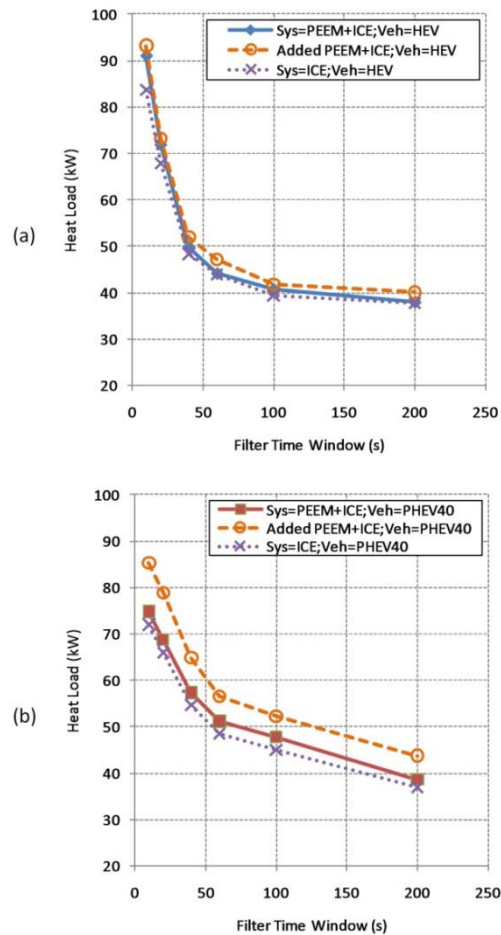


Figure 1. Heat load curves of combined ICE and PEEM systems (solid line), ICE heat load (dotted line), and sum of the individual ICE and PEEM heat load curves (dashed line) over 227 in-use drive cycles. (a) HEV; (b) PHEV40.

The PHEV configurations illustrated a more dramatic difference. Figure 1b shows the same information as Figure 1a, except for the PHEV40 configuration. The PHEV showed a larger difference

between integrated heat load (solid line) and added heat load curves (dashed line). From the results for the simulated PHEV configurations, the PHEV could be a better candidate for integrating the PEEM cooling system with the ICE coolant system.

The hurdles associated with using high temperature coolant for PEEM thermal management systems [5] led to another option to integrate the low-temperature liquid-cooled PEEM system with other vehicle systems that could benefit from a low-temperature liquid coolant. In [6] the use of a low-temperature liquid coolant loop was proposed for the air conditioning (AC) condenser. The work outlined in [6] mentioned that supplying 60°C coolant to the liquid-to-refrigerant condenser ensured adequate AC performance. The highlighted AC temperature requirement is compatible with existing cooling loops for commercial HEV applications [7]. As a result of the temperature compatibility, a focus was placed on a proposal to integrate the low-temperature coolant loop for the PEEM system with a liquid-to-refrigerant AC condenser.

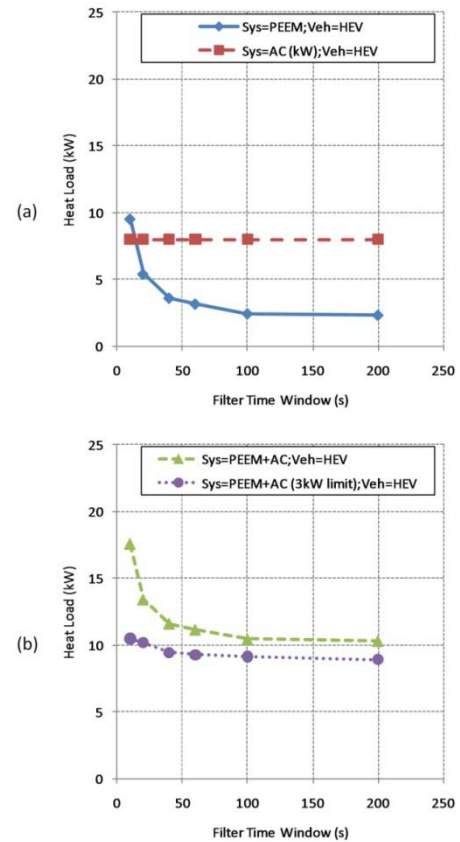


Figure 2. PEEM and AC condenser heat load curves over 227 cycles. (a) PEEM (solid line) and fixed 8 kW AC condenser heat load (dashed line); (b) Combined PEEM and AC heat loads: AC always on (dashed line) and AC off when PEEM heat is over 3 kW (dotted line).

For the proposed low-temperature system, the misalignment of the peak heat loads was possible through control of the AC system operation. Figure 2 shows the impact of controlling the AC system on the integrated heat load. Figure 2a highlights the individual system-specific heat load curves for the PEEM components and the AC condenser. The AC condenser heat load was fixed at 8 kW to illustrate a worst-case scenario of full AC operation. Integrating the PEEM and AC condenser heat loads with the AC always on resulted in the combined heat load curve shown in Figure 2b (dashed line). The impact of turning off the AC during brief periods when the PEEM heat load exceeded 3 kW is shown in Figure 2b (dotted line). Controlling the AC system to turn off during transient high power operation of the PEEM system produced a significant transient and continuous heat load reduction for the integrated system.

Conclusions

The proposed heat load curve provided a method for evaluating the transient and continuous heat loads of individual components and integrated thermal management systems over actual in-use conditions. The developed analysis techniques were applied to alternative vehicle configurations with electric drive systems. Two primary integration options were analyzed involving the PEEM system using a high temperature coolant loop and a low-temperature coolant loop. The high temperature thermal management system, integrating the PEEM and ICE systems, showed a potential application especially for PHEV configurations. However, the high temperature coolant remains an issue for current commercial PEEM systems [5]. The low-temperature thermal management system integrated the PEEM system with the vehicle AC system. The combined system showed similar operating temperature requirements and a potential synergy in the heat load versus time, depending on the control of the AC system.

The integration of the low-temperature PEEM thermal management system with other vehicle systems took the work [6] a step further to investigate integration opportunities related to alternative vehicle propulsion technologies. Specifically, applications include propulsion systems with electric drive systems such as HEVs, PHEVs, FCVs, and EVs. A liquid-cooled AC condenser improves front-end packaging, reduces refrigerant lines, and increases AC condenser package flexibility [6]. The PEEM system benefits by sharing the cost of the low-temperature coolant loop.

System thermal and fluid models and heat exchanger sizing models showed the potential of integrating the power electronics and electric machine cooling with the AC system. While there appear to be synergies related to temperature and heat loading, a more thorough analysis of an implementable concept is required. The next step in the analysis appears justifiable based on the potential viability and benefits of the system.

References

1. Fulton, W., Giesler, J., and Patton, H. "Cooling System for Internal Combustion Engines." U.S. Patent 1,306,000, June 10, 1919.
2. Gonder, J., Markel, T., Simpson, A., and Thornton, M. "Using GPS Travel Data to Assess the Real World Driving Energy Use of Plug-In Hybrid Electric Vehicles (PHEVs)." Presented at the Transportation Research Board (TRB) 86th Annual Meeting, Washington, D.C., Jan. 21-25, 2007.
3. Markel, T. and Pesaran, A. "PHEV Energy Storage and Drive Cycle Impacts." Presented at the 7th Advanced Automotive Battery Conference, Long Beach, California, May, 2007.
4. Bennion, K. "Plug-In Hybrid Electric Vehicle Impacts on Power Electronics and Electric Machines." NREL Milestone, NREL/MP-540-36085, September 2007.
5. Hsu, J., Staunton, R., and Starke, M. "Barriers to the Application of High-Temperature Coolants in Hybrid Electric Vehicles." Oak Ridge National Laboratory Technical Report ORNL/TM-2006/514, 2006.
6. AP, N-S., Guerrero, P., Jouanny, P., Potier, M., Genoist, J., Thuez, J. "UltimateCooling™ New Cooling System Concept Using the Same Coolant to Cool All Vehicle Fluids", 2003 Vehicle Thermal Management Systems Conference (VTMS6), IMechE C599/010/2003, May, 2003.
7. FreedomCAR and Fuels Partnership. Electrical and Electronics Technical Team Roadmap (November 2006) [Online]. Available: www.eere.energy.gov/vehiclesandfuels/pdfs/program/eett_roadmap.pdf.

P. Medium-Duty Plug-in Hybrid Electric Vehicle Analysis

Robb Barnitt (Principal Investigator) and Matthew Thornton
National Renewable Energy Laboratory
1617 Cole Boulevard
Golden, CO 80401-3393
(303) 275-4489; robb.barnitt@nrel.gov

DOE Vehicle Systems Analysis Activity Manager: Lee Slezak
Voice: 202-586-2335; Fax: 202-586-1600; E-mail: Lee.Slezak@ee.doe.gov

Objective

Assess the potential benefit of medium-duty plug-in hybrid electric vehicle (PHEV) platforms.

Approach

Leveraging other Advanced Vehicle Testing Activity (AVTA)-funded projects, acquire and analyze vocational duty cycle data.

Utilizing vehicle characteristics and measured fuel economy data (via ReFUEL) to develop and validate a model of an existing medium-duty HEV.

Model cost, mass, and fuel consumption impacts of adding battery capacity and more robust components.

Accomplishments

Parcel delivery vocational duty cycle data were collected and analyzed. Evaluation of relevant real world duty cycle data resulted in a focused selection of drive cycles for chassis dynamometer testing and vehicle simulation.

With industry partner support, a model was developed of a pre-production gasoline hybrid electric parcel delivery vehicle (gHEV), currently deployed in service by FedEx.

Measured fuel economy data over three “vocationally relevant” drive cycles were used to validate a parcel delivery platform model.

Simulated fuel consumption was evaluated over a range of battery energy capacities, several representative drive cycles, daily vehicle miles traveled (dVMT), and battery and motor power ratings.

Future Directions

Expand the drive cycle database to ensure accuracy of modeling efforts.

Model a range of platforms/vocations for a PHEV prototype.

Down-select vocations/platforms for retrofit and prototype efforts.

Partner with industry and leverage cost-share opportunities to develop one or more ground-up PHEV prototypes.

Initiate in-use vehicle demonstration utilizing National Renewable Energy Laboratory (NREL) analysis, data collection, and chassis dynamometer test capabilities.

Develop medium-duty PHEV test-bed.

Introduction

Medium-duty vehicles are typically represented by classes 3 through 6, with a gross vehicle weight rating(GVWR) range of 10,000 to 26,000 pounds. There has been considerable research focus on PHEV technology in the light-duty vehicle segment, which due to its large volume of fuel consumed and well-matched user driving behaviors, make it an excellent application for PHEV technology. While also large fuel consumers, heavy-duty vehicles typically do not exhibit characteristic drive cycles (transient intensive) that render them appropriate for PHEV application. The medium-duty vehicle segment has received less scrutiny for PHEV application, despite several compelling attributes:

- Many transient intensive drive cycles conducive to PHEV application.
- Fleet-based vehicles that return to a home base, facilitating overnight charging.
- Potential for significant fuel savings per vehicle.
- Attractive value proposition, given the potential for reduced maintenance costs, longer periods of vehicle ownership and social pressures to green corporate image.

Approach

Several other AVTA-funded projects and industry collaborations were leveraged toward progress on medium-duty PHEV analysis activities in fiscal year(FY) 2009. These activities were grouped around the analysis and evaluation of pre-production gasoline hybrid electric parcel delivery trucks currently being operated by FedEx in Southern California. These efforts included collection and analysis of parcel delivery vocational duty cycle data, and chassis dynamometer testing of a FedEx gHEV at NREL’s ReFUEL Laboratory.

With assistance from industry partners FedEx and Azure Dynamics, a model of the gHEV was developed. It was then validated using measured fuel economies from ReFUEL testing. Finally, energy storage and component resizing were explored, seeking an optimal PHEV configuration that will optimize for fuel consumption and cost,

given insight into real world vocational usage patterns.

Results

Eight FedEx vehicles were instrumented with GPS-based data loggers, and over 62route days of spatial speed-time data were collected. These data were used to confirm daily route consistency, and to characterize each route over 55 drive cycle metrics. Key drive cycle characteristics of three study vehicles are summarized in Table 1.

Table 1. Study Vehicle Key Drive Cycle Characteristics

Vehicle #	242292	242294	242295
Average Driving Speed (mph)	16.8	16.9	16.2
Daily VMT (miles)	43.8	47.2	21.3
Stops/mile	3.86	3.80	4.24
Avg. Acceleration (ft/s ²)	2.27	2.11	2.10
Avg. Deceleration (ft/s ²)	-2.61	-2.58	-2.56
Accelerations per mile	20.90	20.88	23.08
Decelerations per mile	20.36	19.83	22.81
Kinetic Intensity (ft ⁻¹)	0.00059	0.00055	0.00075

Calculated kinetic intensity was used to compare real drive cycles to existing stock drive cycles, and frame chassis dynamometer test cycle selection and vehicle simulation activities. Based upon observed drive cycle kinetic intensities, the Orange County Bus Cycle was selected as a cycle that best approximated the routes driven by three study vehicles, while the New York City Cycle (NYCC) and HTUF4 Cycle were selected as upper and lower boundaries for vocational kinetic intensity.

A gHEV was transported from California to NREL’s ReFUEL laboratory for emissions and fuel economy measurement. Fuel economy results over three drive cycles are presented in Table 2.

Table 2. gHEV Fuel Economy Results

	Drive Cycle	gHEV FE (mpg)
	HTUF4	10.5
	Orange County Bus	8.6
	NYCC	6.8

Using vehicle specifications and physical characteristics shared by FedEx and Azure Dynamics, a model of the gHEV was developed. Approximations were made for the vehicle engine map and hybrid control strategy. The model was validated by comparing simulated fuel economy to measured fuel economy for the three cycles tested at ReFUEL. Simulated fuel economy was within 1 to 9% of measured fuel economy, depending upon the drive cycle.

Using this validated gHEV parcel delivery platform model, preliminary analyses of PHEV configurations were conducted. Simulations focused on the daily fuel economy (dFE) achieved with hardware changes such as battery capacity, and also with variability in driving behaviors like cycle intensity and dVMT. Preliminary results are illustrated in Figure 1.

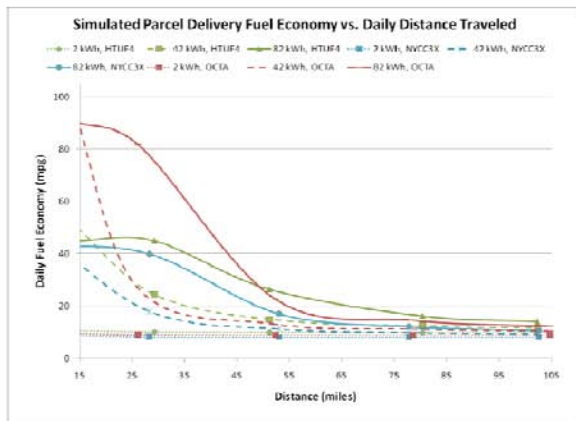


Figure 1. Simulated Fuel Economy Results

These results show the incremental fuel economy benefit realized through increasing battery energy.

The baseline three trends represent simulated fuel economy versus dVMT for a 2-kWh battery, similar in capacity to the baseline gHEV but with a charge-depleting control strategy. Six other trends illustrate the relationships between dFE and dVMT over three drive cycles and two battery energy capacities (42 and 82 kWh). Tables 3 and 4 illustrate simulated fuel economy dependence upon battery energy, drive cycle, and dVMT (20 and 45 miles). The referenced baseline is the 2-kWh battery with a charge-depleting control strategy.

Table 3. Simulated Fuel Economy, 20 dVMT

Drive Cycle	Battery Energy (kWh)	dFE (mpg)	% Increase Over Baseline
NYCC	2	8.8	0
	42	28.0	220%
	82	43.0	391%
OC Bus	2	9.3	0
	42	51.5	457%
	82	89.0	862%
HTUF4	2	10.5	0
	42	39.0	273%
	82	46.0	340%

Table 4. Simulated Fuel Economy, 45 dVMT

Drive Cycle	Battery Energy (kWh)	dFE (mpg)	% Increase Over Baseline
NYCC	2	8.2	0
	42	12.2	49%
	82	23.8	190%
OC Bus	2	9.1	0
	42	14.4	59%
	82	31.0	243%
HTUF4	2	10.2	0
	42	16.5	63%
	82	36.0	255%

Conclusions

As has been shown in light-duty PHEV analyses, drive cycle intensity and daily VMT are important variables in the prediction of daily fuel economy. However, due to the daily consistency in routes typical of medium-duty vocations such as parcel delivery, transit bus, school bus, and utility, medium-duty PHEV design can be tailored to specific drive cycle and dVMT characteristics.

Knowledge of these usage patterns through duty cycle analysis can aid original equipment manufacturers (OEM) in targeted design, and aid end-users like FedEx in deploying PHEVs on the most appropriate routes.

In FY 2010, more detailed modeling of PHEV parcel delivery configurations will be linked to performance and cost trade-offs. In addition, expanding the in-use medium-duty vehicle duty cycle database will allow for simulation of relevant real world usage patterns, and more focused vehicle design across parcel delivery and other medium-duty vocations.

Publications

PHEV Parcel Delivery Truck Model – Development and Preliminary Results, *Hybrid Truck Users Forum*. October 2009.

Q. Energy Storage Life and Cost Study to Identify Cost-effective Vehicle Electrification

*Aaron Brooker (Principal Investigator), Matthew Thornton and John Rugh
National Renewable Energy Laboratory
1617 Cole Boulevard
Golden, CO 80401-3393
(303) 275-4392; Aaron.Brooker@nrel.gov*

*DOE Technology Manager: Lee Slezak
Voice: 202-586-2335; Fax: 202-586-1600; E-mail: Lee.Slezak@ee.doe.gov*

Objective

Estimate the improvement of energy storage life or cost that makes vehicle electrification cost effective relative to current and future conventional and hybrid electric vehicles (HEV).

Approach

Validated the vehicle fuel economy, performance, cost, and battery life models with published industry data.

Implemented a variation of the in-use PHEV fuel economy estimation method described in “Deriving In-Use PHEV Fuel Economy Predictions from Standardized Test Cycle Results,” IEEE Vehicle Power and Propulsion Conference, Dearborn, Michigan, 2009 (NREL/CP-540-46251) by J. Gonder, A. Brooker, R. Carlson, J. Smart.

Estimate the cost effectiveness based on the sum of vehicle cost and present fuel cost.

Accomplishments

Evaluated the cost effectiveness of conventional vehicles, HEVs, plug-in hybrid electric vehicles (PHEV), and electric vehicles (EV) using data reflecting near-term industry battery technology.

Compared the cost effectiveness again assuming battery replacement, opportunity charging, or direct electric power along a small fraction of heavily traveled roadway.

Although it requires an improvement in connection technology and infrastructure along a small fraction of heavily traveled roadway, found that an HEV powered by external electricity (similar to today’s trolleybuses) is the most cost-effective option to the consumer—even if the connection device is an extra \$1,000.

Found that reducing the battery cost from \$700/kWh to \$300/kWh or improving battery life by a factor of 10 made PHEVs cost effective, indicating the need for continued battery research and development for EVs and PHEVs.

Future Directions

Improve the in-use fuel consumption estimate of PHEVs and update the results.

Introduction

Electrifying transportation can reduce or eliminate dependence on foreign fuels, emission of green house gases, and emission of pollutants. One challenge is finding a pathway for vehicles that gains wide market acceptance to achieve a meaningful benefit.

Approach

This project evaluated several approaches aimed at making EVs and PHEVs cost effective, including opportunity charging, replacing the battery over the vehicle life, improving battery life, reducing battery cost, and providing electric power directly to the vehicle during a portion of its travel. Many combinations of PHEV electric range and battery power are included. For each case, the model accounts for battery cycle life and the national distribution of driving distances to size the battery optimally.

Cost Estimate

A large share of the market must switch to electric vehicles in order to realize the national and global benefits of vehicle electrification. According to the J.D. Power and Associates’ 2008 Alternative Powertrain Study, most consumers will purchase a fuel-saving vehicle if the fuel savings pays back the extra upfront cost [3]. Alternatively, most would not be willing to purchase a fuel-saving vehicle if it didn’t payback the extra upfront cost [4] Therefore, this study uses cost effectiveness as a metric to reflect the potential success to achieve the individual, national, and global goals.

Cost effectiveness is estimated by comparing the net present vehicle and fuel cost of each electric vehicle against today’s options. Since insurance, maintenance, and repairs have not been consistently higher or lower for advanced vehicles such as HEVs [5], they were not included.

Component costs were based on previous study estimates [5] shown in Table 1. The exception is the \$700/kWh battery energy cost coefficient. This was calibrated to match estimates of a range of today’s HEV, PHEV, and EV vehicles as seen in Figure 1.

Table 1. Component Costs.

Battery	\$22/kW + \$700/kWh + \$680
Motor/controller	\$21.7/kW + \$425
Engine	\$14.5/kW + \$531
Markup factor	1.75

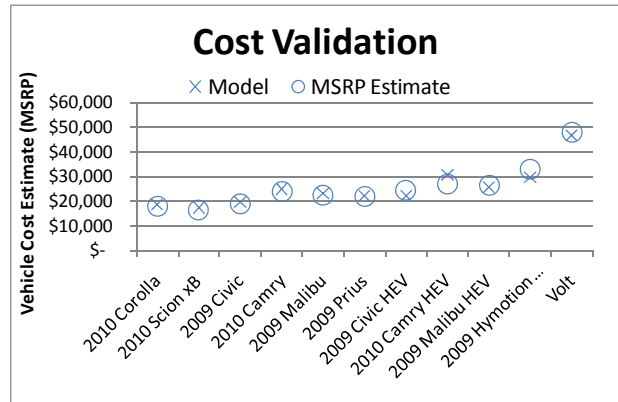


Figure 1. Cost Validation.

Distribution of Driving Distances

This study’s assumption on driving distance between recharge expanded the constant distance assumption used in other studies to a distribution of distances. This had important impacts on battery life, control strategies, and fuel economy. A constant distance is often used to represent a consistent commuting distance. Commuting, however, only represents one third of the miles driven[9]. Therefore, most driving may not be a consistent distance. To improve this assumption, this study uses a distribution of daily driving distances based on national statistics [9]. Figure 2 was generated using the 2001 National Household Travel Survey (NHTS) DAYPUB database and filtering consistent with SAE J2841. The frequency of occurrence assumed 2-mile bins with a total of 600 bins, which was required to capture the maximum daily driving distance of 1,200 miles. While long trips are infrequent, they are important because their length can make them a significant portion of the total miles traveled.

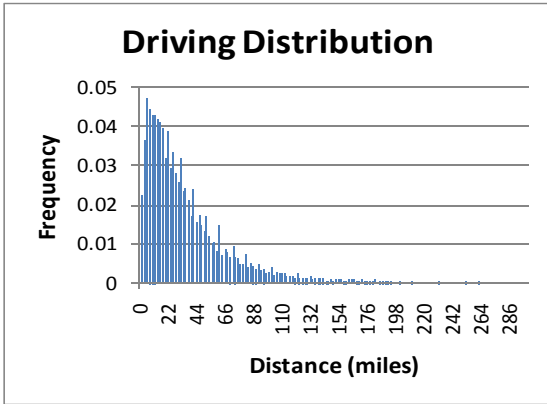


Figure 2. Distribution of driving between recharges.

Battery Life and Sizing

The driving distribution has important implications on battery life and sizing. For PHEVs and EVs, the trip length is used to estimate the level of discharge to the battery based on the vehicle's charge-depleting efficiency. Each discharge causes a specific level of battery wear based on data from Johnson Controls [10], as seen in Figure 3. The average charge-depleting wear per mile was calculated using the trip driving distribution data, battery discharge efficiency, and battery cycle life data. The acceleration and regenerative braking cycle wear per mile based on the drive cycle simulations, which can account for as much as 5% of the wear for low-range PHEVs, was then added to calculate the total wear per mile.

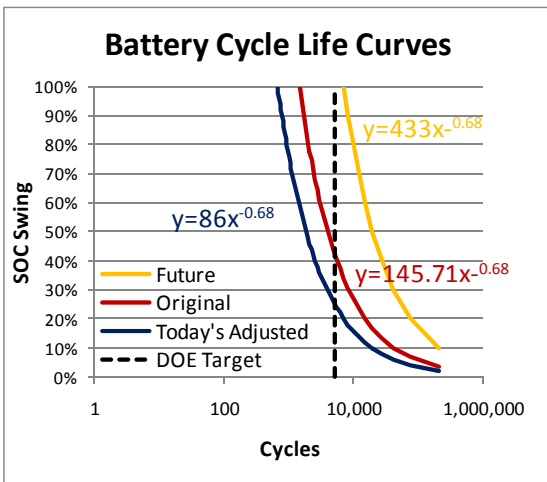


Figure 3. Battery life estimates.

The original battery life curve in Figure 3 represents the published data. Because this data does not

consider calendar, temperature, or power level effects for the current technology case, the trend was adjusted to match published Nissan Leaf [11] and Chevy Volt [12, 13] battery life expectations. The future case was adjusted to match the 7,000 cycle life published by A123 Systems [14], which is similar to the Department of Energy's (DOE) target [15]. It is used for the future improved case because it too does not include the calendar, temperature, or power level effects that would occur for a vehicle application.

Dynamic Plug-in

This study also expands on the type of PHEV evaluated. Although it would require an improved connection, it assesses a vehicle that plugs in dynamically, similar to the way trolley buses or streetcars currently do. Because it is connected while driving, it does not need a large battery to gain PHEV fuel economy benefits, although it does need infrastructure along a small fraction of roadway. The fraction of infrastructure is small because most travel occurs on just a few roads. The interstate, for example, makes up 1% of the miles of roadway, but carries 22% of the vehicle miles traveled [17, 18]. This scenario assumes that 40% of the distance driven is connected dynamically. It also assumes an additional \$1000 cost to the consumer for the dynamic connection, HEV cost and fuel economy when not connected dynamically, and PHEV charge-depleting fuel economy when connected.

Results

Using today's battery assumptions, while the gasoline consumption decreases significantly, most electrification pathways were not cost effective compared to HEVs or CVs, as seen in Figure 4. The vehicles listed on the figure follow the naming convention of vehicle type, charge-depleting range, and then battery power level. For example, the PHEV10 Low Power stands for a PHEV with 10 miles of charge-depleting range using a low power battery. Increasing battery power had little effect on fuel consumption results because in both cases the battery power can provide most of the driving on the test cycles—so the fuel economy differs only slightly. For the electric powered vehicles, the electricity cost is relatively low, reflecting the low cost of electricity and the high efficiency of batteries and motors. The gasoline, on the other hand, is a

large expense, especially for the conventional vehicle. Even so, the extra battery costs in PHEVs and EVs outweighed the gasoline cost savings.

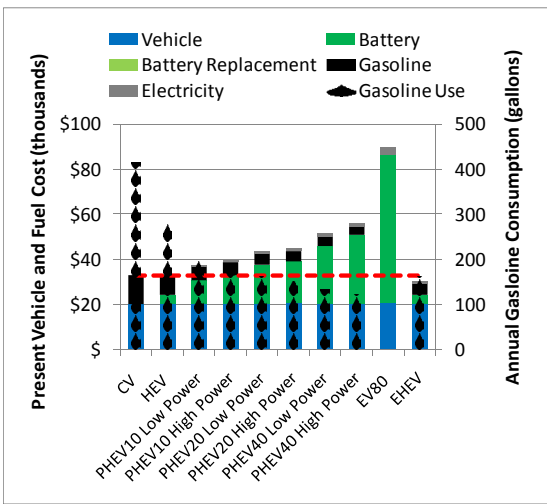


Figure 4. Current battery cost and life results.

One case may warrant further investigation because it reduced total cost to the consumer and it reduced fuel use. This is labeled EHEV, for electrified HEV. This case assumes that an HEV could connect to an external source of energy along some roadways while moving, similar to the way trolley buses or streetcars do in some cities such as Boston, Cambridge, Philadelphia, and San Francisco [22], though it would require research to improve the connection. On the consumer side, the EHEV is cost effective, even with the extra \$1000 cost to the consumer for the connection mechanism. The cost is low because it gains the low cost electric mode operation similar to a battery PHEV without the cost, wear, efficiency losses, and weight of a large battery.

Battery replacement had minor overall improvements in cost effectiveness. These cases reduced the size of the battery but used it more aggressively to reduce upfront cost and weight, and to take advantage of lower future battery costs. The advantages, however, were mostly balanced out by the increase in battery wear, as seen in Figure 5.

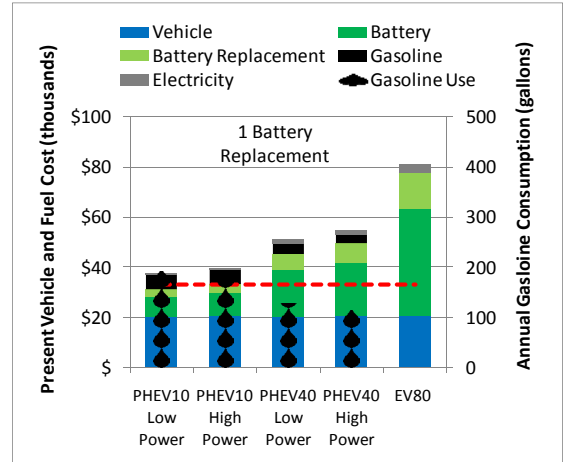


Figure 5. Current technology with battery replacement.

Opportunity charging further decreased PHEV gasoline consumption, and thus gasoline cost, but at a greater increase in battery cost. Opportunity charging increases the use of the battery. In order to sustain the additional use and wear, the battery energy had to be increased from 6.3 kWh to 11.1 kWh. This added over \$6,500 to the vehicle cost.

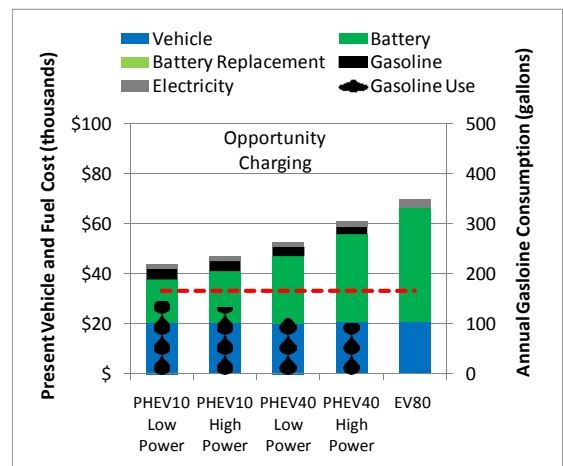


Figure 6. Current technology with opportunity charging.

Additional analyses that reduced the battery cost from \$700/kWh to \$300/kWh or improved battery life by a factor of 10 also made PHEVs cost effective, indicating the need for continued battery research and development for EVs and PHEVs.

Conclusions

Three different improvements may make vehicle electrification cost effective:

- Reduce the battery cost from \$700/kWh to \$300/kWh.
- Increase battery life by a factor of 10.
- Improve dynamic connections, similar those used by trolleybuses that could power HEVs electrically while traveling along heavily traveled roadways.

Publication

A. Brooker, M. Thornton, J. Rugh, "Technology Improvement Pathways to Cost-effective Vehicle Electrification," submitted to SAE World Congress, 2010.

References

1. U.S. Energy Information Administration. www.eia.doe.gov. Accessed July 10, 2006.
2. Highway Statistics 2004. U.S. Department of Transportation. Federal Highway Administration. <http://www.fhwa.dot.gov/policy/ohim/hs04/index.htm>.
3. J.D. Power and Associates, "J.D. Power and Associates 2008 Alternative Powertrain Study," July 2008.
4. J.D. Power and Associates, "J.D. Power and Associates 2002 Alternative Powertrain Study," 2002.
5. Mello T., "The Real Costs of Owning a Hybrid," <http://www.edmunds.com/advice/hybridcars/articles/103708/article.html>, July 23rd, 2008, retrieved 10/12/08.
6. Simpson, A., "Cost-Benefit Analysis of Plug-In Hybrid Electric Vehicle Technology," 22nd International Battery, Hybrid and Fuel Cell Electric Vehicle Symposium and Exhibition (EVS-22), Yokohama, Japan, October 23-28, 2006.
7. "At \$40,000 the Volt Would Result in No Profit for GM," posted 3/25/08, retrieved 10/13/09, <http://gm-volt.com/2008/03/25/at-40000-the-volt-would-result-in-no-profit-for-gm/>.
8. Shiau, Ching-Shin Norman, Samaras, Constantine, Hauffe, Richard, Michalek, Jeremy J., "Impact of battery weight and charging patterns on the economic and environmental benefits of plug-in hybrid vehicles," Energy Policy (0301-4215), July 2009. Vol.37,Iss.7;p.2653-2663.
9. Hu, P., Reuscher, T., "2001 National Household Travel Survey, Summary of Travel Trends," December 2004.
10. Dr. Duvall, M., "Batteries for Plug-In Hybrid Electric Vehicles," presented at The Seattle Electric Vehicle to Grid (V2G) Forum, June 6th, 2005.
11. Nissan USA Q&A, <http://www.nissanusa.com/leaf-electric-car/?dcp=ppn.39666654.&dcc=0.216878497#/car/index>, posted 8/10/09, retrieved 10/13/09.
12. Lienert, A., "GM Hustles to Bring Chevrolet Volt to Market by November 2010," <http://www.edmunds.com/insideline/do/News/articleId=125465>, posted 4/4/08, retrieved 10/13/09.
13. Interview with Chevrolet Volt Vehicle Chief Engineer Andrew Farah, http://www.coveritlive.com/mobile.php?option=com_mobile&task=viewaltcast&altcast_code=073e2147ec, retrieved 10/12/09.
14. "Life, Thousands of Low Rate Cycles. Chart 1/4," <http://www.a123systems.com/a123/technology/life>, retrieved 10/13/09.
15. Howell, D., "FY 2008 Progress Report for Energy Storage Research and Development", page 3, January 2009.
16. Gonder, J., Brooker, A., Carlson, R., Smart, J., "Deriving In-Use PHEV Fuel Economy Predictions from Standardized Test Cycle Results," presented at the 5th IEEE Vehicle Power and Propulsion Conference, Dearborn, Michigan, 2009 (NREL/CP-540-46251).
17. Federal Highway Administration, "Federal - Aid Highway Length - 2004 Miles by System", <http://www.fhwa.dot.gov/policy/ohim/hs04/xls/hm15.xls>, posted October 2005, retrieved 10/15/09.
18. Federal Highway Administration, "Annual Vehicle Distance Traveled in Miles and Related Data - 2004 1/By Highway Category and Vehicle Type," <http://www.fhwa.dot.gov/policy/ohim/hs04/xls/vm1.xls>, retrieved 10/25/09.

19. Gonder J, Simpson A., "Measuring and reporting fuel economy of plug-in hybrid electric vehicles," presented at the 22nd International Battery, Hybrid and Fuel Cell Electric Vehicle Symposium and Exhibition (EVS-22), Yokohama, Japan, 2006 (NREL/CP-540-40377).
20. Tesla Motors,
<http://www.teslamotors.com/buy/buyshowroom.php>, retrieved 10/22/09.
21. Wikipedia, "AC Propulsion eBox",
http://en.wikipedia.org/wiki/AC_Propulsion_eBox, retrieved 10/22/09.
22. Wikipedia, "Trolleybus",
http://en.wikipedia.org/wiki/Trolleybus#United_States_of_America, retrieved 10/22/09.

R. Medium and Heavy-Duty Vehicle Simulation

Aymeric Rousseau (project leader), Antoine Delorme, Dominik Karbowski

Argonne National Laboratory

9700 South Cass Avenue

Argonne, IL 60439-4815

(630) 252-7261; arouseau@anl.gov

DOE Technology Manager: Lee Slezak

Objectives

Integrate state-of-the-art component data and drive cycles into Powertrain System Analysis Toolkit (PSAT).

Develop specific control strategies for medium- and heavy-duty vehicles.

Approach

Review literature to define specific development required.

Work with original equipment manufacturers (OEM) to develop and implement specific test and control strategies into PSAT.

Accomplishments

Integrated state-of-the-art component data through collaboration with OEMs.

Developed specific control strategies through collaborations with OEMs.

Developed reference conventional vehicles for several applications.

Developed specific post-processing calculations.

Future Directions

Evaluate the impact of advanced technologies on fuel consumption.

Introduction

Medium- and heavy-duty vehicles represent a significant portion of the fuel consumed in transportation activities. While their applications differ from those of light-duty vehicles, numerous technologies can be shared across classes.

First, to properly assess the impact of different technologies, specific control strategies and component data must be developed. Second, conventional vehicle models representing state-of-the-art technologies are needed as reference.

Control Strategy Development

A new shifting algorithm was created with OEM inputs to represent specific requirements of medium- and heavy-duty applications (Figure 1). The main difference from light-duty vehicles resides in the shape of the curve. In addition, because a higher gear number is considered (up to 18), particular attention was required to avoid any overlap of gear shifting. The algorithm has been validated against proprietary information. The algorithm will now be used to provide shifting logic for any combination of engines and transmissions.

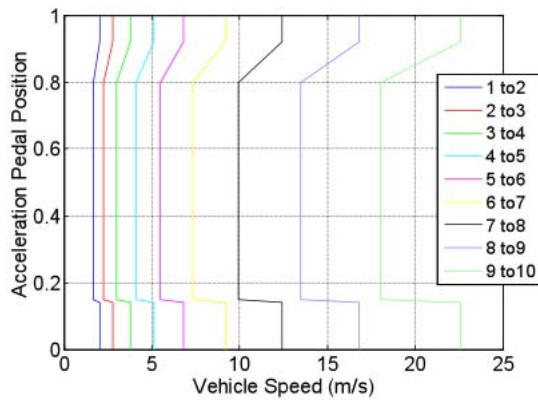


Figure 1. Shifting Curve Example for 10-Speed Long Haul (Note: m/s = meter per second)

The StateFlow algorithm was modified to allow gear skipping during upshift and downshift. Members of the group visited OEMs to test-drive trucks to better understand how shifting was performed.

Since torque converters do not lock up and release under the same conditions as light-duty vehicles, a specific algorithm was developed in collaboration with OEMs.

The engine algorithm was modified to allow jake braking during deceleration for long haul. Engine

data was implemented from OEMs so that the engine negative torque could be represented properly.

Reference Vehicles for Several Applications

Working with OEMs, state-of-the-art component data was implemented in PSAT for the critical components, including the engine, transmission, and torque converter.

Two generic sets of torque converter specifications, including speed and torque ratio and K-factor, were also generated based on proprietary OEM data.

Data for each major vehicle application were collected from several sources, including from both public and proprietary information. Table 1 shows an example of a set of components implemented for a Class 8 long-haul.

As shown in Figure 2, eight vehicle applications were developed and simulated on representative drive cycles. Their rates of fuel consumption were successfully compared with data from the literature.

Table 1. Examples of Component Selection for Long-haul Application

Engine	Cummins ISX 14.9L 317kW
<i>Transmission</i>	Fuller FRM 15210B Manual 10 Speed Ratios : 1 st gear 14.8, 10 th gear 1.0
<i>Final Drive Ratio</i>	2.64
<i>Tire</i>	P295/75R22.5 Radius = 0.51054 m Rolling Resistance = 0.005
<i>Vehicle Losses</i>	Drag Coefficient = 0.565 Frontal Area = 10.38 square meters (m ²)
<i>Curb Weight</i>	8936 kg (tractor) – 6,759 kilograms (kg) (empty trailer)
<i>Gross Vehicle Weight Rating</i>	36,280 kg
<i>Maximum Payload</i>	20,586 kg

Figure 2. List of Applications of Conventional Vehicles

Specific Post-Processing Development

Because the efficiency of trucks is defined by how efficiently they carry a specific payload, specific post-processing was developed to properly assess the impact of new technologies.

Figure 3 shows the difference between fuel economy and load specific fuel consumption (LSFC) for different payloads for a long-haul vehicle. As the figure shows, while only a 25% decrease in fuel economy is observed, the LSFC is divided by eight.

technologies for different vehicle applications. Several conventional reference vehicles were developed.

Future activities will focus on enhancing the existing control strategies and available sets of component data. Specific requirements will be developed for each application so that additional powertrain configurations, including for HEVs and PHEVs, can be developed and their benefits analyzed.

Publications/Presentations

A. Rousseau, "Heavy Duty Vehicle Modeling & Simulation," Presentation to DOE Merit Review, May 2009.

A. Rousseau, A. Delorme, "Update on Development of Medium and Heavy Duty Models," Presentation to DOE, September 2009.

A. Rousseau, "Status of Heavy Duty Vehicle Simulation Tools and Challenges for Regulations," Presentation to National Academy of Science, December 2008.

Figure 3. Importance of Metric Selection

Conclusions

Specific component data and control strategies were implemented to represent state-of-the-art

S. Medium Truck Duty Cycle (MTDC) Project

Principal Investigator: Helmut E. (Bill) Knee
Oak Ridge National Laboratory (ORNL)
National Transportation Research Center
2360 Cherahala Boulevard
Knoxville, TN 37932
Voice: 865-946-1300; E-mail: kneehe@ornl.gov

DOE Technology Development Manager: Lee Slezak
Voice: 202-586-2335; E-mail: lee.slezak@ee.doe.gov

ORNL Program Manager: David E. Smith
Voice: 865-946-1324; Fax: 865-946-1262; E-mail: smithde@ornl.gov

Objectives

Collect duty cycle data and performance measures for class-6 and class-7 medium trucks, from real world operating environments.

Analyze data and information gathered from the Medium Truck Duty Cycle (MTDC) Project (as well as data and information previously collected for the Heavy Truck Duty Cycle (HTDC) Project) with regard to performance characterization and fuel efficiencies.

Establish a real world-based heavy and medium truck performance database capable of supporting the needs of the Department of Energy (DOE), researchers, and private industry. Support Argonne National Laboratory by providing data and information for the development and validation of Powertrain System Analysis Toolkit (PSAT) modules for heavy and medium trucks.

Seek inexpensive and efficient technologies to collect duty cycle data and information for a large number of commercial vehicles operating in real world environments.

Continue leveraging DOE's MTDC efforts with the Department of Transportation's (DOT) Federal Motor Carrier Safety Administration's (FMCSA) interest in commercial vehicle safety; in particular, the collection and analysis of brake and tire performance data from real world operating environments.

Seek strong involvement of private industry and other Federal agencies in the conduct of this program.

Approach

Identify relevant duty cycle and performance measurement data that supports Argonne's PSAT development, as well as other major research programs such as DOE's 21st Century Truck Partnership (21CTP), FMCSA's Commercial Motor Vehicle Roadside Technology Corridor (CMVRTC) and the Environmental Protection Agency's (EPA) SmartWay Program.

Identify sources of duty cycle and performance measurement data from existing onboard sensors/databus, and identify any additional sensors that are necessary, affordable, minimally invasive, and do not disrupt normal business activities of the volunteer fleets.

Seek private industry fleet partners that would allow data collection from their vehicles at no charge to the program.

Develop and maintain six data acquisition systems (DAS) used to collect data from the test trucks.

Instrument up to six medium trucks (test trucks) at one time and collect up to 60 channels of information at 5 Hz for 12 months for four selected vocations (class-7 combination vehicle, transit bus, wrecker, and utility truck) to obtain a detailed profile of medium truck operations in realworld environments.

Download data wirelessly and in near-real-time from the volunteer fleets.

Review the collected data as they are obtained to identify any problems related to the sensors, DAS, or the data.

Enter the reviewed data into a heavy truck/medium truck (HTMT) database residing at the Oak Ridge National Laboratory (ORNL).

Develop a prototype Duty-Cycle Generation Tool (DCGenT) capable of statistically generating duty cycles based on characteristics specified by the user and for a user-specified duty-cycle duration period.

Develop a data search tool that can be utilized by non-ORNL staff to extract data files of interest to the user.

De-instrument the test trucks upon completion of field testing.

Identify fuel efficiency studies that can be conducted utilizing the collected data and select and conduct one or more studies for the heavy/medium truck data.

Support ANL in data needs for development and/or validation of PSAT.

Continue and enhance the program's partnership with DOT's FMCSA, and seek a partnership with EPA for leveraging funds and resources.

As possible, support DOE's 21CTP.

As possible, be responsive to data and information requests received by ORNL and/or DOE.

Keep DOE informed of program progress through monthly/quarterly/yearly progress reports, and project review meetings.

Prepare final reports for the MTDC efforts.

Accomplishments

The HTDC Final Report was completed and published as an ORNL Technical Memorandum. More than 150 copies were distributed to interested parties from other Federal agencies, private industry, academia, and other research organizations.

Memorandums of Understanding (MOUs) were developed to engage in partnerships with the H. T. Hackney Corporation, (for class-7 combination vehicles) and the Knoxville Area Transit (KAT) (for transit busses) to collect data from three vehicles each from their fleets.

The six HTDC DASs were modified and tested for use in the MTDC Program. The DASs were instrumented with wireless download capabilities so that data could be downloaded from each vehicle remotely and daily. Modifications to the DASs were also made and tested to assure that they could communicate with and extract data from the test vehicle's databus (J1939 for the Hackney trucks, and J1708 for the transit busses).

Using the data collected in the HTDC project, ORNL staff completed a data analysis aimed at determining the effect of speed change (55mph versus 65mph) on fuel efficiency. The information was generated using the existing HTDC database. The information was compiled by truck and trailer tire type and topography (i.e., roadway grade) for all of the six participating HTDC trucks. Results

indicated that in all cases, higher fuel efficiency was achieved when traveling at 65 mph than when traveling at 55 mph.

Another study that was conducted utilizing the HTDC database involved the effects of weight on fuel efficiency. A logarithmic relationship was found between fuel efficiency and weight. Publication of the study is being considered.

ORNL developed a capability to look at different driver performances on similar segments of highway. Such information is valuable in determining the impact of various driver behaviors on fuel efficiencies. An analysis of the HTDC data showed that in some cases, the fuel efficiencies of drivers traveling on the same segment of highway with the same vehicle, with the same payload, under similar conditions varied by as much as 50%. (A poor driver required 18 gallons of fuel versus 12 gallons of fuel to travel 180 km).

At the request of DOE, ORNL developed five realworld class-8 heavy truck duty cycles using the information collected in the HTDC project. These duty cycles involved trucks at nearly the legal weight limit traveling on different terrains (i.e., different topography), and in both rural and urban environments.

Partnerships were sought with DOT's FMCSA and DOT's National Highway Traffic Safety Administration (NHTSA), and was achieved with the FMCSA. The partnership involves allowing the FMCSA to put brake and tire pressure sensors on the MTDC combination vehicles. FMCSA will share its capabilities for wireless downloads with the program in exchange for allowing brake and tire pressure monitoring sensors to be put onto the MTDC combination vehicles. A total of 80 channels of data are being collected for the MTDC combination vehicles.

The six test vehicles (three from H. T. Hackney and three from KAT) were instrumented and put into service collecting data in the second quarter of fiscal year (FY) 2009. ORNL received funding from FMCSA to install instrumentation and sensors for the collection of brake and tire pressure data on the MTDC combination vehicles.

ORNL organized the first DOE/DOT Heavy Truck Synergy Meeting at DOT Headquarters in Washington, DC in March 2009. The meeting was well-attended by representatives from DOE's Vehicle Technologies Program (VTP), FMCSA, NHTSA, Federal Highway Administration (FHWA), the Research and Innovative Technology Administration (RITA), and the EPA. Regular meetings between DOE and various agencies of DOT regarding commercial vehicle operations are planned.

A formal MOU signing was held at the National Transportation Research Center (NTRC) in Knoxville, Tennessee on July 7, 2009. Signing participants included representatives from DOE's VTP, H. T. Hackney, KAT and ORNL. Representatives from FMCSA were also present. The event was well-covered by television and newspaper. About 50 people were on-hand for the signing. The signing ceremony was followed by a meeting between representatives from DOE's VTP and FMCSA's Wireless Roadside Inspection (WRI) Program to discuss a Large Scale Duty Cycle (LSDC) project that would collect data from a large number of vehicles wirelessly. Positive results came out of the meeting and a conceptual design study was suggested for FY2010.

Improvements were made to the Duty Cycle Generation Tool (DCGenT) that allows duty cycles to be developed from conditional probabilities between velocities and accelerations. This improves the previous approach which used only histograms of velocities and accelerations.

ORNL established a secure system to store and manage the HTDC and MTDC databases. The data is multiply replicated in various locations to assure that the collected data is secure. Data is backed up daily and maintained for a 30-day window.

Future Directions

ORNL will complete MTDC data collection for the combination vehicle and transit bus in FY2010.

ORNL will initiate MTDC data collection on the wrecker and utility truck vocations in FY2010.

ORNL will initiate efforts to investigate the feasibility of collecting duty cycle data from a large number of vehicles in different vocations across the continental United States. Various approaches are being considered, including the use of commercial mobile radio services and cellular technologies. This LSDC project is seeking partnership with DOT.

ORNL is helping establish a technology evaluation clearinghouse in support of FMCSA's safety and regulatory needs. A complementary capability (i.e., a capability to assess the fuel efficiency benefits [or dis-benefits] from various emerging technologies) will be discussed with DOE's VTP. A joint technology evaluation clearinghouse for the assessment of safety and energy efficiencies associated technologies could be reasonably leveraged between the two agencies.

As funding allows, specialized studies will be conducted regarding the fuel efficiency characteristics of the class-6, -7 and -8 test vehicles.

As possible, refine the DCGenT.

Seek stronger alignment with the 21CTP's SuperTruck Program, and the National Transportation Research Center, Inc.'s (NTRCI's) "Safe Truck" concept.

Seek further integrative energy efficiency and safety research including cross-agency (e.g., DOT) research.

Seek opportunities to collect real world operations experience from fleets utilizing heavy hybrid technologies.

Introduction

Nearly 80 percent of U.S. domestic freight revenue involves the use of heavy trucks. Current trucking industry issues encompass a fine balance of concerns related to the economical, safe, and secure operation of heavy trucks on our highways. In order to move toward an effective solution set that optimally balances such concerns, a firm understanding of the nature and characteristics of heavy and medium truck driving and their associated duty cycles in the United States is critical.

The U.S. trucking industry involves considerable use of heavy trucks (class-8 and class-6 being the classes which consume the most fuel), operates in relatively small fleets (50% of the fleets in the United States are less than 100 trucks, and 25% are less than 10 trucks), operates on small profit margins, and is faced with considerable regulatory and economic pressures (e.g., issues related to hours of service and reduction of truck idling time). Making heavy trucks more efficient through new technologies or congestion avoidance protocols is a goal that would contribute to larger profit margins and contribute to

a reduced dependence on oil and reduced emissions. Since efficient systems are also typically more inherently safe, lives could also be saved.

A practical dilemma involves knowing what the true benefits of new energy efficient technologies are. Most benefit assessments are based on existing information on heavy truck operation. Much of this information is stylized and based on duty cycles that are meant to test various emission or fuel economy measurements. For example, the FTP Transient Cycle is a transient engine dynamometer cycle for heavy-duty truck and bus engines. It includes segments designed to simulate both urban and freeway driving and is used for emissions certification testing of heavy-duty diesel engines in the United States. Another example is the Urban Dynamometer Driving Schedule (UDDS), which is an EPA transient chassis dynamometer test cycle for heavy-duty vehicles. While cycles such as these are based on an understanding of the vehicle technology and how best vehicles might be tested to assess emissions and fuel economy, they do not really reflect real world driving and the real demands placed on the vehicle, driver, or vehicle systems.

Despite common beliefs, how trucks actually operate on our highways is not well known. With hours of service rules, recurring congestion in urban environments, anti-idling regulations, differing fleet management philosophies, weather, the need to deal with incidents of non-recurring congestion, and various topological conditions, only the most highly experienced heavy truck driver has a true situational awareness of the characteristics of driving on our nation's highways. A better understanding of the effects of these impacts on driving, as captured via a field test of heavy and medium vehicle driving, would provide a valuable asset to DOE, other Federal agencies, and the trucking industry in evaluating technologies for energy efficiency, safety, emissions, fleet management, etc.

For DOE, such data and information would provide a basis on which to make decisions related to new technologies being developed to reduce fuel consumption, provide alternative power sources (e.g., hybrid engine technologies and fuel cells), transition to alternative fuels, and reducing emissions. In particular, a database that reflects true driving experiences across various parameters such as geographic terrain, fleet size, fleet type, driving environment, and driving protocols, can provide a rich source of information that could be utilized to make sound energy efficiency-based technology decisions.

These and similar complementary data needs of various agencies of DOT, EPA, and the trucking industry require data and information on how trucks are actually utilized and driven in real world environments, the geography over which they are operated, information related to the driving situation, and the protocols and regulations that govern their operation. In addition, much of the current thinking and research related to long haul, and regional and urban/city driving are based on anecdotal information. A quantitative profile of the driving behavior of heavy and medium trucks does not currently exist. A thorough understanding of the operation of heavy and medium trucks within duty cycles that reflect real world conditions is an asset that would have great benefit to DOE, other Federal agencies, and the overall trucking industry.

Approach

This program involves efforts to collect, analyze, and archive data and information related to heavy and medium truck (classes 8, 7, and 6) operation in real world driving environments. Such data and information will be usable to support technology evaluation efforts, as well as provide a means of accounting for real world driving performance within heavy truck analyses. Additionally, the data collected will generate data, information, and duty cycles that will support Argonne's development of PSAT and could contribute to other major programs. For example, the HTDC and MTDC databases could provide baseline data and information for DOE's 21CTP's SmartTruck Program, or duty cycle data and information for EPA's SmartWay Program.

Industry is also finding the HTDC and MTDC efforts valuable. Industry partners in this program to date have included Michelin Americas Research and Development Corporation, of Greenville, South Carolina; Dana Corporation of Kalamazoo, Michigan; and Schrader Trucking of Jefferson City, Tennessee. Class-6 and -7 partners include: Dillard-Smith Construction (e.g., electrical line utility bucket trucks) of New Market, Tennessee; Fountain City Wrecker Company of Knoxville, Tennessee; KAT of Knoxville, Tennessee; and H. T. Hackney (e.g., straight and combination trucks [dry-box and refrigerated]) of Knoxville, Tennessee. These partners are interested in the vehicle and driver behavior and performance in real-world driving environments in order to support their interests in fuel efficiency and improved operations, and to support future fleet investment decisions.

The program partners have provided significant in-kind contributions, including: no-cost access to test vehicles, test equipment, and engineering services; and six sets of new tires for class-8 testing. Figure 1 shows a typical class-7 H.T. Hackney delivery truck (with non-refrigerated, refrigerated, and frozen compartments) that is being used in the MTDC portion of the program.



Figure 1. Typical Class-7 H.T. Hackney Delivery Truck with Non-Refrigerated, Refrigerated, and Frozen Compartments

The program has involved a Pilot Test, class-8 data collection and analysis, and currently, a class-6/7 data collection and analysis effort. During FY 2009, the final report for the class-8 data collection and analysis effort was completed and 150 copies of the report was distributed to other Federal agencies, industry, academia, and research organizations. Initial MTDC efforts supporting class-6/-7 data collection effort were initiated.

Initiation of the Class-6/Class-7 Medium Truck Duty Cycle (MTDC) Efforts

In FY2009, the six DASs utilized in the HTDC efforts were modified for use on the MTDC platforms. This involved making them compatible with both the J1939 and J1708 data busses (for the H. T. Hackney vehicles and KAT vehicle, respectively). In addition, technologies were added that allowed for the collection of data wirelessly, and in near-real-time (if desired). In the HTDC efforts, data was collected onboard for onetotwo weeks and manually downloaded on weekends involving roundtrips of more than 150 miles. Software was also developed to automatically download data once per day, and to scan the data for errors (missing data, data out of range, etc.) Each of the six test vehicles generates data on 60 parameters at 5 HZ. The six instrumented vehicles were launched into data collection efforts in the second quarter of FY2009, and will collect data for 12 months.

A Memorandum of Agreement signing event was held at NTRC in Knoxville, Tennessee and involved participants from DOE's VTP, H. T. Hackney, Corp. and KAT.

The MTDC effort in FY2009 also benefited from forming a partnership with DOT's FMCSA. FMCSA shared wireless roadside technology capabilities for the privilege of adding brake and tire pressure sensors to the H. T. Hackney test vehicles. This also involved the collection of an additional 20 channels of data. This DOE/DOT synergistic relationship stimulated the first joint meeting between representatives from DOE's VTP, various agencies of DOT (FMCSA, NHTSA, FHWA, and RITA), and the EPA on the topic of heavy truck operation and performance. This meeting was organized by ORNL, was well-attended, and will involve follow-on meetings.

The MTDC data collection effort for the first two vocations (class-7 combination vehicle and transit bus) will be completed in 2010, at which time the six DASs will be moved to the second two vocations (wrecker and utility truck). Data analyses will be initiated on the data collected from the first two vocations.

The Duty Cycle Generation Tool (DCGenT)

The DCGenT prototype allows a user to specify characteristics of interest related to the collected data and to compile all data collection segments in the database that meet the specified characteristics. Users may specify "AND" and "OR" Boolean operations during the search. Characteristics can, for example, relate to road grade, tires, time-of-day, weather, speed, and location (urban, rural, metro, etc). Characteristics related to payload will be added in the future. For the applicable segments, conditional probabilities related to velocity and acceleration are generated (a new feature added in FY2009), and statistical integration is performed to generate a single characteristic duty cycle that reflects the velocity and acceleration profiles of the applicable segments. In the extremes, users can generate a duty cycle for one specific segment traveled by an individual test truck (on one extreme), or can generate a single duty cycle for all segments of the data within the database. More likely will be the generation of a duty cycle that relates to a selected set of characteristics. The user

can also specify the desired duration of the duty cycle.

At the request of DOE, ORNL developed five real world class-8 heavy truck duty cycles using the information collected in the HTDC project. These duty cycles involved trucks at nearly the legal weight limit traveling on different terrains (i.e., different topography), and in both rural and urban environments.

The Data Access Tool

In order to allow users to utilize the database for purposes other than duty cycle generation, a prototype data access tool exists that allows for the extraction of all of the raw data associated with user-specified performance characteristics. The resulting compilation of raw data segments can then be utilized by users for specialized analyses.

Special Studies Conducted

In order to demonstrate the value of the collected data for purposes other than duty-cycle generation, a number of special studies were conducted.

Using the data collected in the HTDC project, the ORNL staff completed a data analysis aimed at determining the effect of speed change (55mph versus 65mph) on fuel efficiency. The information was generated using the existing HTDC database. The information was compiled by truck and trailer tire type and topography (i.e., roadway grade) for all of the six participating HTDC trucks. Results indicated that in all cases, higher fuel efficiency was achieved when traveling at 65 mph than when traveling at 55 mph.

Another study that was conducted utilizing the HTDC database involved the effects of weight on fuel efficiency. A logarithmic relationship was found between fuel efficiency and weight. Publication of the study is being considered.

ORNL developed a capability to look at different driver performances on similar segments of highway. Such information is valuable in determining the impact of various driver behaviors on fuel efficiencies. An analysis of the HTDC data showed that in some cases, the fuel efficiencies of drivers traveling on the same segment of highway

with the same vehicle, with the same payload, under similar conditions varied by as much as 50% (a poor driver required 18 gallons of fuel compared to 12 gallons of fuel to travel 180 km).

Future Directions

This program will provide a valuable asset for making heavy and medium truck energy efficiency technology decisions based on real world performance data. In particular, it will provide input for developing, calibrating, testing and evaluating Argonne's PSAT, and will result in the development of a prototype duty-cycle generation tool capable of generating custom duty cycles for various user-specified long-haul characteristics. Future directions for this work will be to enrich the database with data that provides greater breadth and depth to enhance its applicability to fuel efficiency analyses. This includes continuing to collect and analyze data on class-6/7 vocational applications, situational circumstances, operational protocols, etc., and to extend data collection to a large-scale by inexpensively collecting duty cycle data from a large number of vehicles operating in real world environments across the United States. A conceptual design study for a LSDC project will be initiated in FY2010. If this study shows that such a large and rich data source can be tapped into relatively inexpensively, the variation in duty cycles within a particular vocation can be studied and better understood.

Such capabilities support the establishment of a national data archive for heavy/medium truck performance data, and would be a valuable national asset for heavy truck energy efficiency research. Inclusion of safety data and information might also be a long-term goal that could receive cross-agency attention and support.

Many Commercial Off-the-Shelf (COTS) technologies make fuel efficiency claims that are unsubstantiated. This program should support the laboratory, test-track, and/or field testing of these technologies. If viable, the testing could support greater adoption of these technologies by the private industry. It should be noted that DOT's FMCSA has established a Commercial Motor Vehicle Roadside Technology Corridor (CMVRTC) in East Tennessee (due to the significant amount of truck traffic in the area) for testing and evaluating safety and

enforcement technologies. A complementary testing and assessment capability for energy efficiency technologies might offer another opportunity for leveraging resources between DOE and DOT

Lastly, a future goal is to gain a deeper understanding of heavy truck operations on our nation's highways.

Data for the HTMT database should continue to be added and analyzed. Additional data in the post-MTDC era should be accomplished by piggybacking data collection on other national truck-based programs, including programs by other Federal agencies (e.g., DOT's FMCSA).

Fuel efficiency analyses should also become a major thrust of this program.

The availability of a national data archive of heavy truck performance data and an emphasis on energy efficiency-based data analysis could support the establishment of a Center of Excellence in Heavy Truck Performance Research and should be considered by DOE.

Analyses should also become a major thrust of this program. Special studies such as the fuel efficiencies of 55 mph versus 65 mph, utilizing data from the HTMT database, should be conducted.

Lastly, many COTS technologies make fuel efficiency claims that are unsubstantiated. This program should support the laboratory, test-track, and/or field testing of these technologies. If viable, the testing could support greater adoption of these technologies by the private industry.

T. Technical and Market Penetration Challenges of Plug-in Hybrid Electric Vehicles

Michael Kintner-Meyer (Project leader)
Pacific Northwest National Laboratory, P.O. Box 999
Richland, WA 99352
(509) 375-4306; Michael.Kintner-Meyer@pnl.gov

DOE Technology Manager: Lee Slezak
(202) 586-2335; Lee.Slezak@ee.doe.gov

Participants
Zoran Filipi, Richard Curtin, John Sullivan, Walter McManus, John Lee, University of Michigan

Objectives

Analyze the market adoption of plug-in hybrid electric vehicles (PHEV) and their integration into the grid. A joint project between Pacific Northwest National Laboratory (PNNL) and the University of Michigan (UM) was designed with the following sub-objectives:

- Evaluate optimal battery and prime mover sizing for PHEVs using real driving from southeastern Michigan and determine the charging cycles.
- Perform a national survey to investigate attitudes and beliefs regarding PHEVs.
- Develop a market penetration model using an agent-based modeling approach.
- Analyze the impacts of PHEVs on the reliability of the electric grid.

Approach

This is the second year of a two-year joint project between the UM and PNNL. UM primarily focused on the vehicle-related research and development (R&D) aspects that provided market penetration curves of PHEVs, which then were utilized by PNNL to assess impacts of the emerging PHEV load on the current and future electric , wholesale costs, and overall emissions.

Accomplishments

University of Michigan's accomplishments:

- Completed vehicle simulations to address the optimal battery and prime mover sizing for South-East Michigan Naturalistic Data Set.
- Completion of a national survey to explore customers' attitudes regarding PHEVs and their willingness to pay a premium for fuel efficiency and additional features of PHEVs. The survey results provided valuable information to the market acceptance and market adoption modeling community.
- Completion of two market adoption modeling efforts. One uses an agent-based model approach simulating key stakeholders impacting the purchasing decisions of new and used vehicles. The other uses the classical Bass model with a high resolution of demographics of future PHEVs buyers.
- Completion of a reliability analysis based on probabilistic risk assessment to determine the likely changes on the outage based on new PHEV load.

Future Directions

This project was completed in fiscal year (FY) 2009.

VEHICLE SIMULATIONS (ZORAN FILIPI)

Introduction

The main objective of this task was to characterize the tradeoffs between PHEV attributes and cost. Rather than using repetitions of Federal driving schedules for estimations of PHEV all-electric range (AER) and energy consumption, we utilized the University of Michigan Transportation Research Institute’s (UMTRI) naturalistic driving data generated through Field Operational Tests of instrumented vehicles. The naturalistic driving data by and large captures more aggressive driving behavior than Federal driving schedules.

Two representative PHEV configurations, a power-split hybrid and a series hybrid, were modeled using Powertrain System Analysis Toolkit(PSAT). Then the performance and energy/power usage metrics were obtained by simulating the vehicle behavior over the naturalistic drive cycles recorded in southeastern Michigan.

Design and cost tradeoffs were characterized by setting up the PHEV optimization study to establish the optimum sizing of components for any desired AER or charge-depleting range (CDR). The optimization was carried out by (1) coupling the predictive PHEV simulation to non-gradient-based algorithm DIRECT and (2) utilizing representative real world cycles. Specifying different distances as a target AER or CDR resulted in the generation of several optimal configurations that define a trade-off between the CDR and component sizes. The trade-off with respect to battery size is particularly interesting because battery dominates the cost. The mathematical problem is non-linear for both the series and the power-split configurations. This is because battery capacity increases more rapidly with desired CDR due to more aggressive features of naturalistic driving during longer commutes.

PHEV Design Optimization and AER/Battery Size Trade-off

The objective of the optimization study was to find a battery and motor combination with minimal(most efficient) battery energy usage to achieve a desired

all-electric driving range subject to power constraints of the battery and the motor. The PHEV configuration model used in this analysis was based on the Chevy Volt. The model was built in PSAT by choosing individual components and modifying the control strategy to restrict the engine usage only to sustain battery state-of-charge (SOC). To generate a synthetic drive cycle (from 10 to 40 miles) we developed a methodology based on Markov chains.

The series configuration uses the engine only to sustain battery charge; hence engine size is calculated separately depending on the optimal battery and motor size. The battery size required for the all-electric range is chosen to have sufficient power and energy to complete the driving cycle. The motor has to fulfill peak power demand.

Figure 1 shows the results of the optimization for different desired AER. The green line is obtained by using repetitions of the urban dynamometer driving schedule (UDDS) cycles rather than synthetic real world cycles.

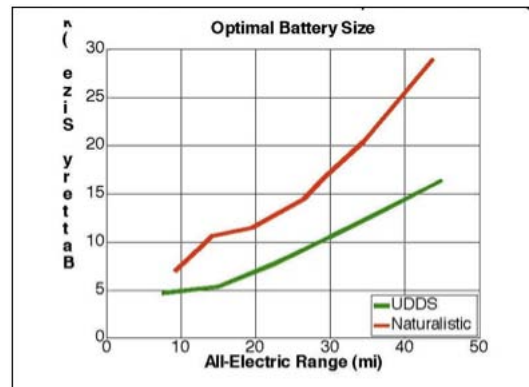


Figure 1. Optimal Battery sizes tradeoff with desired AER for series vehicle configuration

The abrupt changes of slope observed at low range (~15 miles) are the result of transitioning from power constraint to energy capacity constraint. Simply, for relatively short cycles, power requirement dominates size selection; but after a point, the battery becomes large enough to fulfill all power requirements. The overall shape of the naturalistic curve is non-linear at the high end, because longer commutes generally lead to more high-speed driving and higher energy/mile

consumption. Consequently, the difference in optimal battery sizes calculated for naturalistic driving versus UDDS becomes progressively larger.

Daily Driving and Resting schedules

A 24-hour driving mission is the combination of all driving trips during a 24-hour period starting at midnight. Our series PHEV model was used to simulate the 24-hour mission that includes driving and charging. Starting with an SOC of 90%, the battery is depleted to reach a charge-sustaining SOC limit of 40% during the second trip. After that, the engine ensures normal vehicle operation. We also observe that the vehicle is resting for a significant amount of time at home (12 hours – mostly at night) and work (10 hours). Figure 2 shows the results in terms of SOC at resting times for various locations.

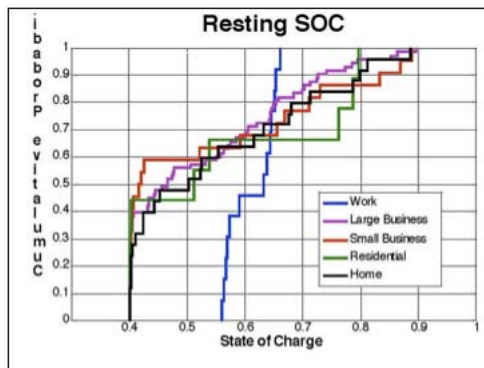


Figure 2. Cumulative Distribution of SOC on arrival at different resting locations

Summary

The PHEV simulator developed in PSAT and an optimization framework were used to characterize the trade-off between component size and cost and AER. Two vehicle configurations were considered: a power-split and a series PHEV. Rather than relying on repetitions of Federal driving schedules originally designed for emission certification, we utilized real world driving data (UMTRI's naturalistic driving data). Based on these data, a methodology for generating representative synthetic cycles was developed by the UM team based on the Markov chain.

Optimal component sizes were obtained for AER between 8 and 45 miles. The optimization is non-linear due to more aggressive features of naturalistic driving over longer distances. Predicted battery sizes

for any given electric range are much higher when naturalistic driving is considered rather than Federal emission certification tests. This finding emphasizes cost concerns and stimulates thinking about strategies involving multiple charging during the day. Daily driving habits are of consequence for charging patterns. Hence, the database was mined to obtain complete information about PHEVs' 24-hour daily missions. Simulating these missions with the PHEV simulator and assuming charging with the 120-V outlet vehicle models provides distribution of battery SOC upon arrival at different locations. Combining these SOC distributions with the time spent at each location, we identified that apart from home, work was the most ideal location for charging the battery. Significant charging can also be achieved at retail locations.

Publications, Presentations

Brian Adornato, Rakesh Patil, Zevi Baraket, Tim Gordon, Zoran Filipi, "Characterizing Naturalistic Driving Patterns for Plug-in Hybrid Electric Vehicle Analysis", Proceedings of the IEEE Vehicle Power and Propulsion Conference, Paper # 171, Dearborn, MI, September 2009.

Rakesh Patil, Brian Adornato, Zoran Filipi, "Impact of Naturalistic Driving Patterns on PHEV Performance and System Design", SAE Paper 2009-01-2715, presented at the SAE Powertrains, Fuels and Lubricants Conference, San Antonio, November 2009.

Rakesh Patil, Brian Adornato, Zoran Filipi, "Design Optimization of a Series Plug-in Hybrid Electric Vehicle for Real-World Driving Conditions", paper 10PFL-0759 in review for the 2010 SAE World Congress, April 2010.

June 19 2009, Invited talk at the International Workshop *Facing the Challenge of Future CO2 Targets: Impact on European Passenger Car Technologies*, "Pathways for Reducing Vehicle CO2 Emission Based on Hybrid and Plug-in Hybrid Propulsion Concepts", Turin, Italy.

October 2009, Invited talk at the 2009 ASME Dynamic Systems and Control Conference "V2G Integration: Impact of Real-world Driving Conditions on PHEV Design, Control and Charging Schedules", Frontiers Session on Progress and

Challenges in the Configuration, Control, and Battery Management of Vehicle-To-Grid (V2G) Integration Systems.

NATIONAL SURVEY TO INVESTIGATE ATTITUDES AND BELIEVES REGARDING PHEVS (RICHARD CURTIN)

Introduction

Vehicle purchases are important economic decisions for individual consumers and have important consequences for the nation as a whole. PHEVs represent a significant change in technology with which most consumers are currently unfamiliar. PHEVs are expected to reduce the cost of fuel by recharging batteries from electrical outlets, but the vehicles are anticipated to cost significantly more than a conventional vehicle. Recharging batteries would require a significant shift in consumer habits and in the infrastructure of the nation's electrical grid. PHEVs are expected to reduce overall carbon dioxide emissions, counteract global warming, and contribute to the energy independence of the nation. Environmental and other non-economic attitudes represent a potentially important component of PHEV purchase decisions.

The goal of this research was to assess the current state of knowledge and opinions about PHEVs among U.S. consumers. Interviews were conducted from July to November 2008 with a nationally representative sample of 2,513 adults. Questions covered their potential interest in hybrid electric vehicles supplemented questions about their current vehicles, their driving habits, mileage and gasoline expenditures, and parking location. Official government data was also used, including the cost of gasoline, electricity, and the fuel economy of the vehicle driven. Data on the economic and demographic characteristics of the household were supplemented by a range of environmental and other non-economic attitudes toward the new technology embodied in PHEVs. The purpose of this study was to examine the conditions under which consumers would purchase a PHEV. Rather than focus on "first adopters," the research focused on the potential pool of purchasers in the first several years after the introduction of PHEVs.

Survey Results

PHEVs were described to survey respondents in general terms, with the implicit assumption that these vehicles were like conventional vehicles in every way except for how the vehicle was powered and refueled. Consumers were asked to consider two key factors about these hybrids: (1) the savings achievable on fuel costs and (2) the added cost premium to purchase the vehicle. The questions were based on estimates of the likely fuel savings and cost premiums for the hybrid vehicles in five to ten years (in today's dollars). The costs premiums presented to consumers for PHEVs were \$2,500, \$5,000, and \$10,000 and the fuel savings was estimated at 75% compared with a conventional gasoline engine. Consumers' preferences for new vehicles were elicited in terms of purchase probabilities or the likelihood of a future purchase.

With an additional cost of \$2,500, the mean purchase probability for a plug in hybrid electric vehicle was 46%, which dropped to 30% for a PHEV that cost an additional \$5,000, and to 14% at an additional cost of \$10,000. This large response in purchase probabilities to increasing price premiums was greater than could be justified based on purely economic rationales. Based on consumers' actual gas expenditures with their current vehicles, the average payback period for the added premium to be offset by fuel savings ranged from 2.0 to 8.5 years at an inflation adjusted discount rate of 3%. To be sure, new technology entails risks that may entail higher costs or a lower resale value, which would mean that these payback periods were underestimated. At a real discount rate of 10%, the payback period ranged from 2.2 to 12.9 years. Indeed, other studies of purchases of energy efficient household appliances have found even longer payback periods implied by the actual purchase decisions of consumers, up to a 20% discount rate.

Three general sets of factors were investigated to gain a better understanding of how consumers judged the potential purchase of a PHEV. The first general factor was the characteristics of the vehicle that consumers currently own and how the vehicles were driven, determining the cost implications of vehicle purchasing decisions. The second general factor focused on the socio economic characteristics of the household, its geographic location, and

recharging capabilities. The third factor was environmental and other non-economic attitudes that may be related to preferences for hybrid vehicles.

The impact of these three general factors can be summarized as follows: although economic considerations had a significant influence on hybrid purchase probabilities, environmental and other non-economic attitudes had an even larger impact. It is a rather commonplace finding that the utility that consumers draw from vehicles depends on more than a strict economic cost-benefit calculation. Even when vehicles are equivalent in every way from an economic point of view, different makes, models, and styles connote different social messages about the owner. A strong appeal of plug-in hybrids is that consumers believe such a purchase would vividly demonstrate their commitment to a cleaner environment. Such beliefs are important for the introduction of plug-in hybrids, acting to off-set some of the higher economic costs by conferring social benefits. Such positive social benefits can be expected to be inversely proportional to the number of hybrid owners. At some point, the positive social benefits of owning a hybrid may shift to rising negative social implications about those who shun these more fuel efficient vehicles. Such a purely social dynamic, however, cannot exist independent of economic factors, especially since vehicles are generally the second most expensive purchase made by consumers.

The first buyers of PHEVs are likely to currently own vehicles with relatively high fuel efficiency ratings and favor the purchase of the vehicle for environmental reasons. The economic justification for the purchase will not be great since the payback period to offset the cost premium will be longer than for someone who owns a low mileage vehicle. The first time buyer will be highly educated and think it is important to signal their commitment to a cleaner environment to others. First time PHEV buyers are likely to own their own home with convenient access to an electric outlet and relish the opportunity to avoid gas stations and recharge their vehicles overnight at off-peak pricing. Although a first time PHEV buyer is likely to have relatively high income, these consumers were as sensitive as moderate or lower income consumers to the potential size of the premiums on PHEVs.

The economic challenges to the successful introduction of PHEVs are diverse, although the reactions to the premiums charged for PHEVs were nearly universal. As the premiums for PHEVs doubled from \$2,500 to \$5,000 and doubled again to \$10,000, there was a uniform decline in purchase probabilities across all of the socio economic characteristics measured, across all differences in the characteristics of the vehicles they currently owned and how they were used, and across all of the environmental attitudes measured. On average, the purchase probabilities declined by 16 percentage points for each doubling of the initial cost premium. This was true no matter how high or low the subgroup's initial purchase probability was from the overall average. Each doubling prompted the same decline in the likelihood of purchase. This was the most vivid and convincing demonstration of the sensitivity of consumers to the price of PHEVs. At a premium of \$10,000, 56% of all respondents reported that there was no chance that they would ever purchase a PHEV, double the 23% response at a premium of \$2,500. The average purchase probability at the \$10,000 premium fell by 70%—to just a one-in seven chance of purchase from nearly a one in two chance at the \$2,500 premium.

Given that a tax credit amounting to \$7,500 dollars will be available to buyers of PHEVs, this would make PHEV purchases much more likely, at least in theory. The problem is that most buyers would have to finance the total price of the vehicle including the premium before they could claim the tax credit. This would limit the already narrow group of new vehicle buyers to those who were more likely to pay cash rather than finance the vehicle. If this tax credit could be converted into a reduction of the purchase price, its impact on sales would be much greater and more equitable to those who purchased on credit. The data provide strong evidence that a combination of economic and social incentives may be the most effective for the successful introduction of PHEVs. Indeed, social forces play an important role in most purchases, including vehicles. The survey documented the significant influence of hybrid vehicles in signaling people's commitment to a clean environment. Nonetheless, the importance of the attitudes toward the environment in explaining hybrid purchase probabilities provides less compelling evidence of the underlying demand than if preferences for hybrids were mostly based on

economic criteria. The presumption is that following the introduction of PHEVs, if the vehicle is priced so that consumers can recoup their initial investments over a reasonable time period, consumers would find ample economic justification for the purchase of a PHEV. The critical role of environmental and other non-economic attitudes is to provide the initial burst of interest and sales to propel the appeal of PHEVs to the mass market.

Publications and Presentations

Richard Curtin, “When we build it, will they come,” Plenary Panel, “The Business of Plugging In: A Plug-in Electric Vehicle Conference,” sponsored by the University of Michigan, DTE Energy, General Motors, and The Center for Automotive Research, and held in Detroit MI Oct 19-21, 2009.

PHEV MARKETPLACE PENETRATION. AN AGENT-BASED SIMULATION (JOHN SULLIVAN)

Introduction

This work explores an agent-based approach to understanding future vehicle markets. The approach is a simulation method that creates a computer-based (virtual) market built out of finite collection of heterogeneous individuals that participate in the market. These individuals are called “agents” and encompass new and used-car consumers, manufacturers, fuel-suppliers, and governments—all making decisions. Consumers’ decisions are based on their individual preferences and willingness-to-pay. The model incorporates interactions between agents, such that one individual’s decisions may be influenced by the decisions of her neighbors or co-workers. The model also permits exogenous “shocks,” such as sudden changes in fuel supply, or government regulations. The approach does NOT produce forecasts of future markets; rather it produces possible outcomes given sets of assumptions of how the individual agents decide. The agent-based “virtual automotive market place model” (VAMMP) is used for estimating PHEV penetration into the U.S. light-duty vehicle fleet.

Model Description

The VAMMP model is an agent-based model that simulates the automobile marketplace, which is

comprised of four classes of decision makers in software: consumers, government, fuel producers, and vehicle producers/dealers. These agents, virtual decision makers in the software, interact with one another and the environment (especially economic) based on their individual needs and/or organizational objectives. Each cycle (one month), consumers briefly review the status of their driving distance, fuel costs, and whether it’s time to buy another car. If it is determined that there is a need to change driving distance or buy a car, they act in a way to remain at least budget-neutral and meet their driving needs and model preferences. Nominally, agents can choose from twelve models of vehicles produced by three original equipment manufacturers (OEMs). At the end of each cycle, car dealers review sales and revenues, replenish the new car lots consistent with demand, and adjust the prices of used cars based on virtual market supply and demand. Government monitors system-wide fuel use, carbon emissions, and vehicle introductions and implements policies (fuel tax, vehicle tax incentives, etc.) to meet policy objectives. Finally, fuel producers provide fuels for automotive application and change prices both exogenously (petroleum induced gasoline price shock) and endogenously (competition between two fuel types).

Consumers (vehicle buyers) have home and work addresses, incomes, transportation budgets, vehicle preferences (size, performance, and sometimes brand and special features), driving needs (city and highway driving for errands, commuting, and discretionary trips), and preferred duration of vehicle ownership before buying another vehicle. The consumer agents live in neighborhoods consistent with their income and transportation budgets. In every time period (one month), consumers not only review their transportation distance driven and associated costs, but also whether it is time to buy another vehicle.

Cars come in three sizes (small, medium, and large, denoted 1, 2, and 3) and three performance levels (low, medium, and high, denoted 1, 2, and 3). All vehicles have city and highway fuel economy as well as prices. Generally, large, high-performance vehicles (short 0 to 60 times) are priced higher and tend to have lower fuel economy than average; whereas just the opposite is the case for small, low-performance vehicles. Permuting this range of

vehicle attributes results in nine vehicle segments, though all are not present (e.g., no large low performing vehicles are included). As there are three OEMs, some segments have vehicle entries made by competing OEMs. There are a total of 12 models of vehicles in the vehicle population, though in some cases some new types of vehicles are added to the population. The introduction of HEVs or PHEVs takes the vehicle model population beyond 12 models to between 13 and 15 vehicles. All cars have two stages to their lifetime, one as a new car and one as a used car. After these two stages, the vehicle is scrapped. The price for a new car ranges between about \$12,000 for a small, low-performance vehicle to \$33,000 for a large, high-performing vehicle.

Car lots come in two varieties, new and used. Every cycle, numbers of and revenues from vehicle sales are tracked. In the case of new vehicles, these numbers are used to generate demand- and revenue-based values for restocking new car lots with vehicles acquired from OEMs on an unlimited basis with the various models available.

Government's role in the model is to monitor fuel sold, fleet vehicle fuel economy, and carbon emitted and to implement policies depending on various environmental and energy security considerations. In this study, we explored the following government policy instruments: subsidies for PHEV production, tax rebates on PHEV sales, gasoline tax increases, and sales tax exemptions. More details of this are given in the HEV and PHEV sections.

Fuel Producers: There are two fuels germane to the PHEV market penetration case addressed herein: gasoline and electricity. For conventional and HEV fleet scenarios, gasoline is the relevant fuel. Fuel prices are set exogenously and in this simulation gasoline prices range from \$2/gal to \$4/gal; electricity prices remain fixed at \$0.095/kWh.

Results: Penetration of PHEVs into the U. S. Auto Marketplace

This part of the study is to model specific policy initiatives and their influence on PHEV marketplace penetration. We are interested in near-term sales and fleet penetration behavior, more specifically at five and ten years out from the start of the simulation.

Results for PHEV penetration curves are shown in Figure 3. These curves show considerable variation, especially approaching simulation terminations. The curves displayed either show or will ultimately show an S-shaped logistics-type form of the penetration curves—though none have to reach their asymptotic limit.

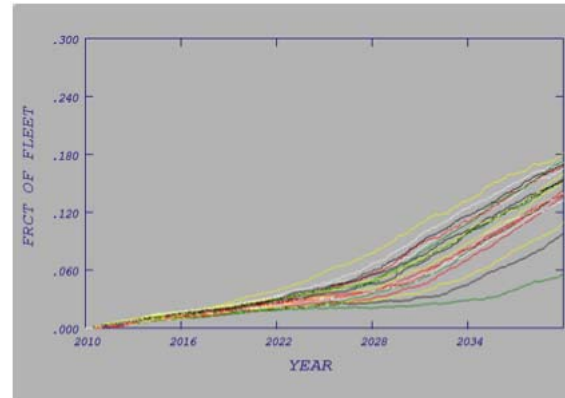


Figure 3. Penetration of PHEVs into the simulated market place; 20 runs; for full tax rebates, OEM subsidies and a tax sales tax break

All scenarios in the PHEV study start with the base case. The *base case* for the PHEV simulation study assumes that the current Federal tax rebate program for PHEVs is in place. The purpose of that program is to encourage new car purchasers to buy a PHEV using a tax credit, which ranges between \$2,500 and \$7,500 based on energy capacity in the battery.

Figure 4 presents a more detailed view of the shifts in the vehicle ownership distribution over the course of the simulation for scenario 4-Y-N. The dash marks in the figure show the ownership distribution at the simulation start. The bars represent it at simulation conclusion. It is clear that many consumers are opting for the cheapest, most fuel efficient vehicles, namely models 1, 6, and 9 as well as the PHEV models 5, 10, and 15. Overall, ownership of larger, higher performing, less fuel-efficient vehicles is down, relative to simulation start time.

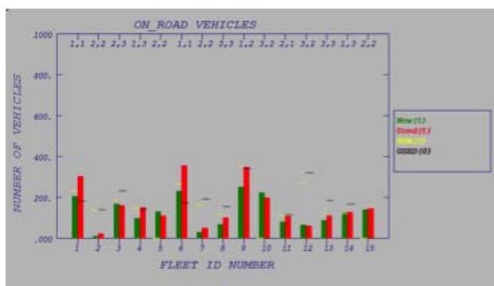


Figure 4. Fleet vehicle model ownership by vehicle ID number; numbers at top denote size and performance; dashes (reference marks) denote ownership levels at simulation start time

Conclusions

The simulation tool (VAMMP model), is a dynamic model that includes four classes of decision makers: consumers, government, vehicle dealers (and OEMs), and energy suppliers.

The model was applied to estimating the penetration of PHEVs into the U.S. auto marketplace. The results of the agent-based modeling study of PHEV penetration into the U.S. auto marketplace show that tax rebates, PHEV subsidies, and sales tax exemptions have a significant impact on PHEV penetration levels. Our simulation results show that a suitably incentivized auto marketplace can facilitate PHEV penetration levels into the U.S. automobile fleet. More specific results are as follows:

- By 2015, sales could reach 2 to 3% with fleet penetration of around 1%.
- By 2020, sales could reach around 4 to 5% with fleet penetration a little more than 2%.
- Without subsidies, the current policy case would result in a fleet penetration level of less than 1% in ten years.
- Subsidies are critical; sales tax exemptions can help if applied to scenarios where OEM subsidies are in place.

Because the individual vehicle replacement rate is a limiting factor in any market turnover scenario, it will take time to turn over the fleet even if new vehicle technologies have marketplace acceptance. A gasoline tax increase of about 5¢ per gallon would support government funding to incentivize PHEV sales. Finally, a PHEV fleet penetration of around

18% would reduce gasoline consumption by over 20% and decrease fossil carbon emissions by about the same amount.

Publications and Presentations

J. L. Sullivan, I. Salmeen, and C. Simon, PHEV Marketplace Penetration, An Agent Based Simulation, UMTRI Technical Report 2009-32, July 2009.

The Virtual Automotive Marketplace Model (VAMMP), A Case for the Plug In Hybrid Electric Vehicle, J. L. Sullivan, I. Salmeen, and C. Simon, The North American Association for Computational Social and Organization Science (NAACSOS) Conference, Phoenix, Arizona, Oct. 23, 2009.

MARKET MODELS PREDICTING PHEV ADOPTION AND DIFFUSION (WALTER MCMANUS)

Introduction

Complex system models (or agent-based models) and market models represent distinct but complementary approaches. Market models focus on predicting aggregate market-level outcomes, such as product units produced and sold, selling price, production cost, and the ultimate size of the potential market. Economic theory links the aggregate market outcomes to the underlying choice behavior of individual consumers, dealers, or other entities that participate in the market. In effect, all individual consumers are aggregated into a single “representative consumer” who is a rational economic optimizer. Agent-based modeling, on the other hand, starts with agent (buyer, dealers, government) preferences and basic behavior rules and allows them to interact, thus projecting into the future and looking for collective responses (market penetration). This may or may not be optimal. The two approaches working together permit a thorough elucidation of the behavior of the players and a better sense of the likely success of PHEVs in the automobile marketplace.

Market and Demographic Assumptions

The common assumptions describe the household market for all light vehicles for 2010 through 2050, including sales of new vehicles, growth in the

installed base of all light vehicles, and scrappage rates for all light vehicles. We started with the 2010-2050 forecasts of vehicle stocks and sales presented in the AEO (2009). Since AEO forecasts include vehicles owned by business, government, and households, we adjusted our forecasts to exclude business and government using U.S. Bureau of Economic Analysis (2009) and U.S. Census Bureau (2007).

Models with a Fixed Saturation Level

We developed four “benchmark” models that predict the diffusion of PHEVs. These include Bass, Generalized Bass, Logistic, and Gompertz models. All four models have a fixed saturation level, and three (Bass, Logistic, and Gompertz) generate unconditional predictions because they are single-variable functions of time. In Generalized Bass, sales depend on time, price, and the value of fuel saved. Thus, in order to predict sales one needs first to predict price and value of fuel saved. In models with a fixed saturation level, price and other variables operate to change the shape of the diffusion curve, but not the ultimate market potential.

Bass and Generalized Bass describe the diffusion of new products as the result of social interaction between users and potential users of the product. Like many economic models, Bass models predict the aggregate market outcomes with parameters estimated on aggregate data, which are then interpreted in terms of the behavior of individual consumers.

The Benchmark Models

The producers (sellers) of a new product can influence the rate at which potential users become users through the four Ps of marketing—product, price, place, and promotion. The rate at which potential users become users is also influenced by social and economic interaction between users and potential users—word-of-mouth and plainly visible (and even conspicuous) consumption choices of neighbors, co-workers, and co-commuters. The four Ps are external interventions that aim to directly influence some potential users to become users. Word-of-mouth and conspicuous consumption are channels of influence that are internal parts of the social/market system.

Results with a Fixed Saturation Level

The benchmark models results shown in Figure 5 imply a small market for the PHEV.

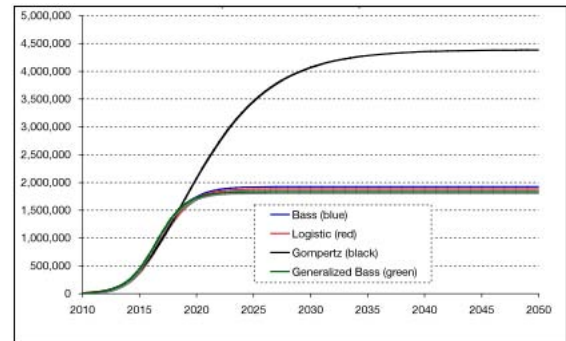


Figure 5. Benchmark Scenario Predictions of Cumulative PHEV Adoptions

The Gompertz scenario predicts an ultimate market more than twice that predicted by the other benchmark scenarios. However, in a market with more than 200 million vehicles in use, there is not much practical difference between an installed base of two million and one of four million PHEVs. Similarly, peak annual sales of between 340,000 and 370,000 PHEVs would not have much impact in a market with 15 million annual sales. These predictions have some caveats. We assumed HEVs and PHEVs are analogous products, not just generations of the same product. If we had assumed they were generations of the same product, then our market predictions would be even smaller. Only Generalized Bass has behavioral variables (price premium and fuel costs), but in the Generalized Bass model, these variables change the shape of the path to saturation but not the ultimate market potential.

Models without a Fixed Saturation Level

To overcome some of the limitations of the benchmark models, we developed two models that do not have fixed saturation levels. Each of these models examines a different set of factors that could have an impact on the ultimate market potential. One model, presented in Centrone in 2007, incorporates demographic factors that describe the growth of the population of potential adopters in terms of birth and death rates. The other model, which we call the consideration-purchase model (suggested by Struben and Sterman in 2008),

incorporates factors from the domains of consumer choice and vehicle stock-flow dynamics.

Summary of Research Findings

We developed the consideration-purchase model (suggested in Struben and Sterman [2008]) to build on the strengths of the benchmark and Centrone models, while overcoming some of their limitations. The model explicitly incorporates a consumer choice component that can be expanded well beyond its current simplified form. The highly simplified form was chosen to match the “choice experiment” in the PHEV survey (Curtin et al. 2009) for the \$2,500, \$5,000, and \$10,000 price premiums. The model also accounts for the dynamics of vehicle sales, stock, and scrappage. The results are shown in Figures 6 for annual sales and Figure 7 for vehicle stock.

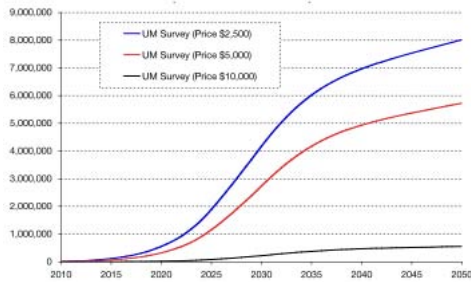


Figure 6. Survey Price Scenario Predictions of PHEV Sales

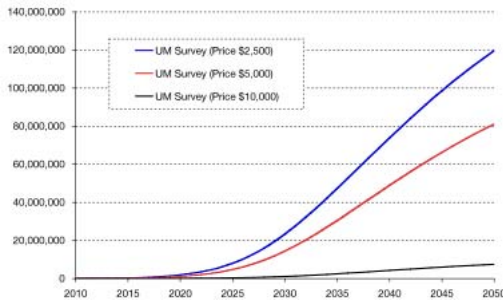


Figure 7. Survey Price Scenario Predictions of PHEV Stocks

Conclusions

We examined predictions of PHEV market diffusion derived from six market models. Four models assumed fixed saturation levels and were used as benchmarks: Bass, Generalized Bass, Logistic, and Gompertz. One model used demographic factors to

describe growth in market potential in terms of births and deaths of the population of potential adopters (Centrone). Our preferred model used factors related to consumer consideration and purchase choice and factors related to vehicle stocks and flows to describe PHEV adoption and diffusion as a complex dynamic system.

The predicted saturation level of adoptions is just under two million for the Bass, Logistic, and Generalized Bass models; and 4.4 million for the Gompertz model. The benchmark models track very closely for the first nine years after introduction, attaining 1.5 million cumulative adoptions. Thereafter, the Gompertz cumulative adoptions curve rapidly diverges from the others. These predictions have some caveats. We assumed HEVs and PHEVs are analogous products, not just generations of the same product. If we had assumed they were generations of the same product, then our market predictions would be even smaller. To overcome some of the limitations of the benchmark models, we developed two models that do not have fixed saturation levels. Each of these models examines a different set of factors that could have an impact on the ultimate market potential.

Our consideration-purchase model predictions for PHEV sales are extremely sensitive to price premiums. Five years after introduction, in 2015, sales range from 118,793 units (at a premium price of \$2,500) to 4,726 units (at a price of \$10,000). This range grows rapidly. Fifteen years after introduction, in 2025, sales range from 1,891,576 units (at a price of \$2,500) to 84,341 units (at a price of \$10,000). Twenty-five years after introduction, in 2035, sales range from 6,021,141 units (at a price of \$2,500) to 379,615 units (at a price of \$10,000).

IMPACTS OF PHEVS ON THE RELIABILITY OF THE ELECTRIC GRID (JOHN LEE)

Introduction

The increasing interest in a large-scale introduction of PHEVs into the market raises the concern that the reliability of current distribution circuits will be adversely impacted, especially in residential areas. This study presents the development of probabilistic reliability models for distribution circuits. The study focused the reliability impacts of distribution

systems due to the new load expected from the growing PHEV fleet. The study was based on outage events recorded in the DTE Energy’s system outage and data analysis (SODA) in an attempt to analyze how the reliability indices may be changed as a result of serving the additional PHEV load.

Of the entire 2,732 circuits for the DTE system providing 11 GWe to 2.2 million customers, this study is limited to the analysis of 167 circuits in the Ann Arbor area, which serves 146,115 customers.

Probabilistic Model for Circuit Reliability Analysis

We introduce a fault tree (FT) model to obtain the probability that a load point will lose power. Figure 8 shows all the basic events that can lead to load point failure in the circuits we are analyzing. For example, let λ_{OHL} and λ_{UGL} be the failure rate of overhead line and underground cable, respectively. During a mission time T , the probability of overhead line failure P_{OHL} is given by:

$$P_{OHL} = 1 - \exp(-\lambda_{OHL}T) \approx \lambda_{OHL}T. \tag{1}$$

Similarly, we set $P_{UGL} \approx \lambda_{UGL}T$. After some manipulation, we obtain the total failure rate of the conductor as:

$$\lambda_{conductor} = \lambda_{OHL} + \lambda_{UGL}.$$

The failure rate of the top event *Loss of Power to Load Point* can similarly be obtained by summing up the basic event failure rates (Figure 8). Most load points are served by either an overhead or an underground transformer. In either case, only one transformer is in the fault tree. However, if multiple line paths can reach a load point, and the transformers are not fused, then faults from other transformers may affect the load point. In such a case, our fault tree structure will remain the same, but now the *transformer fault* event will need to account for other transformers as well.

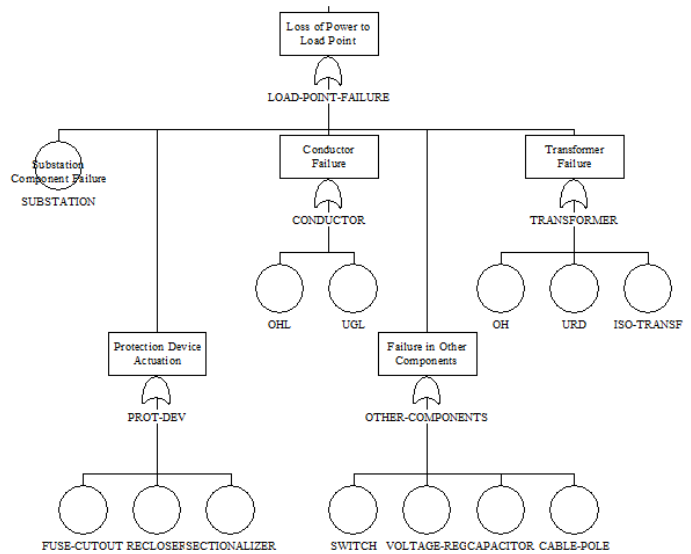


Figure 8. Fault tree showing key events leading to loss of power to load point represented as the top event

Reliability Indices for Ann Arbor Circuits

Stochastic reliability calculations were performed on 167 circuits within the Ann Arbor region. This accounted for 29,356 load transformers serving 146,115 customers over 2,074 miles of overhead lines and 1,145 miles of underground cables. The aggregated failure rates and repair times of components that were extracted from SODA files between 2005 and 2008 are expressed in commonly used reliability indices and summarized in Table 1.

Table 1. Reliability Indices for Ann Arbor

	SAIFI	SAIDI	CAIDI
OVERALL	1.8	17.9	9.8
Substation	7.80%	2.40%	1.64%
Load Transformer	1.37%	2.32%	1.62%
Overhead Line	71.33%	76.37%	77.63%
Underground Cable	3.63%	3.14%	1.97%
Fuse Cutouts	2.67%	2.59%	2.55%
Cable Pole	0.86%	1.00%	0.59%
Recloser	3.92%	3.45%	3.56%
Sectionalizer	5.29%	4.85%	6.43%
Step Up/Down Transf.	1.46%	2.21%	2.45%
Capacitor Bank	1.53%	1.63%	1.53%
Disconnect Switch	0.14%	0.05%	0.03%
Voltage Regulator	0.05%	0.00%	0.00%

SAIFI: System Average Interruption Frequency Index, denotes the average number of times a customer loses power per year. SAIDI: System Average Interruption Duration Index represents the average duration of outages a customer is expected to experience in a given year. CAIDI: Customer Average Interruption Duration Index measures average customer outage duration in a year.

Overhead lines by far contributed the most to reliability indices by over 70% followed by substation failures and underground cables.

A FT model was developed that attempts to represent the underlying physical causes of failure in the Ann Arbor system. The model was benchmarked with Ann Arbor circuit reliability indices after excluding weather related outages, which contributed about 20% toward the SAIFI.

Life of Transformers due to PHEV Charging

To analyze the impacts on distribution system failure due to the emerging PHEV load, we assess the transformer load-dependent probability of failure.

IEEE developed standards to calculate the transformer loss-of-life as a function of its load ratio. The loss-of-life in transformers is primarily caused by the accelerated aging (and ultimate breakdown) of the windings insulators as a function of the cumulative history of the internal temperature.

Using an approximate load profile scaled for a 50-kVA transformer, Figure 9 shows a load profile with and without PHEV loading.

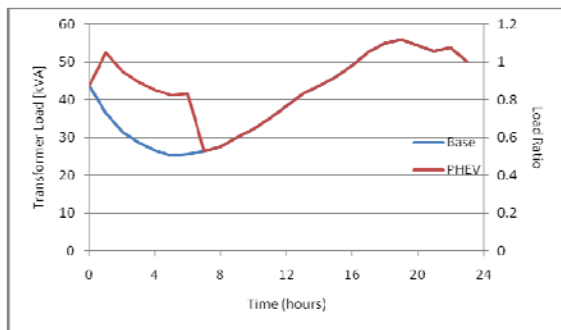


Figure 9. Load profile for a transformer over 24 hours with and without PHEV load

Assumed are eight PHEVs charging at a rate of 2 kW from 1 a.m. to 7 a.m. Table 2 shows the loss-of-life impacts as a function of charging profiles. The charging schedule over night (1 to 7 a.m.) has only a 6% increase on the loss-of-life. Charging coincident with the other loads (5 p.m. – 11 p.m.) will increase the aging of the transformer by 95 months after oneyear of operation.

Table 2. Transformer aging over one year as a function of charging time

	Aging (months)	% impact
NO PHEV	1.7	0
5 PM - 11 PM	95	5400
8 PM - 2 AM	36	2000
11 PM - 5 AM	4.6	170
1 AM - 7 AM	1.8	6

Expressed in terms of failure rate, if the transformer operates at the constant load ratio of 1.4, then the transformer failure rate will increase from 1.7%/yr to 12%/yr. In this case, the overall reliability index of the circuit remains small because of the transformer’s small contribution to the overall reliability (1.3% to the annual SAIFI).

Summary and Conclusions

The analysis of DTE’s Ann Arbor distribution system failure events indicates the major contributions to outages represented in the three reliability indices (SAIFI, SAIDI, CAIDI) are overhead lines, substation failures and underground cables.

Using the IEEE guide on transformer aging, we have studied the impact of different load profiles on the mean life of the service transformer. We have considered different starting times for a 2-kW, six-hour battery charging superimposed on a generic load profile for a 50-kVA residential transformer to determine the impact of the accelerated aging on the transformer. In the worst scenario, where the PHEV charging takes place around the peak load, the mean life of the transformer could be shortened from a nominal value of 60 years to 40 years. Although there is considerable uncertainty in our estimation of the mean life of transformers in place in the DTE circuits, it is clear that some of the older units would be much more susceptible to early failures than newer units. Given diversity of transformer ages in DTE’s footprint, co-incident charging could have a significant impact on the health and lifetime of transformers in DTE’s grid. This also indicates the need to implement optimal PHEV charging schedules through the growing AMI infrastructure.

U. Predicted Impact of PHEVs to the U.S. Power System

Michael Kintner-Meyer (Project leader)
Pacific Northwest National Laboratory, P.O. Box 999
Richland, WA 99352
(509) 375-4306; Michael.Kintner-Meyer@pnl.gov

DOE Technology Manager: Lee Slezak
(202) 586-2335; Lee.Slezak@ee.doe.gov

Objectives

Perform a comprehensive grid impact analysis of plug-in hybrid electric vehicles (PHEV) on the U.S. grid. The analysis focused on the following specific objectives:

- Evaluate the impacts of a high concentration of PHEVs in distribution systems.
- Evaluate the production cost and emissions impacts of PHEVs in U.S. bulk power systems.

Approach

This is the second year of a two-year joint project between the University of Michigan (UM) and Pacific Northwest National Laboratory (PNNL). UM primarily focused on the vehicle-related R&D aspects that provided market penetration curves of PHEVs. The results of the UM work were utilized by PNNL to assess impacts of the emerging PHEV load on the current and future electric infrastructure with respect to reliability, production cost of electricity, and associated emissions.

Accomplishments

PNNL's accomplishments:

- Completion of the distribution system impact assessment.
- Completion of a structured survey to estimate future PHEV market adoption for PHEVs under different market conditions.
- Developed a set of charging profiles based on the Department of Transportation's (DOT) 2001 National Household Travel Survey.
- Completion of the modeling runs for production cost and emissions impacts.

Future Directions

Final reports for the impacts assessments will be completed in early 2010. Additional analyses on grid impacts will be performed focusing on the interactions of electric vehicles and renewable energy resources. This will be performed in collaboration with NREL.

DISTRIBUTION SYSTEMS ANALYSIS

Introduction

Charging PHEVs from residential electrical outlets is both practical and convenient from the owner's perspective. The existing electric power delivery

system offers a natural advantage in being already built with the capacity to serve peak loads. As a consequence, it tends to be under-utilized during off-peak periods. If charging strategies can be planned and coordinated to match the availability of this off-peak capacity, a national fleet of PHEVs could be accommodated with little need to increase the

energy delivery capacity of the existing grid infrastructure. In practice, this ideal opportunity may be compromised by several factors, including the size and distribution of the PHEV fleet and the timing of vehicle charging activity.

PNNL addressed three basic questions concerning how typical existing electrical distribution systems could be impacted by the addition of PHEVs to residential loads. These questions are:

- How many vehicles can the existing power delivery system support in the near future?
- What time of day are PHEVs being charged?
- Where vehicles are being charged?

This study complements other research performed for the Department of Energy (DOE) by UM in collaboration with PNNL on various issues relating to PHEV adoption, marketability, and impacts on the electric power grid.

Focus of the Present Study

The present study has a close relationship to the work of Lee et al. of UM summarized earlier because it expands consideration of the impacts PHEVs may have on the electric power grid. While Lee et al. focused on the load-dependent reliability impacts of distribution systems by modeling life reductions in secondary transformers, this analysis analyzes the limiting factors and components in distribution system as a result of high concentrations of new PHEV loads. This analysis is based on electric load flow techniques for selected PHEV penetrations to observe which, if any, components of main distribution feeders that exceed their capacity.

This analysis also addresses the impact of the additional load on the distribution transformers serving each individual load. As the principal measure of this type of impact, the peak percent loading (provided by the relationship of kW load to transformer kVA capacity) is estimated for the existing loads and then compared to load conditions when PHEV load was added. In both portions of the study, three electric utilities located in Washington State: Franklin Public Utility District (PUB), Snohomish PUD, and Puget Sound Energy (PSE) collaborated by providing information that allowed system-specific feeder modeling.

PHEV Charging Profiles

The key assumptions that drive the outcome of this impact analysis are (1) the assumptions related to the time of day when the vehicles are likely to be recharged, (2) the locations where the vehicles are connected to the electric grid, and (3) the rate at which the PHEVs are recharged (fast versus slow charging). Fast charging would likely require charging at higher voltage and current ratings when compared to the commonly used 120-V, 15-A rated outlets of most residences. Charging at 240 V and 30 A or even at 50 A would significantly increase the rate of electricity transfer to the battery. Thus, it is likely to have higher impacts on the electric infrastructure both at the charging premise (in most cases the home) as well as the distribution system as a whole.

The market adoption estimates of PHEVs were treated somewhat differently than applied in other studies. Rather than estimating a certain penetration of PHEVs that impact the U.S. distribution system, we framed the problem by first hypothesizing a number of PHEVs per residential home (single detached homes), and then analyzing the likely impacts. Specifically, we defined a 100% PHEV scenario, meaning one PHEV per residential customer (home), and a 50% scenario, in which every second home has a PHEV.

Charging Scenarios

In the absence of established real world data on PHEV charging patterns, this study assumed plausible charging scenarios based on DOT's 2001 National Household Travel Survey. A set of charging profiles were developed that were derived from approximately 32,000 individuals who logged trips performed with a personal vehicle. From these logs, driving patterns and resting periods at the home were computed. The following six charging cases represent scenarios covering the most likely range of charging strategies to be expected when PHEVs become more common:

- **Case 1** – 120-V charging at home.
- **Case 2** – 120-V charging at home and work.
- **Case 3** – 120-V charging at home delayed until after 10 p.m.

- **Case 4** – 50% of all vehicles at 120V, 50% of all vehicles at 240V (50/50 at 120/240V) charging at home.
- **Case 5** – (50/50 at 120/240V) charging at home and work.
- **Case 6** – (50/50 at 120/240V) charging at home delayed until after 10 p.m.

The charging cases that include opportunity charging at work were modified to only account for the charging at home. This modification became necessary because the opportunity charging at work would impact that distribution system at a commercial or industrial location where the incremental increase in load would likely be much smaller than the impacts of one or two PHEVs at home. It should also be noted that there is a difference in the residential electricity consumption for a PHEV that is exclusively charged at home versus one that has the opportunity to charge at work. The energy requirements for home charging are less when the battery was recharged at work.

We named the modified cases as (a) Case 2M – 120-V charging at home and work – home only, and (b) Case 5M – 50/50 at 120V/240V charging at home and work – home only.

Figure 1 shows the charging profiles for the six scenarios investigated. All curves represent the actual load measured at the battery of the PHEV, assuming that the battery charging circuit has a round-trip efficiency of 87% (Duvall, 2002). A PHEV 33 is assumed at the current distribution into vehicle weight classes as described in (Kintner-Meyer, 2007). Load duration in each case accounts for the transfer of sufficient energy to recharge the PHEV battery until either the battery is full or the vehicle is being disconnected from the grid. Each curve is modified to represent the actual load seen at the secondary of the distribution transformer serving the individual residence. For the “Charge at Home and Work” curves (Cases 2M, 5M), only the electricity delivered at home was considered.

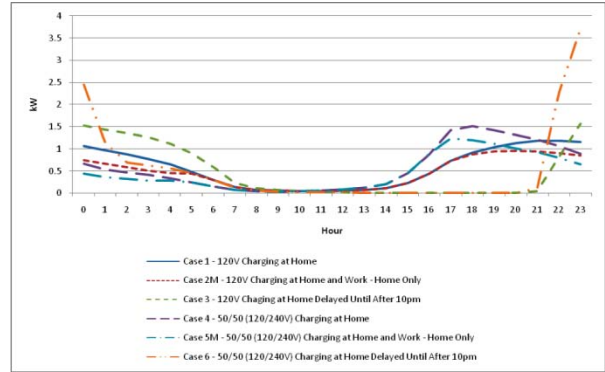


Figure 1. Charging Profiles

Feeder Characterization

To assess the differential impacts of PHEV charging, it was necessary to establish a baseline characterization of the domestic feeders involved in terms of representative hourly load profiles and load composition. To capture diversity in how different utility companies design and size distribution system components, we analyzed representative distribution system feeders with primarily residential customers from three electric utilities in the Pacific Northwest, one investor owned utility (IOU) and two public utility districts. To mask some of the proprietary data of these collaborating utility organizations, we assigned numbers to the utility organizations, such as utility No. 1, 2, and 3. Each utility partner provided very detailed infrastructure data of its distribution systems. This included the topology of the feeder configuration, detailed physical and electrical characteristics of each component in the distribution system to perform accurate power flow analyses. A total of 50 feeders were analyzed.

Study Methodology

An analysis of PHEV impact was performed on each representative feeder superimposed on present feeder loads and load configurations. The impacts at two levels of hypothetical PHEV load penetration were investigated: 50% and 100% PHEV per residential customer.

The analysis is based on several primary assumptions:

- PHEVs are distributed evenly through the system; there are no location-specific concentrations of PHEVs.

- PHEVs are charged only at single-family residences. This excluded public charging stations.
- Impacts are analyzed for today’s system. Load growth was not considered.

For this study, power flow simulations were performed with new PHEV loads applied at single-family residences. Power flow analyses were performed using the SynerGEE analysis package (SynerGEE, 2009) for a representative day (24 hours) for all feeders with the 50% and 100% penetration rates and for the six charging profiles.

Load curves for a representative feeder in utility No. 1 are shown in Figure 2 for the 100% penetration rates assuming 120V/12 A charging.

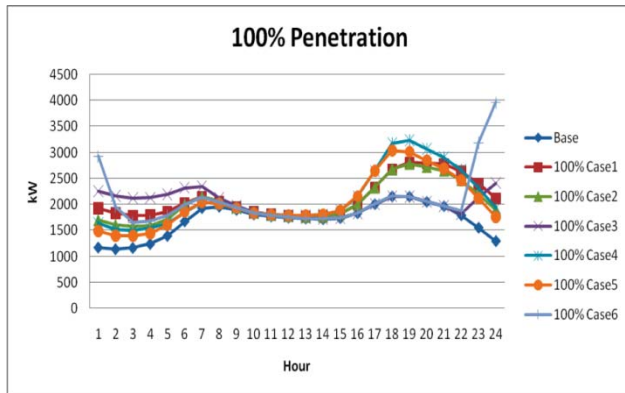


Figure 2. Representative Feeder Load Curve for 100% PHEV Penetration, Utility No.1

The results were used to determine whether or not the rated capacity of any feeder components (i.e., conductors, switches, fuses, and other protection and control devices) was exceeded. In addition, the adequacy of distribution transformer capacity was analyzed.

Results: PHEV Impacts on Infrastructure Loading

The distribution system components that failed from overloading and the number of feeders affected are indicated in Figures 3 and 4 for the various charging cases and PHEV penetration rates. The results are shown only for utility No.1, but they are representative for the other two utility organizations.

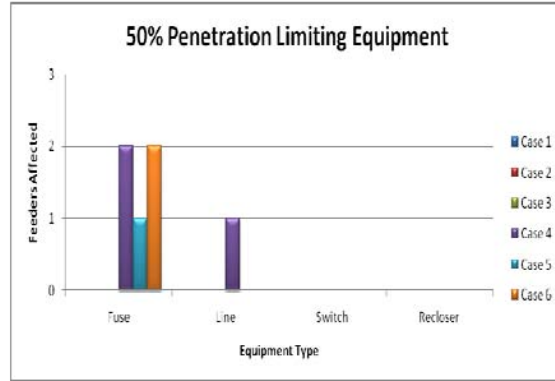


Figure 3. Number of Feeders with Equipment Failures by Type for 50% PHEV Penetration, Utility No. 1

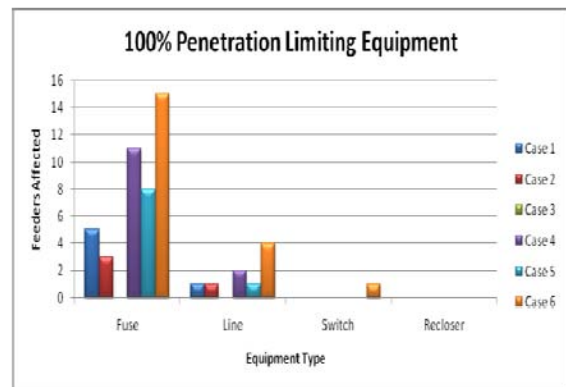


Figure 4. Number of Feeders with Equipment Failures by Type for 100% PHEV Penetration, Utility No. 1

Infrastructure Impacts of Fast Charging

In an earlier analysis (Schneider, Gerkenmeyer, Kintner-Meyer, Fletcher, 2008), a fast charging scenario was investigated for feeders in the Pacific Northwest. In the fast charging scenario, it is assumed that all PHEVs would begin charging system-wide within a three-hour period directly after individuals arrive home from work. The resulting charging profile is shown in Figure 5. It assumes minimal diversity and a 240-V/30-A charger. The impacts on the electrical distribution infrastructure for the fast charge scenario are evaluated using the same methodology as described above and presented below.

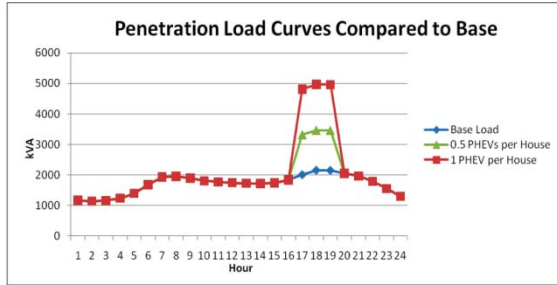


Figure 5. Feeder Load Curve in Fast Charge Scenario, Utility No. 1

Equipment failures, feeder penetration support, and load curves are shown in Figure 6 for utility no 1.

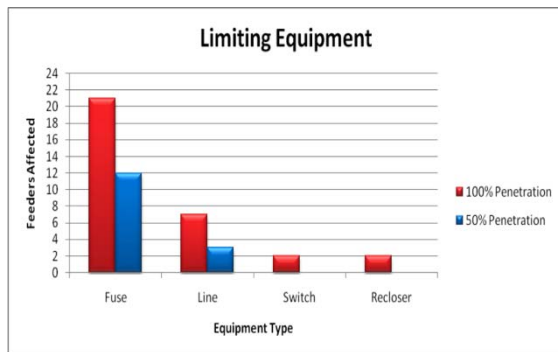


Figure 6. Number Feeders with Equipment Failures by Type in Fast Charge Scenario, Utility No. 1

Impacts on Secondary Distribution System Transformers

The addition of a PHEV load can have a more significant impact on the individual distribution transformers than on the system as a whole. While overloading a transformer may not have immediate impacts, when a transformer is loaded beyond its nameplate rating, the life of the transformer will be diminished based on the duration and the severity of the overload condition (IEEE Std. C57.91). In the second part of this study, load flow analyses were performed for each hour of a typical day to compare the rated kVA of each transformer with the peak load it experienced. The results are shown below for selected charging cases.

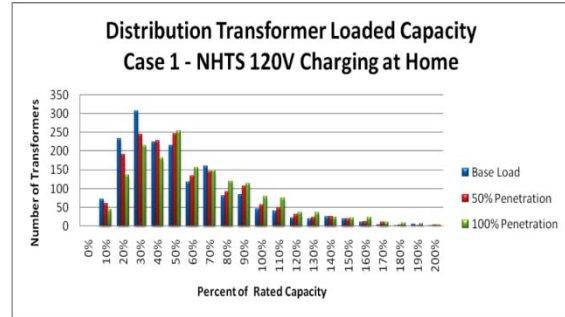


Figure 7. Transformer Loading for Case 1, Utility No. 2

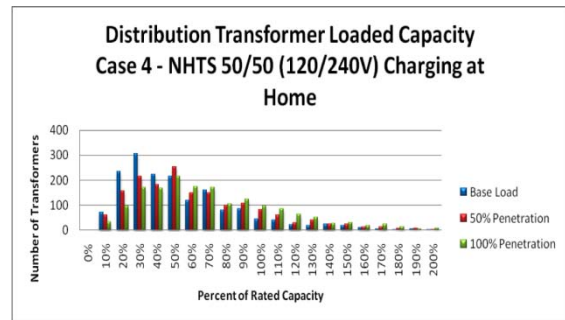


Figure 8. Transformer Loading for Case 4, Utility No. 2

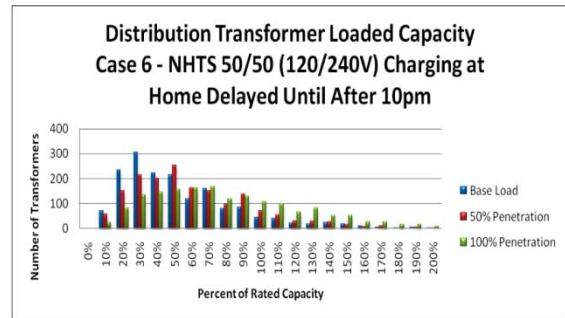


Figure 9. Transformer Loading for Case 6, Utility No. 2

Diversity Across Utilities

As seen in Figures 7, 10, and 11, there is significant diversity in how utility organizations size the system components. Furthermore, there has been a significant difference in the system component sizing practices over the years. Older distribution systems were sized for much smaller total residential loads than they are now.

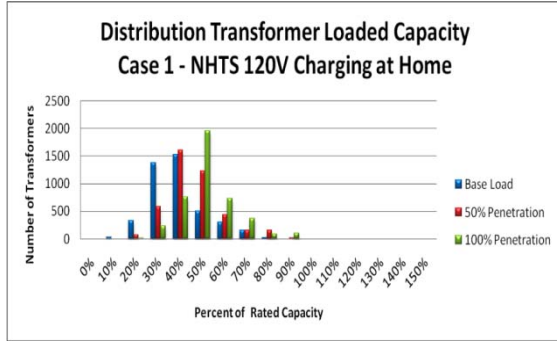


Figure 10. Transformer Loading for Case, Utility No. 1

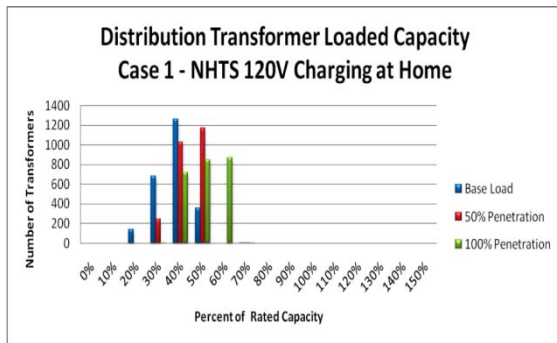


Figure 11. Transformer Loading for Case 1, Utility No. 3

Discussion of Results and Conclusions

Analysis of PHEV charging impacts on the representative feeders of three utilities in the Pacific Northwest showed that for the most part the rated capacity of individual distribution system components was not exceeded assuming diversified 120-V/12-A charging scenarios and a combination of 120-V and 240-V charging. Even at the penetration of 100% (one PHEV per home), a relatively small number of components exceeded their rated capacity. Most of those components were low-cost fuses, which is why most cases are sized very conservatively as the first line of defense in the protection schemes. We tested the options of using higher current rated fuses in an attempt to eliminate the load bottleneck. In most cases, the fuses were set very conservatively and could easily be upsized to support a higher load flow. In only a few cases an upsizing of the fuse revealed that other limiting power flow constraints remained, which were more costly to upsize.

In contrast, the fast charging scenario with little diversity has a broader range of system impacts.

Not only are fuses, switches, and reclosers impacted by higher loadings, but several line segments are as well. While distribution system lines can be operated under conditions beyond the rated capacity, their life expectancy is reduced. In some circumstances, overhead line sagging combined under high load conditions can interfere with vegetation (trees) and cause ground shortening. Thus, overall fast charging strategies are likely to have a higher impact on all distribution system components than do slow charging strategies at 120V.

Furthermore, in some cases, the additional load introduced by PHEV charging was found to increase the time secondary distribution transformers operate in excess of rated capacity. Supported by the findings of Lee et al. (2009), this will tend to have a direct impact on transformer life. Depending on whether a utility loads its transformers lightly or heavily, these results could be significant. Those utilities that have heavily loaded transformers should be able to use these results and the results of related studies (e.g., the UM study by Lee et al.) to determine how the life of the transformer will be impacted. In contrast, utilities with lightly loaded transformers may be able to verify that the additional PHEV load will not affect the life of their transformers.

The load curves developed in this analysis can be used by electric utilities to modify their own load curves to prepare for the emergence and increased deployment of PHEVs and other electric vehicles. Utilities can use the results and further extrapolate them to create new formulas for calculating the diversity factor that is used to size transformers for new and existing services.

Publications

Schneider, K.; Gerkenmeyer, C.; Kintner-Meyer, M.; Fletscher, R. Impact Assessment of Plug-In Hybrid Vehicles on Pacific Northwest Distribution Systems, IEEE PES General Meeting, July 20, 2008. Pittsburgh.

PHEV MARKET PENETRATION ANALYSIS (DELPHI APPROACH)

There are many analytical approaches that attempt to model customer acceptance and purchasing

decisions of new and used vehicles. For the purpose of this study, we performed a Delphi approach, which was based on structured interviews of industry professionals to elicit expert opinions of what a plausible and defensible penetration potential for PHEVs could be. Industry professionals from the automotive, battery, automotive supplier, and research communities were contacted by email. The email included survey questions and information on a prototypical penetration curve as represented by a logistic function. The interviewees were requested to provide specific loci on the logistics penetration curve for three distinct scenarios. For the purpose of this study, the second scenario was chosen as the most realistic yet optimistic penetration scenario. This study was predicated on the conditions that (a) DOE's cost and performance targets for PHEVs can be met, as specified in "Plug-In Hybrid Electric Vehicle R&D Plan" and (b) the tax incentives and positive regulatory environment governing current hybrid technologies are extended to PHEVs. The specific cost and performance targets for PHEVs include:

- \$4,000 marginal cost of PHEV technology over existing hybrid technology.
- 40-mile all-electric range.
- 100 miles per gallon equivalent.
- PHEV batteries meet industry standards regarding economic life and safety.
- Tax incentives, regulations, and technical standards favor PHEVs.

It should be mentioned that since the interviews in late 2007, the Emergency Economic Stability Act (EESA) of 2008(enacted on October 3, 2008) now provides a tax credit for plug-in electric drive motor vehicles, which includes electric vehicles (EVs) as well as PHEVs sold after January 1, 2010. These specific tax credits, not known at the time of the interviews, were presumed to be made available for future PHEV purchasers. In hindsight, the EESA substantiated the somewhat hypothetical assumptions postulated in the interviews. The resulting penetration curve is shown in Figure 12.

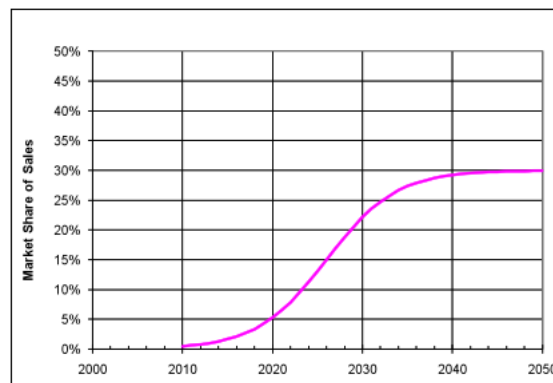


Figure 12. PHEV market penetration curve according to Balducci assuming that DOE's R&D goals are met.

The combined expert judgment suggests that the long-term potential of PHEV at about 30% of the total annual sales of new vehicles with a market penetration of about 23% in 2030.

This result is qualitatively in agreement with more recent studies performed by Sentech, Oak Ridge National Laboratory (ORNL) and UM. Sullivan et al. and McManus suggested a modest penetration of PHEVs when considering all of the competing vehicle propulsion technologies. Sullivan projected for the 2040 timeframe approximately 20% market adoption. McManus estimated less than 20% market penetration for 2050. Also, SENTECH, Inc. and ORNL recently published a report on the study of market introduction for PHEVs, in which the market penetration of all PHEVs (cars and light trucks) was at about 20% of the annual sales in 2030. It should be noted that the more recent results of various market penetration analyses point to a significantly lower market adoption rate than the 2007 Electric Power Research Institute (EPRI) and National Development and Reform Commission (NDRC) results, which for the 2050 long-term projection, projected 61% for the medium penetration scenario and 80% for the high scenario.

This resulting penetration trajectory was used as a key driver of all of PNNL's grid impact assessments.

PHEV IMPACTS ON PRODUCTION COST IN U.S. BULK POWER SYSTEMS

The following sections provide some preliminary results PHEV/grid impact assessment for the Western Grid (Western Electricity Coordinating

Council, WECC). Results for the Eastern Interconnect and the Texas grid (Electric Reliability Council of Texas) are currently being compiled.

Definition of Charging Profiles

In the absence of the real world data on charging patterns of PHEVs, one needs to postulate plausible charging scenarios that are based on driving patterns—particularly resting periods of vehicles that would allow the vehicle owner to recharge the PHEV battery. Although DOE is currently collecting vehicle data from retrofit PHEVs that include charging patterns, these data sets are in the early stages of covering a sufficient degree of regions and customer driving patterns. Thus, they were considered not ready to be the sole sources for developing comprehensive charging profiles valid for the U.S. as a whole.

As an alternative approach to real driving data, this study developed charging profiles based on simulations derived from DOT's 2001 Household Traveling Survey. This data set comprises representative U.S. driving patterns for privately owned vehicles derived from individual respondents' daily traveling diaries. The survey provided approximately 32,000 samples of daily trips using light duty vehicles. Given the starting time, locations, the destinations and arrival times of each trip in the survey, we determined the resting locations of a vehicle and its arrival and departure times at that location. Only two resting locations were of interest for the purpose of this study: (a) home and (b) work. At such locations, any vehicle would reside for longer periods of time (i.e., more than 15 minutes) and be able to be plugged-in for battery charging. Shorter durations such as those for brief errands were considered not suitable for battery charging opportunities. Furthermore, the estimated travel distance was used to determine the battery's state-of-charge (SOC) at the point of arrival. The SOC determined the maximum electric energy that can be transferred into the battery until the battery is fully charged.

Figure 13 shows the resulting charging profiles of a diversified population of vehicles.

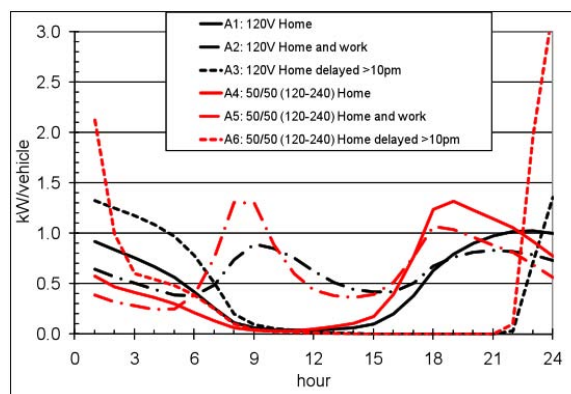


Figure 13. Set of charging profiles derived from DOT's 2001 Household Traveling Survey

Impacts of PHEVs on the Western Grid

This section discusses the preliminary results of the Western Grid. The impacts were determined for a 2030 scenario, for which we determined a plausible number of PHEVs on the road, as well as assumed a fleet of power plants that will be built between today and 2030.

We utilized the PHEV market adoption results based on the Delphi Approach mentioned above. The adoption trajectory for PHEVs is shown in Figure 14. It is expressed in terms of market share in percent of annual sales in the United States. We derived the number of available PHEVs in the fleet by inventorying old vehicles leaving the market being replaced by new vehicles. In addition, we applied a 1.4% annual growth rate of U.S. LDV. Using these assumptions, a total of 37 million vehicles are presumed to be in the total U.S. fleet. The 37 million PHEVs were apportioned based on existing vehicle registrations by State.

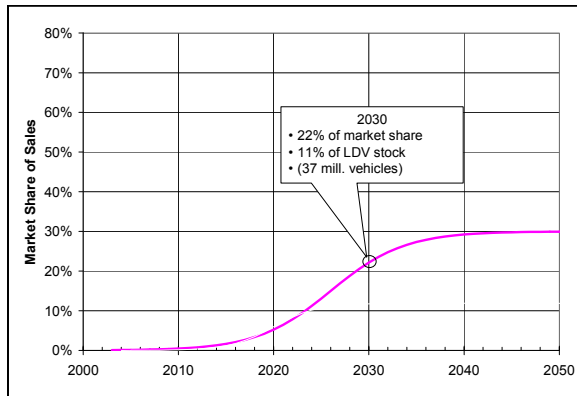


Figure 14. PHEV Penetration Projections based Balducci’s Delphi Approach

Methodology

We employed a commercially available production cost modeling software called PROMOD by Ventyx to perform a security constrained unit commitment and optimal power flow simulation for the entire Western Grid (WECC). This software is based on a rich and detailed representation of the cost-performance characteristics of over 1900 generator units in the WECC footprint, as well as the transfer limits among 64 balancing zones. To set up the scenarios for the PHEV and grid impacts analysis, we added the additional PHEV load and included the likely generation capacity additions as determined by the Annual Energy Outlook (AEO) 2009, Reference case for the 2030.

Production Cost Results

Figure 15 presents the average monthly production cost averaged across the entire WECC footprint for the year 2030. Across the three charging profiles, the “Home and Work” profile results in the largest average increase. This is particularly noticeable during the high load summer months when the available supply is tight. The higher production costs are due to the use of higher cost, gas-fueled, single cycle steam turbines and some combustion turbines, which are primarily used for only a few hours during peak load conditions. The “Home and Work” charging profile had the highest contribution toward the peak load conditions. Conversely, the production cost for the night charging (delayed until 10p.m. profile) resulted in the lower average cost for all of the three charging profiles utilizing low cost generation capacity during the off-peak periods.

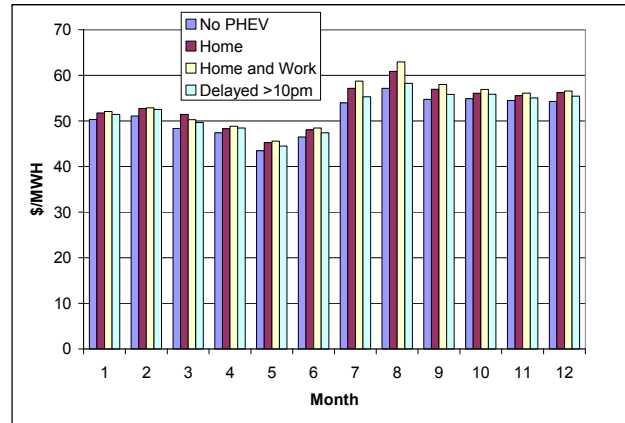


Figure 15. Average production cost of WECC in 2030 by months

Locational Marginal Price (LMP) Results

While the average production cost is a good indicator for the estimated cost necessary to generate and deliver the electricity to customers within the bulk-power system, the LMP provides a better indicator for the likely market response to the new PHEV load. The LMP is the marginal cost of the last generator necessary to deliver electricity to a certain balancing zone or node in the bulk power network. The locational aspect is of particular relevance when transmission lines or power transfers across or inside balancing areas are congested.

Table 1 shows the average hourly LMP for California and Arizona. The elevated average LMP for California is a clear result of congestion within the California footprint. Congestion was prevalent even without the PHEV (A0) scenario, which is a clear indication that the capacity additions as adopted from the AEO 2009 reference case was not sufficient for the load growth as assumed in the PROMOD software. Arizona, on the other hand, showed almost no congestion. Because of the congested conditions in California, the impact of day-charging (home and work) exacerbate the congestion cost with 40% increase in the average LMP compared to the base case (A0, no PHEV). The price impacts of day-charging during peak hours under unconstrained conditions are much more moderate, increasing the LMP by less than 4% (60 \$/MWh compared to 57.8 \$/MWh). These results are indicative for potential price response that could be expected when PHEVs are charged during peak periods when the grid is highly congested.

Conversely, there will be regions within the WECC where charging of PHEV would probably have less impact even during peak periods.

Table 1. Locational marginal prices for selected zone

Selected Zone (charging profile)	Locational Marginal Prices in \$/MWh
	Average
California(A0)	165.7
California(A1)	207.8
California(A2)	229.9
California(A3)	174.5
Arizona(A0)	57.8
Arizona(A1)	59.3
Arizona(A2)	60.0
Arizona(A3)	58.7

Marginal Emission Results

Of interest in the debate regarding the net carbon emissions of electric vehicles is the question on the emissions that could be assigned to PHEV. In other words, the emission on the margin that would be caused by dispatching power plants that otherwise would not be utilized in the absence of PHEVs. We evaluated the marginal generation by plant category for the entire WECC and then determined the carbon content of that generation. Because PROMOD did not allow us to determine the CO₂ emissions by hour by plant type, we determined the emissions using EPA emission coefficients as found in Energy Information Administration (EIA) form 1605, the heat rate as provided by PROMOD and the hourly generation by plant type in the model solution.

Figure 16 shows the marginal generation contrasting the two charging profiles A2 (charge a home and at work) and A3 (charge at home with a delay until after 10p.m.).

When we analyze the emission associate with the marginal generation of PHEVs, we found that the carbon content for the day charging (A2) is lower than that for night charging (A3). This result is due to the fact that more coal generation is utilized for night charging as percentage of the total generation to meet the PHEV load that during the full day charging. It should also be noted that on the margin the carbon content of the generation is significantly

larger than for the emissions based on the entire generation. This result is not surprising because of the large contribution of emission-free hydropower, which reduces the average carbon intensity. While the average carbon emission content for the WECC and in particular the Pacific Northwest is very low, on the margin, however, the generation is primarily based on the fossil fuel resources.

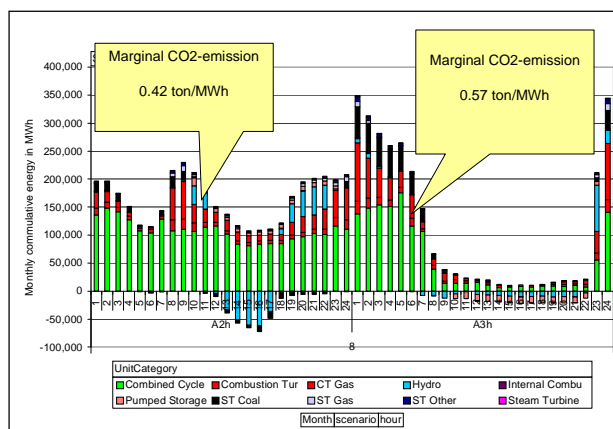


Figure 16. Marginal Generation for WECC for 2030 in August

Conclusions

Preliminary results were generated for the WECC. The results indicate that while the emerging PHEV load may only impact the average production cost of electricity to a small extent for the entire footprint, there may be zones within the WECC—most notably California, where the impacts of PHEVs may be felt more severely particularly when vehicles are charged during the day. Regarding the impacts on the CO₂ intensity of electricity (ton of CO₂ per MWh), for the WECC, it is likely that day charging may be associated with fewer carbon dioxide emissions per unit of electricity generated than during the night. This result indicates that there could be a conflict between charging at lowest cost and charging with the lowest carbon footprint. Under a future carbon cap and trade legislature, when the carbon emissions are monetized, we anticipate that the lowest cost and the lowest carbon intensity charging solutions will be one and the same if the price of carbon emission is sufficiently high.

III. INTEGRATION AND VALIDATION

A. Battery Hardware-in-the-Loop Testing

Neeraj Shidore (project leader)
Argonne National Laboratory
9700 South Cass Avenue
Argonne, IL 60439-4815
(630) 252-7416; mailto:nshidore@anl.gov

DOE Technology Manager: Lee Slezak

Objective

Use battery hardware-in-the-loop (BHIL) to analyze plug-in hybrid electric vehicles (PHEV), focusing on battery performance, life, and cost in the context of vehicle systems. In particular,

Analyze the impact of battery parameters on vehicle performance and fuel economy indices and

Analyze the impact of vehicle energy management on battery use in a vehicle, and relate it to battery life and performance.

Approach

Build a battery test stand in which the battery is connected to a bidirectional power supply that acts as a power source/sink.

Control the bidirectional power supply that acts as a power source/sink to/from the battery so that the instantaneous battery power is equivalent to the instantaneous battery power in a PHEV running a drive cycle.

Use Powertrain Systems Analysis Toolkit-PRO (PSAT-PRO) computer simulation software to emulate a PHEV, and control the direct-current (DC) power supply so that the battery can be evaluated in a closed-loop, real-battery/virtual-vehicle scenario (HIL concept).

Accomplishments

Completed a study on the trade-offs between fuel efficiency and battery cycle life, with a cost analysis. In this collaborative effort, Argonne's economic analysis team worked on the cost analysis with inputs from Johnson Controls-Saft (JCS).

Began a new experiment on managing PHEV energy to achieve a fast rise in battery temperature and quick improvement in engine efficiency at cold temperatures. Gold-Peak batteries will supply the battery modules necessary for this experiment.

Using battery HIL to develop the model-based design process for Argonne's "Autonomie" software.

Conducting experiments in support of SAE J1711 and J1634 task forces for developing PHEV and battery-electric vehicle (BEV) test procedures.

Future Directions

Complete the experiment on managing energy at cold temperatures.

Develop and validate the model-based design process for Argonne's Autonomie software.

Consider using an air-cooled battery pack to study energy management at high temperatures. More specifically, to examine how to manage vehicle energy to control battery usage and limit the rise in battery temperature, and to investigate the impact of such energy management strategies on fuel economy.

Link Argonne’s battery HIL and engine HIL tools for a simultaneous study of two key PHEV components.

Continue to support test procedure development.

Introduction

PHEVs have been identified as an effective technology for displacing petroleum. With regular charging, they draw significant off-board energy from the electrical grid. Rechargeable energy storage systems (e.g., batteries) have a much larger energy capacity than currently produced charge-sustaining (CS) hybrids. This larger energy storage system can be used to power a significant all-electric range (AER) or selectively power low-load portions of the driving demand. The battery’s response to variations in control choices will have a significant impact on vehicle-level performance. The needs of the battery under these control scenarios are of critical interest to battery developers. As such, emulation, modeling, and HIL testing techniques for a plug-in battery system have been developed to help accelerate the development of PHEVs for a mass market.

The most significant technical barrier to commercially viable PHEVs is in the energy storage system. The challenge here is to develop batteries that can meet the requirements imposed by a PHEV system, while meeting market expectations in terms of cost and life. In this context, a vehicle system approach becomes necessary in order to investigate the operational requirements specific to PHEV technology. Vehicle-level investigations determine (1) the relationship between component technical targets and vehicle system performance and (2) the entire system design’s potential to displace petroleum use. Battery HIL is an important tool in this vehicle-level investigation of PHEV batteries.

Approach

In BHIL, the battery is connected to a DC power source, which is controlled by a real-time simulation model that emulates the rest of the power train, for

PHEV operation (Figure 1). The vehicle model is derived from a simulation model developed using PSAT.

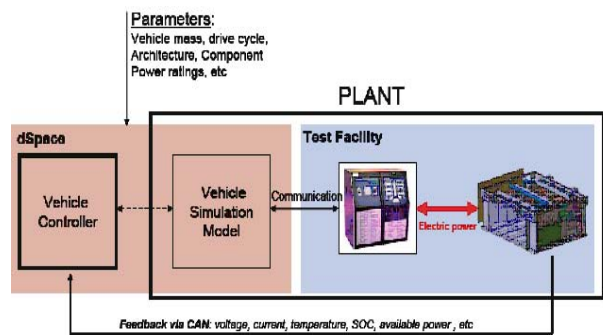


Figure 1. Battery HIL Represented as a Closed-Loop Plant-Controller-Feedback System

Accomplishments for Fiscal Year 2009

1. Completed a Study on Trade-offs between Fuel Efficiency and Battery Cycle Life, with Cost Analysis

Battery utilization was studied by using BHIL for a given virtual vehicle (Table 1) with a JCS battery.

Table 1. Vehicle Powertrain

Parameter	Value
Engine power (kW)	90
Motor power (kW)	80
Energy storage system (ESS) power (kW)	60 kW at 50% state-of-charge (SOC) for 30 seconds (physical battery)
ESS capacity (Ah)	41 (physical battery)
Number of cells for ESS	72 (physical battery)
Total vehicle mass (kg)	1,921

Battery utilization results were used to estimate equivalent battery cycle life. Then the trade-offs between cycle life and fuel economy gains based on

battery use were studied (Figure 2). For each energy management strategy, the amount (in dollars) of the net present value (NPV) of savings in gasoline (due to lower consumption) over the life of the vehicle was compared with the gasoline consumption of a conventional vehicle in the same vehicle class.

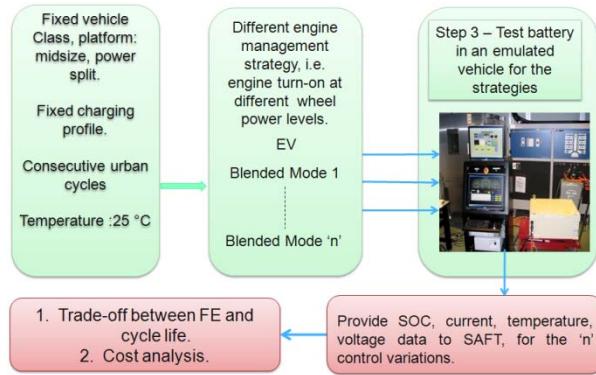


Figure 2. Experimental Process

A summary description of the vehicle and the energy management strategies is provided in Table 2.

Table 2. Virtual Vehicle, Drive Cycle, and Energy Management Summary

Vehicle	Power-split configuration; midsize vehicle with a mass of 1,921 kg.
Drive profile	Consecutive Urban Dynamometer Driving Schedule (UDDS) cycles for 40 miles of travel.
Energy management	Engine turns on the basis of the wheel power demand threshold. The threshold is varied to change battery utilization and engine fuel consumption values. Engine turn-on thresholds based on wheel power demand are 10, 15, 20, 25, 30, and 50 kW.
Battery temperature	Initial temperature of 25°C.
Battery SOC's	Initial SOC is ~90% for each test; battery is CS at 30% SOC.

The trade-offs between battery cycle life and fuel consumption based on different energy management strategies are shown in Table 3 and Figure 3, respectively, for 40 miles of UDDS driving.

Table 3. Battery Cycle Life and Fuel Consumption for the Different Energy Management Strategies

Engine ON threshold wheel power (kW)	Fuel consumption * (L/100 km)	Depth of discharge swing	Estimated battery cycle life (# Deep discharge cycles).	Normalized # deep discharge cycles
10	4.12	11%	x*50	50
15	3.22	26%	x*12.5	12.5
20	2.2	45%	x*2.5	2.5
25	1.56	~60%	x	1
30	1.4	~60%	x	1
50	1.5	~60%	x	1

* “Hot” start conditions assumed.

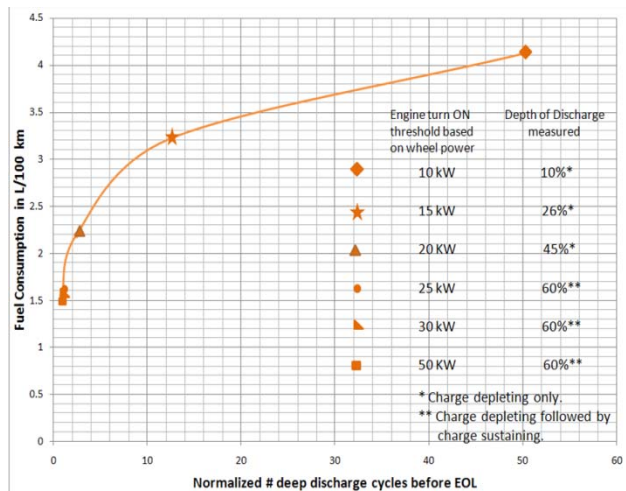


Figure 3. Trade-offs between Fuel Economy and Battery Cycle Life

The × in Table 3 represents the estimated cycle life for a 60% SOC swing. The U.S. Advanced Battery Consortium (USABC) target for the cycle life for 70% swing is 5,000 deep-discharge cycles. From Figure 3, the following observations can be made:

- A slight increase in fuel consumption results in a significant improvement in battery cycle life.
- $\frac{\Delta \text{Fuel consumption}}{\Delta \text{Battery cycle life}}$ is highly nonlinear. This is especially true for regions of the plot where battery life is less than or equal to vehicle life (normalized number of deep-discharge cycles is <10). This region of the plot is relevant for practical considerations.

- Fuel consumption and electrical consumption per mile have an inverse but linear relationship. However, this relationship is not true for battery life and electrical consumption. Battery cycle life increases nonlinearly with a decrease in electrical consumption.
- A common method of comparing PHEVs is to use a plot of alternating current (AC) in Wh/mi versus fuel in L/100 km, allowing for comparison of the location of their electrical and gasoline consumption points (in charge-depleting [CD] mode). If battery cycle life can be accurately predicted, two or more PHEVs can be compared by using a three-dimensional plot of fuel versus electrical AC versus battery cycle life.

The NPV calculations of the amount paid for gasoline (\$) saved over the life of the PHEV (when compared with a conventional vehicle) are shown in Figure 4. The NPV calculations are based on costs of \$3 per gallon for gas and 10 cents per kilowatt-hour for electricity.

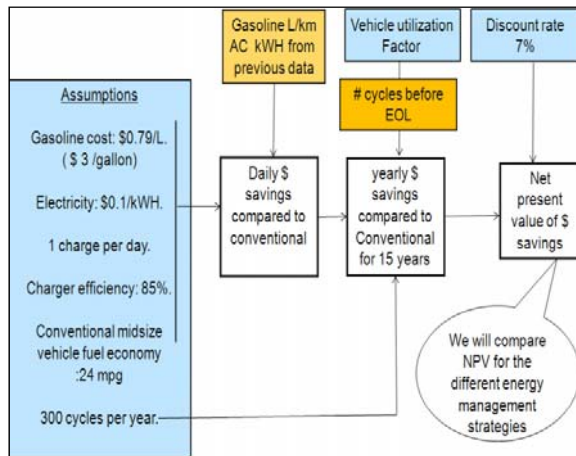


Figure 4. NPV Calculations for Each Strategy

The results of the NPV value calculations for the different energy management strategies are shown in Figure 5. The curve in the figure can be understood by splitting it into three sections for analysis. Two vertical dashed lines separate the three sections (left, center, and right). The x's on the curve represent the number of deep-discharge cycles until end-of-life (EOL).

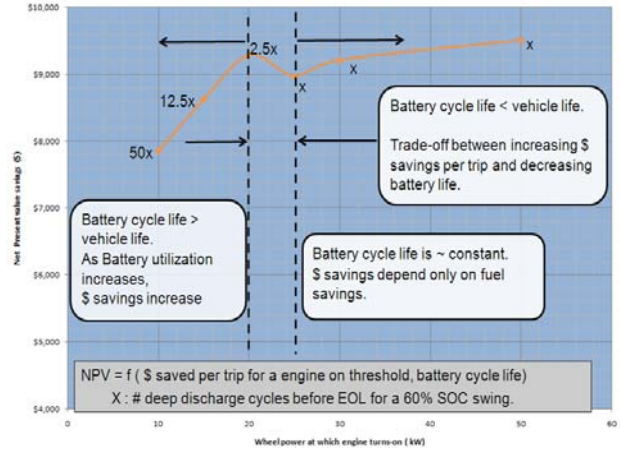


Figure 5. NPV Values for the Different Strategies, with Trade-offs Observed

- The section to the left is where the engine starts at wheel demand thresholds of 10, 15, and 20 kW. This results in a battery cycle life of 50, 12.5, and 2.5x. These three cycle lives are more than the vehicle life. Therefore, battery cycle life does not have a negative impact on gasoline fuel savings over the life of the vehicle. Naturally, as the engine turn-on threshold increases (higher battery consumption), the NPV dollar savings increase.
- The section to the right is where the engine starts at thresholds of 25, 30, and 50 kW. In each case, the battery cycle life is more or less the same (x) and possibly less than the vehicle life. Therefore, when the NPV of gasoline savings (\$) for 25-, 30-, and 50-kW cases are being compared, the battery cycle life does not count as a factor. Again, the higher the engine turn-on threshold (i.e., the lower the engine utilization), the higher the NPV of gasoline \$ savings. This section of the curve has a milder slope than the section on the extreme left. This is because 30- and 50-kW wheel power demands do not occur very often in the UDSS cycle, and battery/engine utilization does not change much from one control to the other. Therefore, gasoline fuel consumption increases slightly from the left to right in this section.
- In the central part of the curve, there is a trade-off between decreasing battery cycle life and increasing fuel savings. When the engine

turn-on threshold is 20 kW, the battery cycle life (2.5×) is definitely greater than the vehicle life. When the engine turn-on threshold is 25 kW, the battery cycle life (×) may be lower than the vehicle life. Therefore, as one progresses from 20 to 25 kW on the horizontal axis, battery cycle life starts factoring into the NPV \$ savings. As battery life decreases from 25-kW to 20-kW wheel power engine turn-on, NPV \$ savings decrease because of this factor. Also, engine utilization decreases from the left to the right; therefore, NPV \$ savings increase as a result of the increase in engine usage. Thus, the trade-off between decreasing battery life and increasing gasoline savings that results from lower engine usage decreases the NPV \$ savings in this part of the curve.

From the Figure 5 curve, the following observations can be made:

- An electric vehicle (EV) strategy (engine turn-on at 50-kW wheel power demand) does not necessarily translate into higher gasoline \$ savings. In the figure, the savings for the 50-kW case are marginally more than those for the 20-kW case. However, given the margin of error in battery cycle life assumptions and other approximations in this study, this difference is insignificant.
- The NPV savings for the higher engine turn-on thresholds (25, 30, and 50 kW) are concentrated in the early years of the vehicle, with no savings in the later years because the battery has reached EOL. For the lower engine turn-on thresholds, the NPV savings are spread over the life of the vehicle.
- The depth and spread of the trade-off region (central section) is sensitive to × (i.e., any change in the × value changes the trade-off region).
- From the strict perspective of NPV gasoline savings (\$), the ideal engine turn-on threshold on the basis of wheel power demand is about 20 kW (if the savings are to be spread over the life of the vehicle).
- Ideally, maximum NPV \$ savings will be gained for an engine turn-on threshold that is between 20- and 25-kW wheel power demand. This is also the wheel power demand that

leads to the battery life and vehicle life being exactly the same.

Although the NPV \$ savings depicted in this curve are sensitive to the assumptions about 1) gasoline and electricity costs, 2) the number of deep-discharge cycles per year, and 3) the number of grid charges per day, the trade-off between cycle life and fuel savings would always exist for different battery utilizations. The shape of the trade-off region would change. For example, if the price of gasoline increased, the impact of decreased battery life would be even more significant, and the negative slope in the trade-off region would be much larger.

The analysis presented above is for 40 miles of UDDS cycle driving. The same analysis was repeated for 40 miles of LA92 driving, with different energy management strategies for the same vehicle (engine turn-on at 20-, 25-, 30-, and 40-kW wheel power thresholds). Variations in NPV savings observed for 40 miles of LA92 driving and for UDDS driving were similar, as shown in Figure 5.

In addition, for the LA92 case, the analysis was repeated for different distances (10 to 100 miles of daily driving). Figure 6 shows the NPV \$ savings for different energy management strategies over different driving distances. Although the higher Wh/mi in the blended mode (higher EV operation) does not result in the greatest NPV savings, there is an optimum energy management due to the trade-off between battery cycle life and gasoline fuel savings. But, again, the energy management strategy with the highest Wh/mi (40-kW engine turn-on) does not result in maximum NPV savings.

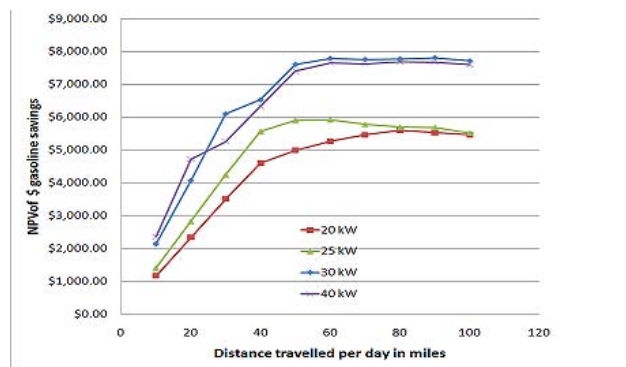


Figure 6. NPV Savings for Different Energy Management Strategies and Driving Distances

If battery cycle life is less than vehicle life, the PHEV operation of the vehicle will cease before the vehicle’s EOL, and there will be no savings in the vehicle’s later years. Therefore, there is the potential for battery replacement to extend the benefits of PHEV operation until the end of vehicle life. The LA92 section of the analysis was extended to evaluate battery replacement scenarios. Battery cost equations from prior published papers on battery cost were used. Battery cost is proportional to battery power, energy, and production volume. Figure 7 shows the NPV savings with and without battery replacement. With the battery cost estimates used in this study, the increase in PHEV savings is offset by the battery cost, and there is a net decrease in PHEV gasoline \$ savings.

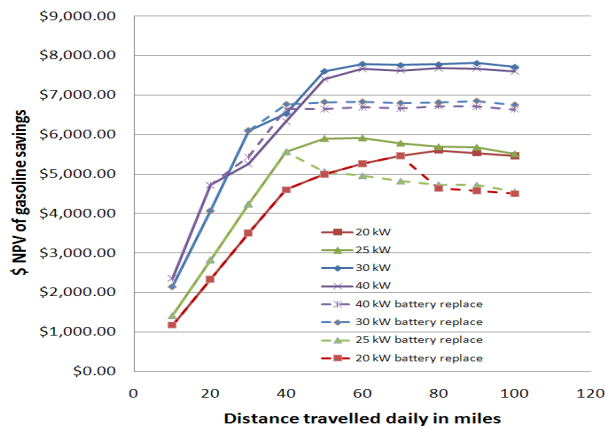


Figure 7. NPV Savings for Different Energy Management Strategies and Driving Distances, with Battery Replacement

From the completed study, the following conclusions can be drawn:

- Battery cycle life is one of the key variables in deciding the optimum energy management strategy for a vehicle. Current optimization studies are for a per-trip optimization and thus neglect this important variable.
- The NPV of gasoline saved (\$) over the life of a PHEV is a better performance index for comparing PHEV energy management strategies than L/100 km or Wh/mi. This is because NPV \$ gasoline savings considers not only L/100 km and Wh/mi, but also battery cycle life.
- The optimum energy management strategy suggested by the NPV \$ savings calculations

is different from optimization results on a per-trip basis (which suggests CD mode until the end of the trip) or maximum EV operation as needed for credits.

2. Support SAE J1711 and J1634 Test Procedures

BHIL was used to evaluate shortcuts proposed for the J1711 and J1634 procedures. BHIL is an ideal tool for understanding the impacts of battery-specific scenarios (e.g., SOC estimation, cell balancing, and tests that end because of a lack of battery power) on a vehicle. The impact of these issues on the test procedure results can be minute, and they can be confounded by test-to-test variations in vehicle parameters for chassis dyno testing. Also, some testing was battery specific, and conducting the tests on BHIL saved valuable time on the chassis dyno. Tables 4 and 5 show some BHIL tests to evaluate a proposed shortcut to the J1634 procedure.

Table 4. Comparison of Proposed Abbreviated Range Determination and a Full J1634 Test

	Shortcut Test # 1	J1634 Test # 1	Shortcut Test # 2	J1634 Test # 2	Shortcut Test # 3	J1634 Test # 3
Range (mi)	123.4	127.31	124.48	122.17	124.48	122.18
Discharge Wh/mile	161.709	165.9	161.51	166.55	161.49	166.86

Table 5. Comparison of Proposed Abbreviated Range Determination and a Full J1634 Test

	Shortcut Test # 1	J1634 Test # 1	Shortcut Test # 2	J1634 Test # 2
Charge Consumption (AC Wh/mi)	197.7	194.4	193.6	193.4

3. Use BHIL to Develop Model-Based Design Process for Argonne’s Autonomie Software

The Autonomie software developed at Argonne could be used as an environment for vehicle system modeling and simulation software-in-the-loop (SIL), controller-in-the-loop HIL, component-in-the-loop HIL, and potentially for developing embedded controls for an actual vehicle. Modifications need to be made to the Autonomie blocks that have been developed for simulation in order for them to be

used for component-in-the-loop HIL. BHIL will be used as the HIL platform to test Autonomie for component HIL. The current PSAT-PRO Simulink battery block for BHIL is shown in Figure 9(a), and the Autonomie block being developed is shown in Figure 9(b).

For HIL, Autonomie will include additional blocks for signal measurement and monitoring, checking limits on commands and feedbacks, E-Stop regulation, etc.

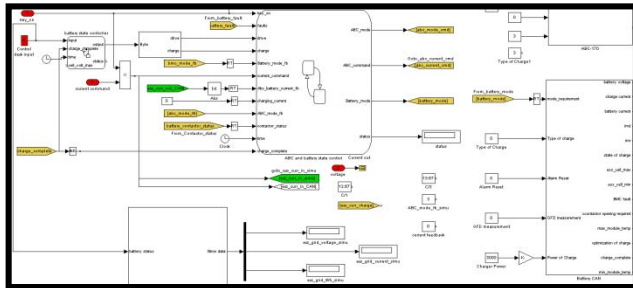


Figure 9(a). PSAT-PRO Block for Battery HIL

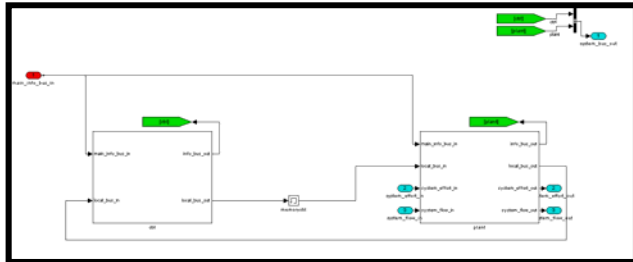


Figure 9(b). Autonomie Battery Block Being Developed

4. Began New Study on PHEV Energy Management to achieve Fast Rise in Battery Temperature and Quick Improvement in Engine Efficiency at Cold Temperatures

Because the plating effect at cold temperatures necessitates a battery management system (BMS) reduction in usable battery power, the battery pack must be brought back to its normal temperature of operation. At the same time, the engine temperature must be increased as fast as possible to improve engine efficiency. To achieve this goal, the same amount of energy available (based on road load) has to be optimally shared between the battery and the engine. This experiment will:

- Investigate optimum energy management to achieve the two conflicting goals (rise in both battery and engine temperature);
- Use Argonne’s battery systems HIL facility, with the battery module in an environmental chamber at cold temperatures; and
- Include a validated engine thermal model that predicts engine temperature rise and efficiency as a function of speed and torque usage history.

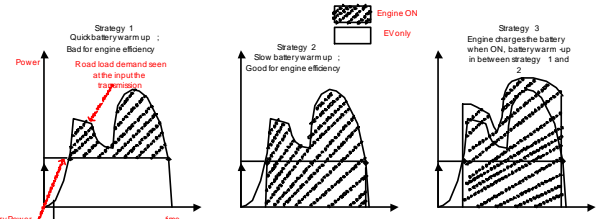


Figure 10. Three Different Energy Management Strategies and Their Implications on Engine and Battery Temperature Rise

Conclusions

Battery HIL was used to evaluate the trade-off between energy management and battery cycle life. The trade-off was evaluated by measuring and comparing the NPV \$ savings over the life of a PHEV and conventional vehicle. Battery HIL is being used to support the PHEV and BEV test procedures. Autonomie development for HIL will be tested on BHIL. This will contribute to the model-based design process possible with Autonomie. A new experiment on energy management at cold temperatures using Battery HIL was started.

Papers/Presentations

Shidore, N., J. Kwon, and A. Vyas, *Trade-off between PHEV fuel efficiency and battery cycle life with cost analysis*, presented at the IEEE Vehicular Power and Propulsion Conference, Detroit, MI, Sept. 2009.

Shidore, N., and M. Duoba, *Evaluation of J1634 shortcuts*, presented to the SAE J1634 Task Force Web-meeting, Jan. 2009.

Shidore, N., *Battery systems performance studies — HIL components testing*, presented at the 2009 DOE Hydrogen Program and Vehicle Technologies Annual Merit Review.

Shidore, N., *Trade-off between battery cycle life and fuel efficiency using HIL*, presented to the Vehicle Systems Analysis Tech Team (VSATT), USCAR, Dearborn, MI, March 2009.

Papers selected for future publications based on the above work:

Shidore, N., J. Kwon, and A. Vyas, *Comparison of PHEV energy management strategies using NPV of gasoline savings*, 2010 SAE World Congress, Detroit, MI.

Rousseau, A.P., S. Hallbach, and N. Shidore, *Automated Model Based Design Process to Evaluate Advanced Component Technologies*, 2010 SAE World Congress, Detroit, MI.

B. Peak Shaving-PHEV Battery Control Development & Vehicle

Theodore Bohn (Project Leader)

Argonne National Laboratory

9700 South Cass Avenue

Argonne, IL 60439-4815

(630) 252-6592; tbohn@anl.gov

DOE Technology Manager: Lee Slezak

Objectives

Perform studies to measure the energy storage system performance advantages of actively coupling an ultracapacitor array with a lithium (Li)-ion battery as a means to address the following critical shortcomings of present approaches to Li-ion battery pack integration in electrified vehicle applications.

- Although current energy storage systems based on Li-ion batteries for plug-in hybrid electric vehicles (PHEVs) have a reasonable power capability at room temperature, at -10°C it drops to one-fifth that of rated power. This prohibits all-electric vehicle (EV) operation during low-ambient temperature conditions. Ultracapacitors do not exhibit such power degradation at low-ambient temperature conditions.
- High power draw at low states of charge significantly stress Li-ion batteries in terms of usable life and efficiency. Studies performed in fiscal year 2008 confirmed that developing an "Active" combination of ultracapacitors and PHEV batteries have the potential to substantially improve battery low-temperature performance and minimize battery cycle life issues.

Reduce the net cost of energy storage systems (ESS) with increased performance and net energy density. The additional cost of the power electronics and ultracapacitors is postulated to be offset by the lower cost, higher energy density batteries.

Reduce the total volume of the ESS by cutting the battery size by ~50% and adding back ~30% of the volume with ultracapacitors and electronics in the Johnson Controls-Saft (JCS) battery pack.

Approach

Investigate the economic feasibility of these controls with different power electronic converters to evaluate the trade-off between cost and improvement in battery low-temperature performance and estimated battery cycle life.

Evaluate the lithium polymer battery technology at the single-cell level and multi-module sub-system level, in elevated temperature conditions, both with and without ultracapacitor active and passive combinations.

Use an emulated vehicle (using the hardware-in-the-loop [HIL] principle) to verify operation of the various energy storage and control elements against the predicted performance from the circuit-based models.

Accomplishments

Constructed actively coupled capacitor-battery ESS model and completed four iterations of state-of-charge (SOC) regulation, including global optimization routines for tuning.

Confirmed through the results of modeling that in ideal conditions (a priori knowledge of drive cycles), a compact, 72-Wh (40-lb) ultracapacitor bank could achieve the desired transient decoupling goals.

Constructed a full-sized (300 V; 72 Wh) ultracapacitor bank with instrumentation and completed voltage step response checkout tests on ABC170 test stand.

Obtained Brusa BDC412 DC/DC converter and MotoTron ECM hardware. Initiated the development of controls and power lead wiring harness construction.

Future Directions

Continue tuning controller software to balance the SOC window with aggressiveness of peak power reduction from the battery side of the energy storage system by applying insights gained on the battery HIL test stand and ABC170 as DC/DC converter.

Investigate limitations of battery-only ESS at high SOC and low operating temperatures, as well as estimate reduction in power capability at end-of-life. Run the same battery at these conditions with and without an actively coupled ultracapacitor system.

Similarly, implement lower power density, higher energy density battery on battery HIL stand with actively coupled ultracapacitor to illustrate ESS optimized for energy in battery, for power with ultracapacitor via active coupling by using power electronics.

Complete implementation of control software in MotoTron ECM and Brusa BDC412 DC/DC converter. Run system with 300-V, 72-Wh ultracapacitor bank in PHEV and HEV. Investigate the impact on cold weather operation and reduction of system losses for a wider usable battery SOC window.

Work with original equipment manufacturer (OEM) and Tier I suppliers to identify production cost/size of a DC/DC converter that meets requirements for actively coupled ultracapacitor system and energy optimized battery for Chevy Volt-sized PHEV.

Introduction

Argonne has developed a highly dynamic power conditioning electronics interface that acts as an intelligent interactive control to regulate the power-sharing scheme between ultracapacitors and batteries. During the first half of fiscal year 2009, this project investigated the use of these controls with different power electronic converters to evaluate the economic feasibility of combining ultracapacitors and batteries. This was done by measuring the trade-off between cost and improvement in battery low-temperature performance and estimated battery cycle life. Experiments were prepared to use an emulated vehicle (using the HIL principle) to verify operation of the various energy storage and control elements against the predicted performance from the circuit-based models.

The latter half of 2009 has involved preparing for experiments designed to evaluate the lithium polymer battery technology at the single-cell level and multi-module sub-system level, in elevated temperature conditions, both with and without ultracapacitor active and passive combinations.

The goal of this research is to investigate methods to combine the best attributes of power-dense ultracapacitors with energy-dense Li-ion batteries to obtain a net energy storage system that is less expensive than batteries and is a compromise between power and energy density. This goal is achieved by actively coupling the energy from the ultracapacitors, at a very high rate of charge/discharge, in parallel with the battery. In essence, by using power electronics, the ultracapacitors can become the equivalent of “active suspension” to decouple “bumps” from the battery pack during acceleration and braking events. As such, the battery current capability requirements can

be greatly reduced, allowing a lower cost and more energy-dense battery to be used in PHEVs. Another goal of this research is to reduce the total volume of the ESS by cutting the battery size by ~50% and adding back ~30% of the volume with ultracapacitors and electronics.

In addition to reducing power demand stress on the Li-ion battery, the actively coupled ultracapacitor ESS can increase the allowable operating conditions of the Li-ion battery. These include:

- Operation at low temperatures. Below -20°C, Li-ion batteries generally need to limit the discharge rate to lower than C/5, or, for a 41Ah/10-kWh pack, only 8 amps.
- Operation at high SOC: Above 80% SOC, most batteries must progressively limit charge acceptance rate to eventually less than C/2, near 100% SOC.

Operation at low SOC: Battery impedance increases at low SOC, and internal heat generation/losses increase.

One of the practical benefits of separating the energy storage system for a PHEV into two sections is that the ohmic (I^2R) losses can be relocated into the high-current capability ultracapacitors—which have much lower impedance than batteries and better surface area for cooling. In other words, the actively coupled capacitor ESS relocates the heat outside of the batteries, allowing the batteries to be more densely packaged, with thicker electrode material.

The review panel at the Department of Energy (DOE) Annual Merit Review questioned the validity of the claimed benefits and the failure mechanism of Li-ion batteries in the EV/PHEV application. The concern was that insufficient test data were available to prove or disprove that combining ultracapacitors with batteries improves the life or cold temperature performance of the composite energy storage system being studied. To address these unknowns, experiments were designed to evaluate the lithium polymer battery technology at the single-cell level and multi-module sub-system level, in elevated temperature conditions, both with and without ultracapacitor active and passive combinations.

David Howell of DOE’s Vehicle Technologies Program has volunteered to support the Argonne

Chemical Sciences and Engineering Division (CSE) Battery Test Facility to run three 10-module test articles on a long-term cycling study (one set with no capacitors, one set with direct parallel, and one set with emulated active parallel capacitors). The cycling portion of the study is expected to take several years and require ~3,000 cycles.

After a rigorous peer review process, the experiment plan was completed, and the single-cell experiments were set in place in the test stands using 3.8v/5Ah lithium polymer cells from Gold Peak USA. The properties of the cells are listed in Table 1. However, the start of this experiment has been on hold due the limited quantity of available test channels in the CSE Battery Test Facility during their facility upgrade.

The multi-module level experiment apparatus has been fabricated along with the less-aggressive, but more real-world, design of the experiment test plan. These are unattended experiments that need redundant levels of battery protection, monitoring, and cell-level management/balancing. The original battery management system hardware selected did not pass acceptance criteria, and a second vendor was selected (Elithion). Researchers using Argonne’s CSE Battery Test Facility, in general, only tests single-cell battery components with no external protection systems or automated balancing networks—just temperature and voltage monitors that are built into the test stand.

Table 1. Battery Description

Manufacturer	Gold Peak
Part Number	LPC5099130L
Electrical Specifications	
Nominal Voltage	3.8 V
Nominal Capacity (1 C)	5 Ah/22 Wh
Standard Discharge	5 A (1C)
Max Cont. Discharge	15 A (3C)
Max Peak Discharge	30 A (5C<30 s)
Discharge Termination	3 V (recommended)
Charge Algorithm	CC/CV to 4.2 V, <1.5 A taper
Standard Charge	1.2 A (0.2C) ~5-7 h
Fast Charge	5 A (1 C) ~2.5 h
Charge Voltage	4.2 V +/- 50 mV
Specific Energy	123 Wh/kg
Energy Density	243 Wh/L
AC Impedance	<6 mOhms (1 kHz)
Specific Power	613 W/kg (5C rate)
Power Density	1213 W/L (5C rate)
Mechanical Specifications	

Dimensions	3.94 L x 0.26 W x 5.5 H (in.)
Mass	0.25 kg
Temperature Specifications	
Discharge Temp. (°C)	-20 to +60
Std. Charge Temp. (°C)	0 to +45
Fast Charge Temp. (°C)	10 to +45
Storage Temp. (°C)	-20 to +45

The Argonne battery HIL stand is shown in Figure 2 with the dSpace control rack in the center, which runs the vehicle models and sends current commands (via CAN) to the ABC170 power processing unit (shown on the right).

The physical JCS VL41M battery is connected to Channel A; the ultracapacitor bank is connected to Channel B. The thermal chamber on the left can be used for simulating hot or cold operating conditions on the battery or capacitors.

Tasks/Results

1. Peak Shaving-PHEV Battery Control Development and Vehicle Integration

The 100-Wh/300-kW (peak) capacitor bank, voltage protection/monitoring circuits, and active power electronics (60 kW peak, custom DC/DC converter with CAN controls) is shown in Figure 1. This system was configured for the battery HIL stand, which emulates an EV/PHEV without the risk of battery system failures or cost of a full-sized PHEV battery pack. In this case, the emulated system was sized to match the requirements of the Chevy Volt (~400v/16kWh ESS capacity).



Figure 2. Argonne Battery Systems HIL Test Stand

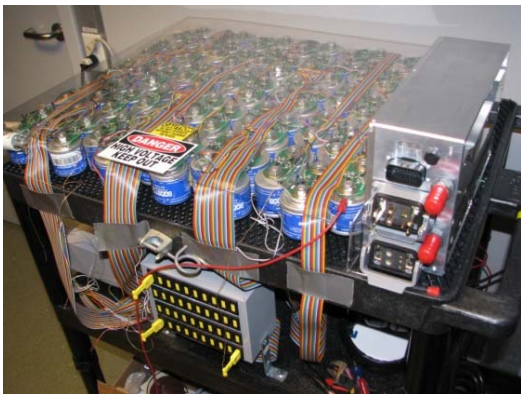
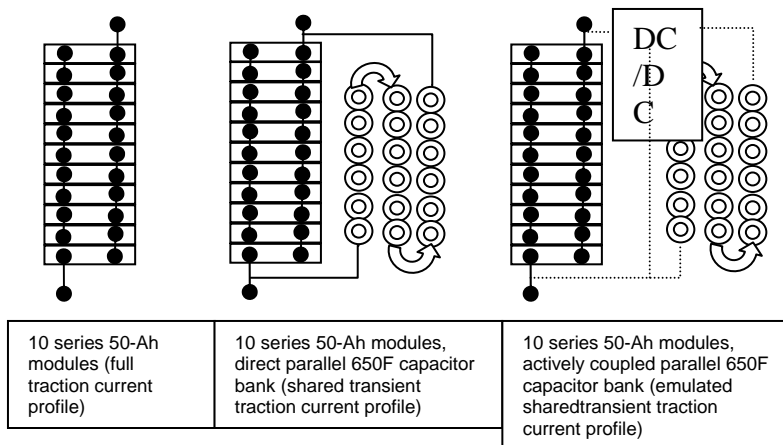


Figure 1. Ultracapacitor Bank and Power Electronics for HIL Battery-Capacitor Experiments

2. Sub-System Multi-Module Battery-Capacitor Experiments

Figure 3 shows a schematic view of the three test article 10-module sub-packs designed to be run on the Argonne battery systems HIL test stand to verify current sharing between the passive and active combination of ultracapacitors and LiMnO₂ chemistry Li-polymer batteries. The start of testing is currently on hold until a safety plan with a battery management/protection system is approved.



**Figure 3. Three 45-V/30-Ah Sub-System Gold Peak Modules (72 cells each — 12S/6P each)
w/650F Ultracap Bank**

3. Single-Cell Experiments (5 effects +1 control test article)

Table 2 provides details on the single-cell experiment test plan for the long-term cycling evaluation to be run on the battery test stand at the CSE facilities. The experiment consists of exposing a high-energy Li-ion battery to a variety of charge/discharge profiles and a parallel connected ultracapacitor Li-ion combination to a variety of charge/discharge profiles. The unpackaged single-cell test articles have delicate copper tabs for terminals. A fixture was designed to address this issue. Figure 4 shows the lithium polymer single cells mounted in a Lexan frame for minimal impact on thermal equilibrium with maximum protection of the terminals and low loss connections.



Figure 4. Gold Peak 5Ah/3.8v Single-Cell Test Articles in Lexan Frame with Robust Terminals for Test Fixture

Table 2. Details of Single-Cell Experiment Test Plan

Exp.	Hardware Configuration	Description of Current Profile	Purpose	Baseline Experiment for Comparison
1	Lithium Cell 5 Ah	0.5 C discharge/1 C charge	Control	none
2	Lithium Cell 5 Ah	PHEV CD Cycling	Evaluate dynamic cycling impact	1
3	Lithium Cell 5 Ah Parallel with 65 F	PHEV CD Cycling.	Evaluate dynamic cycling impact with ultracap	2
4	Lithium Cell 5 Ah Parallel with 650 F	PHEV CD Cycling Table 7	Evaluate dynamic cycling impact with 10x ultracap	2
5	Lithium Cell 5 Ah	PHEV CD Cycling Smoothed to emulate Actively connected ultracap (195°F)	Evaluate dynamic cycling Impact with DC/DC interface to ultracap	2
6	Lithium Cell 5 Ah	3-s charge/3-s discharge	Evaluate extreme dynamic cycling impact	1

Conclusions

The sub-system multi-module battery-capacitor experiments designed to be run in the battery systems HIL test stand are on hold, pending the approval of a safety plan for the battery management/protection system. (The safety plan is required to run these experiments continuously while unmanned.)

The single-cell cycling experiments (5 effects +1 control test article) are also on hold due to the lack of available battery cycling test stands at the CSE facilities. Other battery testing projects in the CSE take priority over this on. We are hoping to find additional funding to enable the purchase of our own battery cycling equipment to accomplish this and similar experiments. The cycling portion of the single-cell experiment is expected to last several years to complete the 3,000 cycles required.

Publications and Interactions

Technical papers have been published using modeling results and preliminary hardware data for SAE Congress, EVS23, IEEE Vehicle Power and Propulsion Conference, Advanced Automotive Batteries Conference, and Advanced Capacitor World Summit. Much interest resulted from the presentation on progress with the UC/Battery combination at the DOE Annual Merit Review in Washington, D.C., May 2009.

C. Impact of PHEV Design Strategies and Fuels on Fuel Economy and Emissions

Henning Lohse-Busch
Argonne National Laboratory
9700 South Cass Avenue
Argonne, IL 60439-4815
(630) 252-9615; HLB@anl.gov

DOE Technology Manager: Lee Slezak

Objectives

Quantify the impact of aggressive engine usage in plug-in hybrid electric vehicle (PHEV) mode on fuel economy and emissions.

Evaluate the impacts of fuel economy and emissions on control strategies in PHEVs.

Investigate emissions reduction through hybrid control.

Approach

The Modular Automotive Technology Testbed (MATT) made this research possible. MATT is a flexible powertrain research tool with an open control system.

The project was a collaborative effort between Argonne and the University of Tennessee.

The study's approach consisted of:

- Benchmarking the baseline emissions and energy consumption,
- Designing an emissions mitigating hybrid control, and
- Testing the new routines on hardware.

The three vehicle modes considered were:

- A conventional vehicle,
- An Urban Dynamometer Driving Schedule (UDDS), all-electric capable PHEV with an "engine optimum" control strategy, and
- A blended PHEV with an "engine load following" control strategy.

Accomplishments

Successfully completed all software and hardware phases of the program.

Observed significantly increased PHEV emissions, compared with the conventional vehicle mode, as a result of prolonged engine OFF periods and more aggressive engine usage.

Reduced PHEV emissions to Super Ultra-Low Emissions Vehicle (SULEV) limits by implementing a proper engine warm-up strategy and improved engine start-up routines.

Future Directions

The impact of different hybrid control strategies will be the focus of future work in this area.

Background and Approach

PHEVs present a new challenge for engine and emissions control, as shown in Figure 1. A PHEV can operate for an extended period without using the engine. As such, the exhaust after-treatment system will take much longer to reach a normal operating temperature, or the catalytic converter may cool down enough between engine usages to become ineffective upon engine start-up. The emissions problem may be compounded by the aggressive use of the engine in some PHEV strategies.

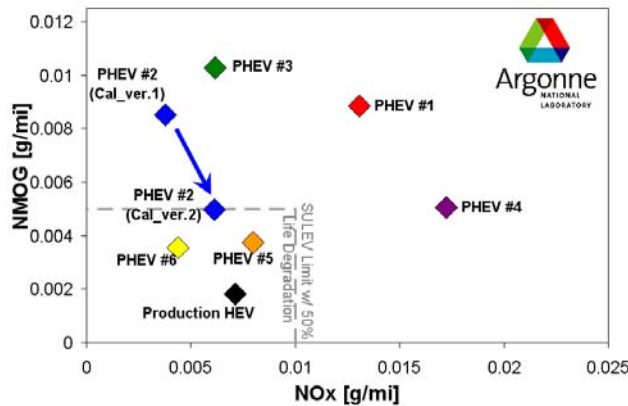


Figure 1. Emissions Behavior of PHEV Testing at APRF

This investigation intends to quantify the impact of aggressive engine usage in PHEV modes on emissions and energy consumption. In a second stage, hybrid control strategy modifications will be used to reduce the emissions. The conventional vehicle results will be presented briefly as a baseline. The actual study is centered on two different types of PHEVs:

- An all-electric capable PHEV with an engine optimum torque split strategy; and
- A blended PHEV with a load following torque split strategy.

The project was divided into two phases. The first phase involved developing the energy management and torque split control strategy in simulation with implementation on MATT. Once the initial code was ready, the baseline tests were completed in the Advanced Powertrain Research Facility (ARPF). A cold start full-charge test was completed and recorded for each hybrid vehicle type. These tests were then used as PHEV emission baselines to

understand the source of the emissions from a control perspective. The second phase began with developing emission mitigation control routines, such as engine warm-up strategies and ramping of the engine load. Then, a new set of cold start full-charge tests was completed and recorded. The emissions and energy consumption of Phase 1 and Phase 2 were then compared.

Results for Phase 1

All-Electric Capable PHEV

The first PHEV test involves the all-electric capable vehicle. Figure 2 shows the full-charge test results. The first two UDDS cycles are the charge-depleting cycles completed in the electric vehicle mode. The third cycle is the transition cycle. The engine turns ON for the first time on Hill 2 at higher speeds. Toward the end of the third cycle, the charge-sustaining phase begins, on the basis of the battery energy usage. The engine temperature warm-up starts on the fourth cycle. The engine does cool off during the longer OFF phases. The engine OFF phases are long, even during the charge-balanced cycles. The engine never reaches the operating temperature of the conventional vehicle. It is always 20°C below the conventional in the engine optimum control mode.

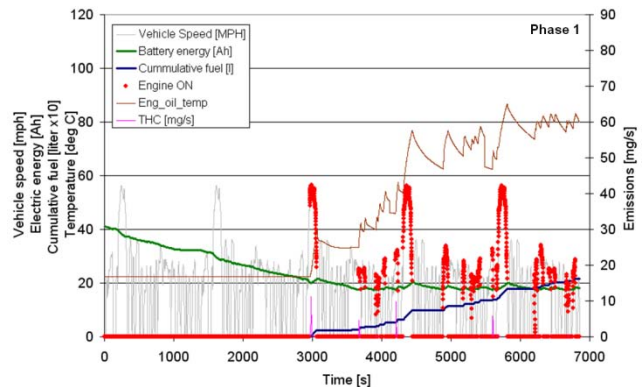


Figure 2. Phase 1 Full-Charge Test Results for the All-Electric Capable PHEV with ‘Engine Optimum’ Control

Figure 3 shows the emissions and engine operating range of the first engine cold start test (which is the third UDDS cycle in the full-charge test). Note that the emissions scale changed from 120 in the conventional vehicle graph to 200 in this graph. The majority of the emissions are still generated on the first engine start. This is a cold start, and the engine

is immediately loaded to 150 Newton-meters (Nm). The second start still produces a large emissions spike. The engine operation is now only in the high load area. Figure 4 shows the emissions and engine operating range for the hot start charge-sustaining test (which is the fifth UDDS cycle in the full-charge test). Even though the engine is still warm from the previous test, the first engine start produces a large emissions spike due to the high initial load applied to the engine. The catalytic converter cools off significantly during some of the engine OFF phases, even on this charge-sustaining test cycle. The engine operation is the same as on the cold start test, except that more engine fuel energy is used compared with the cold start charge-depleting test.

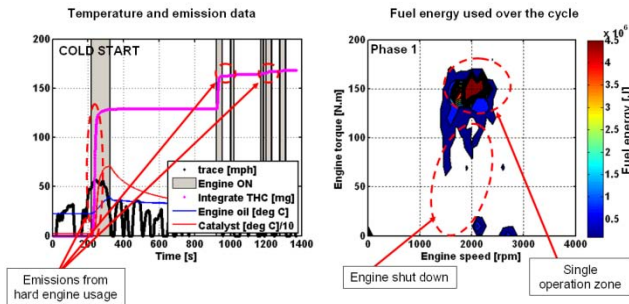


Figure 3. Phase 1 Cold Start Cycle Summary for the All-Electric Capable PHEV with Engine Optimum Control

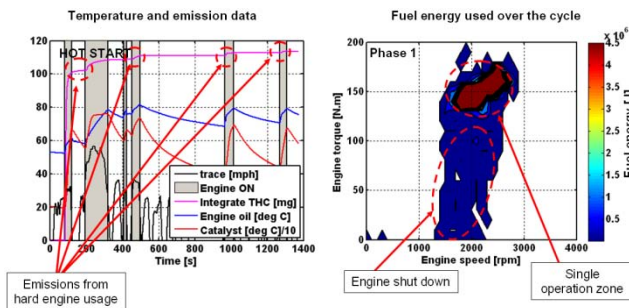


Figure 4. Phase 1 Charge-Sustaining Hot Start Cycle Summary for the All-Electric Capable PHEV with Engine Optimum Control

Blended PHEV

The second PHEV test utilized a blended PHEV control strategy. The blended PHEV’s full-charge test results are shown in Figure 5. In this case, the engine is used on the first UDDS cycle. During the charge-depleting phase, the engine turns ON only

five times during the cycle, which indicates extended engine OFF periods. Nevertheless, over the first three charge-depleting cycles, the engine temperature does rise slowly. During the charge-sustaining phase, the engine reaches an operating temperature close to that of the conventional vehicle operation. The engine OFF time on the charge-sustaining cycle is fairly short compared with the prolonged engine OFF period for the engine optimum charge-sustaining cycle. The first three cycles are charge depleting, compared with only the first two cycles for the all-electric capable PHEV. Once the charge-sustaining phase is reached in the blended PHEV test, the battery energy usage of the load following strategy is much ‘flatter’ compared with the engine optimum control. The load following strategy does not work the battery as hard as the engine optimum strategy.

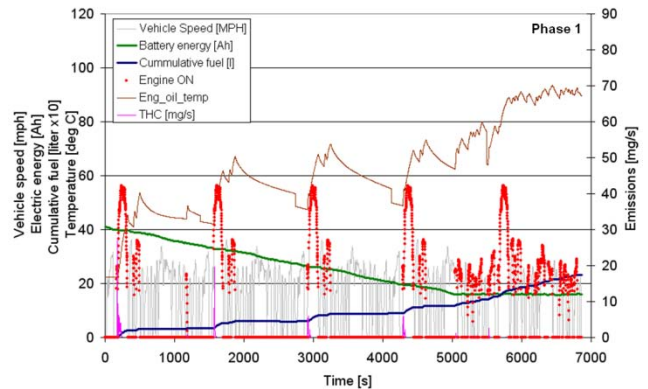


Figure 5. Phase 1 Full-Charge Test Results for the Blended PHEV with ‘Load Following’ Control

Figure 6 summarizes the emissions and engine operating range of the first cold start test of the blended PHEV. This is also the first UDDS cycle of the full-charge test. It should be noted that the emissions scale has changed from 120 in the conventional vehicle graph to 350 in this graph. The engine turns ON only five times in the charge-depleting test. The first engine start causes the majority of the emissions during the test. The engine actually does not start immediately, which causes the large emissions spike. The following engine starts produce only small emissions spikes, which are explained by low engine loads in this load following control strategy. The engine operating range is wide in the load range. However, overall,

only a small amount of fuel energy is used compared with that used in the conventional vehicle operation, which is normal in this charge-depleting test.

Figure 7 summarizes the emissions and engine operating range of the charge-sustaining cycle, which is the fifth and last UDDS cycle in the full-charge test. The engine turns on frequently throughout the cycle, but the total emissions produced are very low. The engine and catalytic converter temperature are close to operating temperature and fairly constant. The engine operating range is quite wide, but the average engine load is higher than that of the conventional vehicle. The engine idle fuel island of the conventional vehicle has also been eliminated by the hybrid operation. The total fuel energy consumed is higher than in the charge-depleting test, which is expected for this charge-sustaining test.

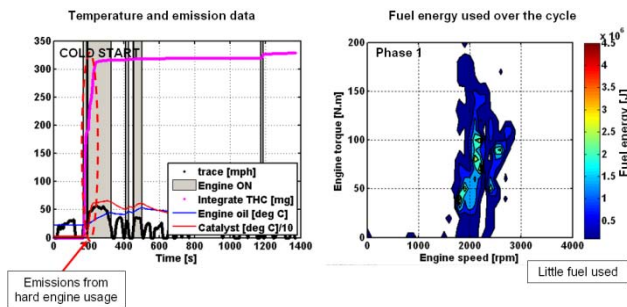


Figure 6. Phase 1 Cold Start Cycle Summary for the Blended PHEV with Load Following Control

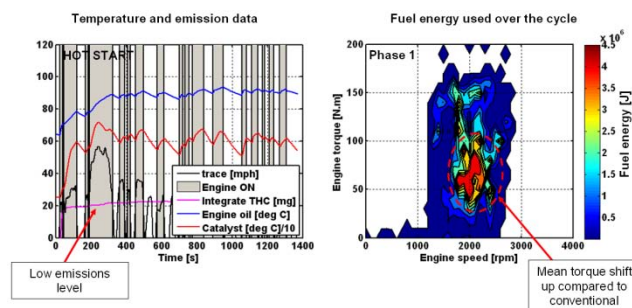


Figure 7. Phase 1 Charge-Sustaining Hot Start Cycle Summary for the Blended PHEV with Load Following Control

Phase 1: Energy Consumption and Emissions Summary

Figure 8 summarizes the energy consumption and emissions test results for the conventional vehicle, the all-electric capable PHEV, and the blended PHEV. The energy consumption graph shows the conventional fuel economy data in black. The cold starts for all test sets are marked in green. The all-electric capable PHEV is shown in red. The first test uses only electric energy. The cold start test uses slightly more electric energy compared with the second UDDS cycle. The third cycle is the transition cycle, which is charge-depleting. The last cycle is charge-sustaining. The fuel economy gain, when compared with the conventional vehicle operation, is 25%. The blended PHEV is shown in blue. The first cycle is marked in green and is slightly offset from the general blended PHEV energy consumption line. The engine cold start losses cause this offset. With the cold start cycle, the first three tests are the charge-depleting cycle. The fourth cycle is the transition cycle. The fifth cycle is the charge-sustaining cycle. The following engine load cycles have a slightly higher fuel consumption, which can be explained by the less efficient engine operation compared with that of the engine optimum strategy.

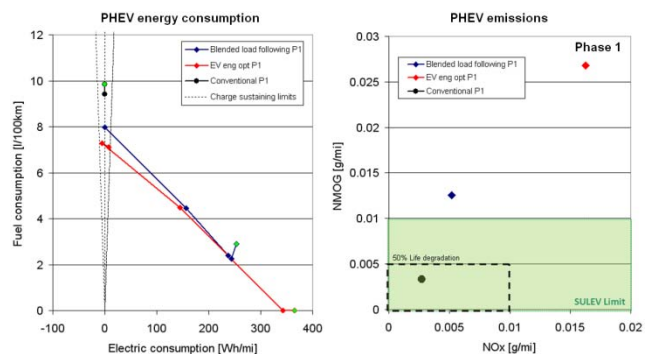


Figure 8. Phase 1 Energy Consumption and Emissions Summary for All Tests

The emissions data are quite revealing. The conventional vehicle achieves SULEV. The blended PHEV is just outside the SULEV limits. The all-electric capable PHEV has the highest emissions. The emissions results in the graph are the average of the five individual full-charge cycles for each vehicle type. In the conventional vehicle, the catalytic converter temperature is always high, and the engine loads are fairly light with mild tip-ins. In comparison, the all-electric capable PHEV with the engine optimum strategy is extremely aggressive on

the engine loads. The engine loads are high, and the tip-ins are immediate. The catalytic converter temperature takes several cycles to reach its operating temperature, but it still cools down significantly during some prolonged engine OFF periods. All these reasons explain why the all-electric capable PHEV with the engine optimum control strategy generates the highest emissions. For similar reasons, the blended PHEV with the load following strategy is between the conventional vehicle and the all-electric capable PHEV in terms of emissions and energy consumption.

Emission Mitigation Routines

From the Phase 1 results, it is clear that the engine load must be reduced until the engine catalytic converter reaches its light-off temperature. Even once the light-off temperature is reached, the engine maximum torque should be limited until the engine and the exhaust after-treatment systems reach operating temperatures. The original idea was to ramp up the maximum engine torque as a function of time. However, after further reflection and discussion, it was decided that the engine torque maximum limit would be ramped up as a function of engine energy output. If a certain amount of energy is produced by the engine, it will guarantee that a certain amount of energy goes to warm up the engine and the exhaust after-treatment system. Ramping the maximum available engine torque based on time is inappropriate. It could result in a situation where the engine idles only during that period, and the desired operating temperature would not be reached.

Figure 9 illustrates that while in conventional mode, the engine cranks out about 2–3 MJ of energy by the end of Hill 2 on the UDDS. At that point, the engine and exhaust after-treatment system have reached their operating temperatures.

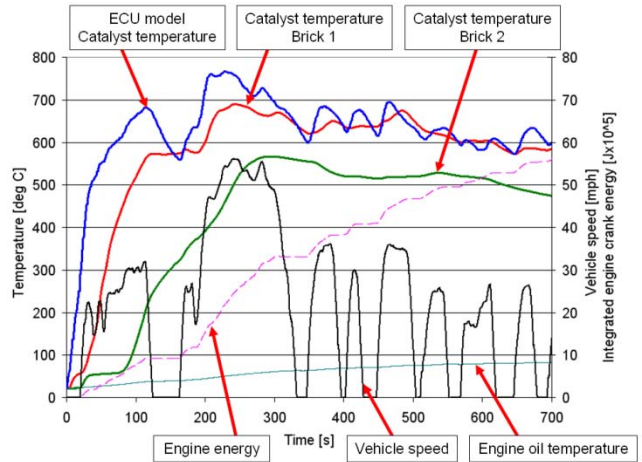


Figure 9. Catalyst Temperatures and Crankshaft Energy on a Cold Start UDDS in Conventional Vehicle Mode

On the basis of the Phase 1 data set, it seems that when the engine is turned ON, the engine load should be ramped in with mild tip-ins compared with the immediate load request commanded in Phase 1. Figure 10 shows the three routines that are implemented in Phase 2 for the first engine start to reduce the engine emissions for these full-charge PHEV tests.

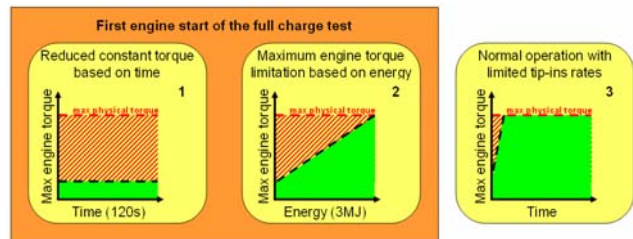


Figure 10. First Engine Cold Start Warm-up Routines

The long engine OFF times in Phase 1 allow the engine and catalytic converter to cool off significantly. Thus, after the first engine start occurs, the catalytic converter temperature is monitored. When the converter’s temperature drops below a target temperature, an engine warm-up routine is initiated. The engine torque is limited and ramped up based on engine output energy. The target energy during this warm-up is much lower. Figure 11 shows the warm-up algorithms for the engine start-up triggered if the catalytic converter temperature drops below its target temperature.

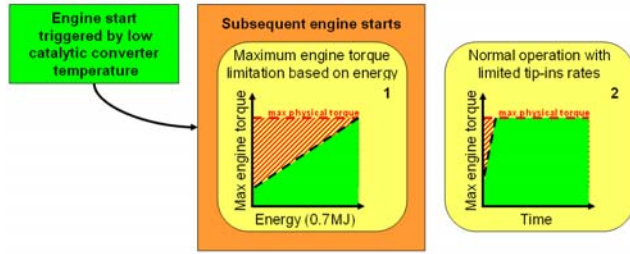


Figure 11. Subsequent Engine Warm Start Warm-up Routines Triggered by a Low Catalytic Converter Temperature

In all cases, the engine starts are always followed by a ramp in of the maximum torque to prevent the aggressive engine usage from Phase 1. All of these routines are not necessary in simulation, but they are required with real hardware to obtain reasonable emissions data. These warm-up algorithms are easily implemented in the open controller on MATT.

Results for Phase 2

The cold start Federal Test Procedure (FTP) schedule tests were performed in the conventional vehicle mode. The fuel economy and emission results were very close to the results of Phase 1, which demonstrates MATT’s repeatability, even with a gap of several months.

All-Electric Capable PHEV

The Phase 2 results for the all-electric capable PHEV are presented in Figure 12. The first two UDDS cycles are still completed in electric vehicle mode. The first engine start occurs at the start of the third UDDS cycle. Note that the engine oil temperature is (and will be, from this point forward) compared with the Phase 1 test. This shows that the engine warm-up strategy is successful. In charge-sustaining mode, the engine ON time is similar to that of Phase 1.

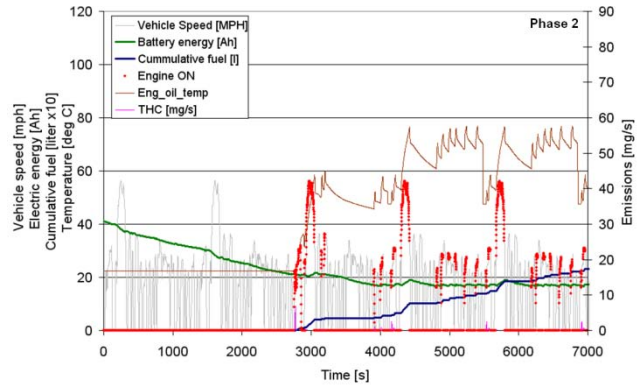


Figure 12. Phase 1 Full-Charge Test Results for the All-Electric Capable PHEV with Engine Optimum Control with Engine Warm-up

For this case, only the cold start test emissions and engine operating range summary are shown in Figure 13. After the first engine start, the engine is ON for an extra 200 seconds. The integrated emissions are three times lower compared with the first engine start cycle in Phase 1. The catalytic converter reaches 800°C in Phase 2, compared with 600°C in Phase 1. More importantly, no large loads are applied to the engine for the first 120 seconds, during which the catalytic converter reaches 600°C. On the engine operating range graph, a few of the warm-up routines are visible. During the initial engine ON phase, the maximum engine load is limited to a constant torque of 25 Nm, as shown in the graph. Also, a small engine idle fuel island reappears because the engine is forced to idle during the 120 seconds when the vehicle is stopped. The engine should not be started and stopped until the exhaust after-treatment system reaches light-off temperature. Finally, the engine load is not contained to 150 Nm as it was in Phase 1. The graph does show an operating range from 50 Nm to 150 Nm. This is the result of the slow ramp-up of the maximum engine torque limit based on the engine energy output.

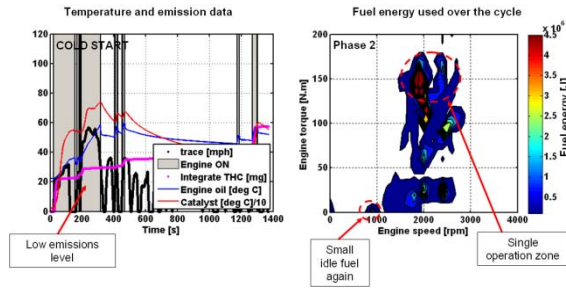


Figure 13. Phase 2 Cold Start Cycle Summary for the All-Electric Capable PHEV with Engine Optimum Control with Engine Warm-up

The power flow graphs for Phase 1 and Phase 2, shown in Figure 14, provide more detail about the impact of the engine warm-up strategies. In Phase 2, the engine turns ON for Hill 1 of the UDDS cycle. During the first hill, the engine power is lower than 8 kW due to the 25-Nm limit, and the motor provides the dynamic tractive power to meet the trace. At the end of Hill 2, the engine idles for about 30 seconds. This represents the end of the 120-second phase, during which the engine is required to turn ON and is limited to a maximum torque of 25 Nm. The engine is used two more times during Hill 2. The graph shows the engine torque ramp during Hill 2. At about 250 seconds, the engine torque is no longer limited. In Phase 1, the engine turns ON during Hill 2 and is immediately loaded to 150 Nm.

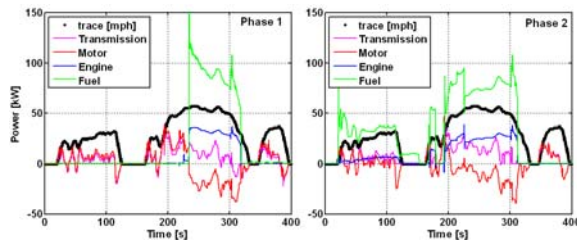


Figure 14. Power Flow Comparison between Phase 1 and 2 of the Cold Start Cycle of the All-Electric Capable PHEV with Engine Optimum Control

Blended PHEV

The Phase 2 full-charge test results for the blended PHEV are presented in Figure 15. The engine is ON more often at the start of the first UDDS cycle than it is in Phase 1. The engine temperature is about 20°C hotter during the charge-depleting phase. In Phase 2, the sixth UDDS cycle is charge sustaining, while that occurs during the fifth UDDS cycle in Phase 1. This is due to the higher engine usage with

the engine warm-up strategy. Thus, less electric energy is used on the UDDS cycle in charge-depleting mode.

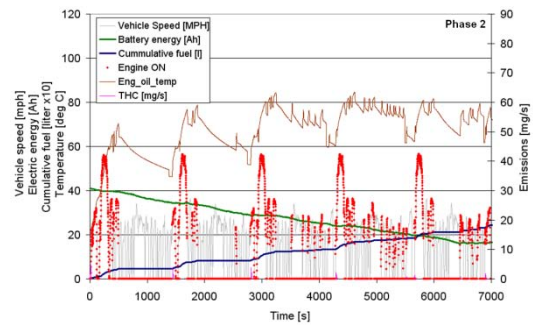


Figure 15. Phase 2 Full-Charge Test Results for the Blended PHEV with Load Following Control with Engine Warm-up

Figure 16 depicts the emissions and engine operating range UDDS cycle summary for the first engine start test on the full-charge test. The engine starts immediately. In the blended PHEV, the engine must be warmed up based on the key start. The engine is ON for the first three hills. In the load following strategy, the engine loads are not as high as in the engine optimum control strategy. This causes the load following case to take longer to finish the warm-up phase (because it is energy based). The integrated emissions level is 10 times lower than in the Phase 1 results. The engine temperature is higher by 10°C on this charge-depleting test than it is in Phase 1. In the engine operating range graph, the idle fuel island reappears, since the engine is forced to idle in the initial warm-up phase. Compared with the Phase 1 test, the low engine torque operation is also new. This result is caused by the fact that when the engine is ON, it is used with the maximum engine torque available.

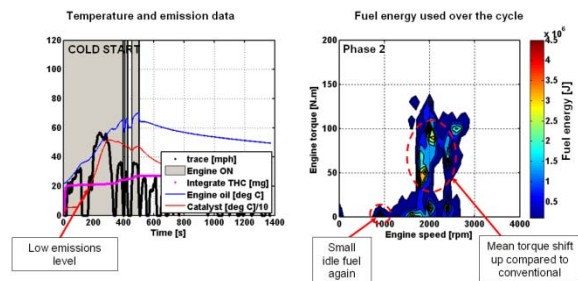


Figure 16. Phase 2 Cold Start Cycle Summary for the Blended PHEV with Load Following Control with Engine Warm-up

Figure 17 presents the power flow graphs for Phase 1 and Phase 2. These graphs provide more details on the impact of the engine warm-up strategies for the blended PHEV. Similar to the engine optimum test, the initial warm-up phase (where the engine torque is limited to 25 Nm) is seen on Hill 2. Also on Hill 2, the motor torque spikes up during hard acceleration, which shows that the engine is still limited during the maximum engine torque limit ramp-up phase.

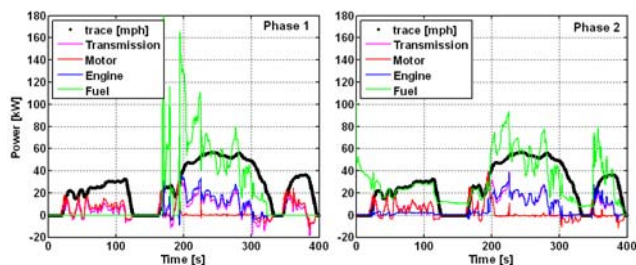


Figure 17. Power Flow Comparison between Phase 1 and 2 of the Cold Start Cycle of the Blended PHEV with Load Following Control

Phase 2: Energy Consumption and Emissions Summary

Figure 18 summarizes the energy consumption and emissions test results for the conventional vehicle, the all-electric capable PHEV, and the blended PHEV. To allow for easy comparison, the color codes and axes on the graphs are the same as those in the graphs for Phase 1 (Figure 8). The conventional vehicle and all charge-sustaining fuel consumption for both PHEVs are the same as in Phase 1 and are shown respectively. This result is as expected. For the all-electric capable PHEV with the engine optimum control, the energy consumption on charge depleting is the same as that in Phase 1. The transmission cycle used more fuel but less energy, which is a consequence of the engine operating more through the engine warm-up routine. For the blended PHEV with the load following control strategy, an extra cycle had to be tested to obtain a charge-sustaining cycle. The charge-depleting cycles all used more fuel, and thus less electricity, as a consequence of the engine warm-up routines.

The real success is apparent in the emissions summary. Both PHEVs achieved SULEV limits. The engine warm-up routines, coupled with the slow engine loading after an engine start, reduce the

emissions level dramatically. The emissions results of Phase 1 are shown in faded grey.

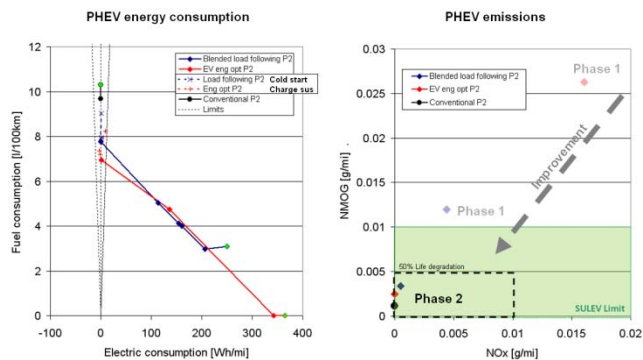


Figure 18. Phase 2 Energy Consumption and Emissions Summary for All Tests

Conclusion

This study investigated the impact of aggressive engine usage on emissions for PHEVs. The conclusion of the first phase showed that the engine should be warm and the exhaust after-treatment system must be higher than the light-off temperature of the catalytic converter before significant engine load demands are applied. Otherwise, large emissions spikes occur.

Further, the immediate high engine load requests after the engine start also cause large emissions spikes, even while the engine and exhaust system are at operating temperatures. Therefore, some warm-up routines are designed. On the first engine start, the engine is limited to a maximum torque of 25 Nm. Next, the maximum available engine torque is ramped up as a function of the engine energy output. The energy output target is calibrated to ensure that the engine and exhaust system reach their operating temperatures. If the catalytic converter temperature drops below a target temperature, the maximum available engine torque is again ramped up as a function of a smaller engine energy output. Finally, the engine loads are ramped in using mild tip-ins to further reduce the emissions spikes.

The engine warm-up strategies reduced the emissions of all the PHEVs to SULEV limits without significantly increasing the energy consumption. This study could not have been performed without the open controller approach and in-depth instrumentation of the MATT research tool.

IV. LABORATORY TESTING AND BENCHMARKING

A. Benchmarking and Validation of Hybrid Electric Vehicles

Danny Bocci

Michael Duoba

Forrest Jehlik

Henning Loehs-Busch

Eric Rask

Argonne National Laboratory

9700 South Cass Avenue

Argonne, IL 60439-4815

(630) 252-6398; mduoba@anl.gov

DOE Technology Manager: Lee Slezak

Objectives

Benchmark production Honda Civic Hybrid to compare to 2nd generation Insight (comparison of cost reduction in effectiveness in production hybrid).

Approach

Purchase vehicle, manufacturers' service manuals, and diagnostic tools for the vehicles tested.

In the case of the Level 1 testing, instrument engine speed, battery current, and battery voltage.

In the case of the Level 2 testing, install (1) an engine torque sensor and (2) a drive shaft torque sensor and use indicated engine torque sensor to determine engine torque from in-cylinder pressure measurement.

Also for Level 1+ testing, determine, scale, and record Controller Area Network (CAN) signals through testing as a means of measuring parameters that would otherwise be too difficult or expensive to obtain.

Run tests for cycle fuel economy, energy consumption, performance testing, and steady-state load for benchmark.

Accomplishments

Successfully conducted Level 2 testing on Honda Civic Hybrid.

Developed CAN signal data acquisition for recording signals that the vehicles monitor or use for controls.

Future Directions

Instrument and evaluate Honda Insight hybrid; compare and analyze levels of technology and energy consumption.

Introduction

For this work, a Level 2 benchmark of a 2006 Honda Civic Hybrid was conducted. The intensive evaluation of this Integrated Motor Assist (IMA) powertrain will serve as the datum to compare technology optimization for the 2nd generation 2010 Honda Insight hybrid, which uses the newest, and more cost effective, IMA system. This comparison will be completed FY 2010, with preliminary data presented at the conclusion of this report.

1.0 Vehicle Data Acquisition

The Honda Civic was outfitted with a PXI-based multi-channel data acquisition board used to collect data from the vehicle (Figure 1). In addition, the vehicle was instrumented with wheel- and engine-flywheel-mounted torque sensors. These conditioned signals were sent to an external PXI chassis and then to the data acquisition computers in a test cell control room.

Thermocouples were integrated to measure the temperatures of vehicle components. These signals were routed to a National Instruments (NI) thermocouple chassis mounted on board the Honda Civic, and then they were passed to the PXI chassis and read in real time.



Figure 1. Vehicle Data Acquisition (DAQ) Layout: 1 Teledyne Engine Torque Sensor, 2 signal conditioning board, 3 NI Thermocouple PXI, 4, Teradyne OBDII interface, 5 power supply

2.0 Vehicle Data Network Acquisition

The 2006 Honda Civic hybrid uses two Controller Area Networks (CANs): one to monitor traditional vehicle architecture (CAN 1) and the second to monitor the hybrid powertrain (CAN 2). For monitoring, the traditional CAN bus was connected to the OBD II interface located under the driver's side dash, while the hybrid CAN bus was spliced into the CAN bus. CAN signals were read into a

computer with a compatible software interface, thereby allowing recognized signals to be measured and recorded.

3.0 Electrical System Measurement

For electrical energy consumption, current and voltage taps were installed in the high-voltage vehicle electrical system. Details about the location are shown in Figure 2. This setup allowed the electrical power flowing through the high-voltage battery and DC-DC converter to be measured.

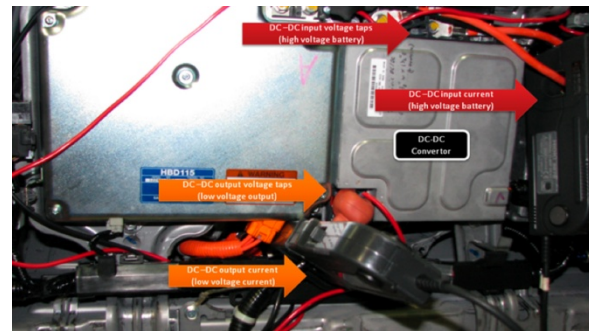


Figure 2. Position of Current Clamps and Voltage Taps

4.0 Fuel Flow Measurements

To measure fuel flow, the production fuel line was spliced, allowing a high-resolution in-line fuel flow meter to be integrated downstream from the fuel tank and pump (Figure 3). A stainless-steel connector was installed to ensure that the production vehicle remained operational during non-test driving. Outputs from this configuration were volumetric flow and temperature of the fuel.

5.0 Torque Sensors

The 2006 Honda Civic was fitted with torque sensors to monitor the combined torque output of the internal combustion engine and motor-generator (ICE-IMA), as well as the vehicle half shafts to monitor the post-transmission axle torque. The ICE-IMA torque sensor uses a strain gage mounted onto the CVT input shaft, mitigating the need for extensive vehicle modification. Three main components comprise the engine torque-sensing unit: the strain gage, antenna, and signal-conditioning unit. The IMA instrumented with the torque sensor is shown in Figure 4.

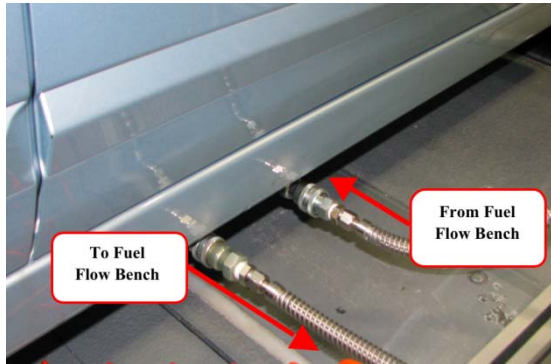


Figure 3. Fuel Flow Meter Connections

The unit measures the physical deformation caused by the ICE-IMA output torque and outputs an analog signal, which can be interpreted into a torque.



Figure 4. Mounted ICE-IMA Torque Sensor

Wheel torque sensors were installed onto the vehicle half shafts as shown in Figure 5. Half shaft torque sensors have no antenna but were directly wired to signal conditioning units. Once conditioned, the signals were passed into the data acquisition system for logging.



Figure 5. Image of Half Shaft Torque Sensor Mounted on Axle

6.0 Temperature Sensors

K-Type thermocouples were installed onto the vehicle to monitor temperatures throughout. Exhaust, CVT, and engine temperatures were monitored; in the IMA, several temperatures were measured and are shown in Figures 6 and 7.

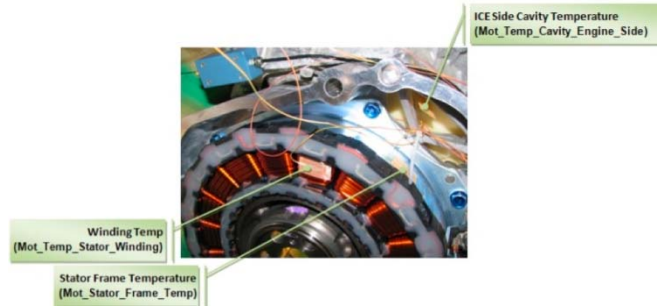


Figure 6. IMA Temperatures; CVT Side

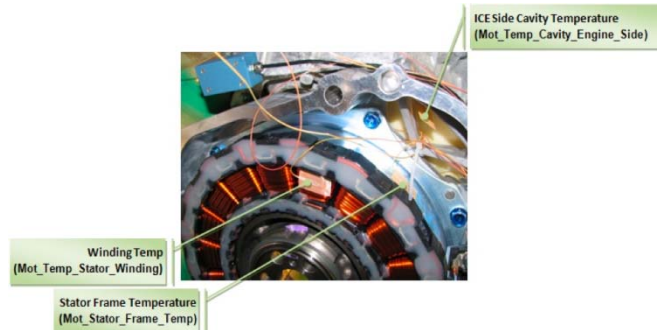


Figure 7. IMA Temperatures; ICE Side

Engine oil temperature was recorded by attaching a thermocouple to the end of the oil dipstick. In addition, thermocouples were implemented into the exhaust system to attain post-catalytic converter exhaust temperatures.

7. Vehicle Setup and Test Procedures

The test vehicle was mounted to the dynamometer with appropriate vehicle restraints for a front-wheel-drive dynamometer configuration. Ratchet straps and a static strapping system were used to secure the vehicle in the front and rear. Vehicle exhaust was connected to the dilution-mixing tee for emissions sampling. The vehicle setup is shown in Figure 8.



Figure 8. Honda Civic Setup on Dynamometer

Vehicle sensors and measurement equipment were then connected to the facilities data acquisition system. The Honda Civic was connected to an additional brake controller to operate the vehicle in proper dynamometer testing mode (overriding the anti-lock braking system [ABS] sensors to allow for regular driving). The facility equipment and dynamometer were then tuned and calibrated for the Honda Civic, thereby ensuring that the correct calibration and proper engineering units were recorded.

The coast down procedure was performed twice to determine the measured losses and to verify that these losses were repeatable. According to SAE, acceptable deviation is 5%; coast down procedures were repeated until this standard was met. Data collection could begin once the vehicle has successfully completed the coast down.

8. Analysis of Testing Results

8.1.1 Engine Fueling Map

Response surface methodology techniques were applied to the experimental engine data to develop an engine fueling rate map as a function of speed, load, and engine temperature. Engine temperature is defined here by the sump oil temperature. Data from cold start Urban Dynamometer Driving Schedule (UDDS), highway (HWY), and US06 cycles were combined, and any engine off or negative torque load points were excluded. Figure 9 displays the speed load points collected during the drive cycles, and Figure 10 illustrates the relationship among engine speed, engine load, and fueling rate.

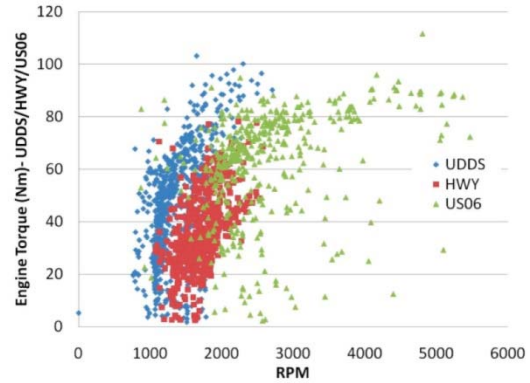


Figure 9. Honda Civic Engine Speed/Load Points during Drive Cycles (negative torque excluded)

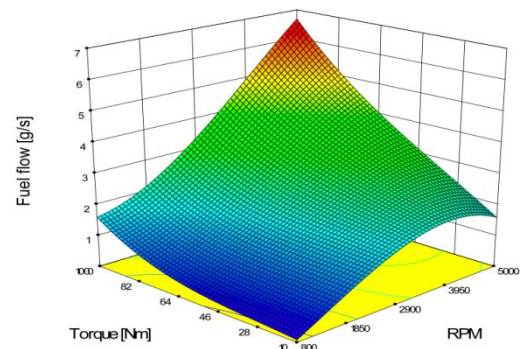


Figure 10. Honda Civic FuelingMap; Oil Temperature 60 C

The thermal state of the engine was observed to have a significant effect on vehicle fuel consumption. Figure 11 illustrates the fuel consumption at a relatively low engine oil temperature of 60°C, while Figure 12 illustrates the fuel consumption at an engine oil temperature of 90°C. Comparing these two charts at identical speed load points reveals that the engine consumes less fuel at 90°C. The engine operates more efficiently at a higher temperature. This trend was also observed in the results of cold start tests versus hot start tests—mileage in cold start tests decreased, with corresponding mileage variations of 50.8, 54.5, and 54.1 mpg observed from cold to hot tests. This change is the result of a reduction in both friction and heat transfer due to smaller thermal gradients as the engine heats.

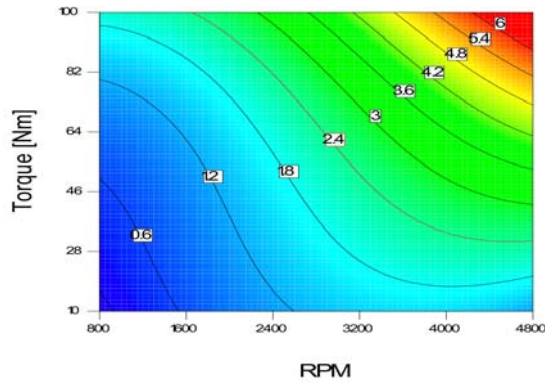


Figure 11. Honda Civic Fueling Map Fueling Contour; Oil Temperature 60 C (compare to Figure 12)

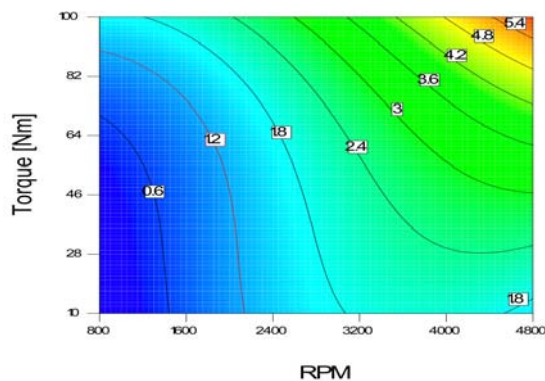


Figure 12. Honda Civic Fueling Map Fueling Contour; Oil Temperature 90 C (compare to Figure 11)

The engine temperature of the Honda Civic was slow to reach steady operating temperatures from cold-start conditions (Figure 13). The final steady operating temperature for the UDDS cycle operation was observed to be approximately 90°C.

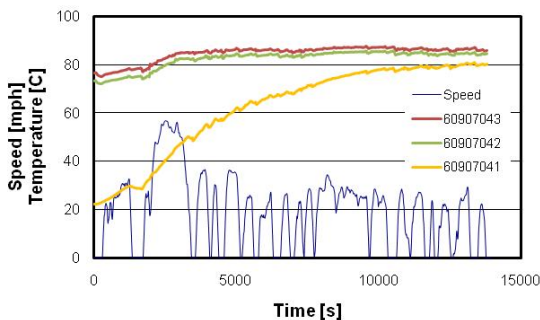


Figure 13. Oil Temperature vs. Vehicle Speed for UDDS Cycles

8.1.2 Engine On-Off Modes

The Honda Civic Hybrid uses cylinder deactivation to reduce fuel consumption. The solenoids regulating oil pressure to the connecting pins of the V-Tech system were initially monitored to determine the engine-operating mode. These data were compared to the measured fuel flow rate to the engine (Figure 14).

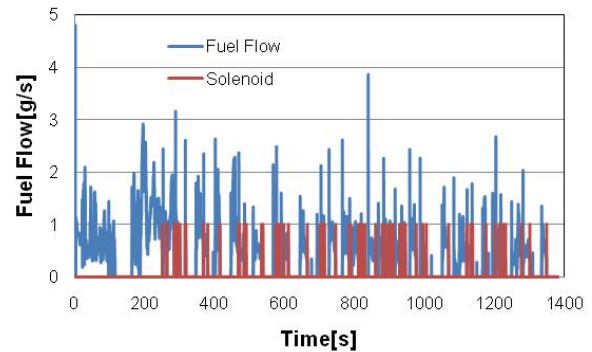


Figure 14. Plot Comparing Engine Off Methods

Periods of operation during which the fuel rate was zero were observed, yet the valvetrain solenoids were not activated. The engine was motoring as no fuel was supplied and had to overcome pumping losses associated with the four-stroke cycle. To observe the fuel savings, engine off was defined by the fuel flow rate to the engine. A threshold fuel rate of 0.10g/s fuel flow was set as the threshold. The engine was considered to be off under any instance during testing when the measured fuel flow was less than 0.10 g/s, while the engine was considered on at points above this threshold.

Figure 15 illustrates the occurrence of fueling rates over the UDDS, HWY, and US06 drive cycles. It was observed that the bin of 0.5–0.1 g/s contained minimal points, while the bin of 0–0.5g/s contained over 3,000 data points. The threshold value was above the fueling rate when the engine was off, providing an accurate measure of the engine off mode. This indicates the aggressive engine off characteristic of the IMA.

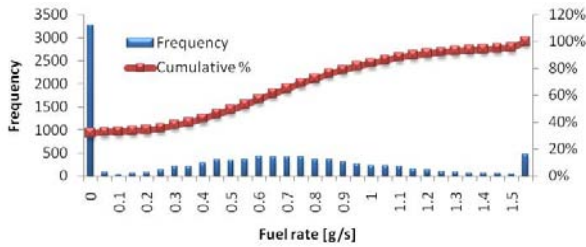


Figure 15. Histogram of Measured Fuel Rate

Engine on-off modes were plotted against the vehicle trace speed for the UDDS cycle (Figure 16), as well as for US06 and HWY.

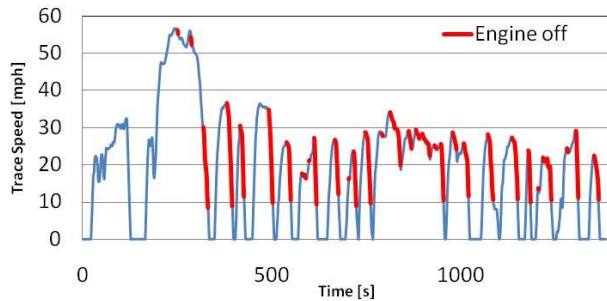


Figure 16. UDDS Engine On-Off Curve

The percentage of engine on and off was calculated by using a similar analysis for the US06, UDDS, and HWY drive cycles. These results are illustrated in Figure 17. Respective engine on percentiles are 66, 53, and 85% for the cycles. The effect of state-of-charge (SOC) was examined for each cycle, but no significant deviation occurred.

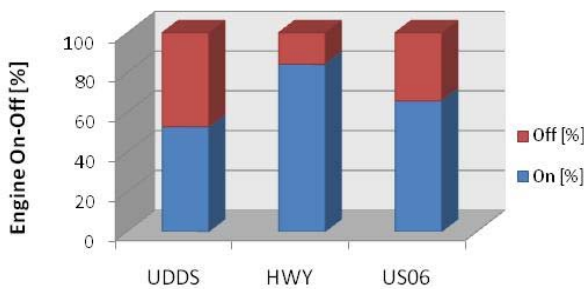


Figure 17. Engine On-Off Comparison for UDDS, HWY, and US06

8.1.3 High- and Low-Speed Cam Profiles

The Honda Civic Hybrid uses variable valve timing to increase performance and power output of the internal combustion engine. Engine modes of operation were engine off, herein referred to as

Mode 0, and engine on, as discussed previously. The engine on mode is further divided into two subcategories: Mode 1 and Mode 2. Mode 1 is defined as engine operation in which the valvetrain follows the low-speed cam profile, while Mode 2 is defined as engine operation where the valvetrain follows the high-speed cam profile. Measurement of the solenoid voltage determined the operational oil passageways within the valvetrain and thus revealed the cam profile followed. The engine operational modes were plotted against the engine speed and engine load. The results are shown in Figure 18.

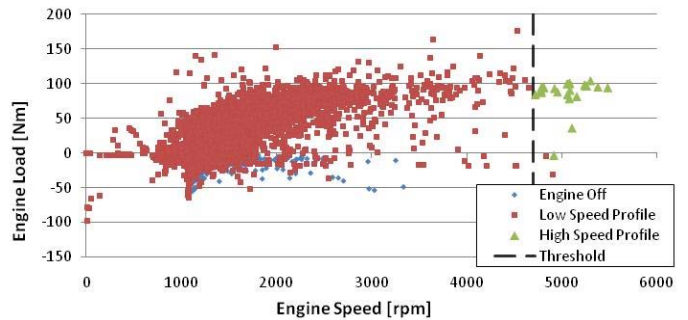


Figure 18. Plot Illustrating Engine Modes at Varying Engine Speeds

From this figure, it was observed that the threshold value between Modes 1 and 2 was near 4700 rpm. If the engine speed were below 4700rpm, the valvetrain would follow the low-speed cam profile; if the speed were greater than 4700 rpm, the solenoids would activate, causing the valvetrain to follow the high-speed profile.

8.2 IMA System Usage

8.2.1 Degree of Hybridization Factor Analysis

The IMA system was used to supplement engine power. To quantify the degree of hybridization of the vehicle, a metric of engine versus total power was developed. This hybridization factor quantifies the amount of input or output of the battery to the input of the internal combustion engine. It is calculated as follows:

$$DoH = \frac{EnginePower [W]}{EnginePower [W] + BatteryPower [W]}$$

Positive engine power is defined as power input to the transmission, and positive battery power is defined by power input to the transmission. By using this convention, a factor of one indicates that the internal combustion engine is the only source of input power. A factor of less than one indicates that the IMA system assists in vehicle propulsion. A factor of zero indicates that the vehicle is fully electric. A value greater than one indicates that the motor acts as a generator; additional work is being performed to generate electricity, in addition to vehicle propulsion. Figure 19 shows the hybridization factor analysis from the combined US06, UDDS, and HWY datasets.

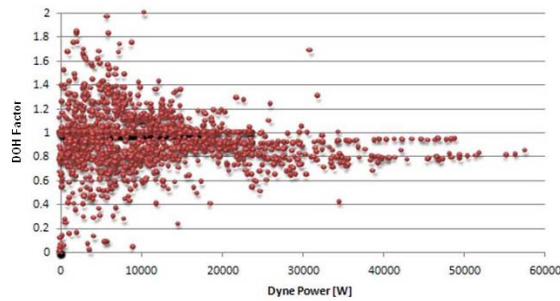


Figure 19. Hybridization Factor vs. Dynamometer Power for Combined DataSet

8.2.2 Charge Sustaining Strategy

Efforts were made to observe the Honda IMA system and analyze its operational points and limits.

From observation of the datasets collected, it was observed that the system uses a charge-sustaining strategy operating between the limits of 30 and 80% battery state of charge (see Figure 20).

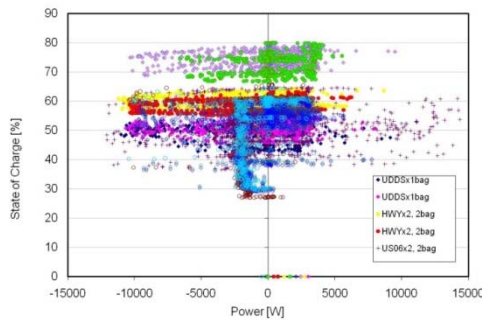


Figure 20. SOC versus Battery Power

The frequency of SOC was determined as illustrated in Figure 21.

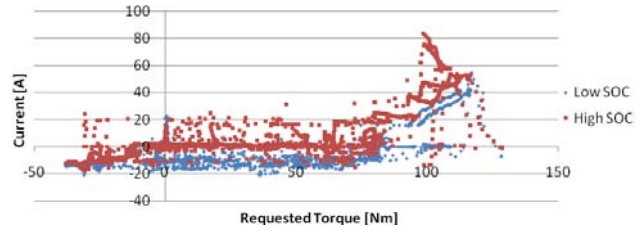


Figure 21. Comparison of Torque Request against Current for High and Low SOC

Observation of the requested torque as read by the CAN bus and the SOC revealed that if the requested torque exceeds 80 Nm, the IMA will not apply additional load to charge the battery, regardless of the SOC (Figure 22).

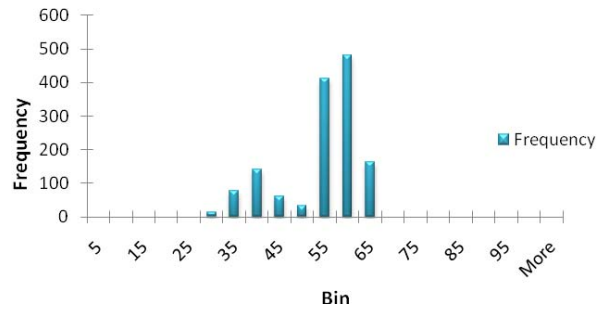


Figure 22. Histogram of SOC Frequency for UDDS Low SOC Test

8.3 Performance

High SOC tests were compared to low SOC tests (see Table 1). The IMA benefits acceleration, and tests in which the IMA contributed more energy to vehicle acceleration had lower passing times.

Table 1. Summary of Passing Time Results

Data Set	Metric	Passing Test			
		35-55	55-65	35-70	55-80
60907050 Avg SOC	Time [s]	5.80	4.50	13.10	12.70
	IMA Assist [kJ]	64.91	41.46	37.18	53.53
60907051 High SOC	Time[s]	6.30	4.80	12.50	12.70
	IMA Assist [kJ]	54.99	42.26	78.08	64.48
60907052 Low SOC	Time[s]	7.70	6.00	12.70	13.10
	IMA Assist [kJ]	-3.87	-2.36	46.59	43.78

8.4 Emissions

The emissions generated by the Honda Civic hybrid are shown in Figure 23 and Table 2. According to the Environmental Protection Agency (EPA) emission standard for lightweight vehicles, the Honda Civic meets SULEV standards, Tier II Bin 2. These standards may be referenced in Table 3.

The cold start UDDS cycle was observed to generate the most emissions, although they were still within SULEV standards. The post-catalytic exhaust temperature is plotted in Figure 24 for comparison of temperature to tailpipe emissions. Test cycles with lower post-catalytic exhaust temperatures were observed to produce higher total hydrocarbon (THC), oxides of nitrogen (NO_x), and methane (CH₄) emissions, while aggressive drive cycles, such as US06, produced higher carbon monoxide (CO) emissions.

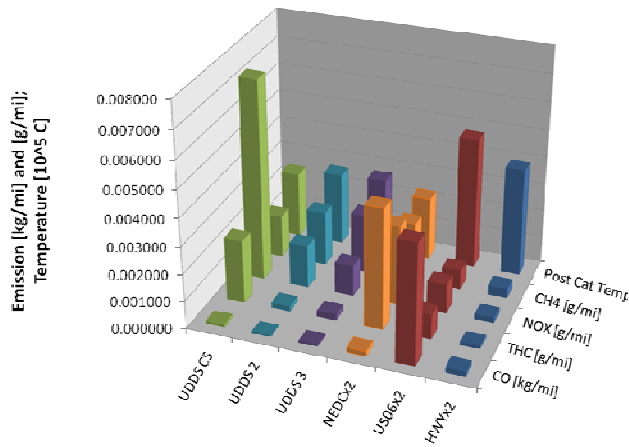


Figure 23. Tailpipe Emissions for Various Drive Cycles

Table 2. Table of Emissions Results for Various Drive Cycles

	UDDS CS	UDDS 2	UDDS 3	NEDC x2	US06 x2	HWY x2
CO [kg/mi]	0.000105	0.000054	0.000077	0.000170	0.004348	0.000173
THC [g/mi]	0.002298	0.000184	0.000215	0.004379	0.000896	0.000113
NO _x [g/mi]	0.007300	0.001562	0.001127	0.002911	0.001092	0.000194
CH ₄ [g/mi]	0.001544	0.001977	0.002152	0.002152	0.000716	0.000341
Post Cat [C]	239.64	264.00	270.73	228.78	477.53	394.46

Table 3. EPA Emission Standards
[http://www.epa.gov/otaq/standards/light-duty/tier2stds.htm]

Standard	Emission Limits at 50,000 miles					Emission Limits at Full Useful Life (120,000 miles) ²				
	NOx (g/mi)	NMOG (g/mi)	CO (g/mi)	PM (g/mi)	HCHO (g/mi)	NOx (g/mi)	NMOG (g/mi)	CO (g/mi)	PM (g/mi)	HCHO (g/mi)
Bin 1	-	-	-	-	-	0	0	0	0	0
Bin 2	-	-	-	-	-	0.02	0.01	2.1	0.01	0.004
Bin 3	-	-	-	-	-	0.03	0.055	2.1	0.01	0.011
Bin 4	-	-	-	-	-	0.03	0.07	2.1	0.01	0.011
Bin 5	0.05	0.075	3.4	-	0.015	0.07	0.09	4.2	0.01	0.018
Bin 6	0.08	0.075	3.4	-	0.015	0.1	0.09	4.2	0.01	0.018
Bin 7	0.11	0.075	3.4	-	0.015	0.15	0.09	4.2	0.02	0.018
Bin 8	0.14	0.100 / 0.125 ^c	3.4	-	0.015	0.2	0.125 / 0.156	4.2	0.02	0.018
Bin 9 ^b	0.2	0.075 / 0.140	3.4	-	0.015	0.3	0.090 / 0.180	4.2	0.06	0.018
Bin 10 ^b	0.4	0.125 / 0.160	3.4 / 4.4	-	0.015 / 0.018	0.6	0.156 / 0.230	4.2 / 6.4	0.08	0.018 / 0.027
Bin 11 ^b	0.6	0.195	5	-	0.022	0.9	0.28	7.3	0.12	0.032

The post-catalytic temperature over time is shown for the UDDS cold start and hot start cycles (Figure 24). It was observed that the catalytic converter would be fully warmed up 300 s into the test, regardless of starting conditions of the test.

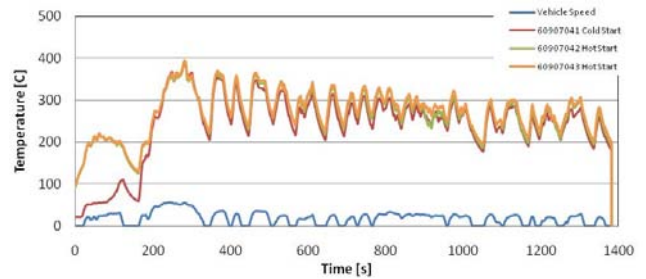


Figure 24. Image of Exhaust Temperature Overtime for UDDS

Emissions data were also observed for cycles comparing high and low SOC (see Figure 25 and Table 4). The initial SOC was not observed to have an effect; the average post-catalytic exhaust temperature dominated the amount of emissions produced.

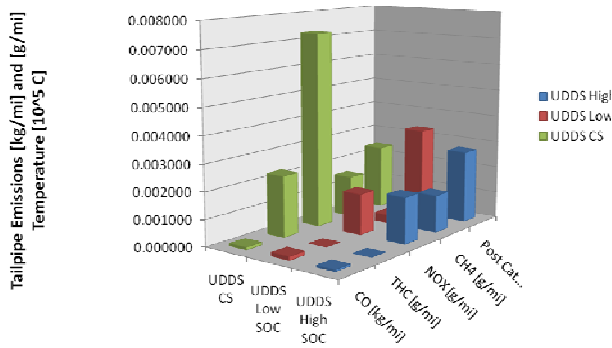


Figure 25. Tailpipe Emissions for UDDS High and Low SOC

Table 4. Comparison of Emissions and Initial State of Charge

	UDDS High SOC	UDDS Low SOC	UDDS CS
CO [kg/mi]	0.000068	0.000145	0.000105
THC [g/mi]	0.000000	0.000000	0.002298
NOx [g/mi]	0.001735	0.001538	0.007300
CH4 [g/mi]	0.001405	0.000312	0.001544
Post Cat Temp [°C]	270.90	331.18	239.60

8.5 Energy Consumption

The energy consumption for the Honda Civic Hybrid is shown in Figure 26. This figure compares the mileage to the amount of electrical energy consumed and thus reveals the effectiveness of the IMA. For this analysis, positive electrical power is defined by the current convention used for this analysis. Positive current is current that leaves the battery and goes to the motor, providing input energy to the continuously variable transmission (CVT), while negative current is current that leaves the electric motor and goes to the battery, taking power off the flywheel.

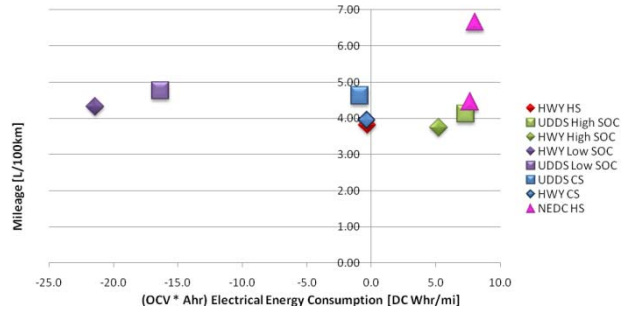


Figure 26. Energy Usage for Honda Civic Hybrid

Tests with a high initial state of charge were able to attain the best mileage. Also, it was observed that drive cycles consisting of high speeds and high accelerations yielded worse mileage. Finally, the difference in mileage for hot start and cold start tests was minimal.

Summary

The Honda Civic hybrid is a less-costly approach to generating an HEV. Through the use of integrated motor-assist power electronics coupled to the engine crankshaft output, the Civic Hybrid is able to achieve relatively low fuel consumption numbers on standardized drive cycles as a result of aggressive engine on-off operation, in combination with motor assist for acceleration events and braking regeneration.

The system consists of an integrated motor assist, with a 15-kW permanent magnet motor powered by a small nickel metal hydride (NiMH) battery. Typical battery use was observed at 0.2~0.3 kWh for a standard UDDS cycle. Aggressive engine shutoff is controlled via (1) a three-step hydraulic-powered rocker arm system that enables all cylinders to be shut off from airflow or (2) a two-step system, resulting in maximum power effort.

Vehicle specifications are listed in Table 5.

Table 5. 2006 Honda Civic Hybrid Specifications

Hybrid System Net Power	110 hp @ 6000 rpm (85kW) 123 lb-ft @ 2500 rpm (167 Nm)
Engine	1.3-L SOHC 8-valve i-VTEC 4-cylinder Variable Cylinder Management (VCM) 93hp @ 6000rpm (70kW) 89 lb-ft @ 4500rpm (123 Nm)
Electric Motor	
Power output	20 hp @ 2000 rpm (15 kW) 76 lb-ft @ 0–1160 rpm (103 Nm)
Motor Type	Permanent magnet DC brushless motor
Voltage	*Data unpublished
Traction Battery	
Power output	
Type	Ni-MH
Voltage	158
Ignition	Direct ignition system with immobilizer
Transmission	Continuously Variable Transmission (CVT)
Drivetrain	Front engine, front-wheel drive
Body construction	Unit-body construction
Suspension	MacPherson strut front suspension Multi-link rear suspension Stabilizer bar
Steering	Electric power-assisted rack and pinion steering
Turning circle diameter, curb to curb (ft)	34.8
Brakes	Power-assisted ventilated front disc/solid rear disc brakes Anti-lock braking system (ABS)/electronic brake distribution (EBD) with brake assist
Traction and Control System	Electronic Stability Vehicle Stability Assist™ (VSA®) with traction control

Conclusions

The APRF at Argonne is a powerful tool for gathering data from the most advanced powertrains at a level of detail not available anywhere else in the industry. The original equipment manufacturer (OEM) partners in FreedomCAR have become close collaborators in terms of sharing time and equipment, and they benefit significantly from the testing programs and studies performed at Argonne’s Center for Transportation Research. In addition, Argonne is constantly introducing new instrumentation methods, like CAN signal data acquisition, which can replace some sensors. This will improve the reliability of data acquisition and reduce the effort and time delays encountered when fabricating and installing intrusive sensors into the vehicle. Such new testing methodologies will also allow us to collect more readings from a larger subset of vehicles being tested.

Preliminary Civic-to-Insight Comparison

In addition to general benchmarking of the Honda Civic, one of the larger goals of the effort was to provide data with which to compare Honda’s existing hybrid vehicle (Civic) to a next-generation vehicle (Insight). In this case, the main goal of the newly developed Insight was to achieve a significant cost reduction while creating a high-fuel-economy vehicle. The new system does offer a significant cost advantage over the existing Civic vehicle: \$19,800 versus \$23,800 base MSRP, but this is at the expense of highway fuel economy. Figure 27 shows the respective label fuel economies for both the Insight and the Civic.

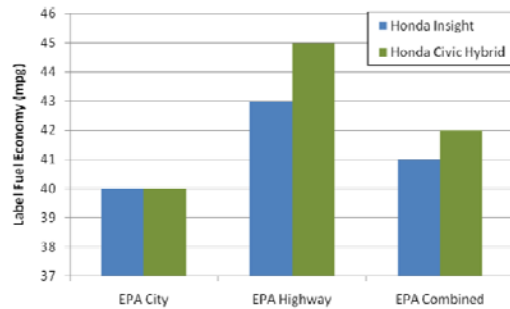


Figure 27. Honda Insight and Civic Fuel Economy

The main tasks associated with comparing the Civic and Insight involve understanding the design-level compromises leading to this lower-cost and slightly lower fuel economy vehicle.

Through some preliminary testing, a few key issues have been identified as likely causes for the difference in fuel economy. The first major differentiator is the amount of regenerative braking capability the vehicles possess. Regenerative braking capability is a direct fuel economy enabler. Thus, any reduction in this capability will directly affect the vehicle’s fuel economy. In several presentations, Honda has claimed that the Insight’s motor-generator has been reduced in size to minimize system costs. This reduction in size will directly reduce the capability of the hybrid system in terms of power and torque capability (at certain speeds). With this design decision in mind, the lower regenerative braking capability shown in Figure 28 is expected, but it speaks directly to the difference in fuel economy. If less regenerative braking energy is

captured, less energy is available to supplement fossil fuel.

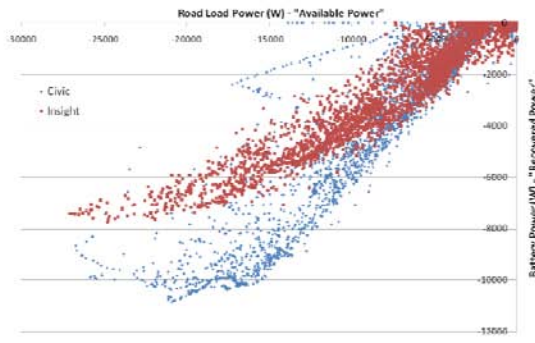


Figure 28. Honda Insight and Civic Regenerative Braking Capability

In addition to reduced regenerative braking capability, the size-reduced motor-generator also contributes to two additional factors that help explain the Insight's reduced fuel economy. Because of the motor's reduced operating envelope, the hybrid system does not use the system as often and therefore must operate at reduced overall efficiency, as compared to the more powerful (and therefore more flexible) Civic system. Figure 29 exemplifies this effect. During a simple highway cruising cycle, the Civic motor shows many more torque peaks where it is working to help increase the system's overall efficiency.

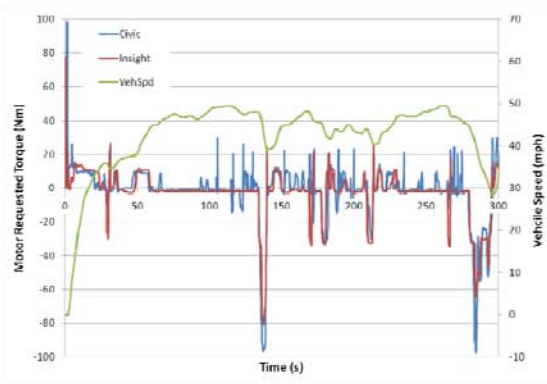


Figure 29. Honda Insight and Civic Motor Requested Torque

Another likely effect of the reduced motor-generator capability is that the Insight's engine must also run at a higher load (power) over a given cycle. This is again largely due to the Insight's weaker system and reduced ability to supplement the engine with power

from the hybrid system. Figure 30 illustrates this point. Note that during a portion of the highway cycle, the Civic engine power is lower than that of the Insight.

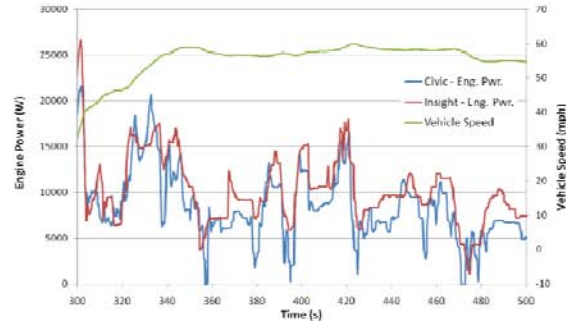


Figure 30. Honda Insight and Civic Engine Power

Argonne has performed a preliminary investigation of the new Honda Insight relative to the Honda Civic. It has been hypothesized that the reduced fuel economy is partially due to the reduced motor-generator size and thus capability. This hypothesis appears true given the previous analysis, but more data and analyses are needed to understand the design trade-offs made in developing the Insight. It is anticipated in FY 2010 that much more knowledge will be gained regarding the Insight and the design decisions that went into developing this low-cost vehicle. Furthermore, this knowledge will help provide Argonne with the groundwork to continually aid in the development of more cost effective and higher fuel economy advanced vehicles.

B. Benchmarking and Validation of Plug-in Hybrid Electric Vehicles

Michael Duoba (project leader)

Argonne National Laboratory

9700 South Cass Avenue

Argonne, IL 60439-4815

(630) 252-6398; mduoba@anl.gov

DOE Technology Manager: Lee Slezak

Objectives

- Gain insight into new, experimental test methods for plug-in hybrid electric vehicles (PHEV) to support SAE J1711 effort.
- Use novel instrumentation and Argonne's capability to "crack" controller area network (CAN) messages to provide a clear view into the internal workings of the PHEV's control strategy and its affect vehicle-level results.
- Provide vehicle-level and detailed component data during chassis dynamometer testing of the following vehicles:
 - End-of-life Hymotion Gen 2 Prius conversion.
 - Hymotion Gen 2 Prius with "Version 2" L5 System.
 - Argonne Prototype Through-the-Road (TTR) PHEV.
 - Plug-in Conversion Corporation Prius, nickel metal hydride (NiMH) PHEV with advanced controls.

Approach

- Test fuel economy and emissions over the Urban Dynamometer Driving Schedule (UDDS), Highway (HWY), and US06 cycles. Repeat with air conditioner (A/C) on.
- Measure energy usage from the vehicle's battery system(s) by using the Hioki Power Meter current and voltage sensors. The Hioki meter also calculates real-time ampere-hour (A•h) and kilowatt-hours (kWh).
- Determine, scale, and record CAN signals through testing as a means of measuring parameters that would otherwise be too difficult or expensive to obtain.

Accomplishments

- Developed calculation tool that summarizes all the components of a PHEV according to the latest J1711 and California Air Resources Board (CARB) procedures in an easy-to-read, one-page printout.
- Produced insightful data on the various operational strategies for the blended-style PHEV Prius, as well as quantified differences in operation of the end-of-life PHEV.
- Upgraded test facility to auto initialize and collect CAN signals and Hioki battery power analyzer data into the facility acquisition system for proper time alignment, timestamp, and data merging. This results in substantial time savings in data analysis and improved accuracy.

Future Directions

- Upgrade four-wheel drive (4WD) dynamometer facility to perform U.S. Environmental Protection Agency (EPA) 5-Cycle (SC03 and extreme cold for the -7°C Federal test procedure [FTP])) tests to quantify and benchmark advanced technology vehicles over a profile of realistic, in-use conditions.
 - Expand similar investigations into dedicated battery electric vehicles.
-

Introduction

A fundamental component of the PHEV R&D plan is the updating of benchmark data of the best-available PHEVs as they become more sophisticated in design over time. Since PHEV conversions first became available, a new, second generation has emerged that incorporates operation constraints that avoid high criteria tailpipe emissions (a controversial issue for aftermarket conversion companies sometimes seen in early generation conversions) and can operate without fuel consumption at higher vehicle speeds.

In addition, the TTR hybrid vehicle platform built by Argonne was fully benchmark tested. It can be run in all-electric mode and can also be operated in blended mode for explicit comparisons of the two methods.

Vehicle benchmarking combines testing and data analysis to characterize a vehicle's efficiency, performance, and emissions. The vehicle is tested over many cycles to deduce the control strategy under a variety of operating conditions. The PHEV benchmarking data can be applicable to virtually every effort in the FreedomCAR and Fuel Partnership, and all of the technical teams benefit from the data collected in Argonne's Advanced Powertrain Research Facility (APRF).

Approach

Argonne is a world leader in PHEV test procedure development. A standard test sequence was developed to maximize test results while meeting procedure requirements within time constraints (including two-day weekend breaks).

Standard Five-Day PHEV Benchmarking Test Schedule

Below is a sample baseline five-day PHEV test schedule used as a baseline for all benchmark PHEV testing. The US06 tests and A/C test are deleted if time is limited. Extra tests are commonly applied to investigate particular aspects of a vehicle's specific design attributes. At a minimum, the charge-depleting and charge-sustaining results of the UDDS and HWY test are found.

- **Day 1**
 - Setup vehicle and instrumentation
 - HWY×2 w/coast downs
 - US06×2 2bag charge-depleting
 - US06×2 2bag charge-sustaining (if time permits)
 - *Charge overnight*
- **Day 2**
 - HWY×2 (cold start) up to 5 pairs charge-depleting
 - If necessary, US06×2 charge-depleting until charge sustaining operation
 - HWY×2 charge-sustaining
 - UDDS prep
 - *Charge overnight*
- **Day 3**
 - UDDS 2bag (cold start) up to 6 cycles charge-depleting
 - If necessary, US06×2 charge-depleting until charge sustaining operation
 - UDDS 2bag charge-sustaining
 - *DO NOT CHARGE OVERNIGHT*
- **Day 4 (Charge-Sustaining Day)**
 - UDDS charge-sustaining 2bag (cold start)
 - UDDS charge-sustaining 2bag
 - HWY×2 charge-sustaining
 - US06×2 2bag charge-sustaining
 - UDDS prep
 - *Charge overnight*
- **Day 5 (A/C Day) (AVTA Specific testing)**
 - UDDS with A/C 2bag (cold start)
 - UDDS with A/C 2bag
 - HWY×2 with A/C
 - UDDS, UDDS, HWY×2 until charge-sustaining with A/C
 - If necessary, US06×2 charge-depleting until charge-sustaining operation
 - UDDS charge-sustaining with A/C 2bag
 - UDDS charge-sustaining with A/C 2bag
 - HWY×2 charge-sustaining with A/C
 - US06×2 charge-sustaining with A/C
 - Dismount vehicle from dyno

PHEV Results Calculation Tool (1-Page Printout)

The final results calculated from PHEV testing require extracting data from a number of tests and calculating multiple output results. The "Full Charge Test," the "Charge-Sustaining" cycles, and the overnight charge event must all be organized and the data extracted and processed according to the procedures outlined in draft SAE J1711 procedures and CARB procedures.

Argonne has written an automated calculating, tabulating, and plotting tool specifically for PHEVs. It leverages the data acquisition and processing tools written in the LabView graphical programming environment.

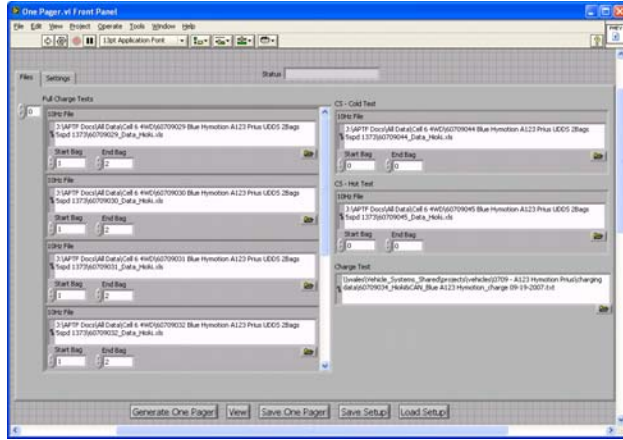


Figure 1. PHEV Calculation Tool Setup Screen

Figure 1 shows the setup screen for the tool. First, the individual test files are identified, then the data fields are initialized. Finally, comments are written and a link to a vehicle picture provides the rest of the information needed to generate a one-page printout.

A sample printout is shown in Figure 2. The first feature is the mix of plots and tables. The plots and tables line up together and auto-scale to fit the page, depending on how many cycles are in the full charge test (FCT). The charge-sustaining test and the charge event are also captured in graphs and tables. Parameters such as all-electric range (AER), charge-depleting cycle range (Rcdc), actual charge-depleting range (Rcda), equivalent all-electric range (EAER), and the electric range fraction (ERF) are calculated from the time-resolved data. Final consumption results are shown using the two utility factor (UF) weighting approaches outlined in J1711: “lumped” and “fractional.” The familiar PHEV two-dimensional(2-D) plot for describing fuel and energy consumption are also shown in the lower left corner.

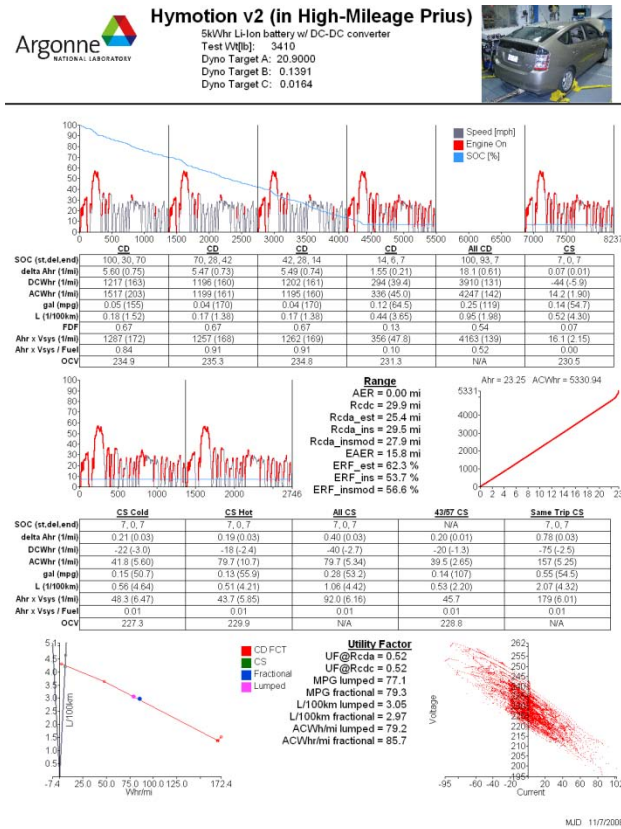


Figure 2. Sample One-Page PHEV Results

Hymotion Gen 2 Prius “Version 2” Results

Hymotion recalled all of its original PHEV field prototype conversion kits and replaced them with “Version 2” kits. Hymotion learned from the initial units and completed crash, safety, and durability testing of the new units over the past year.

Hymotion improved the frame, connectors, and electronics on the basis of the collected data. They shipped the new unit to Argonne with the latest calibrations. Argonne installed this unit in its highly instrumented Prius and completed one week of PHEV testing to benchmark the performance of the new unit (Figure 3).



Figure 3. Argonne Hymotion Prius PHEV "Version 2"

Figure A1 (in the Appendix) shows the results captured in the 2-D consumption results plots. Individual points represent cycles. Lines depict the progression from the first cycle (cold-start) to the last cycles, which are charge sustaining.

Figure A2 shows the same information from the UDDS and HWY cycles from the same Prius with the "Version 1" conversion installed. Notice that the cycle points fall on a very similar line, but the new system is slightly improved, with higher fuel displacement rates evident in high electric consumption results in the charge-depleting mode.

For example, the highest UDDS mpg result for the Version 1 was 161 mpg. For the Version 2 it was 200 MPG; again, the same vehicle driving requirements, but less contribution from the fuel driving the engine. Figure A3 shows all the Version 2 results tabulated in a spreadsheet.

A sample one-page calculation sheet is shown for the Version 2 UDDS tests that were made to show summary results on the urban cycle. They are shown in Figure A3.

End-of-Life Hymotion Gen 2 Prius Conversion

This vehicle is a high-mileage (>160,000 mi) Gen 2 Prius with a Hymotion conversion system installed after the mileage was accumulated (see Figure 4). The vehicle spent a couple of years as a fleet vehicle for accelerated life testing. It was delivered from ETEC in Phoenix, Arizona. The purpose of this test was to look at what the impact of a high-mileage host vehicle would do the PHEV results.



Figure 4. End-of-Life Hymotion Prius PHEV

The host vehicle had the expected visible wear from so many miles. However, according to the "vehicle loss" coefficients calculated during the road load determination on the dynamometer, the driven axle had no significant differences in losses compared to the low-mileage, highly instrumented Argonne Hymotion Prius also highlighted in this report. Of course, there is always the possibility that the rear axle could introduce added loads to vehicle driving.

End-of-Life Hymotion Prius	
Vehicle Odometer:	160,948
Test Wt[lb]:	3410
Vehicle A term:	12.7358
Vehicle B term:	0.2187
Vehicle C term:	-0.0005
Argonne Hymotion Prius w/Ver 2	
Vehicle Odometer:	11,000
Test Wt[lb]:	3400
Vehicle A term:	12.8624
Vehicle B term:	0.2108
Vehicle C term:	0.0002

End-of-Life Hymotion Results

The fuel economy of the high-mileage Prius in stock (sustaining) mode was tested as roughly 10% lower than the low-mileage Argonne Prius. This indicates losses unrelated to the Hymotion system. The electrical energy consumption is actually higher than Argonne's Version 2 vehicle results.

The criteria pollutant emissions of a high-mileage vehicle are of concern when evaluating an end-of-life vehicle. Figure 5 shows all of the conversion

PHEVs cold/hot weighted non-methane organic gas (NMOG) and nitrogen oxides (NO_x) emissions for both charge-depleting (colored dots) and charge-sustaining (white dots) modes. Notice that control of NMOG is still obtained by the high-mileage vehicle. Also, NO_x in stock mode is sufficiently controlled. However, the emissions control of NO_x in the charge-depleting mode is not satisfactory. In fact, it is the highest NO_x emissions measured from any PHEV converted Prius test at Argonne.

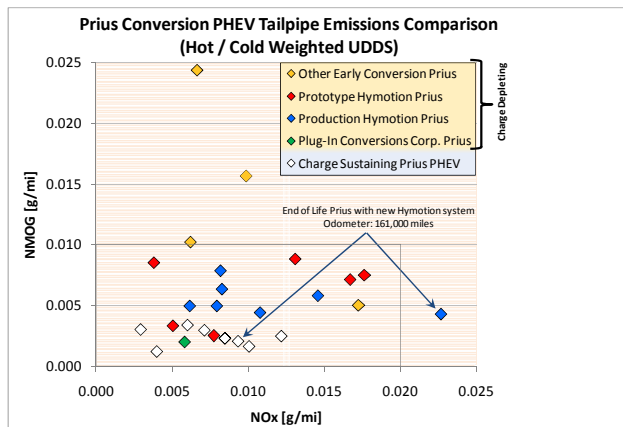


Figure 5. Summary of NMOG and NO_x Emissions from Converted Prius PHEVs

Argonne Prototype TTR PHEV

TTR PHEV stands for through-the-road plug-in hybrid electric vehicle. This vehicle was specifically built to investigate PHEV capabilities and operation without the limitations of a conversion-style, blended, depleting operation.

This prototype TTR PHEV has a separate electric drivetrain in the rear to provide assist and regeneration. A 10-kWh lithium (Li)-ion battery pack is mounted in the rear. An automotive-grade microcontroller using the latest state-of-the-art rapid prototyping tools was used to control the vehicle for proper PHEV operation. Figures 6 and 7 show the vehicle in Argonne’s APRF.

This vehicle actually has similar attributes to Ford’s prototype Escape PHEV, and thus it was run at the same weight and road load as that vehicle. However, in this report, those comparisons are absent because Ford’s test results are CRADA-protected.



Figure 6. TTR PHEV Testing in the 4WD Dynamometer Cell in Argonne’s APRF



Figure 7. TTR PHEV On Test at the 4WD Dynamometer

One interesting study in this test program is comparing and contrasting “blended” with all-electric [Extended-Range Electric Vehicle (EREV)] charge-depleting operation where all other parameters (such as battery size and powertrain characteristics) are kept constant. In the charge-depleting UDDS tests, for example, the blended mode ran four charge-depleting cycles before transitioning into sustaining mode on the fifth UDDS. In all-electric depleting mode, three UDDS cycles were run after transitioning at the beginning of the fourth cycle.

Argonne TTR Results

The all-electric range was 22.5 miles. The calculated “equivalent all-electric range” was 22.0 miles. The

blended mode yielded 24.5 miles with the same calculation. In fact, in blended mode, the vehicle was able to pull out more energy over the depleting cycles than in the all-electric cycles. This dampened the differences between the UF-weighted results of the two scenarios.

The UF favors early use of onboard battery energy. It follows that in real use, if the depletion rate is too slow, some portion of daily driving profiles would result in a vehicle returning home with battery energy still in the pack. This reduces the fraction of electric energy that can displace fuel energy.

Compare the results shown in Figure A5 to A6. The results labeled “MPG fractional” are the best representation of the UF methods. The blended mode calculation yielded 49.7 mpg while the electric-only calculation is 51.8 mpg.

Plug-in Conversion Corporation Prius

There are two unique design features of the Plug-In Conversion Corporation (PICC) Prius (Figures 8 and 9). The first is the battery. This vehicle has a NiMH battery, which has different properties than a Li-ion battery. The battery chemistry differences are observed in the vehicle capabilities and results, as well as in the validity of the assumptions made in test procedures.

The second unique feature of the PICC PHEV is the elevated electric-only speed. Because of planetary gear kinematic speed limitations, the Prius cannot run at speeds higher than 40 mph safely and reliably with the engine at zero speed. What the PICC PHEV does is spin the engine without fueling. This provides higher speed running (up to 50 mph). PICC engineers feel that this helps when the vehicle is driven on urban roads that have 45-mph speed limits.

Figure A7 shows all the test results in the 2-D energy space. Figures A8 and A9 show the analysis printout of the PICC Prius on the UDDS cycle in both the typical blended mode and the EV mode. First, it must be noted that the EV mode cannot operate over 50 MPH, and thus a small portion of the highest speed section of the UDDS could not be driven up to the maximum speed of 56 mph.

The difference in results of the two depleting modes is very noticeable. In the analysis plots, the gray speed trace depicts vehicle speed without the engine on. Red points in the plot depict non-zero engine speed. However, in the case of the PICC Prius in the EV mode, the engine will spin, but all propulsion comes from the electric drive system (looking closely at the speed plot, the limited acceleration can be seen). Notice that in the table placed below the speed plot in Figure A11, no fuel is consumed in the first two UDDS cycles.



Figure 8. TTR PHEV On Test the 4WD Dynamometer



Figure 9. TTR PHEV On Test the 4WD Dynamometer

Plug-in Conversion Corporation Prius Results

Like in the TTR test, the difference between EV mode operation and blended operation are seen in the analysis printouts. The EAER was less than a 2% difference between the two depleting modes,

meaning that both tests used similar amounts of electrical propulsion. However, the UF-weighted mpg results in Figures A8 and A9 show the advantage (in reducing fuel use) of depleting in EV mode. The EV mode results are 94 mpg and the blended operation yielded 88 mpg.

Because the emissions analyzers are always collecting exhaust samples during the cycle testing, it was found that running in EV mode does not mean “zero emissions.” In fact, because the engine is spinning and trace amounts of fuel exist in the intake manifold and also permeating from the oil, hydrocarbon emissions were found to be too high to pass emissions. This finding is of particular interest in to emissions regulating agencies and the conversion companies as a whole.

Conclusions

The APRF at Argonne has become a powerful tool for gathering data from the most advanced powertrains at a level of detail not available anywhere else in the industry.

The OEM partners in FreedomCAR have become close collaborators in terms of sharing time and equipment. They benefit significantly from the testing programs and studies performed at Argonne’s Center for Transportation Research.

In addition, Argonne is continually introducing new instrumentation methods and analysis tools. These activities create a very clear picture of how all the components work in concert and how to make sense of the vehicle-level performance.

PHEVs have such completely different vehicle technology, including more than their electrification. PHEVs have two energy sources being used in a range-dependent manner.

The results of the extensive testing performed in the APRF have provided direction to test engineers for applying suitable test procedures and benchmark analysis to technology developers to be used to calibrate expectations of PHEV technology.

The APRF’s role in continually testing cutting-edge technologies is a key component to tracking and accelerating improved performance and efficacy of electrified vehicles.

Appendix: Graphs and Other Figures

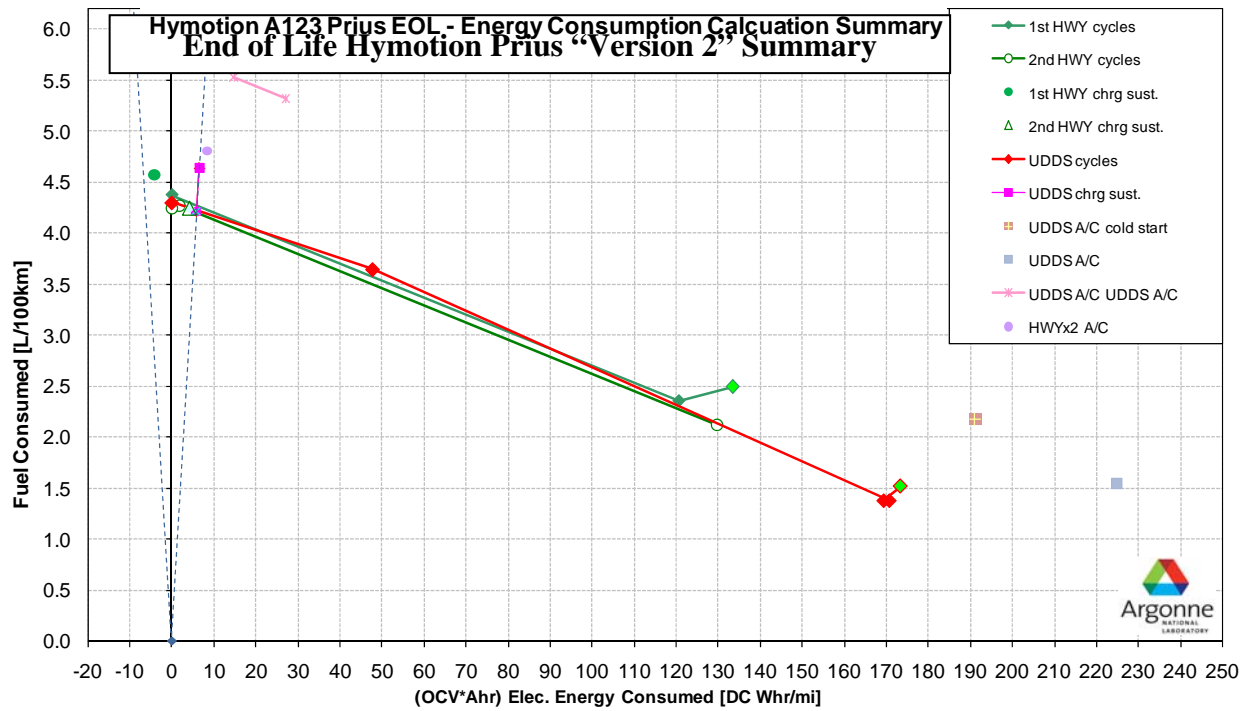


Figure A1. End of Life Prius with Hymotion Version 2 Conversion Results Summary

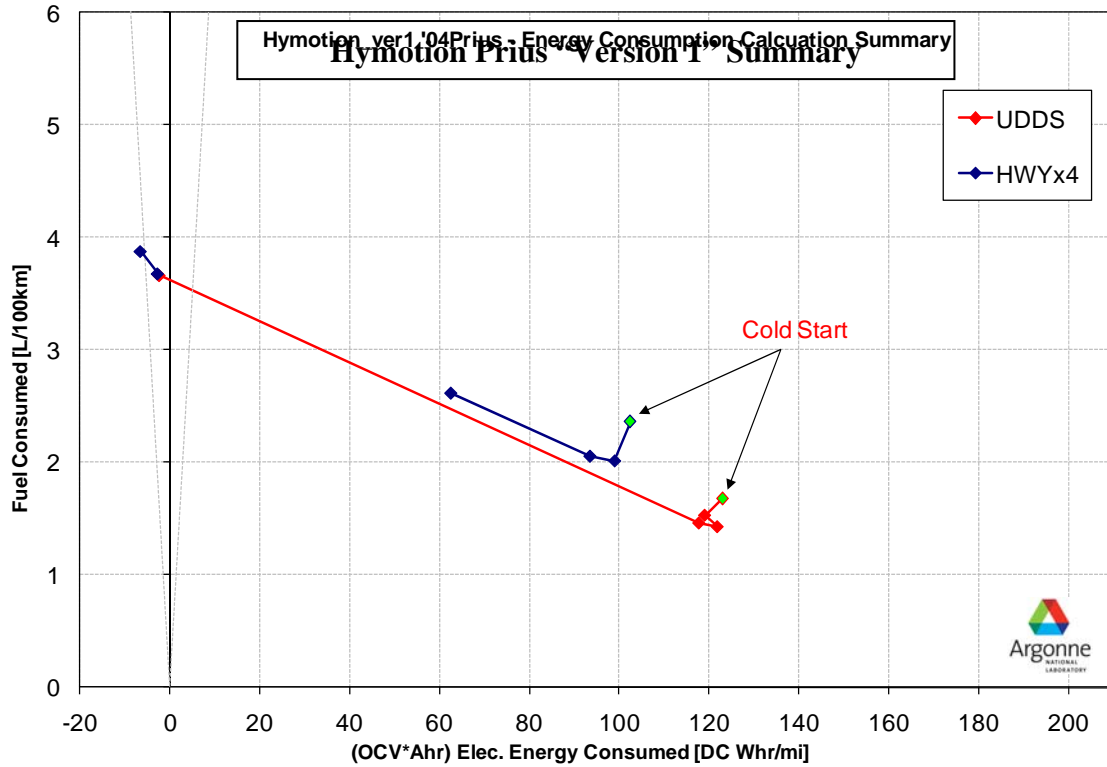


Figure A2. For reference: Hymotion Prius Version 1 Consumption Results Summary

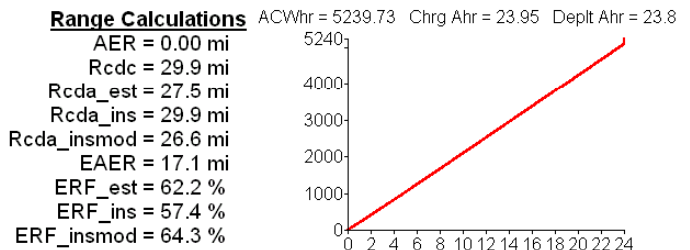
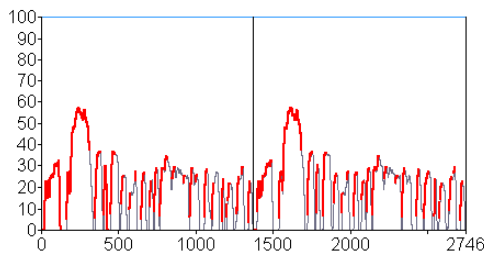
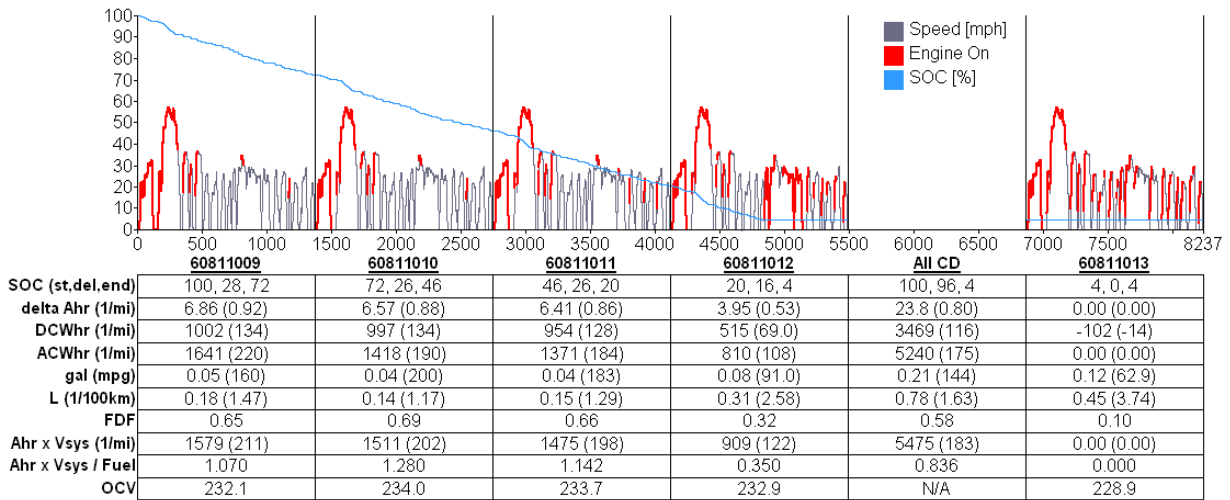
Test #	Cycle Filename	Date	Conditions (hot, cold-start)	Notes Chrg Depl or Chrg Balance	Hioki AC charging WP6 [kWhr]	Hioki Batt Phase1 IH1 [Ahr]	Hioki Batt Phase1+2 [Ahr]	Hioki Batt Phase1 WP1 [kWhr]	Hioki Batt Phase1+2 WP1 [kWhr]	Fuel Scale Phase1 Fuel Consumed [L]	Fuel Scale Phase1+2 Fuel Consumed [L]	Distance Traveled Phase1 [mi]	Distance Traveled Phase2 [mi]	Distance Traveled Total [mi]	Bag 1 Fuel Economy [mpg]	Bag 2 Fuel Economy [mpg]	Bag 1+2 Fuel Economy [mpg]
60811003	US06x2	11/4/2008	HS	CD		3.298	6.294	0.678	1.287	0.559	1.106	8.02	8.01	16.03	53.22	54.08	
60811004	US06x2	11/4/2008	HS	CD		3.016	6.030	0.613	1.236	0.576	1.139	8.02	8.01	16.03	52.01	52.48	
	overnight charging				4.12												
60811005	HWYx2	11/5/2008	CS	CD		5.754	11.166	1.260	2.451	0.349	0.643	10.26	10.26	20.52	112.91	129.13	
60811006	HWYx2	11/5/2008	HS	CD/trans		5.122	5.308	1.134	1.149	0.324	0.930	10.26	10.25	20.51	118.81	63.45	
60811007	HWYx2	11/5/2008	HS	CB		-0.242	-0.427	-0.085	-0.150	0.812	1.437	10.26	10.26	20.52	59.95	61.59	
60811008	UDDS prep	11/5/2008	HS			-0.220	-0.303	-0.070	-0.126	0.288	0.536	3.60	3.87	7.47	48.90	58.66	53.51
	overnight charging				5.16												
60811009	UDDS cold start	11/6/2008	HS	CD		2.020	4.710	0.420	1.003	0.177	0.186	3.60	3.87	7.47	81.14	1703.76	160.18
60811010	UDDS #2	11/6/2008	HS	CD		2.110	4.643	0.451	0.997	0.139	0.147	3.60	3.87	7.47	102.50	1747.69	200.20
60811011	UDDS #3	11/6/2008	HS	CD		1.920	4.449	0.410	0.954	0.146	0.162	3.60	3.86	7.46	97.72	969.06	182.87
60811012	UDDS #4	11/6/2008	HS	trans		1.950	2.543	0.418	0.516	0.140	0.319	3.60	3.87	7.47	101.79	82.83	91.00
60811013	UDDS #5	11/6/2008	HS	CB		-0.334	-0.168	-0.105	-0.102	0.252	0.432	3.60	3.88	7.48	51.18	79.87	62.91
60811014	UDDS #6	11/6/2008	HS	CB		-0.472	-0.333	-0.140	-0.143	0.270	0.453	3.60	3.87	7.46	50.29	79.93	62.25
	overnight charging				5.24												
60811015	UDDS cold start	11/7/2008	CS	CB		-0.490	-0.375	-0.147	-0.159	0.316	0.504	3.60	3.87	7.47	43.77	77.78	56.59
60811016	UDDS #2	11/7/2008	HS	CB		-0.411	-0.428	-0.125	-0.166	0.265	0.457	3.60	3.87	7.46	51.26	75.75	61.57
60811017	HWYx2	11/7/2008	HS	CB		-0.367	-0.466	-0.109	-0.154	0.657	1.266	10.26	10.26	20.52	58.94	63.23	
60811018	US06x2	11/7/2008	HS	CB		-0.214	-0.266	-0.143	-0.237	0.768	1.506	8.02	8.02	16.04	40.16	41.01	

Figure A3. Hymotion Prius Version 2 Tabulated Results Summary

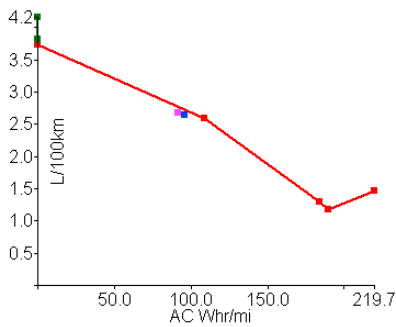


Hymotion ver2 Prius PHEV

5 kWhr Li-Ion battery in addition to the Prius NiMH pack
 Dyno Config:2WD; Test Wt[lb]: 3410
 Dyno Target A: 20.9000
 Dyno Target B: 0.1391
 Dyno Target C: 0.0164

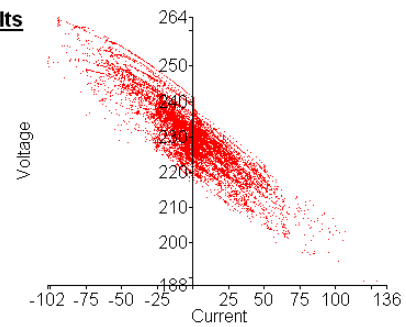


	60811015 - CS Cold	60811016 - CS Hot	All CS	43/57 CS	Same Trip CS
SOC (st.del.end)	100, 0, 100	100, 0, 100	100, 0, 100	N/A	N/A
delta Ahr (1/mi)	0.01 (0.00)	0.00 (0.00)	0.01 (0.00)	0.01 (0.00)	0.02 (0.00)
DCWhr (1/mi)	-159 (-21)	-166 (-22)	-325 (-22)	-163 (-22)	-658 (-22)
ACWhr (1/mi)	2.60 (0.35)	0.51 (0.07)	2.79 (0.19)	1.41 (0.19)	3.16 (0.11)
gal (mpg)	0.13 (56.6)	0.12 (61.6)	0.25 (59.0)	0.13 (59.3)	0.50 (60.2)
L (1/100km)	0.50 (4.16)	0.46 (3.82)	0.96 (3.99)	0.48 (3.96)	1.88 (3.90)
Ahr x Vsys (1/mi)	2.76 (0.37)	0.23 (0.03)	2.99 (0.20)	1.32 (0.18)	3.45 (0.12)
Ahr x Vsys / Fuel	0.001	0.000	0.000	0.000	0.000
OCV	227.6	230.2	N/A	229.1	N/A



UF-Weighted Results

- UF@Rcdc = 0.52
- MPG lumped = 87.83
- MPG fractional = 89.29
- L/100km lumped = 2.678
- L/100km fractional = 2.634
- ACWhr/mi lumped = 91.46
- ACWhr/mi fractional = 96.1



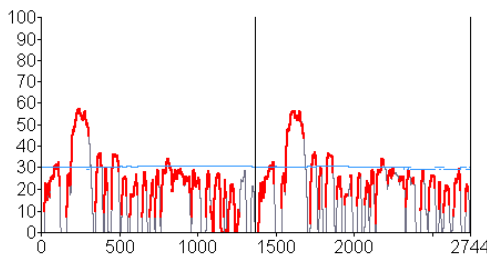
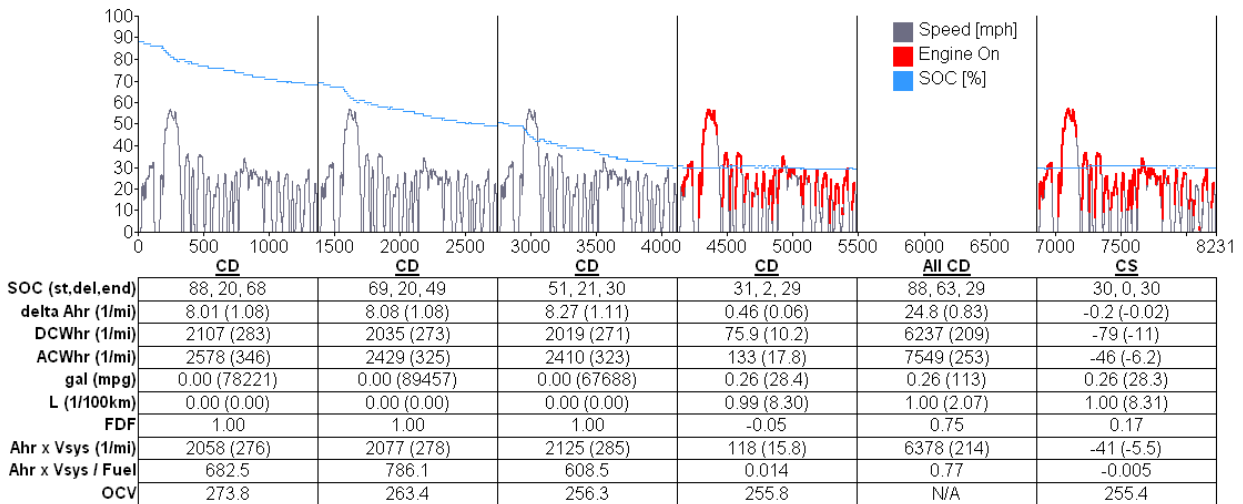
MD 10/29/2009

Figure A4. Hymotion Prius Version 2 Final Results – UDSS tests

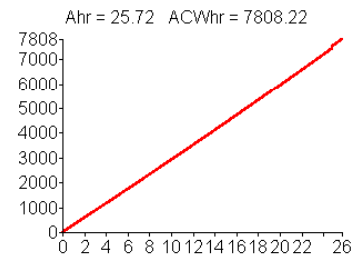


TTR

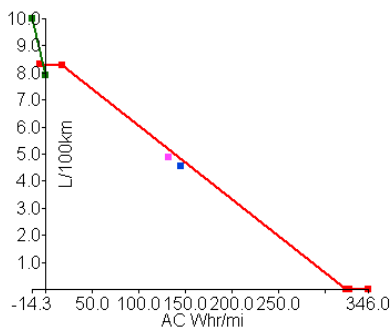
ANL Prototype Through-The-Road PHEV
 Escape Dyno Road Load Used (for comparisons)
 Run in All-Electric CD Mode



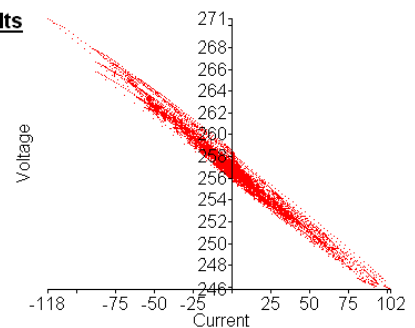
Range Calculations
 AER = 22.5 mi
 Rcdc = 29.8 mi
 Rcda_est = 22.6 mi
 Rcda_ins = 28.1 mi
 Rcda_insmod = 22.4 mi
 EAER = 22.0 mi
 ERF_est = 97.3 %
 ERF_ins = 78.4 %
 ERF_insmod = 98.2 %



	CS Cold	CS Hot	All CS	43/57 CS	Same Trip CS
SOC (st.del.end)	30, 0, 30	30, 0, 30	30, 0, 30	N/A	N/A
delta Ahr (1/mi)	-0.4 (-0.05)	0.00 (0.00)	-0.4 (-0.02)	-0.2 (-0.02)	-0.4 (-0.01)
DCWhr (1/mi)	-131 (-18)	-34 (-4.6)	-165 (-11)	-76 (-10)	-234 (-7.9)
ACWhr (1/mi)	-106 (-14)	1.39 (0.19)	-105 (-7.1)	-45 (-6.0)	-103 (-3.5)
gal (mpg)	0.32 (23.5)	0.25 (29.8)	0.57 (26.3)	0.28 (26.7)	1.06 (27.9)
L (1/100km)	1.20 (10.0)	0.94 (7.90)	2.14 (8.95)	1.05 (8.80)	4.03 (8.42)
Ahr x Vsys (1/mi)	-95 (-13)	1.08 (0.15)	-94 (-6.3)	-40 (-5.4)	-91 (-3.1)
Ahr x Vsys / Fuel	-0.009	0.000	-0.01	-0.004	-0.00
OCV	257.0	257.0	N/A	257.0	N/A



UF-Weighted Results
 UF@Rcdc = 0.52
 MPG lumped = 48.4
 MPG fractional = 51.8
 L/100km lumped = 4.86
 L/100km fractional = 4.54
 ACWhr/mi lumped = 132
 ACWhr/mi fractional = 145



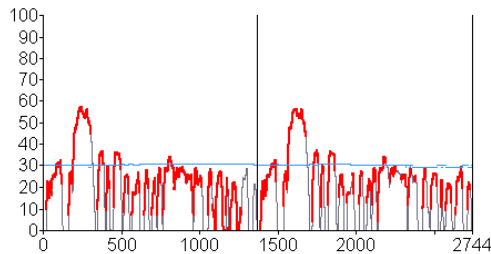
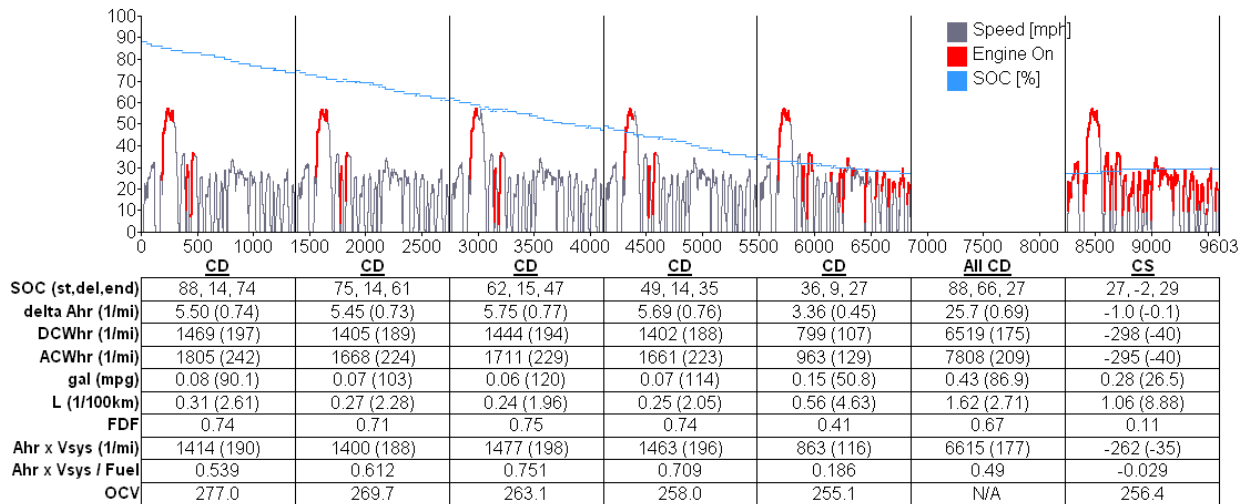
MJD 1/8/2009

Figure A5. Argonne TTR Prototype PHEV in All-Electric Depleting Mode - UDSS tests

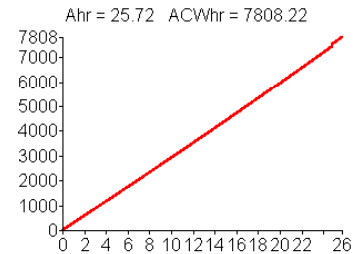


TTR

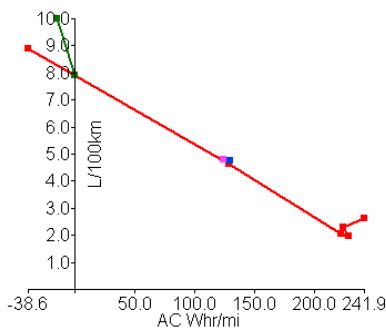
ANL Prototype Through-The-Road PHEV
Escape Dyno Road Load Used (for comparisons)
Run in Blended Mode



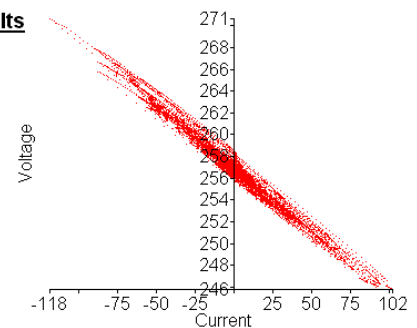
Range Calculations
 AER = 0.84 mi
 Rcdc = 37.3 mi
 Rcda_est = 34.1 mi
 Rcda_ins = 35.2 mi
 Rcda_insmod = 34.2 mi
 EAER = 24.5 mi
 ERF_est = 72.0 %
 ERF_ins = 69.5 %
 ERF_insmod = 71.7 %



	CS Cold	CS Hot	All CS	43/57 CS	Same Trip CS
SOC (st.del.end)	30, 0, 30	30, 0, 30	30, 0, 30	N/A	N/A
delta Ahr (1/mi)	-0.4 (-0.05)	0.00 (0.00)	-0.4 (-0.02)	-0.2 (-0.02)	-0.4 (-0.01)
DCWhr (1/mi)	-131 (-18)	-34 (-4.6)	-165 (-11)	-76 (-10)	-269 (-7.2)
ACWhr (1/mi)	-106 (-14)	1.39 (0.19)	-105 (-7.1)	-45 (-6.0)	-101 (-2.7)
gal (mpg)	0.32 (23.5)	0.25 (29.8)	0.57 (26.3)	0.28 (26.7)	1.31 (28.3)
L (1/100km)	1.20 (10.0)	0.94 (7.90)	2.14 (8.95)	1.05 (8.80)	4.97 (8.32)
Ahr x Vsys (1/mi)	-95 (-13)	1.08 (0.15)	-94 (-6.3)	-40 (-5.4)	-90 (-2.4)
Ahr x Vsys / Fuel	-0.009	0.000	-0.01	-0.004	-0.00
OCV	257.0	257.0	N/A	257.0	N/A



UF-Weighted Results
 UF@Rcdc = 0.59
 MPG lumped = 48.9
 MPG fractional = 49.7
 L/100km lumped = 4.81
 L/100km fractional = 4.73
 ACWhr/mi lumped = 124
 ACWhr/mi fractional = 130



DJB 1/8/2009

Figure A6. Argonne TTR Prototype PHEV in Blended Depleting Mode - UDDS tests

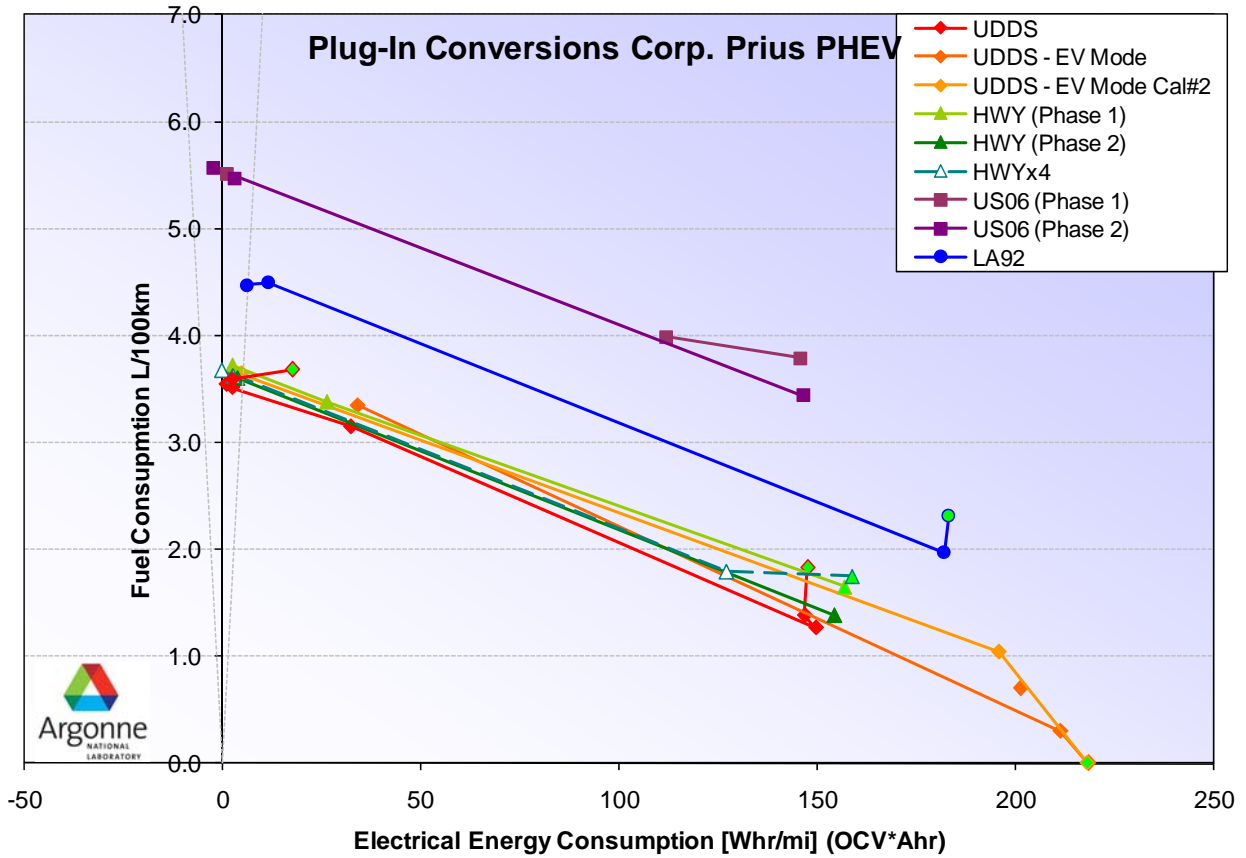
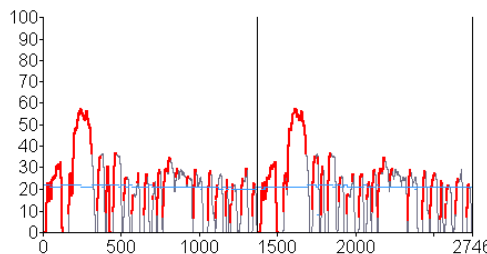
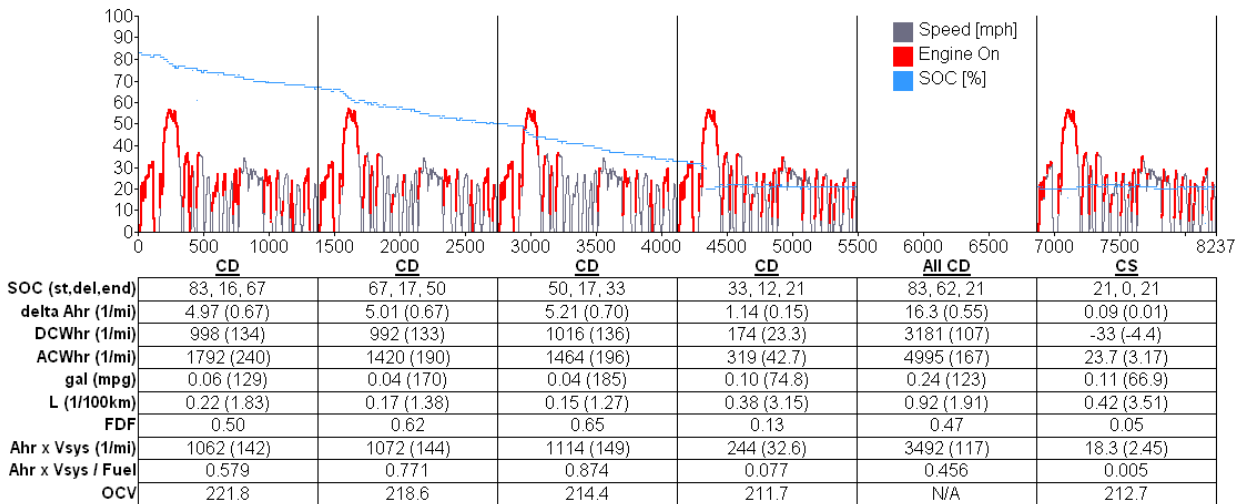


Figure A7. Argonne TTR Prototype PHEV in Blended Depleting Mode - UDDS tests

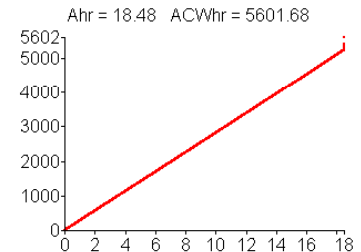


Plug-In Conversions Corp. Prius PHEV

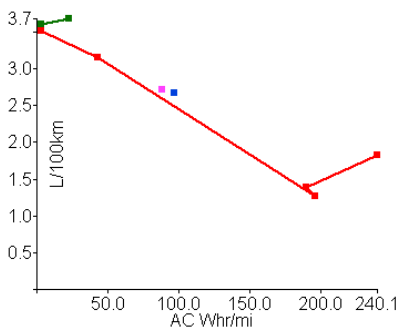
6kWhrRated NiMH battery replaces stock NiMH pack
 Dyno Config: 2WD; Test Wt[lb]: 3500
 Dyno Target A: 21.4500
 Dyno Target B: 0.1391
 Dyno Target C: 0.0164



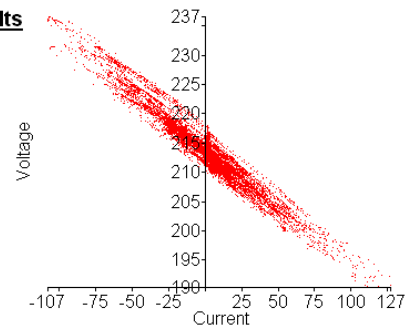
Range Calculations
 AER = 0.00 mi
 Rcdc = 29.9 mi
 Rcda_est = 24.9 mi
 Rcda_ins = 23.6 mi
 Rcda_insmod = 23.5 mi
 EAER = 14.0 mi
 ERF_est = 56.3 %
 ERF_ins = 59.5 %
 ERF_insmod = 59.8 %



	CS Cold	CS Hot	All CS	43/57 CS	Same Trip CS
SOC (st.del.end)	22, 1, 21	21, 0, 21	22, 1, 21	N/A	N/A
delta Ahr (1/mi)	0.61 (0.08)	0.09 (0.01)	0.70 (0.05)	0.31 (0.04)	0.87 (0.03)
DCWhr (1/mi)	76.8 (10.3)	-35 (-4.6)	42.2 (2.82)	13.3 (1.78)	-27 (-0.9)
ACWhr (1/mi)	171 (22.9)	23.9 (3.20)	195 (13.1)	87.0 (11.6)	244 (8.16)
gal (mpg)	0.12 (63.9)	0.11 (65.4)	0.23 (64.7)	0.12 (64.8)	0.46 (65.0)
L (1/100km)	0.44 (3.68)	0.43 (3.60)	0.87 (3.64)	0.44 (3.63)	1.74 (3.62)
Ahr x Vsys (1/mi)	130 (17.5)	18.4 (2.47)	149 (10.0)	66.6 (8.92)	186 (6.22)
Ahr x Vsys / Fuel	0.035	0.005	0.020	0.018	0.013
OCV	214.4	213.9	N/A	214.1	N/A



UF-Weighted Results
 UF@Rcdc = 0.52
 MPG lumped = 86.62
 MPG fractional = 88.15
 L/100km lumped = 2.716
 L/100km fractional = 2.668
 ACWhr/mi lumped = 88.70
 ACWhr/mi fractional = 96.7



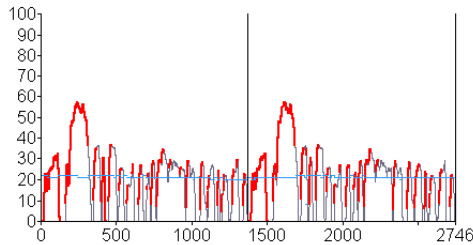
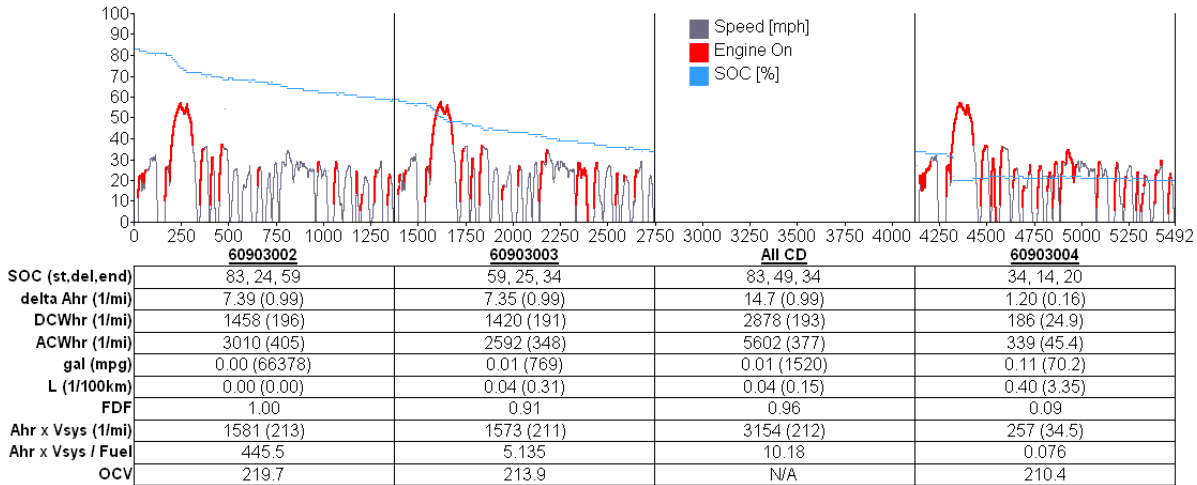
RWC 3/2/2009

Figure A8. Plug-in Conversions Corp PHEV Conversion - UDDS tests

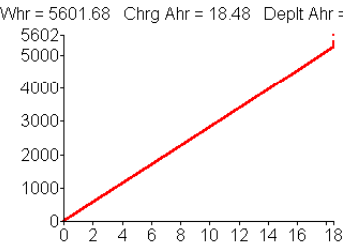


Plug-In Conversions Corp. Prius PHEV - EV Mode

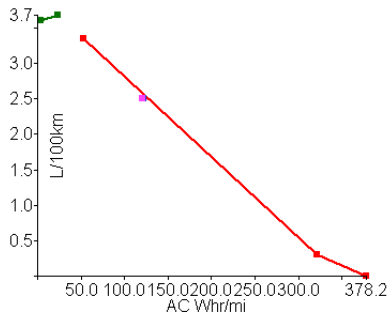
6kWhr Usable NiMH battery replaces stock NiMH pack
 Dyno Config: 2WD; Test Wt[lb]: 3500
 Dyno Target A: 21.4500
 Dyno Target B: 0.1391
 Dyno Target C: 0.0164



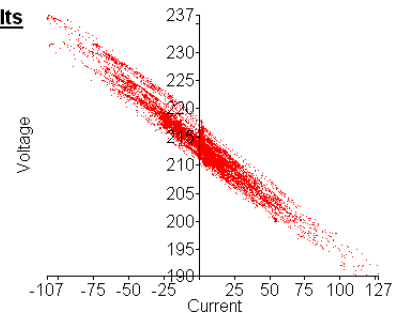
Range Calculations ACWhr = 5601.68 Chrg Ahr = 18.48 Depld Ahr = 14.7
 AER = 0.01 mi
 Rcdc = 14.9 mi
 Rcda_est = 14.9 mi
 Rcda_ins = 14.9 mi
 Rcda_insmod = 14.9 mi
 EAER = 14.2 mi
 ERF_est = 95.7 %
 ERF_ins = 95.7 %
 ERF_insmod = 95.7 %



	60902105 - CS Cold	60902095 - CS Hot	All CS	43/57 CS	Same Trip CS
SOC (st.del.end)	22, 1, 21	21, 0, 21	22, 1, 21	N/A	N/A
delta Ahr (1/mi)	0.61 (0.08)	0.09 (0.01)	0.70 (0.05)	0.31 (0.04)	0.70 (0.05)
DCWhr (1/mi)	76.8 (10.3)	-35 (-4.6)	42.2 (2.82)	13.3 (1.78)	42.2 (2.82)
ACWhr (1/mi)	171 (22.9)	23.9 (3.20)	195 (13.1)	87.0 (11.6)	195 (13.1)
gal (mpg)	0.12 (63.9)	0.11 (65.4)	0.23 (64.7)	0.12 (64.8)	0.23 (64.7)
L (1/100km)	0.44 (3.68)	0.43 (3.60)	0.87 (3.64)	0.44 (3.63)	0.87 (3.64)
Ahr x Vsys (1/mi)	130 (17.5)	18.4 (2.47)	149 (10.0)	66.6 (8.92)	149 (10.0)
Ahr x Vsys / Fuel	0.035	0.005	0.020	0.018	0.020
OCV	214.4	213.9	N/A	214.1	N/A



UF-Weighted Results
 UF@Rcdc = 0.32
 MPG lumped = 93.78
 MPG fractional = 93.98
 L/100km lumped = 2.508
 L/100km fractional = 2.503
 ACWhr/mi lumped = 121.2
 ACWhr/mi fractional = 122



RWC 10/30/2009

Figure A9. Plug-in Conversions Corp PHEV Conversion –Extended EV mode

C. PHEV Test Methods and Procedures Development

Michael Duoba (project leader)

Argonne National Laboratory

9700 South Cass Avenue

Argonne, IL 60439-4815

(630) 252-6398; mduoba@anl.gov

DOE Technology Manager: Lee Slezak

Objectives

Continue work with SAE by chairing the industry/government task force to rewrite SAE J1711 standard for hybrid electric vehicle (HEV) test procedures, specifically addressing plug-in hybrid electric vehicle (PHEV) test procedures.

Publish revised version of the SAE document, SAE J2841, that defines the “Utility Factor” (UF) that can be referenced by the U.S. Environmental Protection Agency (EPA) and is referenced by California Air Resources Board (CARB) legislation. Define the UF for PHEV charge-depleting operation by using the 2001 U.S. Department of Transportation (DOT) data.

Ensure that all stakeholders, including JARI-ISO, CARB, and EPA, have consensus on the general direction and goals of the testing procedure.

Approach

Chair the J1711 SAE task force committee, set agendas, and facilitate decision-making.

Use the vehicles available through the Advanced Vehicle Testing Activity (AVTA), the Argonne-instrumented Prius, the Modular Advanced Technology Testbed (MATT) platform, and the Through-the-Road (TTR) prototype vehicle for testing various uncertain aspects of the new test procedures.

Synthesize existing test data and statistical methods to assess the robustness of the developed procedures and evaluate the error distribution of certain technical decisions.

Accomplishments

The SAE J1711 task force met monthly throughout early fiscal year (FY) 2009 and began to meet bimonthly as the document neared completion. Most of the outstanding unresolved issues have been resolved, and the document is scheduled for completion in early FY 2010.

As in previous years, data from testing in Argonne’s Advanced Powertrain Research Facility (APRF) was critical in reaching several of the major decisions. For example, recent test data from the AVTA vehicles provided guidance when the committee sought to develop a correction procedure for PHEVs having difficulty meeting the existing net energy change (NEC) criterion for charge-sustaining behavior.

Early in FY 2009, Argonne authored the approved SAE J2841 UF Calculations document.

Along with industry and other national laboratories, Argonne oversaw the development of a new and more realistic UF that incorporates driver variability. The study leveraged an existing dataset created by Georgia Tech that was shown to work well with the newly developed methodologies.

Argonne has reached a basic agreement with the International Organization for Standardization (ISO) and JARI in terms of harmonizing the PHEV test procedures and is represented as a voting member on the ISO committee, committed to develop additional PHEV testing standards.

To advance the finalization of the SAE J1711 testing sequence, Argonne has been able to test numerous original equipment manufacturer (OEM) and aftermarket PHEVs, in order to improve and validate the recommended procedure.

Future Directions

The SAE J1711 document is nearing completion and is receiving comments from the standards team and additional technical experts. These comments will be integrated into the document, and the final version of the document will be sent to balloting in early FY 2010.

Argonne has been asked by industry to co-organize the SAE J1634 (battery electric vehicle [BEV] test procedure), with a focus on developing a shortcut method. Argonne's experience with developing a PHEV shortcut method will be useful. Also, electric vehicle (EV) operation of a PHEV must be compatible with results from BEV testing.

Argonne will continue to collaboratively work on assessing consumer driving behavior related to the development of improved utility curves and labeling procedures.

Introduction

In the mid-1990s, the SAE J1711 expired task force (chaired by General Motors [GM]) developed the original J1711 procedure document. However, at that time, no production HEVs or PHEVs existed. In fact, procedure validation was performed at GM with student competition vehicles from University of California-Davis (PHEV) and the University of Maryland (charge-sustaining HEV).

By 2004, the original J1711, like all SAE J-docs after five years, expired. They require re-approval either as-is or after updating. The fundamental procedures used for HEVs are not in contention; it was the PHEV procedures that drew attention. In the literature and in stakeholder focus groups (like those held at the Department of Energy[DOE] in 2006), many widely accepted assumptions for how PHEVs should be tested deviated from the assumptions given in the original J1711. Soon after DOE stakeholder meeting, the industry called upon Argonne to chair the SAE J1711 session, update the PHEV section, and to support consensus decisions with reliable PHEV data.

The SAE J1711 reissue effort has spanned from late 2006 to the current FY 2009. In FY 2008, the focus was on helping CARB with its procedures and freezing the J1711 test concept. In FY 2009, the focus was on solving open issues; refining the document for balloting; and evaluating the procedures using OEM, aftermarket, and Argonne built PHEVs.

Approach

Many of the existing PHEV programs at Argonne heavily leverage the test procedure development activity. Because engineers have had over a decade to consider testing PHEVs, conceptually, nothing is new. The only effort that will help in the development is access to new data to support major decision points. Many of the small investigative experiments were aimed at looking at the impact of various decisions—in other words, asking questions like, “How important or sensitive is the outcome for each procedure or calculation option?”

Given this large background of expertise and knowledge, Argonne has completed several important achievements during FY 2009. The following report will highlight some of these advances in greater detail.

Recommended Test Sequence

One of the most significant accomplishments of FY 2009 was the creation of a recommended testing sequence for running the entire suite of HEV and PHEV tests. The biggest challenge of this task was to incorporate existing legacy test procedures while logically deviating when changes were necessary. Significant effort was spent in creating the recommended sequence and in educating the standards council on the relevant changes to the legacy procedures. Furthermore, finalizing the testing sequence allowed for the procedures to be

tested and validated by using the numerous PHEVs evaluated during FY 2009.

The fundamental procedure development was the creation of a “Full Charge Test” (FCT) sequence to calculate the charge-depleting behavior of a PHEV. This sequence needed to be both technically correct as well as practically reasonable.

When designing the sequence, significant attention was paid to the range of capabilities demonstrated at various OEM and other test facilities. For example, some manufacturers can only test a limited number of back-to-back drive cycles. With this in mind, the test sequence includes both a preferred method and alternative method, between which the expected differences have been minimized. Figure 1 gives an overview of the recommended test sequence.

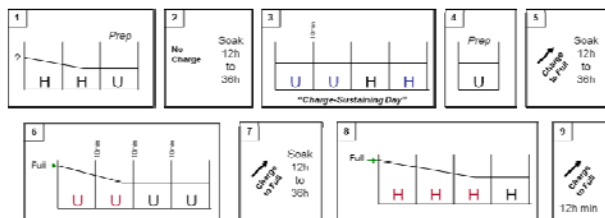


Figure 1. Recommended PHEV Testing Sequence

The basic flow of the test sequence is as follows:

1. The vehicle arrives with an unknown state-of-charge (SOC) and is depleted until charge-sustaining (CS) operation, which must be tested over at least one Urban Driving Dynamometer Driving Schedule (UDDS) cycle during which the NEC charge-balance criteria is met.
2. The vehicle is put into soak conditions for 12 to 36 hours without charging.
3. The CS testing is performed as specified in the existing test procedures.
4. Following the CS testing, a UDDS preparatory cycle is run to condition the vehicle for the FCT sequence.
5. The vehicle is charged to full, soaked, and made ready to test within one hour of being unplugged.
6. The UDDS FCT is run.

7. The vehicle is charged and soaked in the same conditions as Step 5. The recharge energy from Step 7 is used to calculate the total battery usage from the UDDS FCT testing.
8. The highway (HWY) FCT is run.
9. The vehicle is recharged, utilizing the recharge energy from the event as the battery usage for Step 8.

The extensive PHEV testing over the course of FY 2009 was instrumental to finalizing this recommended testing sequence. This testing provided both a sense-check of the resulting procedures and highlighting of areas needing improvement.

Multi-Day Individual Utility Factor

An additional focus area making great strides in FY 2009 was the creation of a more realistic UF for helping to indicate to customers how their PHEVs may perform. The UF is a statistic regarding how probable a given daily driving distance is relative to the greater driving population as a whole. The UF may be calculated as a fraction of total daily miles traveled or total drivers.

Given the amplified impact of a relative few long-range drivers on the daily-miles-traveled-based utility curves, it was decided through the SAE J2841 committee to create a total driver-based utility function. Although the U.S. DOT National Household Travel Survey Data contains information to create a driver-based utility, it also has some critical shortcomings. Namely, the DOT survey has data from only one single day, which does not account for the variability of a driver's daily distance over the course of a year (i.e., several longer trips during the course of the year). With this issue in mind, a single-day-based UF would likely be very optimistic for determining a driver's mix of depleting and sustaining behavior.

Since the DOT survey only contained single-day information, the SAE J2841 committee decided that another dataset needed to be integrated into the calculations. In a joint effort between industry and the national laboratories, a suitable dataset was identified in the form of a Georgia Tech driver study. The study contained multiple-day driver

information for a fairly large cross-section of drivers.

The next collaborative task was to identify and execute a methodology to scale the Georgia dataset to represent national driving behavior. Ultimately, the methodologies proved sound, and the committee was able to create a multi-day individual UF that incorporated the expected variation of driver’s daily distance while properly weighting the utility curve on a fraction of drivers versus total miles traveled basis. Figure 2 shows the different utility curves.

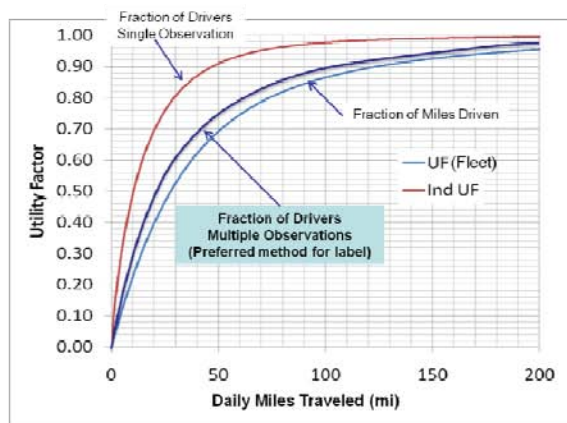


Figure 2. Newly Developed Utility Curves

Expanded Net Energy Change Allowance Window

At the request of several industry SAE J1711 committee members, the current NEC criterion for charge corrected operation was re-evaluated and expanded. The NEC criterion for charge-sustaining operation is to ensure that a vehicle’s behavior over a specific test will be fairly constant over the course of many miles. Without monitoring the energy leaving the battery, a vehicle may store or use excess energy that is not derived from the engine and therefore not sustainable in the long run.

Since PHEV fuel economy includes both charge-depleting and charge-sustaining operation, it is critical that a PHEV must operate within a similar set of NEC criteria. Unfortunately, as battery capacity increases, energy-state estimation errors begin to increase. Thus, the NEC criterion becomes much harder to meet.

Several manufacturers expressed concern that meeting the existing criterion would necessitate

expensive additional effort with little to no benefit to the consumer. Using a mix of vehicle test data and Monte-Carlo-based error estimation techniques, Argonne was able to assess the impact of widening the allowable NEC window and develop a robust procedure for handling the cases when a vehicle cannot meet the previous charge correction window. Furthermore, the entire committee appeared in agreement in backing the new methodology. This progress is particularly notable given that expanded charge correction has been a topic of discussion for many years, with little improvements made in the previous years. As an example output from the analysis study, Figure 3 shows the estimated error distribution created by several of the data-fitting techniques.

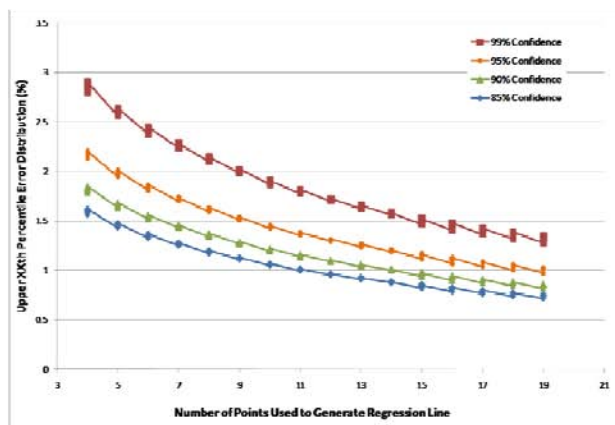


Figure 3. Error Analysis of SOC Correction Method

Conclusions

Argonne’s 12 years of experience in fuel economy and emissions testing of HEVs and PHEVs are unmatched in the DOE system, if not the world. This expertise is the reason industry requested that Argonne lead the J1711 effort.

Challenges that had not been overcome for a decade were addressed by the committee with a fresh look and with data from operational PHEVs, which was never available before. Additionally, Argonne’s importance as an impartial source of expertise has been critical in finalizing this test procedure, while not allowing the development to be biased by the interests of a particular manufacturer or vehicle technology.

There are high-profile questions as to whether the announced GM Volt (and other upcoming PHEVs)

will get a label fuel economy of 230 mpg. Argonne staff is doing everything it can to provide the expertise in test procedure development to cope with such questions in a fair and equitable manner that is technically sound.

As in previous years, Argonne is working very hard online in the committee and offline with OEMs and suppliers. Several OEMs have brought their protected and secret vehicles to Argonne to ensure that they get the best possible data of anywhere in the world. Access to state-of-the-art resources at Argonne has been one reason this project has been so successful.

Through Argonne's hard work, knowledge, and perseverance, the SAE J1711 procedure is nearing completion and balloting. Furthermore, Argonne's standards development activity has contributed immensely to a greater understanding of PHEVs within industry, as well as within the national laboratory system and the greater public.

Publications/Presentations

SAE J2841, "Utility Factor Definitions for Plug-In Hybrid Electric Vehicles Using 2001 U.S. DOT National Household Travel Survey Data" HEV Test Procedure Task Force, March 2009.

Duoba, M., "Calculating Results and Performance Parameters from Plug-In Hybrid Electric Vehicles," SAE paper 2009-01-1328, SAE Congress and Exposition, Detroit, MI, April 2009.

Duoba, M., "Development of PHEV Standard Testing Procedure (SAE J1711)," Test Site Sweden Plug-in Workshop, Gothenburg, Sweden, May 2009.

Duoba, M., "SAE J1711 Development Update - PHEV Testing Standard," SAE HEV Technology Symposium, San Diego, CA, Feb. 2009.

Duoba, M., "Researching PHEV Technology Potential," International Hybrid Technology Development and Large-scale Operation Seminar, Beijing, China, Dec. 2009.

D. PHEV Demonstration Program Prototype Vehicle Testing at APRF

Michael Duoba (project leader)

Argonne National Laboratory

9700 South Cass Avenue

Argonne, IL 60439-4815

(630) 252-6398; mduoba@anl.gov

DOE Technology Manager: Lee Slezak

Objectives

- Benchmark and analyze the Department of Energy(DOE)-funded plug-in hybrid electric vehicle (PHEV) demonstration program vehicles. Report to DOE the capabilities of the original equipment manufacturer (OEM)-designed PHEVs, report lessons learned, and contrast the results to the knowledge base of conversion PHEVs tested at Argonne National Laboratory.
- Provide operational data during chassis dynamometer testing by using novel instrumentation for:
 - TADA Phase 1 Ford PHEV Escape.
 - TADA Phase 2 Ford PHEV Escape.

Approach

- Secure a Collaborative Research And Development Agreement (CRADA) with manufacturer for the testing of the vehicle.
- Instrument the PHEV battery voltage and current, engine speed, and oil temperature.
- Collect operational vehicle information off the Controller Area Network (CAN). The codes that decipher the bus communications were “cracked” by Argonne staff from previous Escape hybrid testing.
- Run test cycles to measure fuel economy and performance, including the experimental SAE J1711 test procedures.

Accomplishments

- Produced fuel economy and emissions dynamometer testing results for both Phase 1 and Phase 2 Ford PHEV Escape prototypes.
- Worked with Ford engineers to analyze results of testing data.
- Evaluated experimental SAE J1711 PHEV test procedures for use on an OEM vehicle.

Future Directions

- Test additional PHEV demonstration vehicles from other manufacturers.

Introduction

Manufacturers have started to develop PHEV prototype demonstration vehicles as a part of the DOE Technology Acceleration and Deployment Activity (TADA) program. Benchmarking these vehicles is important to help direct the future development of PHEVs and to establish the

capabilities of the current technologies available. Testing was performed on two PHEV vehicles developed by Ford (Figures 1 and 2). During this testing, engineers from Ford and Argonne worked together to develop a test plan, test the vehicle, and analyze the resulting data. The results of this testing are protected through the CRADA established between Argonne and Ford.

Approach

Two versions of the prototype Ford PHEV Escape were tested, and additional development and refinement to the controls have been performed between the testing of the two vehicles. The vehicles were tested over Urban Dynamometer Driving Schedule (UDDS), Highway (HWY), and US06 testing cycles in both depleting and sustaining modes according to the SAE J1711 testing methods.



Figure 1. Phase 1 PHEV Escape



Figure 2. Phase 2 PHEV Escape

Because Ford owns the vehicles, extensive instrumentation could not be performed on the vehicle because it would require a significant number of sensors to be installed and modification of the vehicle. Instead, the focus was on key components that were new or different from the baseline HEV Escape vehicle. For both vehicles, the battery's current and voltage were measured to

determine the electrical energy usage. The Phase 1 vehicle also included a flex fuel engine capable of running on E85. For this reason, an advanced combustion analysis system was connected to the engine by using a spark plug with integrated pressure transducer and the stock crankshaft position sensor (Figure 3). Additionally, fuel flow and CAN signals were recorded. For both of the test vehicles, Ford engineers also logged many of the parameters from the vehicle control unit by using proprietary calibration software.

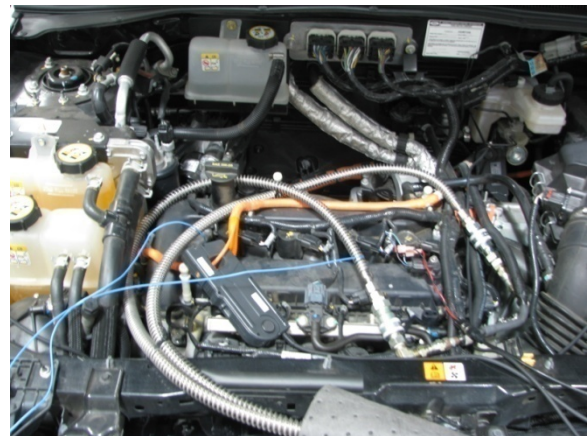


Figure 3. Engine Compartment, including Instrumented Spark Plugs, Current Measurement, and Fuel Flow Measurement Connections

Vehicle Description

Both the Phase 1 and Phase 2 vehicles tested are based on the model year 2010 hybrid Ford Escape powertrain. This includes a 2.5-L Atkinson cycle 4-cylinder engine rated at 153 hp @ 6000 rpm and 136 lb-ft torque @ 4500 rpm. The powertrain uses the same eCVT powersplit transmission as the HEV base vehicle. However, the battery has been upgraded to allow for PHEV operation. The vehicles both use 10-kWh lithium (Li)-ion batteries based on the Johnson Controls 41A•h cylindrical cells. These batteries were packaged in the location of the stock battery, displacing the spare tire beneath the vehicle (but not reducing interior space), as seen in Figure 4.



Figure 4. PHEV Battery Pack

Charging of the vehicles is done through a standard 120-V outlet integrated into the front fender on the driver’s side just ahead of the driver’s door. The plug features a blue illuminating ring to indicate to the operator that power is present at the vehicle, as seen in Figure 5. An LED display behind the rear-view mirror shows the charging status and the current battery state-of-charge(SOC) (Figure 6).

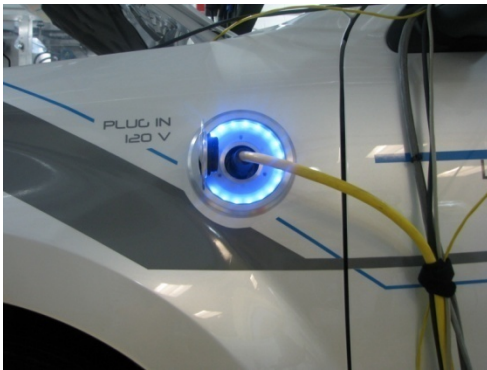


Figure 5. Charge Connector



Figure 6. SOC Display behind the Rear-View Mirror

Both the Phase 1 and Phase 2 vehicles included enhanced telematics packages that showed the power flow of the energy in the powertrain and demonstrated the concept of scheduling off-peak charging. Figure 7 shows a screen that allows the driver to enter the current cost of gas and electricity and to find the actual cost of the current trip.



Figure 7. Telematics Display

Dynamometer Testing Results

The test results from the tests performed during dynamometer testing are protected by the CRADA established with Ford.

Table 2 shows a summary of the amount and level of testing performed on each vehicle. Tables 1 and 3 list the particular cycles tested and how many of each were tested on the Phase 1 and Phase 2, respectively.

Table 1. Summary of Testing

	Phase 1 Testing	Phase 2 Testing
Number of tests	51	65
Miles of testing	466	654
Hours of testing	16.55	21.41
Channels per test	116	111

Table 2. Breakdown of Cycles for Phase 1 Testing

UDDS	22
SC03	3
LA92	4
Japan	2
NEDC	2
US06	4
Highway	6
<i>Misc</i>	8

Table 3. Breakdown of Cycles for Phase 2 Testing

UDDS	29
SC03	3
LA92	6
US06	11
Highway	5
<i>Misc</i>	11

Summary

Two prototype PHEV vehicles from the TADA program were tested at Argonne's Advanced Powertrain Research Facility. The vehicles tested included a Phase 1 and Phase 2 PHEV Ford Escape developed by engineers at Ford. During this testing, the vehicles were run through an exhaustive suite of tests to measure their performance characteristics. The test results were shared with engineers at Ford, along with results from analyses performed by engineers at Argonne. This interaction was critical to the further development of the Ford PHEV Escape demonstrator vehicle, as well as the SAE J1711 test procedure.

E. Comparing PHEV Lab Test Data to On-Road Data

Michael Duoba (project leader)
Argonne National Laboratory
9700 South Cass Avenue
Argonne, IL 60439-4815
(630) 252-6398; mduoba@anl.gov

DOE Technology Manager: Lee Slezak

Objectives

- Collect extensive amounts of PHEV data from fleet use and dynamometer testing and show how and why the results differ.
- The magnitude of the corrections made to raw dynamometer fuel economy results to predict in-use mileage is well studied for conventional vehicles. However, there is an urgent need to provide fundamental insights to determine this relationship in PHEV technology in order to communicate expected real-world PHEV performance the many PHEV stakeholders.

Approach

- Study the various types of vehicle operating conditions for which in-use driving results differ from chassis dynamometer results: aggressive driving, driving in cold temperatures, driving in hot temperatures, and driving while the air conditioner (A/C) runs.
- Conduct a multi-dimensional energy-use analysis to show the areas where dynamometer results match and where they do not.

Accomplishments

- Defined (1) the specific sensitivity of the Hymotion Prius and (2) the dramatic differences in fuel and electricity consumption results between on-road testing and standard dynamometer testing.
- Various relationships were established between driving conditions and where the marginal energy for increased fuel and electric energy usage originate.

Future Directions

- Paid fleet drivers often do not drive in the same way an average driver (who pays for fuel costs). Individual fleet vehicles could be weighted to better match the national data so that in the future, a more representative in-use data set could be compared with the standard dynamometer test results.
- More analyses should be conducted to specifically address mpg labeling of PHEVs.

Introduction

A critical part of the Department of Energy (DOE) research and development (R&D) plan is to benchmark and convey to all stakeholders the fuel efficiency and electrification displacement capabilities of PHEVs. This plan is carried out through the Advanced Vehicle Testing Activity (AVTA) in analyses of chassis dynamometer tests and on-road fleet tests. Argonne is responsible for

using best industry practices to test PHEVs on a chassis dynamometer. Idaho National Laboratory (INL) manages the collection of data from the many fleet vehicles deployed by various operators. Over the past few years, data coming from these two sources have been analyzed. For any vehicle powertrain technology, there is a known and understood difference between the standard dynamometer results and the observed on-road results. PHEVs represent such a dramatic departure

from conventional vehicles that the differences in the data sources do not follow normal trends. Hence, it is vitally important that a comprehensive analysis of the two data sets be performed in order to quantify and explain the differences.

PHEV Testing

PHEVs operate in both charge-depleting (CD) and charge-sustaining (CS) modes. Developing procedures to capture all of the operating modes of a PHEV while maintaining original test conditions and assumptions about the various legacy procedures is a challenging task. In essence, the PHEV test method used by researchers is to repeat the drive schedules back to back until a satisfactory charge-balanced cycle is achieved (at which time the test is ended). Data on the consumption of gasoline fuel and battery energy are captured for each test cycle, and parameters such as the CD range are determined.

The methodology described in SAE J1711 that is used to find the “final answer” from all testing results is called utility factor (UF) weighting. In-use daily driving statistics are applied to carefully weight and combine the results in the CD test with those in the CS test. This methodology provides an estimate of in-use gasoline fuel economy and electric energy consumption. The results of dynamometer testing for the Hymotion Prius are found in Table 1.

Table 1. Depleting, Sustaining, and UF-Weighted Standard Test Cycle Results for the Hymotion Prius

	CD			CS		UF-Weighted		
	MPG	L/100km	Wh/mi	MPG	L/100km	MPG	L/100km	Wh/mi
UDDS	181.1	1.3	131.9	66.6	3.5	91.6	2.57	96.6
HWY	121.0	1.9	119.5	63.5	3.7	85.2	2.76	91.5
US06	52.9	4.4	78.7	43.2	5.4	49.5	4.75	80.9
SC03	91.2	2.6	187.5	38.0	6.2	49.8	4.72	101.0
LA92	88.1	2.7	113.2	50.0	4.7	63.8	3.68	93.5

An important observation is that the vehicle does indeed achieve more than 100 mpg in some cycles while in CD mode. The US06 cycle has very high driving demands, and the SC03 uses the A/C during the elevated temperature test. Consequently, the respective fuel consumption results of these two cycles are much higher.

On-Road Data

ATVA monitors PHEV in-use performance through its fleet demonstration program. In the program, AVTA has collected in-use data from eight different PHEV conversion models, including the Hymotion Prius. These vehicle models are represented in a fleet of 155 vehicles operated in 23 U.S. states and Canadian provinces by more than 75 organizations. The vehicles are equipped with onboard data loggers that record time-history data. More than 360,000 miles have been logged since the program’s onset in late 2007. While the majority of vehicles are operated in commercial fleets, about 10% of the miles driven to date were logged by vehicles in private use.

Summary of Hymotion Prius On-Road Results

The most common question asked about a new fuel-saving technology is “What is the fuel economy?” To answer this question, fleet fuel economy data were processed, and a single aggregate mpg was calculated. Data from 73 Hymotion Priuses equipped with a V2Green data logger from June 1, 2008, to February 28, 2009, were chosen for analysis. Statistics describing these data are shown in Table 2.

Table 2. Large On-Road Data Set Statistics

Number of distinct cars	73
Total miles	242628
Total number of trips	24714
CD miles	87109
CS miles	155519
% CD	0.36
% CS	0.64

Subset of 1,200 On-Road Trips

From the large fleet data set, a more manageable sample of 1,200 trips was selected. Trips for distances of more than 1 mile were randomly selected for this sample. The results from the sample subset (summarized in Table 3) and the parent set are similar. The rest of this paper refers to the 1,200-trip subset, except where noted. This data set was analyzed to find reasons that the on-road gasoline and electric energy consumption results and the results from standard dynamometer test procedures differ.

Table 3. Overall Results of a Subset of 1,200 Trips

	Total mi	Total gal	MPG	Total kWh	wh/mi	% of Dist
CD	5453	87.4	62.4	-708.5	129.9	35%
CS	10134	228.7	44.3	21.3	-2.1	65%
Total	15587	316.1	49.3	-687.2	44.1	

Charging Frequency and Distance between Charging Events

One main assumption used when dynamometer test results are processed to represent “real life” driving is the frequency at which an owner charges a vehicle. The current consensus among researchers is to assume one charge per day of driving. The premise is that the days when a vehicle operator does not charge (perhaps due to forgetfulness or the absence of a charging infrastructure) are offset on other days when “opportunity charging” (charging more than once a day, at home or at locations with charging stations) occurs.

The in-use charge frequency of the entire parent data set is 1.2 charge events per vehicle-day; that is, charging occurs more often than once a day. This premise should weight the final results more toward CD operation. Notice, however, that in both Table 2 and Table 3, the miles travelled in CS mode greatly outweigh those travelled in CD mode. The 2001 National Household Travel Survey (NHTS) data set UF for a PHEV with a 30-mile depleting range is 52%, in contrast to the 35 to 36% found for the data set analyzed in this study.

The bias toward CS mode operation can be understood by looking at the distribution of distances travelled between charging events. One can compare the in-use distance between charge events to the NHTS distribution of daily vehicle miles travelled (VMT), because it is assumed that NHTS vehicles are fully charged before every new driving day. The fleet subset data were compared to the NHTS data to find differences, as shown by the histogram in Figure 1.

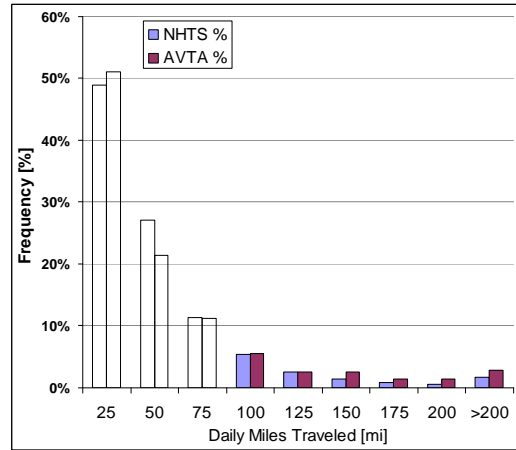


Figure 1. Histogram Comparing NHTS Daily Vehicle Miles Travelled to AVTA Fleet Distance between Charging Events

This comparison shows that vehicles in the AVTA fleet drove distances of more than 125 miles per charging event more often than did vehicles in the NHTS data set. Given that the average CD range of the Hymotion Prius is about 30 miles, this result supports the fact that vehicles in the AVTA fleet drove more miles in CS mode.

A further look at trip distances is shown in the Figure 2 higher-resolution histogram that focuses on shorter distances. Note that this data set includes a larger number of trips of fewer than 5 miles than the NHTS sample set does. The short trips may have been taken in a particular campus area, or many short trips may have occurred during courier duty.

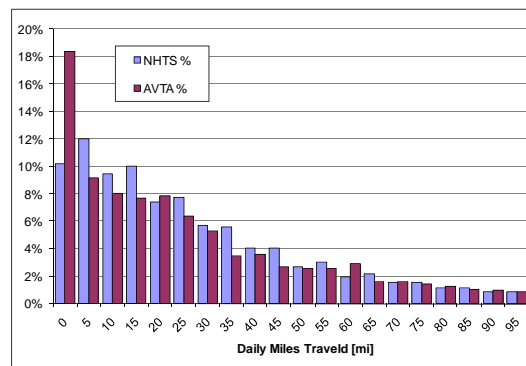


Figure 2. Higher-Resolution Histogram Comparing NHTS Daily Vehicle Miles Travelled to AVTA Fleet Distance between Charging Events

Vehicle Sensitivity to Driving Characteristics and Conditions

When analyzing the fuel economy of a PHEV, one must not forget that two energy sources are being used, so fuel economy alone is no longer an appropriate single efficiency metric. Also, the public is accustomed to seeing vehicle fuel economy with mpg being the relative measure of merit for energy efficiency. For example, vehicles can range from 40 mpg (efficient) down to 15 mpg (inefficient) — a wide, but understood, range. Fuel economy, however, is a poor relative measure of merit for PHEVs because trip MPG can range from the vehicle's CS fuel economy to essentially infinity, depending on the electricity/fuel split. To avoid ambiguity in defining gasoline fuel use when little or no gasoline is used, fuel consumption in terms of liters per 100 kilometers is a preferred metric for analyzing PHEVs in this study.

Some of the fuel economy discrepancies between dynamometer data and the on-road data set are due to the vehicle's response to different driving styles and the proportion of motive energy contributed by the battery. The design objective of the Hymotion Prius PHEV control system is to use as much electrical energy as possible. Because these vehicles are aftermarket conversions, the battery contribution is limited to 20 to 25kW in the Toyota CS HEV design. In analyzing the data, the amount of fuel and battery energy consumed in the on-road data set can be identified.

Engine-on and Fuel Consumption

One would intuitively think that trips in which the engine is kept off more often would result in less fuel consumption. Figure 3 shows this relationship in the fleet data set. Fuel consumption and the engine state are indeed related, but the spread is large because so many other factors determine fuel consumption.

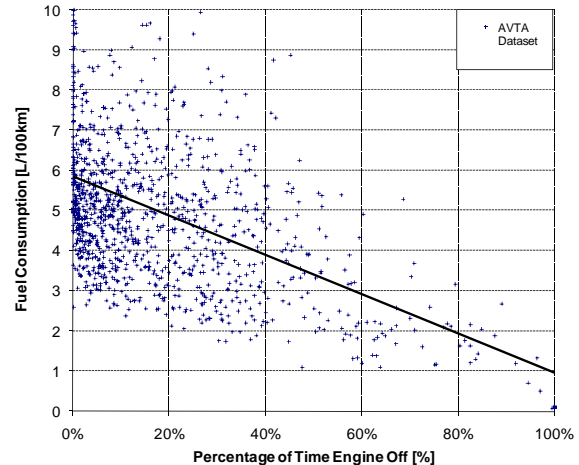


Figure 3. AVTA Fleet Engine-off Time versus Fuel Consumption

Engine-on and Fuel-Battery Energy Split in Charge-Depleting Mode

It has been found that driver aggressiveness plays a large part in energy consumption. Compounding this issue is the difference in bias toward engine operation while the vehicle is in CD mode. There are many conditions that determine if the engine is used for propulsion. Of interest in this section is the power requested by the driver, communicated through the accelerator pedal, and the vehicle speed. Trips driven only in CD mode are investigated here to illustrate the mix of electricity and fuel use.

Driver Demand and Fuel Usage

In defining aggressiveness, it was found that if the driver depressed the pedal by more than 40%, engine start was triggered. Cycle and fleet data on vehicles in both CS and CD mode are analyzed together with regard to fuel consumption in Figure 4. Note in both the fleet and dynamometer data, there is a strong relationship between fuel consumption and the percentage of time that the accelerator pedal is above the 40%-depressed position.

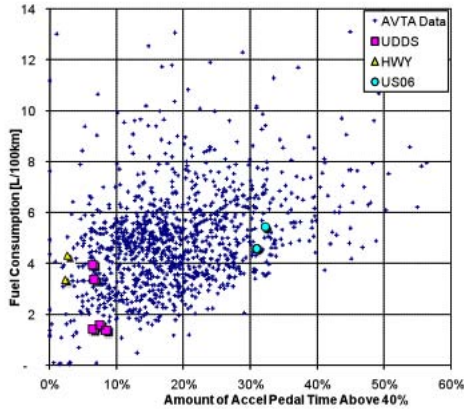


Figure 4. AVTA Fleet Time When Accelerator Pedal Is above the 40%-Depressed Position versus Fuel Consumption

Note the extremely low frequency of time when the accelerator pedal is above the 40%-depressed position in the UDDS and HWY cycles. From the data, one would speculate that these cycles are terrible predictors of the AVTA fleet operating conditions. The US06 cycle predicts aggregate fuel consumption well, but it does so with a much higher >40%-depressed position time. These data suggest that more than pure aggressiveness accounts for the fuel economy shortfall in the on-road data set.

Vehicle Energy Consumption and Ambient Temperature

AVTA vehicles are deployed in locations throughout the United States and Canada and thus operate under diverse climatic conditions. Ambient temperatures are recorded in the vehicle data loggers, so the effect of temperature can be analyzed.

Ambient Temperature and Percentage Battery Energy

Figure 5 shows the ambient temperature and its effect on the percentage of powertrain energy that comes from the battery. The points lying on the x-axis are from CS-mode trips. The Prius has a high-voltage electric-powered A/C system, so as the temperature increases, the battery consumption mix also increases.

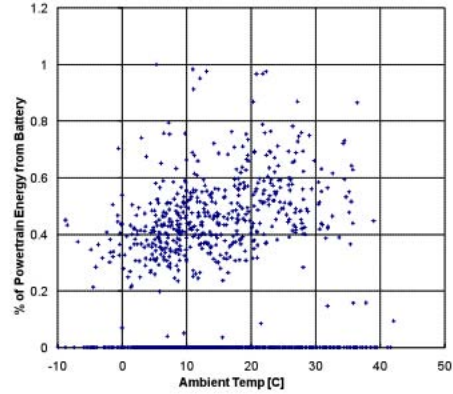


Figure 5. AVTA Fleet Ambient Temperature versus Percent of Powertrain Energy from the Battery

Ambient Temperature and Total Energy Consumption

The plot in Figure 6 was generated to answer the question of whether ambient temperatures above and below the standard test conditions cause more energy consumption. There is a large degree of scatter, although a second-order trend line indicates that the minimum total energy consumption occurs at 23°C.

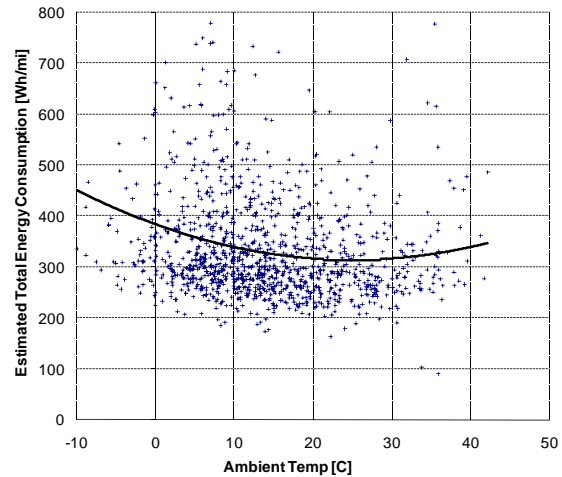


Figure 6. AVTA Fleet Ambient Temperature versus Estimated Total Energy Consumption

Ambient Temperature and Fuel Consumption

Again, fuel consumption garners the most interest; so another plot was generated to show fuel consumption versus ambient temperature. Figure 7 shows the same trend: a high degree of scatter and a trend minimum at roughly 25°C.

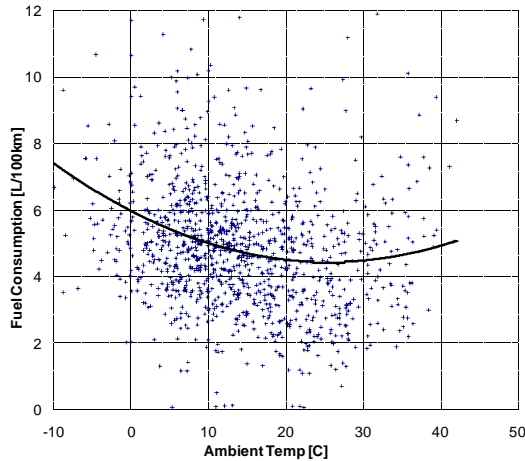


Figure 7. AVTA Fleet Ambient Temperature versus Fuel Consumption

Ambient Temperature and A/C Usage

It has been well documented that A/C usage can greatly increase fuel consumption. In a PHEV, A/C usage can increase both electrical energy and gasoline fuel consumption, depending on conditions. Data loggers in AVTA fleet vehicles record A/C compressor speed over time as an indicator of A/C usage. Trips in the 1,200-trip subset were classified as having the A/C on, on the basis of the occurrence of A/C compressor speeds above 0 rpm. A distribution of the percent of trips with A/C on versus ambient temperature is shown in Figure 8.

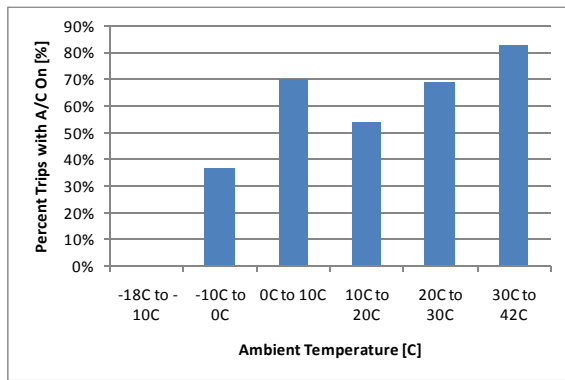


Figure 8. Distribution of A/C Compressor Usage by Ambient Temperature in the AVTA Fleet

There is a surprisingly high proportion of A/C usage at all temperatures above -10°C . Use of the defroster, which engages the A/C to dehumidify air blowing into the cabin, is no doubt responsible for

the high proportion of A/C usage at cold temperatures.

Vehicle Energy Consumption Levels

PHEV results are conveniently shown by an x-y plot of electrical and fuel consumption on the same graph. The full charge test given to PHEVs, which begins in CD mode and repeats cycles until the vehicle reaches CS mode, usually shows the individual cycle results on a relatively straight line of constant efficiencies. If the PHEV is driven in a test cycle in electric-only mode, then the point appears on the zero fuel consumption axis. If the test cycle is charge-balanced, then the result appears on the zero energy consumption axis. Figure 9 describes this energy space for PHEVs.

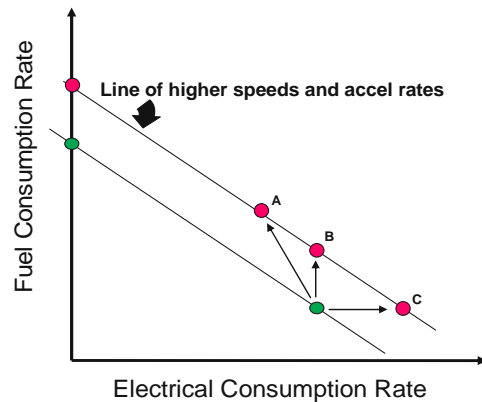


Figure 9. Method for Describing Gasoline and Electricity Consumption Space

In CS mode, when a vehicle is driven more aggressively or at higher road loads, the increased fuel consumption point will be higher on the axis. In CD mode, however, the results can take one of any number of directions up. Typically, a cycle with added load (due to higher speeds or greater accelerations) is on a higher constant efficiency line above the reference line. The added energy required can come solely from the battery (as in point C) or come from both the battery and gasoline fuel. The latter case can result in a constant battery energy-depletion rate (per mile), as shown by point B. However, if the battery power is saturated at its highest level and the added load occurs at higher speeds, the electrical depletion rate per distance actually decreases, and the result is point A.

On-Road Data Set and Dynamometer Results

Figure 10 shows the 1,200-trip data set energy consumption space with the dynamometer drive cycle results. Note the relatively parallel CD and CS lines trading off electricity for gasoline usage, which indicates similar conversion efficiencies. CD points are the points at the lower right; CS points are at or near the y-axis. Points along the line in the middle are cycles that had both CS and CD operation during the cycle (the cycle in which the transition occurred). The highest energy-consuming trend occurred in the SC03 test (high temperature with A/C usage).

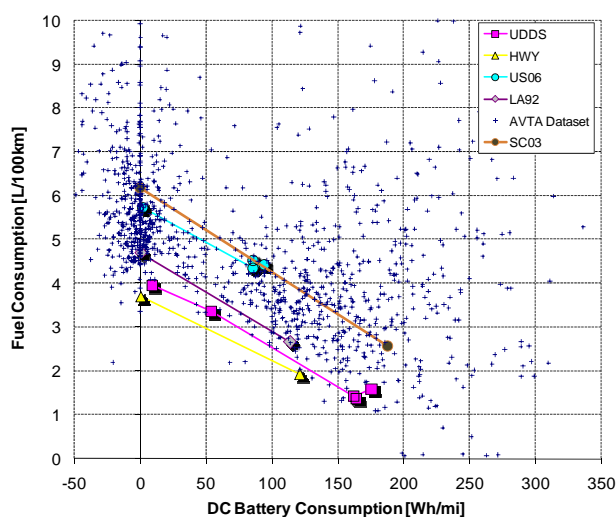


Figure 10. Energy Consumption Space for AVTA Fleet and Dynamometer Drive Cycles

Two main cluster locations dominate the energy-use space: a CS cluster from about 4.5 to 6.5 L/100 km (with some points higher extending up to 9.5 L/100 km), and a CD cloud from 75 to 250 Wh/mi and from 1 to 5.5 L/100 km. The AVTA data show nearly all the CS data with higher fuel consumption than the UDDS and HWY cycles. As described earlier, aggressive driving at higher speeds, like that found in US06, corresponds to lower electric consumption rates per mile in the battery-power-limited Hymotion Prius. Note that the SC03 cycle consumes more energy because of the electrically driven A/C compressor usage, but it does so with driving speeds similar to those of the UDDS cycle. Thus, the location of the CD SC03 point is high on both the electric and fuel consumption axes

(at a location closest to the CD cloud of AVTA points mentioned above).

Conclusions

To understand how a new vehicle technology performs under actual operating conditions for comparison with standard dynamometer testing, it is critical to monitor fleet deployments that implement the technology. In the case of PHEVs, fleet demonstrations also help researchers validate the assumptions used to develop vehicles and establish laboratory testing procedures, such as those related to the frequency of vehicle charging and the distance between charging events. Onboard data loggers that collect detailed information on driving style and conditions, vehicle operation, and charging patterns enable this understanding.

The UDDS and HWY cycles are often times used as reference cycles to describe the achievements of advanced vehicles. When compared to the fleet data set analyzed in this study, they are in fact the least representative of the test cycles used with respect to driving style, vehicle conditions, and ambient temperatures.

On the basis of standard testing procedures and industry-accepted UF weighting, the on-road data set consumed 85% more fuel and 54% less electricity (per mile) than vehicles on the UDDS cycle. Consumption was 73% more on the HWY cycle, with 52% less electricity used. This disparity is partly due to a higher percentage of CS operation in the fleet data set.

Two more aggressive cycles—the LA92 and US06—predict fuel consumption to within 2%. However, they do not represent electricity usage well (on-road consumption was 45 to 51% less).

The UF-weighted SC03 cycle, which includes the A/C-on condition found abundantly in the on-road data set, also did not predict electricity consumption rates well (on-road consumption was 56% less). Nevertheless, given the low driving intensity of this cycle and the high combined gasoline and electricity consumption, as indicated in the previous figure, this cycle demonstrates the significance of non-tractive energy demands (namely, A/C usage) on overall vehicle energy consumption.

The amount of driving in CD mode in the on-road data set was analyzed. The baseline assumption of one charge per driving day was close to the observed 1.2 charge—an encouraging find. However, the NHTS distribution of driving distances was not a good match for the on-road data, since the UF for a 30-mile CD range corresponds to an expectation of 52% CD miles. The on-road percentage of miles was only 35%. More evidence of the bias toward CS operation is the higher frequency of very long trips (many miles beyond the CD range). These characteristics have a fundamental impact on the amount of electricity consumption expected and the relative contribution of fuel consumption.

It was established that the Hymotion Prius is highly sensitive to aggressive operation in the CD mode. Slight increases in accelerator pedal tip-in can prevent electric-only operation and thus preclude fuel displacement.

Loose correlations in ambient temperature and total energy consumed onboard the vehicle and specifically in fuel consumption were found. Ambient temperatures higher or lower than roughly 25°C were found to consume more energy. These findings support the U.S. Environmental Protection Agency's addition of a UDDS cycle tested at -7°C and the SC03 run at 35°C in the "5-Cycle" labelling to better predict in-use energy consumption.

One perhaps surprising find in the data set is the frequency of A/C compressor operation during driving in all but the lowest temperatures. Trips with ambient temperatures between 0 and 10°C involved A/C usage 70% of the time. About 75% of trips at temperatures of more than 20°C involved A/C compressor usage. Given the profound impact of A/C compressor operation, this statistic proves to be a significant factor in the on-road data set results.

Looking at PHEV gasoline and electricity in a two-dimensional consumption space is a powerful method for making comparisons. The summary of the 1,200-trip data set shows that fuel consumption in CS mode matches a combination of the LA92 and US06 cycles. However, CD operation is not well matched by any of the drive cycles. UDDS and HWY results are virtual outliers compared to the on-road data. The SC03 cycle is helpful in representing a consumption space location not characterized by any other cycle (i.e., high required loads at lower

speeds resulting in high fuel and electric consumption).

In summary, many factors contribute to the differences between the on-road data set and results from standard dynamometer testing. However, this conclusion should not discourage developers. The inclusion of additional dynamometer test cycles with varying driving conditions and the use of UF weighting are directionally correct. Also, it is important to note that trends from this study are limited to the driving and charging behavior of the fleet studied. The aftermarket conversion vehicles studied here do not necessarily manifest the performance and sensitivities of future PHEVs. Nevertheless, this study demonstrates the complexity of the PHEV's bi-fuel operation and the importance of evaluating these vehicles across a range of conditions to accurately assess their energy consumption potential.

Publications/Presentations

Duoba, M., et al., *Correlating Dynamometer Testing to In-Use Fleet Results of Plug-In Hybrid Electric Vehicles*, 24th International Battery, Hybrid and Fuel Cell Electric Vehicle Symposium and Exhibition (EVS24), May 13–16, 2009.

F. Maintain an On-Line HEV Test Results Database

Mike Duoba (Project Leader)

Argonne National Laboratory

9700 South Cass Avenue

Argonne, IL 60439-4815

(630) 252-6398; MDuoba@anl.gov

DOE Technology Manager: Lee Slezak

(202) 586-2335; Lee.Slezak@ee.doe.gov

Objectives

- Design and construct a Web-based database repository for the latest technology hybrid vehicle test data.
- Enable free access to the database for industry, universities, and the general public. (Argonne National Laboratory has named it the Downloadable Dynamometer Database, or D³). It is an easy-to-use research tool that allows for the transfer of Argonne's latest advanced vehicle data for analyses and education. The Web address is https://webapps.anl.gov/vehicle_data/.

Approach

- Collect vehicle performance data from testing on Argonne's vehicle test facility — the four-wheel drive (4WD) chassis dynamometer at the Advanced Powertrain Research Facility (APRF).
- Thoroughly review and perform critical analyses of the test vehicle results to verify data accuracy and quality control.
- Reduce the data for upload onto the publicly available Internet site by first directing it to an Argonne Web applet server, after which it will be linked into the database to provide search and reference capabilities.
- Upload new data from Argonne's APRF chassis dynamometer as available, along with any existing vehicle test data.

Accomplishments

- Added new feature to provide a one-page executive summary of vehicle test results, enabling a simple-to-read overview rich in visual content and easy vehicle-to-vehicle comparisons. This feature has proven to be especially useful for reporting test results on plug-in hybrid vehicles (PHEVs).
- Developed an advanced graphical/table calculation tool for PHEV test results calculations. This tool uses all of the new parameters for PHEVs addressed by California Air Resources Board (CARB) regulations and SAE J1711.
- Continued to maintain and update the on-line downloadable database with search capabilities. Uploaded nearly 40 new test data folders to the website for access this past year.

Future Directions

- Increase the visibility of D³ to provide a direct Web address to the Argonne database so that users can find it by using keywords through Google or Yahoo.
- Provide means for two-level access: (1) a basic level for public access that delivers summary one-pagers, simple data sets, and reports and (2) a controlled level, which would require a login/password to gain access to extensive "Level 2" data sets and reports for the Department of Energy (DOE), involved original equipment manufacturers (OEMs), and other national laboratories.
- Refine the user interface to provide more summary data with easy-to-understand graphics.

- Investigate the value to the user of changing the database format from search-based to nested-folder-based, thereby allowing users to see all of the vehicles tested by scrolling through the list of folders.

Introduction

Vehicle benchmarking combines testing and data analysis to characterize efficiency, performance, and emissions as a function of duty cycle, as well as to deduce control strategy under a variety of operating conditions. The valuable data obtained from this effort have been placed in an Internet-accessible database that provides a unique resource not previously available to researchers, students, and industry. This website is available at https://webapps.anl.gov/vehicle_data/.

Benchmarking data are useful to nearly all aspects of the FreedomCAR and Fuel Partnership, and the technical teams also benefit from the data collected in the APRF. It has also become important for test procedure and policy development for DOE, the Society of Automotive Engineers (SAE), CARB, U.S. Environmental Protection Agency (EPA), U.S. Department of Transportation (DOT), and the National Highway Traffic Safety Administration (NHTSA). Test procedures, label fuel economy, and Corporate Average Fuel Economy (CAFE) regulations all depend on these data for development. The importance of maintaining this database is paramount because no other government entity or company has such a data resource available.

Approach

For each of the vehicles tested at Argonne's APRF, a set of data is generated. Depending upon the level and depth of testing, a stream of 50 to 200 different data are collected at the facility standard of 10-Hz data rate.

After testing, all of the data must be inspected, and it must be determined whether the data are complete, thorough, and representative of the vehicle being tested. We use a set of tools that compare and contrast data relative to time and use of the first law of thermodynamics. Because this is a repetitive process, a template to define the time and first law relationships between data is generated. Each new set of data is run against these predefined

relationships and set up for visual analysis and comment (Figure 1).



Figure 1. Standard APRF QC Analysis Tool

Once the data are thoroughly checked, the data are saved and reduced to a predefined subset of data. Each set of data includes:

- **Phase Information:** Summary data for each phase of the test; items include fuel economy and emissions (g/mi), for example.
- **Test Information:** Summary of testing conditions needed to replicate the work at similar vehicle testing facilities; items include road load, dynamometer setting, and test cell environmental conditions, for example.
- **Main Summary:** A one-page test summary with aspects of the phase information, test information, and 10-Hz data combined into a presentable sheet.
- **10-Hz Data:** The raw 10-Hz data for each signal in the vehicle.

After the data quality control step has been performed, data are uploaded to the D³ website (Figure 2). The term D³ is an abbreviation for Downloadable Dynamometer Database. It is in this HTML interface where the relational and searchable database provides functionality (the website is available at https://webapps.anl.gov/vehicle_data/).

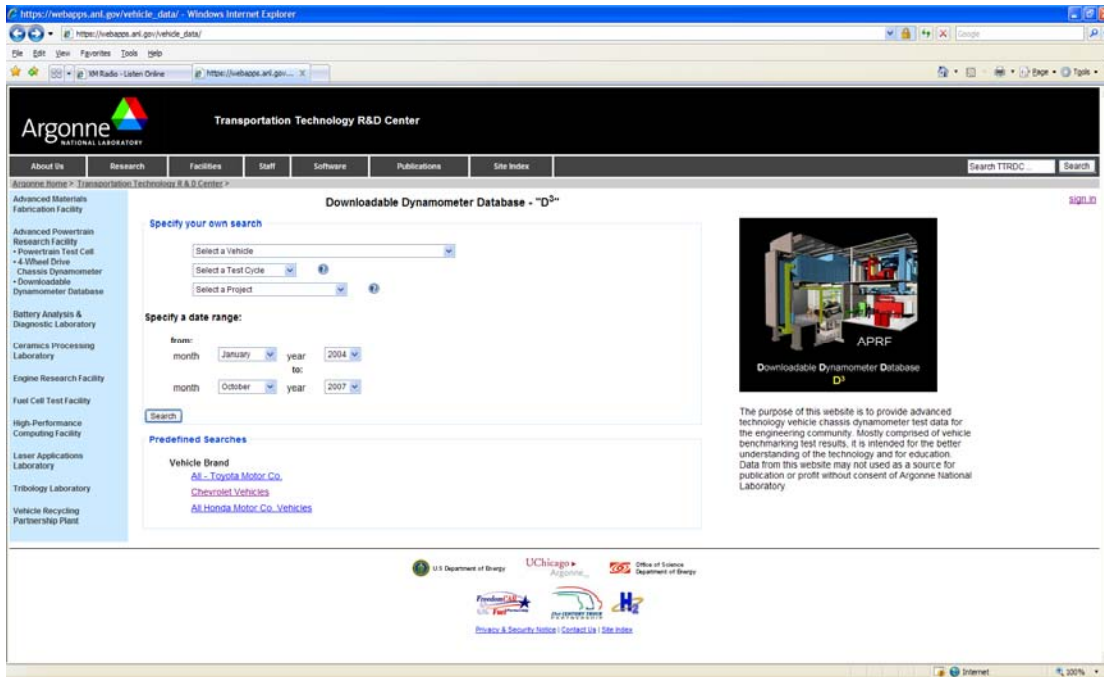


Figure 2. Downloadable Dynamometer Database Homepage

The current interface is designed so that users can easily find data, which are organized either by vehicle or by a virtual project binder. Users have the ability to search the entire database by vehicle, project, test cycle, date of collection, or a predefined search. After the user has completed searching for the requested data, all of the data are sent via http download in a single compressed data file (zip).

Forty-two new test folders have been uploaded to D³ over the past year. (There are more folders ready to go live; the backlog will be filled over the next month or two into fiscal year [FY] 2010). As of September 2009, D³ had 22 advanced vehicles with over 174 sets of data that can be downloaded.

New this year is an automatic one-page reporting tool that visualizes and runs the critical PHEV calculations. Many new parameters unique to PHEVs have been developed in the SAE J1711 and CARB zero-emission vehicle (ZEV) mandate procedures. These parameters relate to energy consumption rates, various definitions of the depleting range, and equivalent electric vehicle (EV) range. The tool also uses utility factors (UF) to weight the final results. An example of one example printout is shown in Figure 3.

Conclusions

The Argonne D³ allows our industry, academic, and government partners access to high-quality vehicle chassis testing data. D³ has been developed with users in mind as a simple and easy-to-use tool that allows for the transfer of useful data for analysis and education. Continuing efforts will be devoted to further develop the database to promote its accessibility and easy-to-comprehend content.

Publications/Presentations

Keller, G., and Gurski, S., et al., “D³ Website,” September, VSATT (Vehicle Systems Analysis Technical Team) Review, 2007.

Keller, G., “Downloadable Dynamometer Database (D³),” DOE Vehicle Technologies Merit Review, 19 May 2009.

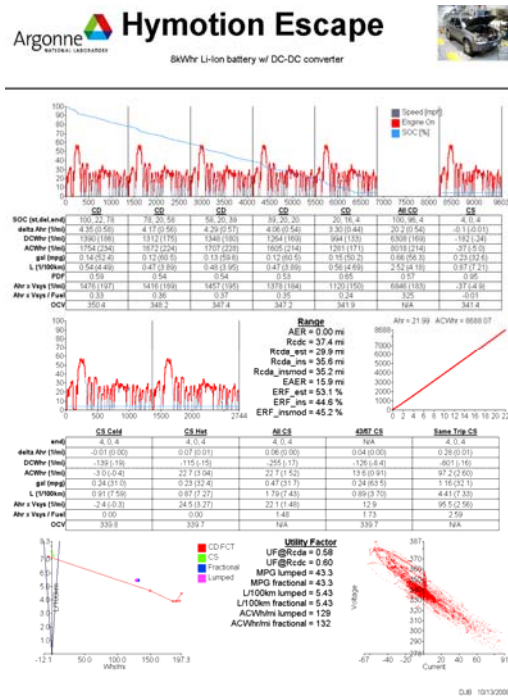


Figure 3. PHEV One-Page Calculation Printout

G. Vehicle Test Procedure for Measuring Air Conditioning Fuel Use

John Rugh (Principal Investigator) and Matthew Thornton

National Renewable Energy Laboratory

1617 Cole Boulevard

Golden, CO 80401-3393

(303) 275-4443; john.rugh@nrel.gov

DOE Vehicle Systems Analysis Activity Manager: Lee Slezak

Voice: 202-586-2335; Fax: 202-586-1600; E-mail: Lee.Slezak@ee.doe.gov

Objective

Develop a vehicle-level test procedure that:

- Measures the fuel use impact of vehicle systems that influence occupant comfort.
- Obtains data to populate the mobile air conditioning (A/C) life cycle climate performance (GREEN-MAC-LCCP) spreadsheet.

Approach

Review and assess industry A/C fuel use measurement practices from a broad group of automobile manufacturers, suppliers, associations, regulatory agencies, and national laboratories.

Consider how different test objectives influence the test requirements.

Assemble a test procedure that measures the impact of vehicle components and systems that influence climate control.

Accomplishments

A vehicle-level A/C fuel use test procedure is recommended that includes:

- Soaking a vehicle with solar lamps that meet SCO3 requirements or with an alternative heating method such as portable electric heaters.
- Operating a vehicle over repeated drive cycles or at a constant speed until steady state cabin air temperature is attained.
- Running A/C-off and A/C-on tests to calculate a cool-down and steady state A/C fuel use.

The A/C system is controlled to approximate how a driver would typically operate it.

Future Directions

Coordinate with and answer questions from regulatory agencies regarding vehicle-level A/C fuel use measurement.

Use the test procedure to measure the reduction of fuel use due to thermal preconditioning of the passenger compartment and potentially other vehicle systems.

Introduction

When a vehicle A/C system is operated, the power required to run the compressor can be a significant power drain on the engine depending on the ambient conditions. A National Renewable Energy Laboratory (NREL) analysis found that the United States consumes seven billion gallons of fuel a year for cooling and dehumidifying light-duty vehicles [1]. In more fuel-efficient vehicles, the impact of the A/C system is more apparent because fuel used for A/C is a larger percentage of the overall fuel use. In advanced vehicles such as plug-in hybrid electric vehicles (PHEVs) and electric vehicles (EVs), total energy management is much more important due to the electric drive capability. If A/C energy use is considered in the design of a PHEV or EV, then the energy storage system (ESS) size will be larger and more costly in order to meet the target performance parameters—compared to if A/C had not been considered.

The use of A/C impacts the charge-depleting (CD) range of PHEVs. NREL performed a simulation of a PHEV40. The vehicle was a mid-sized parallel hybrid sedan with an 81.9-kW engine and a 51.8-kW, 18.5-kWh lithium (Li)-ion battery [2]. Assuming a conventional R134a A/C system, a high cool-down A/C load followed by a lower steady state A/C load was applied to the vehicle. The vehicle was run over repeated drive cycles until charge-sustaining (CS) mode was attained. Figure 1 shows the CD range was reduced by 18% for the US06 drive cycle and 30% over the urban dynamometer drive schedule (UDDS) cycle. Similar results were attained for an EV.

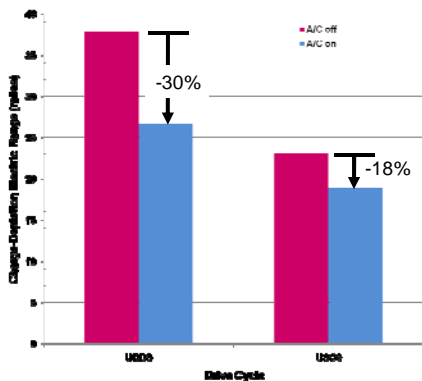


Figure 1. PHEV Charge-Depletion Electric Range over the UDDS and US06 Drive Cycles

In recent years, A/C fuel use has received increased attention from regulatory agencies. In the European Union (EU), one technique available to automobile manufacturers to reduce CO₂ emissions from the mandatory 130 gr CO₂/km to the target 120 gr CO₂/km, is to improve A/C system efficiency [3]. The California Air Resources Board (CARB) has considered green house gas (GHG) emissions from automotive A/C by including a credit for variable displacement compressors (VDC) in the Pavley 1493 bill [4,5] and included credits for reducing indirect A/C emissions in an environmental performance labeling regulation [6]. In June 2009, CARB passed a regulation to reduce the thermal loads in vehicles to reduce GHG emissions due to A/C [7].

For model year 2008 vehicles, the U.S. Environmental Protection Agency (EPA) modified the way fuel economy was calculated for window stickers and included A/C usage [8]. Recently, the U.S. EPA and Department of Transportation (DOT) issued a joint rulemaking proposal to harmonize fuel economy and GHG emissions regulations [9]. As part of the regulation, the EPA is considering credits for A/C system improvements that reduce GHG emissions. While the EPA currently measures the vehicle emissions over the SCO3 drive cycle, there is not an A/C-off test over the same cycle. Therefore, A/C fuel use cannot be directly calculated. As part of the recent joint rulemaking proposal, the EPA has proposed an A/C fuel use test at idle or modifications to the environmental conditions of the SCO3 drive cycle [9].

This increase in regulatory attention has increased the need for a test procedure to quantify the impact of A/C use on fuel consumption. With the development of PHEVs and the negative impact of climate control on electric range, a robust A/C fuel use test procedure is needed to assist designers, engineers, and regulators.

Results

The purpose of the recommended test procedure is to measure the fuel use impact of all vehicle systems and components that impact occupant comfort. This is a research-oriented procedure that is intended to measure approximate real-world A/C fuel use. An additional objective is to provide a process to gather data to populate the mobile A/C life cycle climate

performance (GREEN-MAC-LCCP) spreadsheet with vehicle-level A/C fuel use information. To measure the cool-down as well as steady state A/C fuel use, a thermal soak with solar lamps with the engine off is followed by vehicle operation with the A/C on.

To measure the impact of thermal load reduction technologies and also to enable the measurement of the higher fuel use during cool-down, a thermal soak period is required in an environmental chamber. The thermal soak is followed by an A/C cool-down that is run to passenger compartment thermal steady state. Solar lamps that meet the SCO3 requirement are recommend, as well as a soak long enough to obtain steady state temperatures (~ 1.5 hr). The soak is performed with the windows and doors closed so realistic interior temperatures are attained. Thermal load reduction technologies and the resulting reduced interior temperatures can be assessed with this procedure. Since the vehicle cannot be occupied and driven during the soak, the engine will have to be off prior to driving so this procedure will be a cold start from an emissions perspective. As long as the vehicle control functions the same with the A/C off and the A/C on, the impact of the cold start should not impact the A/C fuel use. The question of whether a solar soak is required for the A/C-off test will need to be determined. If data show the solar load does not have an impact to vehicle systems other than A/C, then a solar load during A/C-off would not be required.

The vehicle will be operated in an environmental chamber with a dynamometer. The solar lamps will be on during the test to provide a realistic thermal load. If the vehicle equipped with a solar sensor, the input into the A/C control algorithm should be realistic. The chamber temperature and humidity should be controlled during testing. A drive cycle is repeated or the vehicle is run at a constant speed until steady state and interior air temperature is attained. This could be defined when a certain temperature is attained or the rate of change of temperature drops to a certain level. Figure 2 shows what the temperature versus time profile of this test procedure might look like. The cool-down A/C fuel use is the average of the A/C fuel use of cycles 1 and 2. The steady state A/C fuel use would be calculated from cycle 4 data.

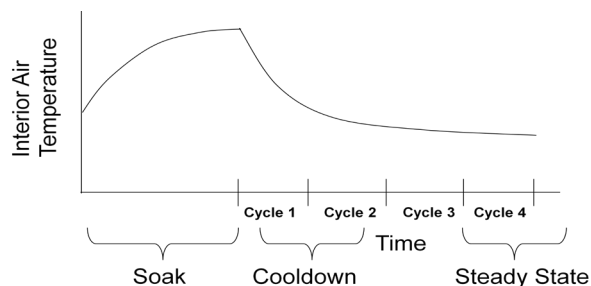


Figure 2. Hypothetical Temperature vs. Time Profile of a Soak and Cooldown A/C Fuel Use Test

This approach offers flexibility with regards to ambient conditions and drive cycle. A/C-off and A/C-on tests are run for all environmental conditions and at as many speeds or drive cycles as required. For example, to obtain A/C fuel use data for the temperature bin data defined in the GREEN-MAC-LCCP model, a single drive cycle could be run at the four temperatures identified in Table 1. If constant speed data is preferred, this table could be filled out for a constant speed. A simplified approach is to run the A/C-off and A/C-on tests for a single environment and a specific drive cycle. For example, a person could use

- 25°C, average air temperature in the U.S. when the A/C is operated [1].
- 66%, average relative humidity in the U.S. when the A/C is operated.
- 850 W/m², SCO3 solar load.
- SCO3 drive cycle.

Table 1. Example Test Conditions and Data Sheet

Temperature °C	RH %	Solar Load W/m ²	A/C Fuel use - Cooldown L/100 km or L/s	A/C Fuel use - Steady state L/100 km or L/s
45	TBD	TBD		
35	TBD	TBD		
25	TBD	TBD		
15	TBD	TBD		

It is recommended to set the vents to the panel setting. For vehicles with automatic temperature control (ATC), adjust the temperature set point to 22°C and allow the blower and recirculation settings to be automatically controlled. This will allow the climate system to be control as designed. For vehicles with manual climate control, set the temperature lever to full cold and adjust the blower and recirculation settings according to a predetermined schedule that would be expected from operation in the field. This might consist of a high blower and outside air at the beginning of the cool-

down, and then transition to lower blower levels and higher recirculation air as the cabin cools down.

Conclusions

Climate control significantly degrades PHEV and EV performance (fuel consumption and range) and detrimentally impacts energy storage system size and cost. A/C fuel use has been subject to increased regulatory activities. There is no automotive industry consensus on a vehicle-level A/C fuel use test procedure.

A vehicle-level A/C fuel use test procedure is recommended that includes:

- Soaking the vehicle with solar lamps that meet SCO3 requirements or with an alternative heating method such as portable electric heaters.
- Operating the vehicle over repeated drive cycles or at a constant speed until steady state cabin air temperature is attained.
- Running A/C-off and A/C -tests to calculate a cool-down and steady state A/C fuel use.

The procedure measures the approximate real-world A/C fuel use. Data is gathered for both cool-down and steady state passenger compartment thermal conditions. The impact of thermal load reduction technologies can be measured using this procedure. It will be possible to characterize the impact of climate control on advanced vehicles, as well as conventional vehicles.

Publication

J. Rugh, "Proposal for a Vehicle Level Test Procedure to Measure Air Conditioning Fuel Use", submitted to SAE World Congress, 2010.

References

7. Rugh, J.; Hovland, V.; and Andersen, S. (2004) "Significant Fuel Savings and Emission Reductions by Improving Vehicle Air Conditioning," Mobile Air Conditioning Summit, Washington, D.C., April 14-15, 2004.
8. Gonder, J.; Markel, T.; Thornton, M.; Simpson, A. (2007). "Using Global Positioning System Travel Data to Assess Real-World Energy Use of Plug-In Hybrid Electric Vehicles." Transportation Research Record: Journal of the Transportation Research Board. Vol. 2017, 2007; pp. 26-32; NREL Report No. JA-540-41444. doi:10.3141/2017-04.
9. Official Journal of the European Union, April 23, 2009, Regulation (EC) No 443/2009, "Setting emission performance standards for new passenger cars as part of the Community's integrated approach to reduce CO2 emissions from light-duty vehicles," <http://eur-lex.europa.eu/LexUriServ/LexUriServ.do?uri=OJ:L:2009:140:0001:0015:EN:PDF>.
10. State of California Assembly Bill No. 1493, <http://www.arb.ca.gov/cc/ccms/documents/ab1493.pdf>.
11. Final Regulation Order, Amendments to Sections 1900 and 1961, and Adoption of new Section 1961.1, Title 13, California Code of Regulations, <http://www.arb.ca.gov/regact/grnhsgas/revfro.pdf>.
12. Manufacturers Advisory Correspondence 2009-01, "Implementation of the New Environmental Performance Label," Mary D. Nichols, Chairman, February 24, 2009, <http://www.arb.ca.gov/msprog/mac/mac0901/mac0901.pdf>.
13. Meeting Minutes, State of California, Air Resources Board, June 25, 2009, Pages 118-273, <http://www.arb.ca.gov/board/mt/2009/mt062509.pdf>.
14. Environmental Protection Agency, 40 CFR Parts 86 and 600, Fuel Economy Labeling of Motor Vehicles: Revisions To Improve Calculation of Fuel Economy Estimates; Final Rule, <http://www.epa.gov/fedrgstr/EPA-AIR/2006/December/Day-27/a9749.pdf>.
15. Proposed Rulemaking to Establish Light-Duty Vehicle Greenhouse Gas Emission Standards and Corporate Average Fuel Economy Standards, ENVIRONMENTAL PROTECTION AGENCY, 40 CFR Parts 86 and 600, DEPARTMENT OF TRANSPORTATION, National Highway Traffic Safety Administration 49 CFR Parts 531, 533, and 537, Pages 257-275,

[http://www.nhtsa.dot.gov/portal/nhtsa_static_file_downloader.jsp?file=/staticfiles/DOT/NHTSA/Rulemaking/Rules/Associated Files/MY2012-2016_CAFE_GHGN_PRM.pdf](http://www.nhtsa.dot.gov/portal/nhtsa_static_file_downloader.jsp?file=/staticfiles/DOT/NHTSA/Rulemaking/Rules/Associated%20Files/MY2012-2016_CAFE_GHGN_PRM.pdf).

V. OPERATIONAL AND FLEET TESTING

A. Plug-in Hybrid Electric Vehicle Testing by DOE's Advanced Vehicle Testing Activity (AVTA)

James Francfort (Principal Investigator), Timothy Murphy (Project Leader)
Idaho National Laboratory
P.O. Box 1625
Idaho Falls, ID 83415-2209
(208) 526-6787; james.francfort@inl.gov

DOE Program Manager: Lee Slezak
(202) 586-2335; Lee.Slezak@ee.doe.gov

Objective

Benchmark the plug-in hybrid electric vehicle (PHEV) concept to determine the probability that PHEV technologies will be adapted for personal transportation use while significantly reducing petroleum consumption.

Benchmark early production and prototype PHEVs from vehicle conversion companies and original equipment manufacturers (OEM).

Reduce the uncertainties about PHEV performance and PHEV battery performance and life.

Reduce the uncertainties about drivers' recharging practices and PHEV acceptance.

Provide PHEV testing results to vehicle modelers and designers, technology target setters, industry stakeholders, and DOE, as well as fleet managers and the general public to support their PHEV acquisition and deployment decisions.

Approach

Document fuel (petroleum and electricity) use over various trip types and distances.

Document PHEV charger performance (profile and demand), charging times, and infrastructure needs, as well as operator behavior impact on charging times and frequencies.

Document environmental factors, such as temperature and terrain, that impact PHEV fuel consumption.

Use PHEV testing specifications and procedures developed by the AVTA that are reviewed by industry, national laboratories, and other interested stakeholders.

Obtain PHEVs for testing to the reviewed PHEV testing specifications and procedures.

Perform baseline performance track and laboratory tests, accelerated on-road tests, and fleet demonstrations on PHEVs.

Place PHEVs in environmentally and geographically diverse test fleets.

Continue to use and develop cost-shared partnerships with public, private, and regional groups to test, deploy, and demonstrate PHEVs and infrastructure technologies in order to highly leverage DOE funding resources with the Advanced Vehicle Testing Activity's (AVTA) 80+ PHEV testing partners.

Prepare testing and data collection methods, and put in place cooperative research and development agreements (CRADA) and non-disclosure agreements (NDA) in preparation for the testing of PHEVs from additional OEMs.

Accomplishments

Continued testing PHEVs in fleet operations and demonstrations with 1.1 million PHEV test miles reached in fiscal year (FY) 2009.

Obtained and tested a cumulative total of 216 PHEVs representing 12 PHEV models (by battery chemistry and manufacturer and vehicle model).

Tested PHEVs with lithium batteries from nine manufactures and non-lithium batteries from two manufacturers.

Completed and published a PHEV charging infrastructure review and costs report.

Conducting cooperative PHEV testing with 80+ non-DOE groups to provide testing access to PHEVs operating in diverse demonstration fleets. The testing partners include: A123Systems, EnergyCS, University of California at Davis, Ohio State University, University of Hawaii, Google, Austin Energy, Central Vermont Public Service Company, Duke Energy, Advanced Energy, Salem Electric, Progress Energy, Portland Gas and Electric, Pacific Gas and Electric, San Diego Gas and Electric, Basin Electric, Buckeye Power, Wisconsin Public Power, Madison General Electric, Reliant Energy, SCANA Energy, Hawaii Center for Advanced Transportation Technologies, State of Hawaii, Hawaii Electric, Maui Electric, BC Hydro, Government of British Columbia, City of Seattle, Tacoma Power, Port of Chelan, Port of Seattle, Puget Sound Clean Air Agency, City of Wenatchee, King County, Fairfax County, Benton County, Chelan County, Douglas County, several Canadian Universities and government agencies, National Rural Cooperative Association, New York State Energy Research Development Agency, and several other organizations.

Conducting geographically and mission-diverse PHEV testing and demonstration activities in 23 states, three Canadian provinces, and Finland. The 23 U.S. states are: Arizona, California, Connecticut, Florida, Georgia, Hawaii, Illinois, Iowa, Kentucky, Michigan, Minnesota, New York, North Carolina, North Dakota, Ohio, Oregon, South Carolina, Tennessee, Texas, Vermont, Virginia, Washington, and Wisconsin.

Developed a three-page PHEV reporting format fact sheet generated from a PHEV database.

Sent 1,200 unique PHEV testing results fact sheets to the AVTA's fleet testing partners.

Continued to operate in a highly leveraged manner, with DOE only purchasing two of the 216 PHEVs in the AVTA data collection and demonstration fleet.

Completed two formal reports on PHEV petroleum and electricity fuel use reports.

Gave 17 formal presentations on PHEV performance and testing at industry conferences and meetings.

Gave another 12 presentations on PHEV performance to Idaho National Laboratory (INL) site visitors and dignitaries

Performed due diligence on other PHEV models to determine their suitability as test candidates.

Future Activities

Continue performing due diligence on potential PHEV suppliers and obtain PHEVs for testing as appropriate

Identified 90 additional PHEVs that will be added to the fleet demonstrations in early FY 2010, including 37 PHEVs in California, at no cost to DOE.

Conduct a PHEV codes and standards review and report on the regulations, standards and codes related to the charging and discharging of electric drive vehicles from and to the electric grid based on current practices in 12 U.S. cities.

Continue to assess the value of fleet requests to provide PHEV fleet data to AVTA.

Obtain future PHEV models and battery technologies for testing.

Develop additional low-cost PHEV demonstration relationships and support the deployment of PHEVs in these testing fleets.

Coordinate PHEV and charging infrastructure testing with industry and other DOE directed entities.

Introduction

DOE's AVTA is evaluating PHEV technology in order to understand the capability of the technology to significantly reduce petroleum consumption when PHEVs are used for personal transportation. In addition, many companies and groups are proposing, planning, and have started to introduce PHEVs into their fleets. Currently, most PHEVs are obtained from local PHEV conversion shops and sometimes at local colleges with automotive education programs (Figure 1). In addition, PHEV conversions often occur at fleet owners' locations (Figure 2).



Figure 1. Port of Chelan lead effort to place PHEVs in Washington state saw several Prius HEVs await the installation of Hymotion PHEV batteries at Wenatchee Valley College.



Figure 2. Green Gears PHEV conversion shop converting a Hymotion Prius at the Maui Electric Company fleet shop.

The vast majority of the PHEVs currently available use an HEV as the base vehicle, and either add a second PHEV battery or replace the base HEV battery with a larger PHEV battery pack (5-kWh PHEV batteries are the most typical size to date). However, some PHEVs are using a single PHEV

battery pack that ranges from 10 to 15 kWh. PHEV control systems and power electronics are also added to the base vehicle to complete the upgrade. These larger additional or replacement battery packs are sometimes recharged by the onboard systems, but all of them must also use onboard chargers connected to the off-board electric grid to fully recharge the PHEV battery packs.

In addition to the battery and control system upgrades, PHEVs in the AVTA test and demonstration fleet also have onboard data loggers installed when the vehicles are converted or when they enter the AVTA demonstration fleet. Experience has shown automated data collection in fleet environments is the only way to ensure accurate data is collected.

The concept of additional onboard energy storage and grid-connected charging raises questions that include the life and performance of these larger batteries; the charging infrastructure required; how often the vehicles will actually be charged; and the actual amount of petroleum displaced over various missions, drive cycles, and drive distances.

Approach

The AVTA supports the introduction of PHEVs by testing the emerging group of PHEV models and documenting vehicle and battery performances, as well as electricity and petroleum use in cost-shared agreements with the AVTA’s fleet testing partners. As a first step, the AVTA developed a 400-page test plan for inspection, dynamometer, test track, accelerated and fleet testing of PHEVs. A total of twelve PHEV models have been obtained and tested in various demonstrations and missions, with additional candidate test PHEVs being considered for testing.

The AVTA has conducted a PHEV charging infrastructure and power electronics study and the documenting report was completed during FY 2009. In addition, two formal reports were completed that discuss PHEV fuel use reporting difficulties and methods, and driving intensity impacts to fuel use. The AVTA has also signed testing, demonstration, and data collection agreements with several additional non-DOE fleets that operate PHEVs. AVTA will collect performance and charging data to

characterize the performance of the PHEVs and the charging infrastructure.

PHEV Testing Methods

Three types of testing methods are used to test PHEVs and they discussed below.

Baseline performance testing during which the PHEV are track and dynamometer tested. The track testing includes acceleration, braking, and fuel use (both electricity and gasoline) at different states-of-charge. The PHEV are also coast-down tested to determine dynamometer coefficients, which are used during the urban and highway dynamometer test cycles. Several PHEVs that were scheduled for baseline performance testing during FY 2009 were not sufficiently capable of completing the testing, so no results are reported. The results for several PHEVs were reported in the FY 2008 report.

Accelerated Testing uses dedicated drivers to complete a series of drives and charges on city and highway streets in the Phoenix, AZ area (Table 1). Note that between each individual 10 to 200 mile drive, the PHEVs are charged from 4 to 12. Several PHEVs completed this testing and the results are discussed below.

Table 1. Revised PHEV accelerated testing distances as of the end of FY 2008.

Cycle (mi)	Urban (10 mi)	Highway (10 mi)	Charge (hours)	Repetitions (N)	Total (mi)	Repetitions (%)	Miles (%)	Cumulative (mi)
10	1	0	4	60	600	37%	11%	600
20	1	1	8	30	600	19%	11%	1,200
40	4	0	12	15	600	9%	11%	1,800
40	2	2	12	15	600	9%	11%	2,400
40	0	4	12	15	600	9%	11%	3,000
60	2	4	12	10	600	6%	11%	3,600
80	2	6	12	8	640	5%	12%	4,240
100	2	8	12	6	600	4%	11%	4,840
200	2	18	12	3	600	2%	11%	5,440
Total	2,340	3,100	1,344	162	5,440			5,440
Av	43%	57%	8.3	18.0				

Fleet testing is normally conducted by PHEVs operating in fleets because government, private, and public fleets are overwhelmingly the earliest adaptors of PHEVs. However, AVTA fleet testing does include operations by the general public. Fleet testing is discussed extensively below. A total of 216 PHEVs were tested by AVTA at the end of FY 2009; the accelerated testing and fleet testing results are discussed below.

The twelve PHEVs that were tested by the AVTA to date are listed below. Only one PHEV, the Renault Kango, completed testing prior to FY 2009. The PHEV models include:

- Ford Escape E85 PHEV (from Ford), with a Johnson Controls / Saft (JCS) lithium battery pack.
- Toyota Prius converted by EnergyCS, with a Valance lithium battery pack.
- Toyota Prius converted by EnergyCS, with a Altair Nano lithium battery pack.
- Toyota Prius converted by Hymotion, with an A123Systems lithium pack.
- Ford Escape converted by Hymotion, with an A123Systems lithium battery pack.
- Ford Escape converted by Electrovaya, with an Electrovaya lithium battery pack.
- Ford Escape converted by Hybrids Plus, with a Hybrids Plus lithium battery pack.
- Ford Escape converted by Hybrids Plus, with a K2 Energy Solutions lithium battery pack.
- Toyota Prius converted by Hybrids Plus, with a lithium battery pack.
- Renault Kangoo with a Nickel Cadmium battery pack.
- Toyota Prius converted by Manzanita with a Thunder Sky lithium battery pack.
- Toyota Prius converted by Manzanita with a lead acid battery pack.

Accelerated Testing Results

Hymotion Prius PHEV (Version II Battery) Testing

(This section discusses the testing results for the Hymotion Prius PHEV conversion that uses the Version II battery from A123Systems. Note that Hymotion is owned by A123 Systems, Boston, MA. Subsequent to the completion of crash testing conducted by Hymotion [not conducted by AVTA], Hymotion redesigned the original Version I battery and replaced all of the Version I Prius PHEV batteries in the field with their crash-tested Version II Prius battery.)

During FY 2009, the Version II Hymotion Prius accelerated testing was conducted by two different AVTA drivers. The first driver was considered an experienced (E) driver due to his experience operating HEVs. As seen in Table 2, driver E drove the 10-mile cycles that resulted in 117.6 mpg, and the first 40-mile all highway cycles that resulted in 103.3 mpg. At this point, a second inexperienced (I) driver was trained in PHEV performance and operations. This driver was assigned to drive the remaining cycles, including the first 40-mile all-urban cycle (62.1 mpg), the first 40-mile mixed cycle (64.3 mpg), and the remaining 60-, 80-, 100-, and 200-mile cycles.

Table 2. Hymotion Prius PHEV with the Version II battery pack accelerated testing results. Note that each total distance was slightly greater than 600 or 640 test miles. *E = Experience PHEV Driver and I = Inexperienced PHEV driver.

Cycle	Urban	High-way	Charge	Reps	Total	Electricity	Gasoline		MPG Recalculated without income-plete charges
(mi)	(10 mi)	(10 mi)	(hours)	(N)	(mi)	kWh	Gals	MPG*	
10	1	0	4	60	600	111.43	5.205	117.6 E	
20	1	1	8	30	600	124.50	8.105	80.1 I	
40	4	0	12	15	600	71.28	9.8	62.1 I	64.2
40	4	0	12	15	600	44.97	7.2	84.2 E	135.6
40	2	2	12	15	600	64.36	9.70	64.3 I	65.5
40	2	2	12	15	600	75.14	6.20	99.8 E	101.7
40	2	2	12	15	600	70.98	6.83	90.6 I	98.9
40	0	4	12	15	600	75.18	6.10	103.3 E	100.0
40	0	4	12	15	600	63.46	8.88	70.8 I	92.4
60	2	4	12	10	600	33.38	10.54	58.8 I	
80	2	6	12	8	640	41.38	10.71	61.8 I	
100	2	8	12	6	600	26.48	10.91	56.5 I	
200	2	18	12	3	600	16.01	10.41	57.7 I	
Total	2340	3100	1404	167	7,840				

When the mpg results for the Version II vehicle were compared to the Version I vehicle (Table 3), it was initially and mistakenly believed that the Version II battery resulted in lower mpg test results. Further analysis suggested that the inexperience of driver I likely was contributing to the lower mpg results.

Table 3. Hymotion Prius PHEV with the Version I battery pack accelerated testing results. Note that each total distance was slightly greater than 600 or 640 test miles.

Cycle	Urban	Highway	Charge	Reps	Total	Electricity	Gasoline	
(mi)	(10 mi)	(10 mi)	(hours)	(N)	(mi)	kWh	Gals	MPG
10	1	0	4	60	600	136.33	4.81	127.2
20	1	1	8	30	600	122.02	5.37	115.9
40	4	0		15	600	84.10	6.05	101.1
40	2	2	12	15	600	87.22	5.78	106.9
40	0	4	12	15	600	79.82	8.54	73.1
60	2	4	12	10	600	55.33	8.98	68.9
80	2	6	12	8	640	43.99	11.36	58.3
100	2	8	12	6	600	35.98	8.43	73.2
200	2	18	12	3	600	15.0	11.02	54.8
Total	1,740	2,500	984	132	5,440	Weighted Average		79.5

Subsequently, Driver E repeated the 40-mile all-urban cycles with a result of 84.2 mpg and the 40-mile mixed cycles with a result of 99.8 mpg. Driver I was then retrained in PHEV operations and re-drove the 40-mile mixed cycles with a result of 90.6 mpg. Therefore, while a limited example, it was thought that driver training can have significant impact on PHEV mpg results. It was not until further data analysis that the impact of ambient temperatures during charging events had on mpg. Individual mpg results during individual trips, as captured by the onboard data logger, indicated there were incomplete charging events that negatively impacted the mpg results. As seen in Figure 4, the incomplete charging events are associated with ambient temperatures of approximately 140°F.

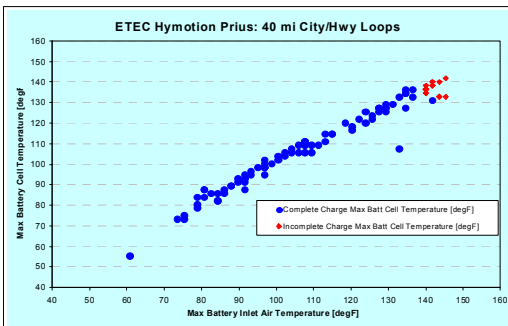


Figure 4. Battery and ambient (measured at battery inlet) temperatures during charging events in the Version II Hymotion Prius PHEV.

When the mpg results were recalculated without the individual 40-mile loops that were driven after incomplete charging events, the result was 135.6 mpg, as seen in the right-most column in Table 2. This is 61% higher than the first reported 84.2 mpg. Another especially large increase in mpg was the

recalculated 92.4-mpg result for the 40-mile all highway cycles, a 31% increase in reported mpg.

Electrovaya Escape PHEV Testing

(This vehicle is owned by the New York State Energy Research Development Agency [NYSERDA] and it was tested in partnership between DOE’s AVTA and NYSERDA in support of NYSERDA’s leadership efforts to support the development of the PHEV industry.)

The Electrovaya Escape PHEV conversion had some problems operating during the initial pass through the accelerated testing, when the results ranged from 29.2 to 43.1 mpg during late FY 2008 and earlier FY 2009. During FY 2009, the Electrovaya Escape was subsequently completely retested and the results ranged from 33.5 to 53.1 mpg (Table 4).

Table 4. Electrovaya Escape PHEV accelerated testing results. Note that each total distance was slightly greater than 600 or 640 test miles.

Cycle	Urban	Highway	Charge	Reps	Total	Electricity	Gasoline	
(mi)	(10 mi)	(10 mi)	(hours)	(N)	(mi)	kWh	Gals	MPG
10	1	0	4	60	600	198.93	11.52	53.1
20	1	1	8	30	600	163.29	13.51	45.7
40	4	0	12	15	600	57.51	14.91	41.1
40	2	2	12	15	600	76.29	15.99	38.7
40	0	4	12	15	600	114.14	11.92	51.5
60	2	4	12	10	600	97.18	13.70	45.3
80	2	6	12	8	640	77.69	16.05	41.3
100	2	8	12	6	600	58.64	15.69	39.8
200	2	18	12	3	600	26.09	17.72	33.5
Total	2340	3100	1344	16	5440	Weighted Average		42.5

The weighted average result at the end of the FY 2009 accelerated testing was 42.5 mpg. It should be noted that this is a 57% higher mpg than the AVTA’s testing results of 27 mpg for the two “normal” Ford Escape HEVs driven for 320,000 miles.

Hybrids Plus Escape PHEV Testing

(This vehicle is also owned by the NYSERDA and it was to be tested in partnership between DOE’s AVTA and NYSERDA in support of NYSERDA’s leadership efforts to support the development of the PHEV industry.)

The accelerated on-road testing for this vehicle was suspended at Hybrids Plus’ request during FY 2009 because this model has undergone battery manufacturer and design changes. It is anticipated

that testing will resume during FY 2010 with a new battery design and control strategy.

Fleet Testing Results

As of the end of FY 2009, there were approximately 650 PHEVs operating in North America. Most of these were in the United States. In order to collect data on PHEVs in fleet operations, at the beginning of FY 2008, AVTA partnered with the two PHEV conversion companies that had performed the most PHEV conversions to date. By the end of FY 2009, AVTA has partnered with more than 80 organizations in the United States, Canada, and Finland. The mix of organizations includes:

- 38 electric utilities (includes the National Rural Electric Cooperative Association)
- 6 city governments
- 6 county governments
- 2 state governments
- 8 universities and colleges
- 2 clean air agencies
- 7 private companies and advocacy organizations
- 3 governments of Canadian provinces
- 1 sea port and 1 U.S. military organization
- Several Canadian and Finnish research centers
- 2 PHEV conversion companies.

The 80 PHEV fleet testing partners have operated 216 PHEVs in 23 states, three Canadian provinces, and Finland (Figure 5) as of the end of FY 2009. Another 71 PHEVs are to be added early in 2010. This brings the total to 287 PHEVs in AVTA's PHEV fleet testing during FY 2010. Note that the AVTA has only purchased two of the 287 PHEVs, making this a highly leveraged testing activity benefiting DOE. Initially, AVTA provided some cost-sharing for the data loggers, but going forward, all data logger, base vehicle, and conversion costs are incurred by the fleets.

The benefit to the vehicle operators in participating in the AVTA PHEV Demonstration is the three-page PHEV fact sheet INL provides to each participant on a monthly basis. The format and content are discussed below. This type of value-for-value

arrangement allows AVTA to operate in a highly funding-leveraged manner, again providing maximum benefit both to DOE and the taxpayer.

The initial 50 vehicles in the test fleet used Kvaser data loggers, which by design include a data logger and a memory card that must be physically removed from the data logger and then either physically mailed to INL or uploaded to INL via the Internet. An additional 141 fleet PHEVs have been added to the PHEV data collection fleet that use GridPoint (formally V2Green) onboard data loggers, GPS units, and cellular communications. The advantage of the GridPoint wireless data collection communication system is significantly increased data collection accuracy and timeliness. There are also some other non-Kvaser and non-Gridpoint data collection devices being used.

About 193 of the 216 PHEVs are Hymotion PHEV conversions of Toyota Priuses; an additional twelve are EnergyCS conversions of Toyota Priuses; and approximately 10 more are Hybrids Plus conversions of Priuses and Ford Escape HEVs. The remaining PHEVs are a mixture of a couple of lead acid PHEV conversions or a couple of Hymotion Escape conversions. The heavy concentration of Hymotion Prius PHEVs reflects the fact that 75% or more of all PHEVs in North America are Hymotion Prius conversions, thus the AVTA's testing partners are mostly operating the Hymotion Prius PHEV conversions. While it is not necessarily desirable to be collecting PHEV data from a single PHEV conversion company model, using the large number of Hymotion Prius PHEVs does allow for data collection in very diverse fleets in very diverse operating and environmental areas.

The first AVTA PHEV test fleet was in the Seattle and Tacoma area of Washington State, with 15 PHEVs in the fleets of:

- City of Seattle / Seattle City Light
- King County
- Port of Seattle
- Puget Sound Clean Air Agency
- Tacoma Power.

Another AVTA PHEV Washington State demonstration of 14 PHEVs is lead by the Port of

Chelan. The University of California at Davis has 13 PHEVs in a test fleet with public drivers that are providing data to the AVTA. The State of California's General Services Administration (CA-GSA) recently acquired 14 Hymotion Prius conversions as part of a total acquisition of 50 of these vehicles. The INL was contacted by CA-GSA who requested that their 50 PHEVs be allowed to participate in the AVTA's PHEV demonstration. This will be the largest single fleet of PHEVs that the INL will be collecting data from. The Government of British Columbia and BC Hydro will have approximately 30 PHEVs participating in the AVTA's PHEV demonstration.

The AVTA also has a testing support agreement with NYSEDA to support fleet testing of 20 PHEVs in New York State fleets; however, deployment was only approximately half completed as FY09 ended.

Hymotion Prius PHEVs with Kvaser Data Loggers Fleet Testing Results

A sample of the types of data being accumulated from the PHEV fleet testing and demonstrations can be seen in the three-page summary report for the North American PHEV Demonstration (Figures 6 through 8). The summary is for the 41 Hymotion Prius PHEVs with Kvaser data loggers that provided data from January 2008 to September 2009.

As can be seen in Figure 6, these PHEVs were driven a total of 269,000 miles during this period. The vehicle operations are broken down into three operations modes:

- **Charge Depleting (CD) Mode:** During each entire trip, there is electric energy in the battery pack to provide either all-electric propulsion or electric assist propulsion.
- **Charge Sustaining (CS) Mode:** During a trip, there is no electrical energy available in the PHEV battery pack to provide any electric propulsion support.
- **Combined (or Mixed) Charge Depleting and Charge Sustaining (CD/CS) Mode:** There is electric energy in the PHEV battery pack available at the beginning of a trip. However, during the trip, the battery is fully depleted.

It should be noted that the only way to recharge the Hymotion A123Systems battery packs is to plug in the vehicle. This PHEV design does not accept energy for recharging during regenerative braking or from the onboard electric generator. The Hymotion design keeps the stock Toyota Prius HEV battery and only this battery can accept onboard energy from recharging or regenerative braking.

As can also be seen in the first page of the summary sheet (Figure 6), the overall fuel economy for the 30,796 trips was 46 mpg. However, for the 17,382 trips in CD mode, it was 61 mpg—a 56% improvement over the 39 mpg for the 10,744 trips taken in CS mode.

As can be seen on page two of the summary sheet (Figure 7), the fuel economy is broken down by city and highway trips, which is binned by average speeds, number of stops per mile, amount of time accelerating, number of stops per mile, number of acceleration events per mile, and the number of seconds cruising per mile. This breakdown by city, highway, and by CD, CS, and mixed modes documents average mpg results that range from 34 to 64 mpg. This figure also shows the impacts on PHEV mpg when drivers drive more aggressively. This is measured by the accelerator pedal position and the amount of time spent during a trip at a higher accelerator pedal position. The higher position is based on how far down the pedal is pushed by the driver; if the pedal is pushed to the floor, it is considered to be in the 100% position—the most aggressive position. In the graph on Figure 7, entitled “Effect Of Driving Aggressiveness on Fuel Economy,” the bottom 0-2 bar represents all trips driven when the pedal position was at 40% or more for only 20% or less time of each individual trip, and the average fuel economy was about 60 mpg. Note that some individual trips had fuel economies between 300 to almost 400 mpg per trip.

The third page (Figure 8) provides recharging information and patterns. The average number of charging events per day when a vehicle is driven was 1.4 charges, the vehicles were driven an average of 29.8 miles between charging events, with 3.4 trips per charging event, and the average charge was for 2.1 hours, and the average energy charged was 1.6 DC kWh.

Page three also shows that the peak drive time was between 4 and 5 p.m., the peak time of day when charging was measured by DC kWh use as between 5 and 10 p.m., and the peak start of charging between 4 and 6 p.m. It should be noted that most of these vehicles are operating in fleets, most of the driving would occur during work hours, and most of the charging would occur either during breaks or at the end of the workday.

Hymotion Prius PHEVs with GridPoint Data Loggers Fleet Testing Results

Another and larger set of fleet testing results that is being accumulated from the PHEV demonstrations can be seen in the three-page summary report for the North American PHEV Demonstration in Figures 9

through 11. This summary is for the 116 Hymotion Prius PHEVs equipped with GridPoint data loggers with GPS and cellular communications that have provided data from April 2008 through September 2009.

As can be seen in Figure 9, these PHEVs were driven a total of 712,000 miles during this period. As with the PHEVs with the Kvaser data loggers, the vehicle operations are broken down into the three operations modes of CD, CS, and mixed CD/CS.

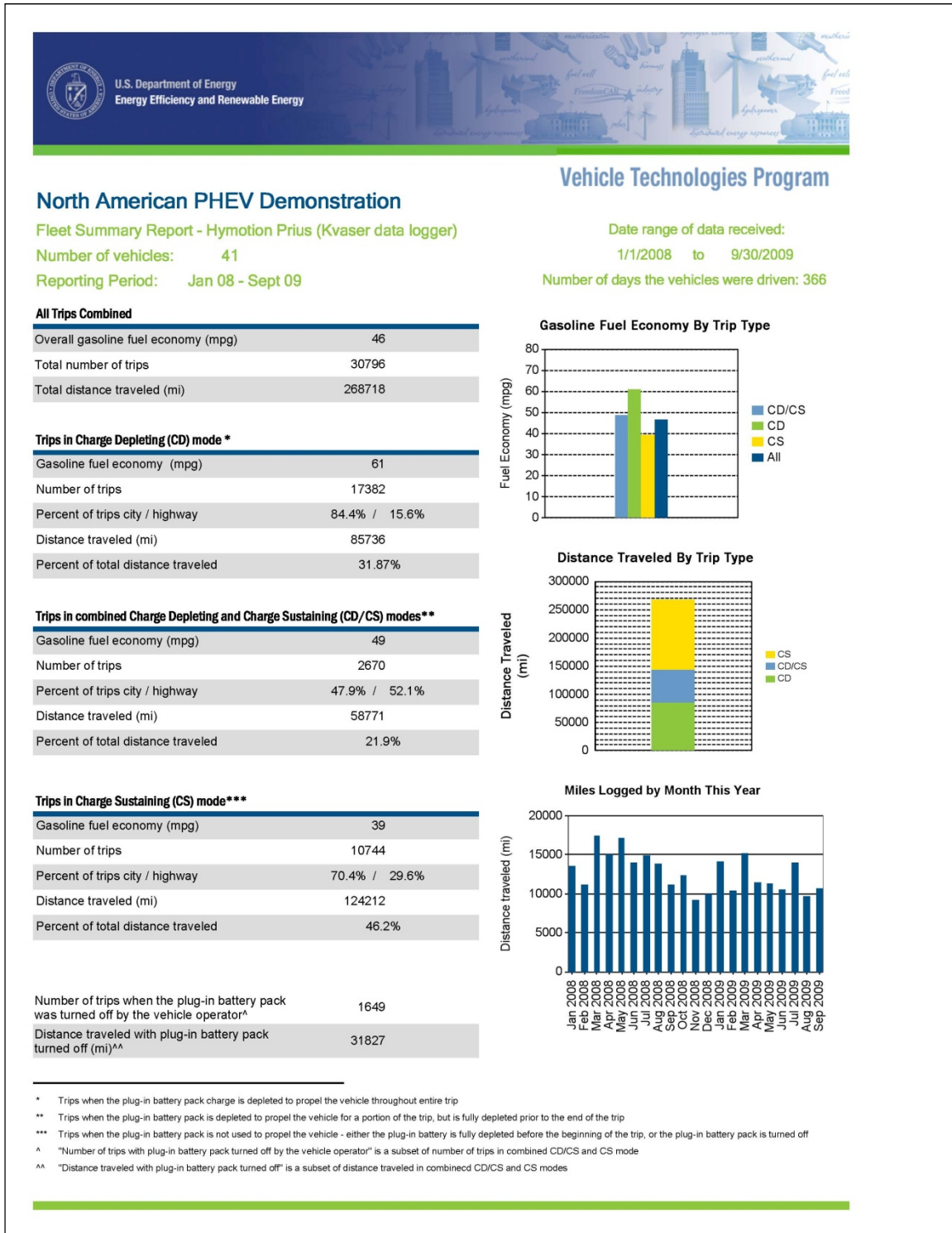


Figure 6. Page 1 of 3 for the PHEV summary report for 41 PHEVs operating January 2008 – September 2009 with onboard Kvaser data loggers.

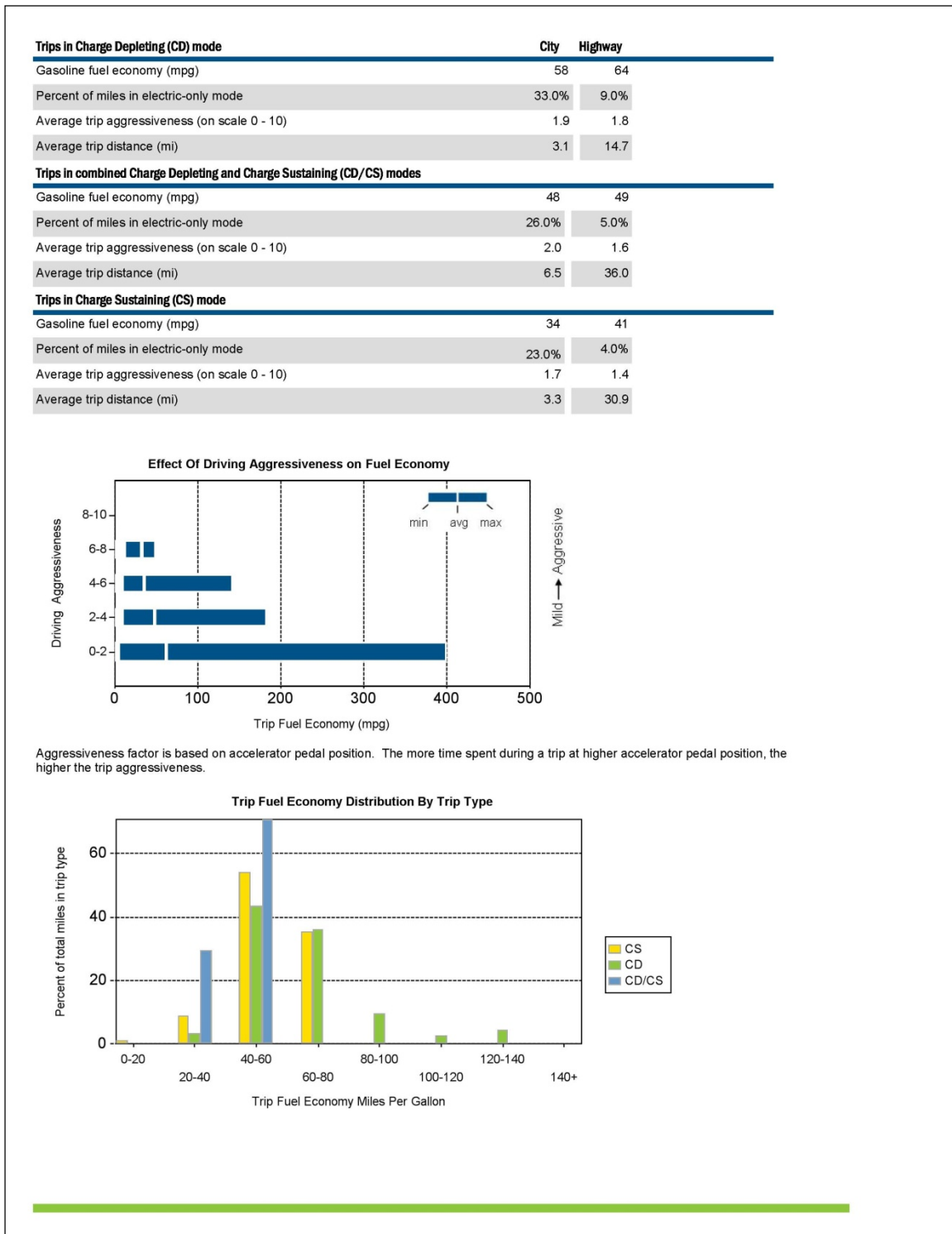


Figure 7. Page 2 of 3 for the PHEV summary report for 41 PHEVs operating January 2008 – September 2009 with onboard Kvaser data loggers.

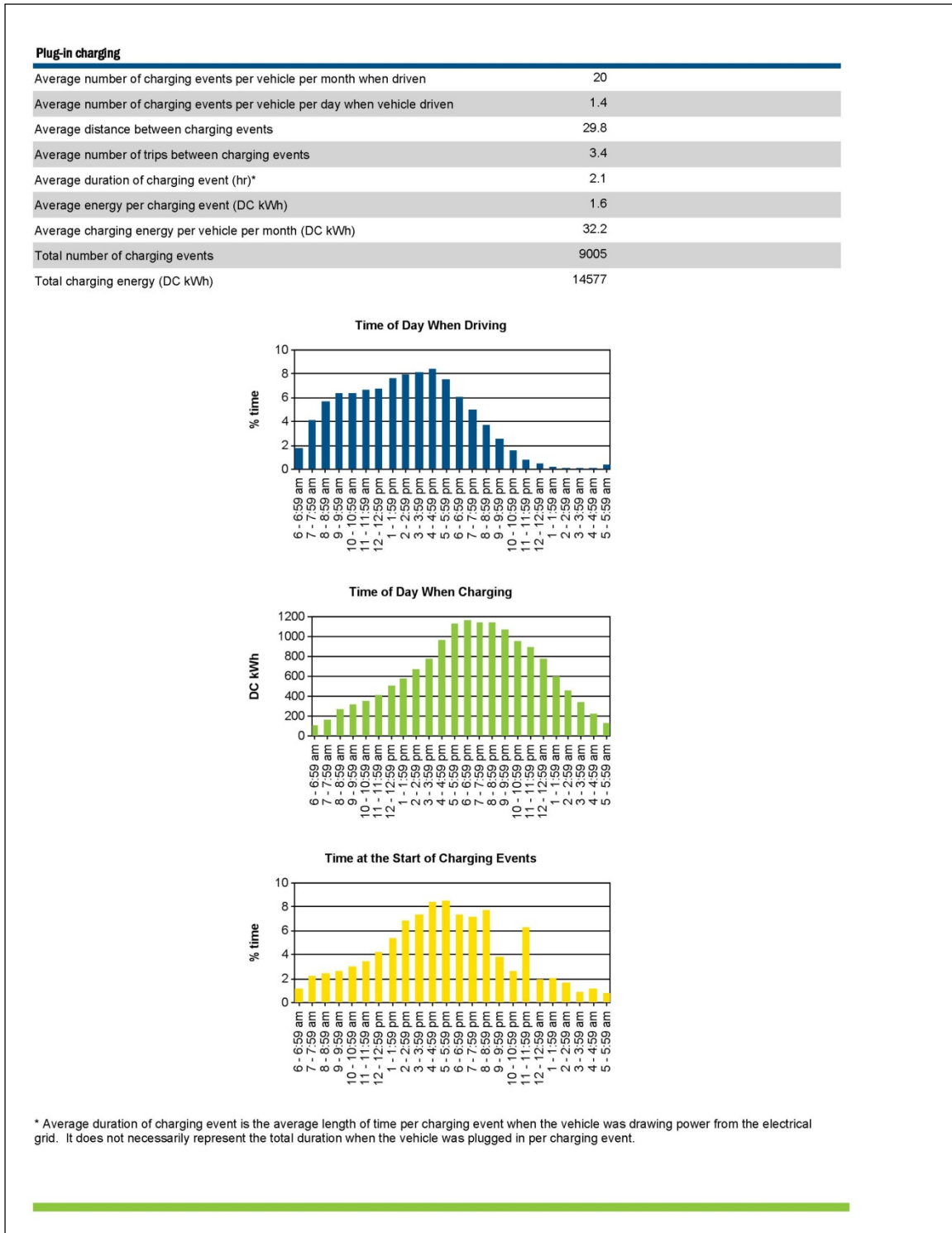


Figure 8. Page 3 of 3 for the PHEV summary report for 41 PHEVs operating January 2008 – September 2009 with onboard Kvaser data loggers.

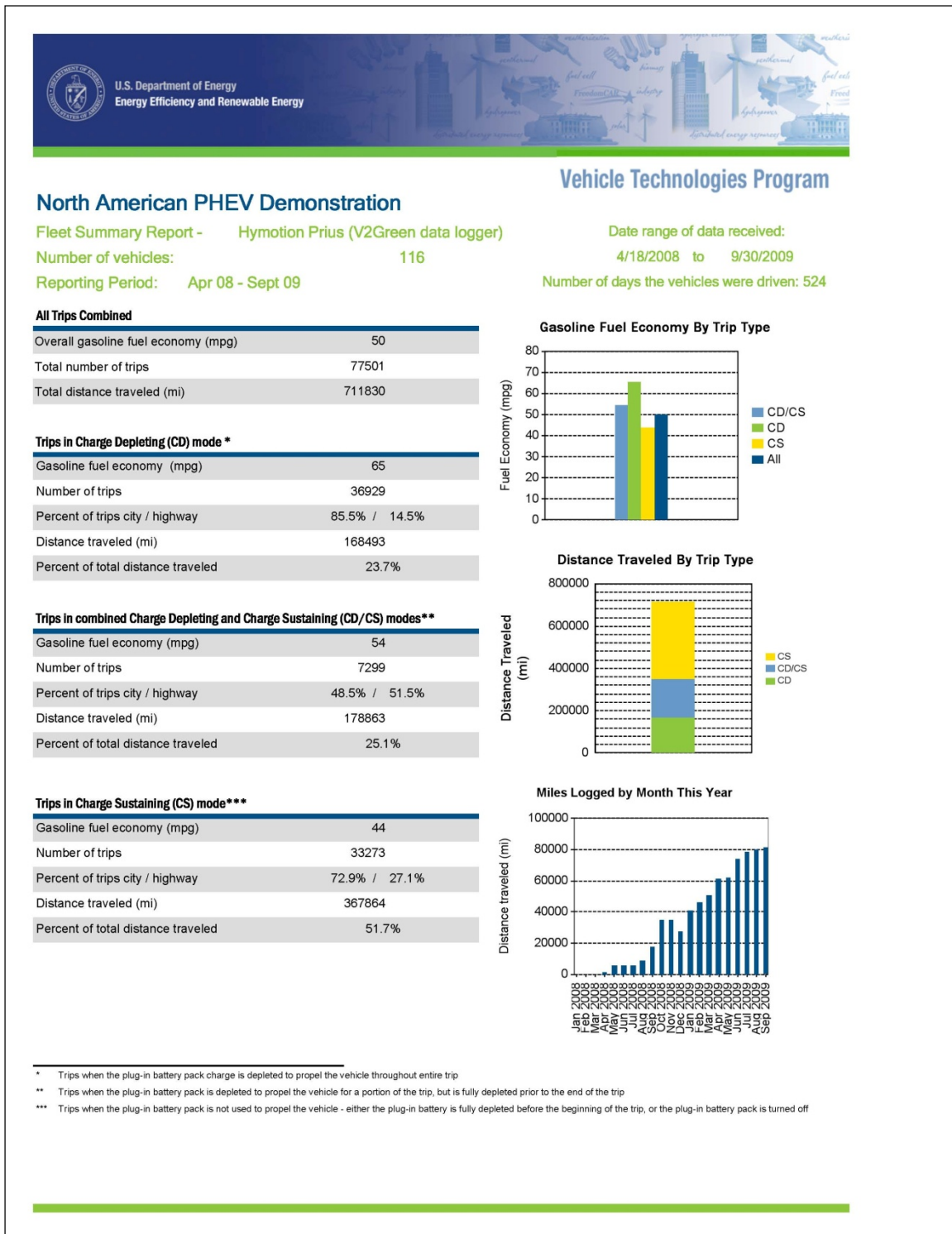


Figure 9. Page 1 of 3 for the PHEV summary report for 116 PHEVs operating April 2008 – September 2009 with onboard GridPoint data loggers.

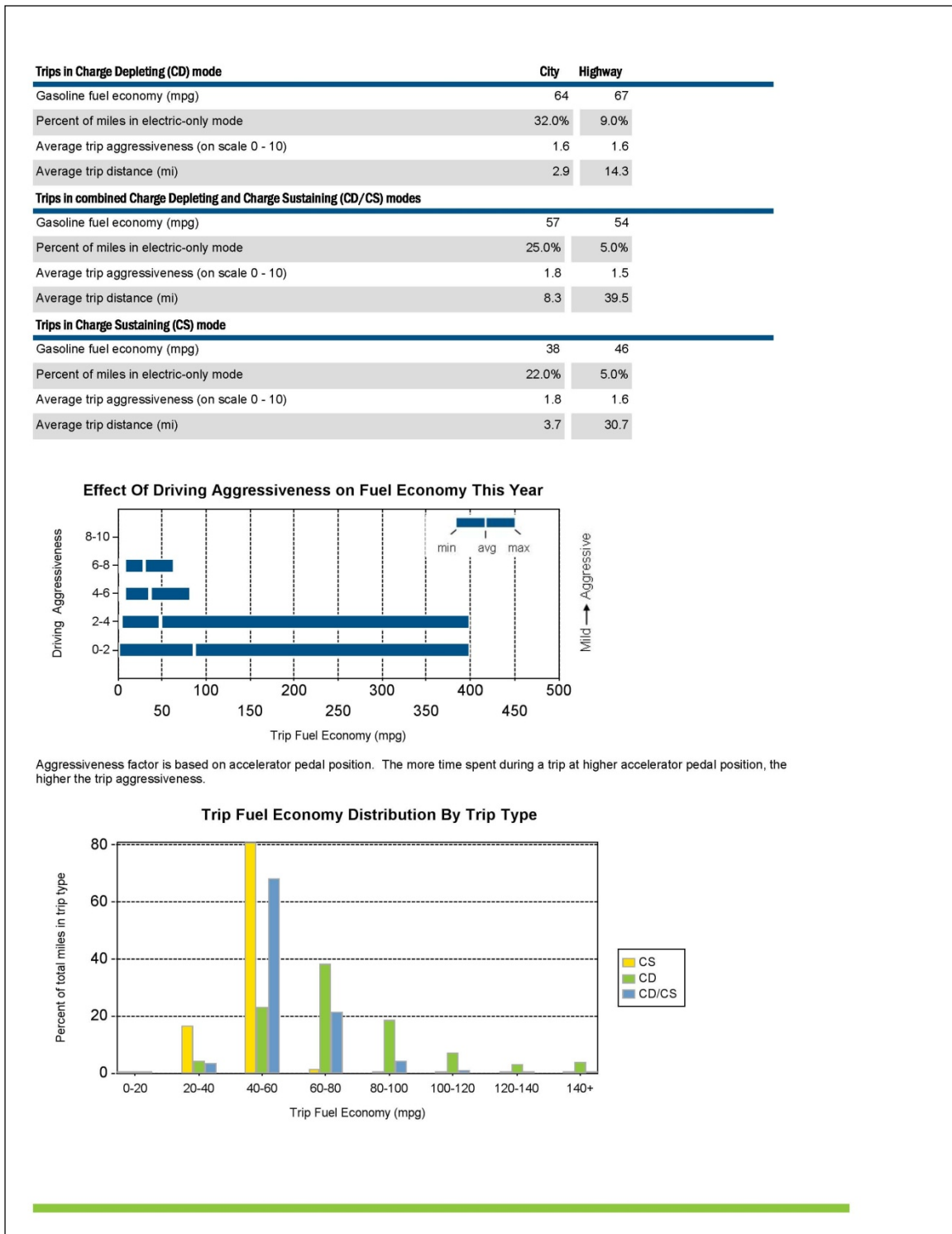


Figure 10. Page 2 of 3 for the PHEV summary report for 116 PHEVs operating April 2008 – September 2009 with onboard GridPoint data loggers.

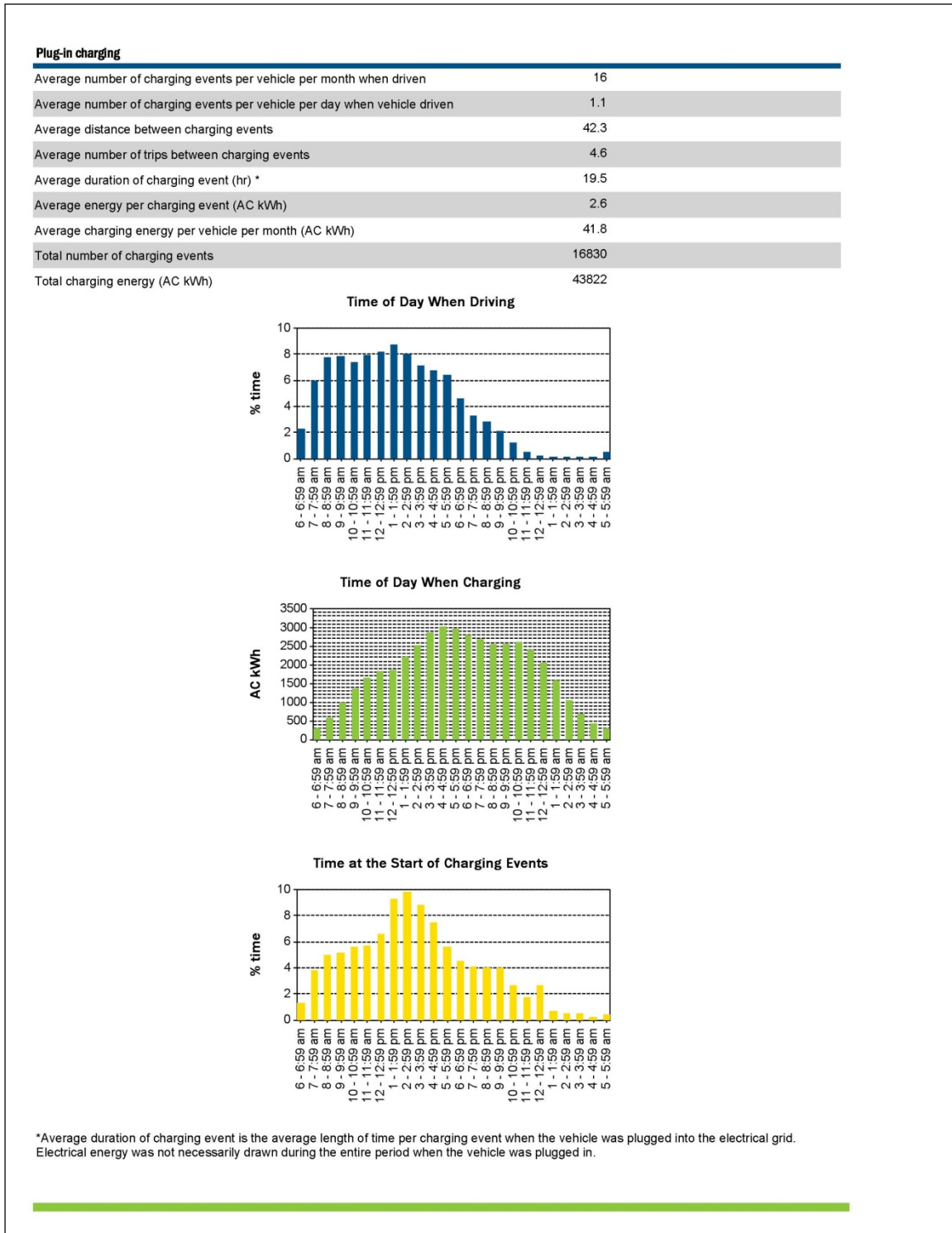


Figure 11. Page 3 of 3 for the PHEV summary report for 116 PHEVs operating April 2008 – September 2009 with onboard GridPoint data loggers.

As can also be see in the first page of the summary sheet (Figure 9), the overall fuel economy for the 77,501 trips was 50 mpg; but for the 36,929 trips in CD mode, it was 65 mpg—a 48% improvement over the 44 mpg for the 33,273 trips taken in CS mode.

As can be seen on page two of the summary sheet (Figure 10), the fuel economy is broken down by city and highway trips, which is binned by average speeds, number of stops per mile, amount of time accelerating, number of acceleration events per mile, and number of seconds cruising per mile. This breakdown by city, highway, and CD, CS, and mixed modes documents average mpg results that range from 38 to 67 mpg, which is 76% higher. Figure 10 also shows the impacts on PHEV mpg when drivers drive more aggressively. In the graph entitled “Effect Of Driving Aggressiveness on Fuel Economy,” the bottom 0-2 bar represents all trips driven when the pedal position was at 40% or more for only 20% or less time of each individual trip. The average fuel economy was about 80 to 85 mpg. Note that some individual trips had fuel economies between 300 to almost 400 mpg per trip.

The third page (Figure 11) provides recharging information and patterns. The average number of charging events per day when a vehicle is driven was 1.1 charges, the vehicles were driven an average of 42.3 miles between charging events, with 4.6 trips per charging event, and the average charge was for 19.5 hours, and the average energy charged was 2.6 AC kWh.

Page three also shows that the peak drive time was between 11 a.m. and 3 p.m., the peak time of day when charging was measured by AC kWh use as between 3 and 6 p.m., and the peak start of charging between 1 and 4 p.m. It should be noted that most of these vehicles are operating in fleets, most of the driving occurs during daytime work hours, and most of the charging occurs either during daytime driving breaks or at the end of the workday.

Operators’ Aggressive Driving Impacts on PHEV MPG

Using the data from 150 of the Hymotion Prius PHEVs with the Kvaser and GridPoint data loggers, and the 22,700 trips that occurred over 151,000 miles in CD mode, Figure 12 shows the percentage of time for each individual trip the accelerator pedal

position is depressed at 40% or more. It can easily be observed that when the pedal is depressed at 40% or more for 30% of a trip or less, the average mpg for each of the 22,700 trips increases.

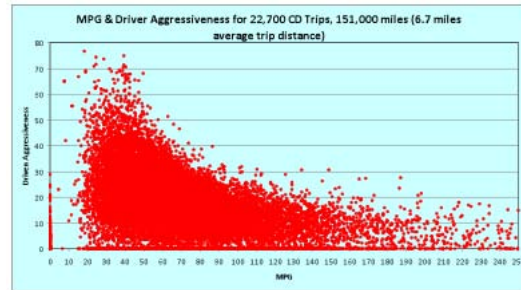


Figure 12. Miles per gallon impacts from aggressive driving during Hymotion Prius PHEVs being driven 151,000 miles and 22,70 trips in charging depleting mode.

Note that Figure 13 shows the average mpg results for each trip in Figure 12 by mpg ranges. The data is presented in Figure 13 by the percentage of miles driven and trips taken. It can be seen that approximately 15% of all trips taken in CD mode result in an average mpg of 100 mpg or greater. Approximately 13% of the trips by miles driven result in an average of 100 mpg or greater. Current PHEV designs are often credited with producing results that exceed 100 mpg; this is correct but only for a small percentage of the time.

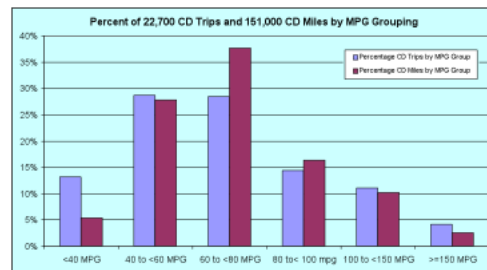


Figure 13. Average miles per gallon results during charging depleting mode operations for 150 Hymotion Prius PHEVs being driven 151,000 miles and 22,70 trips. This is the same trip data as seen in Figure 15.

PHEV MPG Results and Engine Run-Times by Ambient Temperature

Figure 14 shows the average mpg trip results by ambient temperatures for Hymotion Prius PHEVs in CD, CS, and CD/CS operating modes. The mpg results for all three operating modes, as well as the mpg results for all trips combined, demonstrate

significant decreases in mpg results when the vehicles are operated in colder environments compared to the base results at 20 to 30°C. This is especially true for the CD results of approximately 28 mpg at <20°C and CD results of 76 mpg at the 20 to 30°C range. Note that as the ambient temperatures increase above the 20 to 30°C range, there is also a decrease in mpg, but not to the amount seen when the ambient temperature drops.

These decreases and increases in mpg results are not just driven by battery chemistry characteristics at cold and hot temperatures, but also by changes in how the Toyota Prius internal combustion engine (ICE) operates. As seen in Figure 15, the ICE operates at near 100% of the time at the coolest temperatures. This is driven by several factors that range from cabin heating demands to exhaust catalytic converter heating requirements.

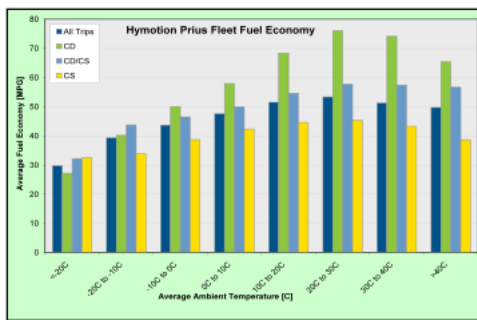


Figure 14. Average miles per gallon results for individual trips driven during various CD, CS, CD/CA operating models, binned by the average ambient Temperatures for each individual trip.



Figure 15. Percentage of miles driven with the Toyota Prius internal combustion engine one by ambient temperatures. This is the same data set as seen in Figure 17.

PHEV Smart Charging Study

In order to provide additional PHEV charging information to the electric utilities that will be providing the charging energy for PHEVs, AVTA partnered with several PHEV fleets in the Puget Sound area (in Washington State) to charge Hymotion Prius PHEVs in several different manners. Please note that this project was lead by Seattle City Light. GridPoint data loggers and vehicle connectivity modules (VCM) are used to control the vehicle charging performance.

Figure 16 documents the normal Hymotion Prius charging ramp-up to 1.2 kW, with some minimal energy use post charge. Figure 17 shows the charging profile when charge time is limited to between 10 p.m. and 4 a.m. Note the 40-W average stand-by power that occurs between the vehicle being plugged in and charging begins at 10 p.m., as well as the average post charge of 5 W. Figure 18 documents the amount of energy drawn outside of the allowable charging window. Note that a total of 35% of the energy is used for charging when communication is not established or lost and charging occurs, and when non-charging energy use occurs both within and outside of the specified charging window.

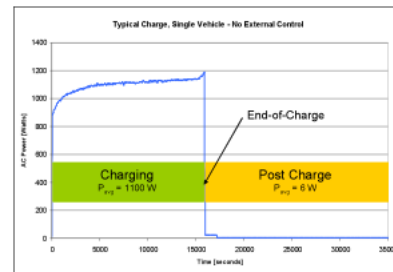


Figure 16. Typical charging profile for a Hymotion Prius PHEV conversion.

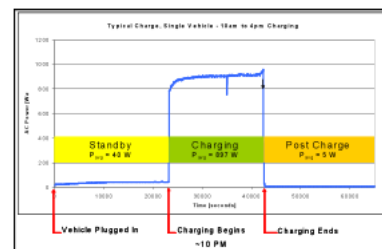


Figure 17. Hymotion Prius PHEV charge pattern when charging is limited to 10 p.m. to 4 a.m.

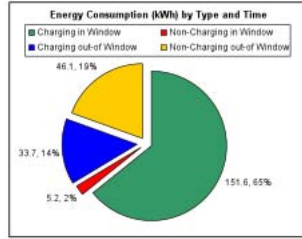


Figure 18. How energy is used for charging a Hymotion Prius PHEV when charging is limited to time of day charging as show in Figure 17. Note 35% of energy is used outside of define charge window.

Figure 19 documents the fragmented charging that occurs in one PHEV when the 13 PHEVs are limited to a cumulative total of 3 kW. Figure 20 documents the charging profile for a single PHEV when charge time is limited to an energy price threshold below 8 cents per kWh. Note the average stand-by power of 139 W for approximately 7 hours before the charging occurs.

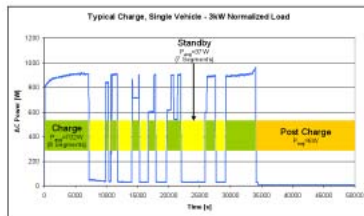


Figure 19. Hymotion Prius PHEV charging pattern when a group of 13 PHEVs are limited to a total of 3 kW of total energy for all 13 PHEVs. Note the 8 charging segments and 7 standby modes.

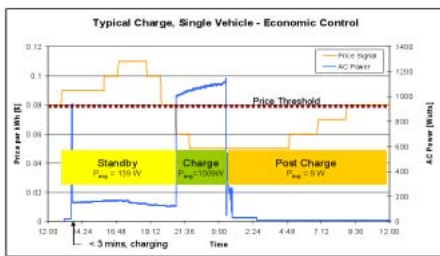


Figure 20. Hymotion Prius PHEV charging pattern when charging threshold is limited to 8 cents per kWh or below.

While limited in sample size, these charge control scenarios demonstrate that charging can be limited by several parameters, but non-charging energy use still occurs due to various factors including lost communications, charging controller energy use, onboard diagnostics, and cooling.

PHEV MPG Reporting

PHEV mpg reporting can be difficult due to the many different ways PHEVs operate and the many significant impacts on mpg results such as drivers, charge frequency, auxiliary use, and environmental impacts. The AVTA report *Plug-in Hybrid Electric Fuel Use Reporting Methods and Results Report* discusses these impacts and provides sample results in detail. The report can be found at:

http://avt.inl.gov/pdf/phev/phev_mpg_report_july09.pdf

Conclusions

The PHEV industry is still very much in its infancy, with approximately 650 light-duty PHEVs deployed in North America as of the end of FY 2009. Total independent test miles on any single PHEV battery pack are still rather limited as is the number of PHEV models to choose from. With the exception of very few PHEVs from OEMS in very restricted fleets, PHEVs from conversion companies have made up the bulk of the vehicles in use to date.

In spite of the limited number of test vehicles (PHEVs represent about 0.0003% of all light-duty vehicles in the United States), initial testing of PHEVs suggests that the technology has great potential for reducing petroleum consumption.

The current cost to convert an HEV to a PHEV ranges from \$10,000 to \$40,000 per vehicle, plus the base cost of the HEV and long-term battery life is unknown. Therefore, on an economic basis, the current cost to the vehicle operator to reduce petroleum consumption with PHEVs is considerable. However, the future incremental cost to convert HEVs to PHEVs, and the cost of ground-built PHEVs from OEMs, are unknown. It is anticipated that future incremental costs will be significantly lower. There have been some price announcements from OEMs and claimed OEMs, but these could not be independently confirmed as FY 2009 ended.

There is also discussion about PHEVs being able to provide electricity back to the electric grid during periods of peak demand. However, the current group of PHEVs is using 110-volt connectors for recharging from the grid, so this concept may remain theoretical at least for the near future due to

limits in the amount of electric energy that can be transferred quickly. Another limiting factor may be battery life, as it is currently unknown what PHEV battery cycle life will be in real world use. Additionally, any sending of electricity back to the grid would further reduce battery life available for electric drive propulsion.

The eventual control systems that future PHEVs will use both for the batteries and propulsion are also unknown. Some in this infant PHEV industry support all-electric ranges, while others support greater use of additional electric assist that will theoretically help maximize battery life. Regardless of these uncertainties, the PHEVs currently in operation have demonstrated the significant potential of PHEVs to reduce the use of petroleum for personnel transportation.

Future Activities

AVTA will continue to test new PHEV models as they become available, as well as previously tested PHEV models that undergo modifications such as new battery designs or chemistries that are believed to provide significant performance enhancements.

PHEV use patterns, and PHEV charging patterns and demands, will continue to be documented in the effort to increase the testing sample size. This will aid in better understanding of charging demands, infrastructure requirements, and costs at the distribution (e.g., building and neighborhood), transmission, and generation levels.

Consideration is being given to testing additional PHEVs in various modes of operation and battery state-of-charge. This will help determine battery life and vehicle performance (1) if the vehicle is charged in scenarios such as every other day, or less often; (2) if the battery is continuously discharged and then charged from 50%, 20% or some other SOC; or (3) if the vehicle is continuously operated at very low SOC and rarely charged. These and other operational modes will be considered for additional testing to examine vehicle and battery performance and life.

Developing additional PHEV testing partnerships will be pursued that support the objectives of testing PHEVs in diverse geographic and electric generation regions. This will support a greater understanding

of vehicle and battery maintenance needs, functionality, operational life, and life-cycle costs. For instance, cold ambient temperatures have been identified as having negative mpg impacts, so the Finnish Government's offer to provide the AVTA with data for their Hymotion Prius at no cost was readily accepted.

Above all else, the AVTA will strive to continue to test PHEVs in a highly leveraged manner in order to accumulate test miles at the lowest cost possible both to DOE and the taxpayer in a technology- and fuel-neutral manner.

Publications

Previous annual reports have identified AVTA's baseline performance testing procedures, vehicle specifications, and pre-FY 2009 reports. All of these documents can be found at: <http://avt.inel.gov/hev.shtml> and http://www.eere.energy.gov/vehiclesandfuels/avta/light_duty/hev/hev_reports.shtml. The PHEV reports published and formal presentations that occurred during FY 2009 are listed below.

1. 2007 Hymotion Escape Accelerated Testing Results – Jan 2009 fact sheet.
<http://avt.inel.gov/pdf/phev/HymotionEscapeAccelTestingResultsReport.pdf>.
2. 2007 Electrovaya Plug-in Hybrid baseline performance fact sheet.
<http://avt.inel.gov/pdf/phev/ElectrovayaEscapeFactSheet.pdf>.
3. 2007 Electrovaya Escape PHEV Accelerated Testing Results – Feb. 2009 fact sheet.
<http://avt.inel.gov/pdf/phev/ElectrovayaEscapeAccelTestingResults.pdf>.
4. M.G. Shirk. September 2009. *Advanced Vehicle Testing Activity (AVTA): PHEV Controlled Charging Demonstration Activities*. Seattle PHEV Stakeholder Meeting. INL/MIS-09-16764.
5. R. Carlson, et al. September 2009. *PHEV Testing and Demonstration Activities Conducted by the U.S. Department of Energy's AVTA – Impact of Extreme Temperature on PHEV Battery Performance*. INL/CON-09-16628.

- PHEV '09 Conference Montreal. Montreal, QC, Canada.
6. J. Gondor, J. Smart, R. Carlson. September 2009. *Deriving In-Use PHEV Fuel Economy Predictions from Standardized Test Cycle Results*. INL/CON-09-16292. IEEE Vehicle Power and Propulsion Conference (VPPC'09). Dearborn, MI.
 7. R. Carlson, et al. July 2009. *The Effect of Driving Intensity and Incomplete Charging on the Fuel Economy of a Hymotion Prius PHEV*. INL/EXT-09-16503. Idaho National Laboratory. Idaho Falls, ID.
 8. H. Iu, J. Smart. May 13-16, 2009. *Determining PHEV Performance Potential – User and Environmental Influences on A123 Systems' Hymotion™ Plug-In Conversion Module for the Toyota Prius*. INL/CON-08-14430. Electric Vehicle Symposium 24. Stavanger, Norway.
 9. M. Duoba, R. Carlson, F. Jehlik, J. Smart, S. White. May 13-16, 2009. *Correlating Dynamometer Testing to In-Use Fleet Results of Plug-In Hybrid Electric Vehicles*. INL/CON-08-15021. Electric Vehicle Symposium 24. Stavanger, Norway.
 10. J. Smart, J. Francfort, D. Karner, M. Kirkpatrick, S. White. May 13-16, 2009. *U.S. Department of Energy – Advanced Vehicle Testing Activity: Plug-in Hybrid Electric Vehicle Testing and Demonstration Activities*. INL/CON-08-14333. Electric Vehicle Symposium 24. Stavanger, Norway.
 11. H. Iu, J. Smart. April 22, 2009. *Report on the Field Performance of A123 Systems' Hymotion™ Plug-In Conversion Module for the Toyota Prius*. INL/CON-08-14430. Society of Automotive Engineers 2009 World Congress. Detroit, MI.
 12. J. Smart. Mar 3, 2009. *Alternative Energy Vehicles*. INL/MIS-09-15524. Taylorview Junior High School Career Fair. Idaho Falls, ID.
 13. J. Smart, D. Lewis. Jan 17, 2009. *Driving a Car: It Takes Energy*. INL/MIS-09-15282 .
 - Museum of Idaho Discovery Day. Idaho Falls, ID.
 14. J. Smart. Nov 6, 2008. INL/CON-08-15046. *US Department of Energy and Idaho National Laboratory PHEV Activity Overview*. Ohio Rural Electric Cooperatives 2008 Fall Marketing, Member Services and Communication Conference. Columbus, OH.
 15. J. Francfort, R. Carlson, M. Kirkpatrick, M. Shirk, J. Smart, and S. White. July 2009. *Plug-in Hybrid Electric Vehicle Fuel Use Reporting Methods and Results*. INL/EXT-09-16343. Idaho National Laboratory. Idaho Falls, Idaho.
 16. J. Francfort. *Virginia EV Road Show – PHEV Operations and Performance*. Virginia Clean Cities and Hampton Roads Clean Cities Coalition. Newport, VA. August 2009. INL/CON-09-16608.
 17. J. Francfort. *Plug-In 2009: PHEV Testing and Demonstration Activities Conducted by the U.S. Department of Energy's AVTA*. Plug-in 2009. Long Beach, CA. August 2009. INL/CON-09-16431.
 18. J. Francfort. *PNWER - AVTA/INL PHEV Testing and Demonstration Activities in North America*. Pacific Northwest Economic Region – 19th Annual Summit. Boise, ID. July 2009. INL/CON-09-16384.
 19. J. Francfort. *Clean Cities Peer Exchange (PA) – DOE/AVTA's HEV, NEV, and PHEV Testing Results and Resources*. Clean Cities Eastern States Coordinator. Pittsburgh, PA. June 2009. INL/CON-09-16262.
 20. J. Francfort. *Advanced Vehicle Testing Activity (AVTA) – Vehicle Testing and Demonstration Activities*. DOE Merit Review. Crystal City, Virginia. May 2009. INL/CON-09-15561.
 21. J. Francfort. *Advanced Vehicle Testing Activity (AVTA): North America PHEV Testing and Demonstrations*. Local Climate Leadership. May 2009. INL/CON-09-15989.
 22. J. Francfort. *Plug-in Hybrid Electric Vehicles (PHEVs) – for Clean Cities*. Clean cities

- Coalition Webcast. Idaho Falls, ID. April 2009. INL/CON-09-15728.
23. J. Francfort. *Advanced Vehicle Testing Activity (AVTA) - North American and Seattle PHEV Testing and Demonstrations*. Seattle Area Chamber of Commerce. Seattle, WA. March 2009. INL/CON-09-15561.
24. J. Francfort. *PHEV Testing and Demonstrations*. NAFA At the Portland International Auto Show. Portland, OR. February 2009. INL/CON-09-15356.
25. J. Francfort. *British Columbia PHEV Demonstration Workshop – AVTA’s PHEV Testing and Demonstration Activities*. Vancouver, Canada. October 2008. INL/MIS-08-14927.
26. J. Francfort. *EPRI – IWC – AVTA’s PHEV Testing and Demonstration Activities. Electric Power Research Institute Working Council – Plug-in Hybrid Electric Vehicle Working Group*. Atlanta, Georgia. October 2008. INL/CON-08-14887.
27. J. Francfort. *PowerUp! Summit – AVTA North America and Washington State PHEV Testing Results*. 2009 PowerUp! Summit. Wenatchee, Washington. May 2009. INL/CON-09-16044.
28. J. Francfort. *Austin Energy AltCar Expo - AVTA’s PHEV Testing and Demonstration Activities*. Austin Energy AltCar Expo & Conference. Austin, Texas. October 2008. INL/CON-08-14944.

B. Hybrid Electric Vehicle Testing

James Francfort (Principal Investigator), Timothy Murphy (Project Leader)

Idaho National Laboratory

P.O. Box 1625

Idaho Falls, ID 83415-2209

(208) 526-6787; james.francfort@inl.gov

DOE Program Manager: Lee Slezak

(202) 586-2335; Lee.Slezak@ee.doe.gov

Objective

Benchmark hybrid electric vehicle (HEV) fuel use, component performance, maintenance requirements, and life-cycle costs.

Provide HEV testing results to vehicle modelers and technology target setters.

Reduce the uncertainties about HEV battery and vehicle life.

Approach

Perform baseline performance and accelerated testing on 18 HEV models and 47 HEVs to date.

Operate at least two of each HEV model over 36 months to accumulate 160,000 miles per vehicle in fleets to obtain fuel economy, maintenance, operations, and other life cycle related vehicle data under actual road conditions.

Test HEV batteries when new and at 160,000 miles.

Accomplishments

Accelerated testing for the HEV fleet, consisting of 47 HEVs and 18 models, exhibited varying fuel economies that ranged from 17.9 mpg for the Chevrolet Silverado to 46.0 mpg for the Gen III 2010 Toyota Prius.

Three additional PHEVs (Gen III Prius, Ford Fusion, and Gen II Honda Insight) were baseline performance tested during fiscal year (FY) 2009, and testing started on a fourth model (Mercedes S400) during FY 2009.

Demonstrated the average decrease in HEV mpg from auxiliary loads (air conditioning) of 21.5%, a range of decreases from 8 to 28.4% by HEV model.

As of September 2009, 4.7 million HEV test miles have been accumulated.

Provided HEV testing results to the automotive industry, the U.S. Department of Energy (DOE), and other national laboratories via the DOE Vehicle Technologies Program's Vehicle Simulation and Analysis Technical Team.

Shared used HEV power electronics parts with the Oak Ridge National Laboratory (ORNL) for their power electronics testing, and made an HEV available to another DOE laboratory for cabin temperature testing.

Provided used HEVs to the Environmental Protection Agency (EPA) for their HEV life cycle testing.

Future Activities

Benchmark new HEVs available during FY 2010, including new HEVs with advanced batteries.

Ascertain HEV battery life by accelerated testing at the end of 160,000 miles.

Continue testing coordination with industry and other DOE entities.

Introduction

Today's light-duty HEVs use a gasoline internal combustion engine (ICE), electric traction motors or electric stop-start technology, along with approximately 1 kWh of onboard energy storage (the battery) to increase petroleum efficiency as measured by higher mpg results compared to comparable vehicle models. HEVs are never connected to the grid for charging the battery. The HEV batteries are charged by an onboard the vehicle ICE-powered generator, as well as by regenerative braking systems.

Sixteen of the eighteen HEV models being tested to date by AVTA use nickel metal hybrid (NiMH) battery chemistries as the onboard HEV battery. Only one HEV model, the 2004 Chevrolet Silverado, uses a lead acid battery, and the new Mercedes Benz S400 uses a lithium-ion battery. It has been anticipated that future HEVs would use lithium battery technologies. However, a recent press release from the Advanced Lead Acid Battery Consortium (ALABC) stated that Mazda will use Panasonic lead acid batteries in their future stop/start HEVs.

In addition to providing benchmark data to modelers and technology target setters, AVTA benchmarks and tests HEVs to compare the advantages and disadvantages of each technology, and also provides testing results to the public and fleet managers.

Approach

As of the end of FY 2009, AVTA has performed, or is performing, accelerated and fleet testing on 47 HEVs, comprised of 18 HEV models. The HEV models and number of each model tested are listed below:

- Generation (Gen) I Toyota Prius - 6
- Gen II Toyota Prius - 2
- Gen I Honda Insight - 6
- Honda Accord - 2

- Chevrolet Silverado - 2
- Gen I Honda Civic - 4
- Gen II Honda Civic - 2
- Ford Escape - 2
- Lexus RX400h - 3
- Toyota Highlander - 2
- Toyota Camry - 2
- Saturn Vue - 2
- Nissan Altima - 2
- Chevrolet Tahoe - 2
- Gen II Honda Insight - 2
- Gen III Toyota Prius - 2
- Ford Fusion - 2
- Mercedes S400 - 2.

Baseline performance testing has been completed on 17 of HEV models, with the Mercedes S400 testing just starting as FY 2009 ended. Note that the difference between fleet and accelerated testing is that some vehicles are placed in fleet operations without a deliberate effort to place maximum miles on a vehicle (fleet testing). While in HEV accelerated testing, two of each HEV model will each accumulate 160,000 on-road miles in approximately 36 months by being placed in a bank courier fleet in Arizona.

All testing has been completed on the following HEV models:

- Generation (Gen) I Toyota Prius
- Gen II Toyota Prius
- Gen I Honda Insight
- Honda Accord
- Gen I Honda Civic
- Ford Escape
- Lexus RX400h
- Chevrolet Silverado

- Toyota Highlander
- Toyota Camry
- Gen II Honda Civic
- Nissan Altima.

Results

As of the end of FY 2008, the 47 HEVs had accumulated 4.7 million total accelerated and fleet test miles (Figure 1). During FY 2009, the HEVs accumulated a total of 557,000 miles, averaging 46,000 test miles per month (Figure 2). The average fuel use per HEV model ranged from 17.9 mpg for the Silverado to 46.0 mpg for the Gen III Prius (Figure 3).

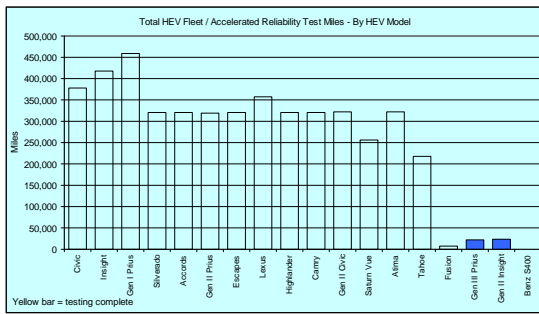


Figure 1. Total HEV test miles by vehicle model.

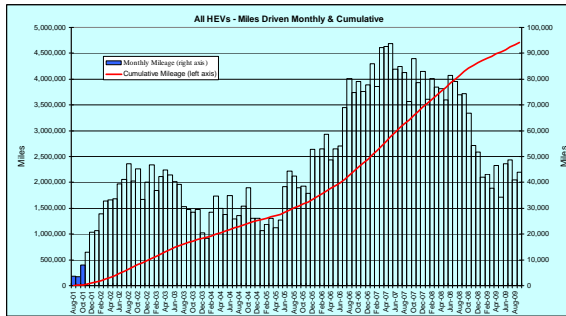


Figure 2. Monthly HEV test mile accumulation during fleet and accelerated testing. The graph runs from August 2001 until September 2008. (Note that September 2009 is graphed but the label does not appear).

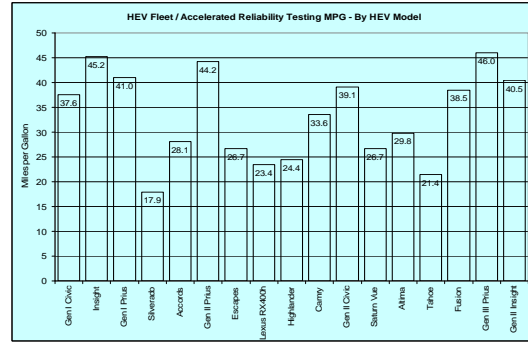


Figure 3. HEV fuel economy (mpg) test results for each HEV model in fleet and accelerated testing.

All of the HEVs in use to date have exhibited reductions in fuel economy results due to auxiliary loads such as air conditioning. The impact from using the air conditioning is most evident from the baseline performance testing results (Figure 4), when the average HEV mpg results decreases 9 mpg when the air conditioning is on during dynamometer testing. In terms of mpg, the negative air conditioning impact varies from 2.8 mpg for the Silverado to 15.0 mpg for the Gen III Prius and 15.8 for the Gen II Civic. In terms of percentage impacts, the air conditioning impact varies from 8.0% for the Vue to 28.4% for the Gen II Civic, with an average negative impact of 21.5% (Figure 5). Note that the baseline performance testing was just starting for the Mercedes S400 as FY 2009 ended. The results for the Ford Fusion were still undergoing the quality assurance process and were unavailable at the time of this report.

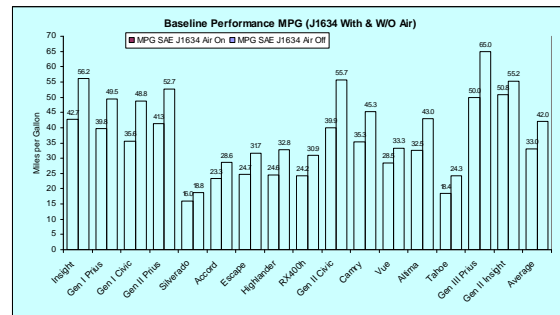


Figure 4. Baseline performance fuel economy test results for SAE J1634 drive cycle testing with the air conditioning on and off.

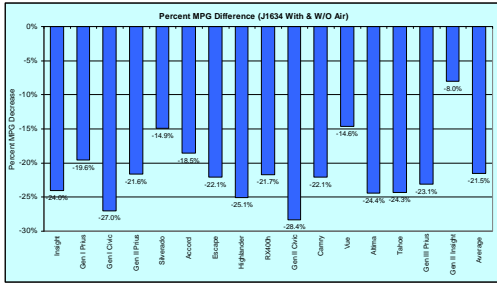


Figure 5. Percentage decrease in baseline performance fuel economy test results for SAE J1634 drive cycle testing when the air conditioning is turned on during the testing.

In addition to the HEV fuel economy and total test miles data being collected, all maintenance and repair event data (including the event costs, whether the event was covered under warranty, dates, and vehicle miles when an event occurred) is collected to compile lifecycle vehicle costs. This data is presented on AVTA's Web pages as both a maintenance fact sheet (Figure 6) and an HEV fact sheet, which includes miles driven, fuel economy, mission, and lifecycle costs on a per-mile basis (Figure 7).

AVTA posted 16 HEV battery test reports during FY 2009 and these can be found at <http://avt.inl.gov/hev.shtml>. In addition to information on the HPPC and Static Capacity testing, the most recent battery test reports (Figures 8 through 13) include the following graphed information:

- Voltage versus Energy Discharged
- Charge Pulse Resistance versus Energy Discharged
- Charge Pulse Power versus Energy Discharged
- Discharge Pulse Resistance versus Energy Discharged
- Discharge Pulse Power versus Energy Discharged
- Peak Power Values with DOE Performance Goals
- Useable Energy.

U.S. DEPARTMENT OF ENERGY | Energy Efficiency & Renewable Energy

HEV Fleet Testing

Advanced Vehicle Testing Activity

Maintenance Sheet for 2008 Chevrolet Tahoe

VIN # 1GNFC13518R207400

Date	Mileage	Description	Cost
7/31/2008	7,363	Changed oil and filter and rotated tires	\$20.30
8/22/2008		Purchased spare tire	\$362.43
10/14/2008	22,316	Changed oil and filter	\$31.28
11/6/2008	28,888	Changed oil and filter	\$15.74
11/25/2008	34,005	Changed oil and filter and rotated tires	\$32.54
1/21/2009	47,076	Changed oil and filter and rotated tires	\$51.54
2/4/2009	53,168	Changed oil and replaced air filters	\$61.07
3/5/2009	58,420	Changed oil and filter and replaced, balanced and aligned two tires	\$688.60
4/14/2009	66,807	Changed oil and filter	\$33.45
5/16/2009	73,322	Changed oil and filter and rotated tires	\$33.45
6/1/2009	82,050	Changed oil and filter	\$36.95
6/8/2009	83,624	Replaced and balanced two tires	\$459.16
6/24/2009	88,682	Changed oil and filter and inspected brake system	\$30.80
8/6/2009	98,691	Changed oil and filter and replaced front struts and shocks	\$597.25
8/19/2009	106,352	Changed oil and filter and inspected brake system	\$32.53
8/24/2009	107,159	Evaluated A/C system (leak detected), replaced A/C compressor and accumulator	\$1877.56
9/3/2009	107,159	Replaced 12 volt battery	\$117.62

eere.energy.gov

Figure 6. Actual Toyota Camry maintenance sheet is provided as an example of a HEV maintenance sheet.

FREEDOMCAR & VEHICLE TECHNOLOGIES PROGRAM

**HEV Fleet Testing
Advanced Vehicle Testing Activities**



**2005
Honda Accord**
VIN #
JHMCN36495C000657

A Strong Energy Portfolio for a Strong America
Energy efficiency and clean, renewable energy will mean a stronger economy, a cleaner environment, and greater energy independence for America. Working with a wide array of state, community, industry, and university partners, the U.S. Department of Energy's Office of Energy Efficiency and Renewable Energy invests in a diverse portfolio of energy technologies.

Fleet Performance

Description:
This vehicle is operated throughout the valley of Phoenix, Arizona by JP Morgan Chase Bank of Arizona's courier fleet. It is operated six days a week, transferring documents between branches and a central processing center on city streets and urban freeways as well as intrastate courier routes.

Major Operations & Maintenance Events:
Repaired electrical door lock @ 79,722
Cost: \$321.17

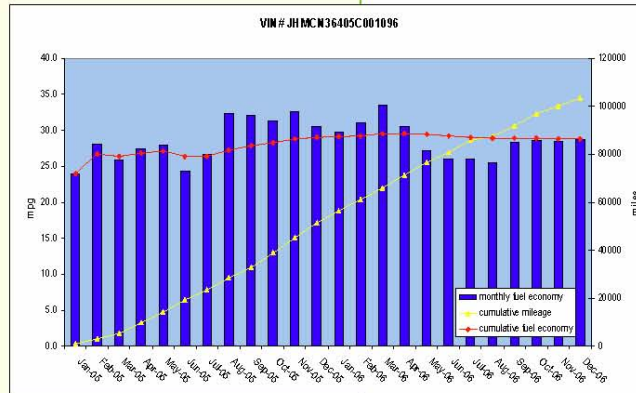
Operating Cost:
Purchase Cost: \$32,945 (12/04)*
Kelly Used Vehicle Price: \$16,935 (1/07)
Sale Price: In Operation
Maintenance Cost: \$0.038/mile
Operating Cost: \$0.13/mile
Total Ownership Cost: \$0.32/mile

Operating Performance:
Total miles driven: 103,646
Cumulative MPG: 29.5

Vehicle Specifications

Engine: I-VTEC V6
Electric Motor: 11.9 kW
Battery: Nickel metal hydride
Seatbelt Positions: Five
Payload: 952 lbs
Features: Front wheel drive, regenerative braking

See HEVAmerica Baseline Performance Fact Sheet for more information.



For more information contact:
EERE Information Center
1-877-EERE-INF (1-877-337-3463)
www.eere.energy.gov

* Purchase includes dealer price with options plus taxes. It does not include title, license, registration, extended warranty or delivery fee costs. Gas figured at \$2.45/gallon.



Figure 7. Actual Honda Civic fact sheet is provided as an example of a HEV fact sheet.



U.S. Department of Energy
Energy Efficiency and Renewable Energy
Bringing you a prosperous future where energy is clean, abundant, reliable, and affordable

2010 Ford Fusion-4699 Hybrid BOT Battery Test Results



Hybrid System Specifications

<u>Battery Specifications</u>	<u>Vehicle Specifications</u>
Manufacturer: Sanyo Type: Nickel-Metal Hydride Number of Modules: 204 Nominal Module Voltage: 1.35 V Nominal System Voltage: 275 V Nominal Pack Capacity: 5.5 Ah	Manufacturer: Ford Model: Fusion Year: 2010 Number of Motors ¹ : 1 Motor Power Rating ² : 60 kW VIN #: 3FADP0L32AR194699

Battery Lab Test Results

<u>HPPC Test</u> Peak Pulse Discharge Power @ 10s ³ : 22.4 kW Peak Pulse Discharge Power @ 1s ³ : 34.1 kW Peak Pulse Charge Power @ 10s ³ : 17.3 kW Peak Pulse Charge Power @ 1s ³ : 28.0 kW Maximum Cell Charge Voltage: 1.5 V Minimum Cell Discharge Voltage: 1.0 V	<u>Static Capacity Test</u> Measured Average Capacity: 5.29 Ah Measured Average Energy Capacity: 1,370 Wh <u>Vehicle Mileage and Testing Date</u> Vehicle Odometer: 272 mi Date of Test: September 2, 2009
---	---

Analysis Notes:

1. Motor refers to any motor capable of supplying traction power.
2. Motor power rating refers to the manufacturer's peak power rating for the motor(s) supplying traction power.
3. Calculated value based on selected battery voltage limits and at 50% SOC.

Page 1

Figure 8. Page 1 of the Ford Fusion HEV being-of-life (BOF) HEV battery test report.

Test Results

Test results for the beginning-of-testing battery testing are provided herein. Battery test results include those from the Static Capacity Test and the Hybrid Pulse Power Characterization (HPPC) Test¹.

Static Capacity Test Results

Static capacity test results are summarized in the fact sheet. The test was performed on September 2, 2009 with a vehicle odometer reading of 272 miles. The measured average C/1-rate capacity was 5.29 Ah compared with the manufacturer's rated capacity of 5.5 Ah. The measured average energy capacity was 1,370 Wh.

Figure 1 is a graph of battery voltage versus energy discharged. This graph illustrates the voltage values during the constant current discharge versus the cumulative energy discharged from the battery at a C/1 discharge rate.

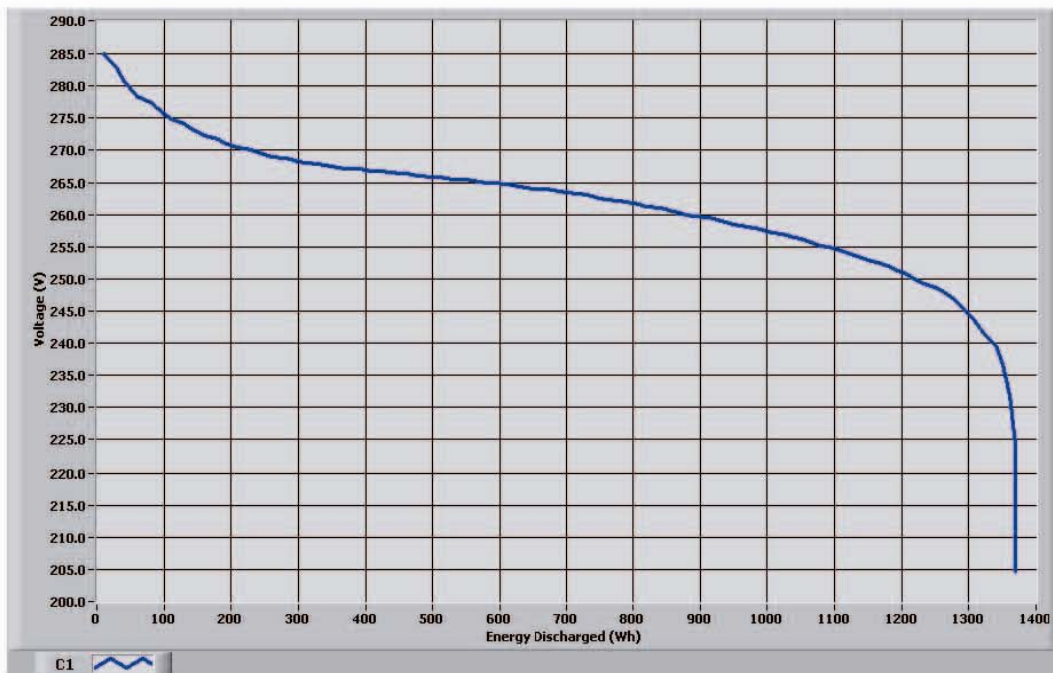


Figure 1
Voltage vs. Energy Discharged

1. Static Capacity and Hybrid Pulse Power Characterization test procedures were performed in accordance with FreedomCAR Battery Test Manual for Power-Assist Hybrid Vehicles, DOE/ID-11069, October 2003 procedures 3.2 and 3.3 respectively.

Figure 9. Page 2 of the Ford Fusion HEV being-of-life (BOF) HEV battery test report.

HPPC Test Results

HPPC test results are summarized in the fact sheet. The peak pulse discharge power at 10 seconds and 1 second into the pulse are 22.4 kW and 34.1 kW at 50% SOC respectively. The peak pulse charge power at 10 seconds and 1 second into the pulse are 17.3 kW and 28.0 kW at 50% SOC respectively. The maximum and minimum cell voltages used for this analysis were 1.5 V and 1.0 V respectively.

Figures 2 and 4 illustrate the battery's charge and discharge pulse resistance graphs which show internal resistance at various depths of discharge. Each curve represents the resistance at the end of the specified pulse interval.

Figures 3 and 5 illustrate the battery's charge and discharge pulse power graphs which show the useable power at various depths of discharge. Each curve represents the pulse power at the end of the specified pulse interval at the cell voltage limits.

Figure 6 is a plot of the battery's HPPC 10 second pulse power as a function of state of charge. The graph shows the power values over the range of state of charge as well as the DOE target performance goals of 25 kW discharge power and 20 kW regenerative power for a hybrid minimum power assist battery. The battery did not meet the DOE power performance goals for any battery state of charge range at the time of testing.

Figure 7 is a plot of the battery's useable energy² as a function of power. The x-axis indicates a desired discharge or charge power level and the y-axis indicates the useable energy at that power. The dashed horizontal line shows the DOE Minimum Power Assist HEV energy performance goal of 300 Wh. The dashed vertical line shows the DOE Minimum Power Assist power performance goal of 25 kW. The Focus battery's useable energy curve falls above and to the left of the intersection of the DOE energy and power performance goals. The maximum power that can be delivered while meeting the DOE energy performance goal is 20.8 kW at 300 Wh. The battery does not meet the DOE power performance goal for any calculated energy value. This indicates that at the time of testing, the Focus battery performance was below the DOE performance goals.

These tests were performed for DOE's Advanced Vehicle Testing Activity (AVTA). The AVTA, part of DOE's Vehicle Technology Program, is conducted by the Idaho National Laboratory and Electric Transportation Engineering Corporation.

2. The plot of the battery's useable energy was generated with the point for 80% SOC on both charge and discharge power being excluded as an outlier to the trend of the rest of the data. Including this point would cause non-linearity and make further analysis impossible.

Figure 10. Page 3 of the Ford Fusion HEV being-of-life (BOF) HEV battery test report.

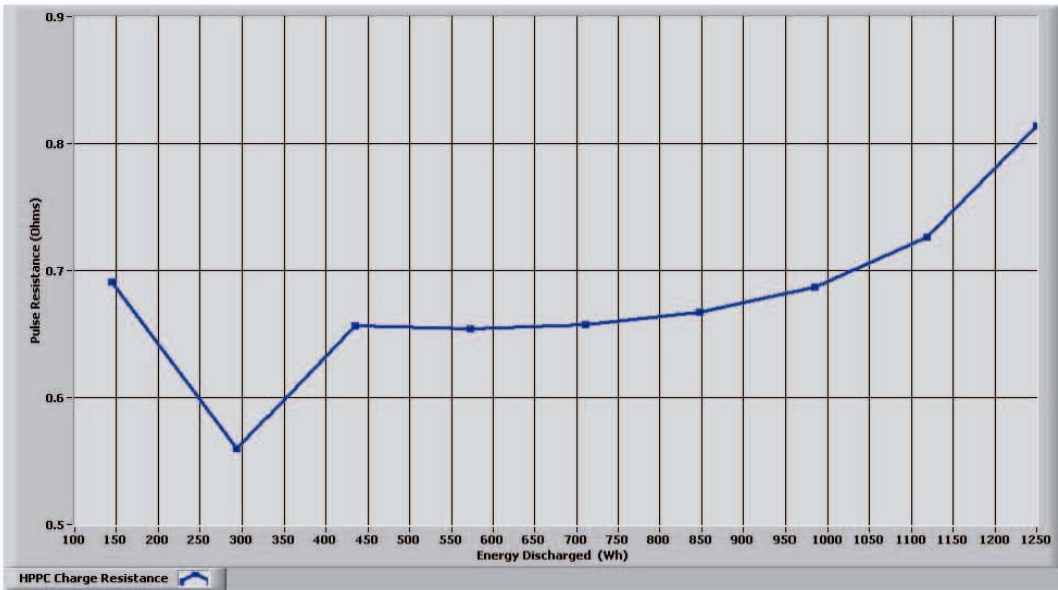


Figure 2
Charge Pulse Resistance vs. Energy Discharged

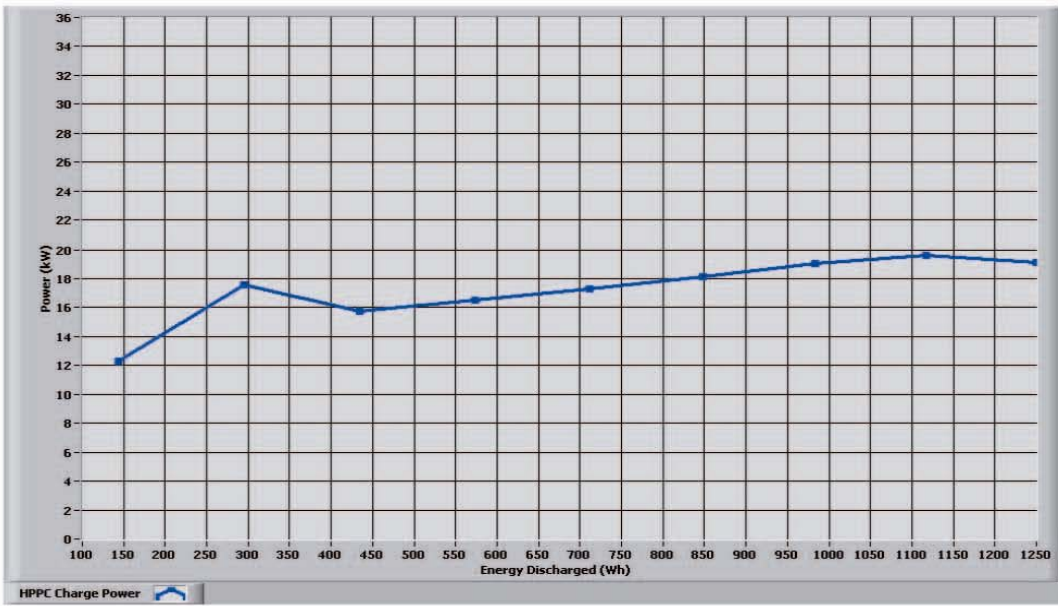


Figure 3
Charge Pulse Power vs. Energy Discharged

Figure 11. Page 4 of the Ford Fusion HEV being-of-life (BOF) HEV battery test report.

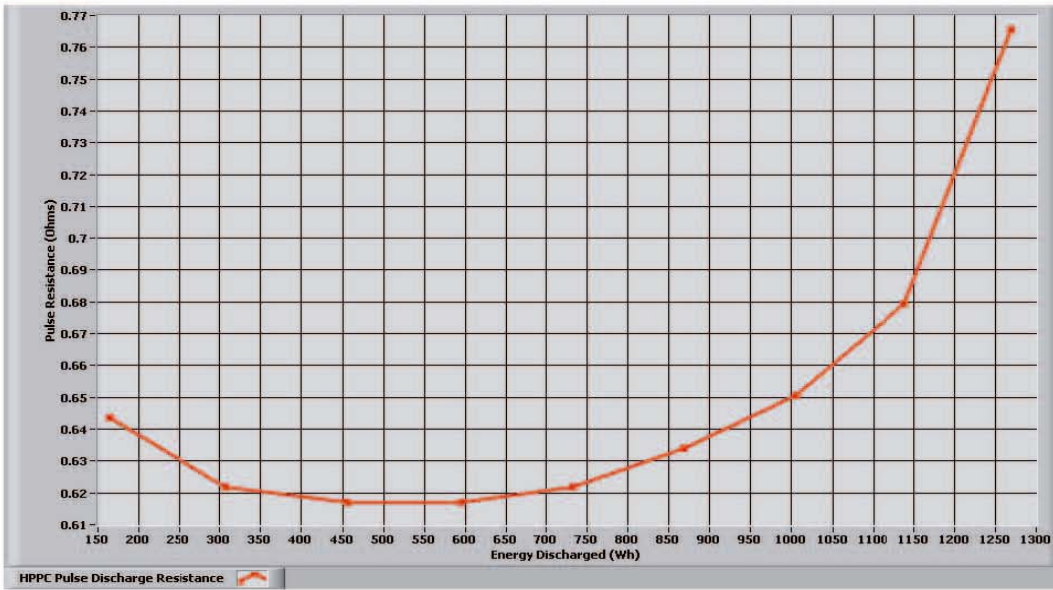


Figure 4
Discharge Pulse Resistance vs. Energy Discharged

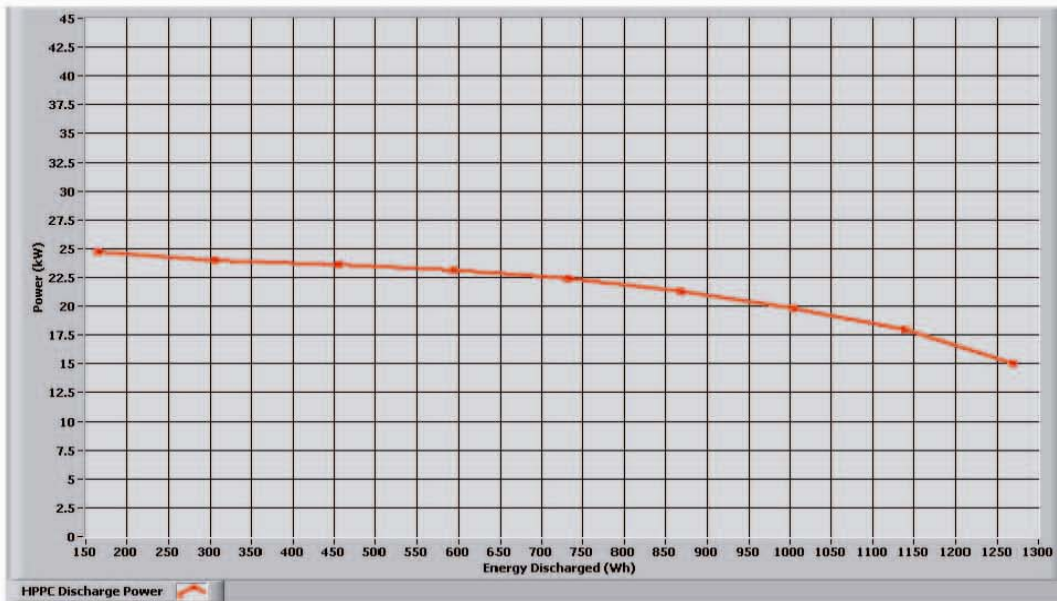


Figure 5
Discharge Pulse Power vs. Energy Discharged

Figure 12. Page 5 of the Ford Fusion HEV being-of-life (BOF) HEV battery test report.

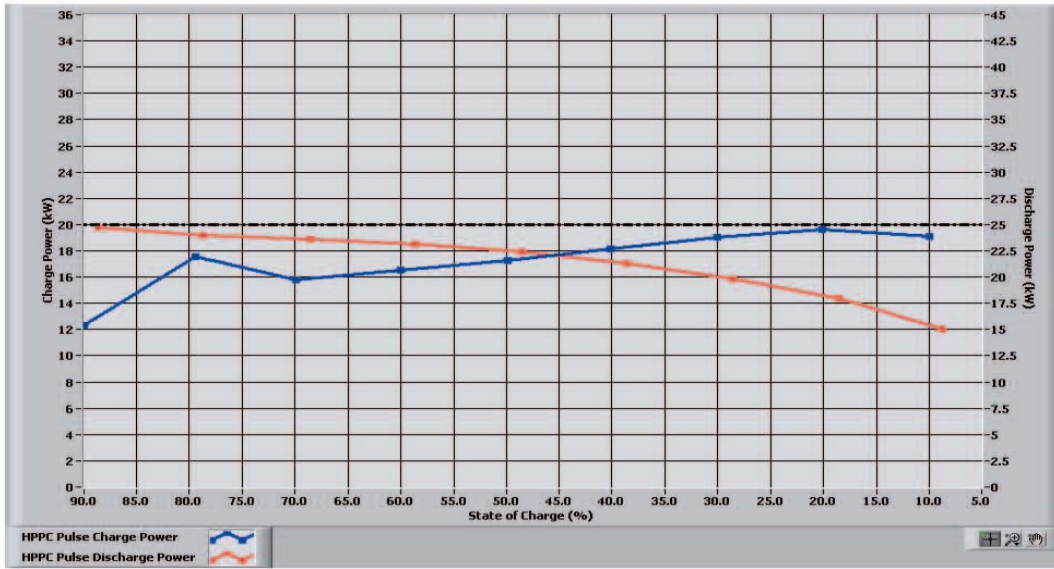


Figure 6
Peak Power Values with DOE Performance Goals

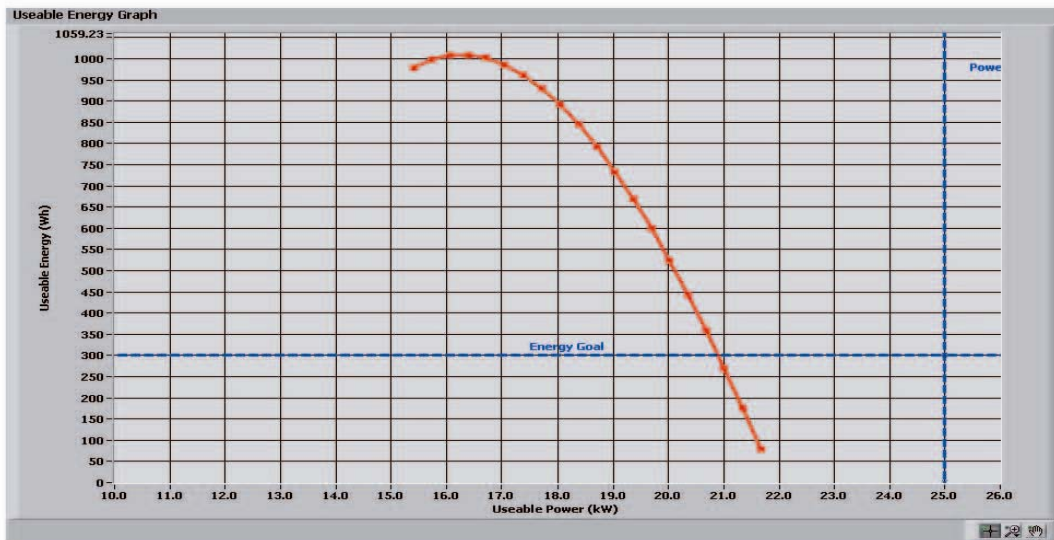


Figure 7
Useable Energy

Figure 13. Page 6 of the Ford Fusion HEV being-of-life (BOF) HEV battery test report.

Conclusions

The single largest negative impact on fuel economy (mpg) is from the use of the air conditioning—when all of the HEV models are operated with the air conditioning on during warm months.

The HEV battery packs generally appear to be robust from an economic viewpoint. As of the end of FY 2009 and 4.7 million test miles, there were five NiMH traction battery failures, but all were covered under warranty by the two OEMs involved.

One OEM's NiMH HEV battery pack failure was due to a battery controller failure at 75,000 miles. This should not be attributed as a pack failure, as the battery controller completely and fatally discharged the HEV battery pack. The same OEM's second NiMH pack failed at 147,000 miles and was again replaced under warranty.

The second OEM had two NiMH pack failures on a single vehicle at 22,000 and 56,000 miles, before this HEV test vehicle was totaled in a crash at 103,000 miles. In addition, the same OEM's other HEV NiMH battery pack also failed in the second test HEV at 90,000 miles. There appears to be a problem with this HEV battery, as all have failed between 22,000 and 90,000 vehicle miles. Both of these vehicles represent the same HEV model from the second OEM.

Excluding the three pack failures from this one HEV model, there was only a single high-mileage HEV battery pack failure out of 4.7 million test miles which suggests that most of the NiMH HEV batteries are very robust.

AVTA has partnered with private fleets to conduct the high mileage HEV testing. All 4.7 million HEV test miles have been accumulated with no driver costs to DOE. In addition, several of the HEV models get secondary test value after completing the 160,000 miles of HEV testing. ORNL uses many of the HEV power electronics subsystems for end-of-life testing and the EPA has also taken several HEVs at AVTA testing completion so they can conduct their own end-of-life testing to support their HEV life-cycle models.

Future Activities

New HEVs available from U.S., Japanese, and European manufacturers will be benchmarked during FY 2010. These will introduce advanced technologies such as lithium or advanced lead acid designs. Most new HEVs will be tested to reduce uncertainties about HEV technologies, especially the life and performance of their batteries, and any other onboard energy storage systems. The first example of this is the testing of the Mercedes S400, which in addition to being the first HEV from Europe available in the U.S., is the first HEV from anywhere with a lithium-ion HEV battery pack.

Publications

Approximately 125 HEV baseline performance, fleet, and accelerated testing fact and maintenance sheets, reports, and presentations have been generated by AVTA and all are available on the AVTA's Web pages. The HEV baseline performance testing procedures and vehicle specifications were also updated and republished on the AVTA's Web pages. New HEV reports and papers published during FY 2009 are listed below.

In addition to the below testing fact sheets, reports, and papers, the maintenance requirements and fuel use fact sheets are generated every three months for all of the HEVs. All of these documents can be found at: <http://avt.inl.gov/hev.shtml> and http://www.eere.energy.gov/vehiclesandfuels/avta/light_duty/hev/hev_reports.shtml.

The below reports were completed and posted during FY 2009. Note that some of the reports are for battery testing when the vehicles were new and some are for the battery testing that occurs at 160,000 miles.

1. 2010 Toyota Prius Gen III VIN 0464 New Battery Testing Fact Sheet
<http://avt.inl.gov/pdf/hev/batterygenIIIprius0462.pdf>
2. 2010 Toyota Prius Gen III VIN 6063 New Battery Testing Fact Sheet
<http://avt.inl.gov/pdf/hev/batterygenIIIprius6063.pdf>
3. 2010 Ford Fusion VIN 4699 New Battery Testing Fact Sheet
<http://avt.inl.gov/pdf/hev/batteryfusion4699.pdf>

4. 2010 Ford Fusion VIN 4757 New Battery Testing Fact Sheet
<http://avt.inl.gov/pdf/hev/batteryfusion4757.pdf>
5. 2010 Honda Insight VIN 0141 New Battery Testing Fact Sheet
<http://avt.inl.gov/pdf/hev/batteryinsight0141.pdf>
6. 2010 Honda Insight VIN 1748 New Battery Testing Fact Sheet
<http://avt.inl.gov/pdf/hev/batteryinsight1748.pdf>
7. 2008 Chevrolet Tahoe VIN 7400 New Battery Testing Fact Sheet
<http://avt.inl.gov/pdf/hev/batterytahoe7400.pdf>
8. 2008 Chevrolet Tahoe VIN 5170 New Battery Testing Fact Sheet
<http://avt.inl.gov/pdf/hev/batterytahoe5170.pdf>
9. 2006 Honda Civic VIN 8725 160k-Mile Battery Testing Fact Sheet
<http://avt.inl.gov/pdf/hev/battery Civic8725.pdf>
10. 2006 Honda Civic VIN 9329 160k-Mile Battery Testing Fact Sheet
<http://avt.inl.gov/pdf/hev/battery Civic9329.pdf>
11. 2005 Ford Escape VIN 5881 160k-Mile Battery Testing Fact Sheet
<http://avt.inl.gov/pdf/hev/batteryescape5881.pdf>
12. 2005 Ford Escape VIN 8237 160k-Mile Battery Testing Fact Sheet
<http://avt.inl.gov/pdf/hev/batteryescape8237.pdf>
13. 2005 Honda Accord VIN 0657 160k-Mile Battery Testing Fact Sheet
<http://avt.inl.gov/pdf/hev/batteryaccord0657.pdf>
14. 2005 Honda Accord VIN 1096 160k-Mile Battery Testing Fact Sheet
<http://avt.inl.gov/pdf/hev/batteryaccord1096.pdf>
15. 2004 Toyota Prius VIN 1052 160k-Mile Battery Testing Fact Sheet
<http://avt.inl.gov/pdf/hev/battery Prius1052.pdf>
16. 2004 Toyota Prius VIN 2721 160k-Mile Battery Testing Fact Sheet
<http://avt.inl.gov/pdf/hev/battery Prius2721.pdf>

C. Hydrogen Internal Combustion Engine (ICE) Vehicle Testing

James Francfort (Principal Investigator), Timothy Murphy (Project Leader)

Idaho National Laboratory

P.O. Box 1625

Idaho Falls, ID 83415-2209

(208) 526-6787; james.francfort@inl.gov

DOE Program Manager: Lee Slezak

(202) 586-2335; Lee.Slezak@ee.doe.gov

Objectives

Assess the safety, and operating characteristics of 100% hydrogen fueled internal combustion engine (HICE) vehicles.

Identify any engine and vehicle system degradations when operating HICE vehicles on 100% hydrogen.

Perform independent testing on candidate 100% HICE vehicles.

Quantify vehicle use patterns and fuel use per mile for the HICE vehicles currently providing data to the Advanced Vehicle Testing Activity (AVTA).

Approach

Use the Integrated Waste Hydrogen Utilization Project (IWHUP) in Vancouver, British Columbia as a source of inexpensive high volume hydrogen to fuel eight 100% HICE pickups converted from natural gas fuel to 100% hydrogen fuel operations.

Four additional same model HICE pickups are operating in four U.S. states

AVTA collects, analyzes and reports the results from the data collected from the onboard data loggers on the twelve HICE pickups that are owned and operated by non-AVTA fleets.

Accomplishments

Fleet testing of the HICE vehicles has demonstrated no safety problems during vehicle fueling and operations as the vehicles demonstrated consistent, reliable behavior.

The vehicles averaged 13.2 miles per gasoline gallon equivalent (mpgge) after 55,000 miles of fleet operations.

This is a very low-cost data collection effort for the Department of Energy (DOE) as no AVTA funds are being used to purchase, fuel, maintain, and operate the vehicles.

Future Directions

Continue to document the operations of the twelve vehicles and fuel use, vehicle performance, and any effects hydrogen has on vehicle subsystems.

Continue to evaluate candidate test vehicles and when appropriate, perform baseline performance and fleet testing on them.

Introduction

In past fiscal years (FY), AVTA was very actively involved in monitoring the Arizona Public Service Alternative Fuel Pilot Plant and testing 100% HICE vehicles, as well as ICE vehicles operating on blends of hydrogen and compressed natural gas (CNG). Four different HICE vehicle models that operated only on 100% hydrogen fuel, plus three additional vehicle models that operated on 15 to 50% hydrogen blended with CNG, were subjected to baseline performance and emissions testing. In addition, a small fleet of approximately 15 ICE vehicles that accumulated 240,000 test miles while fueled on hydrogen/CNG blends were also tracked for fuel use and operations.

During FY 2009, AVTA hydrogen work was limited to tracking a group of 12 eTec/Roush Chevrolet Silverado pickups that were converted to operate on 100% hydrogen. It should be noted that no OEMs were involved in converting these vehicles to operate on hydrogen.

Approach and Results

Given the decreased interest in hydrogen, this vehicle technology has not been an area of major research for AVTA. However, AVTA has continued to collect data on the eight eTec/Roush pickups operating at IWHUP in Vancouver, BC, as well as the four same model pickups operating in four U.S. states. All vehicle costs, from purchase to fueling, operations, and maintenance are paid for by the fleets operating the vehicles. Therefore, this is a very low-cost testing activity for AVTA.

The twelve vehicles are all compressed natural gas Chevy Silverado base vehicles converted to operate on 100% hydrogen fuel. The vehicles are of a “crew cab” configuration, with six seat belt positions. All use three Dynetek carbon-fiber-wrap aluminum-lined tanks installed in the bed of the pickup (Figure 1) for onboard hydrogen storage. The nominal pressure is 5,000 psi (at 25°C) with a maximum pressure of 6,350 psi. The total fuel capacity for all three tanks is 10.5 gasoline gallon equivalents. In addition to the fuel tanks, other modifications included a supercharger, hydrogen fuel rails, hydrogen injectors, and significant engine mapping control testing and modifications.

As of June 2009, the twelve vehicles had been operated for 55,000 miles. Based on the onboard data loggers, they are averaging 13.2 mpgge of hydrogen (Figures 2 and 3). The vehicles have been driven on 9,300 trips, during which they had an average trip distance of 6 miles.

The average idle time per trip is 16%, as measured as a percentage of the total engine run hours. Note that the fuel used per mile appears to be heavily influenced by the idle time per trip. As seen in Figure 2, bottom left graph, trips with engine run times approaching 100% can have fuel use rates approaching 20 mpgge. At the other extreme, trips with idle times exceeding 80% (20% engine run time idling in the graph) will have fuel use results of 5 mpgge or less. Note that the mpgge conversion used is: 1 GGE = 1.012 kg H₂.



Figure 1. Dynetek hydrogen fuel tanks in the bed of the pickup.

Average trip speed also clearly has an impact on mpgge results. As seen in Figure 3, bottom right graph, as the average speed per trip approaches 40 mpg or greater, the per-trip mpgge will always be higher than the overall average of 13.2 mpgge. However, since 69% of all 9271 trips (Figure 3, top graph) have an average trip speed of 10 to 20 mph (3063 trips) or 20 to 30 mpg (3337 trips), the 13.2

mpgge average result may be an under reporting of the average mpgge potential of the HICE technology. If the vehicles were operated at more highway types of speeds, the average mpgge would likely have been in the 15 or greater mpgge range. Note that the calculated average speed of the vehicle when moving did not include any time in which the vehicles were at idle.

Another likely negative impact on the average mpgge result is the trip length distribution (Figure 3, bottom graph)—82% of all the trips were of a distance of 10 miles or less. This type of driving likely included many cold starts, which also contribute to lower mpgge.

Future Activities

Unless DOE directs AVTA to test a technically interesting or innovative HICE vehicle, AVTA is only planning on continuing to collect and analysis the data from the onboard data loggers on the twelve HICE pickups.

Publications and Presentations

Various publications document the pre-FY 2009 HICE testing. These documents, as well as the two-page HICE fleet fact sheet, can be found at <http://avt.inel.gov/hydrogen.shtml>. The two-page eTec/Roush HICE vehicle fleet testing fact sheet can be found at <http://avt.inl.gov/pdf/hydrogen/FactSheetChevy1500HDHydrogenICE.pdf>

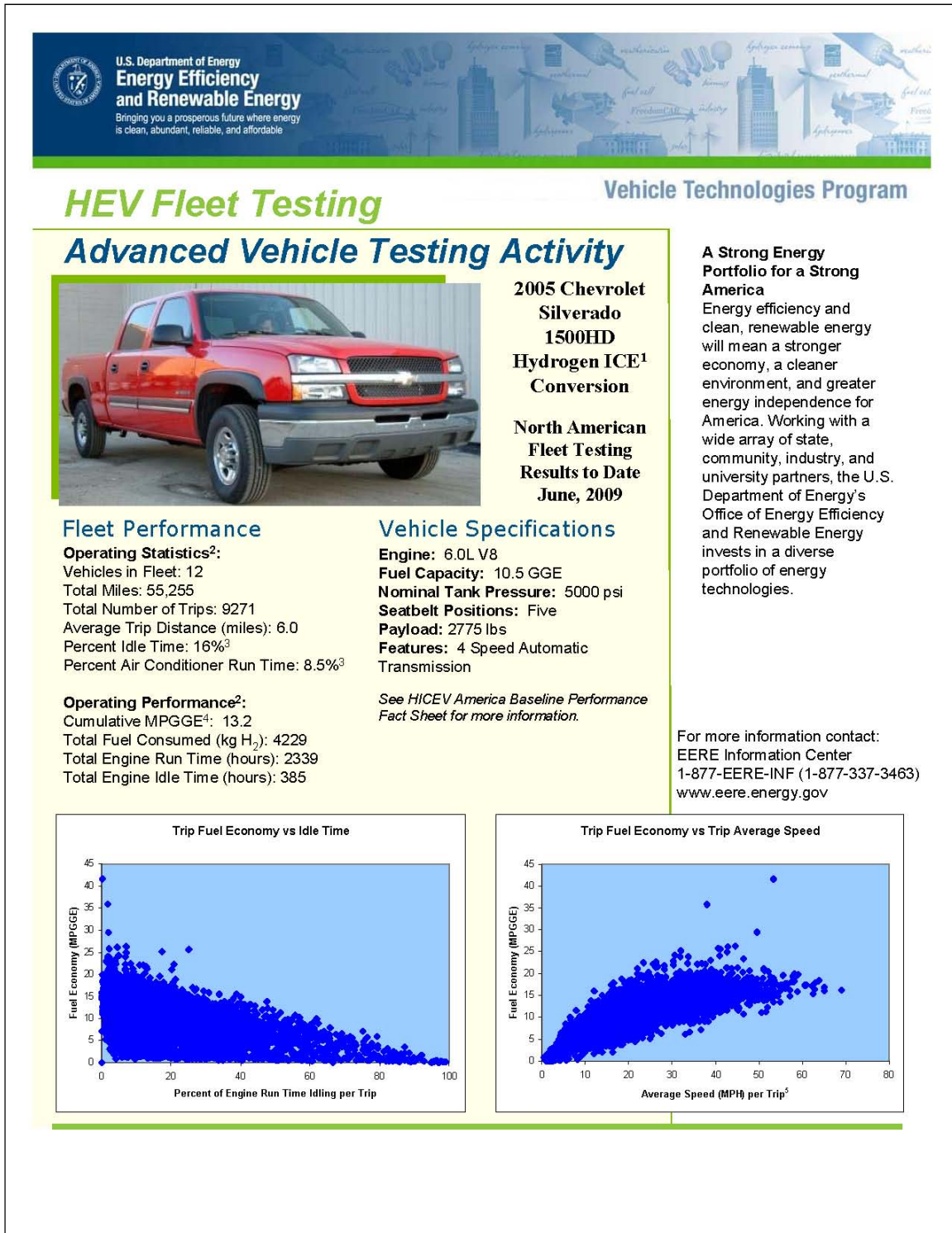
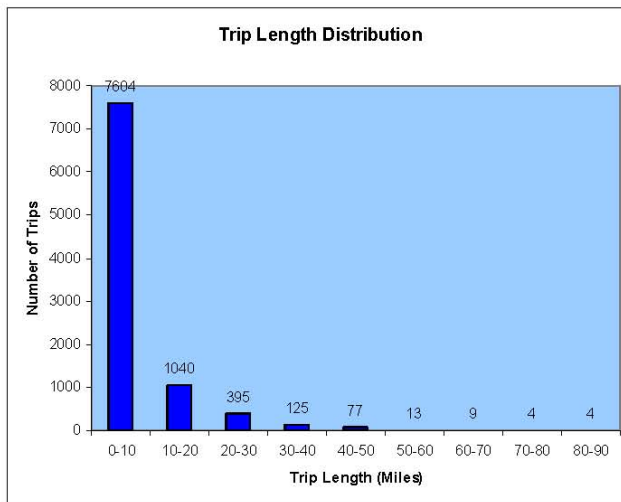
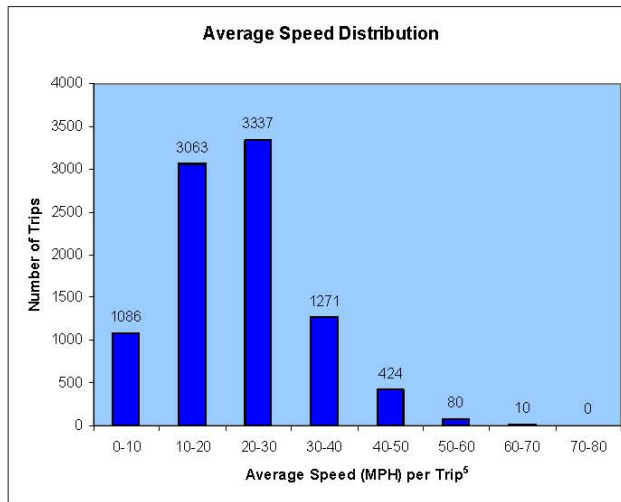


Figure 2. Page 1 of the eTec/Roush Chevrolet Silverado fleet testing activity fact sheet.



Notes:

1. Internal Combustion Engine
2. Data presented represents all electronically logged data, which is a subset of the overall fleet mileage
3. Percentage of total engine run hours
4. Miles per gallon gasoline equivalent (1 GGE = 1.012 kg H₂)
5. Average speed of vehicle when moving, idle time not included in calculation



U.S. Department of Energy
Energy Efficiency and Renewable Energy
 Bringing you a prosperous future where energy is clean, abundant, reliable, and affordable

Figure 3. Page 2 of the eTec/Roush Chevrolet Silverado fleet testing activity fact sheet.

D. Neighborhood Electric Vehicle Testing

James Francfort (Principal Investigator), Timothy Murphy (Project Leader)

Idaho National Laboratory

P.O. Box 1625

Idaho Falls, ID 83415-2209

(208) 526-6787; james.francfort@inl.gov

DOE Program Manager: Lee Slezak

(202) 586-2335; Lee.Slezak@ee.doe.gov

Objective

Support Federal and other fleet requirements for quality test data on neighborhood electric vehicle (NEV) models.

Support the California Air Resource Board's (CARB) decision requiring all NEV models sold in California be tested by AVTA in order to be eligible for CARB incremental funding and zero emission vehicle credits.

Maintain documented test procedures and capabilities to support the continued introduction and operations of neighborhood electric vehicles in fleet environments, and expand the NEV test base.

Approach

Answer all CARB questions regarding NEV testing history, test procedures development, conduct of testing, and AVTA objectives.

Conduct NEV testing on new NEV models as requested by industry and other NEV stakeholders.

Results

Supported CARB's requirement that all NEV models sold in California are to be tested by the AVTA NEVAmerica baseline performance testing procedures.

Conducted NEVAmerica baseline performance testing on three new NEV models from two NEV manufactures during FY 2009, for a total of 22 NEV models tested to date.

Respond to questions and inquires from numerous NEV manufacturers and perspective manufactures as to the testing process, costs, and schedules.

Future Activities

Given the potential of this market and the expanding use of NEVs, when manufacturers introduce additional NEVs, AVTA will continue to test suitable new entrants. As FY 2009 ended, AVTA was in discussion with several additional NEV manufactures regarding the testing of additional NEVs.

Introduction

NEVs are defined by the National Highway Traffic Safety Administration (NHTSA) as low-speed electric vehicles with attainable speeds of more than 20 mph, but not more than 25 mph. NEVs are generally allowed to operate on public

streets with posted speeds up to 35 mph and are licensed as a motor vehicle.

NEVs are growing in popularity among fleets and the public because of improvements in technology and their inherently low operating costs. In response to this increasing popularity, AVTA

continued to maintain testing procedures and to update them based on past testing experience.

Approach

During FY 2009, AVTA tested three new NEV models to the NEVAmerica test procedures. In addition, AVTA answered NEV manufacturers’ inquiries as to testing processes, schedules, and costs. The three new NEVs tested during FY 2009 were:

- 2009 Vantage Pickup EVX1000, two-passenger pickup NEV.
- 2009 Vantage Van EVC1000, two-passenger van.
- 2008 Roush Pickup Truck, two-passenger pickup NEV.

Results

These three NEV models are discussed here along with the other 19 NEV models previously tested (total of 22 NEV models tested) for comparison purposes.

Per Federal Motor Vehicle Safety Standard (FMVSS) 500, the top speed of NEVs cannot exceed 25 mph. As seen in Figure 1, six of the eight most recently tested NEVs have top speeds of between 24.8 and 25 mph, while the previously tested vehicles had an average top speed of 23.5 mph. The two Vantage NEVs tested in FY 2009 had top speeds of 23.8 and 24.1 mph, still closer to the allowable 25 mph than the earlier test NEVs.

As also seen in Figure 1, all three of new NEVs have test ranges in excess of 60 miles per charge. The average for all 22 models is 45.8 miles per charge. It should be recognized that actual “real-world” miles per charge will be lower generally by about 25%.

Figure 2 shows the time required to recharge each NEV to 100% state-of-charge and the battery capacity of each NEV. All of the graphed testing results are for 110-volt charging with the exception of the two earlier tested Frazier-Nash NEVs and the FY 2009 tested Roush REV pickup, which were all fast charged. The Frazier-Nash sedan was recharged in 0.93 hours and the Frazier-Nash pickup was recharged in 0.97 hours. The

Roush vehicle was charged in 1.4 hours. Recharge times for the graphed 19 NEVs Level I charged, ranged from 6 to 11.7 hours, with an average recharge time of 8.1 hours. The two Vantage NEVs tested in FY09 required 11.1 and 11.7 hours of charging. The 22 NEV models had from 5.3 to 12.96 kWh of onboard storage (Figure 2), with an average onboard storage of 7.1 kWh. The most recently tested NEVs from Miles, Vantage, and Roush had an average of 11.2 kWh of onboard energy storage while the earlier tested 17 NEVs had an average of 5.8 kWh of onboard energy storage.

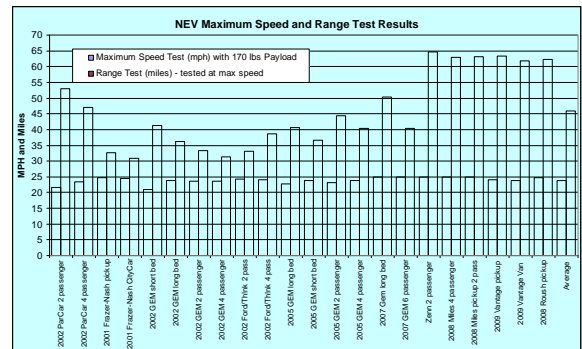


Figure 1. NEV maximum speed as tested on a closed test track, with the accelerator pedal held to the floor (“brick test”), and the range per charge also conducted on a closed track during the “brick test” method.

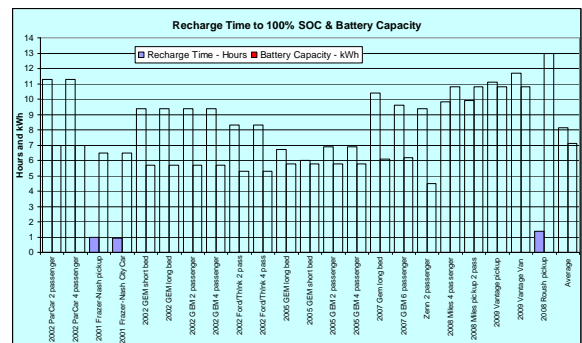


Figure 2. NEV recharge times to 100% state of charge (SOC) and battery capacity for each NEV. All testing results are for 110 volt charging (Level 1 charging) with the exception of the two Frazier-Nash NEVs and the Roush pickup which were all fast charged.

Figure 3 shows the 0 to 20 mph acceleration testing results. The most recent eight NEVs tested during FY 2008 and FY 2009 had an average acceleration time of 5.1 seconds. The average for

the previous 14 test models was 8.1 seconds, which was influenced by the results for the first two NEVs tested and their acceleration times over 16 seconds each. For all 22 NEV models tested, the average acceleration time is 7.0 seconds.

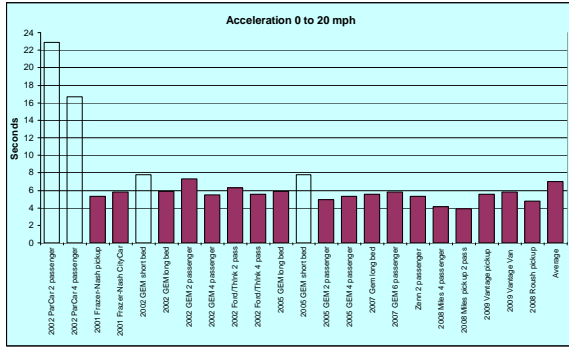


Figure 3. NEV acceleration test times in seconds to accelerate from 0 to 20 mph.

Figure 4 shows the charging efficiency for 20 of the NEV models (the two Frazier Nash NEVs were fast charged and the efficiency was incorrectly captured), as measured as AC Wh used per mile. The overall average for the 20 NEVs was 171.6 AC Wh per mile, while the average for the three recent NEVs tested was 192.9 AC Wh per mile. The average charging efficiency for the first 17 NEVs tested was 167.8 AC Wh per mile. This 168 to 193 decrease in charging efficiency per mile is likely related to the increase in vehicle weight. The first 17 NEVs tested with charging efficiency results weighted an average of 1,512 pounds, while the three FY 2009 test vehicles weighed an average of 2,628 pounds each.

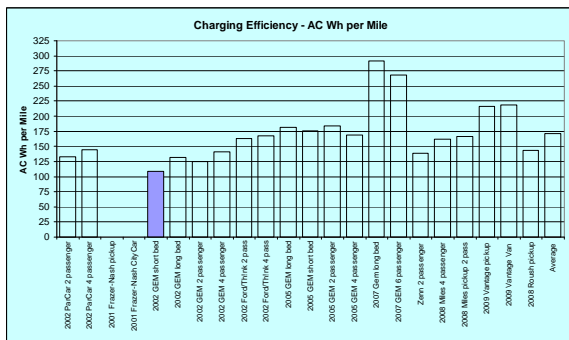


Figure 4. NEV charging efficiency, in AC Wh per mile, for the 20 NEV models with accurate data. The two Frazier-Nash NEVs were charged at Level 3, and the 2002 data for charging efficiency is not available.

Figure 5 shows the miles per AC kWh efficiency for the 20 NEVs reporting AC kWh per mile. NEVs can be a fairly fuel efficient transportation option given the average efficiency of 6.2 miles per kWh. Using the national average price of electricity of 10 cents per kWh, the average price of fuel would be 1.6 cents per mile.

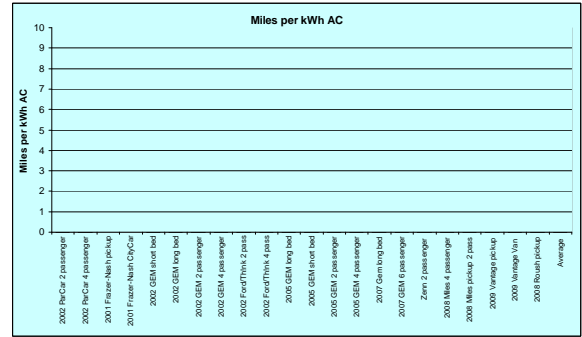


Figure 5. NEV vehicle efficiency as measured in miles per kWh AC. The two Frazier-Nash NEVs were charged at Level 3, and the 2002 data for charging efficiency is not available.

Future Plans

As FY 2009 ended, several additional NEV manufacturers have approached AVTA for information on testing their NEVs. In addition, past NEV manufacturers have indicated that they will be submitting new NEV models for testing.

Publications

The 22 NEV baseline performance testing fact sheets, testing specifications and procedures, and various other NEV testing reports on NEV use, performance, and fleet placement can be found at: <http://avt.inel.gov/nev.shtml>.

NEVAmerica testing reports published by the AVTA during FY 2009 are listed below:

1. 2009 Vantage Pickup EVX1000 pickup NEVAmerica baseline performance testing fact sheet. http://avt.inel.gov/pdf/nev/nev_vantage_pickup_EVX1000.pdf
2. 2009 Vantage EVC1000 van NEVAmerica baseline performance testing fact sheet. http://avt.inel.gov/pdf/nev/nev_vantage_van_EVC1000.pdf

3. 2008 Roush REV pickup NEVAmerica
baseline performance testing fact sheet.
<http://avt.inl.gov/pdf/nev/roush2008nevamerica.pdf>

E. Advanced Technology Medium and Heavy Vehicles Testing

Kevin Walkowicz (Principal Investigator)

National Renewable Energy Laboratory

1617 Cole Blvd.

Golden, CO 80401

(303) 275-4492; kevin_walkowicz@nrel.gov

DOE Technology Manager: Lee Slezak

Objective

Validate the performance and costs of advanced technologies in medium- and heavy-duty applications.

Provide results to interested parties to further optimize and improve the systems.

Facilitate purchase decisions of fleet managers by providing needed information.

Approach

Work with fleets to collect operational, performance, and cost data for advanced technologies.

Analyze performance and cost data over a period of one year or more.

Produce fact sheets on advanced heavy-duty vehicles in service.

Provide updates on current applications to DOE and other interested organizations, as needed.

Results in Fiscal Year 2009

Completed a draft final report on Eaton diesel hybrid delivery vans operating in Phoenix, AZ.

Completed a draft interim report on Azure gasoline hybrid delivery vans operating in Los Angeles, CA.

Completed a draft final report for plug-in hybrid electric school buses manufactured by IC Corporation in four locations.

Completed and validated the fleet duty cycle creation and analysis tool.

Future Activities

Complete evaluations on current fleet vehicles and initiate new evaluations.

Coordinate modeling and testing activities with other Department of Energy (DOE) projects such as the 21st Century Truck Partnership and the Advanced Heavy Hybrid Propulsion Systems (AHHPS) activity.

Monitor and evaluate promising new technologies and work with additional fleets to test the next generation of advanced vehicles.

Introduction

Understanding how advanced technology vehicles perform in real-world service, as well as their

associated costs, is important for enabling full commercialization and market acceptance. DOE's Advanced Vehicle Testing Activity (AVTA) works with fleets that operate these vehicles in medium-

and heavy-duty applications. AVTA collects operational, performance, and cost data for analysis. The analyzed data typically covers one year of service on the vehicles so that any seasonal variations are captured. Because of this, evaluation projects usually span more than one fiscal year (FY). The AVTA team also works on shorter term projects designed to provide updates on current applications to DOE and other interested organizations.

Approach

The AVTA activities for FY 2009 included:

- Fleet evaluations
- Fleet Duty Cycle Creation Tool

Fleet Evaluations

In FY 2009, AVTA worked with three commercial fleets to evaluate the performance of advanced technologies in service. These included:

1) Package Delivery Trucks – Azure/FedEx

Fed Ex has recently purchased 20 pre-production gasoline hybrid electric parcel delivery vehicles (gHEV) and deployed them in Southern California. AVTA-funded activities including industry collaboration have resulted in a robust project involving:

- Collection and analysis of parcel delivery vocational duty cycle data.
- Chassis dynamometer testing of a FedEx gHEV at the National Renewable Energy Laboratory's (NREL) ReFUEL Laboratory.
- A 12-month in-use evaluation.

Eight FedEx vehicles were instrumented with GPS-based data loggers, and over 62 route days of spatial speed-time data were collected. These data were used to confirm daily route consistency, and to characterize each route over 55 drive cycle metrics. From this data, three hybrid study vehicles were selected for a 12-month in-use study. Key drive cycle characteristics of the three selected study vehicles are summarized in Table 1.

Table1. Study Vehicle Key Drive Cycle Characteristics

Vehicle #	242292	242294	242295
Average Driving Speed (mph)	16.8	16.9	16.2
Daily VMT (miles)	43.8	47.2	21.3
Stops/mile	3.86	3.80	4.24
Avg ₂ Acceleration (ft/s ²)	2.27	2.11	2.10
Avg ₂ Deceleration (ft/s ²)	-2.61	-2.58	-2.56
Accelerations per mile	20.90	20.88	23.08
Decelerations per mile	20.36	19.83	22.81
Kinetic Intensity (ft ⁻¹)	0.00059	0.00055	0.00075

Calculated kinetic intensity was used to (1) compare real, collected drive cycles to existing stock drive cycles, and (2) select chassis dynamometer test cycles. Based upon observed drive cycle kinetic intensities, the Orange County (OC) Bus Cycle was selected as a cycle that best approximated the routes driven by three study vehicles, while the New York City Cycle (NYCC) and HTUF4 Cycle were selected as upper and lower boundaries for vocational kinetic intensity.

A gHEV and comparable diesel were transported to NREL's ReFUEL Laboratory for emissions and fuel economy measurement. Fuel economy results over three drive cycles are presented in Table 2. It was found that (1) fuel economy improvements (on an energy/volume equivalent comparison) were possible on the NYCC (~21%) and that (2) fuel economy will decrease slightly for the HTUF4 Cycle and the OC Bus cycle. This is likely due to the lower thermal efficiency of the gasoline engine in the HEV versus the diesel vehicles that were used for comparison. This comparison (gasoline HEV versus diesel) was used to illustrate the fleet options available in Los Angeles. Emissions of NO_x and particulate matter (PM) were considerably less for the gHEV as compared to the diesel (~75-90% reduction in NO_x and a ~90% reduction in PM).

Table 2. Fuel Economy Results

Drive Cycle	gHEV FE (mpg)	gHEV Diesel Equivalent FE (mpg)	Diesel FE (mpg)	gHEV Advantage (%)
CILCC	11.22	12.19	NM	NA
HTUF4	10.45	11.36	11.66	-2.60%
OC Bus	8.61	9.36	9.52	-1.71%
NYCC	6.75	7.34	6.08	20.65%

Three gHEVs and three similar diesel parcel delivery trucks are the focus of the 12-month in-use evaluation. To date, five months of in-use fueling and maintenance data have been collected and analyzed. In-use fuel data were collected via retail fuel data supplied by FedEx, and via on-board fuel logs completed by vehicle drivers and faxed to NREL. Due to occasional gaps in on-board fuel log data, the more comprehensive retail fuel data set was analyzed. Fueling data for the study period are presented below (Figure 1).

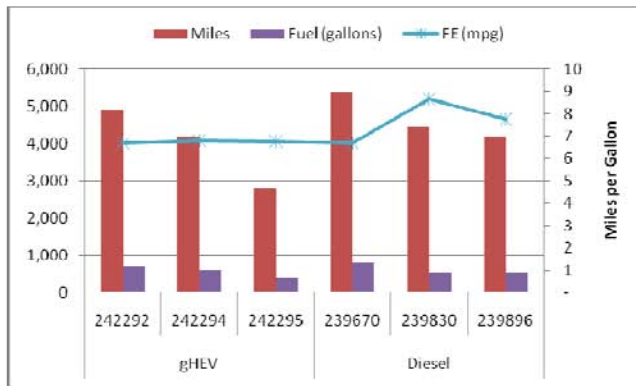


Figure 1. Five-Month In-use Fuel Economy Results

Over five months, the gHEV and diesel groups averaged 6.75 and 7.54 mpg, respectively. Total operating costs per mile for each of the study groups are presented in Figure 2.

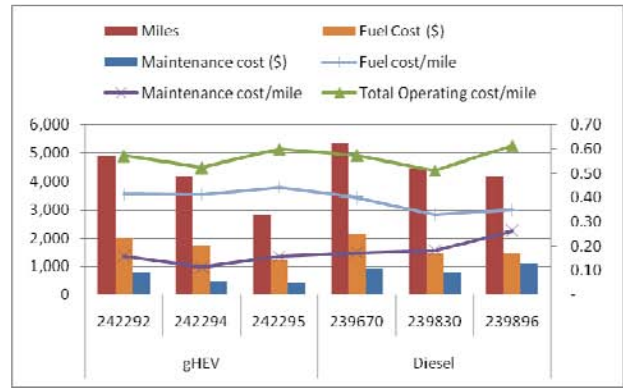


Figure 2. Total Operating Costs

Over five months, the gHEV and diesel groups' total cost of operation per mile are \$0.56 and \$0.57, respectively.

An interim (six month) report is scheduled for December 2009, and a final report containing all data is scheduled for release in June 2010.

2) PHEV School Bus – Enova/IC Corporation Gasoline Hybrid

In 2008, AVTA began to work with three fleets to evaluate gasoline hybrid buses that are currently operating in 14 different locations around the country. In 2009, an additional fleet in Austin, TX was added to the studies in Wake County, NC, Napa, CA, and Manatee, FL school districts, which were chosen due to their data collection capabilities. The buses, manufactured by IC Corporation (a division of International Truck and Engine Corporation) are 33.5-ft front-engine school buses with a gross vehicle weight (GVW) of 29,800 lbs. The buses are equipped with International VT365 engines and have the Enova 'post transmission' hybrid system added. A 330VDC Valence lithium battery pack is utilized. The data collection activity will summarize one school year's worth of data (approximately September through May 2008).

In September 2009 a draft interim report was submitted to the Department of Energy (DOE) to document a school year's worth of data collected at the four sites. These buses were compared with the conventional diesel and compressed natural gas (CNG) buses that were also in operation in the fleets. Highlights of the draft interim report are as follows:

Vehicle Usage: Figures 3 through 6 show the bus usage between the hybrid and diesel buses in all four locations.

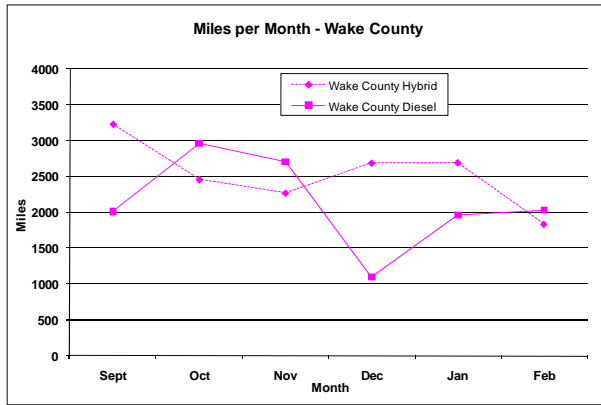


Figure 3. Monthly Mileage for Hybrid and diesel buses at Wake County School District

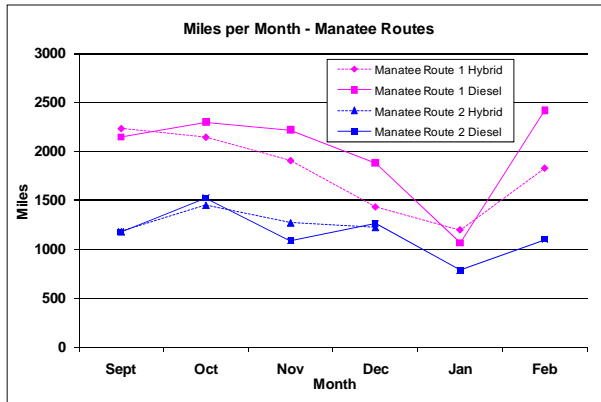


Figure 4. Monthly Mileage for hybrid and diesel buses at Manatee School District

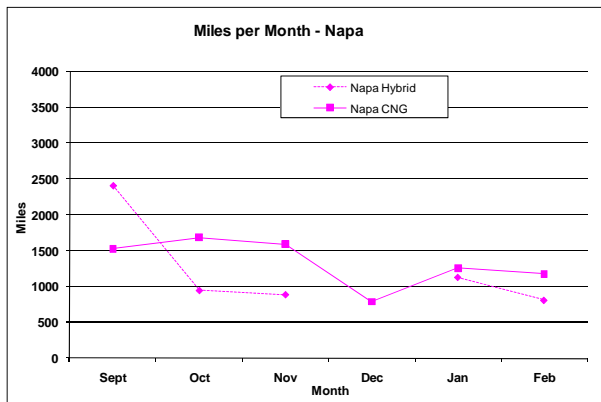


Figure 5. Monthly Mileage for hybrid and diesel buses at Napa School District

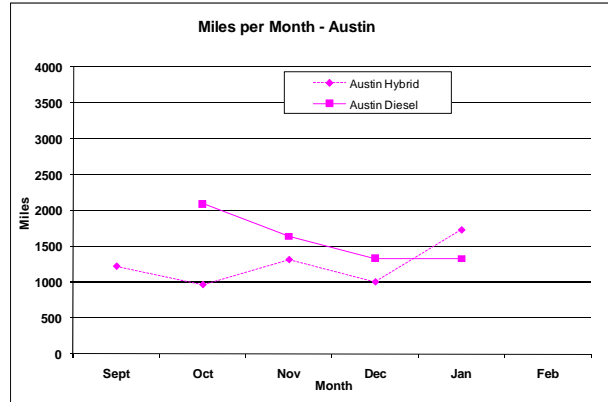


Figure 6. Monthly Mileage for hybrid and diesel buses at Austin School District

On-Road Fuel Economy: Table 3 shows the fuel economy differences between the hybrid and diesel buses in all four locations. Differences ranged from 12 to 30% improvement for the HEVs, although data from vehicle usage shows it is evident that the routes were significantly different. Thus, a direct comparison between buses at each location may not be appropriate. An observed range of fuel economy for the diesels at three locations (Napa uses CNG) was 6.51 to 7.14 mpg. The hybrids showed a range of 8.0 to 9.1 mpg.

Bus	Usable Mileage	Gallons Consumed	Miles per Gallon	Fuel Cost/Gallon (\$) ¹	Fuel Cost/Mile (\$)
Hybrid 606 (route 1)	9,981	1,159	8.61	2.58	0.30
Hybrid 607 (route 2)	4,970 ²	601	8.27	2.58	0.30
Manatee Hybrid Group	14,951	1,760	8.49	2.58	0.30
Diesel 604 (route 2)	6,929	1,253	5.53	2.58	0.47
Diesel 605 (route 1)	11,599	1,591	7.29	2.58	0.36
Manatee Diesel Group	18,528	2,844	6.51	2.58	0.40
Wake County Hybrid	14,330	1,792	8.00	2.61	0.33
Wake County Diesel	11,945	1,674	7.14	2.61	0.37
Napa Hybrid ³	2,833	313	9.05	2.81	0.31
Napa CNG	8,032	1,392	5.77	2.70	0.47
Austin Hybrid	3,968	476.9	8.32	2.38	0.29
Austin Diesel	6,333	923.7	6.86	2.38	0.35

Table 3. Fuel Economy for hybrid and diesel buses at all 4 locations

Laboratory Fuel Economy: A 2007 model year hybrid was obtained from Adams County School District in Adams County, CO. A 2007 model year conventional bus that performs similar operation within the Adams County fleet was also obtained for comparison testing. The buses were both tested on three drive cycles, which were selected based on GPS data obtained from Adams County, Austin School District, and a study conducted in North

Carolina. The three cycles selected for laboratory testing were the Rowan University Composite School Bus Cycle (RUCSBC), the urban dynamometer driving schedule (UDDS), and the Orange County Transit Authority (OCTA) Cycle. Figure 7 shows fuel economy as observed for all three cycles, and the HEV bus data is broken down into charge depleting (CD) mode, charge sustaining (CS) mode, and ‘HEV off’ where applicable. Fuel economy improvements for buses tested on these three cycles in CD mode showed a 55 to 113% improvement compared to the bluebird non-hybrid diesel. They showed a 44 to 108% improvement versus the same IC Corporation bus with the HEV system turned off. CS mode fuel economy of the hybrid bus was roughly equivalent to the diesel bus and also to the bus with the hybrid system off.

Testing indicated that improvements can be expected for roughly 13 to 39 miles based on the cycle.

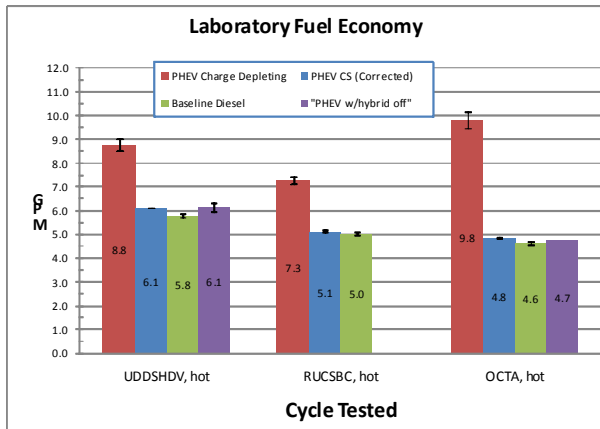


Figure 7. Laboratory Fuel Economy Summary

Energy Storage: Enova chose to use lithium ion batteries for energy storage instead of NiMH or lead acid batteries more commonly used in hybrid buses. The lithium ion batteries work well for the larger state-of-charge(SOC) variations associated with PHEV duty cycles. In addition, the lithium ion batteries have a longer life expectancy compared to other battery types. IC Corporation has a two-year warranty for the batteries. The battery pack used in these charge depleting vehicles are charged overnight using a 220V, 30 amp, single-phase circuit. Full charge will take approximately four

hours with the 220V circuit. A 110V option is also available and will approximately double the charge time to eight hours.

During the first year of service and a portion of the evaluation period for some buses, a manufacturing issue was identified. Due to improper packaging of the battery pack, the battery pack was located on one side of the bus chassis. Not having a split battery pack, IC Corporation corrected the issue with another, equally weighted ballast on the opposite side of the chassis, which added extra weight. Once a split battery pack was available from the battery supplier (Valence), the ballast was removed and the split/balanced mass pack was installed into the buses. This added retrofit activity does show up in the downtime on some of the buses. Figure 8 is a photo of this battery pack.



Figure 8. Enova PHEV battery pack

Operational Costs: Total operational costs for the hybrid buses (fuel and maintenance costs) were \$0.35 to \$0.52/mile at the three locations reporting data and \$0.36 to \$0.42/mile for the diesels.

Overall, the school districts have been satisfied with the buses. A next-generation bus is being planned by IC Corporation and will be studied as part of the FY 2010 DOE AVTA task.

3) UPS Hybrid Package Delivery

UPS obtained new HEV delivery trucks in their fleet in 2007. AVTA initiated an evaluation for these MD package delivery vehicles equipped with an Eaton’s parallel hybrid systems (with lithium battery) to assess the performance and feasibility of this technology in a UPS fleet in Dallas, TX. However, in the spring of 2008, UPS informed NREL that the Dallas fleet was not available to

study and it was not representative of their fleet. They requested changing the study location. A new group of 10 vehicles in Phoenix, AZ was selected for the study and detailed evaluation was restarted. The intent of the project is to compare these lithium battery parallel hybrid trucks with conventional diesel powered trucks. Duty cycle data acquisition was completed in August of 2008 in Phoenix. The 12-month study period was identified to be January through December 2008.

In September 2008, AVTA produced a draft interim project report for six months of data on the trucks in service (January through June 2008). A final published report is expected in 2009. Highlights of the final report are as follows:

Delivery Van Use and Duty Cycle: The hybrids had a usage rate that was 20% less than that of the diesel vans. The hybrids were consistently driven a fewer number of miles throughout the evaluation period and experienced some downtime at the end of the evaluation. The hybrids spent more time idling and operating at slower speeds than the diesels did, and the diesels spent slightly more time operating at greater speeds; this resulted in the hybrids' fewer monthly miles.

Fuel Economy: The six-month average fuel economy for the hybrid vans is 13.1 mpg; 28.9% greater than that of the diesel vans 10.2 mpg (two-tailed P value = 0.0002). Figure 9 shows the average monthly mpg for each van group and the cumulative average mpg as well.

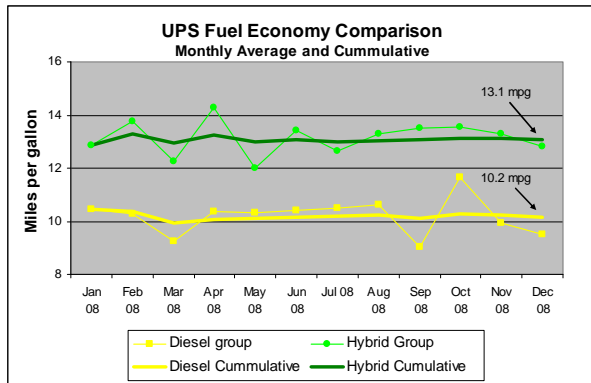


Figure 9. Average monthly fuel economy

Maintenance Costs: There was no statistically significant difference between the study groups in

regards to total maintenance cost per mile or propulsion maintenance cost per mile.

Laboratory Fuel Economy and Emissions Results: Two vans similar to those tested in Phoenix were tested at NREL's ReFUEL Laboratory to determine emissions and fuel economy benefits of the hybrid electric powertrain being evaluated at UPS. The tests were conducted over three driving cycles: the Combined International Local and Commuter Cycle (CILCC), the West Virginia University City (WVU City) Cycle, and the Central Business District (CBD) Cycle. Vehicle exhaust emissions and fuel consumption were measured for repeated test conditions. The hybrid showed a fuel economy improvement of 31 to 37%, while emissions results were mixed (see Tables 4 and 5).

	CILCC	WVU City	CBD
Conventional P100 (mpg)	9.1	6.87	6.83
Hybrid P100 (mpg)	11.99	9.38	9.16
Fuel Economy (mpg) % increase w/hybrid	31%	37%	34%
P Value	0.0010	0.0014	0.0024

Table 4. Laboratory Fuel economy results for UPS HEV

	CILCC				WVU City				CBD			
	Diesel	Hybrid	Hybrid % diff	P Value	Diesel	Hybrid	Hybrid % diff	P Value	Diesel	Hybrid	Hybrid % diff	P Value
CO ₂ (gram/mile)	1026	773	-25%	0.0005	1333	933	-30%	0.0001	1396	1017	-27%	0.0021
NO _x (gram/mile)	7.52	9.69	29%	0.0014	9.22	10.42	13%	0.0137	10.56	10.56	NS	0.98
THC (gram/mile)	1.47	1.27	-14%	0.0413	3.85	3.27	NS	0.48	1.34	1.17	NS	0.61
CO (gram/mile)	7.59	5.38	-29%	0.0025	14.31	12.07	-16%	0.0097	8.31	8.80	NS	0.13
PM (gram/mile)	0.142	0.064	-55%	0.0148	0.120	0.214	NS	0.15	0.116	0.114	NS	0.37

*NS - % difference is not reported because the P Value indicates the difference is not statistically significant at the 95% confidence level.

Table 5. Laboratory Emissions results for UPS HEV

4) Fleet Duty Cycle Creation and Analysis Tool

The AVTA team identified a need by fleet operators and researchers to quickly and accurately be able to assess what type of drive cycles vehicles are operating on. In response to this need, the AVTA team has initiated an effort to devise a computational tool that is capable of analyzing user-acquired GPS time-speed data and creating a compressed 'custom' duty cycle based on the inputs that will have the same fuel economy (if tested) as the large data set. The tool was designed to take an unlimited amount of data (such as a group of vehicles operating over a number of days) and filter this data with the

intention to compress it down to a 30-minute test cycle for vehicle testing or modeling activities. An additional function of this tool is that it is also able to provide comparative data, which will allow the user to assess which ‘standard’ duty cycle is closest to the data provided. This tool has been utilized in AVTA projects to select routes and determine which duty cycles are representative for further modeling and laboratory testing. Additional output will include statistics on various parameters of interest. Figure 10 shows a general screen shot of the output of this tool.

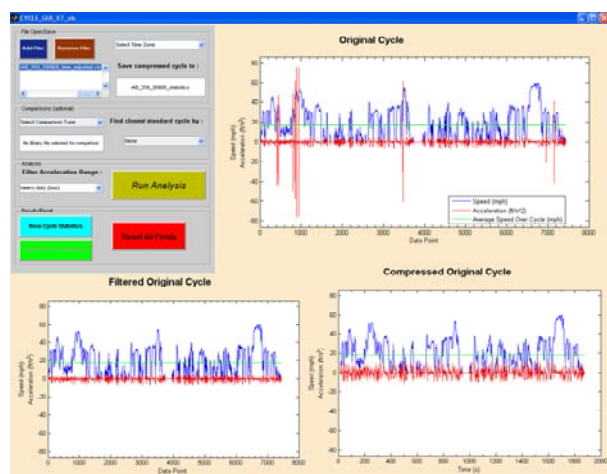


Figure 10. Screen shot of duty cycle analysis and creation tool

In FY 2009, the AVTA team refined the analysis functions and validated it based on modeling activities. Fuel economy (mpg), when modeled for any type of vehicle model available (conventional, HEV, and fuel cell vehicles), was found to be generally within a 5% difference for the large data sets or the shortened 30-minute cycle generated by the tool. The ‘closest matching cycle’ fuel economy was also representative of the fuel economy of the entire data set. This tool will continued to be used in FY 2010, and several industry partners have requested access to it for similar use.

Overall AVTA Results

Results from AVTA fleet evaluations have been anticipated and well received by the industry. Specific results for each evaluation are described as a part of the project sections above.

Future Plans

The team will continue working with fleets to investigate the latest technology in medium-and heavy-duty vehicles. The team will track the latest developments in advanced vehicles and select those with the most promise for further study. Future plans include working with simulation and modeling teams at DOE laboratories to ensure that relevant vehicle data are collected to verify and enhance the various simulation models.

FY2009 Publications / Presentations

Lammert, M. (September 2009). UPS: Final Evaluation of Diesel-Electric Hybrid Delivery Vans. 37 pp.; NREL/TP-540-44134.

alkowicz, K. (September 2009). Final Report on PHEV School Bus Project. 30 pp.; NREL/TP-540-46704.

Barnitt, R.A. (February 2009). In-Use Performance of Orion BAE Hybrid Buses at New York City Transit (Presentation). Presented at the SAE Hybrid Symposium.

Barnitt, R.A. (September 2009). Interim Report on Fed Ex HEV Evaluation Project. 25 pp.; DOE FY2009 Milestone Report.

VI. AERODYNAMIC DRAG REDUCTION

A. DOE Project on Heavy Vehicle Aerodynamic Drag

Project Principal Investigator: K. Salari

Co-Investigator: J. Ortega

Lawrence Livermore National Laboratory

P.O. Box 808, Livermore, CA 94551-0808

(925) 424-4635; salari1@llnl.gov

Contractor: Lawrence Livermore National Laboratory

Contract No.: W-7405-ENG-48, W-31-109-ENG-38, DE-AI01-99EE50559

Objective

Class 8 tractor-trailers comprise 11-12% of the total U.S. petroleum use. At highway speeds, 65% of the energy expenditure for a Class 8 truck is used in overcoming aerodynamic drag. This project's objective is to improve the fuel economy of Class 8 tractor-trailers by providing guidance on methods for reducing drag by at least 25%. This reduction in drag would represent a 12% improvement in fuel economy at highway speeds—equivalent to about 130 midsize tanker ships per year. The specific goals of this project include:

- In support of the Department of Energy's (DOE) mission, provide guidance to industry to improve the fuel economy of class 8 tractor-trailers through the use of aerodynamic drag reduction.
- On behalf of DOE, expand and coordinate industry participation to achieve significant on-the-road fuel economy improvement.
- Join with industry in getting devices on the road.
- Demonstrate new drag-reduction techniques and concepts through the use of virtual modeling and testing.
- Perform full-scale wind tunnel validation of selected devices with industry collaboration and feedback.
- Establish a database of experimental, computational, and conceptual design information.

Approach

Apply computational fluid dynamics (CFD) tools to understand the aerodynamic flow around heavy vehicles in order to assess the design and performance of drag reduction devices.

Investigate the performance and optimization of aerodynamic drag reduction devices(e.g., base flaps, tractor-trailer gap stabilizers, underbody skirts, wedges and fairings, and blowing and acoustic devices, etc.).

Provide industry with design guidance and insight into the performance of add-on devices utilizing both experimental and computational results.

Generate an experimental database to understand the accuracy of CFD results.

Provide industry with conceptual designs of drag-reducing devices.

Join with industry to perform a full-scale wind tunnel validation test of candidate devices at the National Full-Scale Aerodynamics Complex (NFAC).

Accomplishments

For the fiscal year 2009, the DOE this project achieved two primary objectives. The first and foremost is the planning and preparation for the full-scale wind tunnel investigation of aerodynamic drag reduction devices that have shown significant drag reduction on the track or on the road. The study will be performed in the 80'x120' wind tunnel at NFAC, operated by the U.S. Air Force at NASA Ames Research Center (Figure 1). The anticipated start date for this test is mid-December 2009 for duration of two months. During this test, the performance of drag-reducing add-on devices from six different commercial companies and a government laboratory will be assessed on combinations of two tractors (day-cab and sleeper-cab models) and four trailers. The commercial devices were selected based upon a number of criteria, such as prior fuel economy improvement data, weight penalty, level of driver intervention, cost, durability, and installation difficulty. The selected devices will target the vehicle underbody, tractor-trailer gap, and trailer base. In addition to the commercially available devices, a selected number of research devices will be evaluated during the wind tunnel study. CFD simulations have played a key role in the vehicle installation in the tunnel test section (Figures 2 and 3). In particular, we have investigated the sensitivity of the aerodynamic forces to the vehicle height above the tunnel floor and to minor changes in the vehicle yaw angle.

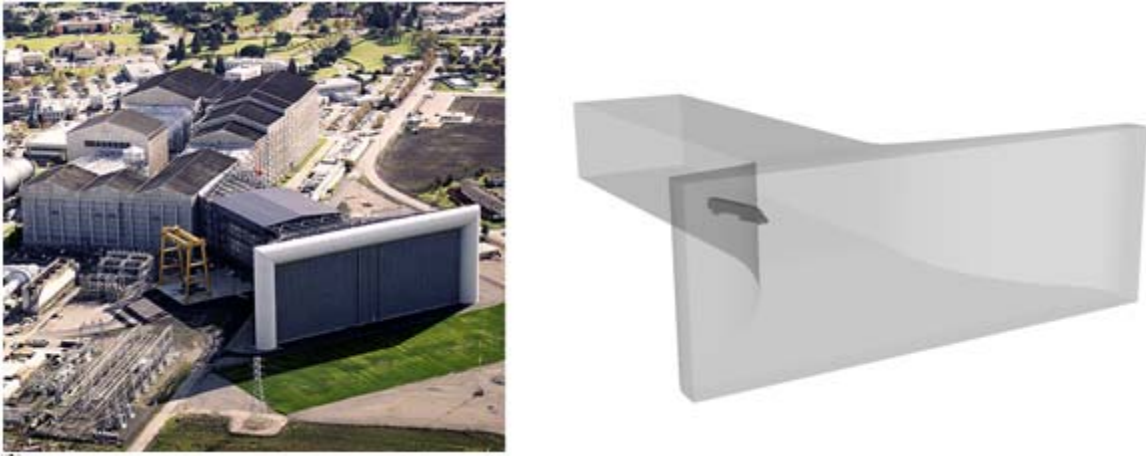


Figure 1. The National Full-scale Aerodynamic Complex (NFAC) 80'x120' wind tunnel at NASA Ames Center (left, actual; right, computational model)

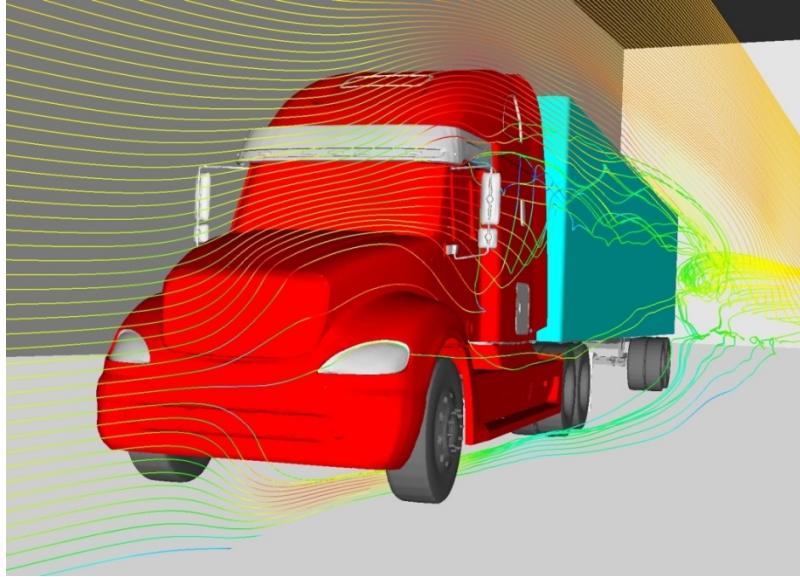


Figure 2. Velocity streamlines about a class 8 heavy vehicle at 6.1 degrees yaw angle in the 80'x120' wind tunnel (CFD simulation)

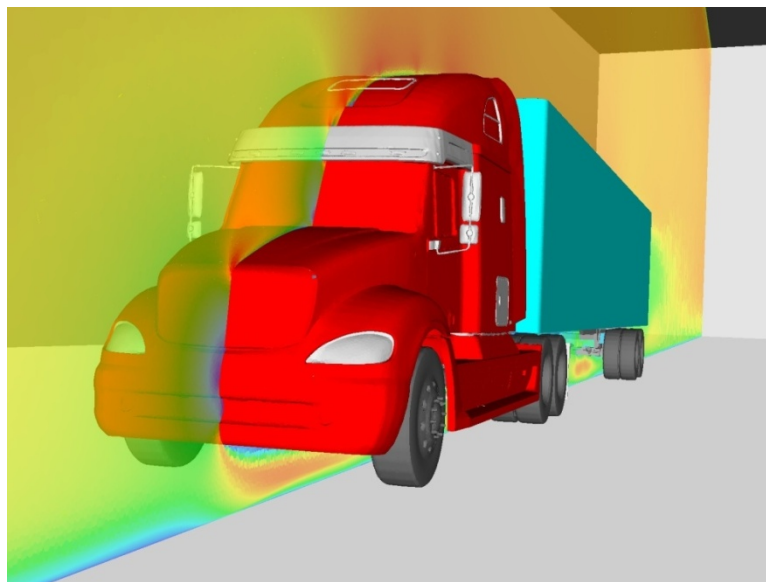


Figure 3. Velocity magnitude contours on a vertical cutting plane within the 80'x120' wind tunnel produced by a heavy vehicle at 6.1 degrees yaw angle (CFD simulation)

The second accomplishment is the preliminary investigation of tanker-trailer aerodynamics. Throughout the United States, there are approximately 200,000 tanker-trailers in operation. These vehicles are typically used to haul aluminum and petroleum, chemical, food-grade, and dry-bulk products [1]. It is estimated that a 1% improvement in the fuel economy of tanker-trailers could result in an annual fuel savings of approximately 30×10^6 gallons throughout the United States. A review of the literature revealed that there have been relatively few studies on tanker-trailer aerodynamics. The first study that we know of occurred in 1978 and was a wind tunnel investigation of $1/10^{\text{th}}$ scale dry and liquid cargo tankers [2]. Due to the model scale and limitations on the maximum tunnel speed, the Reynolds number of the flow about the tanker model was about an order of magnitude less than that of a full-scale vehicle. Additionally, the authors present only drag coefficient data at 0° and 20°

vehicle yaw angles. The next study in the literature does not appear until 2009, in which the authors investigate the aerodynamics of a full-scale tanker-trailer and a simplified tractor geometry using CFD simulations[3]. To reduce the computational resources, a symmetry boundary condition was employed along the vehicle centerline, thus limiting the study to a 0° vehicle yaw angle. Through various geometric modifications of the tanker-trailer, the authors report a reduction in the drag coefficient by 23%. To provide realistic data on a more representative tanker-trailer, we have begun to perform CFD simulations on a detailed day-cab tractor and tanker (Figure 4). The preliminary results of this study demonstrate that the full-scale vehicle has a drag coefficient of approximately 1.0 at highway speed within a typical crosswind. We will present this preliminary data in November 2009 at the annual American Physical Society Division of Fluid Dynamics conference.



Figure 4. Tanker-trailer geometry

Future Direction

Complete the full-scale wind tunnel study at NFAC and document the results by generating internal documentations, conference publications, and presentations.

Utilize the data obtained from the wind tunnel study to down-select the drag reduction devices to be investigated in the DOE grant, "Fleet Evaluation and Factory Installation of Aerodynamic Heavy Duty Truck Trailers" (DE-PS26-08NT01045-03), which will commence in fiscal year 2010.

Begin a detailed investigation of the major aerodynamic drag sources on tanker-trailers and design devices to mitigate these drag sources.

Partner with Navistar, Inc., in the SuperTruck Initiative.

References

1. National Tank Truck Association, www.tanktruck.org.
2. Weir, D.H., Strange, J.F., Heffley, R.K., 1978, Reduction of Adverse Aerodynamic Effects of Large Trucks, Report FHWA-RD-79-84.
3. Buil, R.M. & Herrero, L.C., 2009, Aerodynamic Analysis of a Vehicle Tanker, *J. Fluids Eng.*, 131:041204-1-17.

Acknowledgments

This work was performed under the auspices of the U.S. DOE by Lawrence Livermore National Laboratory under contract DE-AC52-07NA27344.

VII. THERMAL MANAGEMENT

A. Agreement # 14758 – Thermal Conditions Underhood: Nanofluids

Principal Investigator: Jules Routbort

(coworkers: Wenhua Yu, David France, Elena Timofeeva, Dileep Singh, David Smith, and Roger Smith)

Argonne National Laboratory

9700 South Cass Avenue, Building 212, Argonne, IL 60439

phone: (630) 252-5065; fax: (630) 252-5568; e-mail: routbort@anl.gov

DOE Technology Development Manager: Lee Slezak

(202) 586-2335, Lee.Slezak.ee.doe.gov

Contractor: UChicago Argonne, LLC

Contract No.: DE-AC02-06CH11357

Objectives

- In conjunction with the Nanofluid Development Project, in which nanofluids (nanoparticles suspended in liquids) are characterized in terms of base fluid properties, particle physical attributes (material, concentration, shape, size, and size distribution), nanofluid thermal properties (effective density, specific heat, viscosity, and thermal conductivity), and additive properties, determine the thermal characteristics of engineered nanofluids.
- Design, fabricate, and operate specialized experimental facilities to determine and optimize heat transfer rates in engineered nanofluids. (Heat transfer rate is the ultimate measure of nanofluid effectiveness for the transportation industry.)
- Improve and optimize the efficiency of heavy-vehicle cooling systems, with the goal of a minimum cooling system size reduction of 5%.

Approach

- Experimentally and theoretically investigate and optimize the thermal effectiveness of engineered nanofluids for application to the transportation industry.
- Investigate and improve theoretical approaches for predicting nanofluid thermal properties to direct nanofluid characterization and heat transfer studies and to aid in engineering and optimizing nanfluids for the transportation industry.
- Experimentally measure heat transfer coefficients of various selected nanofluids in conjunction with the Nanofluid Characterization Program.
- Experimentally measure and determine nanofluid heat transfer characteristics with regard to stability, agglomeration, and settlement of nanoparticles suspended in the nanofluids.
- Develop theoretical models of nanofluid heat transfer coefficients for designing and engineering nanofluids optimized for vehicle thermal control and other heat transfer applications.
- Perform cooling system tests in collaboration with the transportation industry.

Accomplishments

- Conducted a very detailed and comprehensive review of the physical mechanisms and mathematical models of the effective thermal conductivities of nanofluids.

- Upgraded the heat transfer test facility with (1) an Endress Hauser Promag flow meter to provide more stable and accurate flow rate measurements, (2) Labview data acquisition software to allow more flexible control, and (3) an Agilent multiplexor for data acquisition to increase data throughput rates.
- Experimentally measured heat transfer coefficients of SiC-water nanofluids with the particle volume concentration of 4.1% for four different particle sizes.
- Completed a systematic study of the effects of the nanoparticle size on the heat transfer performance of SiC-water nanofluids.
- Experimentally measured heat transfer coefficients of SiC-50/50 ethylene glycol/water nanofluids.
- Published 3 journal papers, submitted an extensive review paper (accepted for publication), and filed a U.S. patent.

Future Directions

- Identify, develop, characterize, and optimize nanofluids with the combination of stable suspension, low viscosity, high thermal conductivity, and high heat transfer coefficient based on a fundamental understanding of nanofluid heat transfer characteristics.
- Conduct systematic experiments to quantify the heat transfer performance of 50/50 ethylene glycol/water based nanofluids compared to their base fluids and to provide data and predictions necessary for industrial applications.
- Refine comprehensive models of the nanostructure-enhanced and nanoparticle-mobility-enhanced thermal conductivity and heat transfer coefficient of nanofluids for simulation of cooling system performance.
- Conduct tests of cooling-system heat transfer in collaboration with the transportation industry.

Introduction

Due to trends toward higher power outputs and stringent emissions levels, heat rejection requirements are ever-increasing; and the cooling issue for engines has thus been brought to the forefront of the transportation industry. Conventional cooling methods have been optimized to their limits, including design of the radiator air-side fins. However, engine fluids themselves, such as lubricants and coolants, are inherently poor heat transfer fluids and contribute to the limitations on engine cooling rates. Therefore, there is a strong need for higher performance coolants to be used in thermal control systems for vehicles.

Nanofluids are nanotechnology-based heat transfer fluids engineered by uniformly and stably dispersing a very small quantity (typically <5% by volume) of nanometer-sized particles in conventional heat transfer fluids. Nanofluids combine the advantages of both the high thermal conductivity of solid nanoparticles and the convective heat transfer capacity of base fluids. It has been demonstrated by many research groups worldwide that adding nanoparticles in traditional heat transfer fluids can

greatly increase the effective thermal conductivity of nanofluids. Studies on other aspects of nanofluids such as viscosity and heat transfer coefficient have also been conducted. However, detailed studies on the connection between the component properties and the nanofluid thermal performance are still rare.

The goal of this project is to develop nanofluids with enhanced thermal performance over their base fluids (traditional coolants) to improve engine cooling and thereby allow (1) reduction of the size and weight of heavy vehicle cooling systems (radiator, oil cooler, pump, etc.) and (2) vehicle front end design for aerodynamic drag reduction. While such nanofluids are among the most promising coolants for the transportation industry, a better understanding of the thermal enhancement and stability of nanofluids is necessary for achieving the project goal. Therefore, we are conducting the following tasks to attain this understanding: (1) explore and exploit the unique properties of nanoparticles to identify and develop heat transfer fluids with high thermal conductivity and heat transfer rates, (2) experimentally characterize nanofluid physical attributes, (3) determine the basic mechanisms of enhanced thermal conductivity and stability of nanofluids, (4)

develop techniques to lower the viscosity of nanofluids, (5) experimentally determine heat transfer rates and pressure drops in flowing nanofluids, (6) develop and validate new thermal models for nanofluids, (7) develop nanofluid technology for increasing the thermal transport of engine coolants and lubricants, and (8) conduct cooling tests in conjunction with industry. This task is part of the Argonne nanofluid research program and focuses on nanofluid heat transfer.

Results and Discussion

Thermal Conductivity Model Review

A review, which summarizes considerable progress made on the physical mechanisms and mathematical models of the effective thermal conductivities of nanofluids, has been conducted. Specifically, the physical mechanisms and mathematical models of the effective thermal conductivities of nanofluids were reviewed, the potential contributions of those physical mechanisms were evaluated, comparisons of theoretical predictions and experimental data were made, and opportunities for future research were identified.

The studies of physical mechanisms and mathematical models of the effective thermal conductivity of nanofluids are essential for understanding the thermal behavior of nanofluids, for optimizing their thermal performance, and for designing practical application systems using them. During the decade-long development of nanofluid technologies, several mechanisms, including particle-fluid interfacial layering, particle aggregation, and particle Brownian motion, have been proposed to explain the effective thermal conductivity enhancement beyond the predictions of the classical effective medium theories. Based on those mechanisms, many new mathematical models have been formulated, most of which result in improvements to the equations based on the effective medium theories. In addition to the particle volume concentration, the mathematical models (developed based on the proposed physical mechanisms) also include the particle size and nanofluid temperature effects on the effective thermal conductivity enhancement of nanofluids, explicitly or implicitly. Even though it cannot be concluded that those mathematical models reflect the exact physical phenomena, they clearly include

more of the physics than previously elucidated, and they provide a basis for further development.

New mathematical models for the effective thermal conductivity of nanofluids containing carbon nanotubes have also been formulated. The predictions of those models agree reasonably well with the majority of the experimental data. Even with this progress in the area, research on physical mechanisms and mathematical models of the effective thermal conductivity of nanofluids is far from over. This conclusion is based on the facts that not all the experimental data are predicted and explained well by the mathematical models and that many mathematical models are of an empirical nature with empirical parameters to be determined from the experimental data. Therefore, in order to engineer effective nanofluids from basic principles, more effort is needed to develop comprehensive physics-based mathematical models that include the major influence factors and that can well predict experimental data. These future research efforts should include, but not be limited to, such topics as physical mechanisms, additive effects, combination models, carbon nanotube-based nanofluids, and experimental databases.

Heat Transfer Test Facility Upgrade

To expand the capability of the experimental system, both hardware and software in the heat transfer test facility has been upgraded. The main hardware upgrade was the replacement of the Rotameter with the Endress Hauser Promag flow meter, which provides consistently more stable and accurate flow rate measurements by sensing the magnetic field change within the flow stream and transmitting it electronically to the data acquisition system. The main software upgrade was the replacement of the IBASIC program with the Labview program, which provides more flexible control over the reading and display of sensor signals. A typical screen display of the Labview program is shown in Figure 1.



Figure 1. Screen display of Labview program

Particle Size Effect Study

While the effective density and specific heat of a nanofluid can be estimated based on physical principles—the viscosity and thermal conductivity of a nanofluid depend on many factors—among which the size of the particles suspended in the nanofluid is very important. The effects of the particle size on the viscosity and thermal conductivity of nanofluids have been reported by many research groups, including the Argonne nanofluid research team, which has provided insight into the influence of the particle size on the heat transfer coefficient of nanofluids—an ultimate indicator of nanofluid heat transfer performance. However, the experimental results have shown that the heat transfer coefficient of a nanofluid is usually beyond those of nanofluid thermal property effects alone. Therefore, experimental measurements of the heat transfer coefficient of nanofluids containing various particle sizes are essential to fully understand their effects on nanofluid thermal performance.

A series of forced convective heat transfer experiments was carried out for the SiC-water nanofluids with the particle volume concentration of 4.1% at four average particle sizes of 16, 29, 66, and 90 nm. The flow rates for all the studies were varied between 0.4 and 1.4 ml/min, which corresponded to Reynolds numbers between 6,000 and 20,000 using water properties with a constant inlet temperature of approximate 30°C. The heat transfer coefficient measured is compared on the basis of constant velocity for the four particle size nanofluids and water in Figure 2. While the heat transfer coefficients for nanofluids with the average particle sizes of 16 and 29 nm are 10.9 and 3.3% lower than

those of water, respectively; the heat transfer coefficients for nanofluids with the average particle sizes of 66 and 90 nm are 1.1% and 1.4% higher than those of water. As seen in Figure 3, the increased heat transfer coefficient of the nanofluids with larger particles (66 and 90 nm) over the base fluid remained consistent at all inlet temperatures tested (30, 43, and 55°C). This result suggests that heat transfer enhancement of a nanofluid is either weakly dependent on, or independent of, temperature. Consistent performance at all temperatures is a valuable and important feature for all heat transfer fluids. This is because they typically undergo a temperature large range during heating and cooling cycles in transportation systems. These results are in agreement with the observed effects of the particle size on the viscosity and thermal conductivity of the nanofluids. Therefore, for a given particle material, particle concentration, and solution pH, larger particles should be used to maximize nanofluid heat transfer potential.

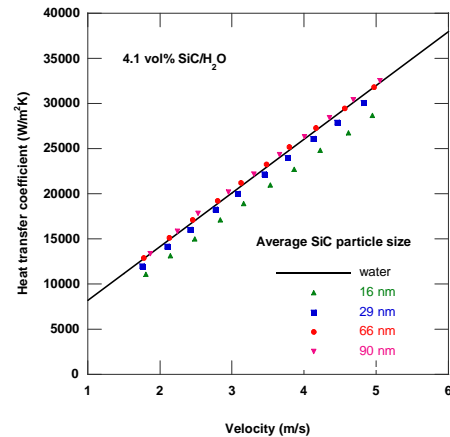


Figure 2. Heat transfer coefficient comparison

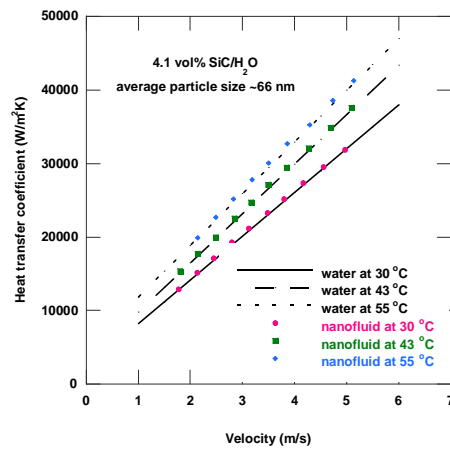


Figure 3. Inlet temperature effect

Ethylene Glycol/Water Based Nanofluids

Preliminary studies of 50/50 ethylene glycol/water based nanofluids have been conducted for a 29nm-SiC-50/50 ethylene glycol/water nanofluid with the particle volume concentration of 3.7%. While the heat transfer coefficient of the nanofluid was decreased by 7% over that of the base fluid at a velocity of 4 m/s (Figure 4), the heat transfer coefficient of the nanofluid was increased about 13% over that of the base fluid at a Reynolds number of 6000 (Figure 5). Recent results from our work, such as these, have redefined how comparisons must be made for applications in the transportation industry. The velocity comparison of Figure 4 is the proper one, and other results from our studies point to the directions to increase the nanofluid heat transfer enhancement when compared on this basis.

The experimental results also show that the heat transfer coefficient is well predicted for the SiC-50/50 ethylene glycol/water nanofluid (Figure 6). This result does not show the increase enhancement beyond fluid properties seen in the SiC-water nanofluid results of Figures 2 and 3. However, it should be noted that although prediction is required for application and fundamental understanding, commercial viability is related to enhancement independent of predictability. During the past year, we have made substantial advancement towards that end.

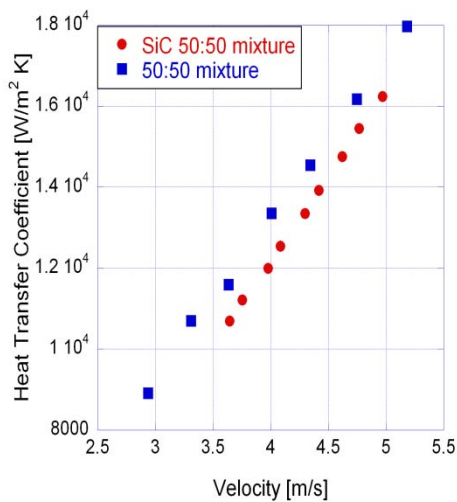


Figure 4. Velocity based comparison

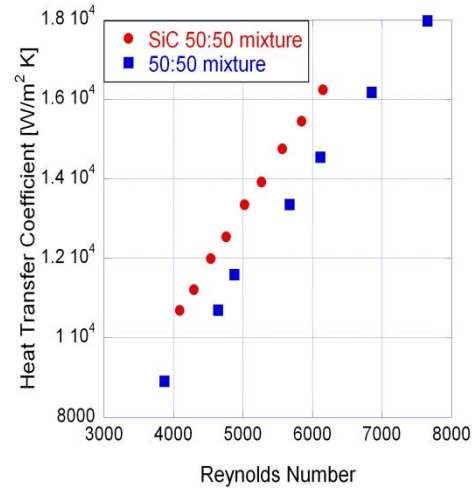


Figure 5. Reynolds number based comparison

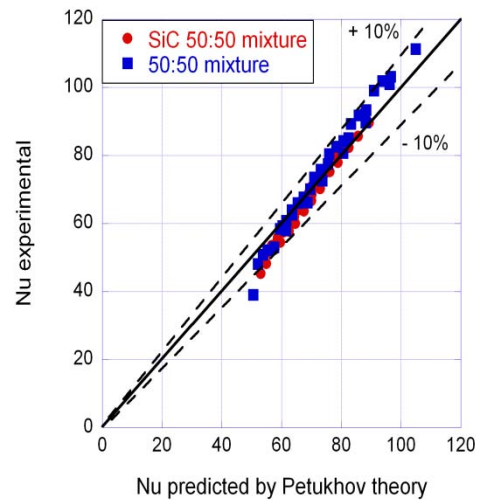


Figure 6. Nusselt number comparison

Conclusions

The theoretical conclusions from the thermal conductivity model studies and the experimental data from the heat transfer studies of SiC-water and SiC-50/50 ethylene glycol/water nanofluids have provided substantial insights in how to develop nanofluids with optimized heat transfer performance including choosing the particle size, controlling the solution pH, utilizing appropriate additives, lowering the effective viscosity, and increasing the effective thermal conductivity. This knowledge will be used in guiding the future development of ethylene glycol/water based nanofluids for vehicle thermal control applications of this project.

Future Directions

Future research will concentrate on developing 50/50 ethylene glycol/water based nanofluids that are optimized with respect to the base fluid properties, nanoparticle properties (material, concentration, shape, size, and size distribution), and additive properties (including pH) to provide the best combination of a stable suspension, low viscosity, high thermal conductivity, and high heat transfer coefficient. We have attracted the interest of a major truck original equipment manufacturer (OEM) who is interested in testing an optimized nanofluid at their test facility.

Publications

W. Yu, D. M. France, J. L. Routbort, and S. U. S. Choi, Review and Comparison of Nanofluid Thermal Conductivity and Heat Transfer Enhancements, *Heat Transfer Engineering* 29 (5) (May 2008) 432-460.

G. Chen, W. Yu, D. Singh, D. Cookson, and J. Routbort, Application of SAXS to the Study of Particle-Size-Dependent Thermal Conductivity in Silica Nanofluids, *Journal of Nanoparticle Research (Special Focus: Thermal Conductivity of Nanofluids)*, 10 (7) (October 2008) 1109-1114.

D. Singh, E. Timofeeva, W. Yu, J. Routbort, D. France, D. Smith, and J. M. Lopez-Cepero, An Investigation of Silicon Carbide-Water Nanofluid for Heat Transfer Applications, *Journal of Applied Physics* 105 (6) (March 2009) 064306.

Wenhua Yu, David M. France, David S. Smith, Dileep Singh, Elena V. Timofeeva, Jules L. Routbort, Heat Transfer to a Silicon Carbide/Water Nanofluid, *International Journal of Heat and Mass Transfer* 52 (15-16) (July 2009) 3606-3612.

Wenhua Yu, David M. France, Dileep Singh, Elena V. Timofeeva, David S. Smith, Jules L. Routbort, Mechanisms and Models of Effective Thermal Conductivities of Nanofluids, accepted for publication in the *Journal of Nanoscience and Nanotechnology*.

Dileep Singh, Jules L. Routbort, Wenhua Yu, Elena Timofeeva, David Smith, David France, Heat

Transfer Fluids Containing Nanoparticles, pending U.S. patent application.

B. Agreement # 16824 – Efficient Cooling in Engines with Nucleate Boiling

Principal Investigator: Wenhua Yu

(coworkers: David France, Jules Routbort, and Roger Smith)

Argonne National Laboratory

9700 South Cass Avenue, Building 212, Argonne, IL 60439

Phone: (630) 252-7361; fax: (630) 252-5568; e-mail: wyu@anl.gov

DOE Technology Development Manager: Lee Slezak

(202) 586-2335, Lee.Slezak@hq.doe.gov

Contractor: UChicago Argonne, LLC

Contract No.: DE-AC02-06CH11357

Objectives

- Investigate the potential of two-phase flow in engine cooling applications.
- Determine limits on two-phase heat transfer (occurrence of critical heat flux or flow instability).

Approach

- Experimentally determine heat transfer rates and critical heat fluxes in small channels with water and a mixture of 50% ethylene glycol in water.
- Perform experiments over a large concentration range of ethylene glycol in water.
- Experimentally determine heat transfer characteristics for subcool flow boiling of water and ethylene glycol/water mixtures.
- Perform experiments with alternative fluids.

Accomplishments

- Completed heat loss calibration tests and data analyses for both the horizontal and vertical test sections.
- Completed single-phase experimental tests and data analyses for the Nusselt numbers and Fanning friction factors of both the horizontal and vertical flows.
- Developed a new procedure based on the ideal mixture and equilibrium assumptions along with Raoult's law to analytically calculate the boiling temperatures and, subsequently, the local heat transfer coefficients, along the test section.
- For horizontal flow boiling:
 - Completed experimental tests and data analyses for the two-phase pressure gradients and boiling heat transfer coefficients to water and ethylene glycol/water mixtures.
 - Developed a pressure drop correlation modified from Chisholm's correlation with a concentration factor to better predict pressure drops for ethylene glycol/water mixtures.
 - Developed a general correlation of boiling heat transfer coefficients(modified from Argonne's boiling heat transfer correlation) with a concentration factor for the prediction of heat transfer rates of flow boiling in small channels, including refrigerants, water, and ethylene glycol/water mixtures.
- For vertical flow boiling, completed experimental tests for the two-phase pressure gradients and boiling heat transfer coefficients to water and ethylene glycol/water mixtures and performed preliminary data analyses for water and 50% ethylene glycol in water mixture.

- A paper from the project, published in the prestigious International Journal of Multiphase Flow, was one of the most cited articles for the years 2002 to 2005 with over 60 citations (as recently identified by the journal).

Future Directions

- Continue systematic data analyses for the two-phase pressure gradients and boiling heat transfer coefficients of vertical flow boiling to water and ethylene glycol/water mixtures. Develop predictive correlations for pressure drops and heat transfer coefficients to provide essential information for design of a nucleate-boiling cooling system.
- Study the effect of vertical versus horizontal flows on two-phase heat transfer.
- Experimentally determine heat transfer characteristics for subcool flow boiling of water and ethylene glycol/water mixtures.
- Perform systematic experiments with alternative fluids.

Introduction

Analyses of trends in the transportation sector indicate that future engine cooling systems may have to cope with greater heat loads because of more powerful engines, more air conditioning, more stringent emissions requirements, and additional auxiliary equipment. Also, reducing the size of cooling systems can reduce vehicle weight, reduce coolant pumping power, and lead to improved aerodynamic profiles for vehicles—all of which contribute to reduced fuel consumption. To achieve these benefits, researchers need to design cooling systems that occupy less space, are lightweight, have reduced fluid inventory, and exhibit improved performance. Among various new cooling systems proposed, nucleate boiling has great potential to meet these challenges. Order-of-magnitude higher heat transfer rates can be achieved in nucleate-boiling cooling systems when compared with conventional, single-phase, forced-convective cooling systems. However, successful design and application of nucleate-boiling cooling systems for engine applications require that the critical heat flux and flow instabilities not be reached. Therefore, a fundamental understanding of flow boiling mechanisms under engine application conditions is required to develop reliable and effective nucleate boiling cooling systems.

Cooling engine areas such as the head region often contain small metal masses that lead to small coolant channels. This geometry, in turn, leads to low mass flow rates that minimize pressure drop. Although significant research has been performed on boiling

heat transfer and the critical heat flux phenomenon, results applicable for engine cooling systems are limited. The purpose of the present study is to investigate the characteristics of coolant boiling, critical heat flux, and flow instability under conditions of small channel and low mass fluxes.

The test apparatus used in this investigation was designed and fabricated to study boiling heat transfer, two-phase pressure drop, critical heat flux, and flow instability of flowing water, ethylene glycol, and aqueous mixtures of ethylene glycol at high temperature (up to 250°C) and low pressure (<345 kPa). Figure 1 shows a schematic of the apparatus.

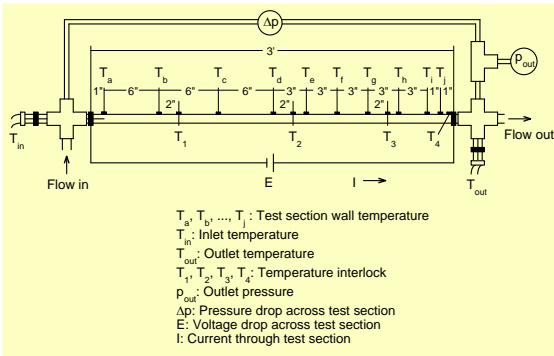
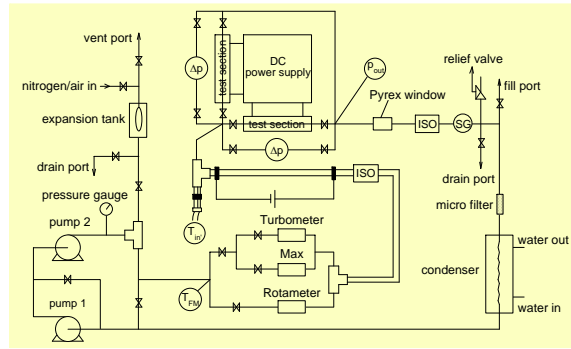


Figure 1. Schematic diagram of test apparatus (top) and test sections (bottom)

The apparatus is a closed loop that includes two serially arranged pumps with variable speed drives, a set of flowmeters, an accumulator, a preheater, a horizontal test section, a vertical test section, and a condenser. The flowmeter set, including various types and sizes, was chosen to cover a large range of flow rates and was calibrated traceable to the National Institute of Standards and Technology (NIST). The estimated uncertainty in the measurements of flow rates was $\pm 3\%$. The bladder-type accumulator allows for stable control of the system pressure. The preheater provides a means to set the inlet temperature of the test sections at various desired levels. Both the preheater and test sections were resistance-heated with controllable direct-current (DC) power supplies. Provisions were made to measure temperatures along the test section for calculating heat transfer coefficients. The pressures and temperatures at the inlet and outlet of the test section were also measured. Pressure transducers and thermocouples were calibrated against standards traceable to NIST. The estimated uncertainty in the measurements of pressures and temperatures were $\pm 3\%$ and $\pm 0.2^\circ\text{C}$, respectively. As a safety precaution, both the preheater and test

sections were provided with high-temperature limit interlocks to prevent them from overheating. After leaving the test section, the two-phase flow was condensed into a single-phase flow, which returned to the pumps to close the system.

To switch between the horizontal- and vertical-flow test sections, an interfacial connector was fabricated (shown in Figure 2). This device establishes a connection between the test-section sensor instruments and the data-acquisition computer system. It allows for easily switching between the horizontal and vertical test sections, which share the rest of the test loop.



Figure 2. Interfacial connector

A data acquisition system consisting of a computer and a Hewlett-Packard multiplexer was assembled to record outputs from all sensors. A data acquisition program, which includes all calibration equations and conversions to desired engineering units, was written. The data acquisition system provides not only an on-screen display of analog signals from all sensors and graphs of representative in-stream and wall-temperature measurements, but also a means of recording temperature and pertinent information such as input power (voltage across the test section and current through the test section), mass flux, outlet pressure, pressure drop across the test section, and outlet quality for further data reduction.

Results and Discussion

Heat Loss Calibration

Although the experimental test section was well insulated thermally from the atmosphere to minimize heat loss to the environment, the heat loss was not negligible during boiling heat transfer tests

because of the small experimental test section, the low fluid flowrates, and the relatively high driving temperatures. Therefore, heat loss tests were performed for the experimental test section wall temperatures up to the boiling heat transfer conditions, and the slight heat loss was subsequently incorporated into the data reduction procedure for boiling heat transfer data. The heat loss was characterized through a special series of experiments with no fluid in the experimental test section. Power was applied to the experimental test section to bring its wall temperature to a selected level. The input power required for maintaining the wall temperature at the selected value is the heat loss rate \dot{q}_{loss}

$$\dot{q}_{loss} = power$$

which is related to the difference between the experimental test section wall temperature T_w and the ambient temperature $T_{ambient}$. By assuming a linear dependence on the driving temperature, the heat loss rate can be expressed approximately as

$$\dot{q}_{loss} = \alpha(T_w - T_{ambient})$$

where the proportional constant α was determined from the heat loss tests. (This constant depends on the heat transfer coefficient and the heat transfer surface area between the experimental test section and ambient for this particular experimental apparatus.) Figure 3 shows the heat loss rate per length as a function of the driving temperature for both the horizontal and the vertical experimental test sections. The test section heat loss was <5% of the applied input power to the experimental test section in all subsequent heat transfer tests.

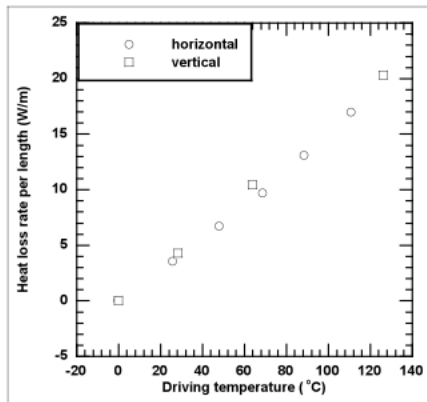


Figure 3. Heat loss calibration

Single-Phase Heat Transfer Verification

To validate the test apparatus, a series of single-phase heat transfer experiments was carried out before two-phase boiling experiments. The single-phase heat transfer experiments were performed at a system pressure of 120–200 kPa, sufficient to keep the test fluids in the liquid phase during heating. During the single-phase heat transfer experiments, the experimental parameters of the test fluids such as temperatures and flowrates were chosen to maintain turbulent flow conditions with their Reynolds numbers >2500. The results of the single-phase Nusselt numbers Nu for the liquid Reynolds numbers in the range of $Re_l = 2250-13000$ and the liquid Prandtl numbers in the range of $Pr_l = 2-18$ were compared with the well-known Gnielinski correlation (Gnielinski 1976)

$$Nu = \frac{(f/8)(Re_l - 1000)Pr_l}{1 + 12.7(f/8)^{1/2}(Pr_l^{2/3} - 1)}$$

where the predicted friction factor f is defined as

$$f = (1.82 \log Re_l - 1.64)^{-2}$$

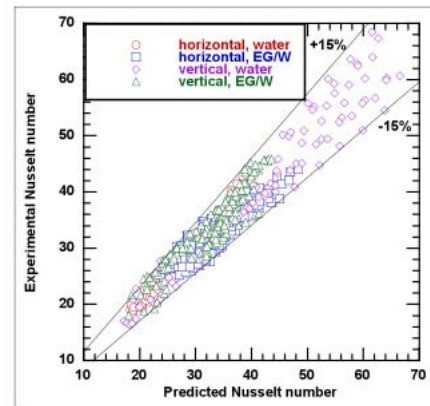


Figure 4. Nusselt number comparison

As shown in Figure 4, where the local Nusselt numbers are plotted, the experimental data are in a good agreement with the predicted values from the Gnielinski correlation with a mean deviation of 7%. Almost all experimental data are within $\pm 15\%$ of the predictions. The Fanning friction factors calculated from the experimental pressure drop data were compared with the standard Blasius correlation (Blasius 1913)

$$f_{\text{Blasius}} = 0.0791 \text{Re}^{-0.25}$$

As shown in Figure 5, the experimental data are in a good agreement with the predicted values from the Blasius correlation with a mean deviation of 9%. These single-phase heat transfer coefficient and pressure-drop results serve as validation of the accuracy of the instrumentation, measurements, data acquisition, and data reduction procedures. They are an “end-to-end” final validation of the experimental apparatus.

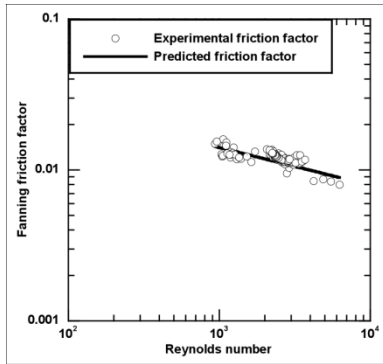


Figure 5. Fanning friction factor comparison

Two-Phase Data Reduction

To calculate local boiling heat transfer coefficients of an ethylene glycol/water mixture, the water-vapor mass fractions, mixture vapor mass qualities, and mixture temperatures, along the experimental test section must be determined. Researchers have used various approaches in making these determinations. Perhaps the simplest approach is to assume that the mixture boiling temperature is constant along the test section and equal to the mean of the zero quality temperature and the temperature at the test section outlet. This approach is not conducive to the determination of local heat transfer coefficients along the length of the test section, as done in the present study. Accuracy can be increased by assuming a linear mixture temperature distribution along the test section. Another approach is to utilize a mixture equation of state, such as the hard-sphere equations. However, ideal mixture and equilibrium assumptions along with Raoult’s law are sufficient to calculate the boiling temperature along the test section and, subsequently, the local heat transfer coefficients with the highest degree of accuracy among the approaches presented. This ideal mixture calculation approach was developed and adopted in

this study. Assuming an ideal mixture and applying Raoult’s and Dalton’s laws to it, one can derive the following equations for determining the water vapor mass fraction F_v , mixture vapor mass quality x , and mixture temperature T_m

$$F_v = \frac{9p_w(p_m - p_{EG})}{31p_m(p_w - p_{EG}) - 22p_w(p_m - p_{EG})}$$

$$x = \frac{31F_m(p_w - p_{EG}) - (9 + 22F_m)(p_m - p_{EG})}{31F_v(p_w - p_{EG}) - (9 + 22F_v)(p_m - p_{EG})}$$

$$T_m = T_{mo} - \frac{\dot{q}/\dot{m} + [F_{vi}i_{fgwi} + (1 - F_{vi})i_{fgegi}]x_i - [F_{vo}i_{fgwo} + (1 - F_{vo})i_{fgego}]x_o}{[F_m C_{pw} + (1 - F_m)C_{pegl}]}$$

where p is the pressure, T is the temperature, F is the mass fraction, x is the mass quality, C_p is the specific heat, i_{fg} is the latent heat of vaporization, \dot{q} is the heat transfer rate, and \dot{m} is the mass flow rate.

Horizontal Flow Boiling

Both experimental tests and data analyses for two-phase boiling heat transfer of horizontal flows to water and ethylene glycol/water mixtures have been completed. The main results are reported below.

Boiling Curve. Figure 6 shows the heat flux as a function of wall superheat for boiling of water and ethylene glycol/water mixtures in small channels. As can be seen from the figure, generally, the saturation boiling in small channels can be divided into three boiling regions: convection dominant, nucleation dominant, and the transition between the two.

Both convective heat transfer and boiling heat transfer exist in all three regions, but their proportions are different in these regions. In the convection-dominant-boiling region, the wall superheat is low, usually less than a few degrees centigrade. Although there is boiling heat transfer, the dominant mechanism is convective heat transfer. As a result, the mass quality and heat transfer rate are quite low compared with those in the other two regions. In the nucleation-dominant-boiling region, the wall superheat is higher than that in the convection-dominant-boiling region but lower than certain upper limits that depend on mass flux. Opposite to the convection-dominant boiling, the boiling heat transfer in the nucleation-dominant boiling is so developed that it becomes dominant,

and the heat transfer rate is much higher than that in convection-dominant boiling. As can be seen from Figure 6, the heat flux in this region is independent of mass flux and can be predicted with a power-law function of wall superheat. This characteristic was used in correlating the heat transfer data. In the transition-boiling region, the wall superheat is relatively high. The heat flux in this region is also high and close to the critical heat flux. The boiling in this region is unstable, and a small change in the heat flux will result in a large change in wall

superheat. If the heat flux increases further, it is possible for the system to reach a critical point, producing an undesirably large increase in the wall superheat.

The above discussion shows that nucleation-dominant boiling is desired in engineering applications for both high heat transfer rate and stable flow boiling without reaching the critical point.

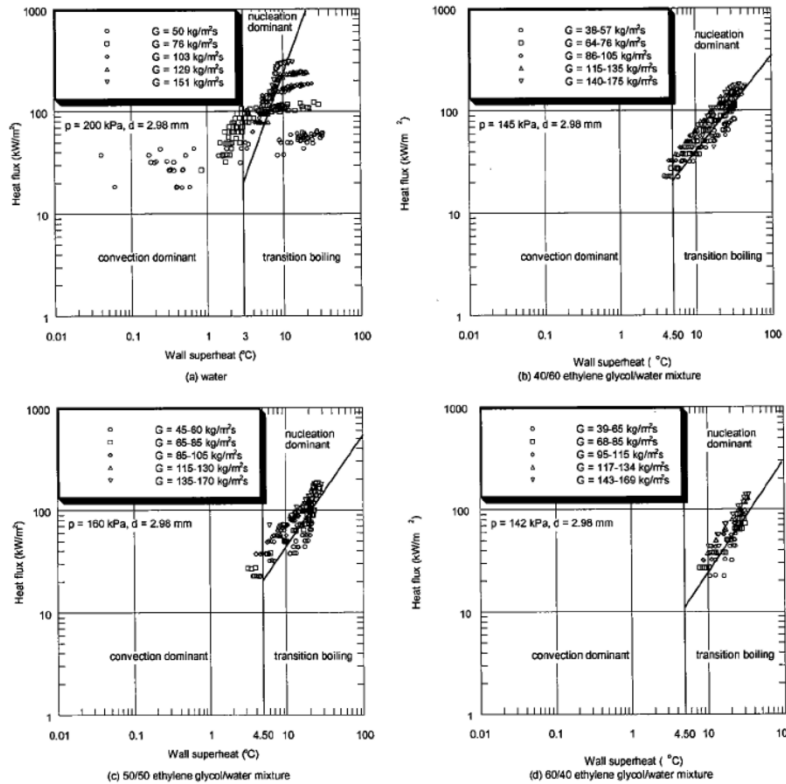


Figure 6. Heat flux as a function of wall superheat

Two-Phase Pressure Drop. The concept of two-phase multipliers proposed by Lockhart and Martinelli (X), and the correlation of those multipliers by Chisholm, were used to compare predictions with the present experimental data. As can be seen from Figure 7, the experimental data are in reasonable agreement with the Chisholm predictions both in values and trends—even though the Chisholm correlation slightly over-predicts the experimental data.

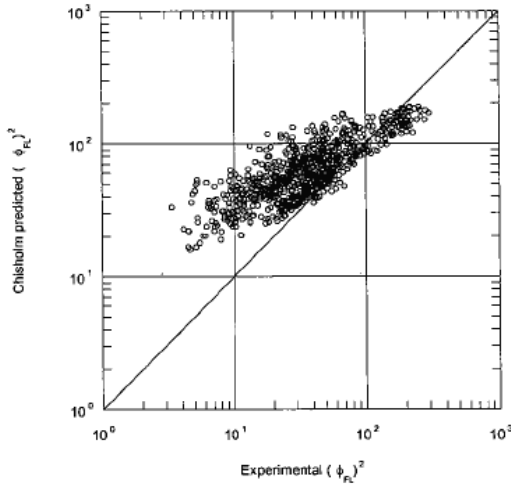


Figure 7. Frictional pressure gradient

To better predict the experimental data and to take the concentration factor into account, the constant parameter $C=12$ in Chisholm’s correlation was modified into a function of the volume concentration (ϕ_v) of ethylene glycol/water mixtures, and Chisholm’s correlation then becomes

$$\phi_{FL}^2 = 1 + \frac{12[1 - 2.8v(1 - v)]}{X} + \frac{1}{X^2}$$

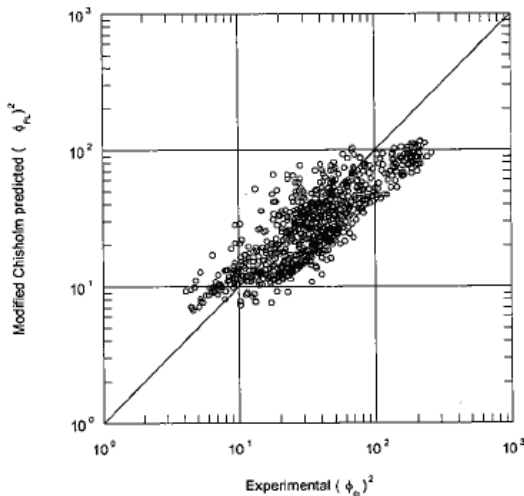


Figure 8. Frictional pressure gradient

This correlation reduces to Chisholm’s correlation for both pure water ($v=0$) and pure ethylene glycol ($v=1$). In Figure 8, the experimental data are compared with the predictions of the modified Chisholm’s correlation. This modification improves the predictions both in values and trends.

Heat Transfer Coefficient. In the present study, the nucleation-dominant boiling data have the following characteristics.

(a) Although both convective heat transfer and nucleate-boiling heat transfer exist, the dominant heat transfer mechanism is nucleate boiling. Because the nucleate-boiling heat transfer rate is much higher than the convective heat transfer, the latter can be neglected.

(b) As shown in Figure 6, the boiling heat transfer is dependent on heat flux but almost independent of mass flux. This finding means that, for a specific fluid, the boiling heat transfer coefficient can be expressed as a function of heat flux.

(c) The heat transfer coefficients have different dependence on heat flux for different fluids. Therefore, deriving a general correlation for boiling heat transfer coefficients requires fluid properties in the correlation.

(d) Argonne researchers employed the dimensionless parameter combinations in the form of boiling number, Weber number, and liquid-to-vapor density ratio in developing different predictive correlations for boiling heat transfer coefficients with different fluids, and the predicted results are quite good.

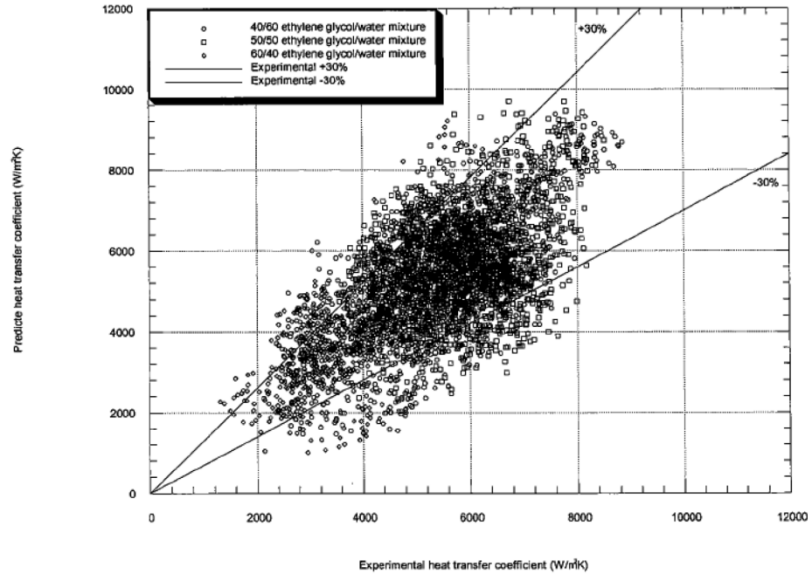


Figure 9. Heat transfer coefficient comparisons (nucleation-dominant-boiling region)

Based on the above facts, Argonne extended the dimensionless property term parameter to include the liquid-to-vapor viscosity ratio, which produced good correlation of boiling heat transfer data (h) for water, 50/50 ethylene glycol/water mixture, refrigerant 12, and refrigerant 134a.

$$h = 135000(BoWe_l^{0.5})^{0.5}[(\rho_l/\rho_v)^{-0.5}(\mu_l/\mu_v)^{0.7}]^{-1.5}$$

In the above equation, ρ is the density, μ is the viscosity, and the boiling number Bo and the Weber number We_l are defined, respectively, as $Bo = q''/(Gi_{fg})$ and $We_l = G^2D/(\rho_l\sigma)$, where q'' is the heat flux, i_{fg} is the latent heat of boiling, G is the mass flux, D is the diameter, and σ is the surface tension. For this heat transfer equation to be used for the prediction of experimental data for ethylene glycol/water mixtures with concentrations other than 50/50, Argonne further modified it with a concentration correction factor, which reduces to 1 for concentrations of $v=0$ and $v=0.5$. The new correlation can be expressed as

$$h/h^* = [1 + 6v(v - 0.5)](BoWe_l^{0.5})^{0.5}[(\rho_l/\rho_v)^{-0.5}(\mu_l/\mu_v)^{0.7}]^{-1.5}$$

where h^* is a characteristic heat transfer coefficient of 135 kW/m²·K for all of the data.

Figure 9 shows the experimental data and the predicted values obtained with the correlation for

ethylene glycol/water mixtures. The predictions are in good agreement with the experimental data, and most are within $\pm 30\%$ of the data. Note that the comparisons are only for the data within the nucleation-dominant-boiling region. The success of the correlation in predicting the heat transfer coefficients of fluids boiling in small channels is directly related to the trend, as presented in Figure 6, that the heat transfer data are dependent on heat flux but not mass flux. The fact that the equation is also heat-flux but not mass-flux dependent is in accord with the experimental data.

Vertical Flow Boiling

In the application of engine cooling, both horizontal and vertical flows exist. Therefore, it is necessary to investigate the impact of vertical versus horizontal flows on two-phase heat transfer.

Experimental tests for two-phase boiling heat transfer of vertical flows to water and ethylene glycol/water mixtures have been completed. Preliminary data analyses for water boiling and 50% ethylene glycol in water mixture have been performed.

Boiling Curve. Figure 10 shows heat flux as a function of wall superheat for boiling water and 50% ethylene glycol in water mixture at various mass flux levels and ambient inlet temperature. As can be seen in the figure, the curve for vertical flow boiling

follows the same trend as that for horizontal flow boiling. However, to reach the same wall superheat, the heat flux (and, in turn, the critical heat flux) for vertical flow boiling is higher than for horizontal flow boiling. This result is expected because the vapor distribution for vertical flow boiling is more uniform than that for horizontal flow boiling due to the influence of gravity. This phenomenon is important for the design of nucleate boiling cooling systems. Because a practical cooling system usually contains both horizontal and vertical channels, the design of a nucleate boiling cooling system will be too conservative if based only on the horizontal-flow boiling data and too optimistic if based only on the vertical-flow boiling data.

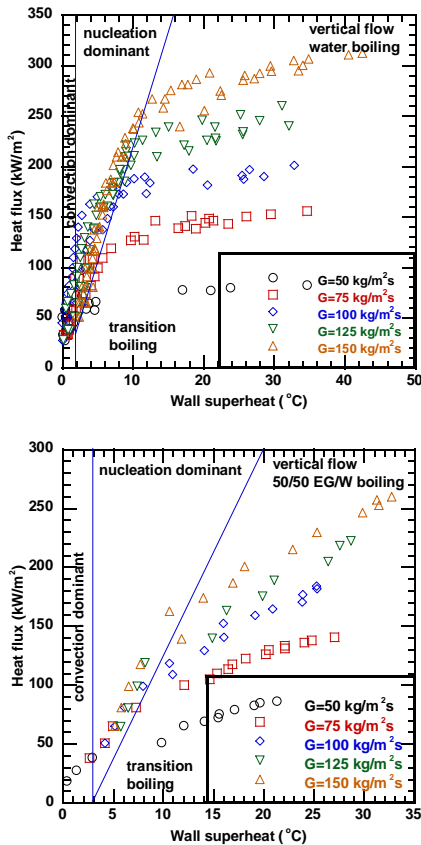


Figure 10. Vertical flow boiling curve

Heat Transfer Coefficient. Figure 11 compares the heat transfer coefficient data of the two-phase vertical flow boiling for water and 50% ethylene glycol mixture with the predictions of the correlation developed by Argonne based on the horizontal boiling data. The limited data show that heat transfer coefficients for vertical flow boiling are greater than those for horizontal flow boiling. It should be noted

that the comparisons are only for the data within the nucleation-dominant boiling region. If further experimental data analyses confirm this trend, it is necessary to develop new correlations to predict vertical flow boiling data.

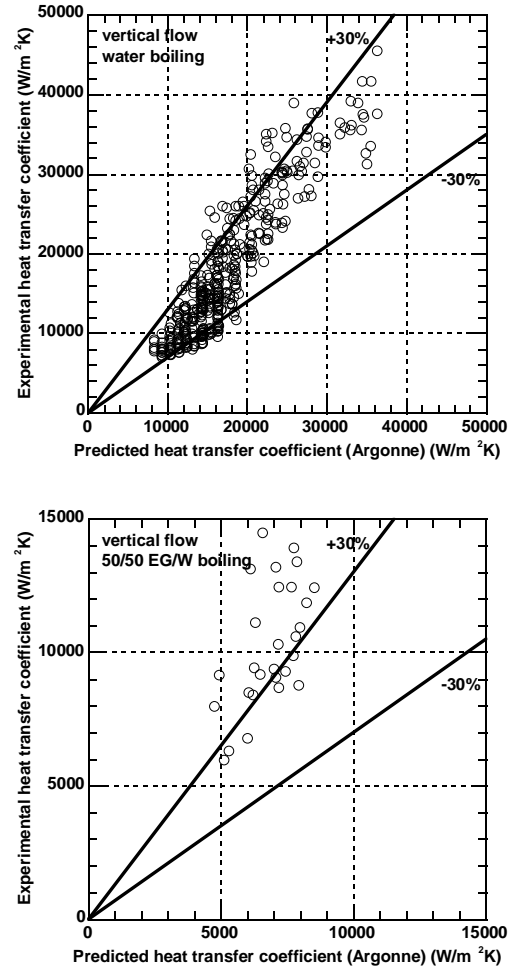


Figure 11. Heat transfer coefficient comparisons

Conclusions

Excellent progress has been made on the experiments and analyses for this project.

(a) A new procedure has been developed that can analytically calculate the boiling temperatures and, subsequently, the local heat transfer coefficients, along the test section by using ideal mixture and equilibrium assumptions along with Raoult’s law. This procedure can be easily used for designing cooling systems with flow boiling.

(b) For horizontal flow boiling, two-phase frictional pressure gradients of ethylene glycol/water mixtures follow similar trends as those of water. The results are in reasonable agreement with the predictions of Chisholm's correlation. A modification has been made to Chisholm's correlation, which reduces to Chisholm's correlation for concentrations $x = 0$ and $x = 1$. This modified Chisholm's correlation improves the predictions of pressure drop for ethylene glycol/water mixtures.

(c) The experiments show a high heat transfer rate with ethylene glycol/water mixtures, which is a positive result for engine cooling. Argonne developed a general correlation based on horizontal flow boiling data for water, ethylene glycol/water mixtures (concentrations 40/60, 50/50, and 60/40), and refrigerants. This correlation predicts the experimental data quite well, and most of the predicted values are within $\pm 30\%$ of the experimental data.

(d) It was found that the boiling heat transfer of ethylene glycol/water mixtures is mainly limited by flow instability rather than critical heat fluxes that usually constitute the limits for water boiling heat transfer. Tests show that stable, long-term, two-phase boiling flow is possible for ethylene glycol/water mixtures as long as the mass quality is less than a certain critical value (approximately < 0.2). The heat transfer rate at this mass quality is significantly higher than that of conventional, single-phase, forced-convective heat transfer.

(e) Results from the preliminary data analyses of vertical flow boiling to water and 50% ethylene glycol mixture show the similar trend of the wall superheat increasing with the heat flux except that, to reach the same wall superheat, the heat flux for vertical flow boiling is higher than that for horizontal flow boiling. These results imply that the critical heat flux for vertical flow boiling is higher than that for horizontal flow boiling. The heat transfer coefficients for vertical flow boiling are greater than those for horizontal flow boiling. These preliminary results will be verified by the ongoing experimental data analyses of vertical flow boiling.

Future Directions

Future research will concentrate on finishing experimental data analyses for vertical flow boiling

of water and ethylene glycol/water mixtures and, if necessary, developing new predictive correlations for two-phase pressure drops and heat transfer coefficients. The final results are expected to provide essential information for the design of nucleate-boiling cooling systems.

C. Agreement # 15529 - Erosion of Materials in Nanofluids

(This project is jointly funded by Propulsion Materials and Heavy Vehicle Systems Optimization)

Principal Investigators: J. L. Routbort and D. Singh
Argonne National Laboratory
9700 S. Cass Avenue, Argonne, IL 60439-4838
(630) 252-5065; fax: (630) 252-5568; e-mail: routbort@anl.gov

DOE Technology Manager: Jerry L. Gibbs
(202) 586-1182; fax: (202) 586-1600; e-mail: jerry.gibbs@ee.doe.gov

Contractor: UChicago Argonne LLC
Contract No.: DE AC02 06CH11357

Objective

- Determine if the use of fluids containing a variety of nanoparticles result in erosive damage to radiator materials and coolant pumps.
- If damage occurs, then develop models to predict the erosive damage.

Approach

- Develop an experimental apparatus to measure erosive loss.
- Conduct experiments to study erosive damage of fluids containing various types and sizes of nanoparticles on typical radiator materials.
- Develop methods to characterize nanofluids and analyze erosion results.

Accomplishments

- Little erosion damage to a typical radiator material (aluminum Al3003) was observed in experiments performed using copper oxide (CuO) nanoparticles in ethylene glycol having impact angles of 30 and 90° and velocities up to 10m/s for impact for a total time of 3620 hrs. Particle concentration varied between 0.1 and 0.85 vol %.
- Utilized small-angle X-ray scattering, dynamic light scattering, and surface area measurements to measure nanoparticle size, distribution, and shape.
- Determined that polymeric gears are degraded by a SiC/water nanofluid.
- Determined that a 130-nm, 2-vol % SiC/water nanofluid does not degrade aluminum Al3003 after over 700 hours of accelerated testing at 8 m/s for 30° and 90° impacts.
- Designed, built, and calibrated a new erosion apparatus to measure the wear in an automotive water pump and the torque required to pump nanofluids.

Future Direction

- Erosion of typical radiator materials using fluids containing a variety of well-characterized nanoparticles will be measured, varying the angle, size of the nanoparticles, impact velocity, nanoparticle volume percent, and temperature.
- If erosion occurs, develop a predictive model.
- Determine wear of nanofluids on automotive pump cast aluminum impeller.
- Measure the pump power of nanofluids and compare to base fluids

Forward

Efforts have shifted away from the in-house production of nanofluids, to development of advanced characterization techniques and establishment of working relationships between companies that produce nanofluids. Our principal partner on a related project for the Industrial Technology Program is Saint Gobain. They have been supplying SiC/water nanofluids for industrial cooling. ANL has been characterizing the nanoparticles, adding ethylene glycol to produce a nanofluid suitable for radiator cooling, and reducing the viscosity by changing the pH. Fluids that show promise from a heat transfer perspective will be characterized by measuring the viscosity, thermal conductivity, and heat transfer coefficients while particle sizes will be measured by small-angle X-ray scattering (SAXS) and dynamic laser scattering (DLS). Finally, liquid erosion tests will be performed to determine the pumping power and if the nanofluid will cause deleterious damage to radiator materials.

Introduction

Many industrial technologies face the challenge of thermal management. Cooling is a crucial issue in transportation. Thermal loads are ever-increasing due to trends toward greater power output for engines and exhaust gas recirculation for diesel engines. The conventional approach for increasing cooling rates is use of extended surfaces such as fins and microchannels. Reducing radiator size will reduce the frontal area and hence the aerodynamic drag. However, current radiator designs have already stretched these approaches to their limits. Therefore, an urgent need exists for new and innovative concepts to achieve ultra-high-performance cooling. Nanofluids seem to show enormous potentials as a coolant for radiators. Literature contains many examples of increased thermal conductivity of fluids by the addition of nanoparticles (see review by Yu, et al. [1]). Enhanced thermal conductivity could lead to enhanced heat transfer. A CFD calculation of a Cummins 500 hp diesel engine using an ideal nanofluid as coolant has shown that the radiator size could be reduced by 5% [2], reducing weight and size, and hence aerodynamic drag.

In order for the enhanced thermal conductivity to be utilized, it must be shown that liquid erosion of typical radiator materials will be tolerable and that the increased pumping power resulting from higher viscosity will not exceed the gain in parasitic energy losses from enhanced cooling. If nanofluids result in excessive erosive wear or very high increased pumping power, they cannot be used. Hence, the Vehicle Technologies Program has funded an investigation on liquid erosion of radiator materials using nanofluids.

Results and Discussion of Erosion

A photograph of the recently built and calibrated liquid erosion apparatus is shown in Figure 1.



Figure 1. Photograph of the liquid erosion apparatus

The apparatus consists of a reservoir containing the fluid and an automotive pump with a cast aluminum impeller attached to a motor controlled electronically to ± 5 RPM. The pump can be isolated and drained and the impeller removed to measure any possible weight loss resulting from erosion. A very accurate, calibrated strain gauge is mounted on the shaft of the motor so that the torque required to pump the nanofluids can be measured and compared to the base fluid.

The flow is measured by a magnetic flow meter that has been calibrated by measuring the weight of fluid/unit time. It is accurate to $\pm 2\%$ and the voltage that is linearly proportional to the flow is measured by a calibrated voltmeter. Flows of about 27 liters/minute are readily achievable. The specimen chamber remains the same as was pictured in the fiscal year (FY) 2007 annual report but is also

shown in Figure 2. The fluid temperature in the reservoir and the specimen chamber are monitored by thermocouples. The velocity in the specimen chamber can easily reach 10m/s for accelerated erosion testing.

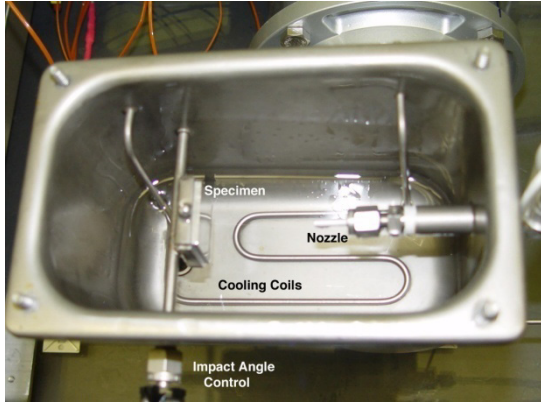


Figure 2. View of specimen chamber with cover removed

A schematic of the pumping system is shown in Figure 3.

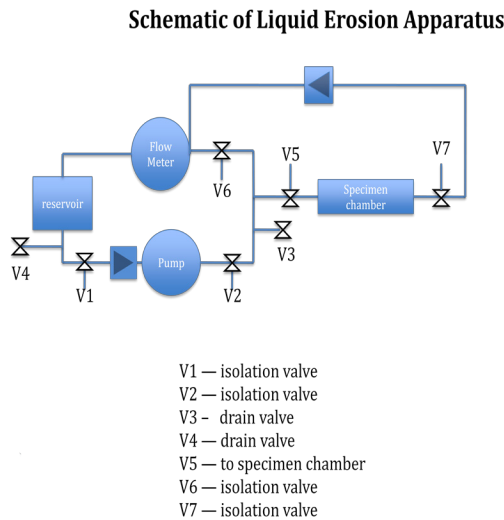


Figure 3. Schematic of new liquid erosion apparatus, torque meter and motor are included in the pump

Figure 4 presents results of the torque measurements for the base fluids and three concentrations of nominal 170nm SiC in water nanofluids. The 170 nm are believed to represent the agglomerated size. Surface area measurements (reported in the section “Nanofluid Development for Engine Cooling Systems” of the FY 2009 Annual Report for Heavy Vehicle Systems Optimization) indicate that the

actual individual particle size is 29 nm [3]. The nanofluids have not been modified for reduced viscosities. The results are as expected: increasing the concentration of nanoparticles increases the torque required to pump them.

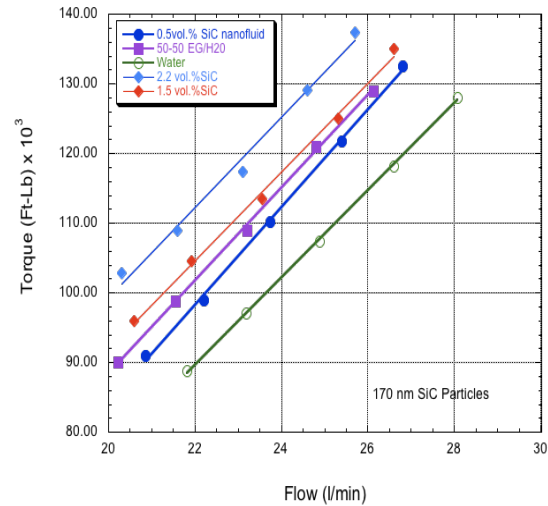


Figure 4. Measurement of the torque as a function of flow rate for water (green), 50% ethylene glycol-50%water (purple), and three different concentrations of SiC-water based nanofluids; each point is the average of between 4 and 6 datum

However, while the torque increases with increasing nanoparticle concentration it should be realized that (1)water has a very low viscosity;(2) a mixture of ethylene glycol and water has a much higher viscosity; and (3) changing the pH and using surfactants can modify the viscosity in alumina [4] or SiC based nanofluids [5]. Additionally, and equally as important, the size can affect the thermal conductivity, viscosity, and heat transfer [4,5]. Larger sizes have a reduced interfacial resistance and hence have a higher thermal conductivity [5]. The above observations open the way of engineering the properties of nanofluids by selecting particle sizes and controlling the chemistry.

SiC is a very promising nanoparticle. It will not oxidize and has a relatively high thermal conductivity—over five times greater than CuO. Also, after 750 hours of testing the 2 vol% SiC/water nanofluid at 8 m/s and at an impact angle of 30°, there was no erosion damage to the aluminum 3003 target. This is most encouraging from an engineering viewpoint.

The above observation was obtained at one condition and does not represent the most severe conditions. Hence, it would be premature to conclude that nanofluids will cause no damage in cooling systems.

Issues & Future Direction

The new liquid apparatus will allow several important parameters to be determined. First, we will be able to measure the increased pumping power resulting from the higher viscosity of the nanofluid. This is extremely important from an energy efficiency point of view. Furthermore, the measurements can be compared to theory and hence can be extrapolated for other nanofluid viscosities.

The new apparatus will allow continued measurements of the erosion of nanofluids on targets made from radiator materials at controlled impact angles and velocities. If erosion occurs, we will use this data, in conjunction with microscopy, to model and predict erosion by nanofluids.

The targets represent conditions that are easy to model. However, we will also be able to measure the erosion of the impellers of the commercial water pump. The water pump is used for a racing vehicle and is not representative of the sealed centrifugal pump units, but it was chosen because the pump can be disassembled to measure the weight of the impellers.

Experiments planned for FY 2010 include an investigation of the torque and erosion of SiC nanoparticles in a 50% ethylene glycol-50% water fluid. The largest sized particles and highest concentration will be used because they represent a combination of the best thermal conductivity and heat transfer properties, with the lowest viscosity increase. Furthermore, if erosion depends on the kinetic energy or critical particle size, they will cause the most damage.

Conclusions

We have built an apparatus that not only allows continuation of well-controlled tests designed to develop the data required to model erosive damage, but will closely replicate “real world” conditions in an automotive water pump and measure the torque required to pump the fluids.

References

1. W. Yu, D. M. France, J. Routbort, S.U.S. Choi, “Review and Comparison of Nanofluid thermal Conductivity and Heat Transfer Enhancements, Heat Transfer Engineering, 29, 432-460 (2008).
2. S. K. Saripella, W. Yu, J. L. Routbort, D. M. France, and Rizwan-uddin, “Effects of Nanofluid Coolant in a Class 8 Truck Engine, SAE Technical Paper 2007-01-21413.
3. Annual Report (FY09), Heavy Vehicle System Optimization, in press.
4. E. Timofeeva, J. Routbort, and D. Singh, “Particle shape effects on thermophysical properties of alumina nanofluids”, JAP 106, 014304 (2009).
5. D. Smith, E. Timofeeva, W. Yu, D. France, D. Singh, and J. Routbort, “Particle Size and Interfacial Effects on Heat Transfer Characteristics of Water-based α -SiC Nanofluids”, submitted.

D. Agreement #18494 – Nanofluid Development and Characterization

Principal Investigator: J. L. Routbort

(co-workers: E. Timofeeva, D. Singh, W. Yu, D. France and R. Smith)

Argonne National Laboratory

9700 S. Cass Avenue

Argonne, IL 60439-4838

(630) 252-5065; fax: (630) 252-5568; e-mail: routbort@anl.gov

Technology Development Manager: Lee Slezak

(202) 586-2335, Lee.Slezak.ee.doe.gov

Contractor: UChicago Argonne LLC

Contract No.: DE AC02 06CH11357

Objective

Exploit the relationships between thermal conductivity and heat transfer rates in nanofluids (nanoparticles suspended in liquids) and their physical attributes (particle material, size, shape, concentration, base fluid properties, and presence of other additives).

Based on fundamental understanding of those relationships, develop a strategy for engineering nanofluids with optimized properties for vehicle thermal control.

Improve/optimize the efficiency of heavy-vehicle cooling systems, with the goal of a minimum cooling system size reduction of 5%.

Approach

Systematically study the effects of different variables in nanofluidic systems: particle material, size, shape, concentration, base fluid properties, and presence of other additives, varying only one parameter, while maintaining other system parameters constant.

Measure the thermal conductivity and viscosity of prepared nanofluids. Correlate dependencies to varied parameters.

Measure and determine nanofluid characteristics with regard to suspension stability and particle agglomeration.

Identify figures of merit that would help minimize the amount of measurements needed for nanofluid evaluation.

Use heat transfer measurement results as a guide to engineering nanofluids.

Develop models describing nanoparticle suspension behaviors that would help in engineering nanofluids for a particular heat transfer application.

Perform cooling system tests in collaboration with transportation companies.

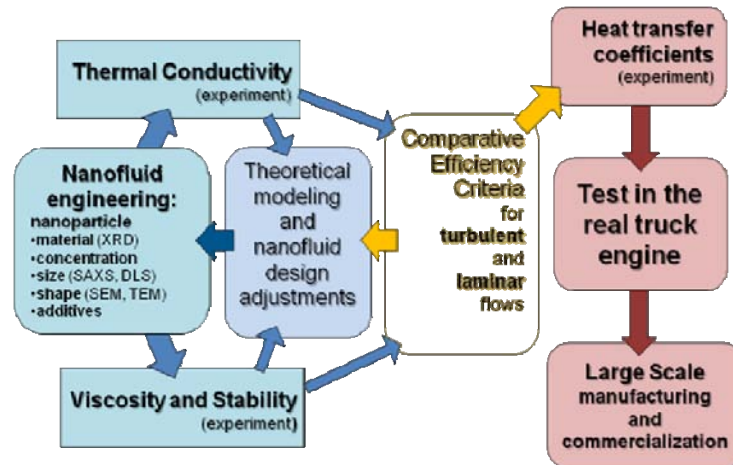


Figure 1. Research to commercialization

Accomplishments

Refined technique of measuring particle sizes using both laser and x-ray scattering techniques[1].

Measured the thermal properties (viscosity and thermal conductivity) of several potential nanofluids (from room temperature to 80°C) [2].

Investigated the effects of particle shape on thermal properties of alumina/EG-H₂O nanofluids [3]. Concluded that for better heat transfer performance, nanoparticles should be slightly elongated spheroids.

Tested the effect of pH on thermo-physical properties of Al₂O₃/EG-H₂O and SiC/H₂O nanofluids. Showed that the viscosity can be significantly modified simply by adjusting the pH of suspensions without affecting thermal conductivity [3, 4].

Studied the effect of average particle size on thermal properties of SiC/H₂O nanofluids[4]. Larger particles are beneficial for both thermal conductivity and viscosity of suspensions, and therefore, the overall heat transfer performance.

Started investigation of the base fluid effect on thermo-physical properties and optimization of SiC/EG-H₂O-based nanofluid.

Published seven journal papers. Two papers are in preparation, and a patent application for “heat transfer fluids containing nanoparticles” has been filed.

Developing a new technique for in-situ production of metal nanoparticles using high-energy X-rays to reduce metal salts in suspension.

Future Directions

Transition from fundamental understanding of nanofluidic systems to optimizing and maximizing the potential of nanofluids as heat transfer fluids. Focus will be on engineering nanofluids for particular industrial applications.

Conduct tests of cooling-system heat transfer in collaboration with the transportation industry.

Refine models of nanostructure-enhanced and nanoparticle-mobility-enhanced thermal conductivity and heat transfer of nanofluids for simulation of cooling system performance. Develop comprehensive model of enhanced thermal conductivity.

Introduction

The requirements for heat rejection in the transportation industry always increase due to trends toward higher power outputs and stringent emission levels, bringing the cooling issue to the forefront. Conventional cooling methods have been optimized to their limits, including design of the radiator air-side fin. However, engine fluids themselves, such as lubricants and coolants, have inherently poor heat transfer characteristics and contribute to the limitations on engine cooling rates. Thus, there is a strong need for higher performance coolants to be used in thermal control systems for vehicles.

Previously, it has been demonstrated that it is possible to improve thermal conductivity of fluids by adding low volume percents (<10%) of nanomaterials to conventional fluids, referred as nanofluids that benefit from high thermal conductivity of solid phase while capable of convective heat transfer mechanism typical for liquids (Figure 2).

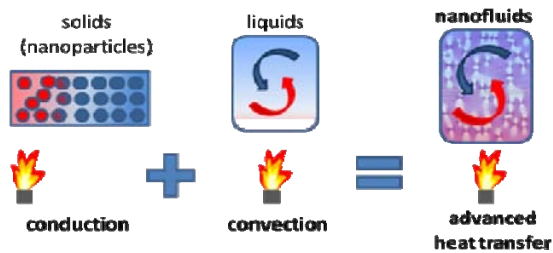


Figure 2. Thermal conductivity benefits

However, the addition of particles to a fluid affects not only thermal conductivity (k), but also other macroscopic properties like viscosity (η), heat capacity (c_p), and density (ρ) that may differently affect heat transfer characteristics of the nanofluid. Therefore, it is clearly important to establish the exact relationship of the nanofluidic system parameters (particle material, size, shape, concentration, base fluid properties, and presence of other additives) to macroscopic system parameters.

A goal of this project is to develop nanofluids that would effectively replace traditional coolants and improve engine cooling—thereby allowing reduction of the size and weight of heavy vehicle cooling systems (radiator, oil cooler, pump, etc.).

To achieve the project goal, better understanding is required of the thermal properties and stability of nanofluids for strategic engineering of nanofluids for heat transfer applications. To attain this understanding, we are conducting the following tasks: (1) explore and exploit the unique properties of nanoparticles to identify and develop heat transfer fluids with high thermal conductivity and low viscosities, (2) experimentally characterize nanofluid physical attributes, (3) determine the basic mechanisms of enhanced thermal conductivity and stability of nanofluids, (4) develop and validate new thermal models for nanofluids, (5) develop techniques to lower the viscosity of nanofluids, (6) develop nanofluid technology for increasing the thermal transport in engine coolants and lubricants using input from heat transfer test results from item ii below, and (7) conduct cooling tests in conjunction with industry.

This project is one of two parts of larger study that was roughly divided into two tasks:

- i) Nanofluid development and characterization.
- ii) Thermal control underhood.

Experimental Details and Results

We have previously demonstrated that evaluation of nanofluids for a particular application requires a proper understanding of all the characteristics and thermo-physical properties of nanoparticle suspensions [3].

The study of particle shape effect on thermo-physical properties was conducted on alumina-EG/H₂O system. The significance of complex interaction between nanoparticles and base fluids in determining the thermal conductivity and viscosity enhancements has been shown. In nanofluids with non-spherical particles, thermal conductivity enhancements predicted by Hamilton-Crosser equation are diminished by the negative contribution of heat flow resistance at the solid-liquid interface (Figure 3).

Using effective medium theory and the assumption that contribution of interfacial effects is proportional to the total surface area of nanoparticles (changes with the shape and size), we obtained a consistent

value of Kapitza resistance from our experimental data.

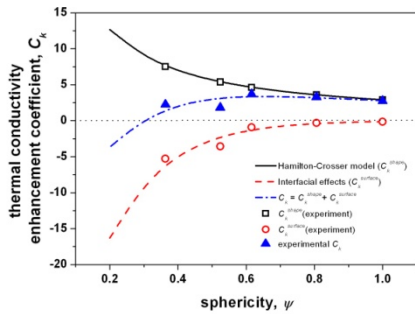


Figure 3. Contribution of particle shape effect(Hamilton Crosser model) and interfacial thermal resistance to the thermal conductivity of alumina/EG-H₂O suspension (5 vol%) at various particle sphericities.

Viscosities of nanofluids were shown to depend on both particle shapes and surface properties of nanoparticles. Elongated particles and agglomerates result in higher viscosity at the same volume fraction due to structural limitation of rotational and transitional Brownian motion. For lower viscosities, spherical particles or lower aspect ratio spheroids should be used. Surface charge at nanoparticles influences particle/base fluid interactions and agglomeration of individual nanoparticles. We demonstrated that viscosity of the alumina and SiC-based nanofluids might be decreased by 30-60% without affecting thermal conductivity by adjusting surface charge with pH of suspension (Figure 4).

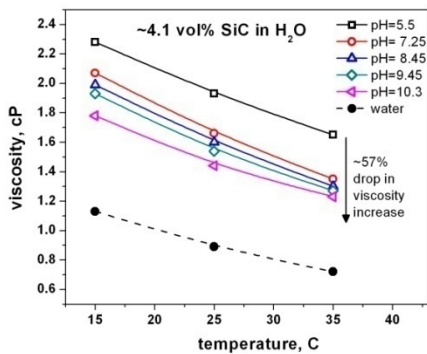


Figure 4. Effect of pH on viscosity of 4.1 vol % a-SiC/H₂O nanofluids with average particle size 29 nm

The effect of average particle size has been studied on a SiC-water system. At all other conditions being the same (pH and particle concentration), smaller

particles provide a higher viscosity increase than larger particles. This is most likely due to the larger surface area of solid/liquid interface and increased effective volume of solids. Thermal conductivity enhancement is higher in nanofluids with larger particles also due to effects of nanoparticle surface area. Solid/liquid interface acts as an obstacle for the heat flow with a negative contribution of interface proportional to the total surface area of nanoparticles.

Viscosity and thermal conductivity are the major parameters defining the heat transfer coefficient in SiC/water nanofluids at specific flow rates. Lower viscosity and higher thermal conductivity are desirable for enhanced performance. It is clear that adding larger particles and optimizing the surface charge can produce a nanofluid that has enhanced heat transfer properties compared to the base fluid (Figure 5). Therefore, particle size is an important instrument in manipulation of nanofluid properties. The limitation to using particle size for nanofluid improvements lies in their stability and erosion resistance.

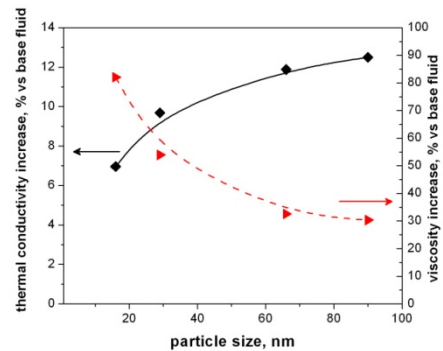


Figure 5. Dependence of thermal conductivity (at 22.5°C) and viscosity (at 25°C) of water based nanofluids on the size of a-SiC particle. Particle concentration is ~4.1 vol%, pH ~9.4.

Analysis of experimental data with figures of merit for laminar [5] and turbulent [6] flows showed, that use of 4.1 vol% SiC nanofluid will be beneficial in laminar flow regime when particles are bigger than ~50 nm, while for turbulent flow average particle sizes should be larger~90 nm (Figure 6).

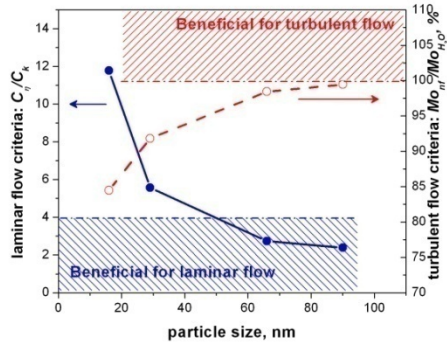


Figure 6. Figures of merit for a-SiC/H₂O nanofluids.

Conclusions

Nanofluids are multivariable systems with basic macroscopic properties like thermal conductivity and viscosity strongly affected by particle shape, size, base fluid composition and presence of additives. Knowledge of those correlations will help in strategic engineering of nanofluids for particular heat transfer applications.

So far, we have established the correlation between particle shape and viscosity and thermal conductivity of nanofluids. This brought us to the conclusion that low aspect ratio spheroid-like particles should be used for the optimization of heat transfer characteristics.

Viscosity of nanofluids can be significantly lowered by adjusting pH to the highest zeta potential achievable in the system. Additionally, this high potential stabilizes nanofluid by electrostatic repulsion mechanism.

Particle size effect favors use of larger particles for higher thermal conductivity and lower viscosity enhancements due to negative interfacial effects. Knowledge achieved in water-based nanofluids will be further transferred to EG/H₂O-based nanofluids.

The effect of base fluid will also be studied to allocate the base fluids that would most benefit from addition of nanoparticles.

Future research will also concentrate on using nanoparticles with higher thermal conductivity. Several choices are under consideration, and their nanofluid solutions must be optimized with respect to volume concentration, particle size, and thermal

conductivity enhancements. Additionally, surfactants and pH modification will be used to lower the viscosity of the nanofluid. In all of these tasks, heat transfer measurement results will be incorporated into the path forward. Also, we hope to cooperate with a radiator manufacturer to measure thermal resistance of an actual radiator using our optimal nanofluid as a coolant.

Acknowledgements

We appreciate the active cooperation of Steve Hartline from Saint Gobain Inc. in supplying nanofluids for this study and on the project in general.

References

- 1 G. Chen, W. H. Yu, D. Singh, D. Cookson, and J. Routbort, "Application of SAXS to the study of particle-size-dependent thermal conductivity in silica nanofluids," *Journal of Nanoparticle Research* 10 (7), 1109-1114 (2008).
- 2 D. Singh, E. Timofeeva, W. Yu, J. Routbort, D. France, D. Smith, and J. M. Lopez-Cepero, "An investigation of silicon carbide-water nanofluid for heat transfer applications," *Journal of Applied Physics* 105 (6) (2009).
- 3 E. V. Timofeeva, J. L. Routbort, and D. Singh, "Particle shape effects on thermophysical properties of alumina nanofluids," *Journal of Applied Physics* 106 (1) (2009).
- 4 E.V. Timofeeva, D. Smith, W. Yu, D. France, D. Singh, and J. Routbort, "The Particle Size and Interfacial Effects on Heat Transfer Characteristics of Water Based a-SiC Nanofluids," (2010).
- 5 R. Prasher, D. Song, J. L. Wang, and P. Phelan, "Measurements of nanofluid viscosity and its implications for thermal applications," *Applied Physics Letters* 89 (13), 133108-133110 (2006).
- 6 R. E. Simons, "Comparing Heat Transfer Rates of Liquid Coolants Using the Mouromtseff Number", in *ElectronicsCooling* (2006), Vol. 12, pp. http://electronics-cooling.com/articles/2006/2006_may_cc.php.

E. CoolCab – Truck Thermal Load Reduction Project

Ken Proc (Principal Investigator)
National Renewable Energy Laboratory
1617 Cole Blvd.
Golden, CO 80401
(303) 275-4424; kenneth.proc@nrel.gov

DOE Technology Manager: Lee Slezak
(202) 586-2335; Lee.Slezak@ee.doe.gov

Objectives

- Investigate the potential to reduce truck cabin thermal load through testing and analysis.
- Develop a tool to help predict heating, ventilating, and air conditioning (HVAC) load reduction in truck tractor sleeper cabins.

Approach

- Work with industry to identify specific needs and development projects in heavy trucks.
- Perform baseline truck testing, data analysis, and model validation work.

Key Milestones

- Engineering Test Report: Infrared Image Field Test at Schneider National, July 2005.
- Status Report: CoolCab Testing with Volvo Truck, September 2006.
- Interim Report on CoolCab Activity, August 2007.
- Presentation of Results of Industry Meetings and Tool Specifications, September 2008.
- SAE Paper: Thermal Load Reduction of Truck Tractor Sleeper Cabins, October 2008.
- Demonstration of Prototype CoolCalc HVAC Load Reduction Tool, September 2009.

Future Activities

- Work with industry partners to validate CoolCalc with truck test data.
- Develop an air conditioning (A/C) model to calculate A/C load data.
- Release a beta version of CoolCalc to select users and industry partners.

Introduction

The trucking industry is faced with increased costs from rising fuel prices, higher maintenance costs, and driver turnover. In addition, excessive idling has been identified as a source of wasted fuel and an unnecessary cost. Survey estimates report that sleeper trucks idle an average of more than 1,400 hours annually [1]. Engine idling consumes more than 800 million gallons of fuel annually in long-

haul (>500 miles/day) trucks [2]. Trucks typically idle to run cabin climate control (heating, cooling, and dehumidification) during driver rest periods and to provide electric power for other amenities. Reducing the amount of truck engine idling can significantly reduce fuel consumption, save money, and reduce tailpipe emissions.

The U.S. Department of Energy's (DOE) Advanced Vehicle Testing Activity (AVTA) initiated a study of diesel truck engine idle reduction technologies in

2002 [3]. This study consisted of several projects that evaluated existing on-board idle reduction technologies, including diesel-fired and electric heaters, electric air conditioning systems, and an auxiliary cab cooler using phase change material. This evaluation demonstrated measured idle reduction and fuel savings with some of the technologies but identified the following issues in meeting driver and operator requirements:

- *Energy storage capacity:* Battery powered and other stored energy cooling systems lacked capacity to meet mandatory driver rest periods in warm ambient temperatures (above 85°F).
- *Driver comfort:* Drivers noted areas within the truck cab where excessive heat penetrated the cabin walls from the environment and the engine exhaust system.
- *Cost:* Some of the technologies tested required significant installation time to retrofit an existing truck. This installation cost, in addition to the hardware cost, was too high to provide sufficient technology payback to the fleets.

To address the identified cost issue, DOE solicited proposals for cost-shared projects to integrate an on-board idle reduction technology at a truck original equipment manufacturer (OEM) [3]. International Truck and Engine Corporation was awarded a contract for the design and factory installation of an idle reduction system.

To address the capacity and comfort issues identified, DOE, through the National Renewable Energy Laboratory (NREL), launched the CoolCab project, which conducted a qualitative study of truck tractor cabins to identify potential areas for improvement. Working with Schneider National, two tractors were analyzed using infrared images to investigate heat loss [4]. This exploratory work noted several areas for improvement in the truck cab insulation, including driver and passenger footwells, sunroof and ceiling pad areas, and the rear of the upper bunk (Figure 1).

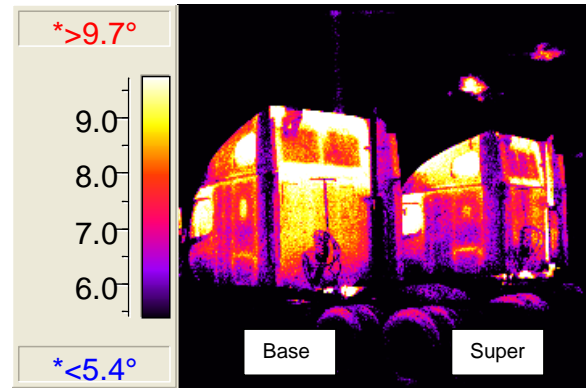


Figure 1. Upper Sleeper Bunk Infrared Image

In fiscal year (FY) 2008, the CoolCab project began to quantify truck cab heat loss and further investigate reducing the thermal load of the truck HVAC system during driver rest periods. Working with truck OEMs Volvo and International, CoolCab tested and analyzed two trucks at NREL's outdoor test facility and modeled the International truck using Fluent CFD software and RadTherm thermal analysis software. This work concluded that applying the standard sleeper privacy curtain and shades reduced the heating load for the sleeper area by up to 21 percent. Insulating the truck cab windows also reduced daytime solar temperature gains by up to 8°C [5].

In FY 2009, the CoolCab project began development of a tool to help predict potential HVAC load reduction in truck tractor sleeper cabins. This tool, called CoolCalc, allows users to create and modify a truck sleeper cabin model to predict cabin temperatures in different environmental conditions and locations. An initial validation of the tool concept was also completed this FY using previous truck test data; this work is the focus of this annual progress report.

Objective

The main objective of the CoolCab project is to identify design opportunities to reduce the thermal load inside truck tractor cabs. Reducing the heating or cooling load is the first step in improving system efficiency to reduce fuel consumption. Reducing this load will enable existing idle reduction technologies and allow more efficient technologies to keep truck drivers comfortable during rest periods.

A secondary objective of reducing cabin thermal load is to decrease heating and cooling loads while a truck or

other vehicle is traveling. This load reduction may provide further gains in reducing fuel consumption and improving fuel economy. In addition, with a trend toward hybrid powertrains in vehicles, energy required for HVAC and other accessories will be at a premium. Load reduction will help reduce these energy demands and help extend vehicle range and efficiency in both light and heavy vehicles.

Approach

CoolCalc is an easy-to-use simplified physics-based HVAC load estimation tool that requires no meshing, has flexible geometry, excludes unnecessary detail, and is less time-intensive than more detailed Computer Aided Engineering (CAE) modeling approaches. It is intended for rapid trade-off studies, technology impact estimation, preliminary HVAC sizing design, and to complement more detailed and expensive CAE tools by exploring and identifying regions of interest in the design space.

CoolCalc is built on NREL’s OpenStudio platform. This was done to accelerate development and leverage off previous and ongoing DOE investment. OpenStudio was developed at NREL and released in 2008. This is a plug-in extension of Google’s SketchUp software. DOE’s EnergyPlus is used as the heat transfer solver by OpenStudio. EnergyPlus is a DOE-funded software, designed for building efficiency analysis, which was found to be general enough to extend to cab thermal modeling.

This year, a prototype version of CoolCalc was developed. The CoolCalc program coding structure was established, providing the foundation on which the current version runs and future developments will be built. In addition to the base coding structure, several critical capabilities were developed: the parametric creation of truck cab geometry, which can then be manually modified by the user; a material definition interface; a construction assignment tool; a construction assignment tool; and a simple object browser that gives access to EnergyPlus’ full capabilities.

While CoolCalc is flexible and does not dictate a specific process, a typical workflow might begin with the creation of geometry using the Parametric Cab creation tool (Figure 2). The Parametric Cab creation window has a series of tabs across the top—

one for each air zone in the model. Each tab has a list of available parametric variables, which will modify the geometry. A model definition file created in the geometry coding framework determines these variables and the parametric geometry relationships. To illustrate this parametric capability, the windscreen angle was changed from 60° to 80° (Figure 3). The cab model quickly updates, allowing for fast modification of the geometry.

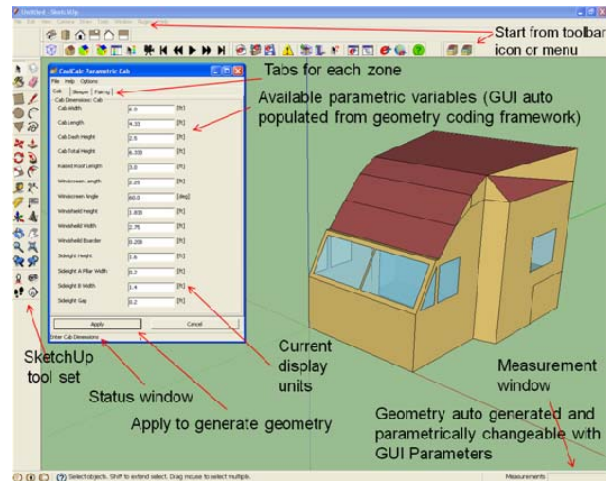


Figure 2. Parametric Cab Geometry Creation

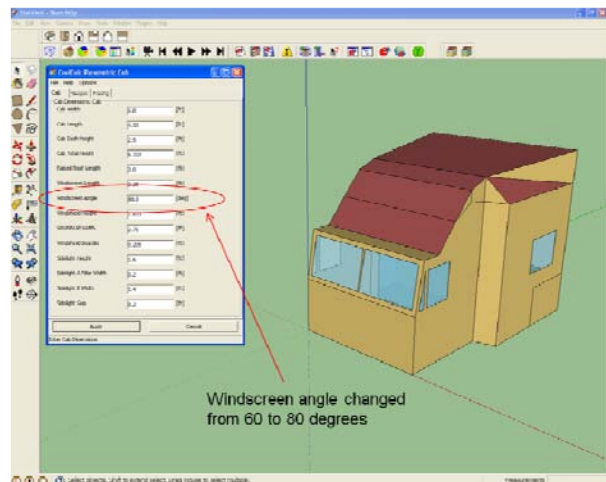


Figure 3. Parametric Cab with Modified Windscreen Angle

Once the cab geometry is established using the Parametric Cab tool, the user can manually modify it. Figure 4 shows an example of a user adding an additional sidelight to the sleeper cab. Double clicking on the surface activated the sleeper cab sidewall. Once activated, the Sketchup drawing tools can be used to modify the geometry. The dashed

lines are construction lines that were created to help quickly draw the sidelight. These can be easily hidden or deleted later. The pencil tool was then used to trace out the construction lines. The pencil tooltip icon can be seen in the top right corner of the sidelight. Once the window shape is closed by the pencil tool, it is automatically recognized as a window and assigned some default properties.

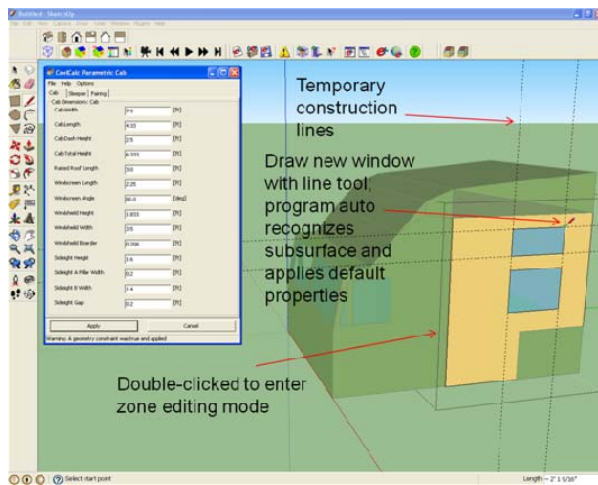


Figure 4. Manual Modification of Geometry –Adding a Sidelight

In EnergyPlus, every component of the model (e.g. walls, materials, location, and solver time step) are treated as an object. In CoolCalc, to modify or define new objects the Object Browser tool is opened (Figure 5). On the left side of the Object Browser window is the object tree, which shows all the objects that are available in the model and allows the creation of new objects. Below the object tree, on the left, is the library window. The library window allows the user to load and manipulate additional libraries of objects. These objects can then be added to the current model by dragging and dropping them into the object tree. On the right is the current object window, the content of which is determined by the object tree selection. The object window can be docked or undocked based on the user’s preference. Some objects have a specific interface window with various boxes and pull-down menus for the user to fill out. Below the specific object window interface, to the right of the object tree, is the text editing window. This window allows for the manual modification of the current object, giving full control to advanced users. For objects where no specific interface has been developed, the

text editing window will comprise the entire right side of the split window.

To modify or define new materials, a material object is selected in the object tree (Figure 5). Based on this object tree selection, the material definition window is displayed on the right. The material definition window provides text boxes or pull-down menus for all the basic material thermal properties: Name, Roughness, Thickness, Conductivity, Density, and Specific Heat. Additionally, there is an option to assign a texture bitmap to a material for display and easy identification in the model. As discussed above, on the bottom right is the text editing window that allows for advanced manual modification of the current material object.

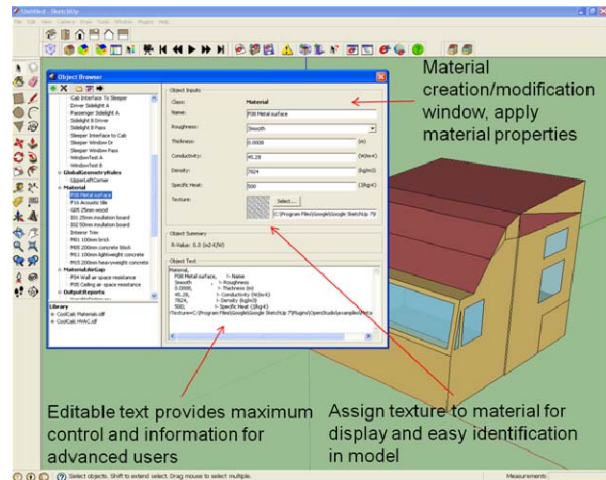


Figure 5. Object Browser and Material Definition Window

Each surface in CoolCalc is treated as multiple-layer 1-D conduction, forming a “sandwich”-type structure. To define this layered structure, a construction object is used. Once again navigating the object tree, a construction object is selected. This changes the current object window (right side) to display the construction definition window (Figure 6). In this window the user selects the materials to include in the construction and can change their order. Materials assigned to the inner and outer layers will determine the solar radiation properties and the texture displayed in the texture rendering mode. The texture preview is shown in the split square, with the outer texture shown in the top left half and the inner texture shown in the bottom right half.

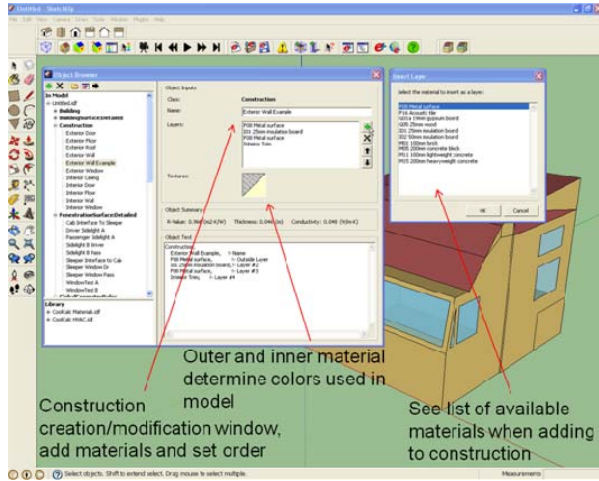


Figure 6. Construction Definition Window

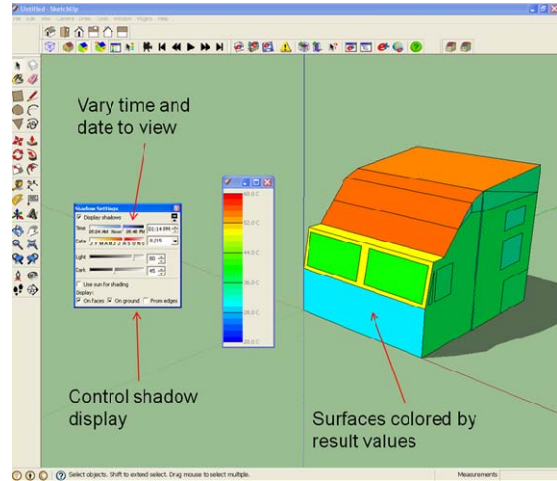


Figure 8. Example Results Displayed

Figure 7 shows the model in texture rendering mode. In this mode, the surfaces are colored by their inner and outer layer material textures. The window to the left of the cab is the Construction Palette. It allows the sorting and selection of constructions and their application to the model using a point-and-click paint can tooltip. This window also allows the drag and drop setting of default construction types using the texture wells at the top of the Construction Palette window.

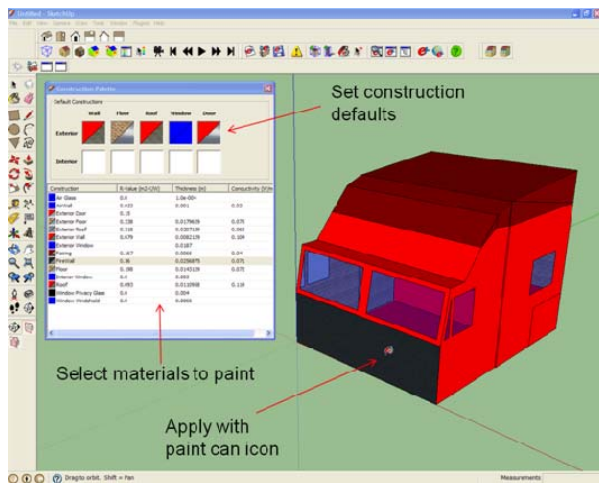


Figure 7. Construction Palette Window and Texture Rendering Mode

Before solving this model, a weather file is selected. There is currently Typical Mean Year (TMY) data available for 2,100 locations worldwide. Custom weather data can also be entered. Once the model is solved, the results can be displayed within the interface (Figure 8).

Results

The CoolCalc concept was validated with an initial test case. A model of an International Truck and Engine Corporation truck cab was developed to compare to test results from CoolCab’s 2007 testing [5]. The model was created using rough geometry information available, best guess assumptions, and test-site weather data. Figure 9 shows a comparison between the model and the measured air temperatures. The front cab results are blue and the sleeper results are pink, with solid lines for model results and dashed for experimental results. This graph shows good agreement both in the peak soak temperature and the overall trends.

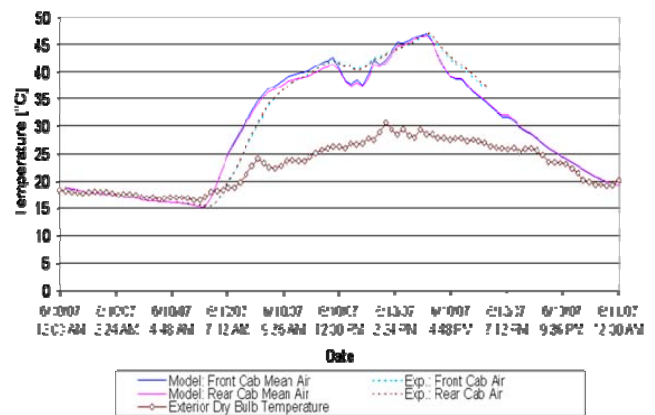


Figure 9. Comparison of CoolCalc Model and Experimental Results

The predicted surface temperatures were also compared to experimental results. Figure 10 shows results for the driver and passenger sleeper side wall

surface temperatures. Since the truck is south facing, the driver side surface temperatures rise in the morning, peak and decline as the sun passes over the vehicle. Likewise, the passenger side surfaces rise in the afternoon, peak, and decline as the sun goes down. The temporal variability seen in the afternoon temperatures for both the experimental and model results were caused by passing clouds on that particular test day.

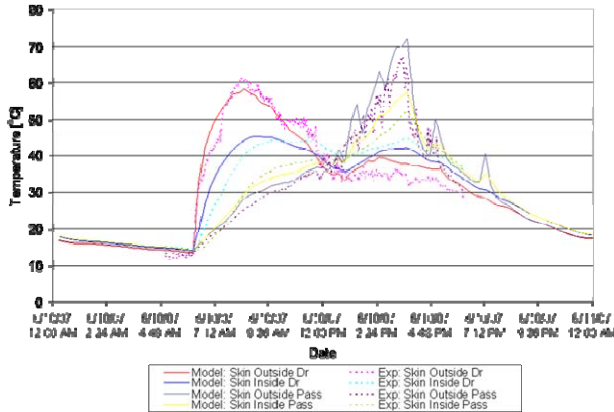


Figure 10. Comparison of CoolCalc Model and Experimental Results for Sleeper Side Walls

The concept validation results also show good agreement between the model and experimental data for the other surfaces that were compared. Additionally, other test days were simulated without changing the vehicle model and similar agreement was found. More detailed model validation is currently being conducted.

References

1. The American Transportation Research Institute. “Idle Reduction Technology: Fleet Preferences Survey.” February 2006.
2. Stodolsky F., Gaines L., Vyas A. “Analysis of Technology Options to Reduce the Fuel Consumption of Idling Trucks.” Argonne National Laboratory, ANL/ESD-43, June 2000.
3. Proc K. “Idle Reduction Technology Demonstrations.” NREL, DOE/GO-102004-1993, November 2004.
4. Rugh J., Farrington R. “Vehicle Ancillary Load Reduction Project Close-Out Report.” NREL, NREL/TP-540-42454, January 2008.
5. Proc K. “Thermal Load Reduction of Truck Tractor Sleeper Cabins.” SAE Paper No. 2008-01-2618, October 2008.

VIII. FRICTION AND WEAR

A. Boundary Lubrication Mechanisms

Principal Investigators: O. O. Ajayi, C. Lorenzo-Martin, R.A. Erck, J. Roubort, and G. R. Fenske
Argonne National Laboratory
9700 South Cass Avenue, Argonne, IL 60439
(630) 252-9021; fax: (630) 252-4798; e-mail: ajayi@anl.gov

Technology Development Manager: Lee Slezak
(202-586-2335, Lee.Slezak@hq.doe.gov)

Contractor: Argonne National Laboratory, Argonne, Illinois
Contract No.: DE-AC02-06CH11357

Objective

- Develop a better understanding of the mechanisms and reactions that occur on component surfaces under boundary lubrication regimes. The ultimate goal is to reduce friction and wear in oil-lubricated components and systems in heavy vehicles. Specific objectives include:
 - Determine the basic mechanisms of catastrophic failure in lubricated surfaces in terms of materials behavior. This knowledge will facilitate the design of higher power density components and systems.
 - Determine the basic mechanisms of chemical boundary lubrication. This knowledge will facilitate lubricant and surface design for minimum frictional properties.
 - Establish and validate methodologies for predicting the performance, and failure of lubricated components and systems.
 - Integrate coating and lubrication technologies for maximum enhancement of lubricated-surface performance.
 - Transfer the technology developed to original equipment manufacturers (OEM) of diesel engine and vehicle components and systems.

Approach

- Characterize the dynamic changes in the near-surface material during scuffing. Formulate a material-behavior-based scuffing mechanism and prediction capability.
- Determine the chemical kinetics of boundary film formation and loss rate by in-situ X-ray characterization of tribological interfaces at Argonne's Advanced Photon Source (APS).
- Characterize the physical, mechanical, and tribological properties of tribochemical films, including failure mechanisms.
- Integrate the performance and failure mechanisms of all structural elements of a lubricated interface to formulate a method for predicting performance and/or failure. This task will include incorporation of surface coatings.
- Maintain continuous collaboration with heavy vehicle system OEMs to facilitate effective technology transfer.

Accomplishments

- Conducted extensive characterization of microstructural changes during scuffing of 4340 steel, through the use of scanning electron microscopy (SEM) and X-ray analysis.
- For metallic materials, developed a model of (1) scuffing initiation based on an adiabatic shear instability mechanism and (2) scuffing propagation based on a balance between heat generation and heat dissipation rates.
- Characterized the mechanical properties and scuffing resistance of a graded nanocrystalline surface layer produced by severe plastic deformation, which results from the scuffing process.
- Conducted preliminary evaluation of scuffing mechanisms in ceramic materials.
- Extended scuffing mechanisms study into ceramics and metals contact pairs, as well as cast iron (typically used as cylinder liner in diesel engine).
- Using X-ray fluorescence, reflectivity, and diffraction at APS, demonstrated the ability to characterize tribochemical films generated from model oil additives.
- Designed and constructed an X-ray accessible tribo-tester for in-situ study of boundary film formation and loss rates.
- Characterized the structure of tribochemical boundary films with different frictional behavior with a new technique that combines focused ion beam (FIB) milling, transmission electron microscopy (TEM), and grazing incidence X-ray diffraction (GIXRD) at APS.

Future Direction

- Continue refinement and validation of the comprehensive scuffing theory for various engineering tribo materials.
- Develop and evaluate methods and technologies to prevent scuffing in high power density oil-lubricated components and systems.
- Continue characterization of tribochemical films formed by model and commercial lubricant additives using FIB, TEM, and X-ray-based surface analytical techniques available at APS.
- Characterize the physical, mechanical, and failure mechanisms of tribochemical films with nano-contact probe devices.
- Evaluate the impact of various surface technologies, such as coating and laser texturing, on boundary lubrication mechanisms.
- Develop a technique to measure real contact temperature needed for tribochemical film formation.

Introduction

Many critical components in diesel engines and transportation vehicle systems such as gears and bearings are lubricated by oil. Satisfactory performance of these components and systems in terms of efficiency and durability is achieved through the integration of materials, surface finish, and oil lubricant formulations often using Edisonian trial-and-error approach. Indeed, experience is likely the sole basis for new designs and methods to solve failure problems in lubricated components. Because of the technology drive to more efficient and smaller

systems, more severe operating conditions are invariably expected for component surfaces in advanced engines and vehicle systems. The trial-and-error approach to effective lubrication is inadequate and certainly inefficient. Departure from this approach will require an improved understanding of the fundamental mechanisms of both boundary lubrication and surface failure in severely loaded lubricated components.

Emissions reduction is another major technical thrust area for the Department of Energy (DOE) in the development of diesel engine technology for

heavy vehicles. With the higher efficiency of diesel engines compared to gasoline engines, significant reduction in emissions will facilitate more use of diesel engines for automotive applications. Unfortunately, some essential components in oil lubricants and additives in diesel fuel (such as sulfur, phosphorus, and chlorine) are known to poison the catalysts in the emission-reducing after-treatment devices of diesel engines. Reduction or elimination of these additives will make emission after-treatment devices more effective and durable. However, this will also make the surfaces of many lubricated components more vulnerable to catastrophic failure. There is therefore a need to develop effective replacement for these essential lubricant additives. Again, such an endeavor will require a better understanding of the mechanisms of boundary lubrication and the failures therein.

Increases in vehicle efficiency will require friction reduction and increase in power density in the engine and powertrain systems. Higher power density translates to increased severity of contact between many tribological components—which, again, will compromise the reliability of various critical components if they are not effectively lubricated. The efficacy of oil additives in reducing friction and in protecting component surfaces depends on the nature and extent of the chemical interactions between the component surface and the oil additives. In addition to reliability issues, the durability of lubricated components also depends on the effectiveness of oil lubrication mechanisms, especially under boundary conditions. Components will eventually fail or wear out by various mechanisms including contact fatigue. Wear is the gradual removal of material from contacting surfaces, and it can occur in many ways, such as abrasion, adhesion, and corrosion. Repeated contact stress cycles to which component contact surfaces are subjected can initiate and propagate fatigue cracks and, ultimately, lead to the loss of a chunk of material from the surface. This damage mode by contact fatigue is often referred to as “pitting.” Wear and contact fatigue are both closely related to boundary lubrication mechanisms. Anti-wear additives in lubricants are designed to form a wear-resistant protective layer on the surface. The role of lubricant additives on contact fatigue failure is not fully understood. However, it is clear that the lubricant chemistry significantly affects contact

fatigue. Again, lack of a comprehensive understanding of the basic mechanisms of boundary lubrication is a major obstacle to a reasonable prediction of the durability of lubricated components and systems.

Significant oil conservation benefits would accrue by extending the drain interval for diesel engine oil, with an ultimate goal of a fill-for-life system. Successful implementation of the fill-for-life concept for the various lubricated systems in heavy vehicles requires optimization of surface lubrication through the integration of materials, lubricant, and perhaps coating technologies. Such an effort will require an adequate fundamental understanding of surface material behavior, chemical interactions between the material surface and the lubricant, and the behavior of material and lubricant over time.

Some common threads are present in all of the challenges and problems in the area of effective and durable surface lubrication described briefly above. The two key challenges are (1) lack of adequate basic and quantitative understanding of the failure mechanisms of component surfaces and (2) lack of understanding of the basic mechanisms of boundary lubrication (i.e., how lubricant chemistry and additives interact with rubbing surfaces, and how this affects performance in terms of friction and wear).

To progress beyond the empirical trial-and-error approach for predicting lubricated component performance, a better understanding is required of the basic mechanisms regarding the events that occur on lubricated surfaces. Consequently, the primary objective of the present project is to determine the fundamental mechanisms of boundary lubrication and failure processes of lubricated surfaces. The technical approach taken in this study differs from the usual one of post-test characterization of lubricated surfaces. Rather, it will include developing and applying in-situ characterization techniques for lubricated interfaces that will use the X-ray beam at Argonne’s APS. Using a combination of different X-ray-based surface analytical techniques, we will study, in real time, the interactions between oil lubricants and their additives and the surfaces they lubricate. Such a study will provide the basic mechanisms of boundary lubrication. In addition to surface

chemical changes, the materials aspects of various tribological failure mechanisms (starting with scuffing) will be studied.

Results and Discussion

Efforts during fiscal year (FY) 2009 were devoted to the two areas of least understood components of boundary-lubricated interfaces (i.e., near-surface material and the tribochemical boundary films). The study of the near-surface material will facilitate a better understanding of scuffing mechanism under severe contact conditions expected in high-power density components and systems. Results of the study can guide the development of scuffing resistant tribological materials and interfaces. Characterization of the chemical boundary films will improve the understanding of boundary film structures and how they relate to frictional behavior. Results of the study can form the basis for the development of a sustainable super-low friction-sliding interface.

Scuffing Mechanisms

In the previous years, our study of scuffing mechanism in hardened steel material (typical used for gears and bearings) led to the development of a scuffing model based on plastic adiabatic shear instability. With this model, the propensity of steel material to scuffing failure can be determined from the pertinent material properties. In internal combustion engines (ICE) (both diesel and gasoline), the cylinder liner is often made of cast iron. In order to increase the power density of the ICE, a better understanding and perhaps a predictive capability are needed for scuffing or catastrophic failure of cast iron liner material. During FY 2009, a comparative mechanistic study of scuffing was conducted for 1080 steel and gray cast iron. Scuffing tests were conducted with both materials using a ball-on-flat contact configuration in reciprocating sliding. The ball is made at a 9.5-mm (1/2") diameter and of hardened 52100 steel. All of the tests were lubricated with a poly- α -olefin (PAO) synthetic base stock fluid. In the scuffing test, the contact severity is progressively increased until a sudden rapid increase in friction (indication of scuffing) occurs. Contact severity can be increased through an increase in load or increase in sliding speed. Both the step load and step speed increase

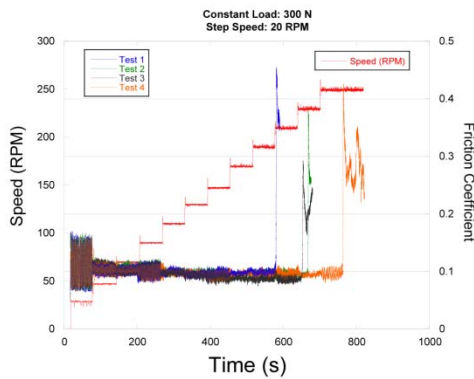
protocols, in which the load or the speed was progressively increased in a discrete manner.

Figure 1 shows the result of the scuffing test for the steel material in both step speed and step load protocols. In both cases, the friction coefficient prior to scuffing was about 0.1, which is a typical value for boundary lubrication regime. Upon scuffing, a suddenly large increase was observed in the friction coefficient. In contrast, the frictional behavior during the test with cast iron is shown in Figure 2. Even though a transition in friction was also observed as the contact severity increased, it was not a sudden or rapid increase. Prior to the transition, the friction coefficient was about 0.075, which is lower than 0.1 for steel (perhaps indicative of the lubricating action of the graphite phase in cast iron). After the transition, the friction coefficient gradually increased to a value between 0.15 and 0.2. Figure 3 illustrates the significant differences in the friction behavior of steel and cast iron materials under severe sliding contact. This is indicative of the differences in scuffing mechanisms of the two materials. Surface profilometry analysis, combined with near-surface microstructural characterization showed that (1) scuffing in steel occurred by rapid severe plastic deformation (adiabatic shear instability) while (2) the friction transition in cast iron coincided with a transition from mild wear to severe wear mode.

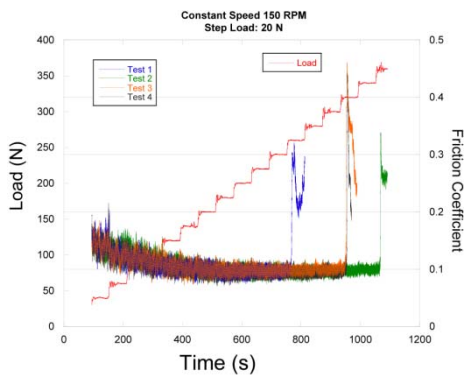
Tribochemical Film Analysis

Frictional behavior of lubricated contact operating under boundary regime is governed to a large extent by the tribochemical surface films formed at the contacting surface. In order to achieve a sustainable and significant reduction in friction, determination of the structural details and properties of these films is essential. From the structural information, film attributes relevant to friction and wear properties, as well as the durability of the films, can be established. In FY 09, tribochemical films produced from different lubricants with similar viscosities were characterized with a combination of aFIB milling technique and TEM. Figure 4 illustrates the frictional behavior of three lubricants with the same viscosity but different additives when applied to a reciprocating line contact between a smooth 52100 steel roller sliding on a hardened case-carburized 4118 steel flat. These are typical bearing and gear steel materials. Since the viscosities of the three

lubricants are the same, and the sliding material pair (including surface roughness) is the same, the contribution of lubricant fluid film and the near-surface material components to the friction at the interface are the same for the three lubricants. Consequently, the differences in the frictional behavior in the figure can be attributed mainly to differences in the structure and properties of the tribochemical boundary films formed by each lubricant.



(a)



(b)

Figure 1. Variation of friction coefficient with time during scuffing test of 1080 steel (a) step speed protocol (b) step load protocol.

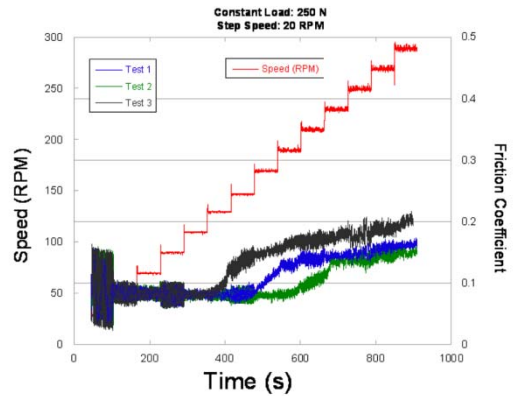


Figure 2. Friction variation with time during scuffing test with cast iron

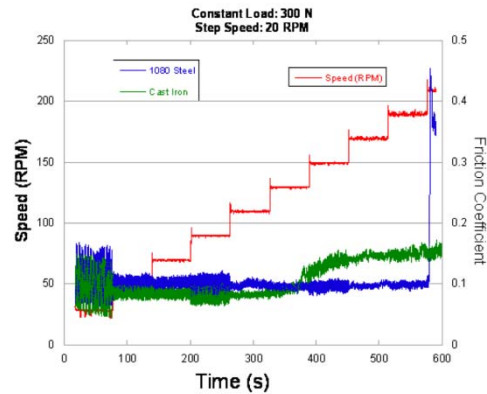


Figure 3. Comparison of friction behavior for 1080 steel and cast iron during scuffing test

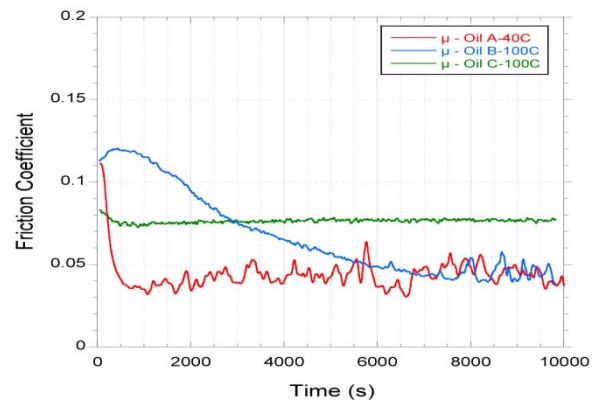
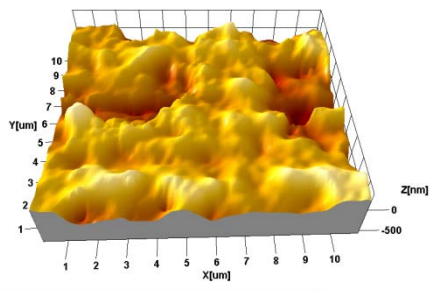
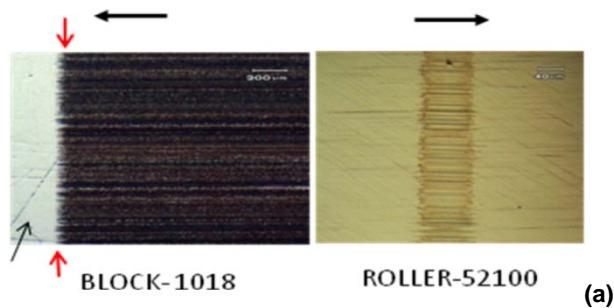


Figure 4. Friction behavior of three different lubricants with different additives

Figure 5 shows an example of the optical micrograph and optical profilometry of tribochemical film from lubricant A. Using a FIB technique, cross-sectional TEM samples were prepared from the three films. A platinum (Pt) layer was first deposited on the surface of local area from which the TEM sample was extracted in order to protect the tribochemical film. Figure 6 shows post-ion milling both sides and extracting TEM samples. The samples were thinned further to make them electron transparent, especially close to the surface area that contains the tribochemical films.



(b)

Figure 5. (a) Optical micrograph of film on flat and roller (b) optical profilometry of tribochemical films on flat formed with lubricant A.

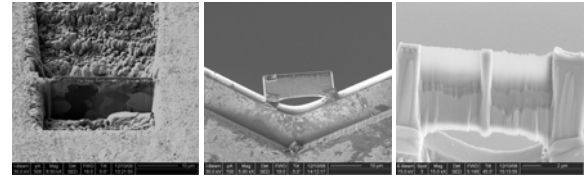


Figure 6. FIB preparation of cross-sectional TEM specimen of tribochemical surface films

Figure 7 shows the TEM characterization of the film from lubricant A. The film has a thickness of about 100 nm (Figure 7b). It is monolayer and relatively homogeneous. With exception of perhaps some local defect, the film also appears to be amorphous (Figure 7c). The film from oil B is also about 100 nm thick, but multi-layer (Figure 8b). It also has an amorphous structure. The tribo-film from lubricant C is about 80 nm thick and primarily consists of a nano-crystalline structure, with a crystal size of 3 to 5 nm (Figure 9b).

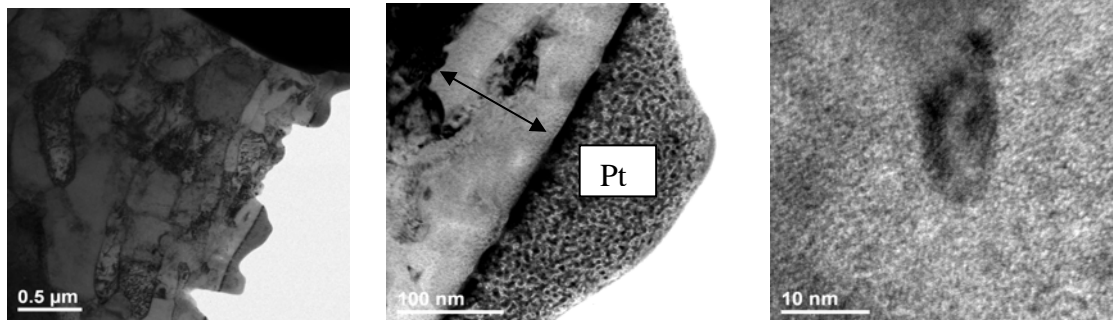


Figure 7. TEM micrograph of Tribochemical film from lubricant A showing the film is about 100 nm thick and amorphous

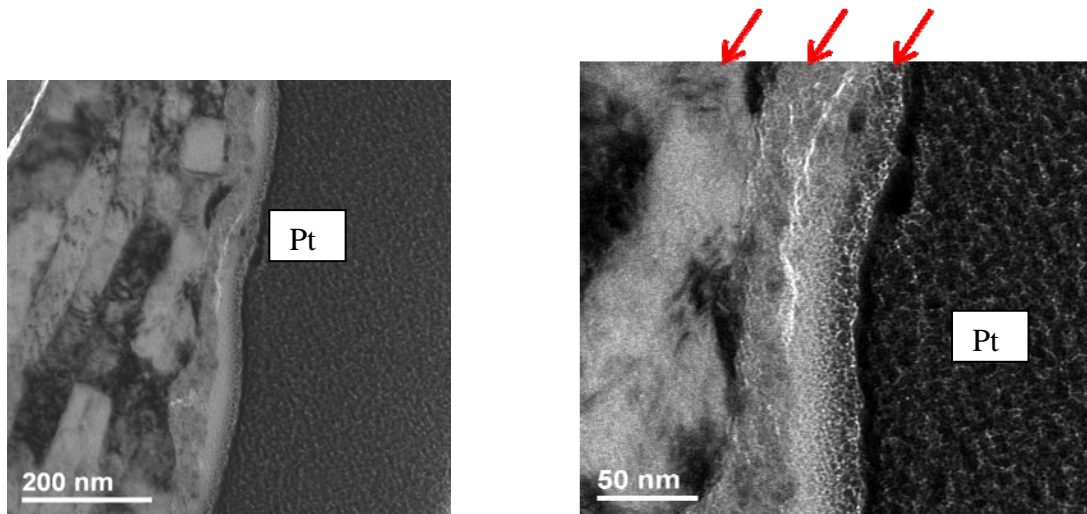


Figure 8. TEM micrograph of Tribochemical film from lubricant B showing the film is about 100 nm thick and multi-layer.

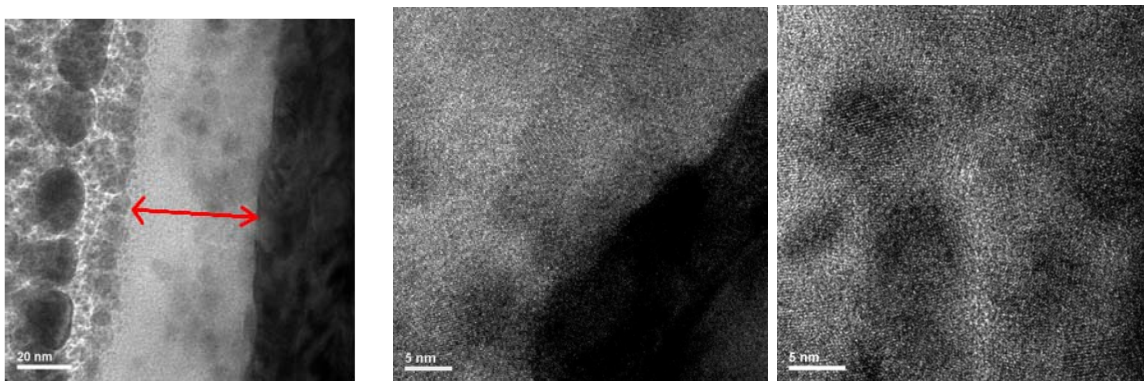


Figure 9. TEM micrograph of Tribochemical film from lubricant C showing the film is about 80 nm thick, monolayer and consists of nano-crystals.

Although still preliminary, the results of FIB/TEM analysis of the three different tribo-films have provided some valuable insight into the structure-friction relationship for boundary films. The two amorphous films showed similar frictional behavior. In both cases, the friction decreased to a relatively low value, although at different rates. On the other hand, the nano-crystalline film showed a nearly constant friction value for the duration of testing, except for a slight decrease at the beginning. Friction in this crystalline film is significantly higher than in the two amorphous films. Work is in progress to further verify this friction-tribo-film structure correlation. GIXRD analysis for several tribochemical films is underway at APS. The combination of FIB/TEM and GIXRD for several

tribochemical films with various frictional behaviors will facilitate the firm establishment of structure-properties relationships for boundary films.

Conclusions

During FY 2009, significant and important progress was made in the two task areas of this project. Scuffing mechanisms in cast iron, an important tribo material in ICE engine, was evaluated. Engine cylinder liners are typically made of cast iron. In case iron, “scuffing” occurs by a transition from mild wear mode into a severe wear mode, which is characterized by rapid removal of material in flake form. Prevention of this transition should enable the design of a high-power density engine.

In the second task of tribo-film characterization, a new and unique technique was developed for analyzing tribochemical boundary film through the combination of FIB and TEM. Three tribochemical films with different frictional behaviors were analyzed with the new technique. Preliminary results showed that the film thickness is between 80 and 120 nm. The lower friction films are amorphous while a constant friction film is nanocrystalline with a grain size of order of 5 to 10 nm. These results will provide guidance for lubricant and surface material integration for predictable and sustainable friction behavior.

Publications

O. O. Ajayi, R. A. Erck, C. Lorenzo-Martin, and G. R. Fenske, "Friction Anisotropy under Boundary Lubrication: Effect of Surface Texture" *Wear* Vol. 267, (2009), 1214-1219.

C. Lorenzo-Martin, O. O. Ajayi, R. A. Erck, N. Demas, and G. R. Fenske, "Characterization of Surface Chemical Boundary Films" Presented at the "Advances in Boundary Lubrication and Boundary Surface Films" International Conference, Seville, Spain, Mar. 29-Apr. 3, 2009.

C. Lorenzo-Martin, O. O. Ajayi, J. K. Lee and A. A. Polycarpou, "Frictional Behavior of Boundary Lubricated Contacts – Effect Tribochemical Surface Films" Proceedings 2009 ASME/STLE International Joint Tribology Conference.

C. Lorenzo-Martin, O. O. Ajayi, R. A. Erck, and G. R. Fenske "Effect of Boundary Films on tribological Behavior of Mild Carbon Steel" Presented at 2009 STLE Annual Meeting, Orlando, FL May 17-21, 2009.

O. O. Ajayi, C. Lorenzo-Martin, R. A. Erck, J. Routbort, and G. R. Fenske, "Boundary Lubrication Mechanisms" 2008 OVT Annual Report (2009), 277- 282.

R. A. Erck, C. Lorenzo-Martin, and O. O. Ajayi, "Friction and Wear Measurements of Hard-Carbon and Nitride Coatings Sliding against 52100 Steel in Commercial Gear Oils at Elevated Temperatures" Presented at 2009 STLE Annual Meeting, Orlando, FL May 17-21, 2009.

Patent

Oyelayo O. Ajayi and Jeffrey Hershberger, "Method for Producing Functionally Graded Nano-crystalline Layer on Metal Surface" Approved by USPTO July 2009. Presented at 2009 STLE Annual Meeting, Orlando, FL May 17-21, 2009.

B. Parasitic Energy Loss Mechanisms

Principal Investigators: George Fenske, Robert Erck, and Nicholas Demas

Argonne National Laboratory

Argonne, IL 60439

Phone: 630-252-5190, Fax: 630-252-4798, e-mail: gfenske@anl.gov

Technology Development Area Specialist: Lee Slezak

(202) 586-2335; fax: (202) 586-2476; e-mail: Lee.Slezak@hq.doe.gov

Participants

Oyelayo Ajayi, Argonne National Laboratory

Zoran Fillipe, University of Michigan

Contractor: Argonne National Laboratory

Contract No.: DE-AC02-06CH11357

Objective

- Develop and integrate mechanistic models of engine friction and wear to identify key sources of parasitic losses as functions of engine load, speed, and driving cycle.
- Develop advanced tribological systems (lubricants, surface metrology, and component materials/coatings) and model their impact on fuel efficiency with a goal to improve vehicle efficiency by 3% in fiscal year (FY) 2012.
- Develop engine component maps to model the impact on fuel efficiency for use in analytical system toolkits.
- Develop a database of friction and wear properties required for models of mechanistic friction and wear of coatings, lubricant additives, and engineered surface textures.
- Validate mechanistic models by performing instrumented, fired-engine tests with single-cylinder engines to confirm system approaches to reduce friction and wear of key components.

Approach

- Predict fuel economy improvements over a wide range of oil viscosities by using physics-based models of asperity and viscous losses.
- Model changes in contact severity loads on critical components that occur with low-viscosity lubricants.
- Develop and integrate advanced low-friction surface treatments (e.g., coatings, surface texturing, and additives) into tribological systems.
- Measure friction and wear improvements on advanced laboratory rigs and fired engines to confirm model calculations.
- Develop component maps of parasitic energy losses for heavy-vehicle system models.

Accomplishments

- Modeled the impact of low-friction coatings and low-viscosity lubricants on fuel savings (up to 4%) and predicted the impact of low-viscosity lubricants on the wear and durability of critical engine components.
- Examined the impact of low-friction technologies on fuel efficiency under high idle conditions.

- Developed experimental protocols to evaluate the friction and wear performance of advanced engine materials, coatings, and surface treatments under prototypical piston-ring environments.
- Evaluated the impact of a commercial additive on the friction properties of base fluids and commercial heavy-duty engine lubricants.
- Developed protocols to deposit low-friction coatings on piston rings and evaluated their impact on the friction of a fully formulated engine lubricant.
- Modified a single-cylinder diesel test stand to measure cylinder-bore friction under motored and fired conditions.
- Developed a lab technique to simulate piston-skirt/liner friction using prototypic components.
- Evaluated the impact of lubricant additives on the friction between the piston skirt and cylinder liner.

Future Direction

- Apply superhard and low-friction coatings on actual engine components and demonstrate their usefulness in low-viscosity oils.
- Optimize coating composition, surface finish, thickness, and adhesion to achieve maximum fuel savings.
- Evaluate the impact of advanced lubricant additives on asperity friction.

Introduction

Friction, wear, and lubrication affect energy efficiency, durability, and environmental soundness of critical transportation systems, including diesel engines. Total frictional losses in a typical diesel engine alone may account for more than 10% of the total fuel energy (depending on the engine size, driving conditions, etc.). The amount of emissions produced by these engines is related to the fuel economy of that engine. In general, the higher the fuel economy, the lower the emissions. Higher fuel economy and lower emissions in future diesel engines may be achieved by the development and widespread use of novel materials, lubricants, and coatings. For example, with increased use of lower viscosity oils (that also contain lower amounts of sulfur- and phosphorus-bearing additives), the fuel economy and environmental soundness of future engine systems can be dramatically improved. Furthermore, with the development and increased use of smart surface engineering and coating technologies, even higher fuel economy and better environmental soundness are feasible.

Integration of advanced lubricant chemistries, textured/superfinished surfaces, and advanced component materials and coatings necessitate

pursuing a systems approach. Changes in one system component can readily change the performance of other components. For example, application of a hard coating on a liner to improve its durability may decrease the durability of the mating rings. Also, lowering the viscous drag will cause certain components (e.g., bearings) to operate under boundary lubrication regimes not previously encountered. This results in accelerated degradation. A systems approach is required not only to identify the critical components that need to be addressed in terms of energy savings, but also to identify potential pitfalls and find solutions.

The primary goal of this project is to develop a suite of software packages that can predict the impact of smart surface engineering technologies (e.g., laser dimpling, near frictionless carbon, and superhard coatings) and energy-conserving lubricant additives on parasitic energy losses from diesel engine components. This project also aims to validate the predictions by comparison with experimental friction and wear data from Argonne National Laboratory. Such information will help identify critical engine components that can benefit the most from the use of novel surface technologies, especially when low-viscosity engine oils are used to maximize the fuel economy of these engines by

reducing churning and/or hydrodynamic losses. A longer-term objective is to develop a suite of computer codes capable of predicting the lifetime and durability of critical components exposed to low-viscosity lubricants.

Starting in 2003, Argonne and Ricardo, Inc. have collaborated to identify engine components that can benefit from low-friction coatings and/or surface treatments. The specific components have included rings, piston skirt, piston pin bearings, crankshaft main and connecting rod bearings, and cam bearings. Using computer codes, Ricardo quantified the impact of low-viscosity engine oils on fuel economy. Ricardo also identified conditions that can result in direct metal-to-metal contacts, which, in turn, can accelerate engine wear and asperity friction. Efforts were also initiated to identify approaches to validate the predictions under fired conditions.

Argonne has focused on the development and testing of low-friction coatings under a wide range of sliding conditions with low- and high-viscosity engine oils. These coatings (such as near frictionless carbon), as well as laser-textured surfaces, were subjected to extensive friction tests using bench-top rigs. The test conditions (i.e., speeds, loads, and temperatures) were selected to create conditions where direct metal-to-metal contacts will prevail, as well as situations where mixed or hydrodynamic regimes will dominate. Using frictional data generated by Argonne, Ricardo estimated the extent of potential energy savings in diesel engines and identified those components that can benefit the most from such low-friction coatings and/or surface treatments. Argonne developed a test rig to simulate engine conditions for piston rings sliding against cylinder liners—one of the major sources of parasitic energy losses identified in Ricardo's studies. The test rig is being used not only to identify candidate technologies that can provide the level of friction reduction assumed in the Ricardo models (e.g., coatings and additives), but also to provide information on the impact of the technologies on material and component wear/durability.

During FY 2009, Argonne analyzed earlier Ricardo simulation studies to determine the impact of (1) low-friction surfaces and low-viscosity fluids on the

overall friction mean-effective pressure (FMEP) and (2) low-viscosity fluids on component durability. Argonne also initiated piston skirt/liner tests to determine the effect of several low-friction additives on skirt/liner friction.

Results and Discussion

Boundary friction and viscosity effects

Phase I and II activities for this project focused on modeling the impact of low-friction surfaces and low-viscosity engine lubricants on friction losses and fuel economy. Figure 1 [1-3] summarizes the results of Ricardo's calculations on the impact of boundary friction and engine lubricant viscosity on the fuel economy of a heavy-duty diesel-powered vehicle. These curves are based on detailed calculations of the FMEP for the piston rings and skirt, valve-train components, and engine bearings under a range of driving conditions. The results predicted fuel savings up to 4-5%, depending on lubricant viscosity grade and asperity friction.

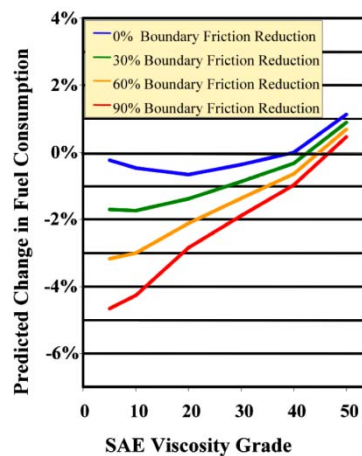


Figure 1. Predicted change in fuel economy as a function of engine lubricant viscosity and boundary friction

In FY 2009, we took a closer look at the role of boundary friction and viscous losses and their impact on FMEP. Figure 2 shows the breakdown of the FMEP into losses to asperity friction and viscous losses at the eight engine modes (load and speed) studied. Graphs are presented for the baseline case (upper left: current asperity friction and 40WT oil); a low-asperity friction/40WT oil case (upper right); a baseline asperity friction, low-viscosity (20WT) oil

(bottom left); and a low asperity friction/low viscosity case (bottom right).

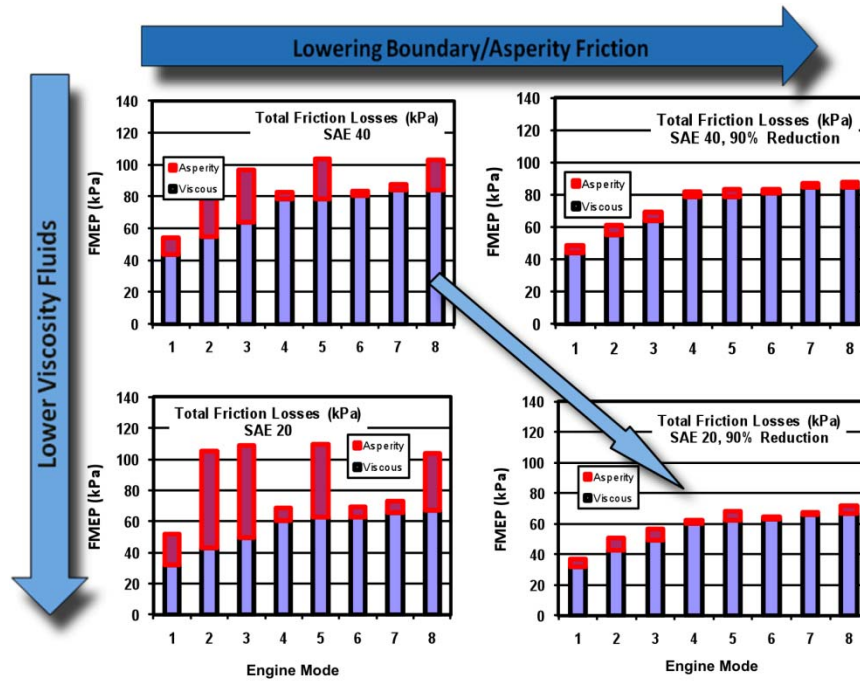


Figure 2. Viscous and asperity FMEP for eight engine modes at different boundary and viscosity

Reducing boundary or asperity friction only, while retaining the same viscosity (40WT) oil, reduces the total FMEP by 10 to 15%. However, the viscous losses still dominate the total FMEP. Reducing the viscosity only, while maintaining the baseline asperity friction, has mixed effects. Under high load conditions (modes 2, 3, 5, and 8), the total FMEP actually increases when the viscosity is reduced due to increased asperity contact with low viscosity fluids. The combined effect of low asperity friction and low viscosity fluids produces the greatest reduction in total FMEP. The results of the analysis suggest the following:

- Reducing asperity friction only can reduce fuel consumption up to 1%.
- Reducing lubricant viscosity only can reduce fuel consumption by 0.5%.
- Reducing both (asperity and viscous losses) together can reduce fuel consumption up to 3-4%.

The fuel savings shown in Figure 1 are for a specific driving schedule in which the fuel consumed at each

mode is weighted with respect to the fraction of time spent at each condition. The amount of time spent at idle (mode 1), where friction can account for more than 50% of the FMEP, significantly impacts the fuel savings – driving schedules with high idle times benefit more from low friction strategies than driving schedules with high-speed modes. This finding suggests that high-speed driving schedules will not benefit as much from low-friction technologies as urban driving schedules. Figure 3 illustrates this effect in greater detail, where the projected fuel savings are plotted as a function of idle time for different lubricant viscosities. The biggest impact of low-friction technologies is accomplished for high idle times (greater than 75 to 80%). While these idle times are not typical of many highway driving schedules, a number of specialty vehicles (e.g., delivery vehicles, garbage trucks, emergency-response vehicles, and military vehicles) spend a large fraction of time at idle.

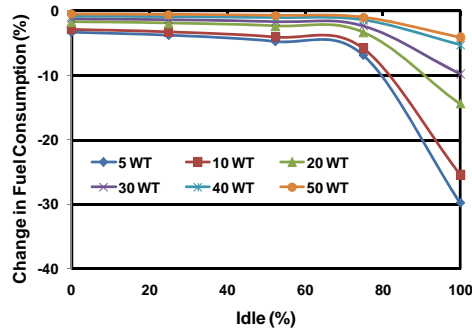


Figure 3. Impact of a 90% reduction in boundary friction on fuel consumption as a function of idle time

Figure 4 illustrates the impact of viscosity on the relative contact severity for different components (e.g., skirt, rings, large end bearing, and small end bearing). The contact severity is based on calculations of the contact loads for the different components. If one assumes the durability is inversely proportional to the load, then the results in the figure can be used to estimate the improvement in the durability required for the components to survive relative to the baseline case (40WT lubricant). For example, operation with a 10WT lubricant would require the use of a ring tribological system (combination of materials, coatings, lubricant additives, surface texture/finish, and/or geometry) that is 3.25 times more durable (wear resistant), while the large end bearings would need to have a tribological system that is 13.5 times more wear resistant than current systems. The results in the figure indicate that the critical component that would be affected by the use of low-viscosity lubricants is the connecting-rod large end bearings. The rings, skirt, and liner will also be affected, but the degree of improvement in wear resistance required to function is not as severe.

Experimental activities during FY 2009 focused on piston-skirt/liner testing. Various variables were studied, including tribochemical film formation, coatings, lubricant additives, and temperature. Results are summarized in the following subsections.

Tribochemical film formation

To investigate the formation of a tribochemical film, experiments were performed using two oils with temperature-activated additives. Figures 5(a) and 5(b) show the friction coefficient of two oils,

designated Oil-A (a commercial gear oil with viscosity of 233.5 cSt at 40°C and 18.7 cSt at 100°C) and Oil-B (an experimental gear oil formulated with low-friction additives and a viscosity of 334.7 cSt at 40°C), at three temperatures (50°C, 70°C, and 120°C), as a function of time. While the focus of these studies is engine oils, using the gear oils serves as a paradigm by providing knowledge about the tribological behavior of additives that may be useful to engine oils. At 50°C, the friction coefficient using Oil-A remained approximately constant at 0.8-0.9 for the test duration of three hours. At 70°C, the friction coefficient was approximately 0.1 at the start of the test, remained constant for 50 minutes, and then gradually decreased to approximately 0.09. Finally, at 120°C, the friction coefficient started higher than 0.1, but quickly decreased (within approximately 20 minutes), reaching a minimum of approximately 0.06—after which it gradually increased, reaching a steady state value of 0.06-0.07 after approximately two hours. At 120°C, the friction coefficient was initially greater than 0.1. That high value is due to the decreased viscosity, which allowed for higher asperity interaction and increased metal-to-metal contact as the film thickness decreased. The subsequent decrease in the friction coefficient may be attributed to the formation of a tribochemical film.

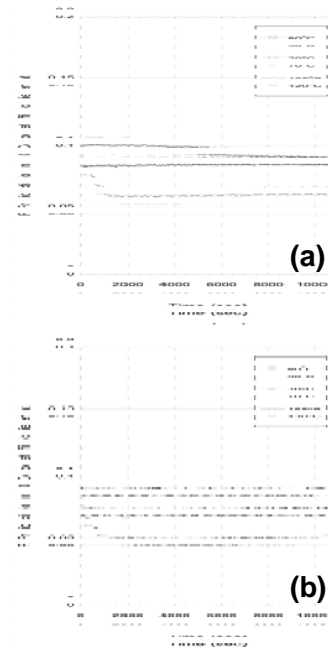


Figure 5. Friction coefficient as a function of time for 3-hour tests using a) oil-A and b) oil-B

The difference in the friction coefficient between 50°C and 70°C may be due to viscosity differences of the oil. The lower viscosity at 70°C may enable a higher number of asperities to contact, where more metal-to-metal contact leads to the higher friction coefficient. The relatively slow formation of a tribochemical film may have occurred, but unlike the case of 120°C, the rate of formation is significantly lower, and its effects on the friction coefficient are not noticed until approximately two hours. Also, at 120°C, the additives in the oil may have been depleted after approximately two hours, at which point a tribochemical film cannot form, leading to the slow gradual increase observed after two hours.

Similar initial trends were observed for Oil-B. However, a gradual decrease in the friction coefficient at 70°C did not occur. That result may be due to the viscosity effects being dominant and the additives not playing an important role at this temperature like in the case of Oil-A. The additives in the case of 120°C may have been depleted after approximately 1.5 hours, at which point no formation of a tribochemical film can occur and the friction coefficient gradually increases, as in the case of Oil-A. Note that friction coefficients as low as 0.05 were achieved with this oil at 120°C.

Coated versus uncoated samples

A different series of tests was performed to compare the tribological behavior between skirt specimens that were either uncoated or coated with a graphite/resin coating. Figure 6 shows the friction coefficient of Oil-A (a) and Oil-B (b) at 120°C as a function of time. The friction coefficient for Oil-A using an uncoated skirt specimen started larger than 0.1, but quickly decreased due to the formation of a tribochemical film. However, using a coated skirt specimen, the friction coefficient did not decrease as quickly and remained significantly higher than in the case of the uncoated skirt specimen. This result may be due to interaction of the additives present in Oil-A with the coating wear debris, which “poisons” the oil and prevents the oil additives from reducing friction. It is also possible that the low-friction tribochemical film is formed on the surface of the coated sample, but is removed as the coating wears.

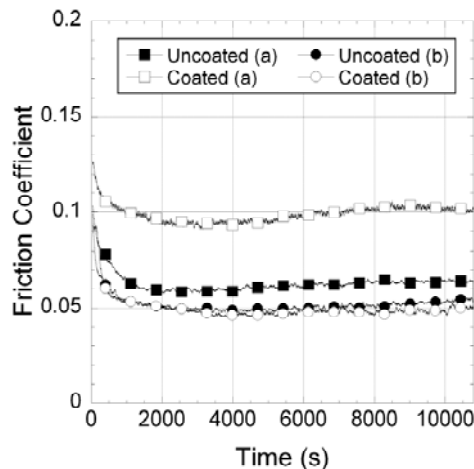


Figure 6. Friction coefficient as a function of time for 3-hour tests with uncoated and coated samples using (a) Oil-A and (b) Oil-B at 120°C

The friction coefficient for Oil-B was approximately the same for both uncoated and coated skirt specimens. Furthermore, the higher friction coefficients may be partially attributed to morphological changes that occur as the graphite/resin coating wears. The wear debris can interact with the oil film thickness, leading to more asperity interaction. The tribological behavior of samples that were either uncoated or coated with a graphite/resin or a-C:H was compared in tests using fully formulated SAE 10W40 oil at 120°C. The results are shown in Figure 7.

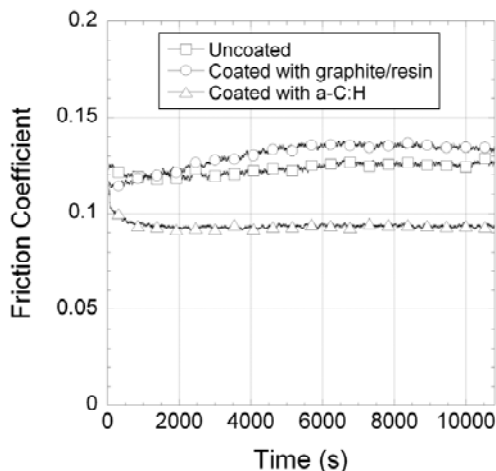


Figure 7. Friction coefficient as a function of time for 3-hour tests with uncoated and coated samples using fully formulated SAE 10W40 oil at 120°C

The friction coefficient was the highest when the skirt specimen was coated with the graphite/resin. However, the difference in the friction coefficient between the uncoated sample and the sample coated with graphite/resin was small. It is possible that as the graphite/resin coating wears, the wear debris interacts with the oil thickness and leads to slightly higher friction coefficient values after approximately one hour. In the case of the a-C:H coated sample, the friction coefficient was the lowest, below 0.10. The inert nature of this coating is responsible for the difference in the tribological behavior.

Effect of additives

The effect of additives on the tribological behavior of uncoated samples in tests using fully formulated SAE 15W40 oil at 100°C was also determined. The results are shown in Figure 8. The fully formulated oil exhibited an initially high friction coefficient, which reached a steady-state value of 0.14. The use of 1 wt% molybdate ester lowered the friction to approximately 0.11, which corresponds to a 20% reduction. Finally, the addition of a 10 wt% boric acid emulsion lowered the friction to 0.08-0.09, a 35% reduction compared to the oil used alone.

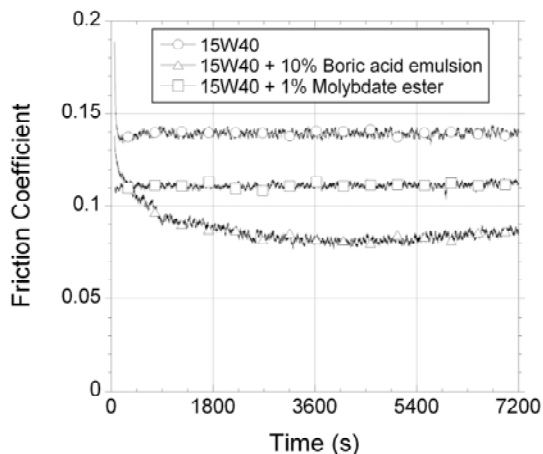


Figure 8. Friction coefficient as a function of time in tests using fully formulated SAE 15W40 oil with and without additives at 100°C

Figure 9 shows photomicrographs of the cylinder liner segments after tribological testing using fully formulated SAE 15W40 oil with no additives, with the addition of 10 wt% boric acid, and with the addition of molybdate ester. Figure 9(a) shows some scratches on the liner surface. While this condition may be attributed to a combination of a

run-in period, initial alignment during the first few strokes of reciprocating motion to a conformal contact of the piston skirt sample is the most probable cause. It is worth mentioning that the initial friction coefficient in all cases is high while a subsequent reduction occurs. This effect is pronounced in the case of the boric acid emulsion, possibly due to morphological changes, as evident from the microscope image of Figure 9(b). For the case with the molybdate ester, Figure 9(c) indicates no damage on the surface of the liner and only the subtle appearance of a wear track produced by polishing wear. Molybdate ester, a known friction modifier, reduces friction by means of molecular adsorption.

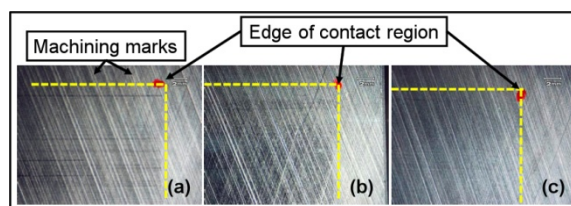


Figure 9. Photomicrographs of the cylinder liner segments after tribological testing using fully formulated SAE 15W40 oil with (a) no additives, (b) the addition of 10 wt% boric acid, and (c) the addition of molybdate ester

The effect of additives on the tribological behavior of uncoated samples in tests using PAO 10 base stock oil was also investigated. Figure 10 shows the resulting friction coefficients as a function of time for 2-hour tests. The PAO 10 oil exhibited an approximately constant friction coefficient of 0.11 for one hour, with a gradual decrease to 0.1 at the end of the test. The addition of 1 wt% molybdate ester initially lowered the friction to approximately 0.1 (a 10% reduction). The friction remained approximately constant with a decreasing tendency toward the end of test to values lower than 0.1.

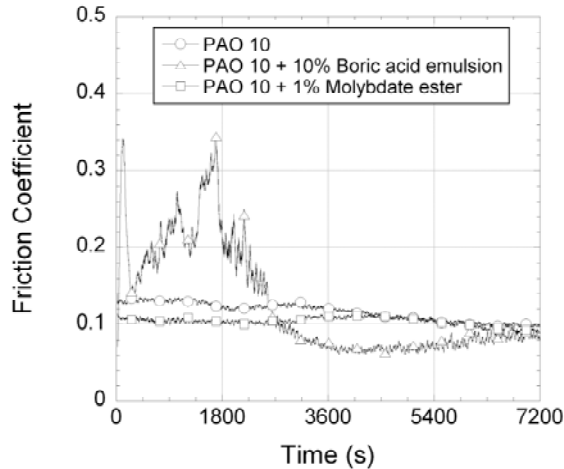


Figure 10. Friction coefficient as a function of time in tests using PAO 10 oil with and without additives at 100°C

Finally, the addition of a 10 wt% boric acid emulsion had a significant effect on the friction coefficient. Initially, the friction coefficient exhibited erratic behavior, reaching greater than 0.3. However, it decreased significantly to a value of 0.08 after one hour. Then the friction increased slightly and reached approximately 0.1. Figure 11 shows photomicrographs of the cylinder liner segments after tribological testing using PAO 10 with no additives, with the addition of 10 wt% boric acid emulsion, and with the addition of molybdate ester. In the case of PAO 10, there is no visible damage except for some minor scratches, similar to the case of SAE 15W40 (compare Figures 9 and 10).

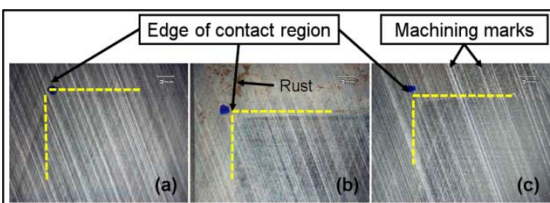


Figure 11. Photomicrographs of the cylinder liner segments after tribological testing using PAO 10 oil with (a) no additives, (b) the addition of 10 wt% boric acid, and (c) the addition of molybdate ester

On the surface of the liner tested in PAO 10 with 10 wt% boric acid, a visible wear track was produced as a result of polishing wear. Finally, in the case of PAO 10 with 1 wt% molybdate ester, unlike the case of SAE 15W40 where no visible wear track occurred due to molecular adsorption, a patchy tribochemical film formed visible under the microscope. Furthermore, when 10 wt% boric acid

emulsion was used as an additive, there was visible rust formation around the wear track. The initially high and erratic friction behavior may have been due to the rust formation and oxidative wear, and after approximately 45 minutes, morphological changes due to polishing wear may have been responsible for the friction reduction. Examination of the piston skirt specimens revealed that the surface texture was removed. Part of the reason for this texture is oil retention between the grooves. Figures 12(a) and 12(b) show photo-micrographs of the piston skirt sample before and after the 2-hour test. The morphology of the sample changed significantly, as shown by the images of Figures 12(c) and 12(d) of the samples before and after testing, respectively. No protection was offered by the addition of 10 wt% boric acid emulsion, and the lowering of the friction coefficient may be attributed to an increase in the apparent area and a decrease in surface roughness as the original texture was removed. This condition could change the lubricating regime and, therefore, the friction coefficient.

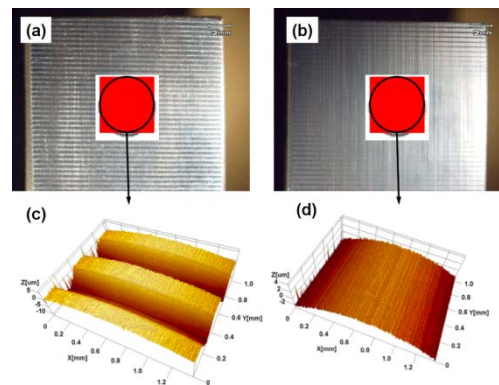


Figure 12. Microscope images of (a) piston skirt segment after testing in PAO 10; (b) piston skirt segment after testing in PAO 10 + 10% boric acid; (c) and (d) corresponding surface profiles for (a) and (b), respectively

More specifically, as groove removal occurs, the boundary lubrication regime will be affected and may change into mixed lubrication, explaining the lower friction coefficient. The addition of the 10 wt% boric acid emulsion resulted in oxidation due to the hydroxyl groups present in the emulsion. Rust formation was not observed with the SAE 15W40 oil, possibly because of the presence of anti-oxidants in the oil.

Effect of temperature

The effect of temperature on the tribological behavior of the interface as a function of speed was also studied. Figure 13 shows the friction coefficient as a function of reciprocating speeds (left y-axis) and the speed profile (right y-axis) at four temperatures. The initial speed was 15 rpm (0.01 m/sec), and it was doubled every 10 seconds up to a maximum of 240 rpm (0.15 m/sec). These short-duration tests were performed at the end of 1-hour tests at 20-100°C, when the friction coefficient had already reached a steady state.

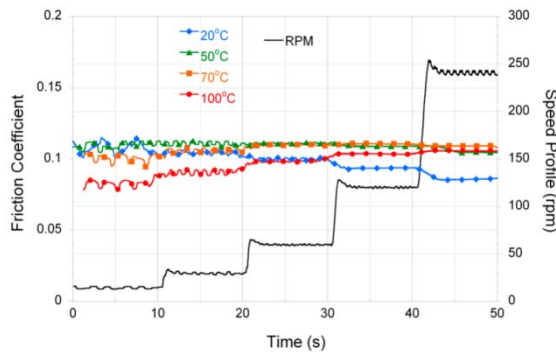


Figure 13. Friction coefficient as a function of speed at 500 N and temperatures of 20°C, 50°C, 70°C, and 100°C for fully formulated 10W30 oil

The friction coefficients at 20 and 50°C were approximately the same in the beginning of the test at the lowest speeds. The initial friction value at both 20 and 50°C was approximately 0.11. As speed increased from 15 rpm (0.01 m/sec) to 30 rpm (0.02 m/sec) the friction coefficient dropped at 20°C. For every stepwise increase in speed, the friction coefficient dropped and reached a minimum between 0.08 and 0.09. At 50°C there was no significant decrease in friction coefficient with increasing speed until 240 rpm (0.15 m/s), before which the friction had remained rather constant. At 70°C the initial friction coefficient started at approximately 0.1, lower than that at 20°C and 50°C. Contrary to what was observed at 20°C, friction increased as the speed increased. A similar but more pronounced trend was observed in the case of 100°C. The friction coefficient was 0.08-0.09 at 15 rpm (0.01 m/s) and increased during every speed increase, reaching a maximum at 0.10-0.11. When the speed was low, pressure did not build up in the oil at all, and the loading was carried by the asperities in the contact area protected by adsorbed molecules of the oil

and/or a thin oxide layer. At this point the contact was in the boundary regime. In the case of 20°C, viscosity was responsible for the initially high friction, while increasing speed decreased the friction coefficient. This effect is also true for the case of 50°C, but it is not as pronounced. Above 70°C, even before any tribological interaction, a chemical film formed on the interface. This film was responsible for the initially low friction coefficients in the cases of 70 and 100°C. However, this chemical film, which is formed due to the temperature-activated additives in the formulated SAE 10W30 oil, was not durable and was quickly removed when the tribological interaction occurred. The viscosity also decreased significantly above 70°C, and the contact moved toward the mixed and elastohydrodynamic lubrication regime, during which the oil-film thickness increased with increasing speed, resulting in a higher friction coefficient.

Summary

The calculated results of parasitic friction losses for eight engine modes suggest that reducing asperity/boundary friction and viscous friction separately are limited in their ability to reduce fuel savings. However, through the combined use of low-friction (coatings and/or additives) technologies coupled with low-viscosity fluids, fuel savings in the 3-4% range can be achieved.

Fuel savings via low-viscosity fluids comes at a price—the reduced viscosity will increase the degree of metal-to-metal contact and hence potentially increase wear and reduce durability or reliability. Analysis of the contact severity loads indicated that the most vulnerable components affected by the increased metal-to-metal contact are the large end bearings, and that the surface finish and/or wear resistance may need to be improved to maintain durability.

Tribological tests were conducted with skirt specimens that were either uncoated, coated with graphite/resin, or coated with a-C:H and were sliding against cylinder liners in various oils. The quick formation of a low-friction tribochemical film was evident at 120°C due to the activation of additives in the oil. At lower temperatures, viscosity effects were dominant, while at 70°C friction was reduced due to the slow formation of a tribochemical film.

The use of a graphite/resin coating in piston skirt specimens, tested in three different oils, did not offer any significant improvement. Testing showed that it was detrimental for one of the oils, as the coating debris may have interacted with the additives, prevented the formation of a tribochemical film due to wear, or interacted with the oil film thickness as it wore. Testing a graphite/resin coating with different oils than those tested in this work should be considered as in different oil formulations. Such a coating may not have a negative effect. The a-C:H coating samples possessed good frictional characteristics and showed significant improvement over the uncoated samples and those coated with graphite/resin.

Tests were conducted on the use of boric acid emulsion and molybdate ester additives to fully formulated oil. While the addition of molybdate ester offered improvement in the friction coefficient, the boric acid emulsion rusted the samples before lowering the friction when used with a base stock oil. Most importantly though, it reduced friction through morphological changes at the expense of polishing wear.

References

- 1) I. Fox, "Numerical Evaluation of the Potential for Fuel Economy Improvement due to Boundary Friction Reduction within Heavy-Duty Diesel Engines," ECI International Conf. on Boundary Layer Lubrication, Copper Mountain, CO, Aug. 2003.
- 2) George Fenske, "Parasitic Energy Loss Mechanisms," *FY 2006 Progress Report for Heavy Vehicle Systems Optimization* (2006).
- 3) George Fenske, "Parasitic Energy Loss Mechanisms: Impact on Vehicle System Efficiency," U.S. Department of Energy Heavy Vehicle Systems Review, April 18-20, 2006, Argonne National Laboratory, Argonne, Illinois.

Publications/Presentations

Fenske, G. R., Erck, R. A., and Demas, N. G., "Parasitic Energy Loss Mechanisms," Heavy Vehicle Systems Optimization, FY 2008 Progress Report (2008).

Demas, N. G., Erck, R. A., and Fenske, G. R., "Tribological Evaluation of Piston Skirt/Cylinder Liner Contact Interfaces under Boundary Lubrication Conditions," *Lubrication Science*, 2009, Accepted.

Fenske, G. R., Erck, R. A., Ajayi, O. O., Masoner, A., and Comfort, A. S., "Impact of Friction Reduction Technologies on Fuel Economy for Ground Vehicles," Proceedings of the 2009 Ground Vehicle Systems Engineering and Technology Symposium (GVSETS), Warren MI, August 2009.

Demas N., Fenske G., and Erck R., "Tribological Evaluation of Piston Skirt/Cylinder Liner Contact Interfaces under Boundary Lubrication Conditions," STLE 64th Annual Meeting, Lake Buena Vista, FL, May 17-21, 2009.

Fenske G., Erck R., Demas N., Eryilmaz, O., and Lorenzo-Martin, M., "Parasitic Energy Losses," US DOE Hydrogen Program and Vehicle Technologies Program Annual Merit Review and Peer Evaluation Meeting, Washington, D.C., May 18-22, 2009.

Argonne is managed by UChicago Argonne, LLC, for the U.S. Department of Energy under contract

C. Agreement # 13723 - Residual Stresses in Thin Films*

**(This project is jointly funded by Propulsion Materials and Heavy Vehicle Systems Optimization)*

Principal Investigators: D. Singh and J. L. Routbort coworkers: Kristen Pappacena

Argonne National Laboratory

9700 S. Cass Avenue, Argonne, IL 60439-4838

630-252-5009 dsingh@anl.gov

DOE Technology Manager: Jerry L. Gibbs

(202) 586-1182; fax: (202) 586-1600; e-mail: jerry.gibbs@ee.doe.gov

Contractor: UChicago Argonne LLC

Contract No.: DE AC03 06CH11357

Objective

- Measure residual stresses in thin films and coatings as a function of film thickness and relate stresses to film properties such as hardness, fracture toughness, and adhesion energy to relate to film processing variables and to predict durability.
- Use techniques developed for measurements of residual stresses in thin films and coatings to measure residual stresses in bulk layered structures produced by joining by high-temperature deformation and to improve their mechanical properties.

Approach

- Develop X-ray technique to measure change of lattice parameter of coating constituents as a function of depth and hence to calculate the lattice strains and stresses.
- Develop indentation and/or scratch techniques to measure hardness, fracture toughness, and adhesion energy of films and coatings.
- Relate stresses, properties, and processing conditions to film durability.

Accomplishments

- Procured ZrN and TiC commercial coatings deposited on steel substrates with varying processing conditions: high-rate reactive sputtering (HRRS) & activated reactive evaporation (ARE).
- Advanced Photon Source (APS) used to measure residual stresses in ZrN and TiC coatings as a function of processing conditions.
- Stresses were found to be sensitive to deposition conditions.
- A commercial scratch tester procured and installed for adhesion energy measurements.

Future Directions

- Develop indentation and/or scratch approaches to measure film adhesion.
 - Develop correlations between processing, residual stresses, adhesion energy for the coating systems studied: MoNCu, ZrN, and TiC. These correlations will help develop processing approaches for the development of coating systems with enhanced durability for applications on heavy vehicle engine components.
-

Introduction

Because of their unusual structural, mechanical, and tribological properties, superhard, nanocrystalline coatings can have an immediate and far-reaching impact on numerous advanced transportation applications including the Department of Energy's (DOE) FreedomCAR and 21st Century Truck Partnerships by reducing parasitic friction losses (hence increasing fuel economy) and wear (hence increasing durability/reliability). They can also be used to overcome toxic emission problems associated with exhaust gas recirculation in diesel engines. Durability of hard coatings is a critical property. The durability is determined by the surface adhesion energy, but is the result, in a large part, of the residual stresses that form as a result of materials, and processing parameters such as deposition bias voltage, ion flux, and temperature.

The approach for this effort is to use the high-brilliance X-rays produced by the Advanced Photon Source (APS) at Argonne National Laboratory and a microfocus beam, to measure the residual stresses/strains of MoN-based thin films and commercial coatings such as ZrN and TiC as a function of depth from the surface through the interface to the substrate. Subsequently, residual stress profiles will be correlated with the film processing conditions, and the resulting film/substrate adhesion and the films tribological properties.

During the past year, focus has been on two coating/substrate systems: (a) ZrN on steel and (b) TiC deposited on steel. Residual stresses as a function of depth in both in-plane and out-of-plane directions have been measured. Mechanical properties evaluation of these coatings was conducted to study the variation of properties as a function of position on the coating. Finally, a scratch tester system was procured and installed. This system will be used for the determination of the adhesion energy of the coatings for correlations with the processing and residual stresses.

Experimental Procedures

Samples

Samples of ZrN and TiC coatings deposited on steel were obtained from a commercial source. These coatings were deposited on tool steel (T-15). Two different processes of deposition were used to fabricate samples of ZrN and TiC: (a) high rate reactive sputtering (HRRS) and (b) activated reactive evaporation (ARE).

HRRS coatings were deposited below 300°C at deposition rates between 2300 Å/min and 4400 Å/min with reactive partial pressures ranging from 0.2-0.5 mTorr and a dc substrate bias of -100V. On the other hand, ARE coatings were deposited between 350-500 °C with deposition rates between 2000-5000Å/min. Carbide samples were fabricated using methane (in Ar carrier gas) in the HRRS process and acetylene in the ARE process. For the nitride samples, nitrogen gas was used in both the processes. Typical sample size was a 0.5inch x0.5 inch square with the deposited coatings approximately 5µm thick.

Residual stresses measurement

X-ray microdiffraction was performed on beamline 34-ID-E at the APS [1]. The X-ray beam was focused by Kirkpatrick-Baezmirrors down to 0.4 (horizontal) x0.6 (vertical) µm². A high-resolution charged coupled device (CCD) X-ray detector was used to collect X-ray diffraction (XRD) patterns from the X-ray microbeam with energy of 8.9 keV (1.39308 Å). Strains and stresses were evaluated from the change in the lattice spacing determined from diffraction pattern of specific diffraction planes of coating materials and their respective stress free states.

The sample was aligned such that one of the edges was perpendicular to the X-ray beam. A schematic of the set-up is shown in Figure 1. The sample was aligned by an X-ray fluorescence method so that the film surface (perpendicular to the page in the figure) was parallel to the X-ray beam. The sample was then scanned with respect to the X-ray beam with a step size of 0.25 µm. Similarly, by rotating the detector or the sample by 90°, out-of-plane strains were determined.

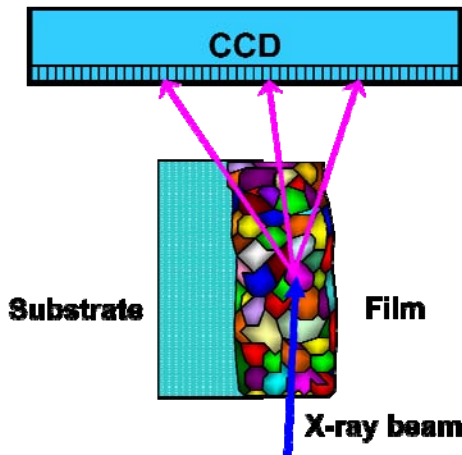


Figure 1. Experimental set-up for residual stress (strain) measurements

Nano-indentation

Nano-indentation on the ZrN-coated sample was conducted to ascertain the variability of the coating properties at various locations, especially near sample edges. Nano-indentation tests were conducted at University of Illinois at Urbana Champaign. The sample surface was divided into four quadrants. Within each quadrant, several measurements were made for hardness and elastic modulus as a function of depth of penetration.

Results and Discussion

Figure 2 shows the diffraction patterns obtained from TiC and ZrN coatings, respectively. The diffraction patterns at various detector orientations are shown for the two cases. The (111) diffraction planes for both coatings were used for the strain measurements. Figures 3 and 4 show the corresponding lattice parameters of TiC and ZrN coatings determined from X-ray diffraction as a function of coating depth. In-plane and out-of-plane values of lattice parameters are plotted as a function of coating depth. The strain-free lattice parameter is calculated from the $\sin^2\psi$ approach [2]. The calculated strains are plotted in Figures 5 and 6 for TiC and ZrN coatings, respectively.

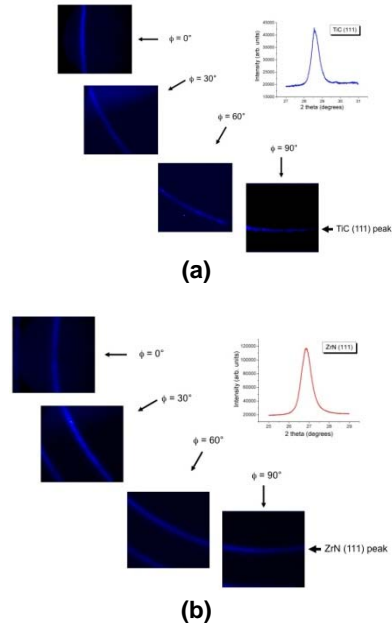


Figure 2. Diffraction patterns from (111) reflections of (a) TiC and (b) ZrN coatings as a function of detector orientation.

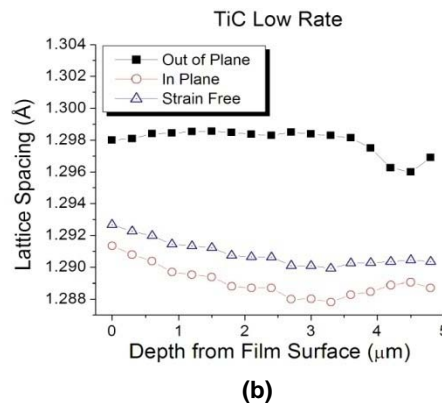
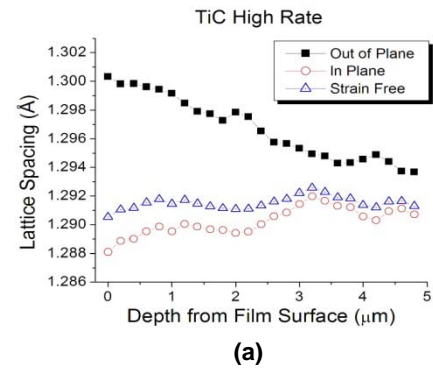


Figure 3. Lattice spacings of TiC coatings as a function of coating depth in in-plane and out-of-plane modes for (a) HRRS and (b) ARE processes.

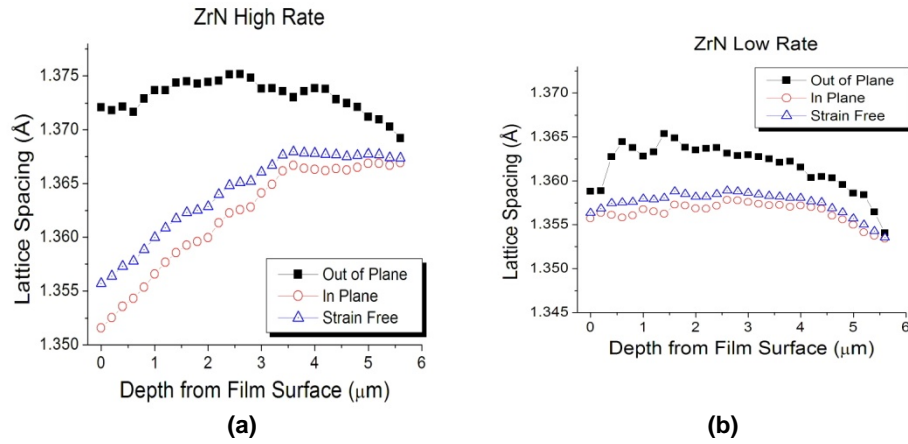


Figure 4. Lattice spacings of ZrN coatings as a function of coating depth of in-plane and out-of-plane modes for (a) HRRS and (b) ARE processes

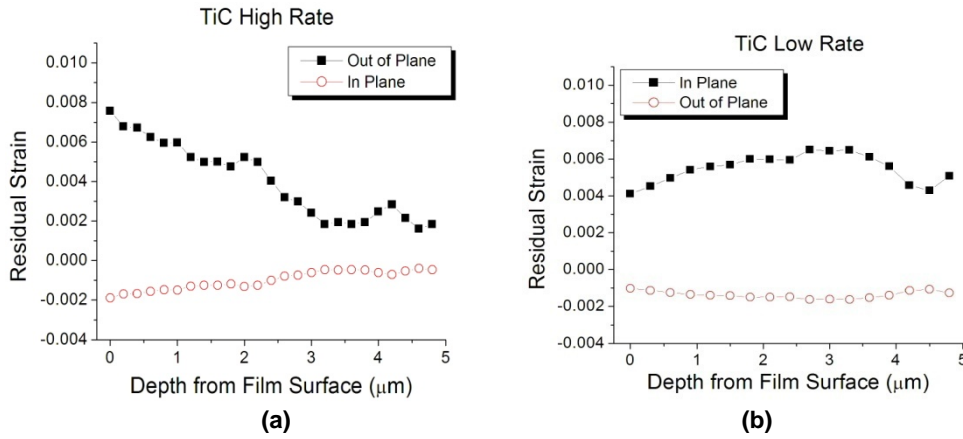


Figure 5. Residual strains of TiC coatings as a function of coating depth in in-plane and out-of-plane modes for (a) HRRS and (b) ARE processes

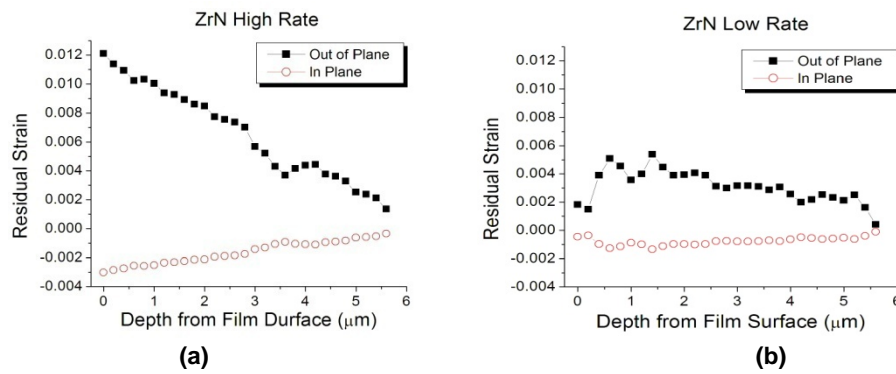


Figure 6. Residual strains of ZrN coatings as a function of coating depth in in-plane and out-of-plane modes for (a) HRRS and (b) ARE processes

Three major observations can be made from the residual strain measurements:

- (a) For TiC coatings, in-plane residual strains are compressive and out-of-plane strains are tensile and their magnitudes decreases from coating surface to the substrate interface.
- (b) for ZrN coatings, strain profiles are quite similar to those observed for TiC samples, i.e., in-plane strains are compressive and out-of-plane are tensile.
- (c) For both ZrN and TiC coatings, the strain variation as a function of coating depth is much steeper for the high deposition rate process (i.e., HRRS, as compared to the ARE process).

As shown in Figure 7, there is significant variability in the measured elastic moduli and hardness as a function of location for the ZrN coating. This figure corresponds to a quadrant in which the lower and right sides correspond to the sample edges. Elastic moduli values vary from 200 GPa to 350 GPa. It is interesting to note that the two lowest elastic moduli (locations 13 and 12) are on the sample edge, whereas, higher elastic moduli are observed for locations (6 and 5) that are away from the sample edge. Similar observations are made in the hardness measurements. These results confirm that there could be processing related local variations in the mechanical properties of the coatings which could contribute to the reduction of the coating durability under service conditions.

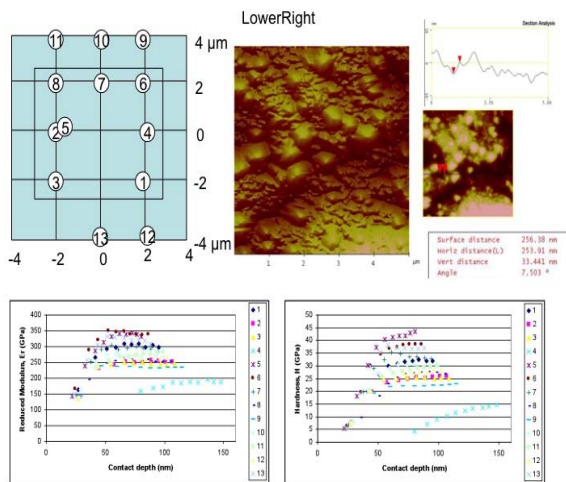


Figure 7. Location of nano-indentations on ZrN coating and the measured elastic moduli and hardness values.

Scratch tester

We have now procured and installed a Romulus scratch tester with a stylometer attachment, manufactured by the Quad Group (Spokane, WA). Figure 8 shows a photograph of the scratch tester. The procedure involves scratching the sample surface using a stylus (125-533 μm radius) at a fixed loading rate that is computer controlled. The system has a built-in acoustic transducer that picks up any coating delamination or fragmentation events. The system also has a microscope that allows one to examine the scratch path (Figure 9) and visually confirm the coating delamination. The load at which the coating delamination occurs is used to determine the adhesion energy of the coating [3].



Figure 8. Computer controlled scratch tester for coating adhesion energy measurements.

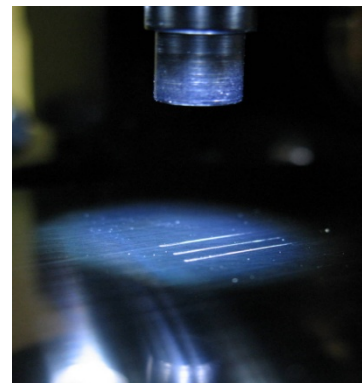


Figure 9. Typical scratches generated during the scratch test.

Conclusions

In conclusion, we have applied a cross-section X-ray micro-diffraction technique to study depth-resolved residual strain in two commercial coatings: ZrN and

TiC, deposited on steel substrates. These coatings were fabricated using two different processing conditions. The nano-indentation technique has been demonstrated as a tool for establishing the variability in the mechanical properties of the coating as a function of the location from the edges to the center of the coatings. To determine the adhesion energy of the coatings, a scratch tester has been procured and installed.

Future Directions

We will continue to develop the scratch test technique to measure surface adhesion energies. Further, residual stress measurements will be correlated to processing conditions and the adhesion energy to develop a protocol for fabricating coatings with long-term durability. Finally, collaboration(s) will be established with a coatings manufacturer for heavy vehicle engine OEMs and technology will be transferred.

References

1. G. E. Ice, B. C. Larson, W. Yang, J. D. Budai, J. Z. Tischler, J. W. L. Pang, R. I. Barabash, and W. Liu, *J. Synchrotron Rad.* **12**, 155 (2005).
2. V. Hauk, *Structure and Residual Stress Analysis by Nondestructive Methods*, (Elsevier, Amsterdam, 1997), Chapter 2.
3. S. T. Gonczy and N. Randall, An ASTM Standard for Quantitative Scratch Adhesion testing of Thin, Hard Ceramic Coatings, *Int. J. Ceram. Technl.*, 2 [5] 422-428 (2005).

This document highlights work sponsored by agencies of the U.S. Government. Neither the U.S. Government nor any agency thereof, nor any of their employees, makes any warranty, express or implied, or assumes any legal liability or responsibility for the accuracy, completeness, or usefulness of any information, apparatus, product, or process disclosed, or represents that its use would not infringe privately owned rights. Reference herein to any specific commercial product, process, or service by trade name, trademark, manufacturer, or otherwise does not necessarily constitute or imply its endorsement, recommendation, or favoring by the U.S. Government or any agency thereof. The views and opinions of authors expressed herein do not necessarily state or reflect those of the U.S. Government or any agency thereof.



2010

DEPARTMENT OF
ENERGY

Energy Efficiency &
Renewable Energy

For more information
1-877-EERE-INF (1.877.337.3463)
programname.energy.gov